



ICES
CIEM

International Council for
the Exploration of the Sea

Conseil International pour
l'Exploration de la Mer

ICES COOPERATIVE RESEARCH REPORT
RAPPORT DES RECHERCHES COLLECTIVES

NO. 318 SPECIAL ISSUE
AUGUST 2013

**ICES Zooplankton Status Report
2010/2011**



ICES Cooperative Research Report

Rapport des Recherches Collectives

No. 318 Special Issue

August 2013

ICES Zooplankton Status Report 2010/2011

Editors

Todd D. O'Brien, Peter H. Wiebe, and Tone Falkenhaug



International Council for the Exploration of the Sea
Conseil International pour l'Exploration de la Mer

H. C. Andersens Boulevard 44–46
DK-1553 Copenhagen V
Denmark
Telephone (+45) 33 38 67 00
Telefax (+45) 33 93 42 15
www.ices.dk
info@ices.dk

Recommended format for purposes of citation:
O'Brien, T. D., Wiebe, P.H., and Falkenhaus, T. (Eds). 2013.
ICES Zooplankton Status Report 2010/2011.
ICES Cooperative Research Report No. 318. 208 pp.

Series Editor: Emory D. Anderson

For permission to reproduce material from this publication, please apply to
the General Secretary.

This document is a report of an Expert Group under the auspices of the
International Council for the Exploration of the Sea and does not necessarily
represent the view of the Council.

ISBN 978-87-7482-125-0
ISSN 1017-6195

© 2013 International Council for the Exploration of the Sea

Above :

Mud shrimp *Solenocera membranacea*
larva, caught in the western Bay of
Biscay. - Juan Bueno, Instituto Español
de Oceanografía (IEO)

Cover image:

Assorted copepods and a decapod
caught in the Mallorca Channel. - Maria
Luz Fernández de Puelles, Instituto
Español de Oceanografía (IEO)

CONTENTS

1	Introduction	4
2	Time-series data analysis and visualization	6
2.1	Time-series data analysis	7
2.1.1	The WGZE time-series analysis	7
2.1.2	Representation of “absence” and zero-value measurements	9
2.2	Time-series data visualization: standard figures	10
2.2.1	Seasonal summary plot	10
2.2.2	Multiple-variable comparison plot	11
2.2.3	Regional overview plot	13
2.3	Time-series supplemental data	15
2.3.1	Sea surface temperature data: HadISST	16
2.3.2	Sea surface chlorophyll data: GlobColour	17
2.3.3	Sea surface wind data: ICOADS	18
2.3.4	Baltic Sea surface salinity data: PROBE–Baltic model	19
3	Zooplankton of the Northwest Atlantic Shelf	20
4	Zooplankton of the Labrador Sea	42
5	Zooplankton of the Nordic and Barents seas	58
6	Zooplankton of the Baltic Sea	78
7	Zooplankton of the North Sea and English Channel	110
8	Zooplankton of the Bay of Biscay and western Iberian Shelf	132
9	Zooplankton of the Mediterranean Sea	162
10	Zooplankton of the North Atlantic Basin	182
11	References	190
12	Site Metadata: Time-series sampling characteristics and contact information	200

1. INTRODUCTION

Todd D. O'Brien, Peter H. Wiebe, and Tone Falkenhaug

In its *Strategic Plan*, ICES recognized its role in making scientific information accessible to the public and to fishery and environmental assessment groups. During ICES Annual Science Conference 1999, ICES requested that the Oceanography Committee working groups develop data products and summaries that could be provided routinely to the ICES community. Since that time, the Working Group on Zooplankton Ecology (WGZE) has produced a summary report on zooplankton activities in the ICES Area, based on the time-series obtained from national monitoring programmes.

This is the ninth summary report of zooplankton monitoring in the ICES Area. This year's report includes twenty-two new survey sites: five in the new Labrador Basin subregion, fourteen in the Baltic Sea, two in the Bay of Biscay and western Iberian Shelf, and one in the western Mediterranean Sea. This report summarizes the North Atlantic Basin and its major subregions using these 62 zooplankton monitoring sites (Figure 1.1) as well as the 40 Continuous Plankton Recorder (CPR) standard areas (Figure 1.2).

Although this report follows previous reports in its general structure and analysis, new standardized data components and graphical visualizations have been added. Each site report begins with a standard figure series demonstrating the seasonal cycles of zooplankton, chlorophyll, and temperature at that site. Multivariate figures then provide a quick overview of zooplankton interactions and/or synchrony with other cosampled biological and hydrographic variables available for the site. Finally, a long-term assessment of each monitoring area is made using a 100-year record of sea surface temperature data, a 50-year record of surface windspeed data, and up to 60 years of CPR zooplankton data (when available near that site). The methods and data sources used for this report are summarized in Section 2.

The monitoring sites in this report represent a broad range of hydrographic environments, ranging from the temperate latitudes south of Portugal to the colder regions north of Norway, Iceland, and Canada (Figure 1.3), and from the lower salinity waters of the Baltic and coastal estuaries to the higher salinity waters of the Mediterranean. Across this broad range of physical conditions, the diversity, abundance, and biomass of zooplankton vary between sites and years, with clear seasonal and cyclical patterns, ranging from a few years to decades in duration, apparent at all sites. Temperature greatly influences the community structure and productivity of zooplankton, causing large seasonal, annual, and decadal changes in population size and in species composition and distribution.

Given the evidence of ocean climate changes and regime shifts as well as the potential effects of acidification and pressures on marine ecosystems from fishing, aquaculture,

and offshore energy developments, it is hoped that in the future, time and expertise can be harnessed and funded to provide a more comprehensive and detailed analysis and synthesis. Increasingly, these data are incorporated into models and syntheses of ecosystems at local to basin scales, providing insights, evidence, and ecosystem perspectives, and relating the impacts of climate and other factors on marine communities. The detailed examination of individual species is beyond the scope of this report. However, changes in ocean climate are likely to affect some species more than others, particularly those at the boundaries of their geographic ranges, where they may be most susceptible to changes in seasonal temperature, food supply, competitors, or predators. Such species may prove to be the best indicators of changes in their environment. The need for high-resolution monitoring of marine plankton that can provide detailed information on seasonal and interannual changes at local, regional, and global scales is becoming increasingly central to our understanding of marine ecosystems and to our advice on the sustainable management of marine services and resources.

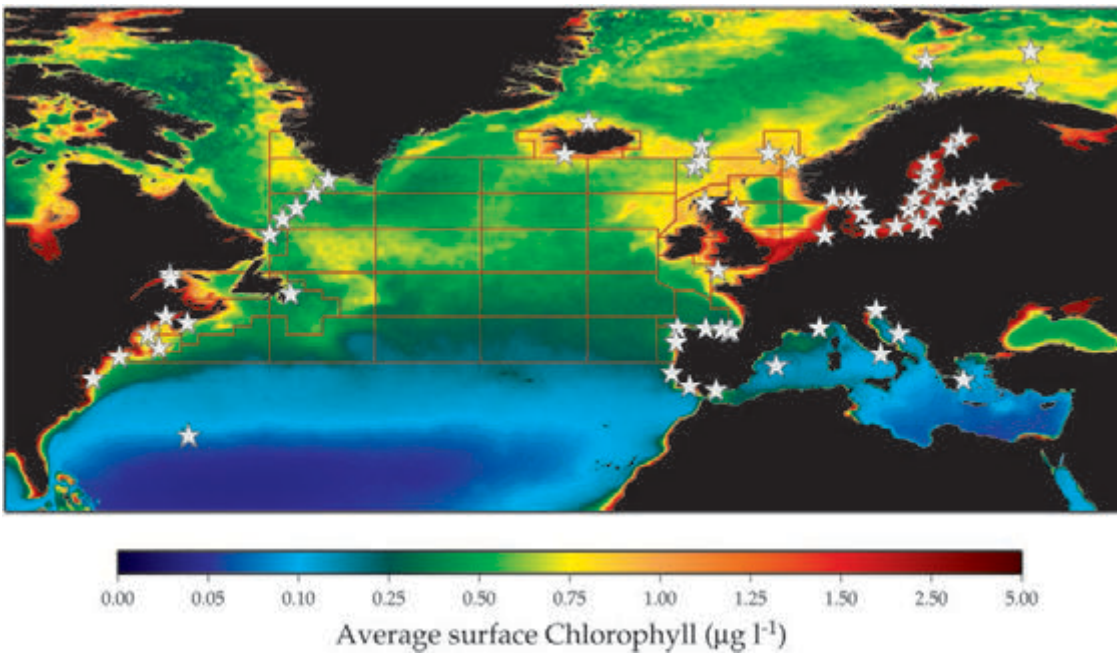


Figure 1.1
Zooplankton monitoring sites within the ICES Area plotted on a map of annual average chlorophyll concentration. Only programmes summarized in this report are indicated on this map (white stars). The red boxes outline CPR standard areas (see Figure 1.2 and Section 10).

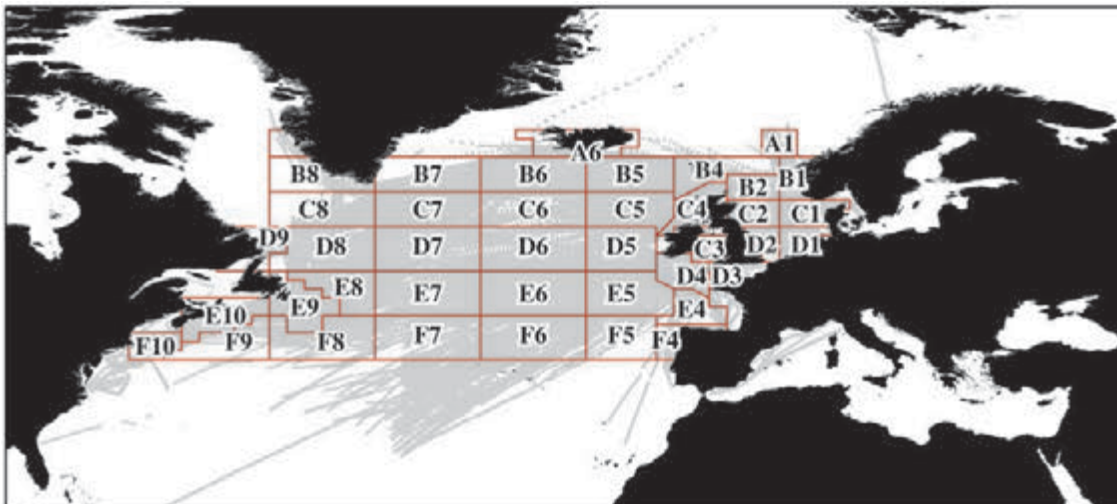


Figure 1.2
Map of CPR standard areas in the North Atlantic (see Section 10 for details). Grey dots and lines indicate CPR sampling tracks.

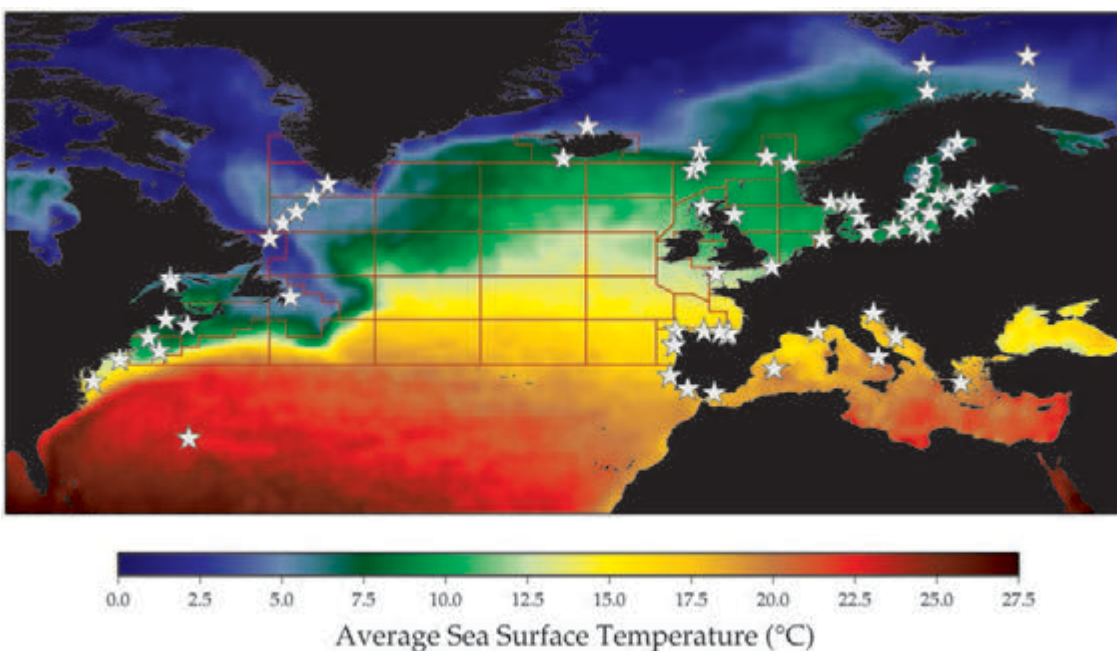


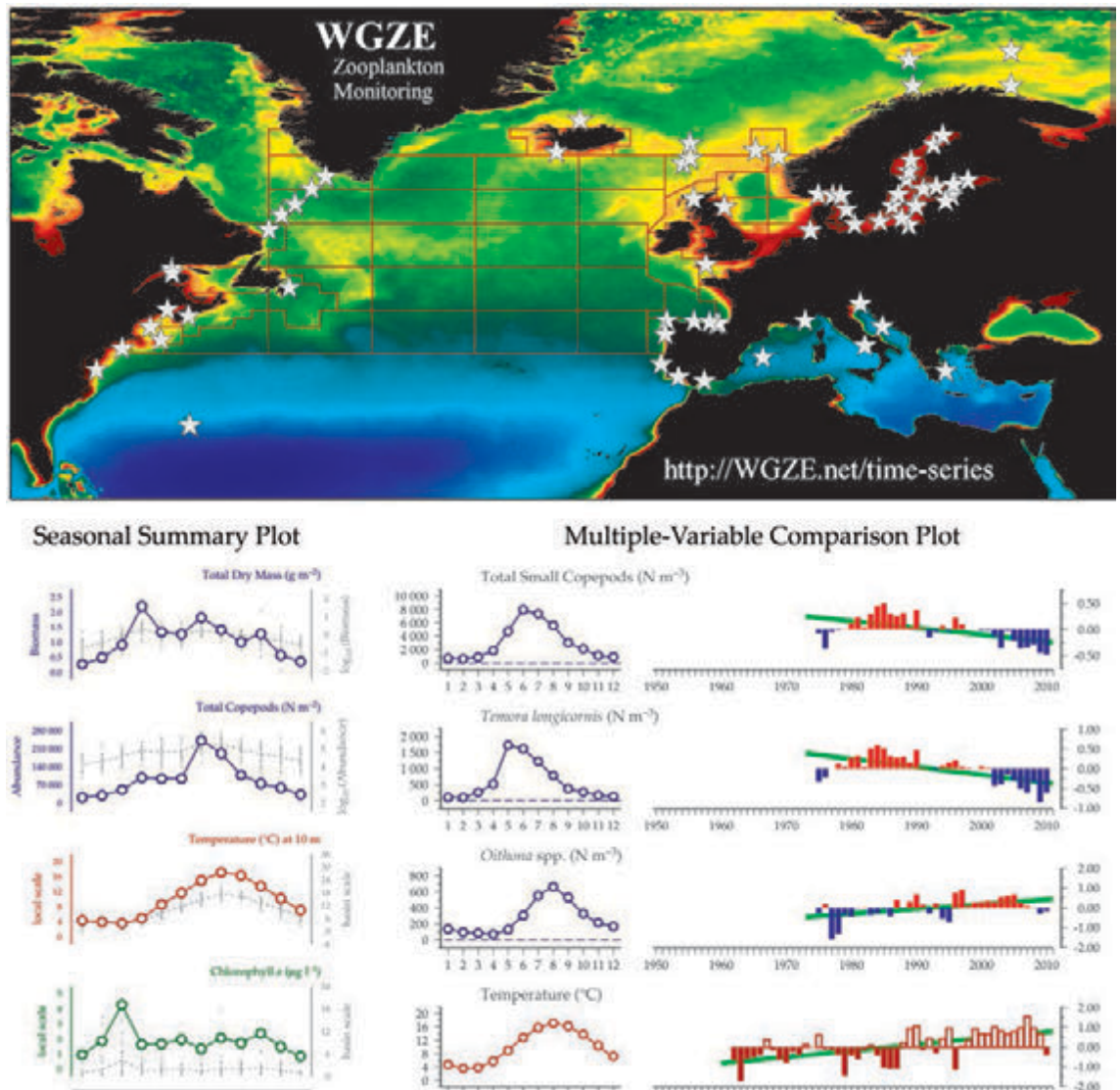
Figure 1.3
Zooplankton monitoring sites within the ICES Area plotted on a map of annual average sea surface temperature. Only programmes summarized in this report are indicated on this map (white stars). The red boxes outline CPR standard areas (see Figure 1.2 and Section 10).

2. TIME-SERIES DATA ANALYSIS AND VISUALIZATION

Todd D. O'Brien

Figure 2.1

Examples of the interactive mapping and visualization tools used for the creation of this report and as available online at <http://WGZE.net>.



The Coastal and Oceanic Plankton Ecology, Production & Observation Database (COPEPOD; <http://www.st.nmfs.noaa.gov/copepod/>) is a global database of plankton survey data, time-series, and plankton data products hosted by the National Marine Fisheries Service (NMFS) of the National Oceanic and Atmospheric Administration (NOAA). Through nine years of scientific collaboration and data-analysis support for plankton working groups such as the ICES Working Group on Zooplankton Ecology (WGZE) and the ICES Working Group on Phytoplankton and Microbial Ecology (WGPME), COPEPOD has developed a collection of plankton-tailored, time-series analysis and visualization tools (illustrated in Figure 2.1), including those used in the creation of this report. These tools in turn became COPEPOD's Interactive Time-series Explorer (COPEPODITE, <http://www.st.nmfs.noaa.gov/nauplius/copepodite/>), a free, online time-series processing

and visualization toolkit that can be used to generate figures and analyses similar to those used in this report (and more). COPEPODITE also features an interactive database that provides information and contact points for hundreds of phytoplankton and zooplankton time-series and monitoring programmes from around the world. This metabase also acts as an access point to all of the sites used in this report as well as those from the concurrent ICES Phytoplankton and Microbial Plankton Status Report (see O'Brien *et al.*, 2012).

This chapter describes the time-series data-analysis methods (Section 2.1), the standard data-visualization figures used throughout this report (Section 2.2), and the supplemental data sources (e.g. sea surface temperature, chlorophyll, and windspeed) included in the standard analyses of each monitoring site (Section 2.3).

2.1 Time-series data analysis

The time-series analysis methods (and visualizations) used in this report were developed in cooperation with the SCOR Global Comparisons of Zooplankton Time-Series working group (WG125), the ICES Working Group on Zooplankton Ecology (WGZE), and the ICES Working Group on Phytoplankton and Microbial Ecology (WGPME). The analyses used for this report use only a small subset of the entire collection of visualizations and analytical approaches created for these working groups. For simplicity, the subset of analysis and figures used in this report is referred to hereafter as “the WGZE time-series analysis”.

2.1.1 WGZE time-series analysis

The WGZE time-series analysis is used to compare interannual trends across a variety of plankton and other hydrographic variables, each with different measurement units and sampling frequencies (e.g. to compare interannual trends in the “number of copepods per cubic meter of water, sampled once a month” with the “average concentration of chlorophyll *a*, sampled weekly”). The WGZE analysis method uses a unitless ratio (or “anomaly”) to look at relative changes in data values over time relative to the long-term average (or “climatology”) of those data.

Each plankton time-series $P(t)$ is represented as a series of log-scale anomalies $p'(t)$ relative to the long-term average \bar{P} of those data:

$$p'(t) = \log_{10}[P(t)] - \log_{10}[\bar{P}] = \log_{10}[P(t) / \bar{P}]$$

If a dataserie at a given site is collected consistently and uniformly for the duration of a monitoring programme, the sampling bias (b) is represented in the equation as follows:

$$p'(t) = \log_{10}[b \times P(t)] - \log_{10}[b \times \bar{P}] = \log_{10}[bP(t) / b\bar{P}]$$

As the sampling bias (b) is present in both the numerator and denominator of the equation, it is cancelled out during the calculation. Likewise, the measurement units of the values are also cancelled out, creating a unitless ratio (the anomaly):

$$p'(t) = \log_{10}[b \times P(t)] - \log_{10}[b \times \bar{P}] = \log_{10}[bP(t) / b\bar{P}] = \log_{10}[P(t) / \bar{P}]$$

By using unitless anomalies, WGZE can make comparisons in the form “copepod abundances doubled during the same time period that chlorophyll *a* concentrations decreased by half”. These unitless comparisons of relative value changes can be made between any variable, within a single site as well as between multiple sites.

The WGZE analysis examines interannual variability and long-term trends by looking at changes in average annual values throughout a time-series. In most regions of the North Atlantic, plankton have a strong seasonal cycle, with periods of high (often in spring) and low (often in winter or late summer) abundance or biomass. As a result of this strong seasonal cycle, calculation of a simple annual average of plankton from low-frequency or irregular sampling (e.g. once per season or once per year) can be greatly influenced by when that sampling occurs (e.g. during, before, or after these seasonal peaks). This problem is further compounded by missing months or gaps between sampling years. The WGZE analysis addresses this problem by using the technique of Mackas *et al.* (2001), in which the annual anomaly value is calculated as the average of individual monthly anomalies within each given year. As this effectively removes the seasonal signal from the annual calculations, this method reduces many of issues caused by using low-frequency and/or irregular monthly sampling to calculate annual means and anomalies.

The WGZE time-series analysis involves a series of calculation steps, illustrated using Figure 2.1.1:

1. The incoming time-series data (i.e. total small copepod abundance sampled weekly at the Helgoland Roads monitoring site, Figure 2.1.1, Site 45 in Section 7.2) are binned into monthly means by year over the entire dataset. During this step, plankton, chlorophyll, and nutrient values are \log_{10} transformed, while temperature and salinity values are not. The distributions of values in each month of each year of the time-series are plotted as the green dots in Figure 2.1.1a, and their value frequency is shown in the green bars in Figure 2.1.1b subpanel. The month-by-year mean values are also shown in the temporal matrix of Figure 2.1.1c, where colours represent value-range categories and white spaces indicate months or years with no data or sampling. Together, these three subplots provide a detailed overview of the data's distribution, variability, and temporal coverage.
2. The long-term average for each month, also known as its climatology, is then calculated. These monthly climatology values are represented by the open red circles in Figures 2.1.1a,b.
3. Each month's climatology value is then subtracted from each month-by-year value (e.g. the matrix cells in Figure 2.1.1c) in order to calculate month-by-year monthly anomaly values for the time-series. In the monthly anomaly matrix (Figure 2.1.1d), months with value greater than that month's climatology (i.e. a positive monthly anomaly) are indicated with a red cell, while months with a value less than that month's climatology (i.e. a negative monthly anomaly) are indicated with a blue cell. Months with no data (no sampling) are left blank (e.g. January through March 2007 in Figures 2.1.1c,d).
4. Annual anomalies for all of the years in the time-series (Figure 2.1.1e) are calculated (per Mackas *et al.*, 2001) as the average of all of the monthly anomalies (Figure 2.1.1d) present within that year. In this figure, annual anomaly values greater than zero are indicated with red, while annual anomaly values less than zero are indicated with blue. An open circle drawn on the anomaly zero line indicates that data were not available that entire year. This symbol for "no data years" is used to distinguish them from near-zero value anomalies, which may plot as a very thin line in the subfigure. (The "no data year" symbol is not present in Figure 2.1.1, but can be found repeatedly in Figure 2.2.2 found in Section 2.2.2.)
5. In Figure 2.1.1e, the green line drawn behind the anomaly bars represents the linear regression of the annual anomalies vs. year. The color and form of this line indicate the statistical significance of this trend (e.g. solid green is $p < 0.01$, dashed green is $p < 0.05$, thin grey is $p > 0.05$).
6. Figures 2.1.1f and 2.1.1g provide useful information about the dataset and/or sampling environment. The left middle subpanel (Figure 2.1.1f) shows the distribution of raw (non-log-transformed) values and their climatological monthly means (green dots and open red circles). This plot shows the full value range of raw values used in the calculations. The left lower subpanel (Figure 2.1.1g) shows the distribution and climatological monthly means of water temperatures at the sampling site. Water temperatures can influence the seasonal cycle of the plankton as they may affect the plankton both directly (e.g. metabolic rates) and indirectly (e.g. water column stratification and subsequent nutrient limitation).

To save printing costs and page space within this report, only Figures 2.1.1f (non-log transformed seasonal cycle) and 2.1.1e (annual anomalies) are presented in the report (see Sections 2.2.1 and 2.2.2). The full figure sets are available online (<http://WGZE.net>) for each time-series site and variable.

Figure 2.1.1 summarizes the seasonal and interannual trends of the dataset as follows:

Small copepods at the Helgoland Roads monitoring site have a seasonal maximum in summer (June/July) and a seasonal minimum in winter (December–February; Figures 2.1.1a,f). The annual average abundances from 1980 to 1990 were above the long-term average (Figure 2.1.1e, red or positive annual anomalies), but have been below the long-term average from 2000 to 2010 (Figure 2.1.1e, blue or negative annual anomalies). Small copepod abundances have been decreasing from the 1980s through 2010 (Figure 2.1.1e, $p < 0.01$, solid green line).

The period of strongest positive annual anomalies (Figure 2.1.1e, years 1983–1988) corresponds to a period of relatively high summer average abundances that extended from spring to autumn (e.g. the large spatial area of red and orange squares in spring–autumn from 1983 to 1988 seen in Figure 2.1.1c). This period also shows positive monthly anomalies throughout most or all months of those years (Figure 2.1.1d), suggesting that the population of small copepods remained high in abundance throughout the year during that period. The period of strongest negative annual anomalies (Figure 2.1.1e, years 2005–2010) corresponds with a period of lower-value winter abundances (e.g. the large spatial area of blue winter values from 2005 to 2010 seen in Figure 2.1.1c). In the latter case, this period corresponds to negative monthly anomalies that extend throughout most of the months within those years (Figure 2.1.1d). Further discussion on the Helgoland Roads zooplankton is presented in Section 7.2.

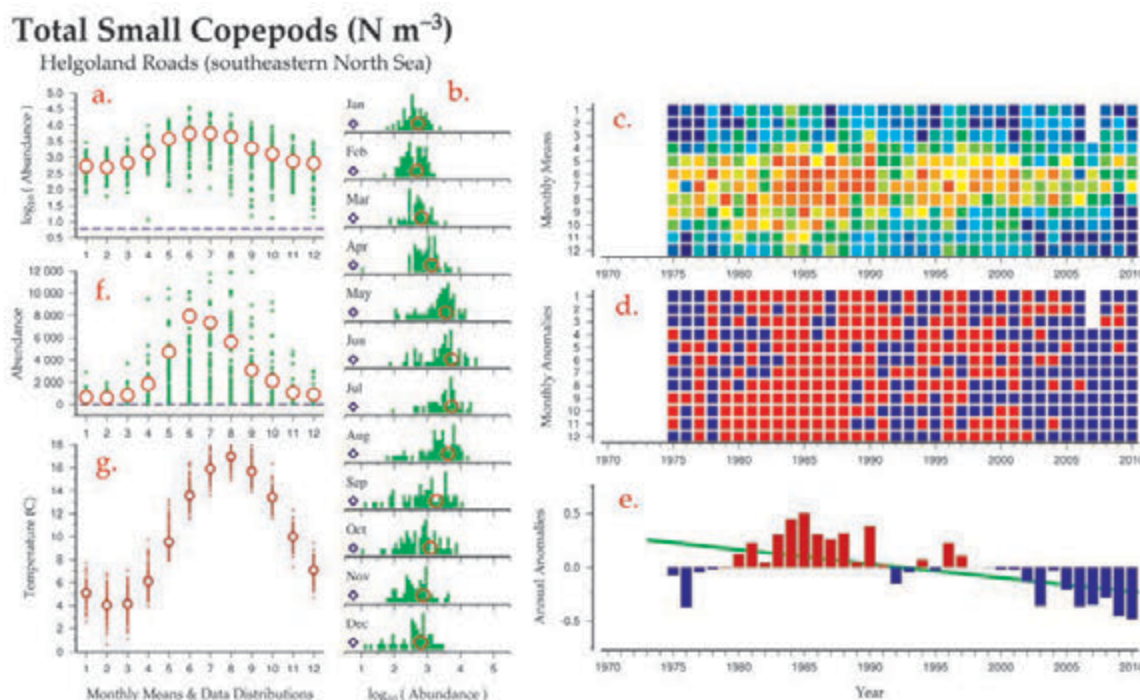


Figure 2.1.1
A collection of standard WGZE time-series visualization figures illustrating the steps and components used in the WGZE analysis for creating annual anomalies of total small copepod abundance from the Helgoland Roads time-series (Site 45, see Section 7.2 for more information on this site).

2.1.2 Representation of “absence” and zero-value measurements

Some plankton groups and species (e.g. meroplankton) have a temporary seasonal presence within a monitoring site and may completely disappear during parts of the year. At the Arendal Station monitoring site (located in the northern Skaggeiak, see Section 7.1), the abundance of cirrepede (barnacle) larvae in the water column is relatively high in spring and early summer but then becomes quite low (and often completely absent) in autumn and winter. Abundance data for cirrepede larvae from this site have zero-value measurements that indicate “looked for and found absent in the sample”. Including these zero values in the standard WGZE time-series analysis is a challenge, however, as the WGZE method log-transforms these data, and $\log(0)$ is an undefined math operation.

One commonly used log/zero-handling solution is to add 1 to all the values before log-transforming them, often referred to as “ $\log(x+1)$ ”. The problem with this solution is that the “ $x+1$ ” offset numerically affects smaller-value-range data (e.g. counts of a rare species with non-zero values ranging from 1 to 20 per unit) at a different magnitude than it numerically affects larger-value-range data (e.g. counts of an entire group of blooming species with non-zero values ranging from 1000 to 20 000). In the latter case, the zero value (“ $x+1$ ” = $0+1$ = 1) is 1/1000th of the otherwise lowest recorded value, and using it will have a greater impact on the calculation of the climatological means and anomalies than that same “ $x+1$ ” offset will have on the smaller range example. An alternate and improved version of the “ $x+1$ ” method is, therefore, to add a value offset that is based on the value range of the data itself (“ $x+0.01$ ”, “ $x+100$ ”), but adding even a small offset still has a non-linear effect on all of the other (non-zero) values in the dataset.

The WGZE zero-handling method does not add any offset. Instead, it replaces any incoming zero value with a fixed “zero-representation value” (Zero-rep), which is equal to one half of the lowest non-zero value seen in the entire datastream for that variable (regardless of year or month). The Zero-rep would be 0.5 for data ranging from 1 to 20, and would be 500 for data ranging from 1000 to 20 000. The Zero-rep method works with both small- and large-range-value sets, without introducing non-linear biases or offsets. This method requires knowing the value range of the data before processing it, calculating the Zero-rep, and then replacing any zero values with this Zero-rep value. While this may be difficult to do by hand, especially with hundreds of variables, it is automatically done by the COPEPODITE toolkit during the data preparation process.

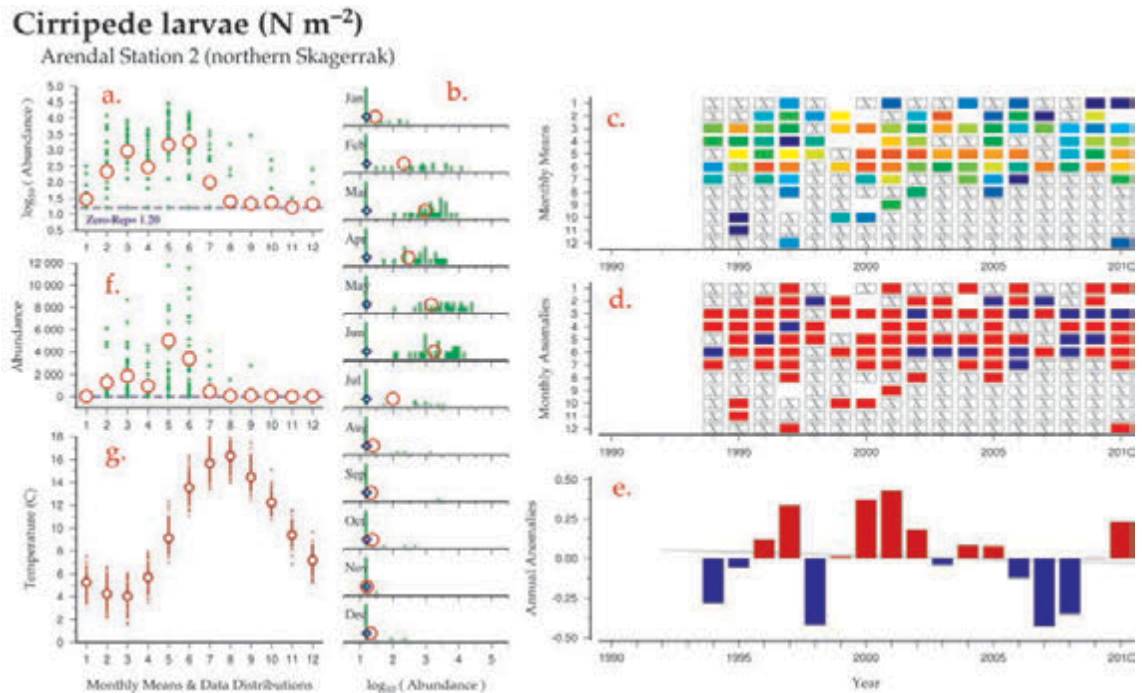
When the Zero-rep function is active for a plankton variable, the standard figures shown in Figure 2.1.1 include some additional graphical elements (see Figure 2.1.2). In the standard figure collection for cirrepede larvae at Arendal Station, the Zero-rep value is indicated as a blue dashed line in Figures 2.1.2a,f and as a blue diamond in Figure 2.1.2b. When cirrepede larvae are absent for the entire month, the month-by-year mean matrix cell for that month is represented with an “[X]”. In Figure 2.1.2c, this symbol differentiates January 2000 (an “[X]” cell, a month in which no cirrepede larvae were found in the samples) from January 1999 and February 2000 (both blank/white cells, months in which no sampling was done). In the monthly anomaly matrix (Figure 2.1.2d), any monthly anomaly based only on this Zero-rep value is also indicated with an “[X]” cell. These monthly anomalies are still involved in the calculation of the annual anomaly averaging calculation (e.g. calculated as the average of all monthly anomalies), with a value equal to the Zero-rep value.

Figure 2.1.2 summarizes the seasonal and interannual trends of cirrepede larvae at Arendal Station as follows:

Cirrepede larvae at Arendal Station have a seasonal maximum in summer (June/July) and a seasonal minimum or absence from August through January (Figures 2.1.2a,f). The decline in abundance begins with the highest water temperatures found in July/August at the site (Figure 2.1.2g), most likely due to benthic settlement of this meroplankton taxa. Seasonally, on a year-to-year basis, the cirrepede larvae

generally follow this pattern (spring/summer abundance, autumn/winter absence) for the duration of the time-series (Figures 2.1.2c,d). On an interannual basis, cirrepede larvae were generally above the long-term average from 1996 to 2005 and below the long-term average from 2006 to 2008. The interannual pattern appears to be cyclical, with no clear linear trends found over the life of the time-series (Figure 2.1.2e, grey line).

Figure 2.1.2
A collection of standard WGZE time-series visualization figures illustrating the steps and components used in the WGZE analysis for creating annual anomalies of cirrepede larvae from the Arendal Station time-series (Site 44, Section 7.1).



2.2 Time-series data visualization: standard figures

With more than 1000 different variables in the full WGZE time-series collection (e.g. taxonomic groups and species abundances and biomasses, temperature, salinity, nutrients and pigments, windspeed, river inflow, and Secchi depth), one of the biggest challenges in creating this report was to find a way of quickly representing these data in a standard visual format within the report itself. These figures need to quickly summarize the seasonal variability, interannual changes, and the presence (or absence) of any long-term trends or patterns. Within this report, each time-series monitoring site summary begins with a standard seasonal summary plot (Section 2.2.1), followed by a more detailed multiple-variable comparison plot (Section 2.2.2) and a regional overview plot (Section 2.2.3).

2.2.1 Seasonal summary plot

The seasonal summary plot (see examples in Figure 2.2.1) shows the seasonal cycle of the general zooplankton population along with the average monthly values of surface temperature and chlorophyll concentrations at each monitoring site. The general zooplankton population can be represented by a total abundance value (e.g. "Total Copepods" or "Total Zooplankton") and/or by a total biomass value (e.g. "Total Dry Mass", "Total Displacement Volume"). In cases where both data types exist within a site, both can be shown (see Figure 2.2.1a).

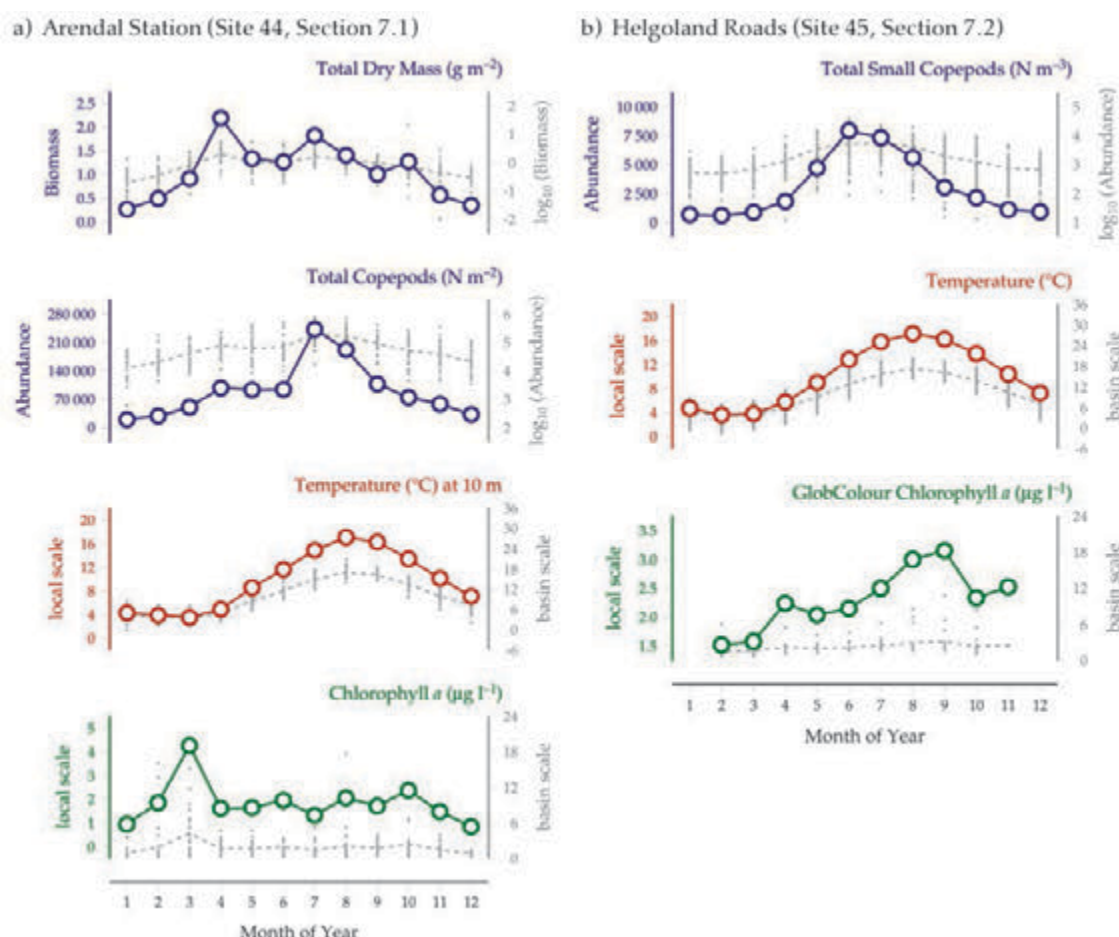
Each subfigure in this plot shows the average monthly values plotted on dual y-axis. The value scale of the left axis is set relatively narrow to highlight the seasonal cycle of the variable and is colour-coded to match the plotted symbols (blue = zooplankton, red = temperature, green = chlorophyll). The value scale on the right, with grey colouration and symbols, shows the values on a broader-value range scale. For temperature and chlorophyll, the

right-scale range is set to cover the range of all values found within this entire report. On this large range scale, one can quickly see how the warmer Mediterranean temperatures compare to the colder Icelandic temperatures, or compare productive to oligotrophic regions. Within the zooplankton population subplots, the left (blue) axis shows raw values while the right (grey) axis shows the \log_{10} transformed values as well as with the general scatter of values used to calculate these monthly means.

The dual axes were adopted because using only the left (tight) axis did not always convey these broad differences found between sites and using only the common right (broad) axis reduced visibility of the seasonal signal (such as the flat grey lines seen in the zooplankton and chlorophyll subplots of Figure 2.2.1).

Figure 2.2.1

Examples of two seasonal summary plots (see Section 2.2.1) showing average month-to-month zooplankton population proxies, water temperature, and chlorophyll at the Arendal Station (Site 44, Section 7.1) and Helgoland Roads (Site 45, Section 7.2) monitoring sites.



2.2.2 Multiple-variable comparison plot

The multiple-variable comparison plot (Figure 2.2.2) presents a seasonal and interannual comparison of select co-sampled variables sampled within a monitoring site. The subfigures in this plot are created by combining subfigures "f" and "e" from the WGZE standard figures discussed in Section 2.1 (see Figures 2.1.1f,e and 2.1.2f,e). The colour of the annual anomalies will not always be blue and red. While annual anomalies of plankton abundance and biomass variables are blue and red, annual anomalies for chlorophyll and pigment variables are green, annual anomalies for temperature variables are dark red, annual anomalies for salinity and density variables are black, and annual anomalies for nutrients, ratios, meteorological values, and anything else is orange (see Figure 2.2.2 for examples).

As described in Section 2.1, the left column of subfigures summarizes the seasonal cycle of each variable, while the right column of subfigures summarizes the interannual patterns and trends of each variable. As described in Section 2.1.1, the trend lines within the annual anomalies subfigures are colour and form coded as follows: green trend lines indicate statistical significant (solid green = $p < 0.01$, dashed green indicates $p < 0.05$), while grey lines indicate a non-significant trend.

Figure 2.2.2 summarizes the seasonal and interannual trends of select variables within the Eastern Gotland Basin as follows:

In the left column of the subfigures, the seasonal cycle plots indicate that the three zooplankton variables were based on only three months of sampling per year and that chlorophyll was based on only five months of sampling data. In contrast, temperature and salinity were based on twelve months of sampling data. In the right column of the subfigures, total [zooplankton] wet mass and *Temora longicornis* annual anomaly values show strong increasing trends ($p < 0.01$, solid green lines), temperature shows a slightly weaker trend ($p < 0.05$, dashed green line), and salinity shows a strong decreasing trend. *Pseudocalanus* spp. shows a decreasing, but non-significant trend (grey line), while chlorophyll shows a slight (but non-significant) increase.

The multiple-variable comparison plot is also useful for highlighting intervariable relationships. In Figure 2.2.2, the copepod taxa *Pseudocalanus* spp. and *T. longicornis* show complimentary, though opposite, trends, which correspond to increasing temperatures and decreasing salinities in the region. This relationship is found because

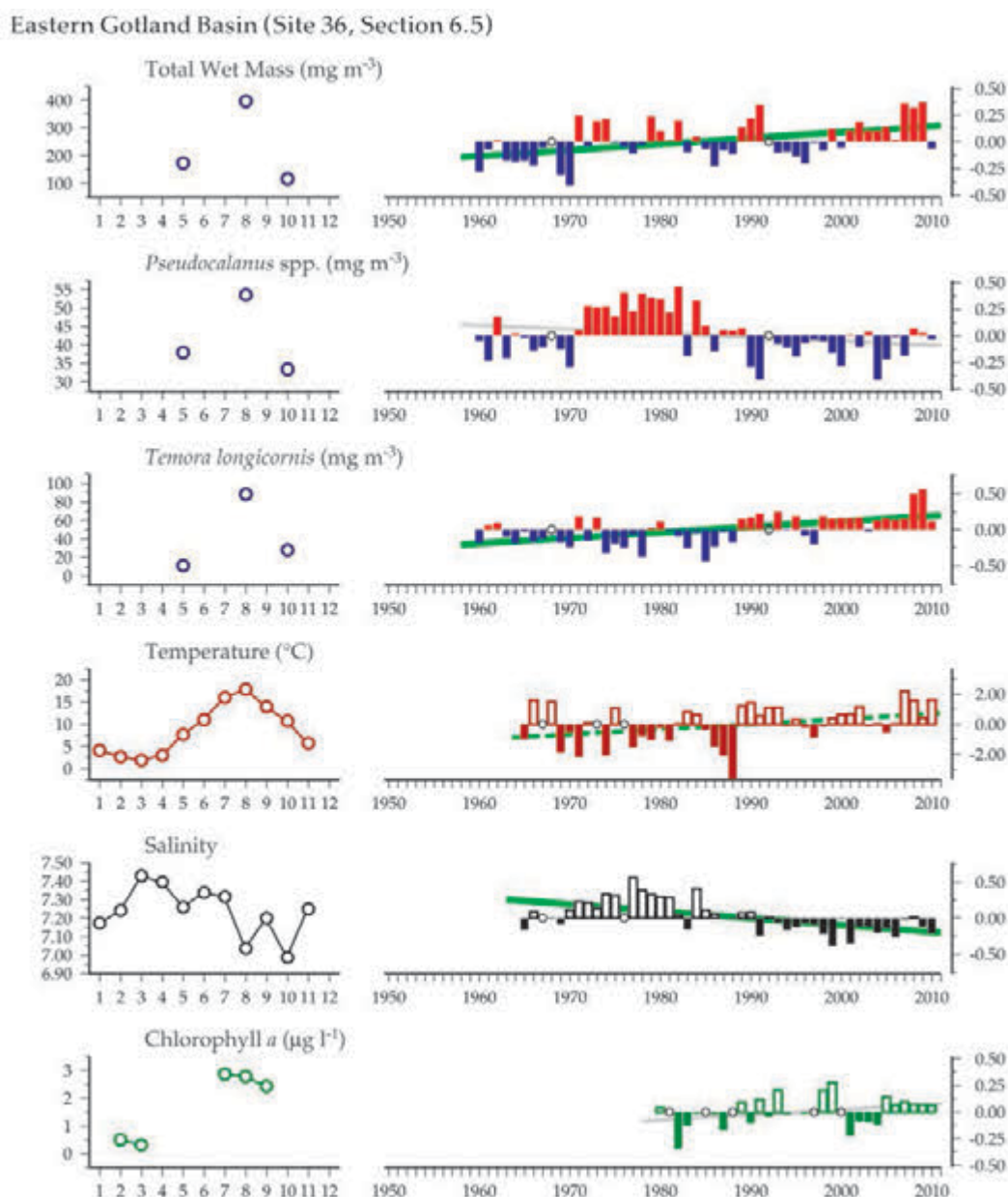
T. longicornis tolerates lower salinities than *Pseudocalanus*, while increasing precipitation in the region (data not shown) is responsible for much of the decreasing salinity (freshening of the waters) in the region. Cases like this, where climate-influenced salinity changes are visible as changes in the zooplankton community, are present in many of the Baltic Sea sites (see Section 6 in general and Section 6.5 for this specific region).

Only a select number of variables and plots are shown for each site to reduce the size of the printed version of this publication. Most of the multiple-variable comparison plots in this report display less than ten variables, while many of the time-series sites have 20 or more variables (including nutrients and additional zooplankton species).

The WGZE times-series site (<http://WGZE.net/time-series>) contains additional variables and visualization figures (such as those of Figures 2.1.1 and 2.1.2) that are not shown in this report document.

Figure 2.2.2
Example of a multiple-variable comparison plot (see Section 2.2.2) showing the seasonal and interannual properties of select cosampled variables at the Eastern Gotland Basin monitoring site (Site 36, Section 6.5).

The green lines drawn in the right subfigures represent the linear regression of the annual anomalies vs. year. The colour and form of these lines indicate the statistical significance of the trend (e.g. solid green is $p < 0.01$, dashed green is $p < 0.05$). A grey line (see *Pseudocalanus* spp. and Chlorophyll) indicates a non-significant trend.



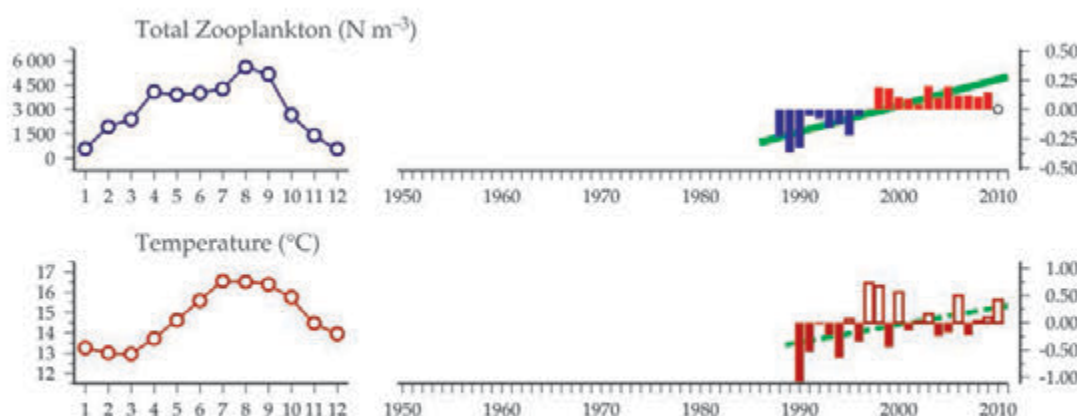
2.2.3 Regional overview plot

Each time-series summary section in this report includes a standard regional overview plot (see Figure 2.2.3) that shows a 50-year summary of sea surface temperatures and wind speeds and a 100+ year summary of sea surface temperatures. These longer-term data are extracted from global-coverage, long-term time-series products such as the HadISST sea surface temperature dataset (see Section 2.3.1) and the ICOADS surface winds dataset (see Section 2.3.3).

The larger spatial scale of the global time-series products as well as the CPR standard areas is not intended to capture the exact local hydrographic and plankton conditions of each site. These data can, however, provide an interesting insight into the longer-term hydrographic and plankton conditions present in the larger areas surrounding that sampling site. For example, while the local influences of coastal currents and upwelling at the A Coruña Transect

(see Section 8.4) are probably not well captured by the HadISST, ICOADS, or CPR datasets, the latter data extending beyond the 1988 starting data of the A Coruña Transect data (Figure 2.2.3a). The extended years of regional data show that surface water temperatures and wind speeds in the region have been increasing over the last 50 years (see Figure 2.2.3b) and that surface water temperatures during the entire 1988–2010 sampling period were above the 100-year average (climatology) found in that region (see Figure 2.2.3c). The total copepods data from the A Coruña Transect and CPR standard area “F04” show different trends. The discussion presented in the A Coruña Transect (see Section 8.4) suggests that this difference is due to local hydrographic upwelling conditions and greater localized production that is not present in the larger region represented by the CPR standard area.

a) 20+ year trends at-site in the A Coruña Transect (Site 52, Section 8.4)



b) 50-year trends in the A Coruña Transect / northwest Iberian Shelf region

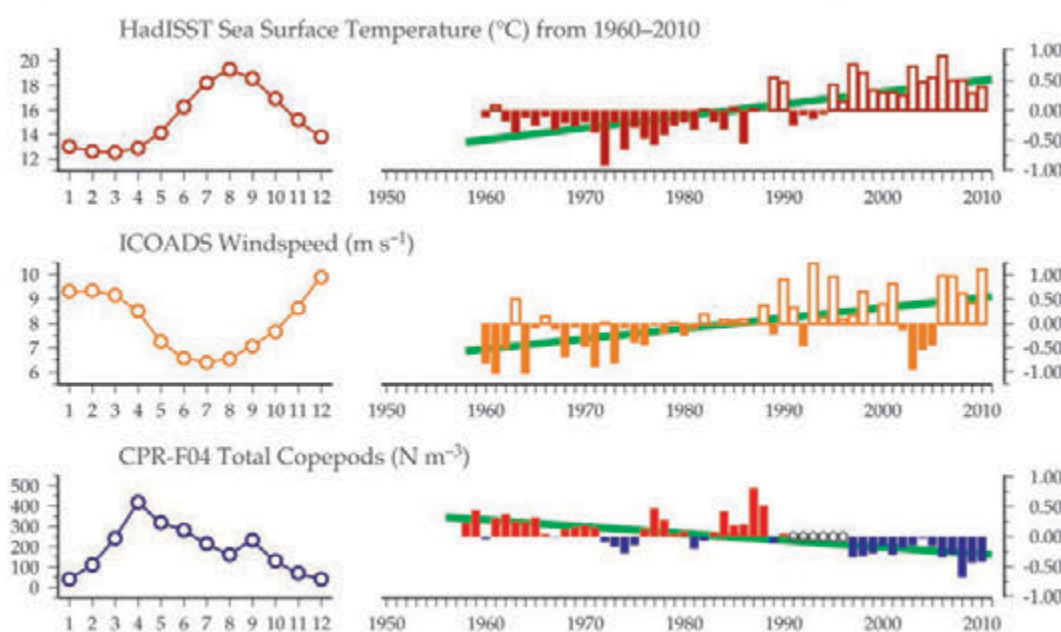
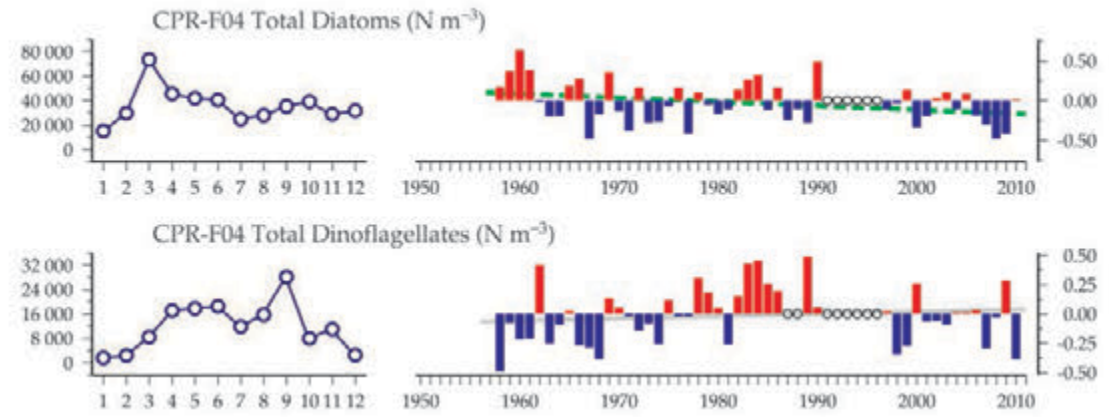


Figure 2.2.3

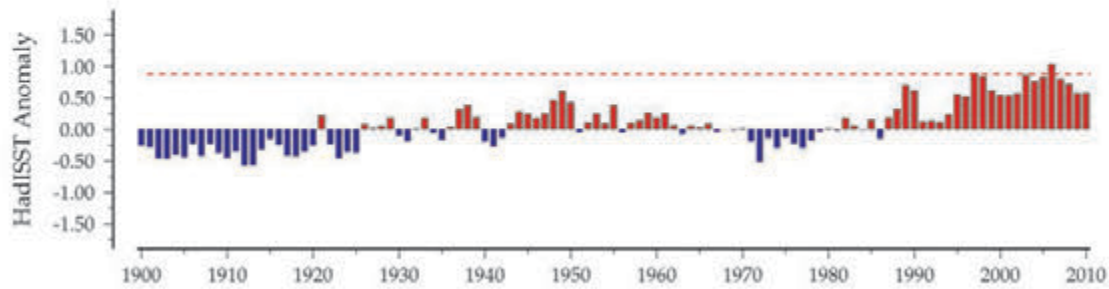
Regional overview plot showing the seasonal and interannual trends of long-term surface water temperatures, wind speeds, and Continuous Plankton Recorder (CPR) plankton data from the northwest Iberian Shelf region surrounding the A Coruña Transect monitoring site (Site 52, Section 8.4).

The “20+ year trends” subpanel at the top of this figure is included for illustrative purposes only and would normally be found in the Multivariable comparison plot (see Section 2.2.2).

Figure 2.2.3
continued



c) 100-year trends in the A Coruña Transect / northwest Iberian Shelf region



2.3 Time-series supplemental data

Water temperature is an excellent indicator of the physical environment in which plankton are living because it affects plankton both directly (i.e. through physiology and growth rates) and indirectly (i.e. through water column stratification and related nutrient availability). Similarly, chlorophyll concentration is an excellent indicator of the average phytoplankton community biomass. While most sites already had *in situ* temperature and chlorophyll data

available, a handful of sites did not. In these cases, the supplemental data sources (summarized in this section) were used to fill in these missing variables. Furthermore, to provide a collection-wide set of uniform-method temperature and chlorophyll data, WGZE included these supplemental time-series data (in addition to all available *in situ* data) with each site. These supplemental datasets are summarized below.

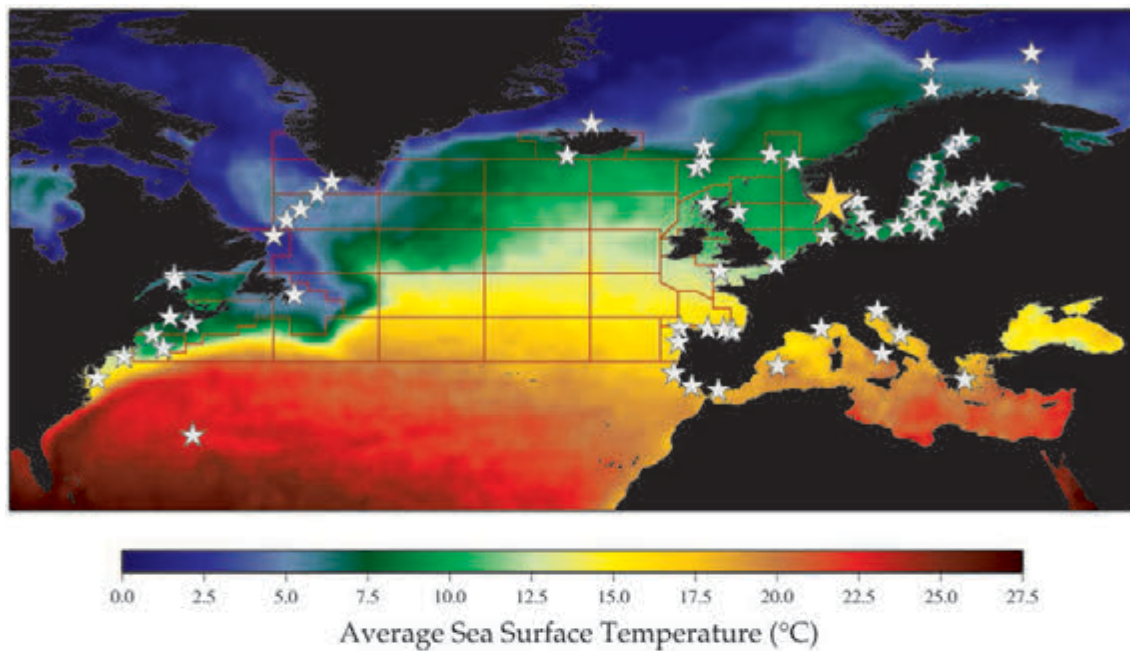
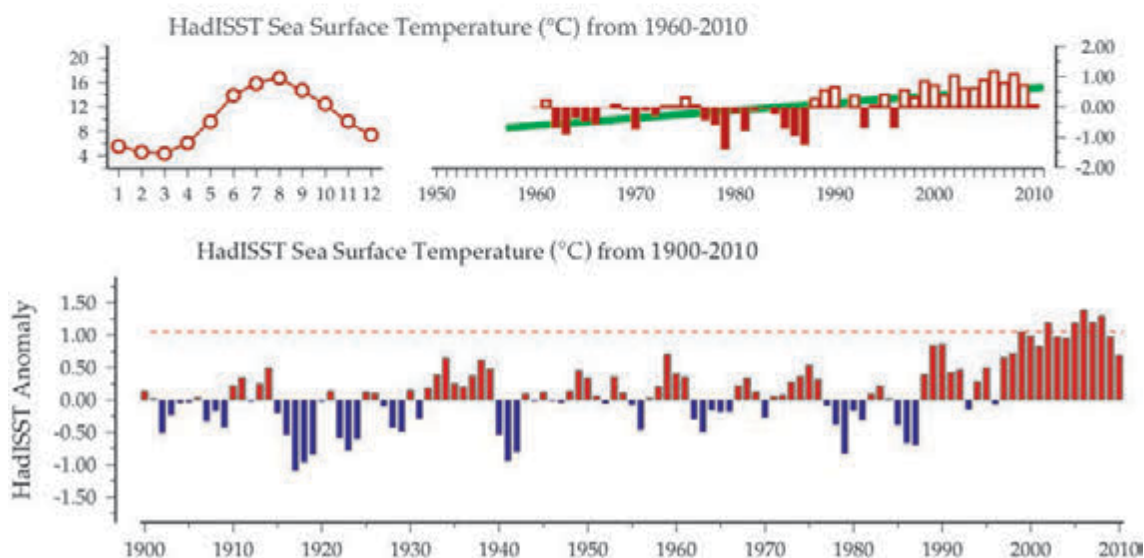


Figure 2.3.1

Map of HadISST sea surface temperature (see Section 2.3.1) overlaid with zooplankton time-series site locations (white and yellow stars) and CPR standard areas (red boxes). The lower subpanel shows examples of seasonal and interannual properties (see Section 2.2.2) of HadISST sea surface temperatures from the northern Skagerrak region (large yellow star on the map, see also Site 44 in Section 7.1).

Arendal Station (Site 44, Section 7.1)



2.3.1 Sea surface temperature data: HadISST

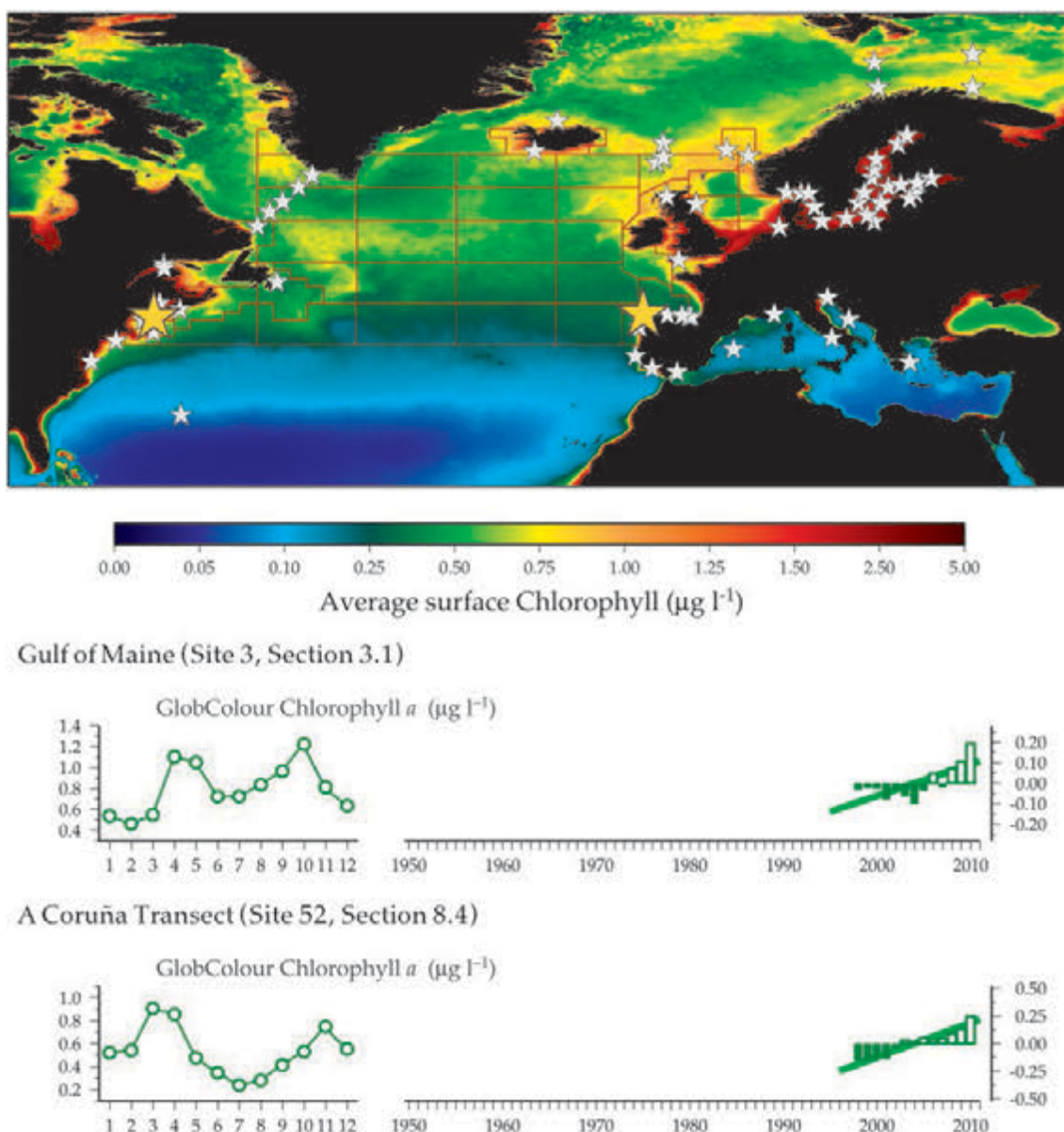
In order to provide a common long-term dataset of water temperatures for every site in the North Atlantic study area, the Hadley Centre Global Sea Ice Coverage and Sea Surface Temperature (HadISST, version 1.1) dataset, produced by the UK Met Office, was used to add standard temperature data to each site (Figure 2.3.1). The HadISST is a global dataset of monthly SST values from 1870 to the present day. This product combines historical *in situ* ship and buoy SST data with more recent bias-adjusted satellite SST and statistical reconstruction (in data-sparse periods and/or regions) to create a continuous global time-series at one-degree spatial resolution (roughly 100 × 100 km). The HadISST data are not intended to represent the exact temperatures in which plankton were sampled, but they do provide a 100+ year average of the general water temperatures in and around the sampling area. These additional data become important as, in many regions of the North Atlantic, temperatures have been increasing over the last 50–110 years (Figure 2.3.1, lower panels), and

plankton growing in those regions may be experiencing some of the warmest water temperatures seen in the last 100 years.

For each plankton time-series, the immediately overlaying HadISST one-degree grid cell was selected. For single-location sampling sites, this one-degree cell included a ~100 × 100 km area in and around the sampling site. For transects and region-based surveys (e.g. Iceland, Norway, Gulf of Maine), the centre point of the transect or region was used to select a single one-degree cell to represent the general conditions of the entire sampling area. (Comparisons with multicell averages revealed no substantial differences.) Once a one-degree cell was selected, all HadISST temperature data were extracted from that cell for the period 1900–2010 and used to calculate annual anomalies.

The HadISST v. 1.1 dataset is available online at <http://badc.nerc.ac.uk/data/hadisst/>.

Figure 2.3.2
Map of GlobColour sea surface chlorophyll concentrations (see Section 2.3.2) overlaid with zooplankton time-series site locations (white and yellow stars) and CPR standard areas (red boxes). The lower subpanel shows examples of seasonal and interannual properties (see Section 2.2.2) of sea surface chlorophyll concentrations from the Gulf of Maine (left-most large yellow star on map, see also Site 3 in Section 3.1) and Northwest Iberian Coast (right-most yellow star, see also Site 52 in Section 8.4).



2.3.2 Sea surface chlorophyll data: GlobColour

In order to provide a common, long-term dataset of chlorophyll for every site in the North Atlantic study area, the GlobColour Project chlorophyll merged level-3 ocean colour data product (GlobColour) was used to add standard chlorophyll data to each site (Figure 2.3.2). This data product is a global dataset of monthly satellite chlorophyll data from 1998 to the present. Although the original product is available at a resolution of 4.63 km, it was binned into a one-degree spatial resolution (roughly 100 km × 100 km) in order to be compatible with the

HadISST dataset. The GlobColour datasets were assigned to corresponding one-degree boxes using the same method outlined for the HadISST datasets (see Section 2.3.1).

The GlobColour Project chlorophyll concentration merged level-3 data product (GlobColour) is available online at <http://www.globcolour.info/>.

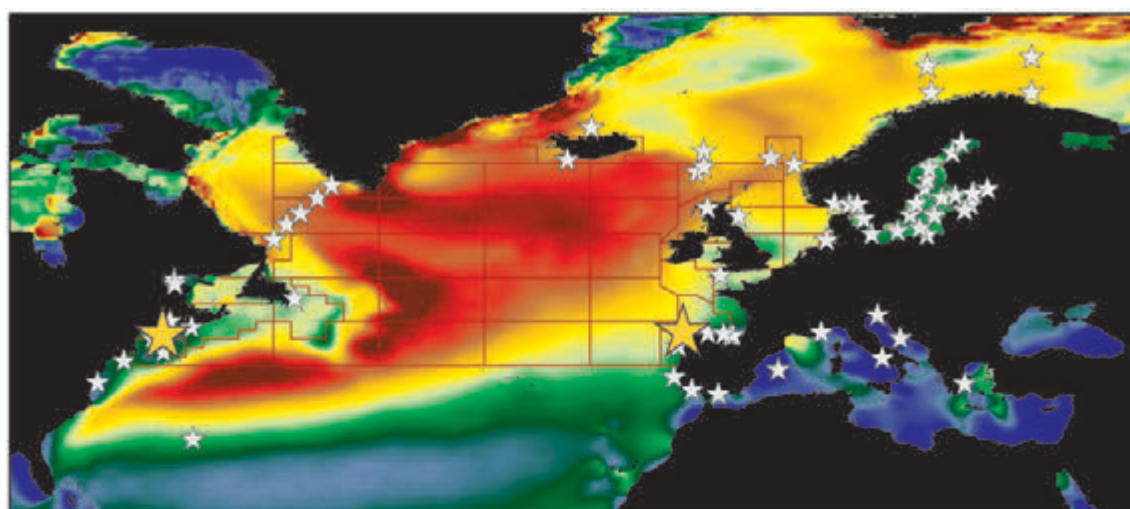
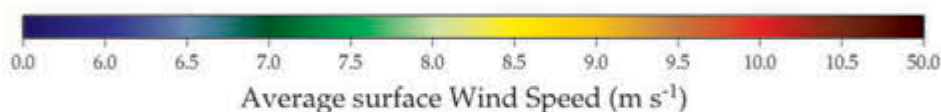
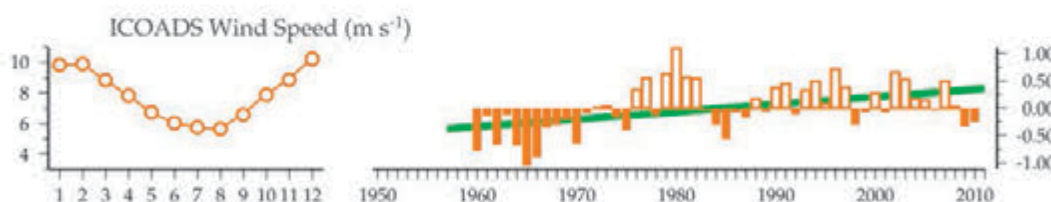


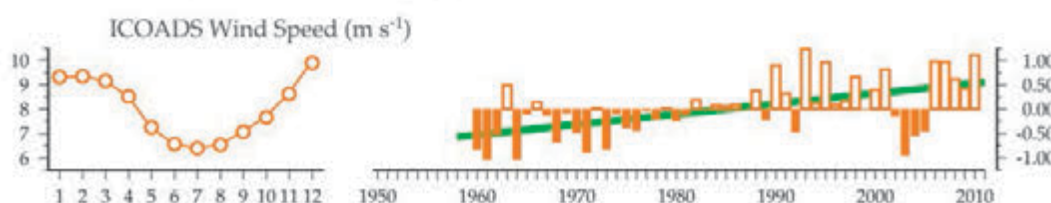
Figure 2.3.3
Map of ICOADS surface windspeed (see Section 2.3.3) overlaid with zooplankton time-series site locations (white and yellow stars) and CPR standard areas (red boxes). The lower subpanel shows examples of seasonal and interannual properties (see Section 2.2.2) of ICOADS surface windspeed from the Scotian Shelf (left-most yellow star, see also Site 6 in Section 3.3) and Northwest Iberian Coast (right-most yellow star, see also Site 52 in Section 8.4).



Gulf of Maine (Site 3, Section 3.1)



A Coruña Transect (Site 52, Section 8.4)



2.3.3 Sea surface wind data: ICOADS

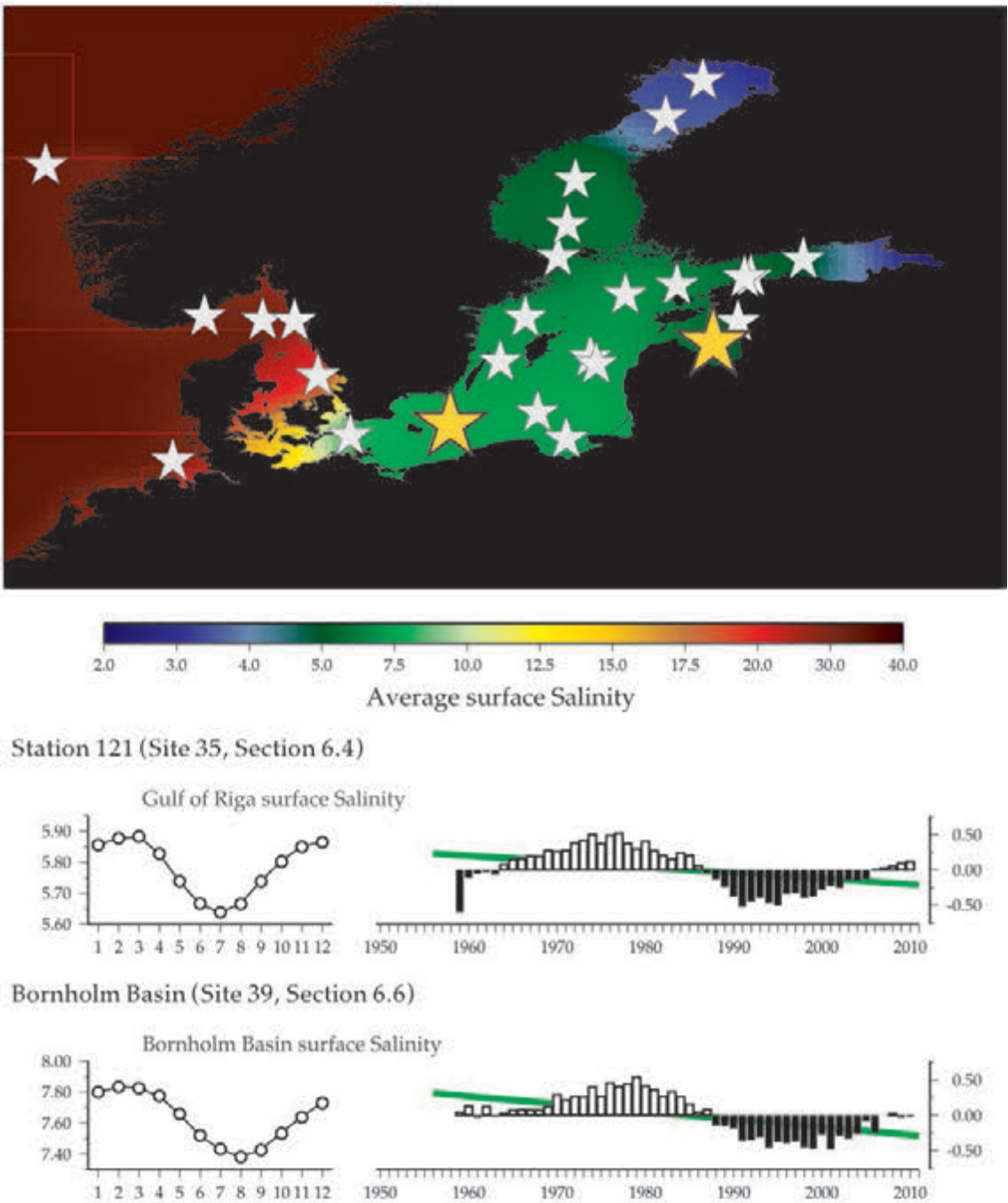
Temperature and wind both play an important role in determining the level of mixing or stratification in the marine environment, which in turn can determine the availability of nutrients and influence plankton production. A recent study by Hinder *et al.* (2012), using scalar wind-speed data from the International Comprehensive Ocean-Atmosphere Data Set (ICOADS), found a strong relationship between Continuous Plankton Recorder (CPR) diatom and dinoflagellate abundances, surface windspeed, and surface water temperatures. This study also noted strong, long-

term increasing or decreasing trends in many regions of the North Atlantic (see Figure 2.3.3).

ICOADS (scalar) surface windspeed data were added as a supplemental variable to each of the monitoring sites in this study. The ICOADS wind data series were assigned to corresponding one-degree boxes using the same method outlined for the HadISST dataseris (see Section 2.3.1).

The ICOADS data is available online at <http://icoads.noaa.gov/>.

Figure 2.3.4
Map of average surface salinity values overlaid with zooplankton time-series site locations (white stars). The lower subpanel shows examples of seasonal and interannual properties (see Section 2.2.2) of PROBE-Baltic surface salinity from the Gulf of Riga (right-most yellow star, see also Site 35 in Section 6.4) and Bornholm Basin (left-most yellow star, see also Site 39 in Section 6.6) regions.



2.3.4 Baltic surface salinity data: PROBE–Baltic model

Zooplankton composition and biomass in the Baltic Sea are influenced heavily by salinity, which, in turn, is driven by freshwater input from land and precipitation in the region, and from occasional influxes of seawater from the North Sea (see Chapter 6 for a full discussion and site-specific examples). In spite of salinity playing such a large role in the zooplankton community, *in situ* co-sampled salinity time-series data were not readily available for all of the Baltic Sea zooplankton time-series sites presented in this report. In these cases, the WGZE study used a time-series of surface salinity calculated from the PROBE–Baltic model, which uses a database of *in situ* data for initialization and validation of the model parameters together with high resolution meteorological and hydrological data as forcing. The model is well documented and the code is freely available (Omstedt, 2011).

The PROBE–Baltic salinity data consist of monthly mean salinity values from 1958 to 2008 (Figure 2.3.4). Unlike the gridded one-degree spatial fields of the HadISST and GlobColour datasets, the PROBE–Baltic data are spatially divided into the major basins of the Baltic Sea (e.g. Bothnian Bay, Bothnian Sea, Gulf of Finland, Gulf of Riga, eastern Gotland Basin, northwestern Gotland Basin). PROBE–Baltic salinity from the corresponding basin was added to each of the Baltic Sea zooplankton time-series sites in Chapter 6.

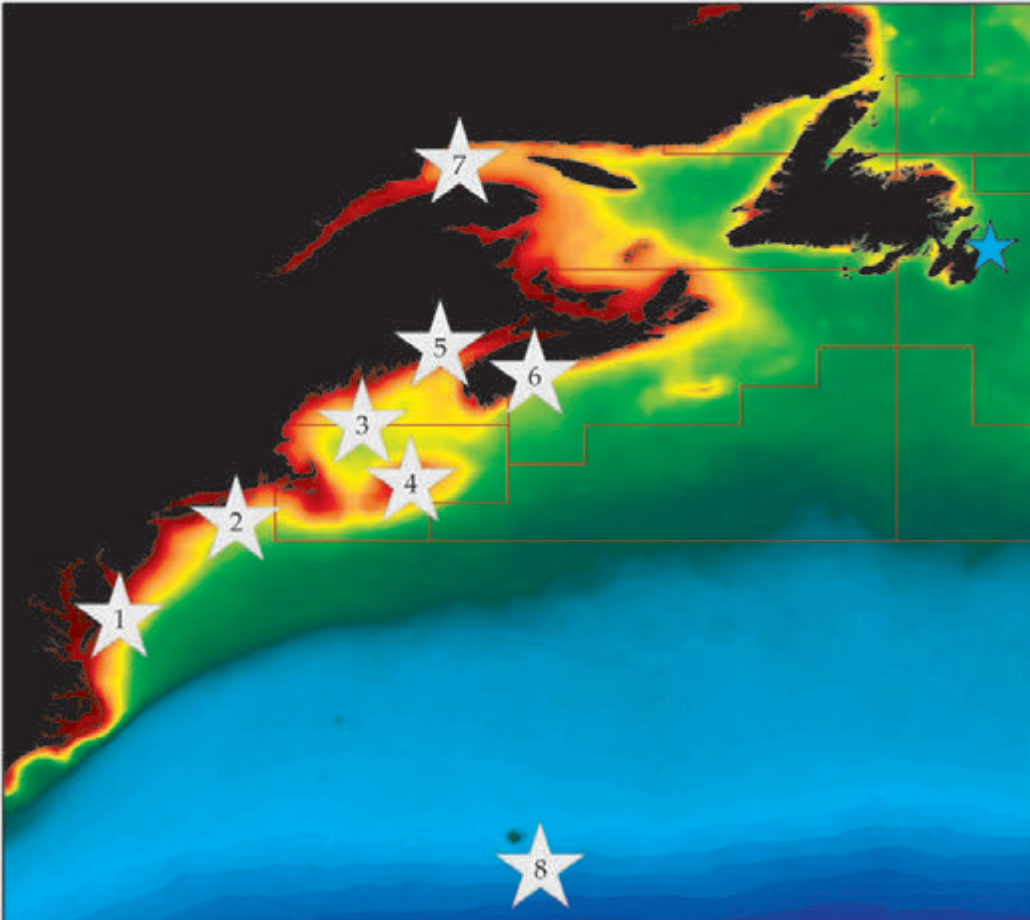
Additional information on the PROBE–Baltic model and data products is available online at <http://www.oceanclimate.se/>.

3Z OOPLANKTON OF THE NORTHWEST ATLANTIC SHELF

Peter H. Wiebe, Jon Hare, Catherine Johnson, Erica Head, Michel Harvey, Stéphane Plourde, and Deborah Steinberg

Figure 3.0
Locations of the Northwest Atlantic Shelf zooplankton monitoring areas (Sites 1–8) plotted on a map of average chlorophyll concentration (see Section 2.3.2).

The blue star indicates a site discussed in Section 4.1 (see Site 9).



Site ID	Monitoring Site (Region)	Section
1	NEFSC Mid-Atlantic Bight (northeast U.S. continental shelf)	31
2	NEFSC Southern New England (northeast U.S. continental shelf)	31
3	NEFSC Gulf of Maine (northeast U.S. continental shelf)	31
4	NEFSC Georges Bank (northeast U.S. continental shelf)	31
5	Prince 3 Bay of Fundy)	32
6	Halifax Line 2 (Scotian Shelf)	33
7	Anticosti Gyre and Gaspé current (western Gulf of St. Lawrence)	34
8	Bermuda Atlantic Time-series Study (Sargasso Sea)	35

The Northwest Atlantic Shelf (Figure 3.0) is influenced by water flowing towards the equator from the Arctic via the Labrador Sea (Loder *et al.*, 1998). On the shelf, cold, relatively fresh water flows southwards from the Labrador Shelf to the Newfoundland Shelf, around the southern tip of Newfoundland, and into the Gulf of St Lawrence through the Strait of Belle Isle. From the Gulf of St Lawrence, water flows out through Cabot Strait and southwestwards along the coast of Nova Scotia, where it mixes with flow from the offshore Slope Water in the central region of the Scotian Shelf. This mixture flows westwards to the Gulf of Maine, where it is joined by inflow from the Slope Water via the Northeast Channel. From the Gulf of Maine, water flows around Georges Bank and along the Mid-Atlantic Bight to Cape Hatteras. The Slope Water includes the water mass northeastward from Cape Hatteras to the Grand Banks, between the continental shelf and the Gulf Stream, and down to the depth of about 900 m (Iselin, 1936).

The changing composition of the water along the shelf is reflected in changes in the zooplankton species composition, with boreal species most abundant in the north and temperate species more important in the south (Head and Sameoto, 2007; Cox and Wiebe, 1979). The Gulf of Maine–Georges Bank–Slope Water region represents a southern boundary for many boreal species and a northern limit for some temperate and subtropical coastal species, although this is changing with the long-term warming trend that is becoming evident in the area. In the Gulf of Maine, broad-scale surveys have revealed that zooplankton abundance and biomass are higher in coastal regions and on Georges Bank than in central deep-water areas, reflecting differences in phytoplankton biomass and production.

An increased influx of Arctic freshwater during the early 1990s was accompanied by increased abundance of Arctic zooplankton species (*Calanus glacialis*, *C. hyperboreus*), first on the Newfoundland Shelf in the 1990s and then on the Scotian Shelf in the 2000s (Head and Sameoto, 2007; Johns *et al.*, 2001). In the Slope Water south of Georges Bank, *C. hyperboreus* was recorded at its farthest position south (39.5°N) in the 1998 CPR survey (Johns *et al.*, 2001). The increase in freshwater input also led to increased stratification on the Northwest Atlantic continental shelf and in the Gulf of Maine, which, in turn, led to earlier starting times for spring blooms (Ji *et al.*, 2008). On the Scotian Shelf and in the Gulf of Maine, the increases in phytoplankton biomass in the 1990s were associated with increases in the abundance of small copepods and with changes in the abundance of larger forms (e.g. *C. finmarchicus*; Pershing *et al.*, 2005; Head and Sameoto, 2007).

On the Scotian Shelf, the spring bloom started particularly early in 1999 and was associated with early reproduction in

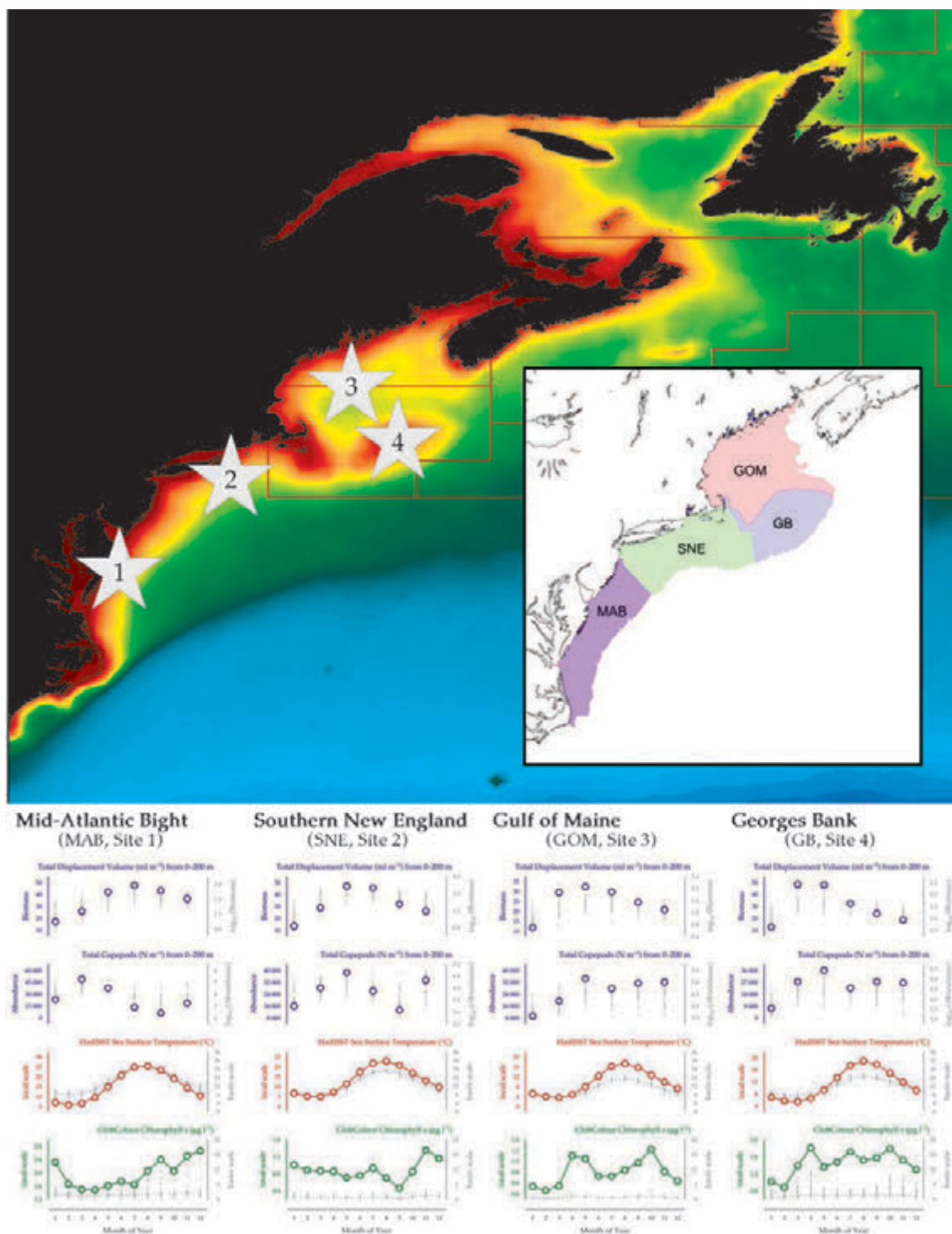
C. finmarchicus and a high level of haddock (*Melanogrammus aeglefinus*) recruitment (Platt *et al.*, 2003; Head *et al.*, 2005). Bloom intensities on the Scotian Shelf were unusually high in 2007, but returned to average values in 2008 (Harrison *et al.*, 2009). Diatoms dominate during the spring and autumn blooms on the Scotian shelf; in the Bay of Fundy, they are dominant year-round.

In the Gulf of Maine, conditions in the early to mid 2000s returned to those seen in the 1980s, with a relatively high North Atlantic Oscillation (NAO) index, lower surface salinities, and higher *C. finmarchicus* abundance (A. J. Pershing, pers. comm.). In the winter of 2009/2010, however, the NAO index took a dramatic negative trend, which may portend major changes in the hydrography and plankton dynamics in the Gulf of Maine and Georges Bank, with a 1- to 2-year time-lag similar to changes experienced in the Gulf of Maine after the 1996 negative NAO index (Greene and Pershing, 2003).

3.1 NEFSC Ecosystem Monitoring Program (Sites 1–4)

Jon Hare and Todd D. O'Brien

Figure 3.1.1
Locations of the NEFSC Ecosystem Monitoring Program areas (Sites 1–4) on a map of average chlorophyll concentration, and their corresponding seasonal summary plots (lower panels, see also Section 2.2.1).



The Northeast Fisheries Science Center (NEFSC) of the National Marine Fisheries Service (NMFS) has a long-standing Ecosystem Monitoring programme covering most of the northeast US continental shelf, which extends from approximately 35–45°N. The NEFSC sampling protocol divides the continental shelf into four regions (Figure 3.1.1), based on their different physical and biological characteristics. NEFSC surveys collect hydrographic and tow data using a randomized spatial sampling technique that samples approximately 30 stations per region per 2-month period. During these surveys, zooplankton are collected using a bongo net (60 cm diameter, 333 µm mesh) towed obliquely from 200 m (or near the bottom) to the surface. The zooplankton time-series in these four areas started in 1977 and continue to the present.

Seasonal and interannual trends (Figures 3.1.2–3.1.5)

Along the northeast US continental shelf, primary production is highest near the shore (Figure 3.1.1, map of chlorophyll, regions of red and yellow coloration). The distribution of zooplankton biomass is similar to that of primary production, with highest levels found during late spring and summer (Figure 3.1.1, lower panels of seasonal summary plots). High levels of primary productivity and zooplankton abundance are also found on Georges Bank. Changes in the northeast US continental shelf zooplankton community have been observed in all regions, with an overall increasing trend in total annual zooplankton biomass (measured as total displacement volume) since the early 1980s (Figure 3.1.2–3.1.5). However, since 1990, zooplankton biomass has decreased somewhat and relatively low levels of zooplankton biomass were observed in 2010 in all four areas. Changes in species composition over this period have been observed in the Georges Bank region (Kane, 2007), with smaller-bodied taxa (e.g., *Centropages hamatus*, *Centropages typicus*, *Pseudocalanus* spp., and *Temora longicornis*) increasing in abundance in the 1990s and decreasing in the 2000s (Figure 3.1.5). There is also some evidence of a shift in seasonality for some zooplankton species (e.g. *T. longicornis*), with the peak abundance period beginning earlier in the season and lasting longer. These changes probably occurred in the Mid-Atlantic region as well.

Since 1960, water temperatures in all of the regions have been slowly increasing (Figure 3.1.6; see also Ecosystem Assessment Program, 2009). Water temperatures are influenced by the influx of cooler, fresher water from the north, and the occurrence of low-salinity events has also increased since the early 1990s (Mountain, 2004).

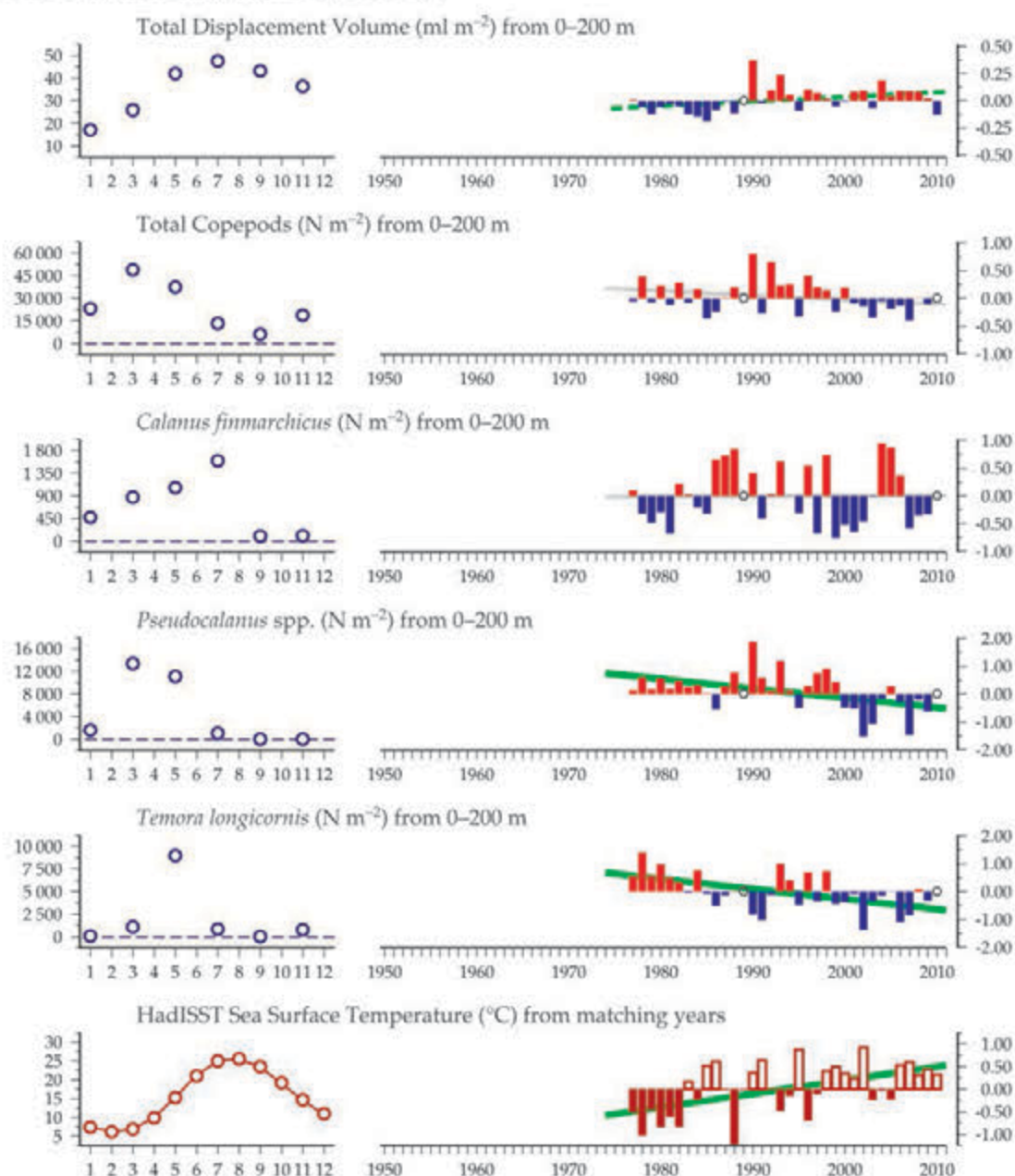
The 100+ year SST trends within each of the regions (Figure 3.1.7) illustrate that temperatures are currently above the 100-year climatological average, and are currently near or below the maximum seen in the 1950s (Figure 3.1.7, red dashed lines).

Stratification within the water column can also be influenced by surface winds, which have also been steadily increasing since the 1960s in all four regions (Figure 3.1.6). Hinder *et al.* (2012) found a strong correlation between increasing surface winds and the Continuous Plankton Recorder survey Plankton Colour Index, attributed to better wind-induced mixing within the water column. CPR Standard Area “F10” (see Figure 10.1 in Chapter 10) encompasses most of the NMFS Georges Bank and Gulf of Maine survey areas. Long-term data from this area (Figure 3.1.8) shows a strong increase in Phytoplankton Colour Index (PCI) and total diatoms, while a clear trend is not evident in the corresponding CPR total copepod data. As the CPR “total diatoms” category does not convey any cell size or species composition information, it is possible that the increasing (total) diatoms include species too small or less preferred within the local copepod diets.

Figure 3.1.2
Multiple-variable
comparison plot (see
Section 2.2.2) showing
the seasonal and interan-
nual properties of select
cosampled variables in
the Mid-Atlantic Bight
monitoring area.

Additional variables are
available online at: <http://WGZE.net/time-series>.

Mid-Atlantic Bight (MAB, Site 1)



Southern New England (SNE, Site 2)

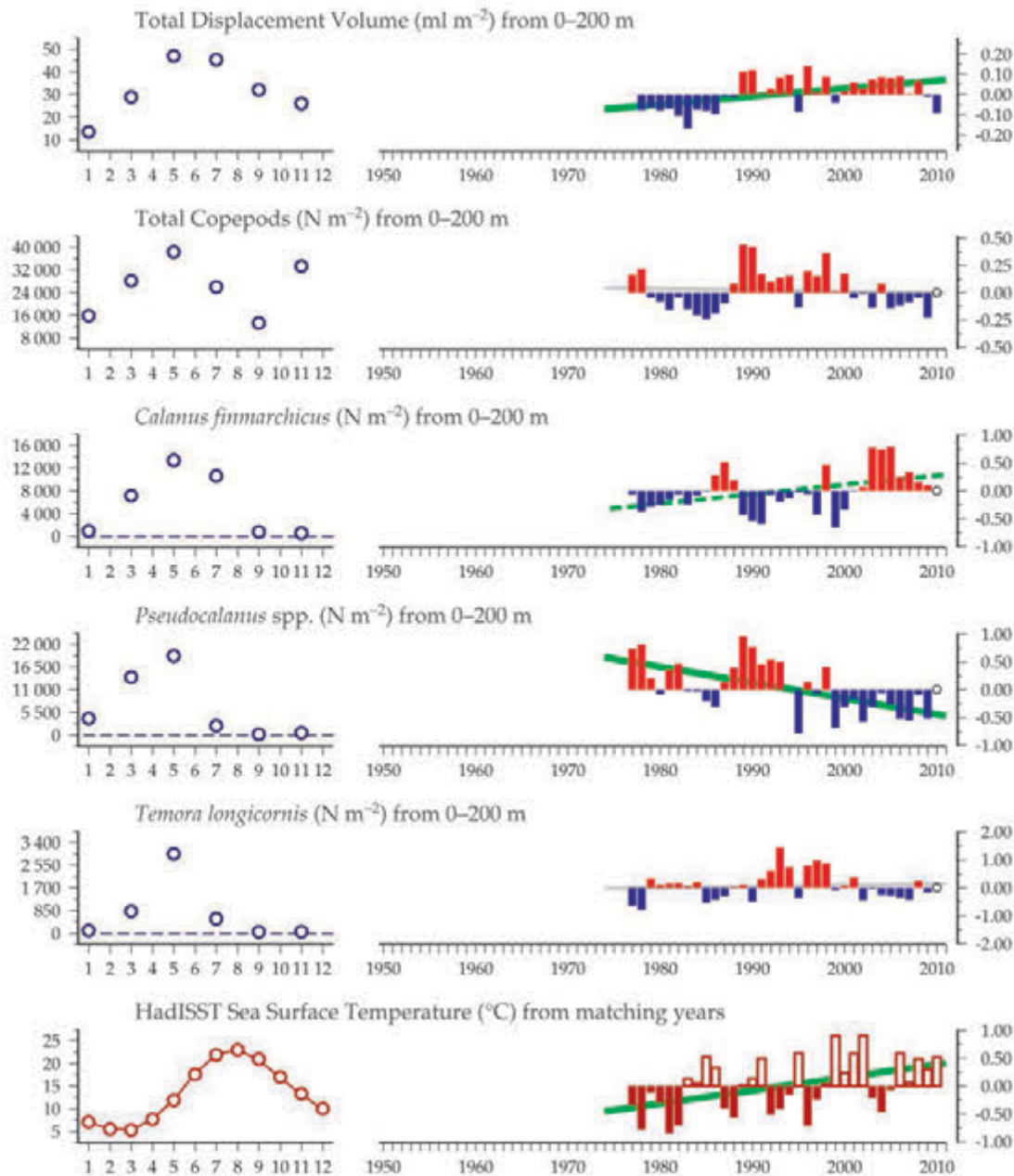


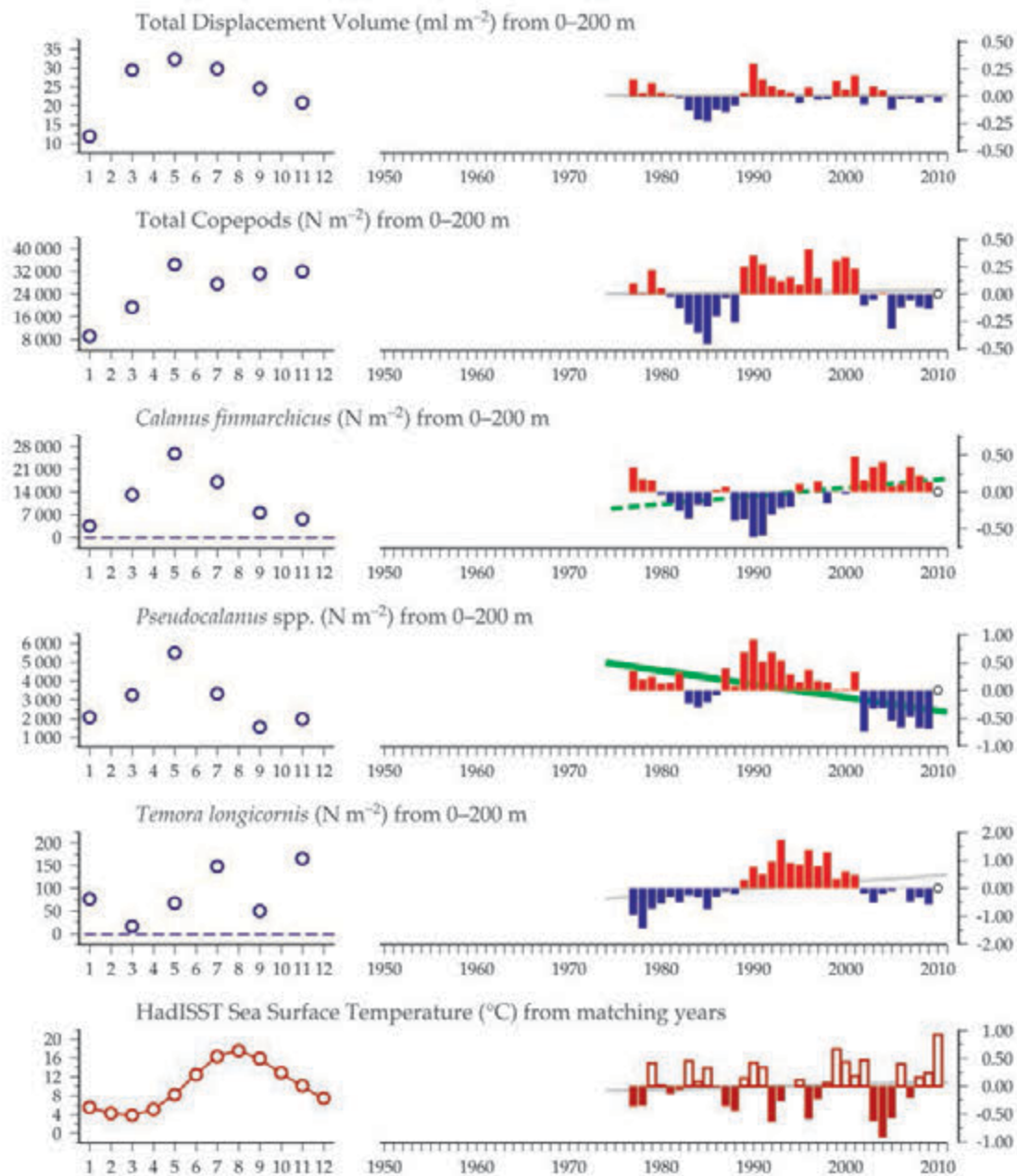
Figure 3.1.3
Multiple-variable comparison plot (see Section 2.2.2) showing the seasonal and interannual properties of select cosampled variables in the Mid-Atlantic Bight monitoring area.

Additional variables are available online at: <http://WGZE.net/time-series>.

Figure 3.1.4
Multiple-variable comparison plot (see Section 2.2.2) showing the seasonal and interannual properties of select cosampled variables in the Gulf of Maine monitoring area.

Additional variables are available online at: <http://WGZE.net/time-series>.

Gulf of Maine (GOM, Site 3)



Georges Bank (GB, Site 4)

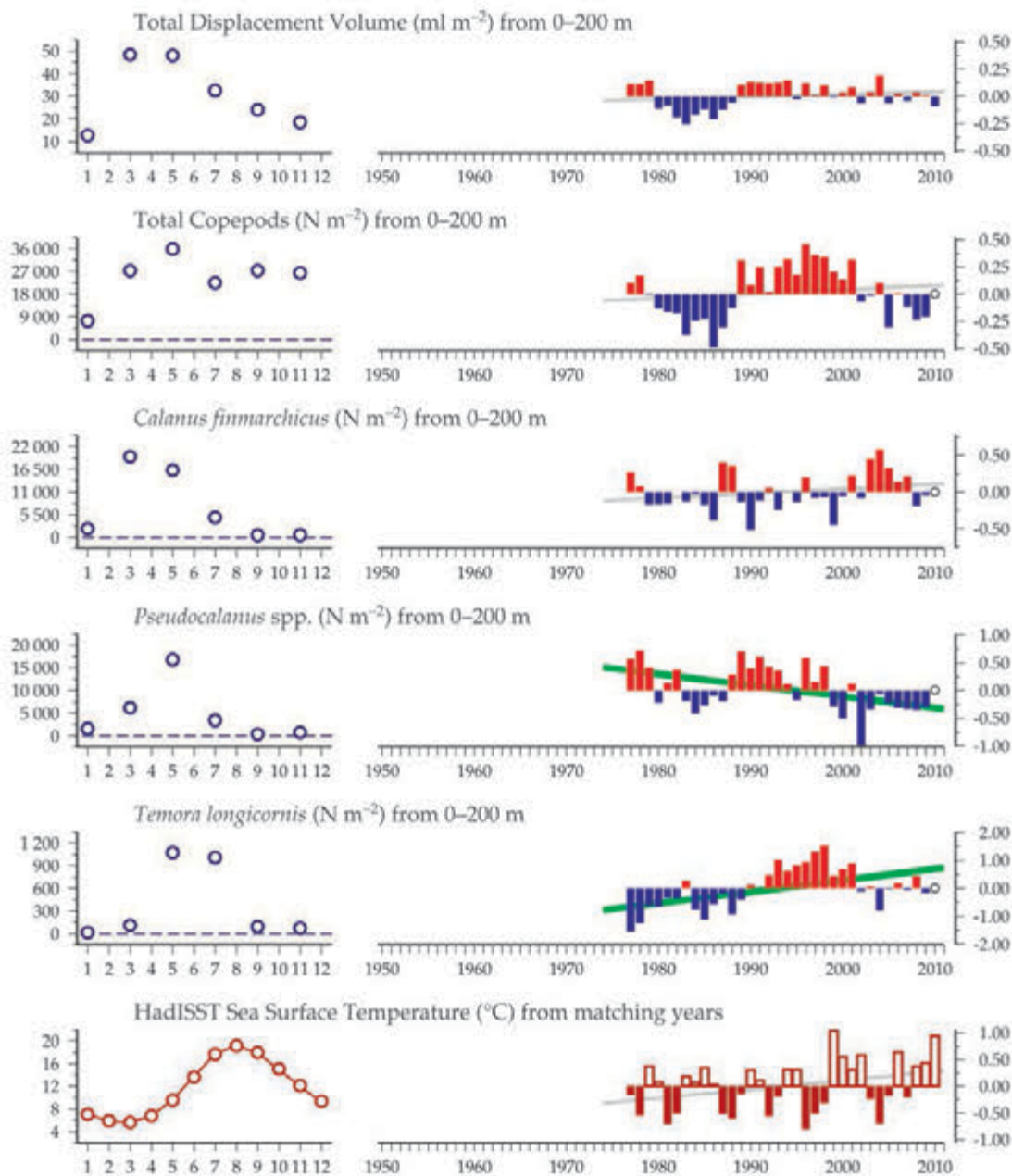


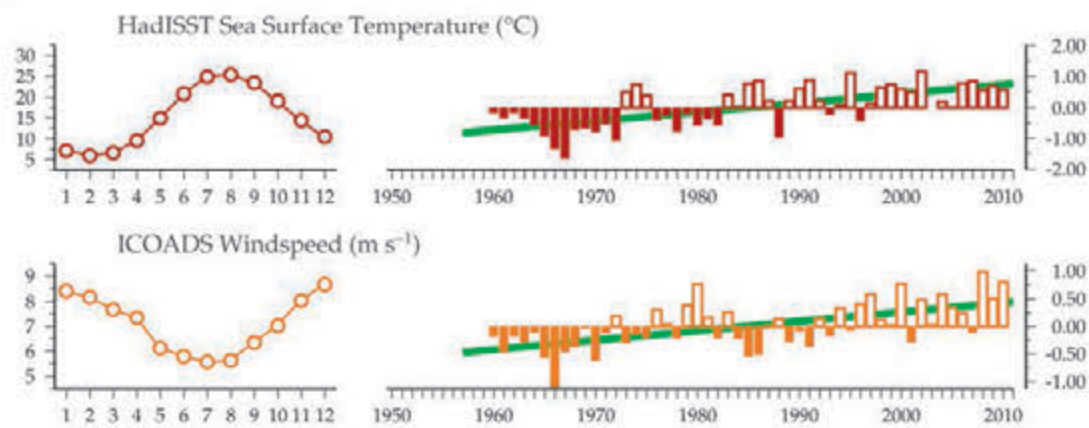
Figure 3.1.5
Multiple-variable comparison plot (see Section 2.2.2) showing the seasonal and interannual properties of select cosampled variables in the Georges Bank monitoring area.

Additional variables are available online at: <http://WGZE.net/time-series>.

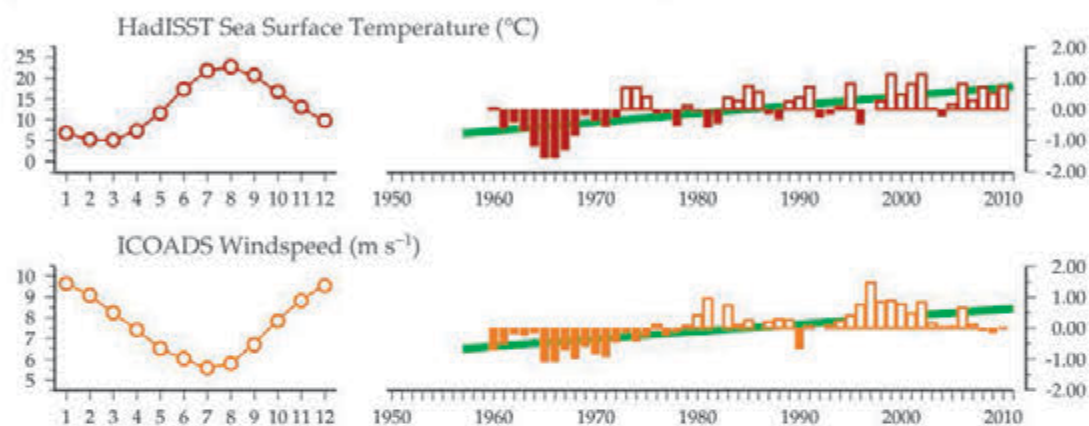
Figure 3.1.6

Regional overview plot (see Section 2.2.3) showing long-term sea surface temperatures and wind speeds in the general region surrounding the Mid-Atlantic Bight, Southern New England, Gulf of Maine, and Georges Bank monitoring areas.

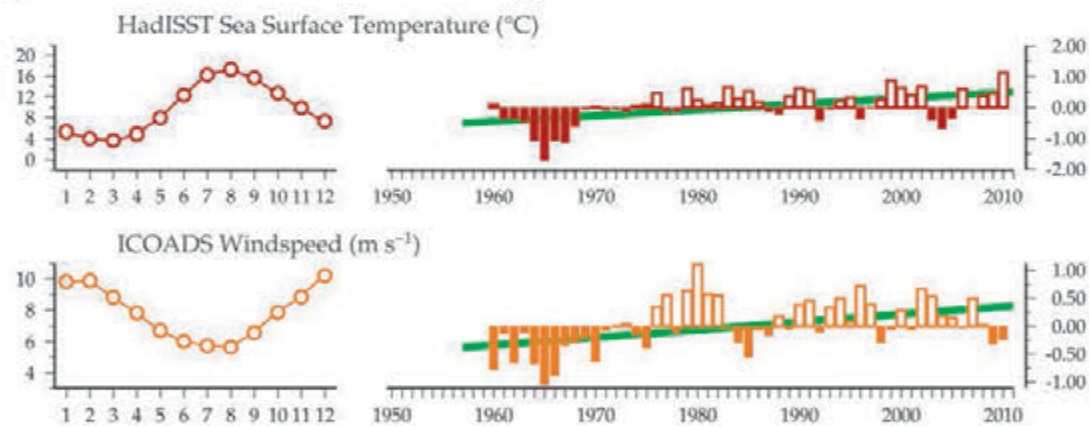
50-year trends in the Mid-Atlantic Bight region



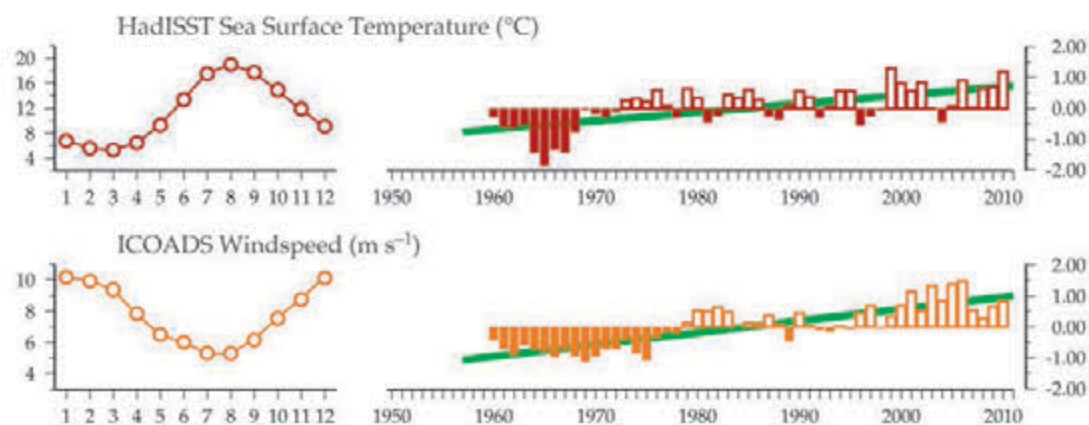
50-year trends in the Southern New England region



50-year trends in the Gulf of Maine region



50-year trends in the Georges Bank region



100-year trends in the Mid-Atlantic Bight region

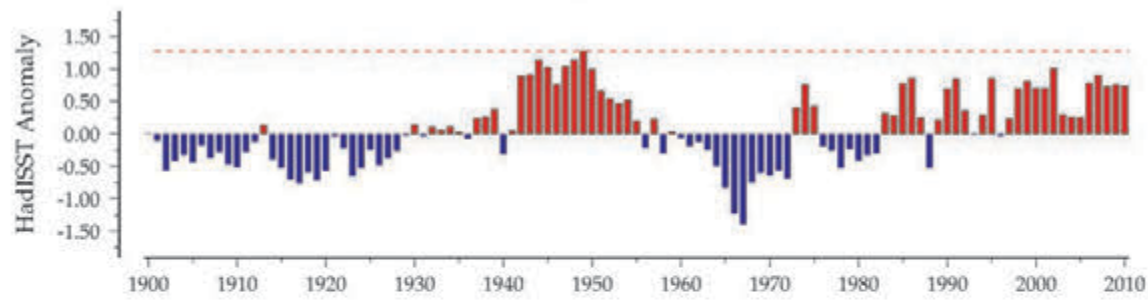
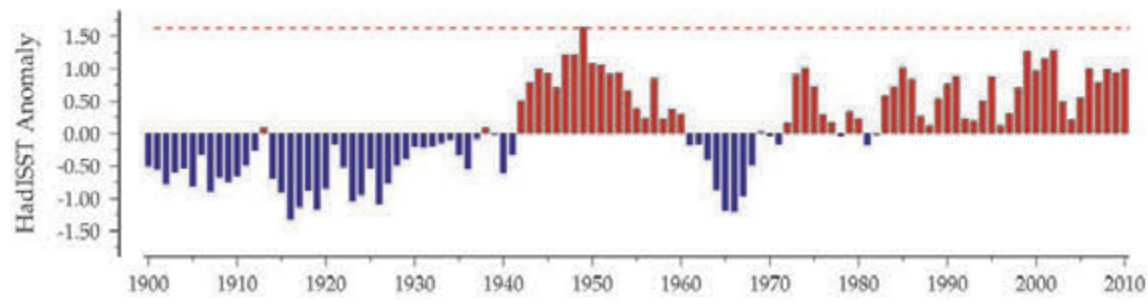
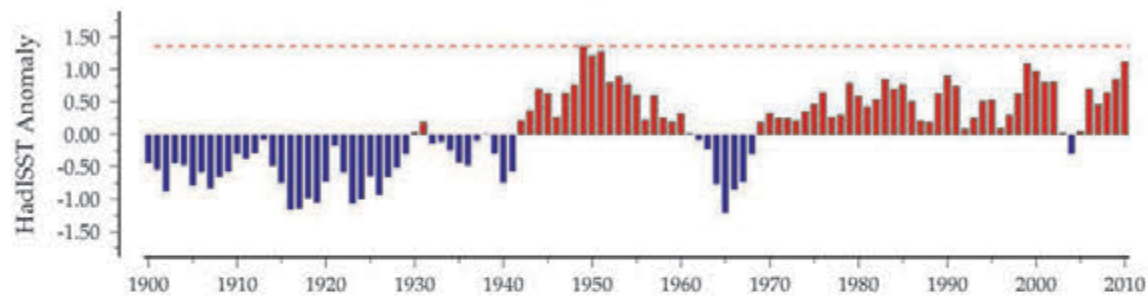


Figure 3.1.7
Regional overview plot
(see Section 2.2.3) showing
long-term sea surface
temperatures in the general
region surrounding the
Mid-Atlantic Bight,
Southern New England,
Gulf of Maine, and Georges
Bank monitoring areas.

100-year trends in the Southern New England region



100-year trends in the Gulf of Maine region



100-year trends in the Georges Bank region

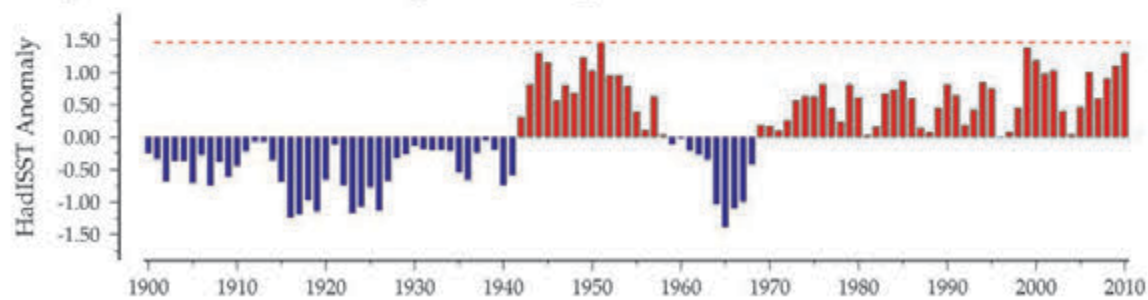
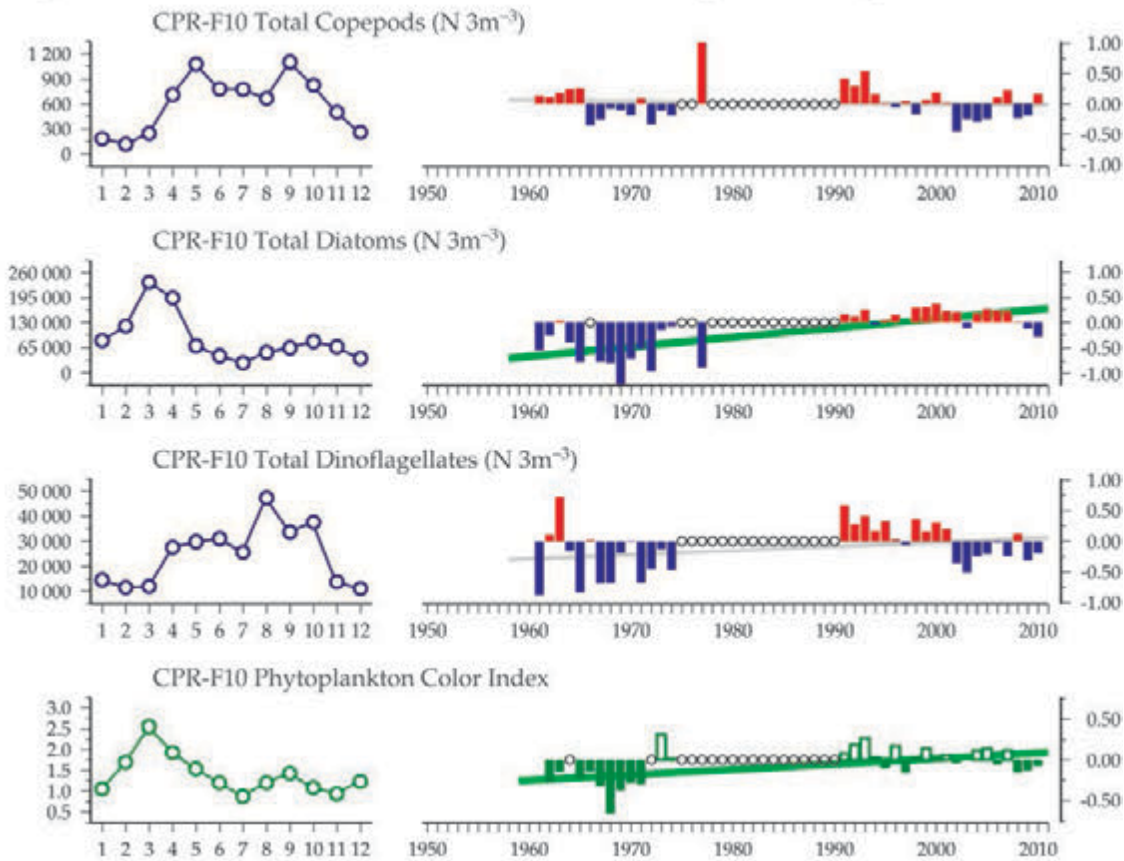


Figure 3.1.8
Regional overview plot
(see Section 2.2.3) showing
select variables from CPR
Standard Area “F10” (see
Section 10), covering the
Gulf of Maine and Georges
Bank monitoring areas.

50-year CPR trends in the Gulf of Maine / Georges Bank region



3.2 Prince 5, Bay of Fundy (Site 5)

Catherine Johnson and Erica Head

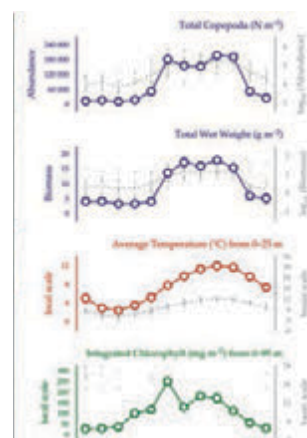
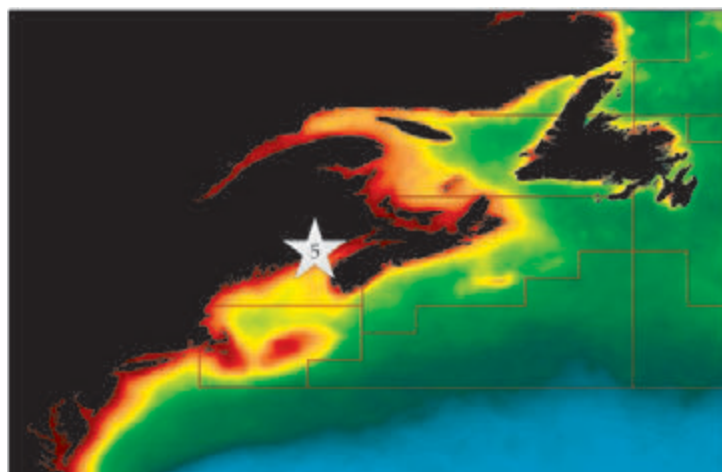


Figure 3.2.1
Location of the Prince 5 monitoring area (Site 5) on a map of average chlorophyll concentration, and its corresponding seasonal summary plot (see Section 2.2.1).

Zooplankton have been sampled by Fisheries and Oceans Canada's (DFO's) Atlantic Zone Monitoring Program (AZMP) semi-monthly (1999 to 2003) or monthly at Prince 5, which is a 100 m deep station located just off Campobello Island in the northwest of the Bay of Fundy, approximately 6 km offshore from St Andrews, New Brunswick (Figure 3.2.1). Zooplankton are sampled at Prince 5 using vertical ring-net tows (0.75 m diameter, 200 μ m mesh) from near-bottom to surface. A small vessel is used as the sampling platform. Conductivity, temperature, and depth (CTD) profiles are recorded, and water samples are collected in Niskin bottles for measuring phytoplankton, nutrients, and extracted chlorophyll. Zooplankton samples are split and one-half is used for size fractionated (< 10 mm and > 10 mm) wet and dry weight determination. The other half is subsampled for taxonomic identification and enumeration. Biomass of the dominant groups is also calculated using individually determined dry weights and abundance data for the dominant species groups (*Calanus*, *Oithona*, *Pseudocalanus*, and *Metridia*). The data are entered into the "BioChem" database at DFO. An ecosystem status report on the state of phytoplankton and zooplankton in Canadian Atlantic waters is prepared every year; the report for 2009/2010 is available at http://www.dfo-mpo.gc.ca/Csas-sccs/publications/resdocs-docrech/2012/2012_071-eng.pdf.

Seasonal and interannual trends (Figure 3.2.2)

The Prince 5 station is tidally well-mixed year-round. Non-living suspended matter has a strong effect on light attenuation at this station, and the phytoplankton growth cycle is typically characterized by an early summer peak with secondary peaks in late summer or autumn (Figure 3.2.1). Monthly average abundance of total copepods is variable (Figure 3.2.1), but values are generally lowest during winter (January–April) and highest in summer to early autumn (June–October). The zooplankton community at this station includes both nearshore and central Gulf of Maine species.

There has been no trend in annual average total copepod abundance anomalies over the 12-year time-series. The highest anomalies were observed in 2001 and 2010 and the lowest in 2002 and 2005 (Figure 3.2.2). In years of low abundance, i.e. years with negative annual abundance anomalies, the summer/autumn high abundance period was often weaker and/or of shorter duration. In addition to copepod abundance, co-sampled time-series of zooplankton wet weight, individual species abundances, integrated chlorophyll, and integrated temperature data are reported for the site (Figure 3.2.2). Although the seasonal cycles of copepod abundance and small (<10 mm) organisms wet weight are similar, their annual anomalies were not correlated, and while late stages of *Calanus finmarchicus* are the biomass dominants in the small organisms wet weight fraction at Prince 5, only abundance anomalies of adult male *C. finmarchicus* were correlated with small organism wet weight.

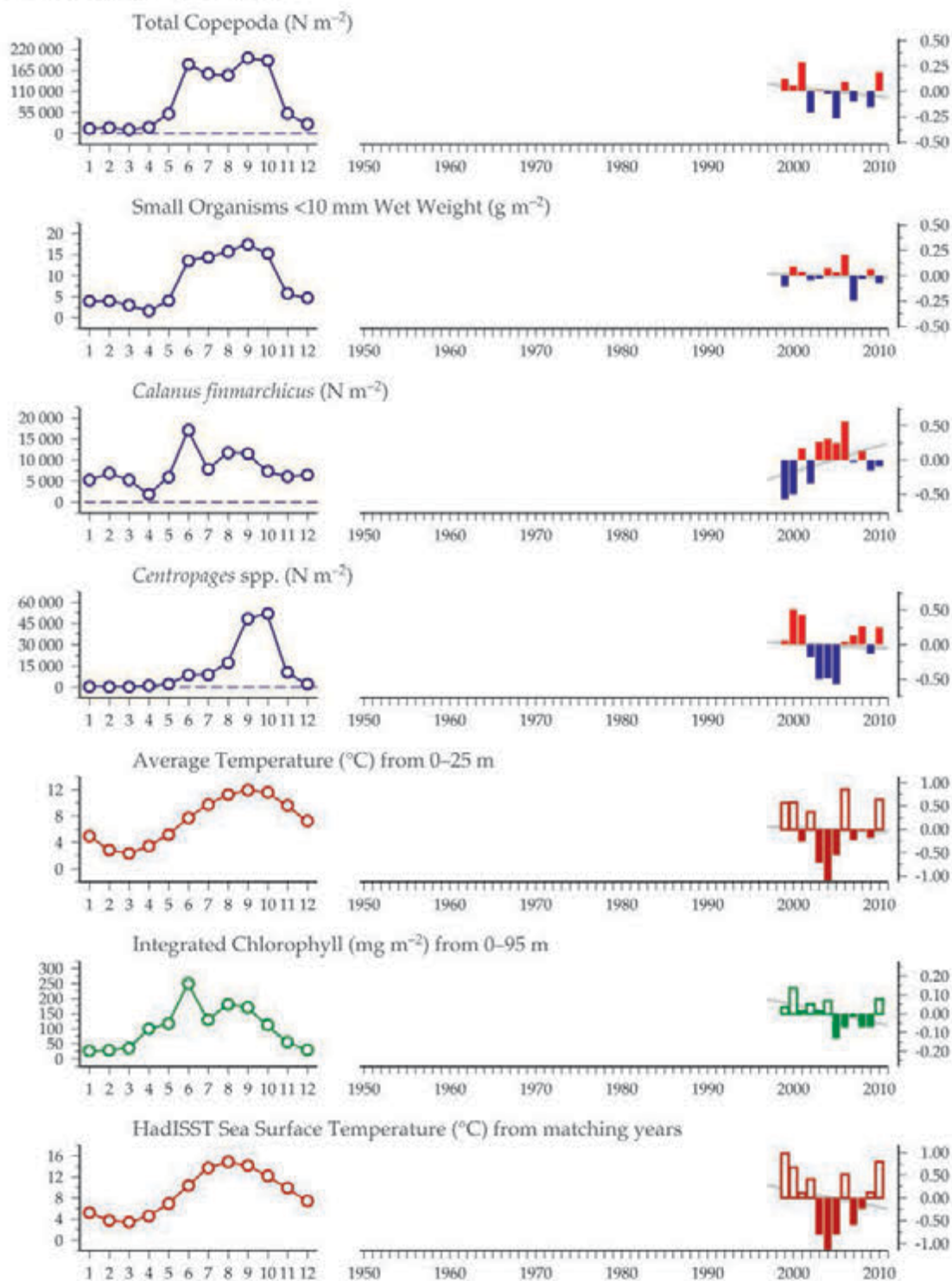
Average temperature sampled at Prince 5 and Hadley SST show similar interannual increases and decreases during 1999 to 2010, with primarily positive anomalies in 1999 to 2002 and in 2006 and 2010 (Figure 3.2.2). The SST values are at the high end of an approximately 50-year multi-decadal trend. *C. finmarchicus* abundance had a significant negative relationship with Hadley SST in 1999–2010, while the warm water copepod *Centropages* spp. had a positive relationship with Hadley SST and average temperature (0–25 m) measured at the site. At Prince 5, cool years appear to favour *C. finmarchicus*, which is a winter/spring coldwater species, while warm years favour *Centropages* spp., which are warm-associated in this region. Chlorophyll anomalies at the site were positive for the first six years of the series, then negative until 2010 when they returned to positive values. Chlorophyll annual anomalies were not correlated with anomalies of any of the zooplankton groups at Prince 5 over 1999–2010.

Figure 3.2.2

Multiple-variable comparison plot (see Section 2.2.2) showing the seasonal and interannual properties of select cosampled variables at the Prince 5 monitoring area.

Additional variables are available online at: <http://WGZE.net/time-series>.

Prince 5, Bay of Fundy



50-year trends in the Prince 5 / Bay of Fundy region

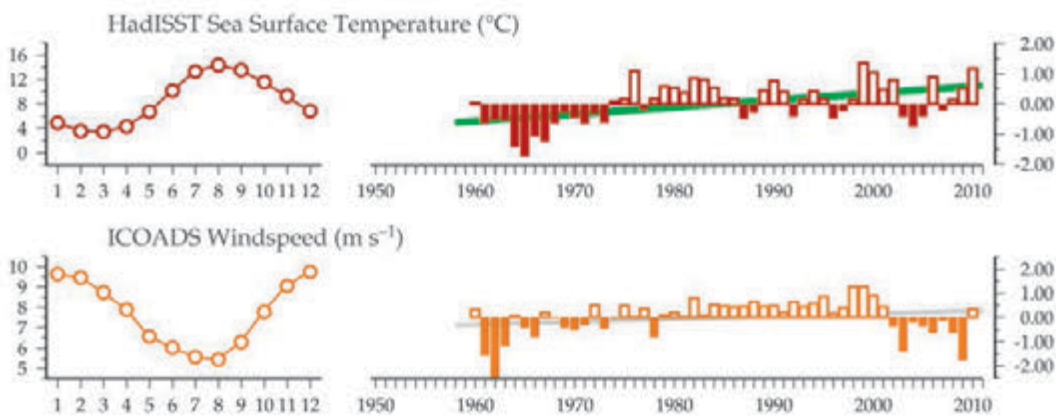
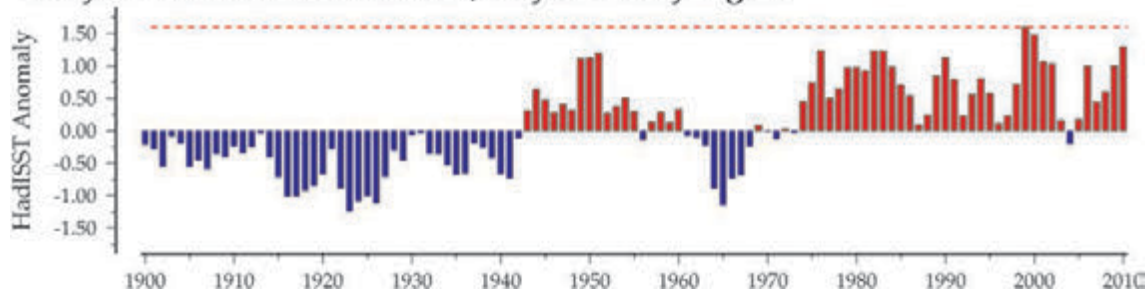


Figure 3.2.3
Regional overview plot
(see Section 2.2.3) showing
long-term sea surface
temperatures and wind
speeds in the general region
surrounding the Prince 5
monitoring area.

100-year trends in the Prince 5 / Bay of Fundy region

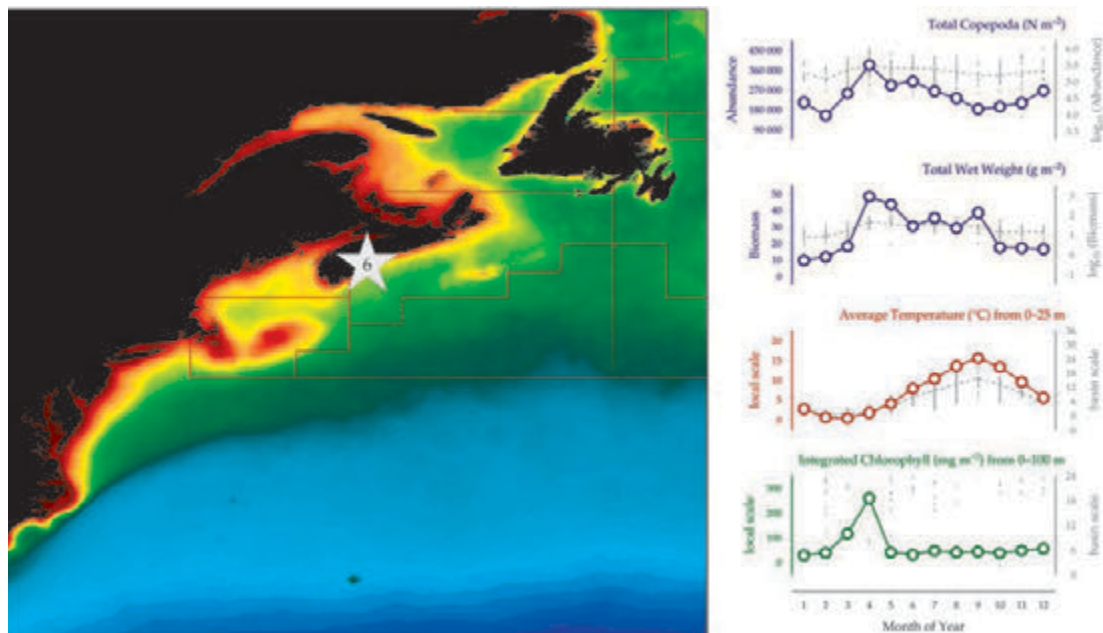


3.3 Halifax Line 2, Scotian Shelf (Site 6)

Catherine Johnson and Erica Head

Figure 3.3.1

Location of the Halifax Line 2 monitoring area (Site 6) on a map of average chlorophyll concentration, and its corresponding seasonal summary plot (see Section 2.2.1).



Zooplankton have been sampled by AZMP every 2–4 weeks since 1999 at Station 2 of the Halifax Line (Halifax 2), which is 150 m deep and located approximately 12 km offshore from Halifax on the inshore edge of Emerald Basin. Zooplankton are sampled using vertical ring-net tows (0.75 m diameter, 200 μ m mesh) from near-bottom to surface. Research ships, trawlers, and small vessels are used as sampling platforms. CTD profiles are recorded, and water samples are collected in Niskin bottles for the measurement of phytoplankton, nutrients, and extracted chlorophyll. Chlorophyll and nutrient concentrations are measured for individual depths, whereas subsamples from each depth are combined to give an integrated sample for phytoplankton cell counting. Zooplankton samples are split, and one-half is used for size fractionated (< 10 mm and > 10 mm) wet and dry weight determination. The other half is subsampled for taxonomic identification and enumeration. Biomass of the dominant groups is calculated using dry weights and abundance data for various groupings (*Calanus*, by species and stage, *Oithona*, *Pseudocalanus*, and *Metridia*). The data are entered into the “BioChem” database at DFO. An ecosystem status report on the state of phytoplankton and zooplankton in Canadian Atlantic waters is prepared every year; the report for 2009/2010 is available at http://www.dfo-mpo.gc.ca/Csas-sccs/publications/resdocs-docrech/2012/2012_071-eng.pdf.

Seasonal and interannual trends (Figure 3.3.2)

At Halifax 2, the water column is well mixed in the winter. Stratification increases in the early spring and is greatest in the late summer–early fall (August–September). There

is an intense spring phytoplankton bloom, and maximum chlorophyll values are generally observed in April (Figure 3.3.2). The seasonal range of variation in total copepod abundance is relatively low at Halifax 2 compared with Prince 5 and other stations in the Gulf of Maine, due to the persistence of small copepods such as *Oithona similis* through the fall and winter at Halifax 2. On average, the maximum copepod abundance is observed in April, and minima occur in February and September. Annual average copepod abundance anomalies were highest in 1999 and 2000, and lowest in 2002, 2007, and 2010. There were no significant trends in total copepod abundance over 1999–2010 and the same was true for the longer time-series derived from CPR observations (Fig. 3.3.3). Annual anomalies of small (< 10 mm) organism wet weight show a significant downward trend since 2000. *Calanus finmarchicus* abundance anomalies tended to be higher at the beginning of the time-series in 1999 to 2003 than in recent years, although they showed no significant trend over time. The recent decline in annual chlorophyll concentrations is thought to be caused by a decline in diatom abundance (Li *et al.*, 2006), although CPR observations indicate that over the long-term near-surface diatom abundance has been higher since the 1990s than it was in the 1960s and 1970s (Fig. 3.3.3). At-site sampled integrated temperature and Hadley SST demonstrate similar interannual increases and decreases, but differ slightly in their seasonal cycles, attributable to the larger spatial region represented by the Hadley data and seasonal changes in the mixed layer depth. Temperature was not related to any of the dominant ring-net zooplankton groups at Halifax 2.

Halifax Line 2, Scotian Shelf

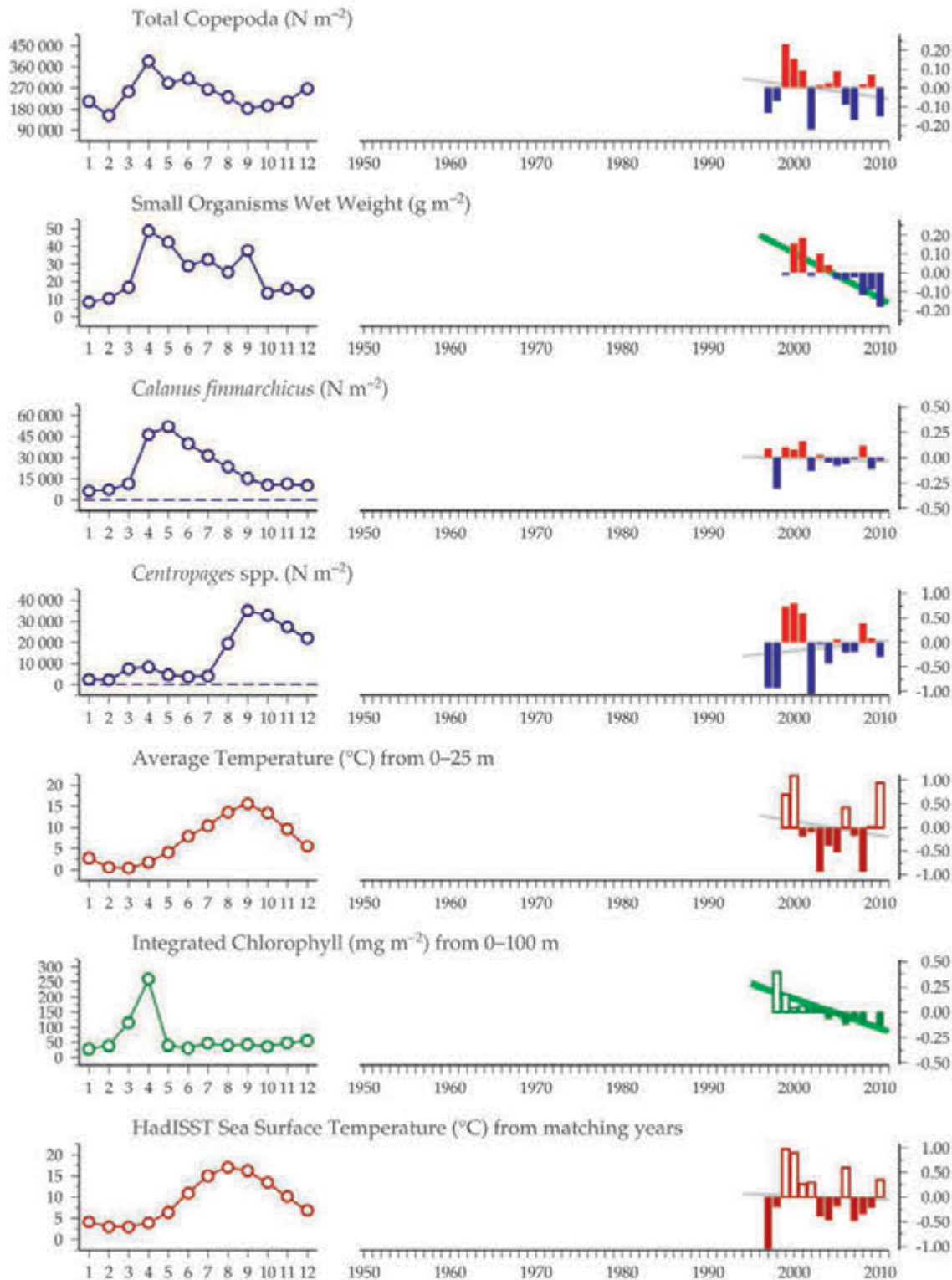


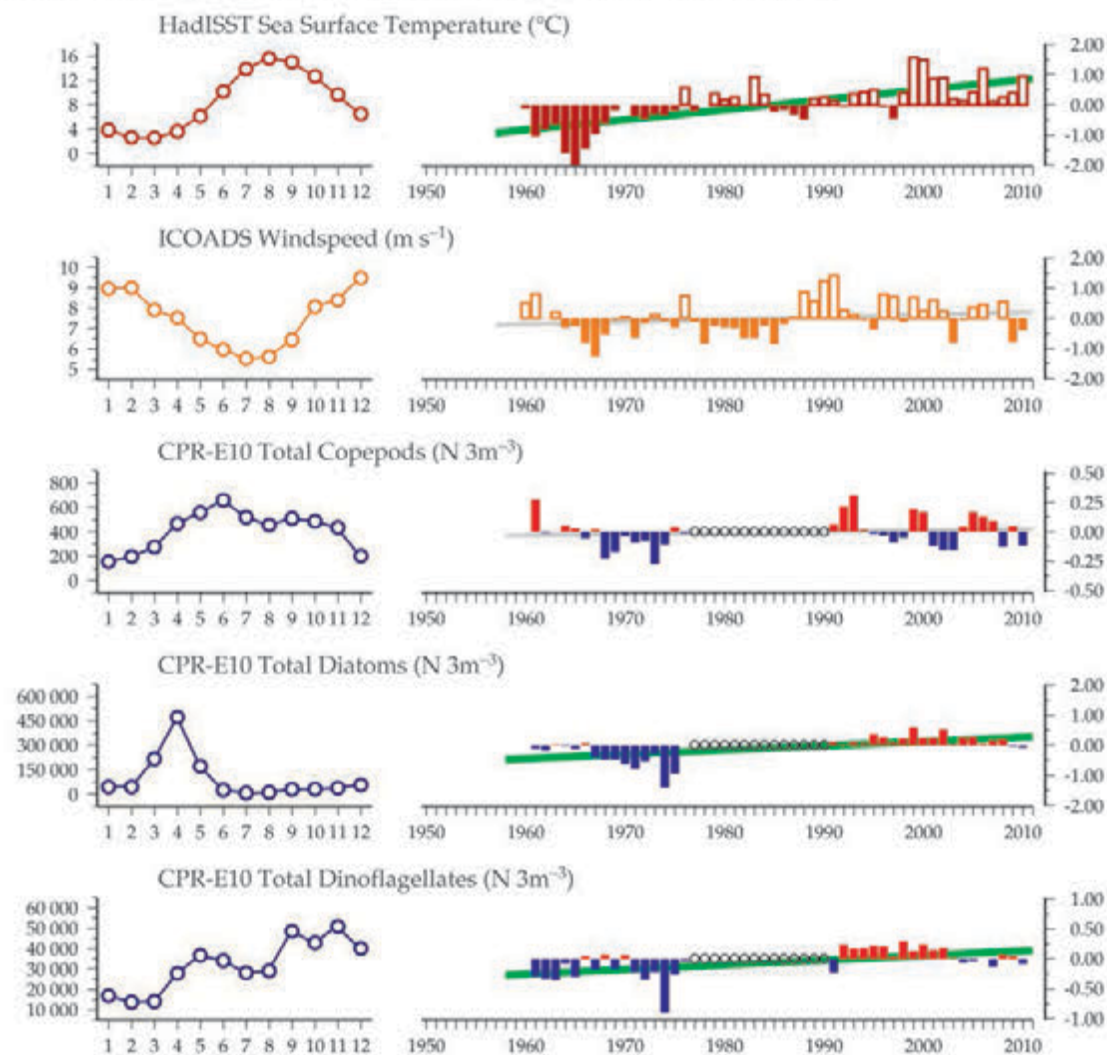
Figure 3.3.2
Multiple-variable comparison plot (see Section 2.2.2) showing the seasonal and interannual properties of select cosampled variables at the Halifax Line 2 monitoring area.

Additional variables are available online at: <http://WGZE.net/time-series>.

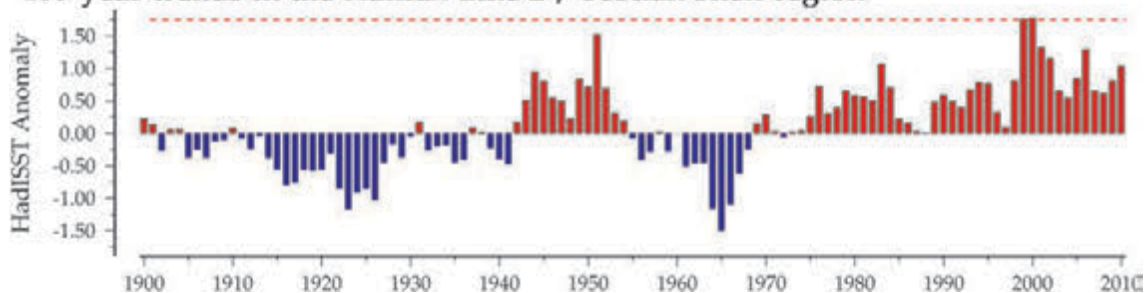
Figure 3.3.3

Regional overview plot (see Section 2.2.3) showing long-term sea surface temperatures and wind speeds in the general region surrounding the Halifax Line 2 monitoring area, along with data from the adjacent CPR E10 Standard Area.

50-year trends in the Halifax Line 2 / Scotian Shelf region



100-year trends in the Halifax Line 2 / Scotian Shelf region



3.4 Anticosti Gyre and Gaspé Current (Site 7)

Michel Harvey and Stéphane Plourde

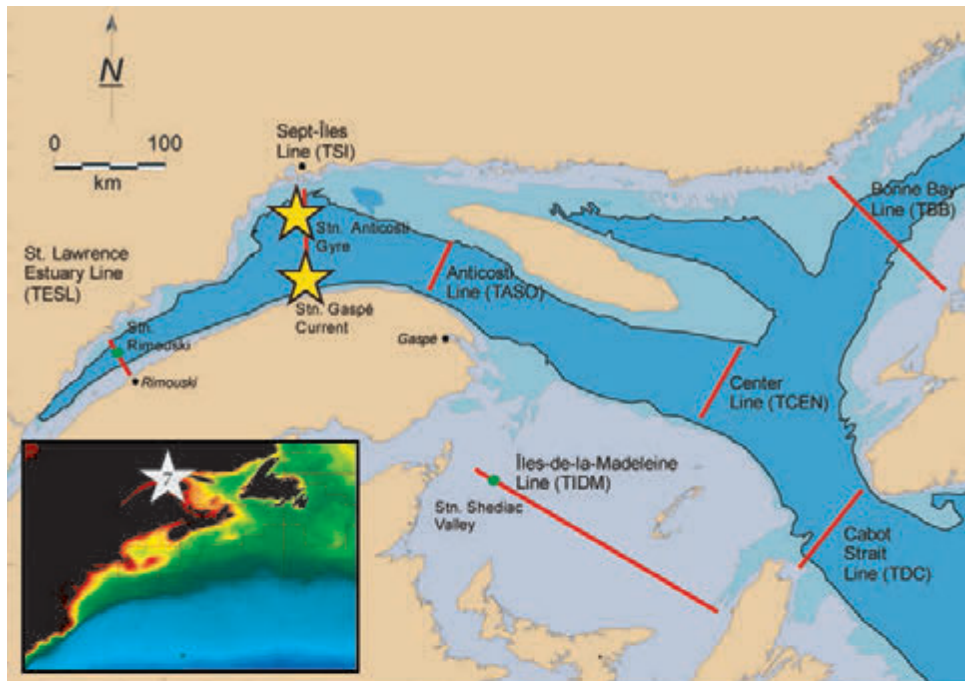
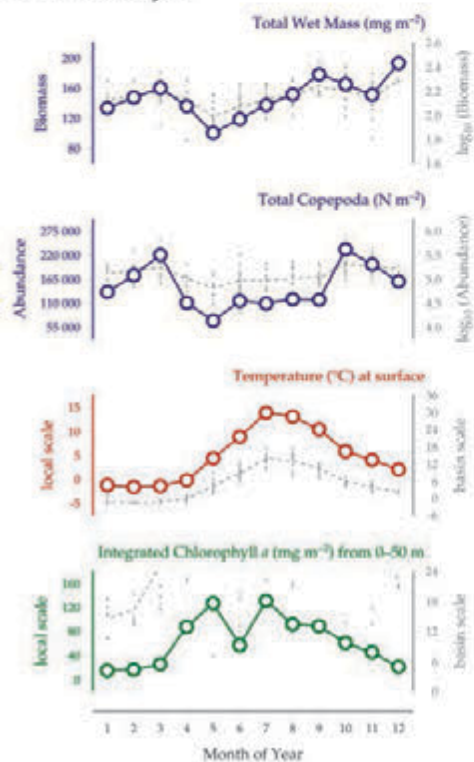
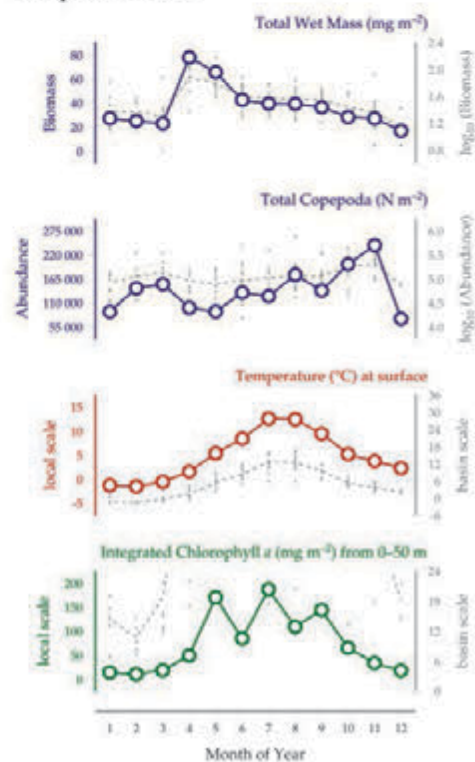


Figure 3.4.1
Locations of the Anticosti Gyre (upper star) and Gaspé Current (lower star) monitoring areas (Site 7), and their corresponding seasonal summary plots (see Section 2.2.1).

Anticosti Gyre



Gaspé Current



The Atlantic Zone Monitoring Programme (AZMP) was implemented in 1998 to collect and analyse the biological, chemical, and physical field data necessary to (i) characterize and understand the causes of oceanic variability at the seasonal, interannual, and decadal scales; (ii) provide multidisciplinary datasets that can be used to establish relationships among the biological, chemical, and physical variables; and (iii) provide adequate data to support the sound development of ocean activities. The key element of AZMP sampling strategy is oceanographic sampling at fixed stations and along sections. Fixed stations are visited approximately every 2 weeks, conditions permitting, and sections are sampled in June and November. Zooplankton are sampled from the bottom to the surface with a ring-net (75 cm diameter, 200 μ m mesh). CTD profiles are recorded, and samples for phytoplankton, nutrients, and extracted chlorophyll are collected using Niskin bottles at fixed depths. Samples are combined to give an integrated sample.

Seasonal and interannual trends (Figure 3.4.2)

The data presented in this summary are from two sampling stations in the northwest Gulf of St Lawrence (GSL): the Anticosti Gyre (AG, depth: 350 m) and the Gaspé Current (GC, depth: 185 m), which together comprise Site 7 (Figure 3.4.1). The GSL is a coastal marine environment with a particularly high zooplankton biomass, relative to other coastal areas, which is dominated by *Calanus* species (de Lafontaine *et al.*, 1991). Zooplankton sampled at the shallow GC site is generally dominated by surface dwelling taxa and 'active' development stages of *Calanus* species whereas deep-dwelling dormant stages of *C. finmarchicus* and *C. hyperboreus* are well represented in samples collected at AG (Plourde *et al.* 2001, 2002, 2003). Zooplankton biomass (total wet mass, Figure 3.4.2) has been generally decreasing at both sites since 2003, whereas copepod abundance at both sites has been increasing since 2000, suggesting a potential trend in zooplankton size structure. Hierarchical community analysis revealed that, numerically, copepods continued to dominate the zooplankton year-round at both fixed stations with no apparent change in copepod community structure was found at either station (Harvey and Devine, 2009).

Zooplankton abundance and biomass do not follow the same seasonal cycle or interannual patterns as chlorophyll. For example, the zooplankton minimum observed at AG in 2001 corresponded to a chlorophyll *a* peak, whereas the zooplankton peak at GC in 2003 corresponded to a chlorophyll *a* minimum. This absence of correlation between zooplankton and algal biomass has been observed in the GSL (de Lafontaine *et al.*, 1991; Roy *et al.*, 2000). The complex estuarine circulation pattern observed at GC and AG is likely to generate this apparent mismatch between surface conditions (chlorophyll *a*) and vertically migrating organisms (zooplankton) at the weekly scale (Saucier *et al.*, 2003; Maps *et al.*, 2011).

Annual cycles of sea surface temperature at both sites are similar, with values below 0°C in winter and peaks above 14°C during summer. Long-term temperatures in the region reveal that temperatures are currently at the high end of an approximately 50-year multidecadal trend. Temperature has been near, or even above, the 100-year maximum (Figure 3.4.3, red dashed line) since 2005. The exact effects of these high temperatures are not fully understood, although total copepod abundance at both regions is currently increasing with increasing temperature at AG and GC.

A detailed ecosystem status report on the state of phytoplankton and zooplankton at these sites is prepared every year. This report is available online at: <http://www.meds-sdmm.dfo-mpo.gc.ca/csas-sccs/applications/publications/index-eng.asp>.

Anticosti Gyre, western Gulf of St. Lawrence

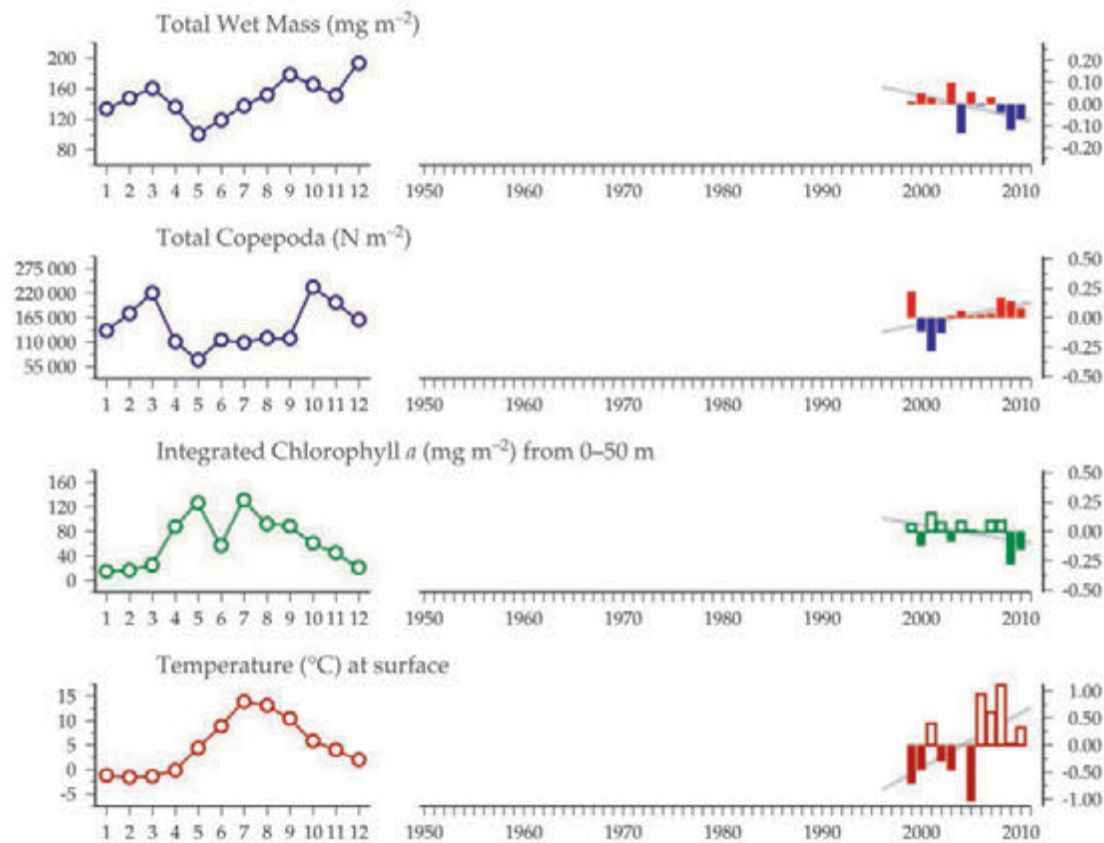


Figure 3.4.2
Multiple-variable comparison plot (see Section 2.2.2) showing the seasonal and interannual properties of select cosampled variables at the Anticosti Gyre and Gaspé Current monitoring areas.

Additional variables are available online at: <http://WGZE.net/time-series>.

50-year trends in the Sargasso Sea region

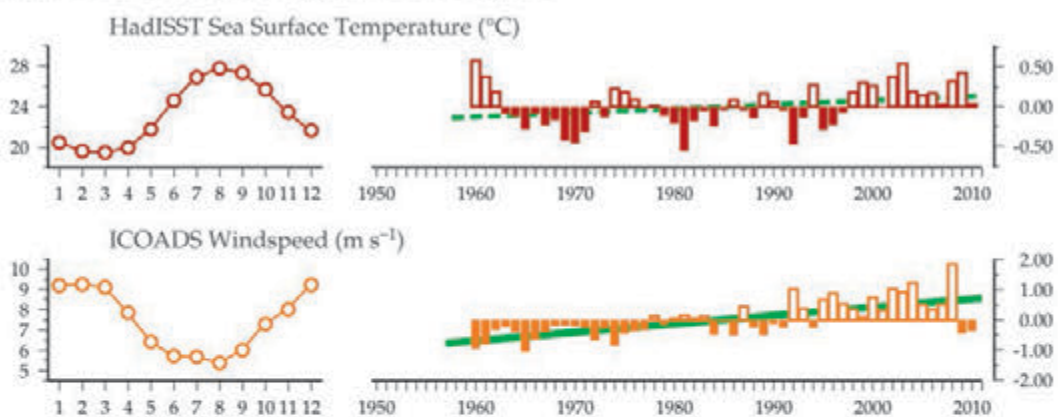
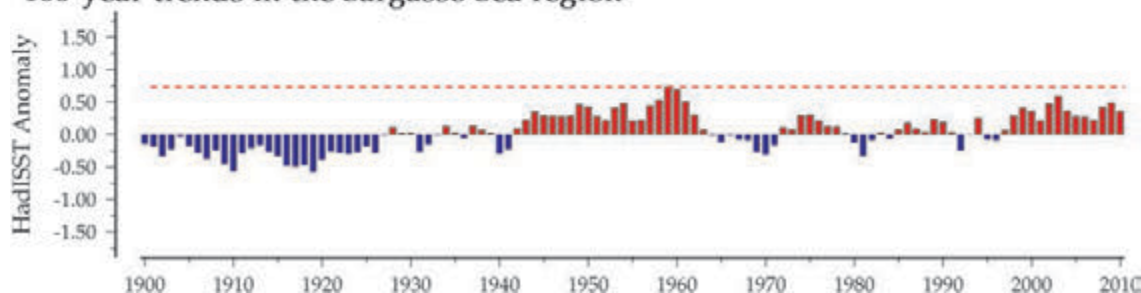


Figure 3.4.3
Regional overview plot (see Section 2.2.3) showing long-term sea surface temperatures and wind speeds in the general region surrounding the Anticosti Gyre and Gaspé Current monitoring areas.

100-year trends in the Sargasso Sea region

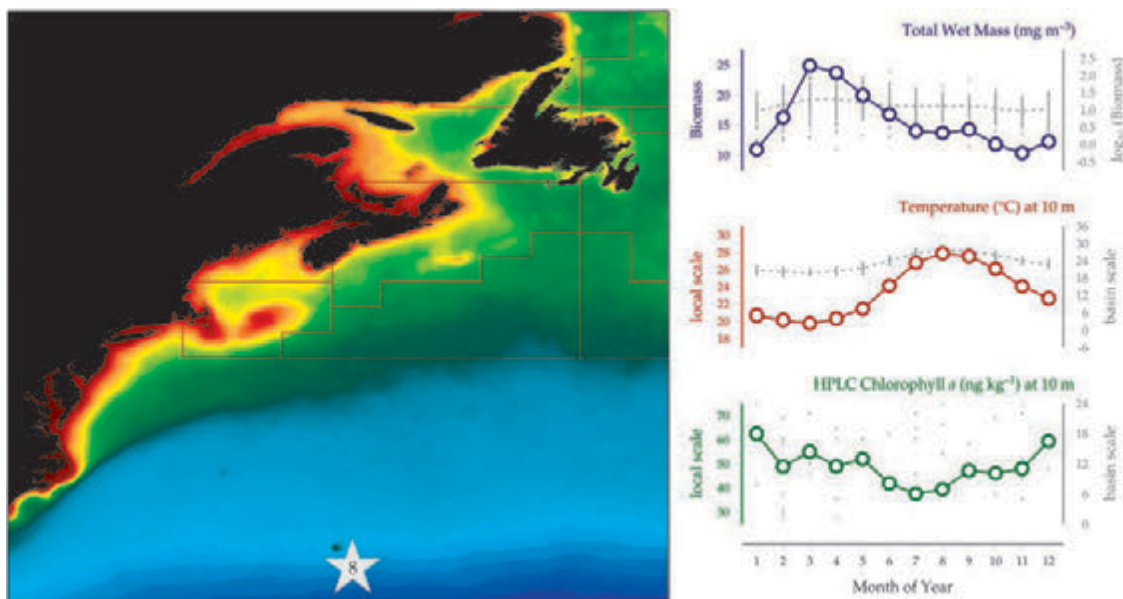


3.5 Bermuda Atlantic Time-series Study (Site 8)

Deborah Steinberg

Figure 3.5.1

Location of the Bermuda Atlantic Time-series Study (BATS) monitoring site (Site 8), plotted on a map of average chlorophyll concentration, and its corresponding seasonal summary plot (see Section 2.2.1).



The Bermuda Atlantic Time-series Study (BATS) site is located in the Sargasso Sea at 31°50'N 64°10'W and is monitored by the Bermuda Institute of Ocean Sciences (BIOS). Zooplankton are collected at least once a month with a 0.8 × 1.2 m rectangular frame net with 202 µm mesh. Two replicate oblique tows are made during the day (between 09:00 and 15:00) and night (between 20:00 and 02:00) to a targeted maximum net depth between 150 and 200 m. Samples from the tows are split on board, with one half-split fractionated by wet sieving through nested sieves with mesh sizes of 5.0, 2.0, 1.0, 0.5, and 0.2 mm for subsequent wet and dry weight analyses, and the other half-split preserved in 4% buffered formaldehyde for taxonomic analysis (Madin *et al.*, 2001; Steinberg *et al.*, 2012).

Seasonal and interannual trends (Figure 3.5.2)

A recent analysis of the dataset (1994–2010) indicated that, during this 17-year period, total mesozooplankton biomass increased 61% overall, although a few short-term downturns occurred over the course of the time-series (Steinberg *et al.*, 2012). The overall increase was higher at night-time compared to daytime, resulting in an increase in calculated diel vertical migrator biomass (mean night minus mean day biomass in epipelagic zone). Night-time biomass values on average are 1.9-fold higher (range = 0.3–12.3) than daytime biomass for the whole time-series, and previous taxonomic analyses (Steinberg *et al.*, 2000) show that migrators such as *Pleuromamma* spp. copepods and euphausiids account for the majority of the night-only biomass. The largest seasonal increase in total biomass was in late-winter to spring (February–April). Associated with the larger increase in late-winter/spring biomass was a shift in the timing of annual peak biomass during the latter half of the time-series (from March/April to a distinct March

peak for all size fractions combined, and April to March for the 2–5 mm size fractions).

Zooplankton biomass was positively correlated with sea surface temperature, water column stratification, and primary production, and negatively correlated with mean temperature between 300 and 600 m (Steinberg *et al.*, 2012). Significant correlations exist between multidecadal climate indices—the North Atlantic Oscillation plus three different Pacific Ocean climate indices—and BATS zooplankton biomass, indicating connections between patterns in climate forcing and ecosystem response. Resultant changes in biogeochemical cycling include an increase in the magnitude of both active carbon flux by diel vertical migration and passive carbon flux of fecal pellets as components of the export flux. The most likely mechanism driving the zooplankton biomass increase is bottom-up control by smaller phytoplankton, which has also increased in biomass and production at BATS, translating up the microbial foodweb into mesozooplankton. Decreases in top-down control or expansion of the range of tropical species northward as a result of warming may also play a role.

Bermuda Atlantic Time-series Study, Sargasso Sea

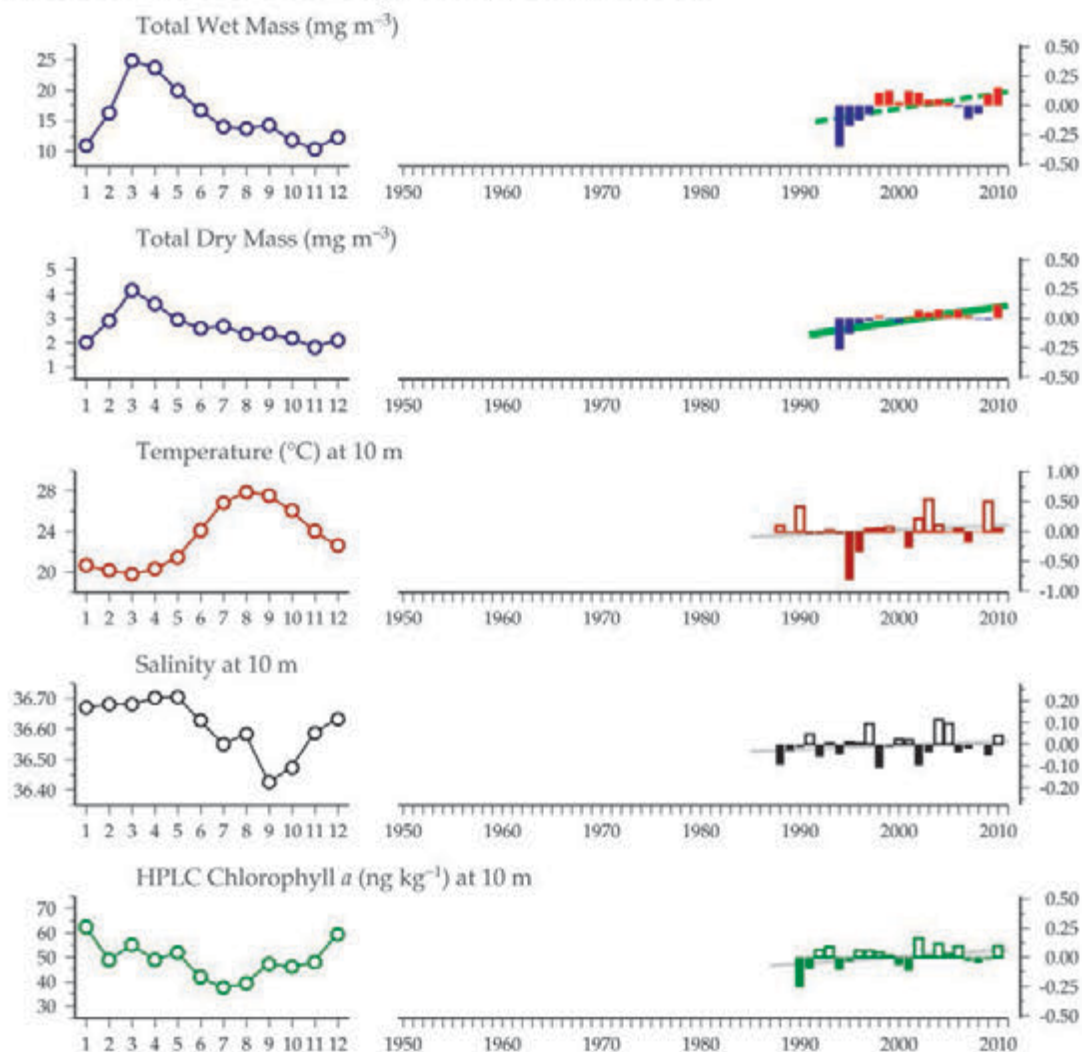


Figure 3.5.2
Multiple-variable comparison plot (see Section 2.2.2) showing the seasonal and interannual properties of select cosampled variables at the BATS monitoring area.

Additional variables are available online at: <http://WGZE.net/time-series>.

50-year trends in the Sargasso Sea region

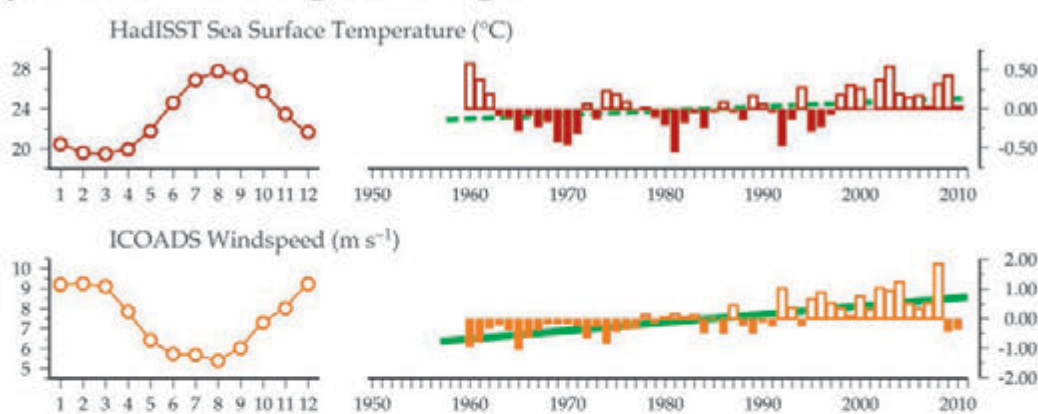
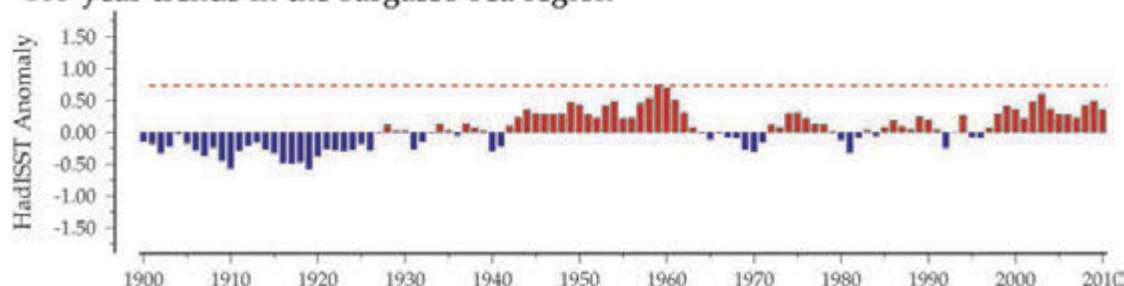


Figure 3.5.3
Regional overview plot (see Section 2.2.3) showing long-term sea surface temperatures and wind speeds in the general region surrounding the BATS monitoring area.

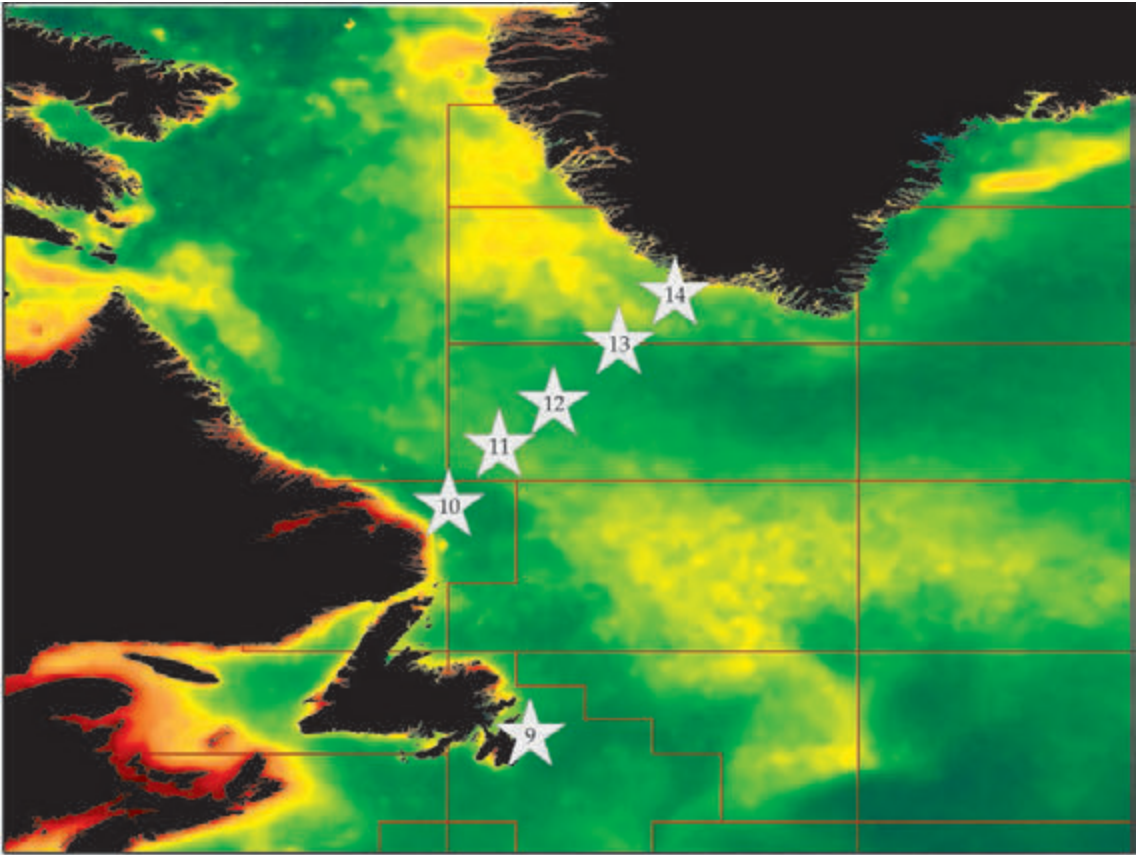
100-year trends in the Sargasso Sea region



4Z OOPLANKTON OF THE LABRADOR SEA

Erica Head and Pierre Pepin

Figure 4.0
Locations of the Labrador Sea zooplankton monitoring areas (Sites 9–14) plotted on a map of average chlorophyll concentration.



Site ID	Monitoring Site (Region)	Section
9	Station 27 (Newfoundland Shelf)	4.1
10	AR7W Zone 1 (Labrador Shelf)	4.2
11	AR7W Zone 2 (Labrador Slope)	4.2
12	AR7W Zone 3 (central Labrador Sea)	4.2
13	AR7W Zone 4 (eastern Labrador Sea)	4.2
14	AR7W Zone 5 (Greenland Shelf)	4.2

The Labrador Sea is located between Greenland and the Labrador coast of eastern Canada. The physical oceanography of this area is described in reports of the Working Group on Oceanic Hydrography (WGOH; Hughes *et al.*, 2011). The broad Labrador Shelf and the narrow Greenland Shelf are both influenced by cold, low-salinity waters of Arctic origin: from the north on the Labrador Shelf via the inshore branch of the Labrador Current, and from the south on the Greenland Shelf via the West Greenland Current, which is formed as the East Greenland Current turns around the tip of Greenland. Warm, saline Atlantic waters flow north into the Labrador Sea on the Greenland side and become colder and fresher as they circulate. There are strong boundary currents beyond the shelf break, which include inputs of Arctic water from the north along the Labrador slope in the offshore branch of the Labrador Current, and of Atlantic water from the south into the eastern region of the Labrador Sea in the Irminger Current. The central basin exceeds 3500 m at its deepest point and is composed of a mixture of waters of both Atlantic and Arctic origin.

The Labrador Sea is one of the few areas in the global ocean where intermediate-depth water masses are formed through convective sinking of dense surface waters. This convection transports cold, dense water to the lower limb of the ocean's Meridional Overturning Circulation. The depth of convection varies from year to year and is strongly influenced by atmospheric forcing, as manifested by the North Atlantic Oscillation (NAO) index. In years when the NAO index is high, there are strong winds from the northwest in late winter, leading to low air temperatures, convection to depths of 1000 m or more, and reduced water temperatures. Conversely, in years when the NAO is low, the winds are not as strong, and air and water temperatures are also warmer.

Changes in Labrador Sea hydrographic conditions on interannual time-scales depend on the variable influences of heat loss to the atmosphere, heat and salt gain from Atlantic waters, and freshwater gain from Arctic outflow, melting sea ice, precipitation, and run-off. Conditions have generally been milder since the mid-1990s. The upper layers of the Labrador Sea have become warmer and more saline as heat losses to the atmosphere have decreased and Atlantic waters have become increasingly dominant (Hughes *et al.*, 2011). The Labrador Sea has a major influence on oceanographic and ecosystem conditions on the Atlantic Canadian continental shelf system, for which it is an upstream source.

Station 27 (Figure 4.0, Site 9) is located 7 km from the coast of Newfoundland and serves to monitor the inshore branch of the Labrador Current and the cold intermediate layer. Interannual variations in environmental conditions at Station 27 are significantly correlated with those at locations up to 300 km away, as in the case of temperature (Ouellet *et al.*, 2003), but this declines as one moves from physical to biological variables. However, Station 27 reflects the combined influence of conditions on the Newfoundland and Labrador shelves, with varying input from the Labrador Sea.

Scientists from Fisheries and Oceans Canada (Bedford Institute of Oceanography) occupy stations along a section across the Labrador Sea between Hamilton Bank on the Labrador Shelf and Cape Desolation on the Greenland Shelf on an annual basis (Figure 4.0, Sites 10–14). This section, the AR7W section (Atlantic Repeat Hydrography Line 7), was first sampled during the World Ocean Circulation Experiment (WOCE) in 1990, when measurements of temperature, salinity, and a comprehensive suite of chemical variables were made. In 1994, sampling of biological variables including bacteria, phytoplankton, and zooplankton was added. Scientists from Fisheries and Oceans Canada (Northwest Atlantic Fisheries Centre) have also carried out year-round sampling of hydrographic, chemical, and biological variables at Station 27 since 1999, with less regular hydrographic measurements dating back to the mid-1940s.

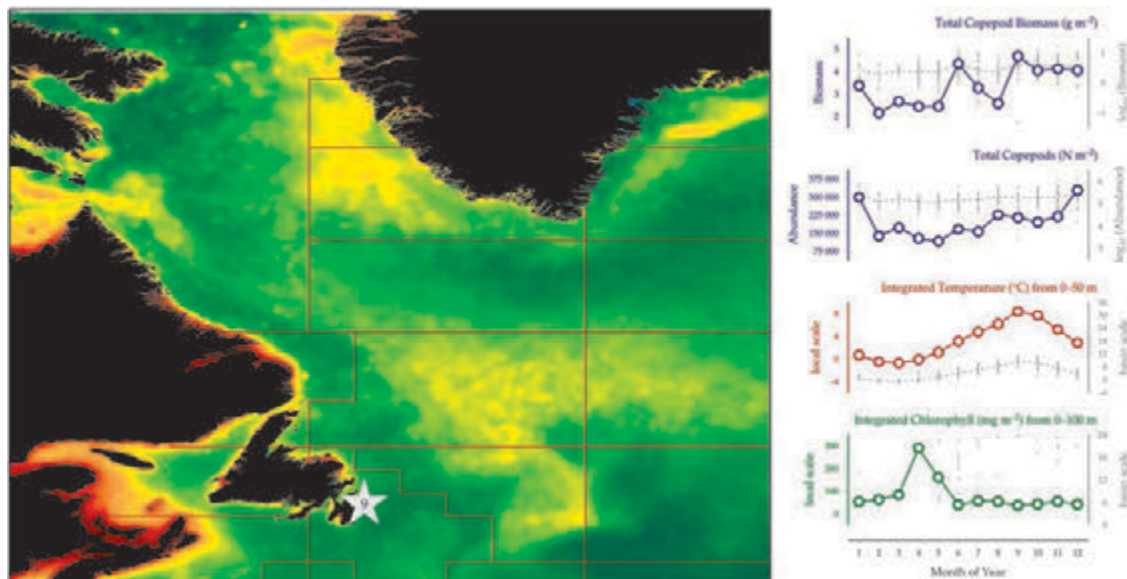
Three species of *Calanus* make up most of the zooplankton biomass along the AR7W section (Head *et al.*, 2003). The North Atlantic species *Calanus finmarchicus* is dominant in the central basin, while the two Arctic species, *C. glacialis* and *C. hyperboreus*, are as important on the shelves. The same three species are equally dominant at Station 27. Annual sampling on the AR7W line is generally during the spring bloom and the reproductive and growth season for *C. finmarchicus* (Head *et al.*, 2000). On the Labrador Shelf, the bloom starts as the winter pack ice recedes north leading to salinity-driven stratification in the surface layer (Wu *et al.*, 2007). The influence of ice-melt on stratification persists as these waters are advected southeast and onto the Newfoundland Shelf and to Station 27. At Station 27, the spring bloom starts earlier when the ice recedes earlier and spring water temperatures are slightly higher, and in years when the bloom is early, *C. finmarchicus* young stages appear earlier, probably because of an earlier start to reproduction and faster development rate (Head *et al.*, 2013). Winter mixing is deepest in the central Labrador Sea basin, and here the timing of the bloom is variable because stratification depends on spring warming of the surface layers. In this region, between the mid-1990s and mid-2000s, satellite determinations of sea surface temperature showed an increasing trend during the March–May period, and ocean-colour satellite measurements of chlorophyll concentration showed that the start of the spring bloom occurred earlier. Over the same period, the proportion of young stages seen in the *C. finmarchicus* population in late May increased from <1% to >30%, probably due to a combination of an earlier start to reproduction and faster development (Licandro *et al.*, 2011). After 2007, sea surface temperatures decreased, as did the proportion of young *C. finmarchicus* stages seen in the western central Labrador Sea in late May (E. J. H. Head, pers. comm.). The bloom occurs earlier in eastern regions of the Labrador Sea than farther west, because melt-water run-off from Greenland leads to enhanced stratification year-round and prevents deep mixing in winter (Frajka-Williams and Rhines, 2010). The bloom generally starts in late April, and young stages of *C. finmarchicus* are abundant by late May, the earliest sampling period for the AR7W line.

4.1 Station 27 (Site 9)

Pierre Pepin

Figure 4.1.1

Location of the Station 27 monitoring area (Site 9) plotted on a map of average chlorophyll concentration, and its corresponding seasonal summary plot (see Section 2.2.1).



Zooplankton are sampled every 2–4 weeks (if possible) at Station 27, using a ringnet (0.75 m diameter, 200 μ m mesh), towed vertically between near-bottom and the surface. Zooplankton are also collected seasonally at stations on a series of transects running perpendicular to the coast of Newfoundland across the Newfoundland and Labrador Shelves and the Grand Banks. Station 27 is located 5 nautical miles east of St John's harbour, on the northwestern edge of the Grand Banks and has a 170 m water depth. In concert with the zooplankton sampling, CTD profiles are recorded, and samples for phytoplankton, nutrients, and extracted chlorophyll are collected using Niskin bottles at fixed depths. For phytoplankton analysis, subsamples from each depth are combined to give an integrated sample.

Zooplankton samples are split, and one-half is used for wet-dry weight determination. The other half is subsampled to give at least 200 organisms that are identified to genus or species and counted. Another subsample is taken containing at least 100 *Calanus* spp. that are identified to species and stage and counted. Biomasses of the dominant groups are calculated using dry weights of various groupings (e.g. *Calanus*, *Oithona*, *Pseudocalanus*, and *Metridia*) and abundance data.

Seasonal and interannual trends (Figure 4.1.2)

At Station 27, total copepod biomass varies seasonally between twofold and threefold, with higher values in autumn than in winter or spring. Interannual variations in total copepod biomass tend to mirror those of the large copepods (*Calanus* and *Metridia* spp.), which dominate the community by weight, but not numerically. The Arctic *Calanus* species, *C. glacialis* and *C. hyperboreus*, reproduce before the spring bloom, whereas the boreal form, *C.*

finmarchicus, reproduces immediately before or during the bloom (Conover, 1988). Thus, the three *Calanus* species are most abundant shortly after the spring phytoplankton bloom. The two Arctic species disappear from the water column by July, whereas *C. finmarchicus* remains abundant throughout the autumn. The biomass of small copepods (*Oithona*, *Pseudocalanus*, *Centropages*, and *Temora* spp.) peaks in late autumn, reflecting the presence of large numbers of *Oithona* species. Overall, there are greater interannual variations in the biomass for the large copepods than for the smaller species.

The seasonal cycle in local *in situ* 0–50 m temperatures differs somewhat from the Hadley SST, although the general pattern in interannual variability is similar. The differences reflect both the wide area of the continental shelf represented in the Hadley estimates relative to the more local measurements taken at Station 27, which is located in the inshore arm of the Labrador Current, and the fact that the 0–50 m depth range includes a seasonally varying proportion of water from the cold intermediate layer, with temperatures close to 0°C. Similarities in interannual variations are the result of large decorrelation scales for SST anomalies in the region (Ouellet *et al.*, 2003). Since 1999, the annual average abundance of *Metridia* spp. has increased significantly at Station 27, while that of *Temora longicornis* and the annual average integrated chlorophyll concentration have both decreased significantly. Other taxa have shown non-significant or no trends. In 2008, the abundances of all three *Calanus* species and those of the smaller copepods *Oithona*, *Pseudocalanus*, and *Temora* spp. were very low, but thereafter, the abundance of *C. finmarchicus*, *C. hyperboreus*, and *Oithona* spp. increased to above-average levels. The abundances of the small copepods *Oithona* spp. and *Pseudocalanus* spp. were at

peak or near-peak levels in 2010, while those of the warm-water species *Centropages* spp. and *Temora longicornis* were below average. Recently, there has been a noted change in the phenology of *C. finmarchicus* and *Pseudocalanus* spp. at Station 27. Since 2005, a greater proportion of C5 copepodites of both species appear to be molting to adulthood during autumn, leading to changes in the relative abundances of adults in spring.

More detailed ecosystem status reports on the state of

chemical and biological oceanographic conditions in the Newfoundland and Labrador region (Canadian Atlantic waters) are prepared every year as Science Advisory Reports or Research Documents.

These reports are available online at: <http://www.isdm-gdsi.gc.ca/csas-sccs/applications/publications/index-eng.asp>.

Station 27, Newfoundland Shelf

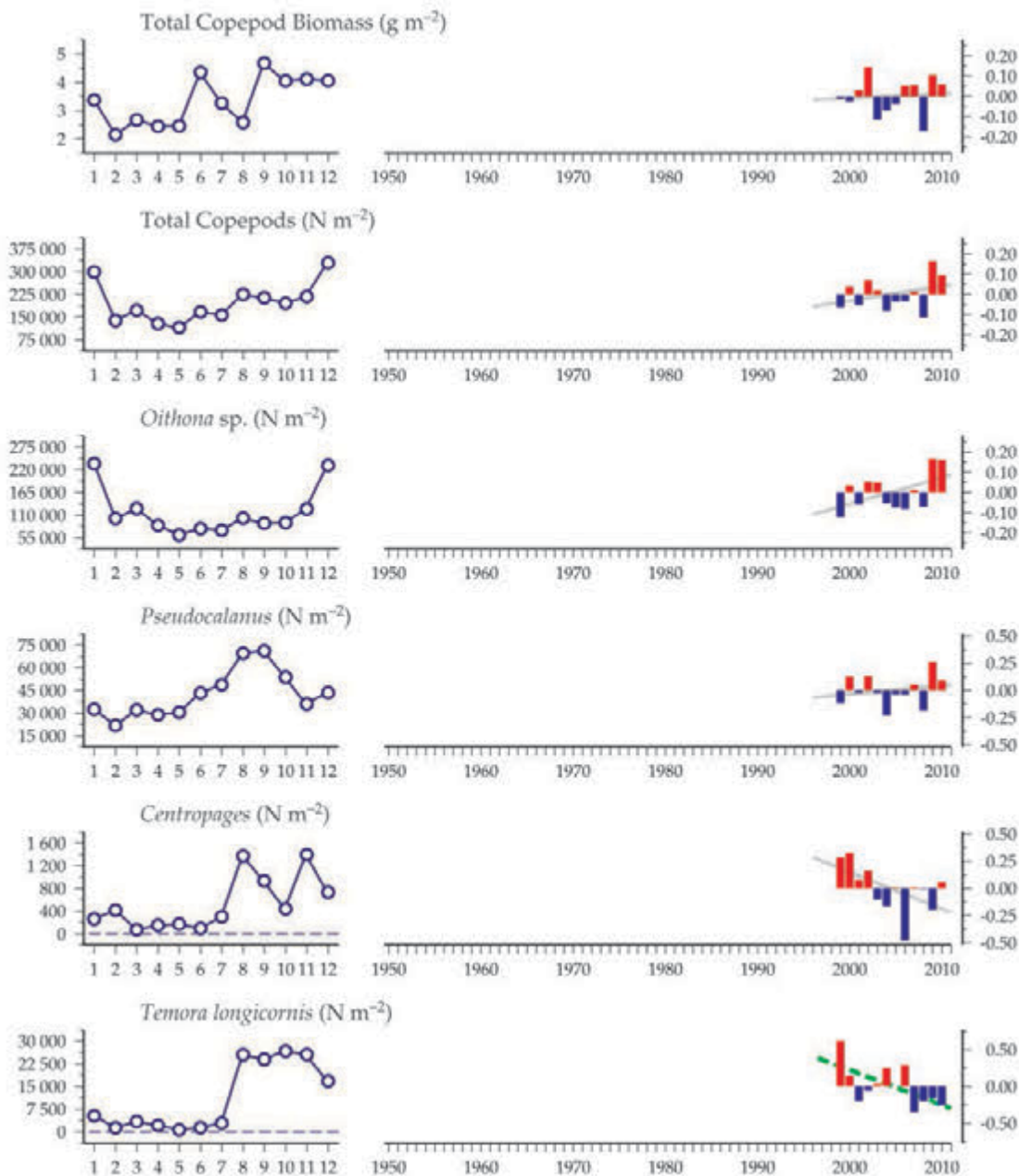
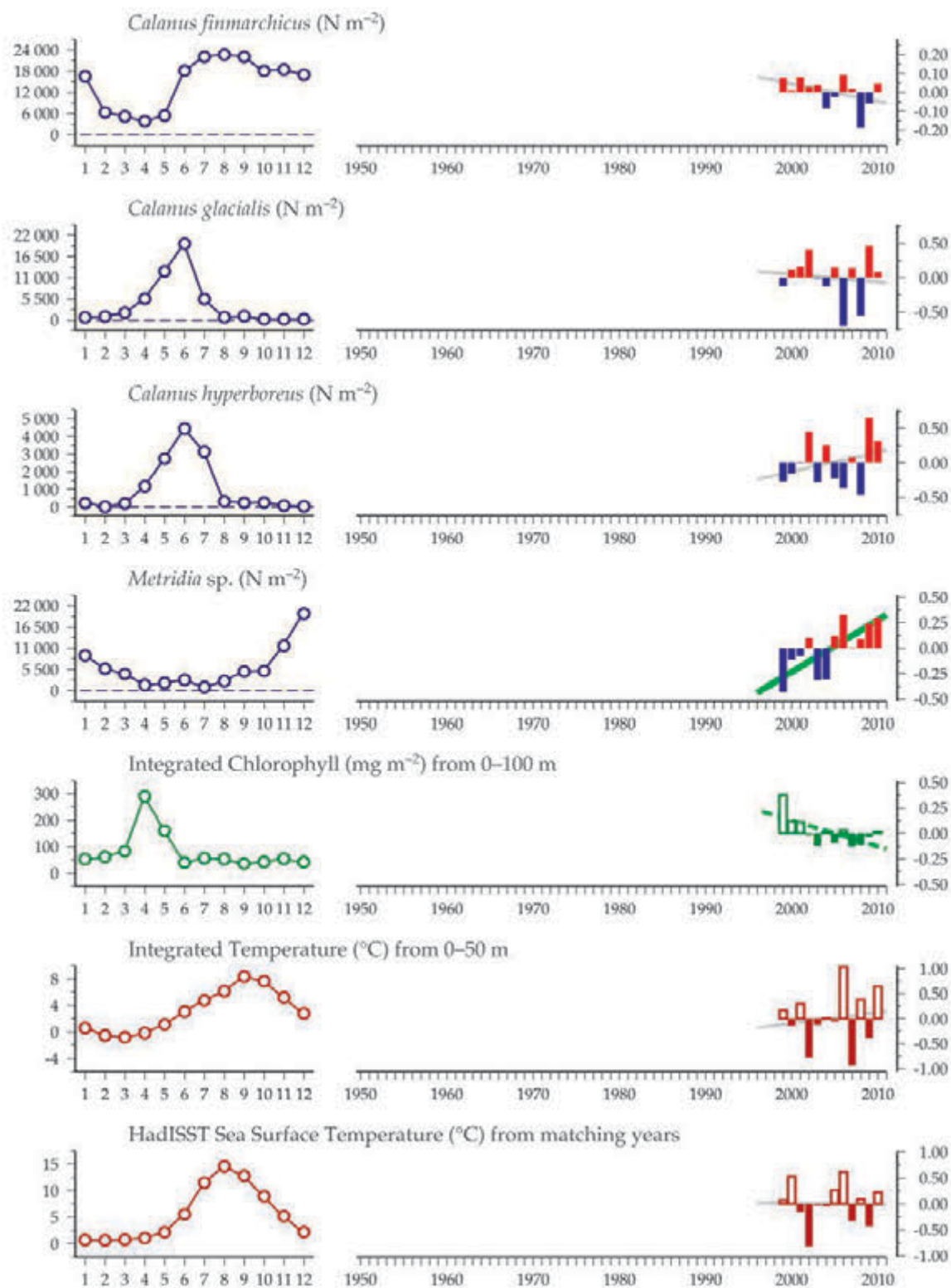


Figure 4.1.2
Multiple-variable comparison plot (see Section 2.2.2) showing the seasonal and interannual properties of select cosampled variables at the Station 27 monitoring area.

Additional variables are available online at: <http://WGZE.net/time-series>.

Figure 4.1.2
continued



50-year trends in the Station 27 / Newfoundland Shelf region

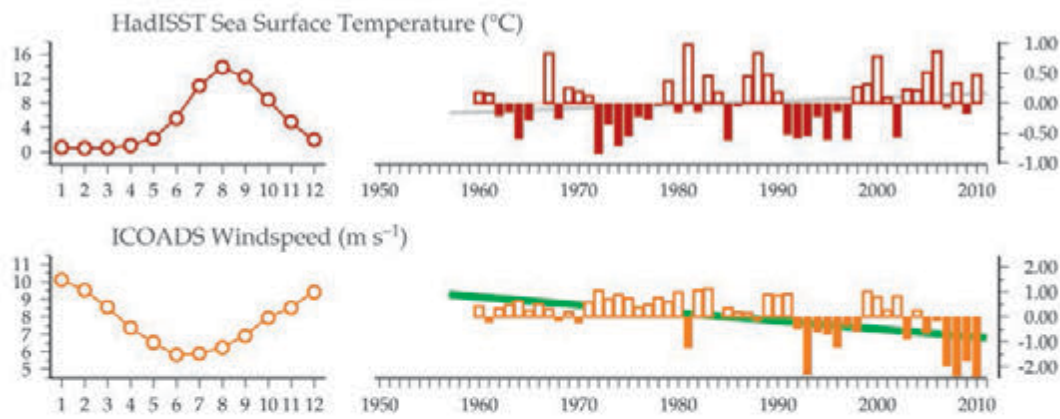
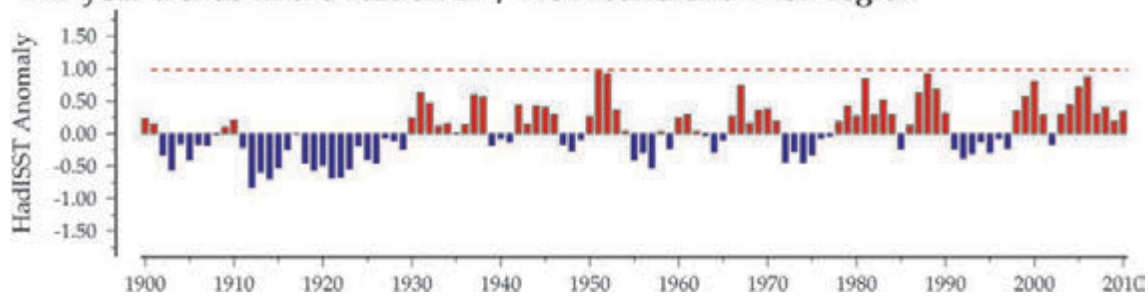


Figure 4.1.3
Regional overview plot
(see Section 2.2.3) showing
long-term sea surface
temperatures and wind
speeds in the general region
surrounding the Station 27
monitoring area.

100-year trends in the Station 27 / Newfoundland Shelf region

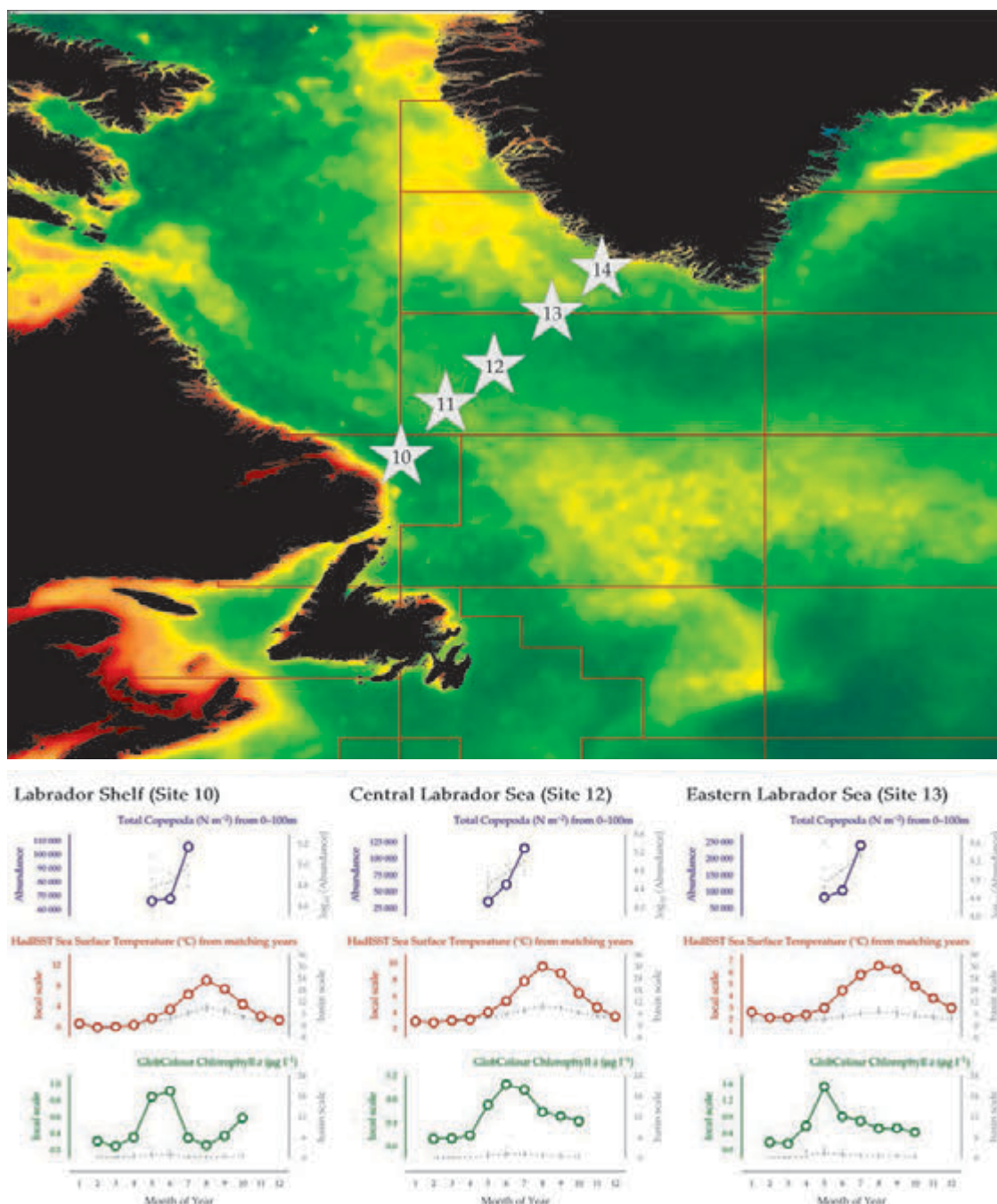


4.2 AR7W Section (Sites 10–14)

Erica Head

Figure 4.2.1

Location of the AR7W Section monitoring areas (Sites 10–14), plotted on a map of average chlorophyll concentration, with corresponding seasonal summary plots (only for sites 10, 12, and 13) shown in the lower panel (see also Section 2.2.1).



Zooplankton are sampled once a year during spring or early summer (May–July) at up to 28 stations along the AR7W section. Most of the occupations have been during late May (1996, 1997, 2000, 2004–2011), with others in June (1998, 2001) and July (1995, 1999, 2002, 2003). In some years, the Labrador Shelf is still covered with pack ice in late May, which prevents sampling at some or all of the stations there. Farther east, the section is ice-free, except for a few icebergs on or near the Greenland Shelf, which can also interfere with sampling at some stations.

Zooplankton sampling is by means of 202 µm mesh ringnets, towed vertically between 100 m and the surface.

Zooplankton are preserved in formalin, identified, and enumerated, and the abundance data are analysed using a multidimensional scaling method that groups stations according to community structure. The stations generally fall into five zones (sites), which correspond geographically to the Labrador Shelf (Site 10), the Labrador Slope (Site 11), the western Central Labrador Sea (Site 12), the Eastern Labrador Sea (Site 13), and the Greenland Shelf (Site 14) (Head *et al.*, 2003). The boundaries between the three central regions are flexible, while the shelf stations are confined by bathymetry.

Zooplankton biomass is determined for groups of organisms that have been picked out and dried in an oven at 60°C for at least 24 h. These groups are for individual stages for three species of *Calanus* and of broader groupings for other taxa (e.g. genus, larvaceans), and the total sample biomass is calculated by summing the dry weights of the groups, using the abundance data where appropriate. Biomass is determined in this way because often the samples contain high concentrations of phytoplankton, which would lead to overestimation of zooplankton biomass, if bulk measurements were to be made.

Seasonal and interannual trends (Figures 4.2.2–4.2.8)

Seasonal cycles of abundance vary among species and regions in the Labrador Sea. For *Calanus finmarchicus*, regional differences in spring bloom dynamics lead to differences in the timing of reproduction. On the Labrador Shelf (LSh, Site 10) and in the Central Labrador Sea (CLS, Site 12), the bloom generally starts in May (see Figure 4.2.1), and populations are dominated by reproductively active adult females (>60%) in late May. In the Eastern Labrador Sea (ELS, Site 13), by contrast, the bloom starts in April, and by late May, young-stage copepodites are abundant and account for >90% of the population. The ELS population in July is more developed, but only slightly more abundant than the LSh and CLS populations. On the LSh, population size has increased by July and young stages (CI–IV) now make up >80% of the total. In the CLS, population size does not change between May and July, and in July, young stages still only make up about 40% of the total, suggesting high mortality and poor recruitment. A similar observation has been made in the central Irminger Sea (Heath *et al.*, 2008). The two Arctic *Calanus* species contribute significantly to the total copepod abundance only on the LSh, with *C. hyperboreus* more abundant in May and June and *C. glacialis*, in July. *C. hyperboreus* reproduce in winter, without feeding (Conover, 1988) and the population is >75% CIV copepodites on the LSh by July and has started to return to depth to overwinter. *C. glacialis* reproduce in early spring, utilizing ice algae as an energy source, and by July, 90% of the population on the LSh are stage CI–CIII, which cannot overwinter and must continue to feed to reach a stage that can. *Oithona* spp. shows no May–July change in abundance on the LSh, but substantial increases in the CLS and ELS. *Oithona* spp. shows no spring–summer increase in abundance at Station 27 (Site 9, see Section 4.1) either, but by contrast, *Oithona* spp. in CPR samples collected in the subpolar gyre, between Flemish Cap and Iceland, are low in abundance in May, increasing to peak values in July (E. J. H. Head, pers. comm.). This regional difference in seasonal cycles could be due to differences in the seasonal cycle of food availability, or species composition, since the population on the shelf is mainly *O. similis*, while the offshore regions, which contain greater proportions of Atlantic water, also contain higher proportions of *O. atlantica*. *Pseudocalanus* spp. were only present in appreciable levels on the LSh, where they did not show the slight increased observed between May and July at Station 27 (see Figure 4.1.2, Section 4.1).

Within Figures 4.2.2–4.2.6, interannual trends in abundance were examined by including only data collected in late May. In general, there were no significant trends in abundance in any of the regions. The only statistically significant trend was an increasing trend for *C. glacialis* abundance in the Central Labrador Sea (CLS, Site 12). In general, the non-significant increasing abundance trends were consistent with increasing temperature trends, but not with the observed *in situ* trends in chlorophyll concentration.

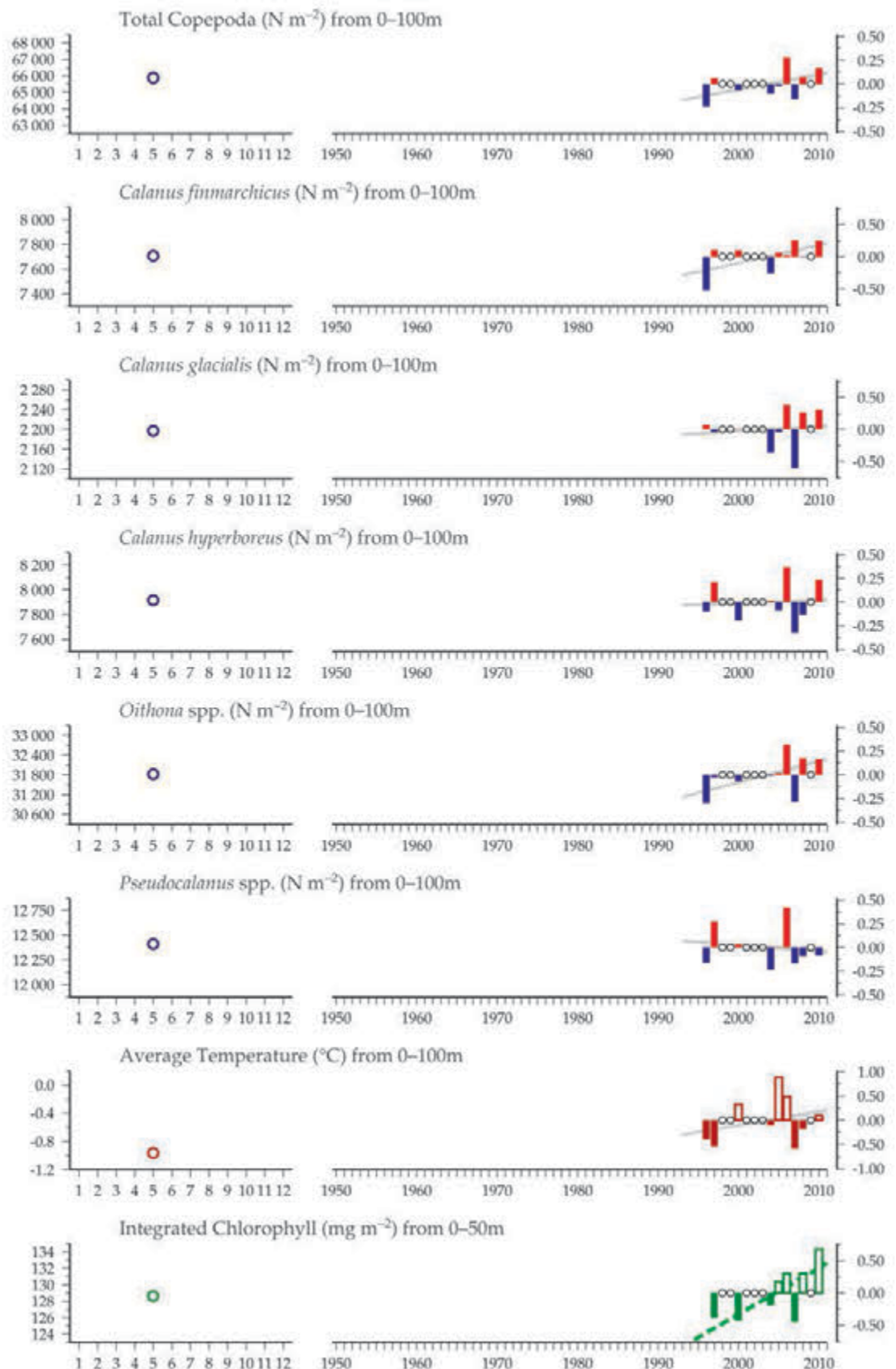
Long-term temperature and windspeeds were increasing at all sites (Figure 4.2.7), with the exception of windspeeds in the Central Labrador Sea (CLS, Site 12). Recent (2005–present) sea surface temperatures in the Labrador Shelf, Labrador Slope, and Central Labrador Sea regions (Sites 10–12) have been near or above the warmest temperatures seen in the last 100 years (see Figure 4.2.8, red dashed lines).

Figure 4.2.2

Multiple-variable comparison plot (see Section 2.2.2) showing the seasonal and interannual properties of select cosampled variables at the AR7W Labrador Shelf zooplankton monitoring area (data collected in late May only).

Additional variables are available online at <http://WGZE.net/time-series>.

AR7W Zone 1, Labrador Shelf (Site 10)



AR7W Zone 2, Labrador Slope (Site 11)

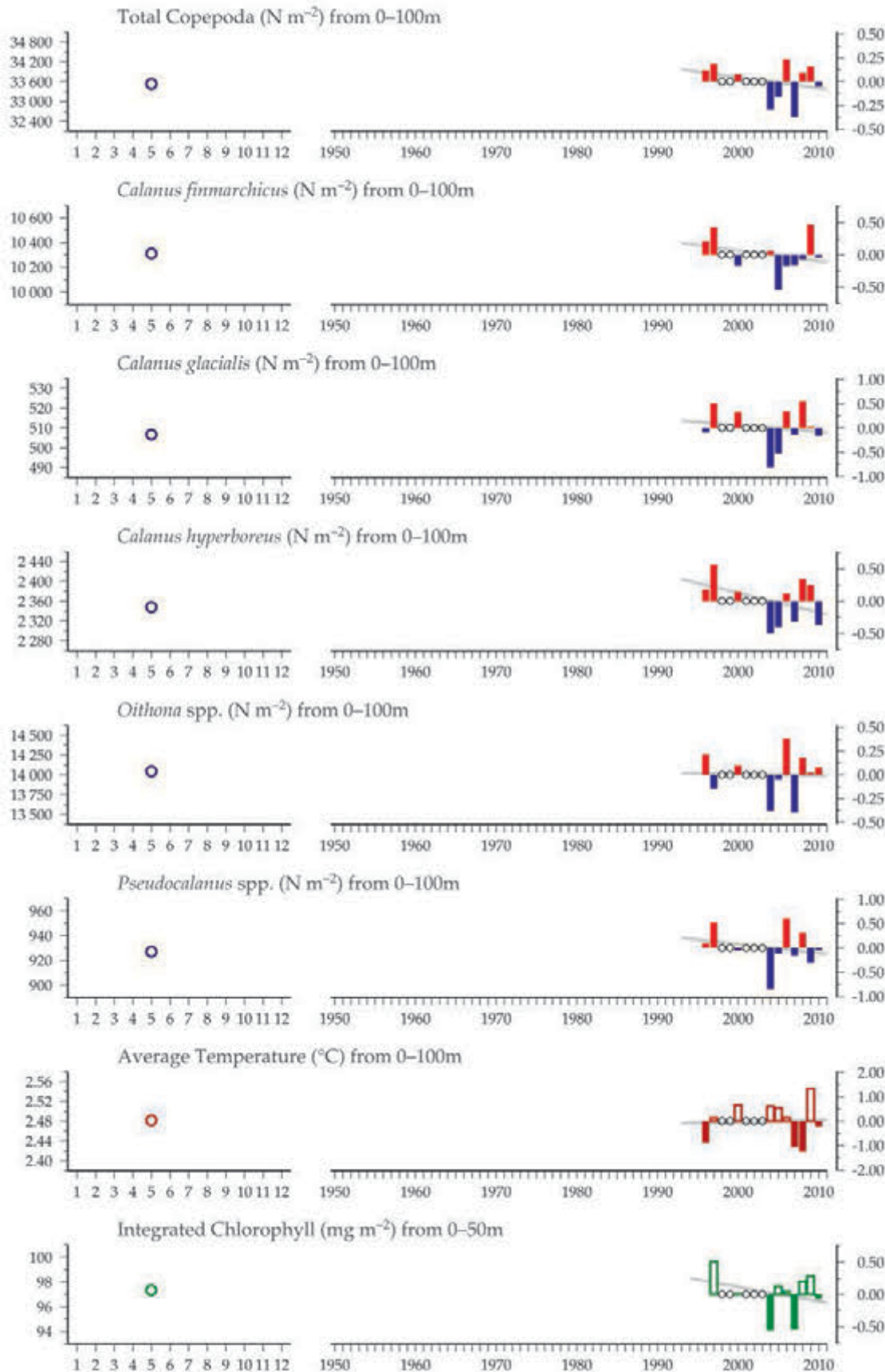


Figure 4.2.3
Multiple-variable comparison plot (see Section 2.2.2) showing the seasonal and interannual properties of select cosampled variables at the AR7W Labrador Slope zooplankton monitoring area (data collected in late May only).

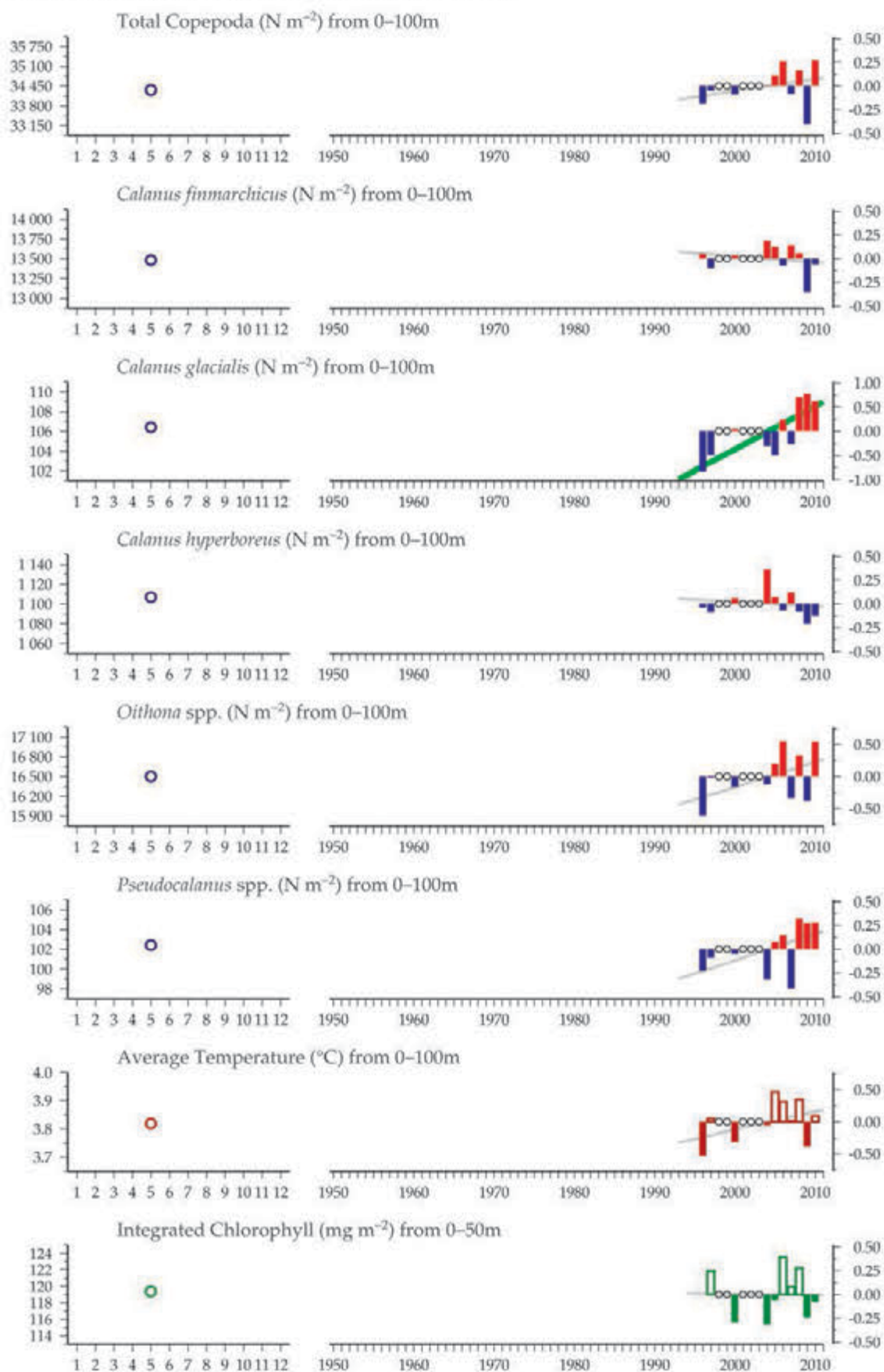
Additional variables are available online at <http://WGZE.net/time-series>.

Figure 4.2.4

Multiple-variable comparison plot (see Section 2.2.2) showing the seasonal and interannual properties of select cosampled variables at the AR7W Central Labrador Sea zooplankton monitoring area (data collected in late May only).

Additional variables are available online at <http://WGZE.net/time-series>.

AR7W Zone 3, central Labrador Sea (Site 12)



AR7W Zone 4, eastern Labrador Sea (Site 13)

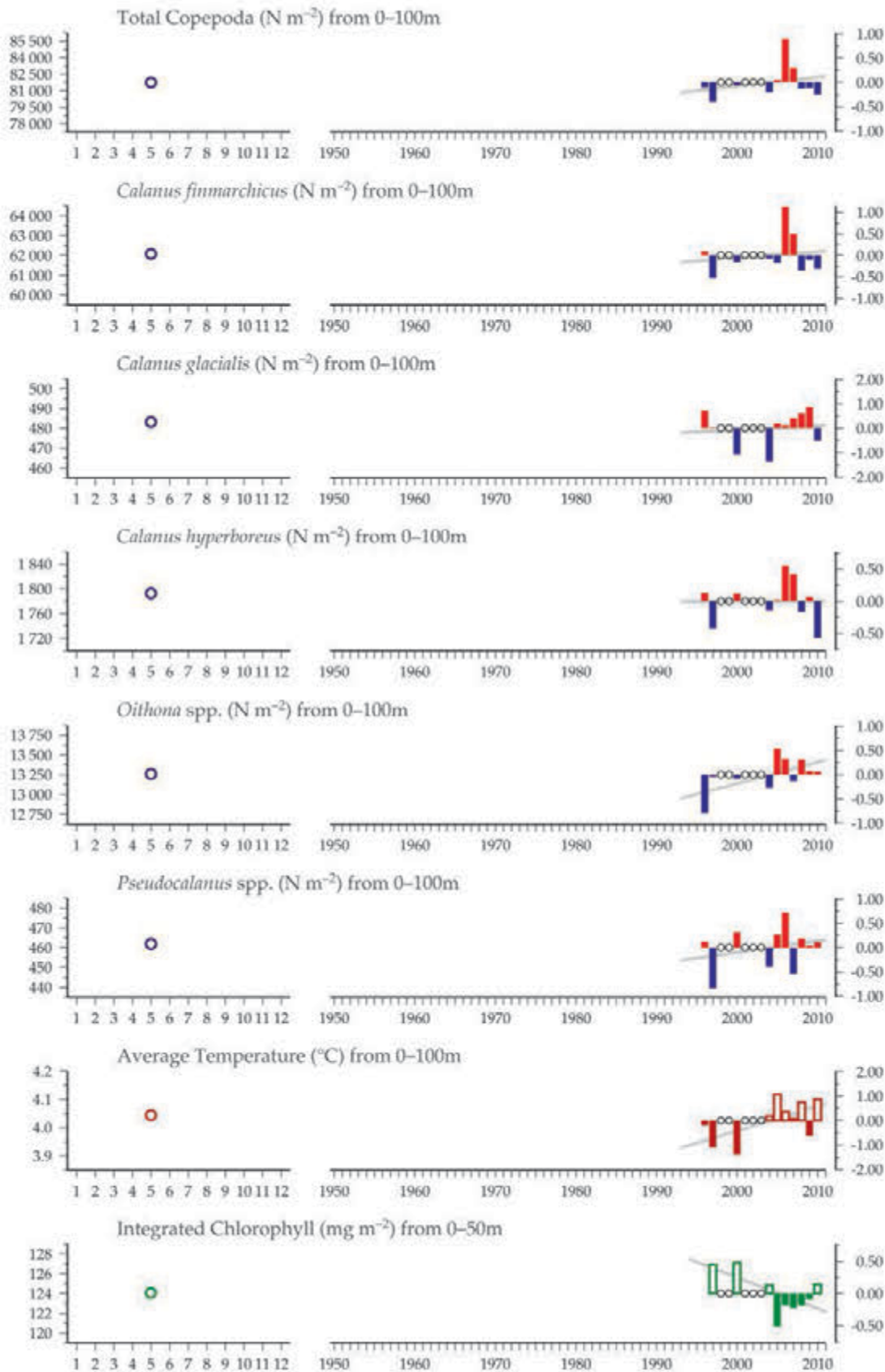


Figure 4.2.5
Multiple-variable comparison plot (see Section 2.2.2) showing the seasonal and interannual properties of select cosampled variables at the AR7W Eastern Labrador Sea zooplankton monitoring area (data collected in late May only).

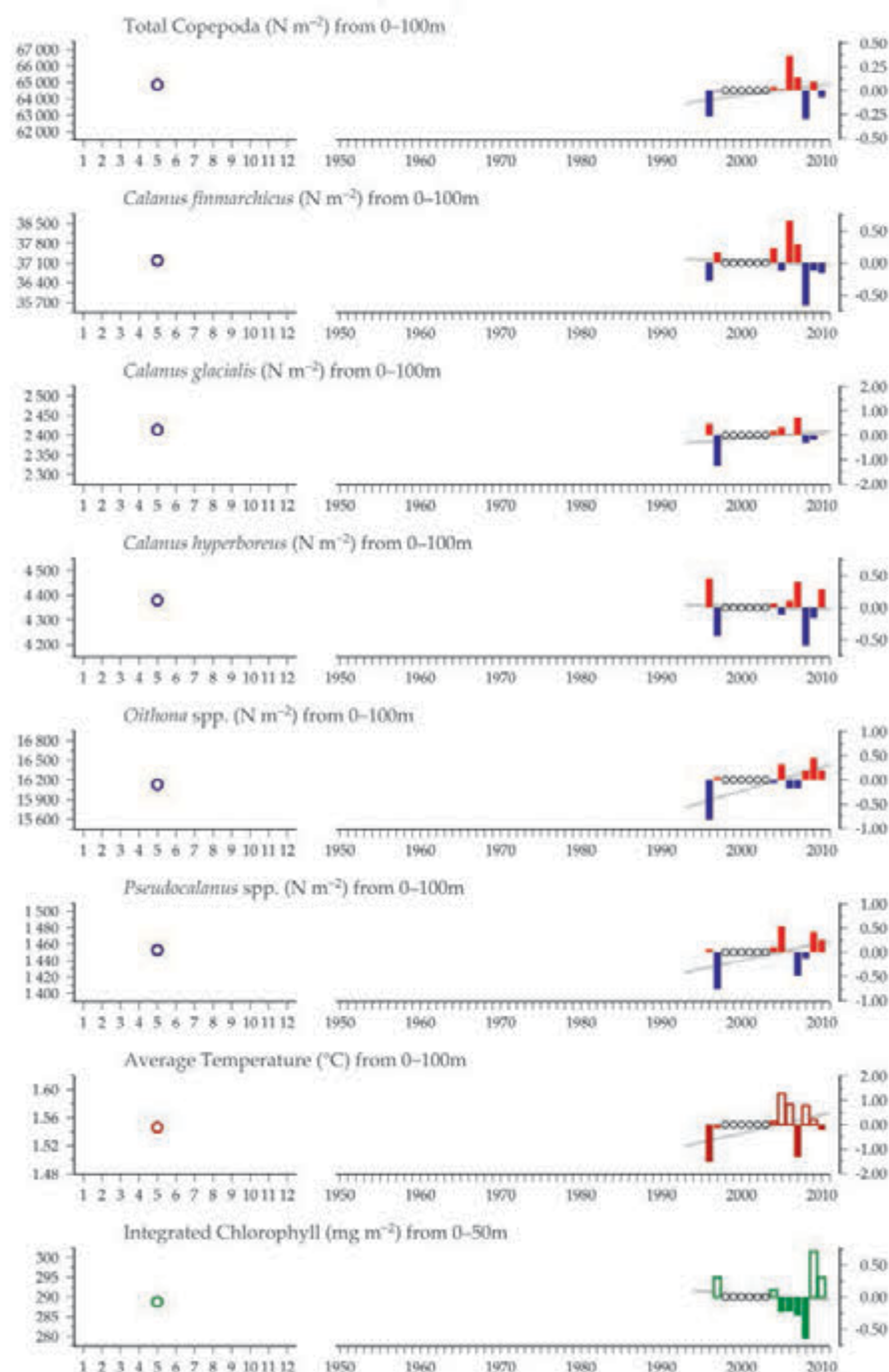
Additional variables are available online at <http://WGZE.net/time-series>.

Figure 4.2.6

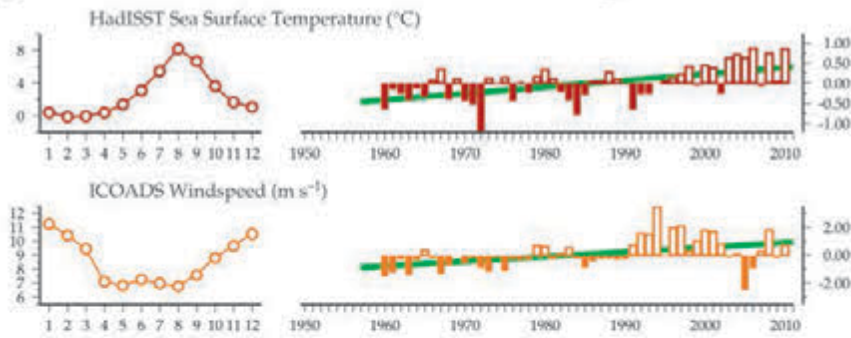
Multiple-variable comparison plot (see Section 2.2.2) showing the seasonal and interannual properties of select cosampled variables at the AR7W Greenland Shelf zooplankton monitoring area (data collected in late May only).

Additional variables are available online at: <http://WGZE.net/time-series>.

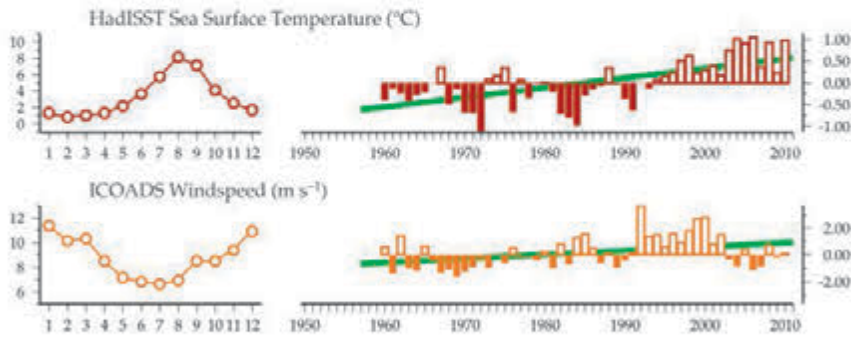
AR7W Zone 5, Greenland Shelf (Site 14)



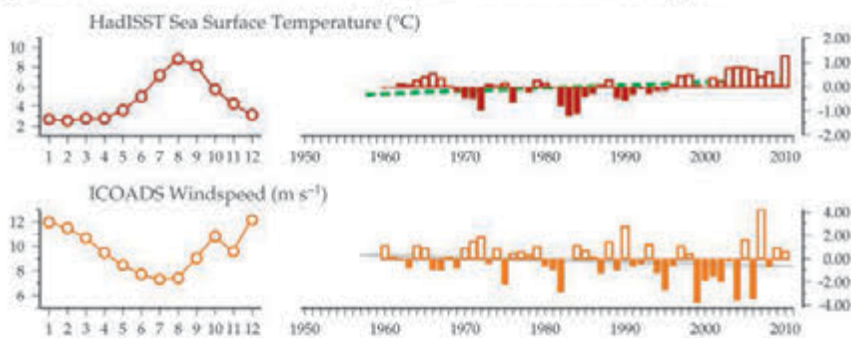
50-year trends in the AR7W Zone 1 / Labrador Shelf region



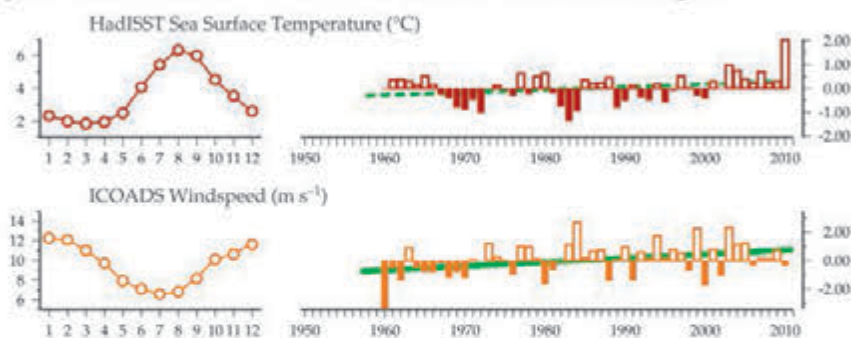
50-year trends in the AR7W Zone 2 / Labrador Slope region



50-year trends in the AR7W Zone 3 / central Labrador Sea region



50-year trends in the AR7W Zone 4 / eastern Labrador Sea region



50-year trends in the AR7W Zone 5 / Greenland Shelf region

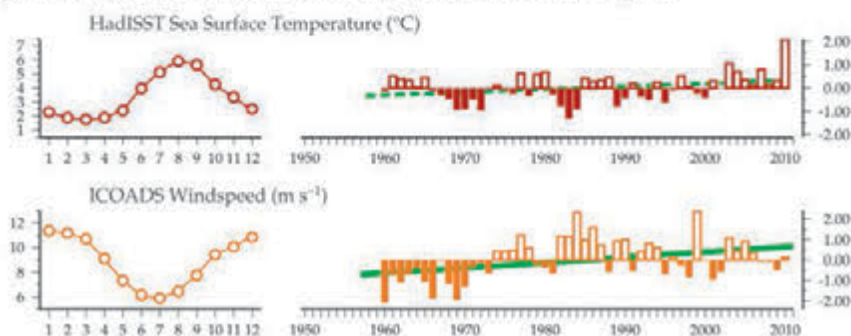
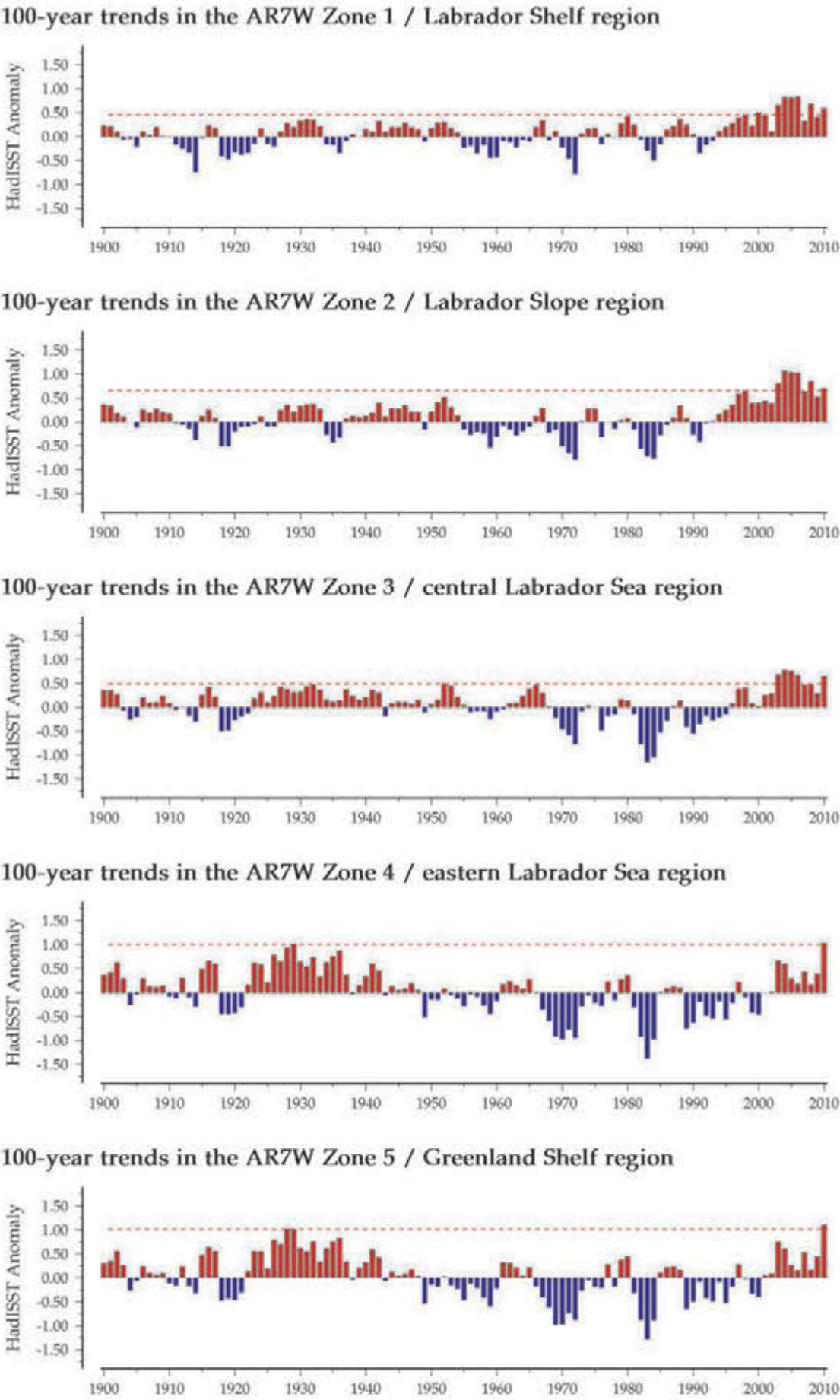


Figure 4.2.7
Regional overview plots
(see Section 2.2.3) showing
long-term sea surface
temperatures and wind
speeds in the general
regions surrounding the
AR7W monitoring areas.

Figure 4.2.8
Seasonal and interannual trends of long-term surface water temperatures in the general region surrounding the zooplankton survey area (see Section 2.2.2 for an explanation of the data sources and figures).



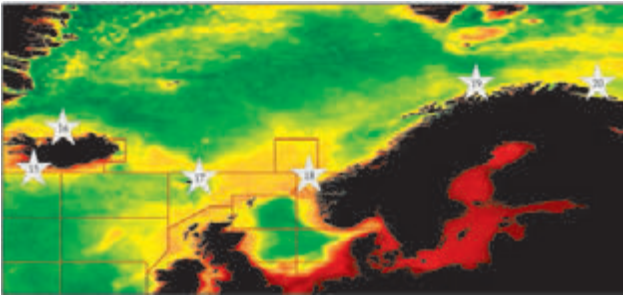


Northern krill Meganyctiphanes norvegica. Source: Jean-François St-Pierre, Department of Fisheries and Oceans, Canada.

5Z OOPLANKTON OF THE NORDIC AND BARENTS SEAS

Astthor Gislason, Eilif Gaard, Hogni Debes, Webjørn Melle, Cecilie Broms, and Padmini Dalpadado

Figure 5.0
Locations of the Nordic and Barents seas zooplankton monitoring areas (Sites 1–8) plotted on a map of average chlorophyll concentration (see Section 2.3.2).



Site ID	Monitoring Site (Region)	Section
15	Selvogsbanki Transect (South Iceland)	51
16	Siglunes Transect (North Iceland)	51
17	Faroe Islands (southern Norwegian Sea)	52
18	Svinøy Transect (Norwegian Sea)	53
19	Fugløya-Bjørnøya Transect (western Barents Sea)	54
20	Vardø-Nord Transect (central Barents Sea)	54

The Nordic and Barents seas (Figure 5.0) are influenced by warm saline Atlantic water entering from the south as the North Atlantic Current. One branch flows west along the south coast of Iceland, north along Iceland’s west coast, then splits into two components at the Greenland-Iceland Ridge. The larger component turns west into the Irminger Sea, whereas the smaller one continues north of Iceland. Atlantic water also enters the Norwegian Sea on both sides of the Faroe Islands. This water flows north along the Norwegian coast as the Norwegian Atlantic Current, past the Svalbard islands, and into the Arctic Ocean. Between Bear Island (south of Svalbard) and the north coast of Norway, a branch of the Atlantic Current flows into the Barents Sea.

Cold, lower-salinity water enters the Nordic and Barents seas from the Arctic Ocean. In the Greenland Sea, Arctic water flows south into the Iceland Sea as the East Greenland Current. North of Iceland, part of this current turns east, mixes with Atlantic water, and enters the Norwegian Sea as the East Icelandic Current. Arctic water enters the Barents Sea in the northeast and flows northwest of the Polar front. Fresh, lower-salinity coastal water flows along the Norwegian coast. The deep ocean basins adjoining the coastal areas are subject to intensive winter cooling and deep convection. Deep return currents carry the convected water back into the deep basins of the North Atlantic.

The populations of zooplankton are dominated by arctic-boreal species and there is a typical seasonal cycle of primary and secondary production, beginning with a spring bloom that is triggered by increasing light and water-column stabilization through stratification. In some places, a secondary autumn peak in production accompanies the onset of the breakdown in summer stratification and increasing inorganic nutrients.

Four species of *Calanus* are among the dominant mesozooplankton species of the region. *C. finmarchicus* is an Atlantic species, overwintering in the deep basins, ascending in late winter and spring, and advected onto the shelf areas. *C. finmarchicus* has a 1-year life cycle, and its main spawning is linked to the phytoplankton bloom. The main habitat of *C. hyperboreus* is the Arctic water of the deep Greenland Sea, and it has a life cycle of two years or longer. It reproduces in deep water during winter, and juvenile stages ascend to the surface layer during spring. *C. glacialis* is regarded as an Arctic shelf species, has a 2-year life cycle, and reproduces during the phytoplankton bloom. *C. helgolandicus* has the southernmost distribution of the four species. It is mainly a shelf species found in the southern parts of the Norwegian Sea. It has a 1-year life cycle, reproduces in autumn, and does not seem to have a typical dormant period.

5.1 Selvogsbanki and Siglunes Transects (Sites 15–16)

Astthor Gislason

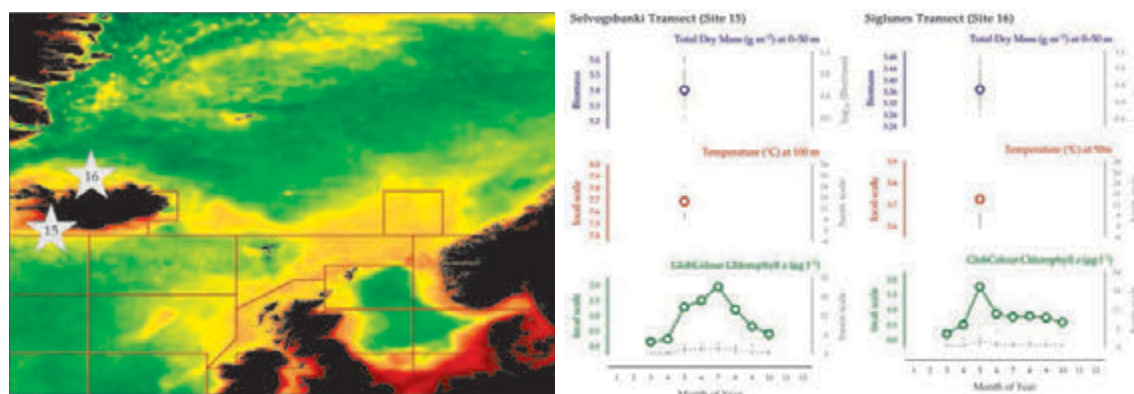


Figure 5.1.1
Locations of the Selvogsbanki and Siglunes transects (Sites 15–16) on a map of average chlorophyll concentration, and their corresponding seasonal summary plots (see Section 2.2.1).

The Icelandic monitoring programme for zooplankton consists of a series of standard transects around Iceland perpendicular to the coastline. In the 1960s, sampling was started at stations along the transects north and east of Iceland. Additional section lines south and west were added in the 1970s. Currently, there are approximately 90 stations. Zooplankton investigations are carried out at these stations every year in May and June. In this summary, long-term changes in zooplankton biomass are examined at the Selvogsbanki (Figure 5.1.1, Site 15) and Siglunes transects (Figure 5.1.1, Site 16). Values for Selvogsbanki are calculated from an average of five stations, whereas values for Siglunes are from an average of eight stations.

At Selvogsbanki, zooplankton biomass has fluctuated rather irregularly, with maxima being observed at 5 - to 10-year intervals (Figure 5.1.2). In spring 2010, zooplankton biomass on the Selvogsbanki transect was higher than the long-term average.

In waters off northern Iceland (Siglunes transect), the high values of zooplankton at the beginning of the time-series dropped drastically with the onset of the Great Salinity Anomaly (GSA) of the 1960s (Figure 5.1.3). Since then, zooplankton biomass has varied, with highs at intervals of approximately 7–10 years. As in the south (Selvogsbanki), zooplankton biomass on the Siglunes transect was above the long-term average in spring 2010.

Copepods (mainly *Calanus finmarchicus* and *Oithona* spp.) generally dominate the zooplankton, comprising >60–70% of the plankton in most years (Gislason *et al.*, 2009). Among the copepods, *C. finmarchicus* tends to be more abundant south of Iceland (~20–70%) than in the north (~10–60%). Temperature and salinity are the most important environmental variables, in terms of explaining the differences in species composition north and south of Iceland, with species and groups such as *Podon leuckarti* and cirripede larvae being relatively abundant south and *C. hyperboreus* abundant north of Iceland. Contrary to results from more southern areas in the North Atlantic (e.g. Beaugrand, 2005), no long-term northward displacement of zooplankton communities is observed around Iceland

(Gislason *et al.*, 2009). However, significant interannual variability in community structure is observed both south and north of Iceland, reflecting oscillations of water masses that characterize the system, with salinity and the nitrate concentrations (an index of phytoplankton production) dictating variability in the south, whereas temperature is the main factor in the north (Gislason *et al.*, 2009).

Zooplankton biomass north of Iceland is influenced by the inflow of warm Atlantic Water (AW). Thus, in warm years, when the flow of higher salinity AW onto the northern shelf is high, zooplankton biomass can be almost twice as high as in cold years, when this inflow is not as evident (Astthorsson and Gislason, 1998; Astthorsson and Vilhjálmsson, 2002). This trend is visible in the annual anomalies (Figure 5.1.3). The reasons for this are probably mainly related to increased advection of zooplankton with AW from the south in warm years. Thus, during both 2000 and 2001, when zooplankton biomass north of Iceland was particularly high, the inflow of warm AW onto the northern shelf was also high. South of Iceland, the links between climate and zooplankton biomass are not as evident as those north of Iceland. Most probably, variability off the south and west coasts is related to the timing and magnitude of primary productivity on the banks, which, in turn, are influenced by freshwater from rivers and by wind force and direction, influencing the mixing regime and nutrient supply.

Currently, sea surface temperature values at both Siglunes and Selvogsbanki are higher than the 100-year averages for each region (Figures 5.1.4 and 5.1.5). The temperatures in both regions appear to follow a 50- to 60-year cycle.

Figure 5.1.2

Multiple-variable comparison plot (see Section 2.2.2) showing the seasonal and interannual properties of select cosampled variables at the Selvogsbanki monitoring area.

Additional variables are available online at: <http://WGZE.net/time-series>.

Selvogsbanki Transect, South Iceland

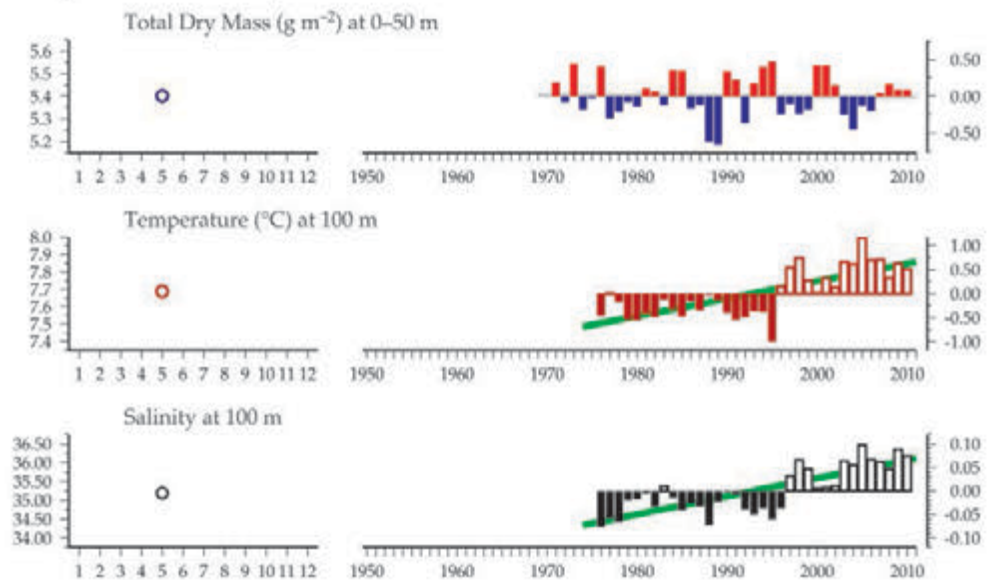


Figure 5.1.3

Multiple-variable comparison plot (see Section 2.2.2) showing the seasonal and interannual properties of select cosampled variables at the Siglunes monitoring area.

Additional variables are available online at: <http://WGZE.net/time-series>.

Siglunes Transect, North Iceland

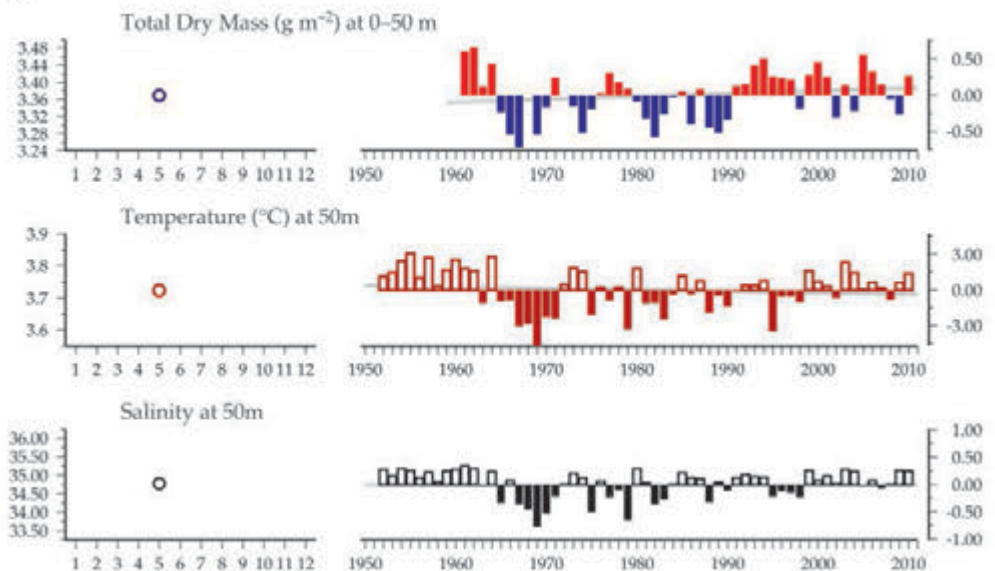


Figure 5.1.4

Regional overview plot (see Section 2.2.3) showing long-term sea surface temperatures and wind speeds in the general region surrounding the Selvogsbanki transect monitoring area, along with data from the adjacent CPR A06 Standard Area.

50-year trends in the Selvogsbanki Transect / South Iceland region

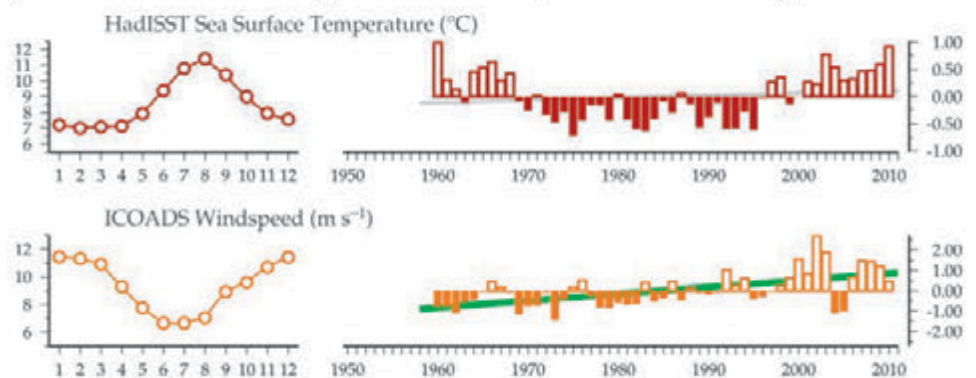


Figure 5.1.4
continued

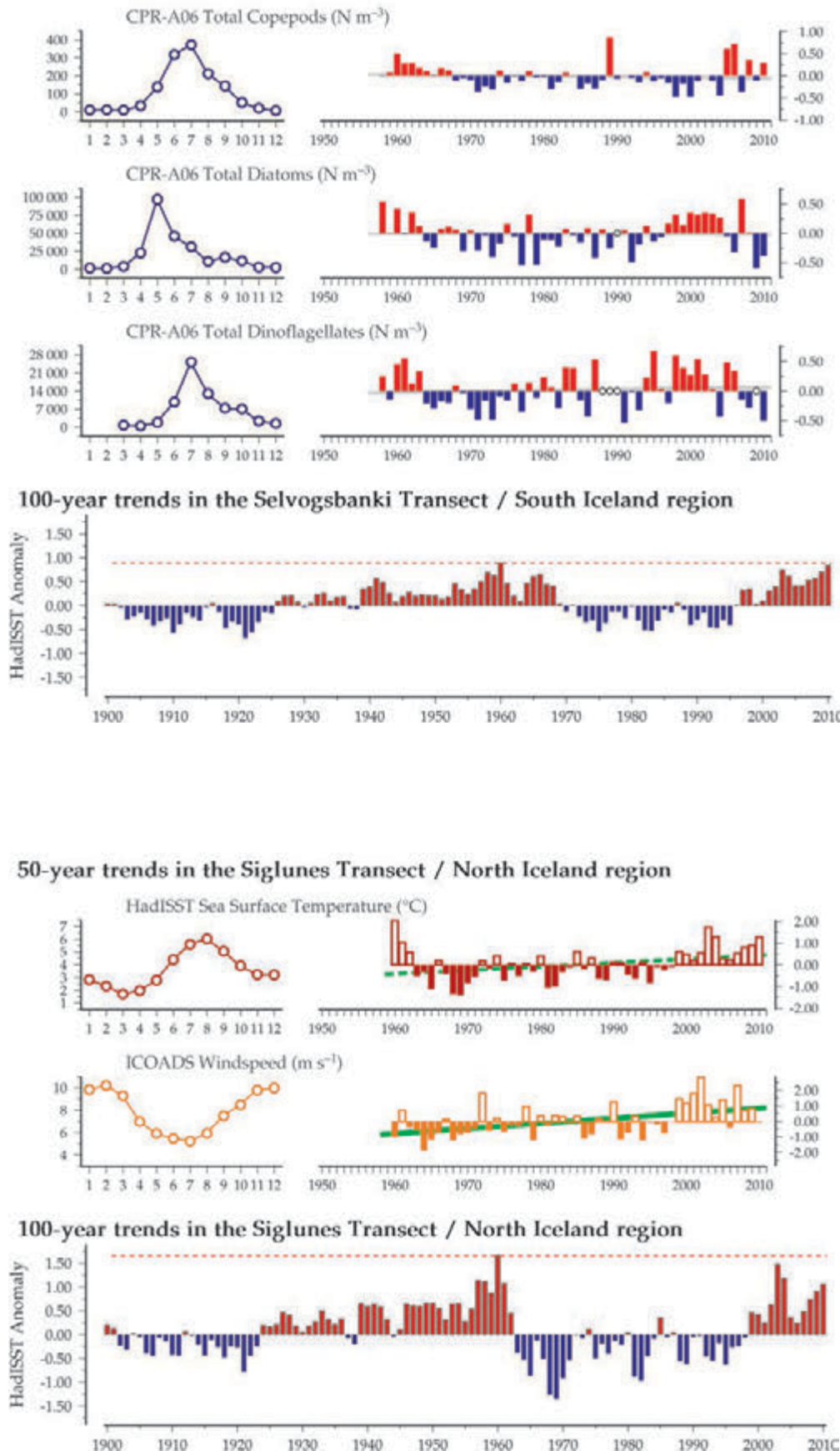
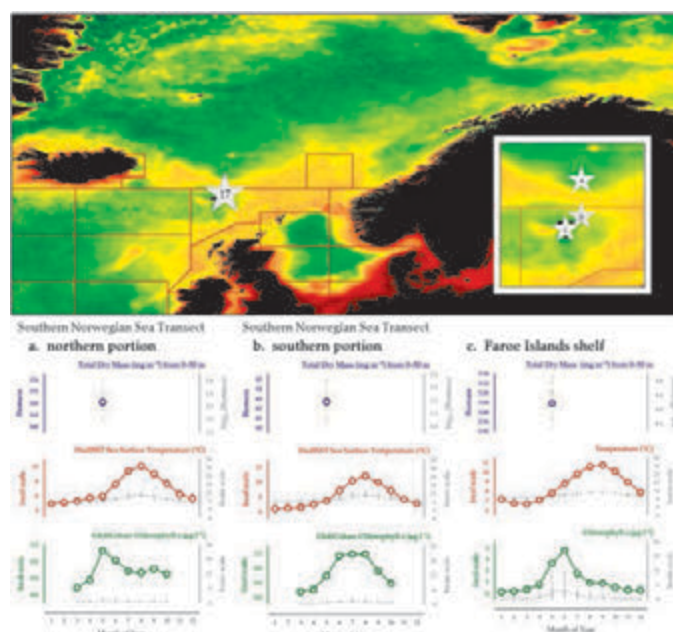


Figure 5.1.5
Regional overview plot
(see Section 2.2.3) showing
long-term sea surface
temperatures and wind
speeds in the general region
surrounding the Siglunes
transect monitoring area.

5.2 Faroe Islands (Site 17)

Eilif Gaard and Hogni Debes

Figure 5.2.1
Location of the Faroe Islands (Site 17) zooplankton monitoring areas, plotted on a map of average chlorophyll concentration, and their corresponding environmental summary plots (see Section 2.2.1).



The Faroe Marine Research Institute (FAMRI) operates a standard transect running from the Faroe Shelf into the southern part of the Norwegian Sea (Figure 5.2.1). FAMRI also operates monitoring on the Faroe Shelf. This section summarizes zooplankton monitoring along the northern and southern portions of the southern Norwegian Sea transect and the Faroe Shelf region.

Southern Norwegian Sea

Zooplankton are collected annually (May 1990–2010) using a WP-2 net (56 cm diameter, 200 μ m mesh) and vertical hauls from a depth of 50 m to the surface. The transect contains 14 stations, 10 nautical miles apart, crossing between two major water bodies. The southern portion of the transect is located in warm Atlantic Water (AW) flowing from the west–southwest, whereas the northern portion is located in cold East Icelandic Water (EIW) flowing from the northwest. In most years, the zooplankton samples were collected close to the phytoplankton spring bloom. *Calanus finmarchicus* is the dominant species in both water masses. Until the early 2000s, biomass was clearly higher in the cold-water mass in the northern portion than in the warmer southern portion. However, since around 2004–2005, this pattern has changed.

The reason for the usually higher biomass in the northern portion in previous years was a higher abundance of overwintering *C. finmarchicus* (CV and adults) (Figures 5.2.2 and 5.2.4), combined with the presence of *Calanus hyperboreus*. In the AW, fewer large individuals, but larger numbers of small stages, were present in May. Due to an earlier start of reproduction in the southern portion prior to 2004, total numbers of *C. finmarchicus* were, on average, usually higher in the AW than in the EIW, despite the lower biomass.

However, since 2003, the abundance of young *C. finmarchicus* copepodite stages in May in the northern portion of the transect has increased significantly, and now no clear differences are evident in the *C. finmarchicus* stage composition in these two water masses (Figure 5.2.4). This indicates earlier reproduction in the EIW in recent years (i.e. since 2003) than in previous years. Thus, in May 1990–2002, the fraction of *C. finmarchicus* recruits in this water mass was only ~10%; in 2003, it increased to ~45% and, since 2004, it has been 75–80%. Another change is that, since 2003, practically no *C. hyperboreus* have been found in the northern portion of the transect. These large copepods were quite plentiful in the first years of the time-series and had a substantial effect on the biomass.

Lower temperatures in the northern portion of the transect (Figure 5.2.4, lower-left subpanel) may explain the generally later *C. finmarchicus* reproduction, compared with the southern portion, in previous years. The difference does not seem to be explained by phytoplankton abundance because chlorophyll *a* concentrations in most years were higher in the cold EIW than in the warmer AW (Figure 5.2.4, lower-right subpanel).

For the time being, it is difficult to identify a cause for the apparently early reproduction of *C. finmarchicus* and for the disappearance of *C. hyperboreus* in the EIW in 2003–2010, compared with previous years in the time-series. Potential weakening of the East Icelandic Current or temperature changes of the EIW (or a combination of both) might explain this change.

Southern Norwegian Sea Transect (northern portion)

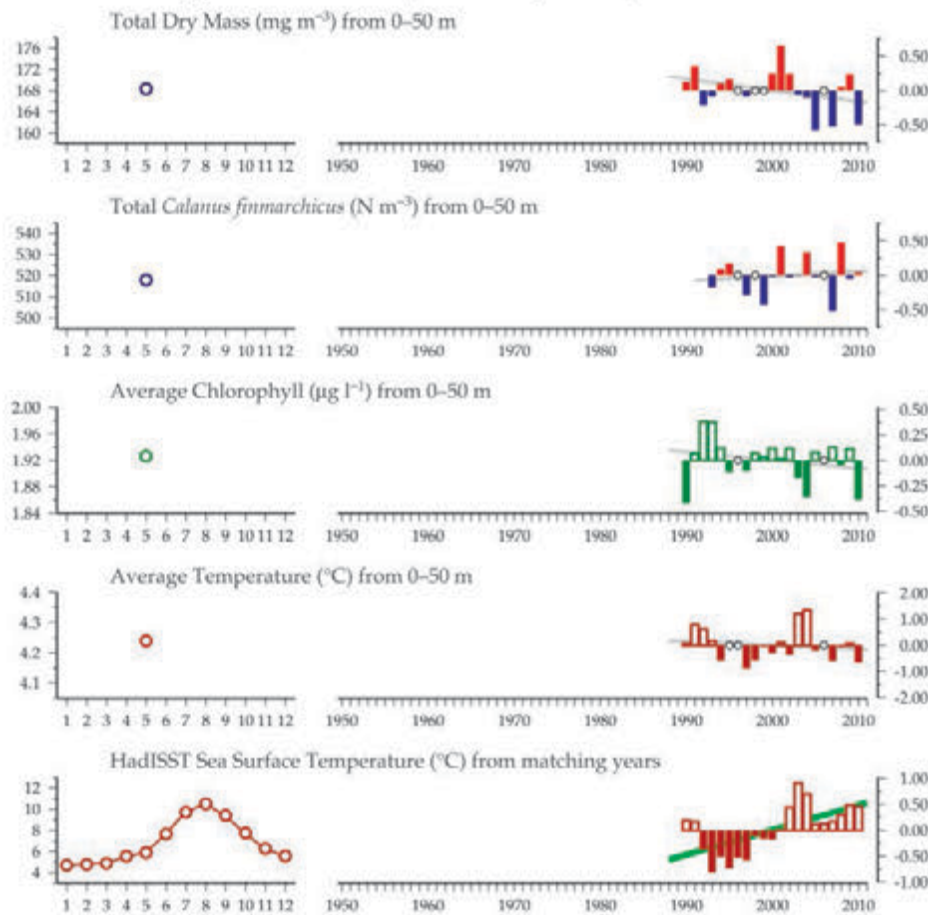


Figure 5.2.2
Multiple-variable comparison plot (see Section 2.2.2) showing the seasonal and interannual properties of select cosampled variables at the southern Norwegian sea transect (northern portion) monitoring area.

Additional variables are available online at: <http://WGZE.net/time-series>.

Southern Norwegian Sea Transect (southern portion)

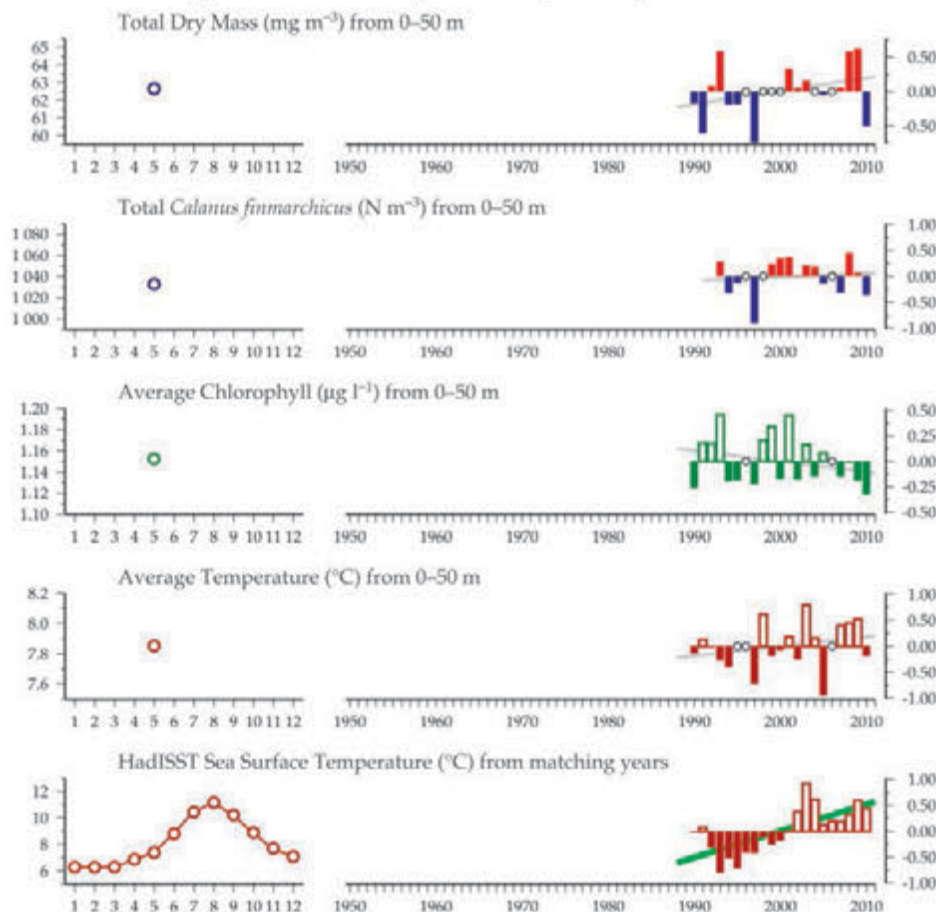
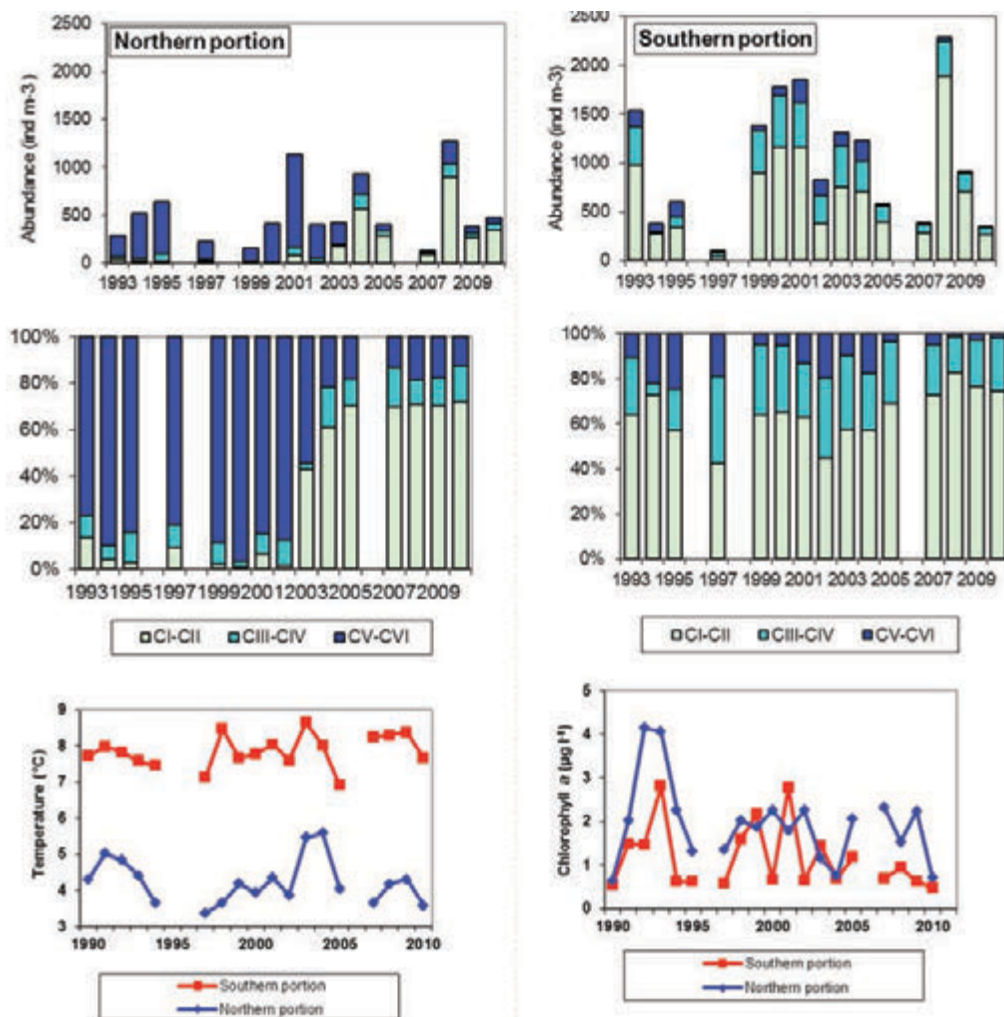


Figure 5.2.3
Multiple-variable comparison plot (see Section 2.2.2) showing the seasonal and interannual properties of select cosampled variables at the southern Norwegian sea transect (southern portion) monitoring area.

Additional variables are available online at: <http://WGZE.net/time-series>.

Figure 5.2.4
Mean abundance of *Calanus finmarchicus* copepodite stages in East Icelandic Water (northern portion of the transect) and in Atlantic Water (southern portion of the transect) in May. Corresponding average temperature and chlorophyll values are plotted in the lower panels.



On the Faroe Shelf, strong tidal currents mix the shelf water very efficiently and result in a homogeneous water mass in the shallow shelf areas. The well-mixed shelf water is separated relatively well from the offshore water by a persistent shelf front that circles the islands at a depth of ca. 100–130 m. In addition, residual currents have a persistent clockwise circulation around the islands. The shelf front provides a reasonable, although variable, degree of isolation between the “onshelf” and “offshelf” areas. This allows the onshelf areas to support a relatively uniform shelf ecosystem that, in many ways, is distinct from offshelf waters.

Although the zooplankton community outside the shelf front (“offshelf”) is dominated by the copepod *C. finmarchicus*, the onshelf zooplankton community is basically neritic, with variable abundance of *C. finmarchicus*. During spring and summer, the zooplankton in the shelf water is usually dominated by *Temora longicornis* and *Acartia longiremis*. *C. finmarchicus* is advected onto the shelf from the surrounding oceanic environment and occurs in the shelf water in interannually variable abundance, which is usually highest in spring and early summer. Meroplanktonic larvae (mainly cirripedia larvae) may also be abundant, and decapod larvae and fish larvae and juveniles are common on the shelf during spring and summer.

In most years, zooplankton summer biomass on the Faroe Shelf is low, and is clearly lower than in the surrounding oceanic environment. This is explained by the higher abundance of *C. finmarchicus* offshelf. This species is much larger than the neritic species and, therefore, strongly affects the total zooplankton biomass (Figure 5.2.5). Owing to the interannually variable abundance of *C. finmarchicus* onshelf, biomass on the shelf is also more variable than that in the surrounding oceanic environment; this is probably the result of the variable amounts of advection onto the shelf.

In 2006–2010, zooplankton biomass on the shelf and in the surrounding offshelf oceanic water was higher than in previous years. This seems to be mainly the result of a higher abundance of *C. finmarchicus* in late copepodite stages (CIV and CV) in both water masses, compared with the dominance of younger stages in the previous years, indicating phenological variability or change.

Another trend in shelf zooplankton is a marked increase in abundance of *T. longicornis*. During 1993–2009, there was a gradual tenfold increase in abundance of *T. longicornis* on the shelf in midsummer; in 2010, the species increased in abundance by a factor of 10 compared to 2009 (Figure 5.2.5).

Faroe Islands Shelf

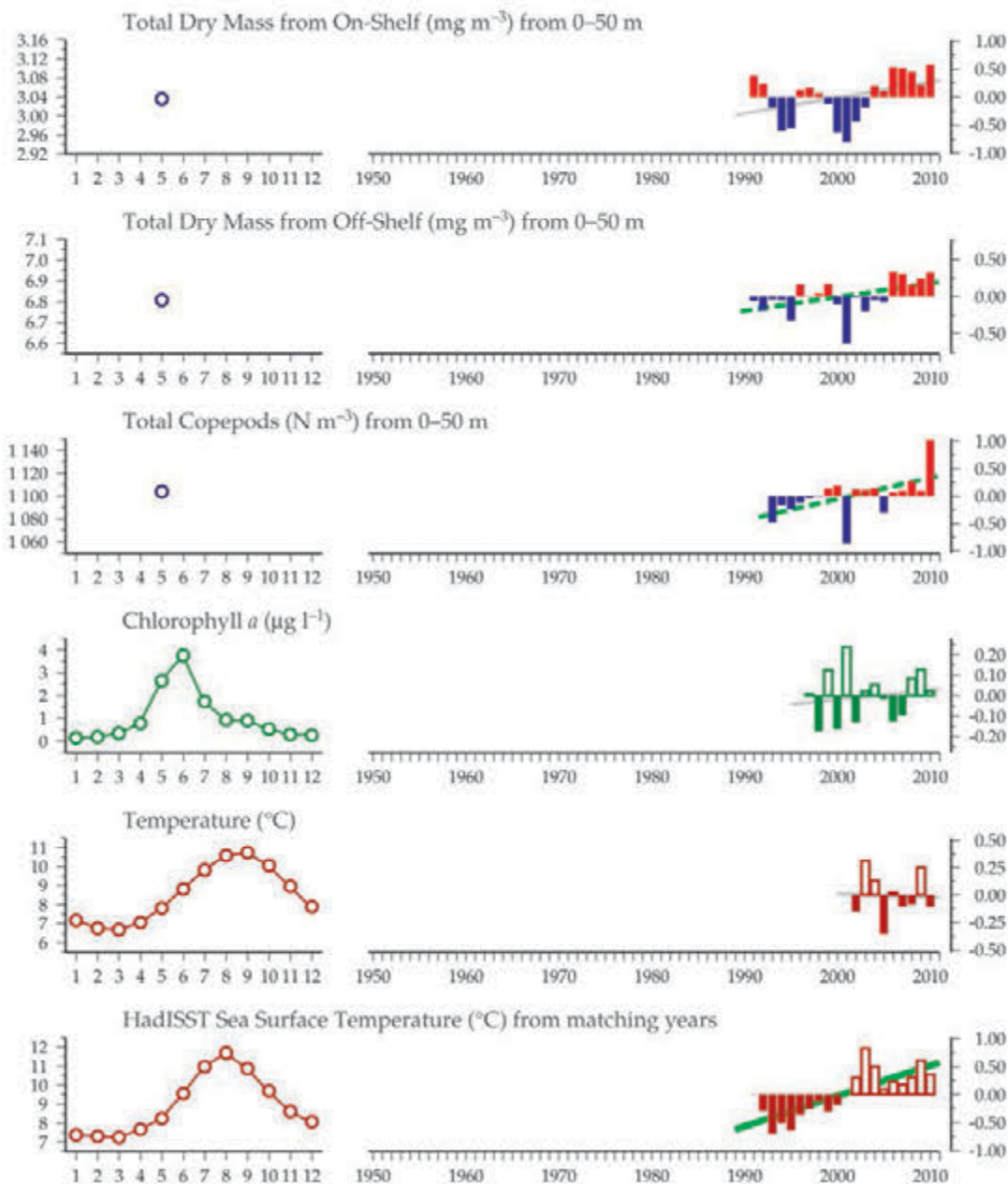


Figure 5.2.5
Multiple-variable comparison plot (see Section 2.2.2) showing the seasonal and interannual properties of select cosampled variables at the Faroe Islands shelf monitoring area.

Additional variables are available online at: <http://WGZE.net/time-series>.

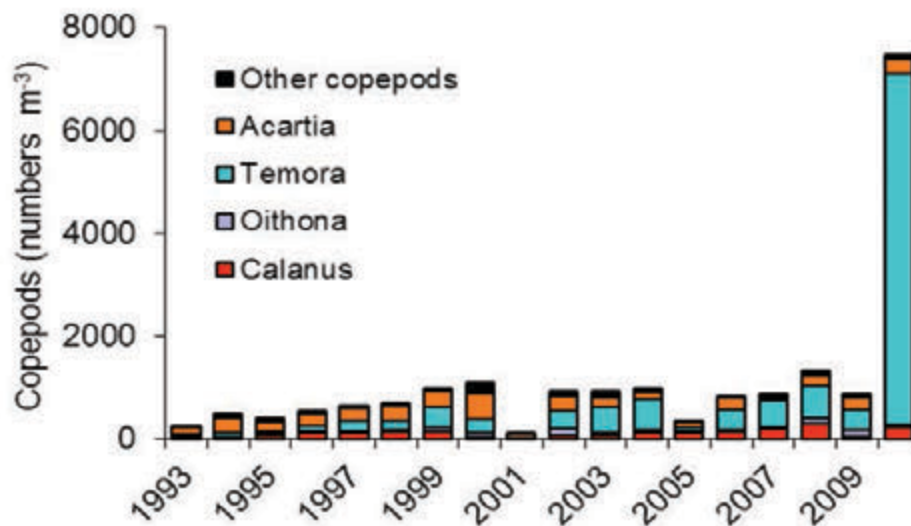
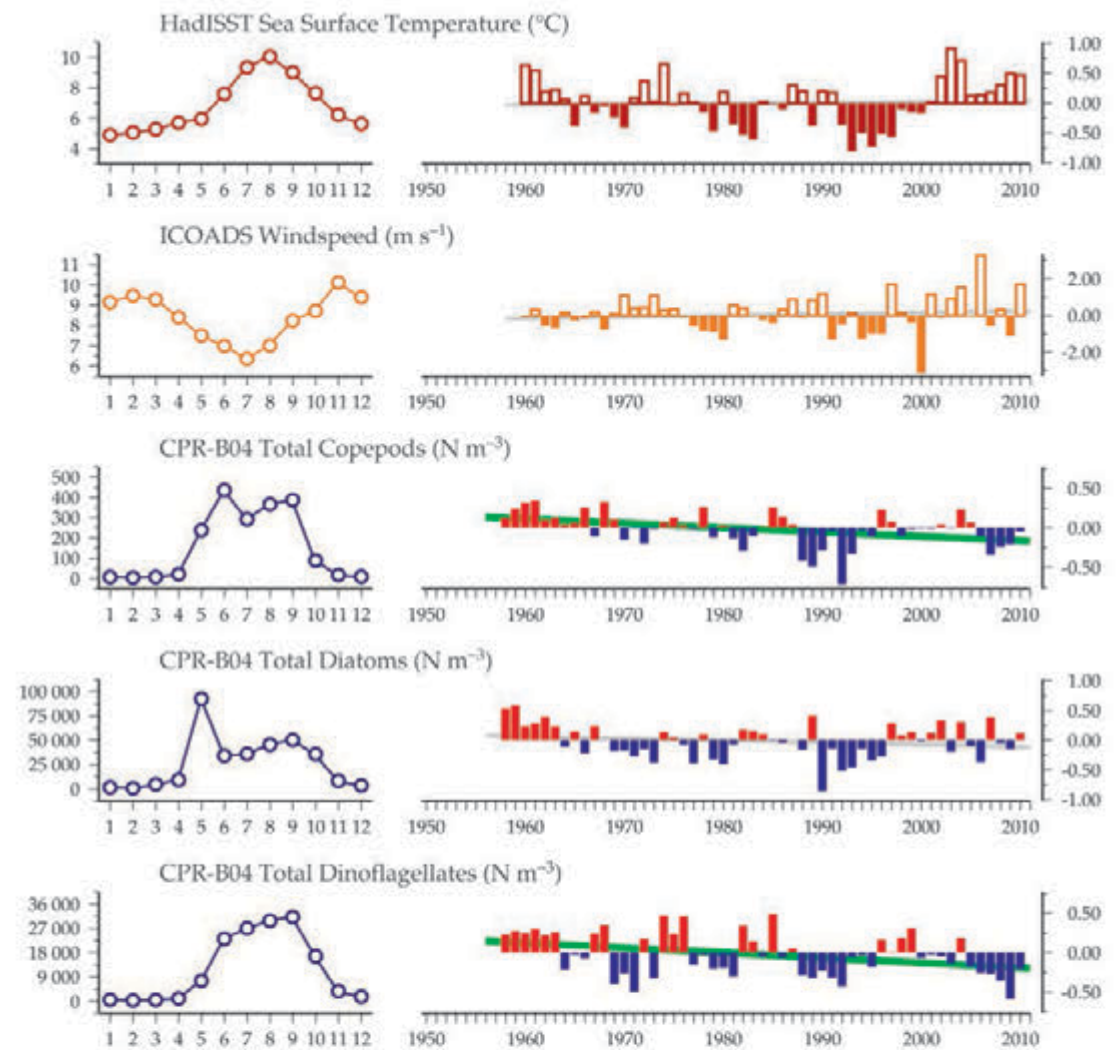


Figure 5.2.6
Mean abundance of copepods on the Faroe Shelf in late June.

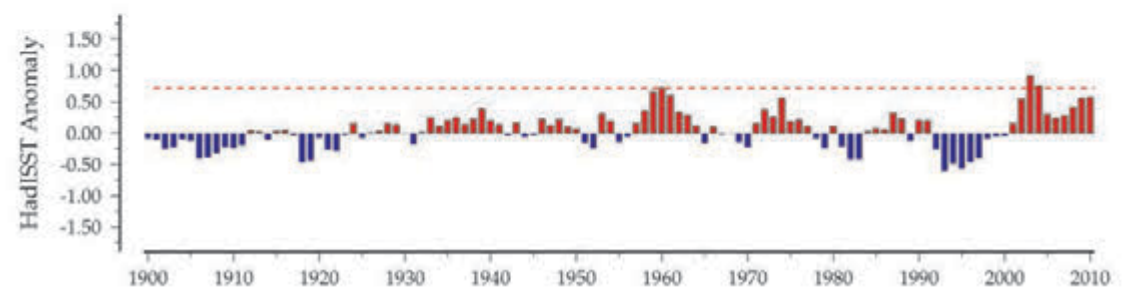
Figure 5.2.7

Regional overview plot
(see Section 2.2.3) showing
long-term sea surface
temperatures and wind
speeds in the general region
surrounding the Faroe
Islands monitoring area.

50-year trends in the Faroe Islands / southern Norwegian Sea region



100-year trends in the Faroe Islands / southern Norwegian Sea region



5.3 Svinøy Transect (Site 18)

Webjørn Melle and Cecilie Broms

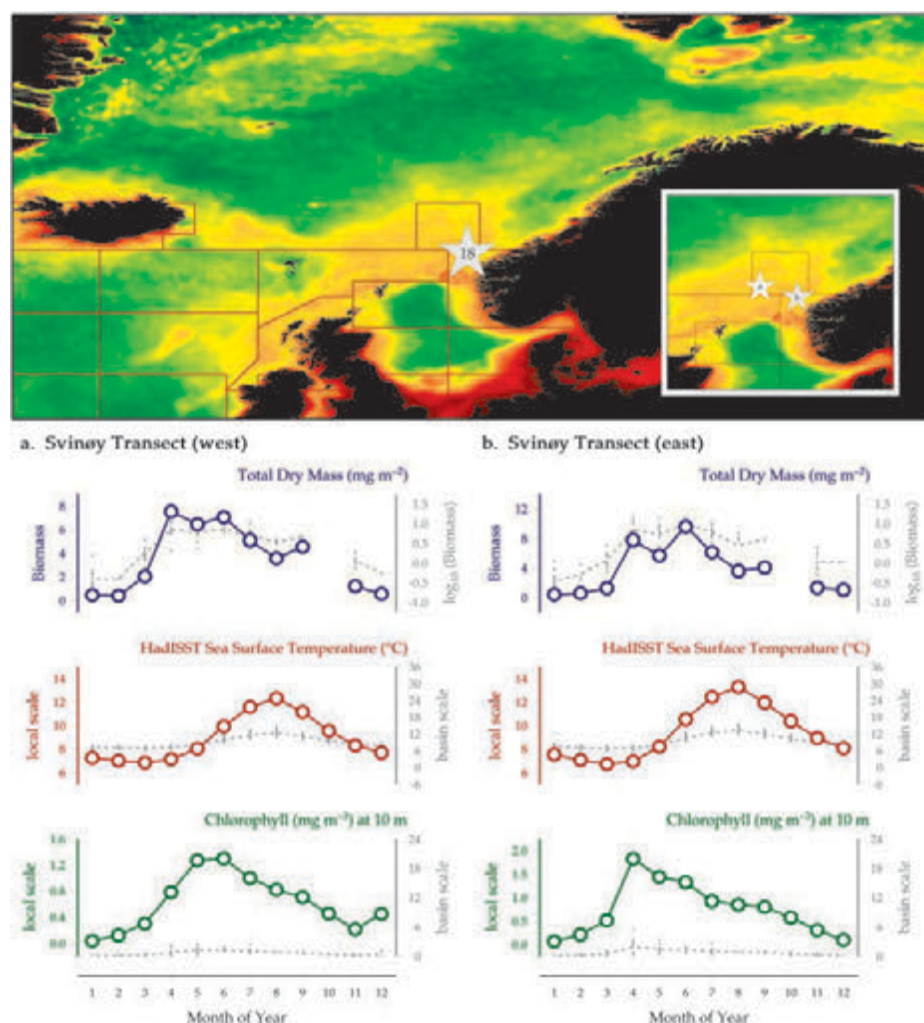


Figure 5.3.1
Location of the Svinøy transect (Site 18) zooplankton monitoring area, plotted on a map of average chlorophyll concentration, and its corresponding environmental summary plots (see Section 2.2.1).

The Institute of Marine Research (IMR) Monitoring Programme samples two fixed transects in the Norwegian Sea: the 15-station Svinøy transect (see Figure 5.3.1, Site 18) and the 10-station Gimsøy transect (not shown). For mesozooplankton, the transects are, by default, sampled four times each year with a WP-2 net (56 cm diameter, 180 µm mesh) from a 200 m depth to the surface. Additionally, the Norwegian Sea is surveyed in May and July/August, both surveys covering approximately 50–100 stations. Data are stored in the local database at IMR, with annual reports made to the Ministry of Fisheries and in the IMR Annual Report on Marine Ecosystems. For the present report, the Svinøy transect is split into two sections called West and East. The western part is generally stations located in Atlantic water, while the eastern part mostly covers coastal water on the shallow shelf.

Seasonal and interannual trends (Figure 5.3.2)

The dominant contributor to mesozooplankton biomass of the southern Norwegian Sea is *Calanus finmarchicus* (Melle *et al.*, 2004). In the Atlantic Water and coastal water,

seasonal dynamics of the species is closely related to the phytoplankton development. There is a tendency for the earlier production of this species in coastal water compared to Atlantic water (Broms and Melle, 2007; Broms *et al.*, 2009; Bagøien *et al.*, 2012). Although *C. finmarchicus* is the dominant species, this difference in timing is not revealed in the seasonal cycles of total zooplankton biomass in the eastern and western parts of the Svinøy section. However, the increase in chlorophyll occurs, on average, as much as one month earlier in the east than the west. The development (timing) of zooplankton biomass in spring at the Svinøy transect does not indicate any shifts in seasonality over the sampling period 1997–2007.

Water temperatures along the Svinøy transect range from 5 to 15°C, with the seasonal high in August and the seasonal low in March/April. A chlorophyll bloom occurs in late April and early May, with a slightly stronger bloom in May along the eastern side of the transect. A protracted post-bloom period persists throughout summer and early autumn along the transect, which is typical for the southern Norwegian Sea.

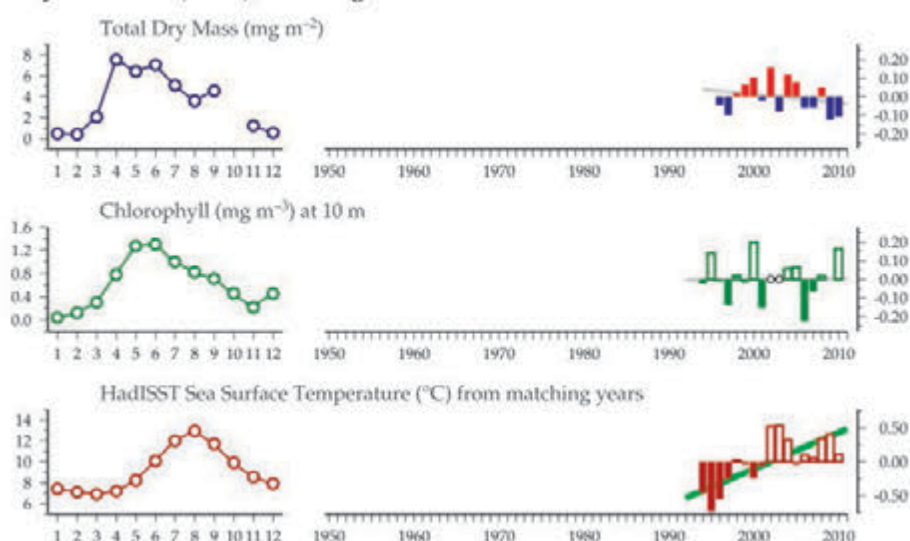
For the duration of the time-series, chlorophyll concentrations in the eastern part of the transect demonstrate a downward trend, whereas water temperatures have been increasing during the same period in both the east and the west. Chlorophyll concentrations in the western part do not show any trend over the sampling period. Both parts of the transect are currently in a period of lower-than-average biomass, a trend coherent with other zooplankton biomass data from the Norwegian Sea. The downward trend in zooplankton biomass may have leveled off in the east. Zooplankton biomass appears to be positively correlated with chlorophyll (in the east) and negatively correlated with temperature during this period.

The nearest CPR standard area is "B01". Interannual trends within CPR copepod abundance correspond fairly well to zooplankton biomass in both the western and eastern (Figure 5.3.3) sections of the Svinøy transect. Long-term SST values along the transect demonstrate that water temperatures since 2000 have been frequently equal to or greater than any seen in the previous 100 years (Figure 5.3.3, red dashed line).

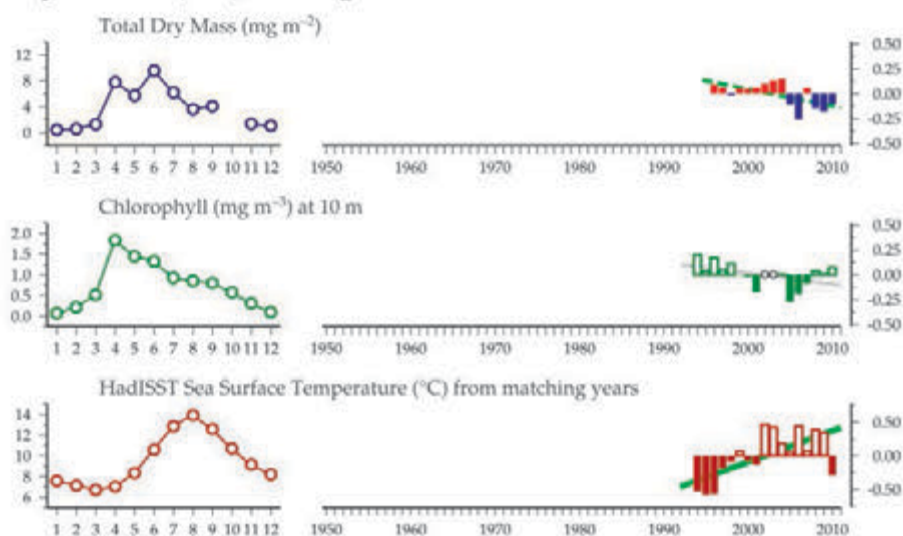
Figure 5.3.2
Multiple-variable
comparison plot (see
Section 2.2.2) showing
the seasonal and inter-
annual properties of select
cosampled variables along
the Svinøy transect.

Additional variables are
available online at: <http://WGZE.net/time-series>.

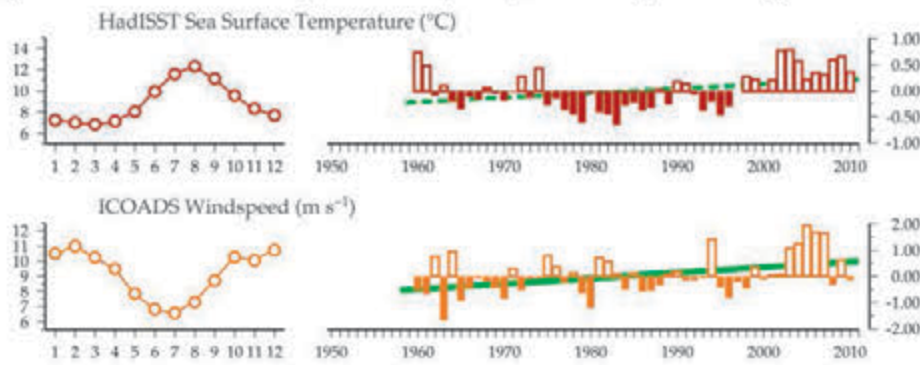
Svinøy Transect (west), Norwegian Sea



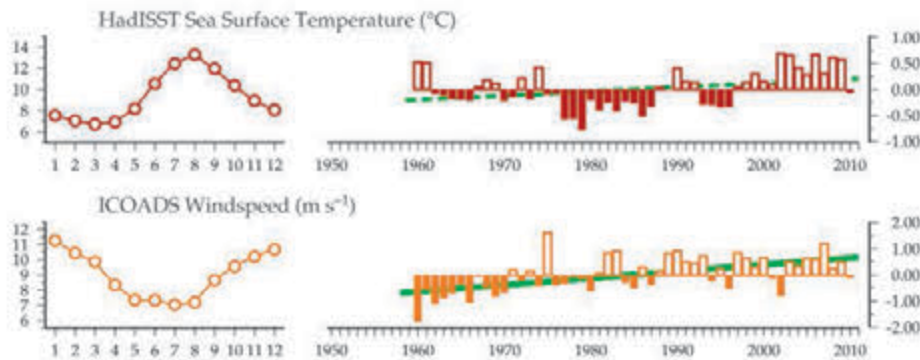
Svinøy Transect (east), Norwegian Sea



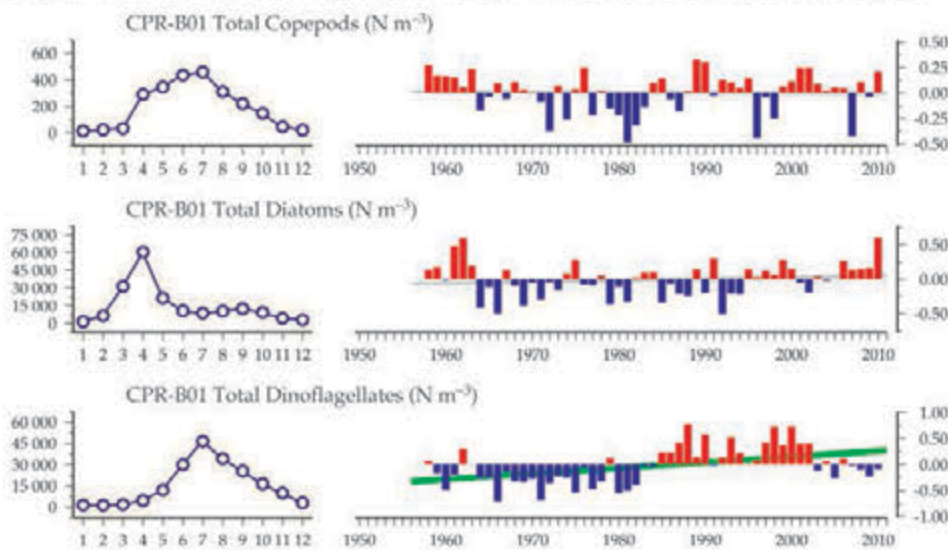
50-year trends in the Svinøy Transect (west) / Norwegian Sea region



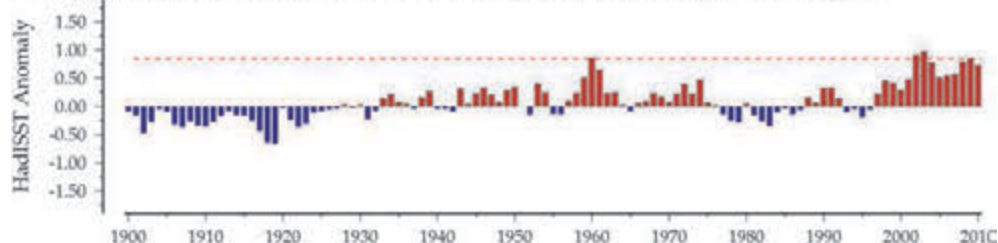
100-year trends in the Svinøy Transect (west) / Norwegian Sea region



50-year CPR trends in the general Svinøy Transect / Norwegian Sea region



100-year trends in the Svinøy Transect (west) / Norwegian Sea region



100-year trends in the Svinøy Transect (east) / Norwegian Sea region

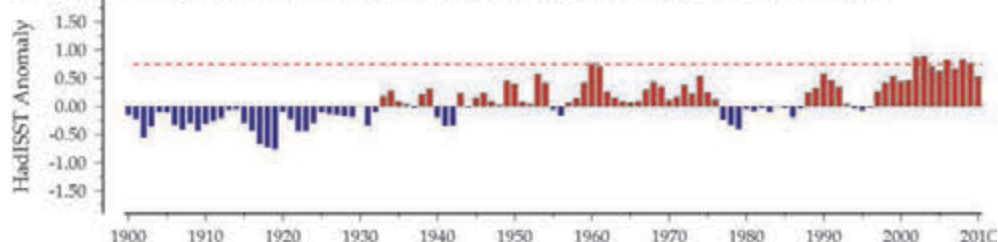


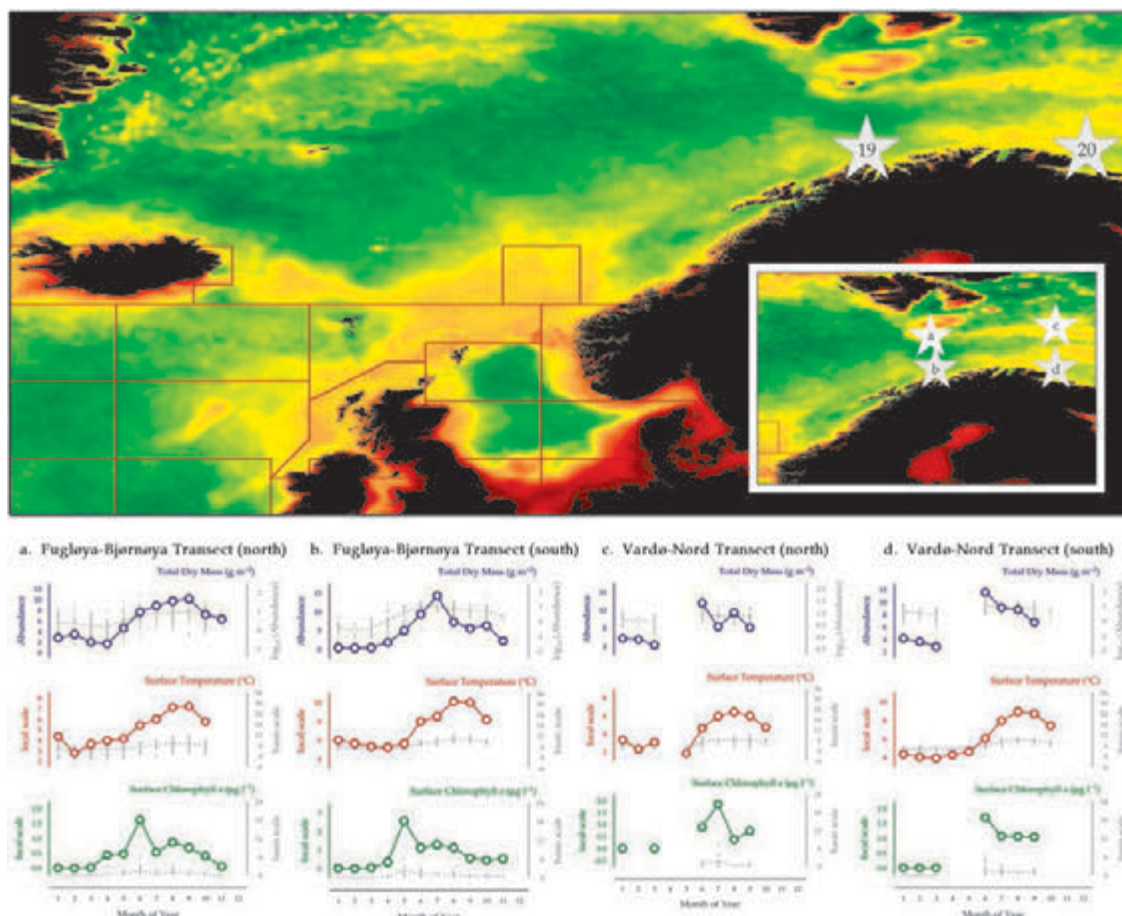
Figure 5.3.3
Regional overview plot (see Section 2.2.3) showing long-term sea surface temperatures and wind speeds in the general region surrounding the Svinøy transect, along with data from the adjacent CPR B01 Standard Area.

5.4 Fugløya–Bjørnøya and Vardø–Nord Transects (Sites 19–20)

Padmini Dalpadado

Figure 5.4.1

Location of the Fugløya–Bjørnøya and Vardø–Nord transects (Sites 19 and 20) zooplankton monitoring areas, plotted on a map of average chlorophyll concentration, and their corresponding environmental summary plots (see Section 2.2.1).



The Norwegian Institute of Marine Research (IMR) Monitoring Programme samples two standard sections in the Barents Sea: the Fugløya–Bjørnøya (FB) transect (Figure 5.4.1, Site 19) and the Vardø–Nord (VN) transect (Figure 5.4.1, Site 20). In addition, the Barents Sea is surveyed in August–September on a basin scale. Data are held within local databases at the IMR, and annual reports are made to the Ministry of Fisheries, in the IMR Annual Report on Marine Ecosystems, and in joint Norwegian/Russian reports. In this report, the FB transect is split into two sections, north ($>72.00^{\circ}\text{N}$) and south ($>72.00^{\circ}\text{N}$), which are each sampled up to 6 times a year with WP-2 plankton net (56 cm diameter, 180 μm mesh) from 100 m and/or from the bottom to the surface in two separate net hauls. The VN transect is also split into two sections: north ($>73.50^{\circ}\text{N}$) and south ($>73.50^{\circ}\text{N}$). The data in this report are from the bottom-to-surface hauls. The zooplankton catch of the net hauls is divided into two halves using a Motoda Splitter. One half is fixed in buffered 4% formaldehyde for subsequent taxonomical analyses and the other half is dried and weighed for dry weight determination. In addition, temperature, salinity, nutrients, and chlorophyll are measured at all sampling stations.

Seasonal and interannual trends along the Fugløya–Bjørnøya transect (Figures 5.4.2–5.4.4)

Zooplankton biomass begins to increase in spring (March–April) in both the northern and the southern sections of the Fugløya–Bjørnøya transect. Peak zooplankton biomass is reached later in the season and extends for a longer period (June–September) in the northern section (Figure 5.4.2), while a strong June/July peak is found in the southern section (Figure 5.4.3). Zooplankton biomass has been steadily decreasing over the duration of the time-series, most noticeably in the $>2000\ \mu\text{m}$ biomass size fraction. The contribution of colder-water zooplankton species in the biomass is associated with the extent of mixing of the Atlantic and Arctic water masses within the FB section. Surface water temperatures in the northern part of the FB section range from 2 to 8°C , with a seasonal high in August–September and a seasonal low in February. In the southern part of the FB section, surface temperatures are warming, ranging from 5 to 10°C , with a seasonal low occurring later in March/April.

Long-term water temperatures along the transect reveal that these temperatures are slightly below the 100-year maximum (Figure 5.4.4, red dashed line). The 50-year trend for the northern part of the FB section shows a strong increase in surface water temperatures, while the southern

part of the section only shows a slight (non-significant) increase.

Seasonal and interannual trends along the Vardø–Nord transect (Figures 5.4.5–5.4.7)

The monthly sampling coverage for the VN transect has large periods of no sampling, making it somewhat difficult to interpret the seasonal dynamics of zooplankton and chlorophyll along the section. Zooplankton biomass along the VN section seems to begin sometime between April and June, peaking in June. Zooplankton biomass has been steadily decreasing over the duration of the time-series, most noticeably in the $>2000 \mu\text{m}$ biomass size fraction.

Lower biomass (during the past four years of sampling) and an overall decreasing trend are common among all sampling sites in the Norwegian and Barents seas. Water temperatures along the Vardø–Nord transect range from 2 to 9°C, with a seasonal high in August in both sections, and a seasonal low in March in the southern section and in April in the northern section. Water temperatures are slightly increasing in both sections and correspond to a slight decrease in both chlorophyll and zooplankton biomass. Although temperatures in the northern section are currently at or near the 100-year maximum for this region (Figure 5.4.7, red dashed line), they are significantly lower than the 100-year maximum for the southern section.

Fugløy–Bjørnøya Transect (north)

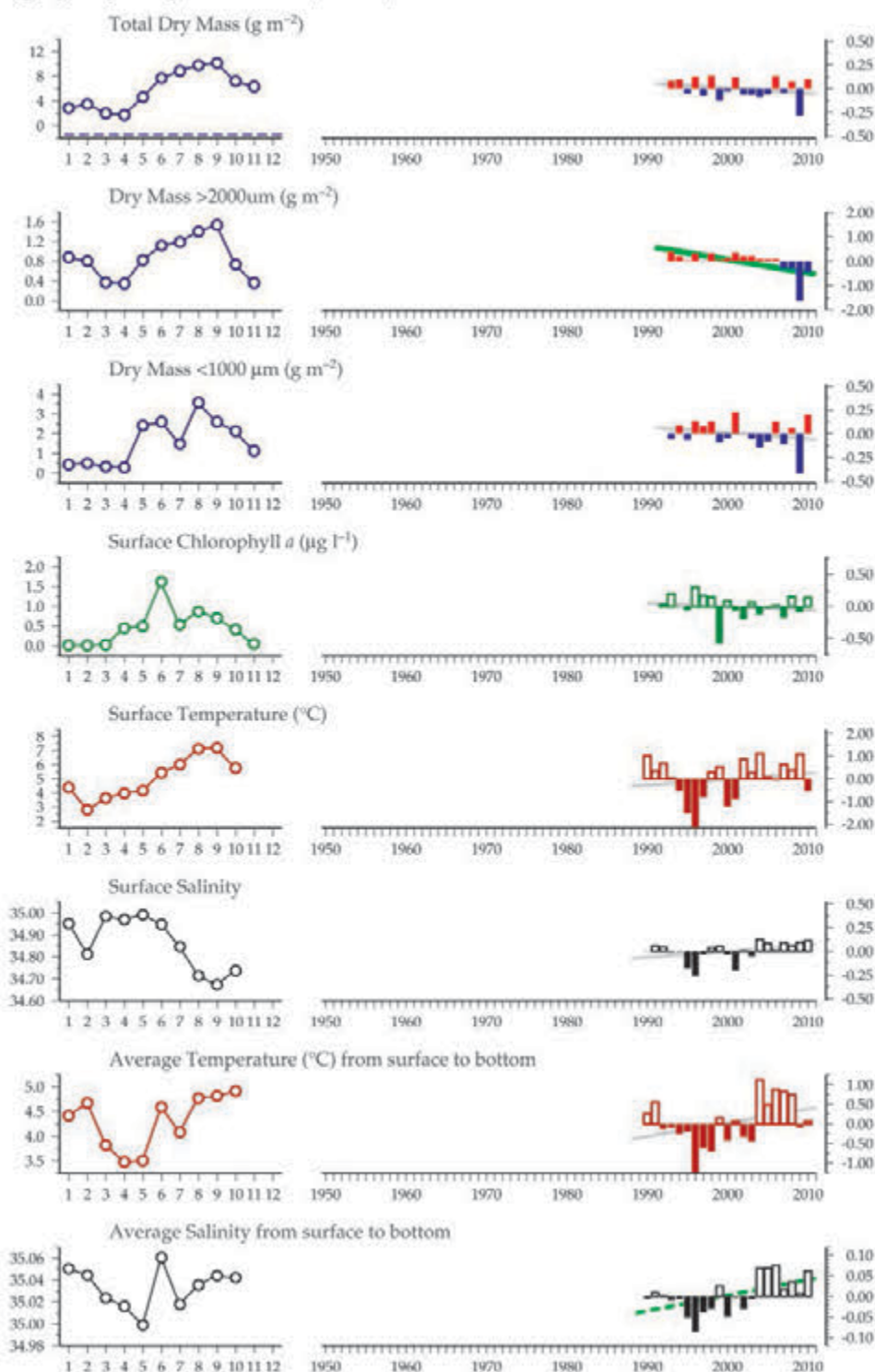


Figure 5.4.2
Multiple-variable comparison plot (see Section 2.2.2) showing the seasonal and interannual properties of select cosampled variables at the Fugløy–Bjørnøya transect (north) zooplankton monitoring site.

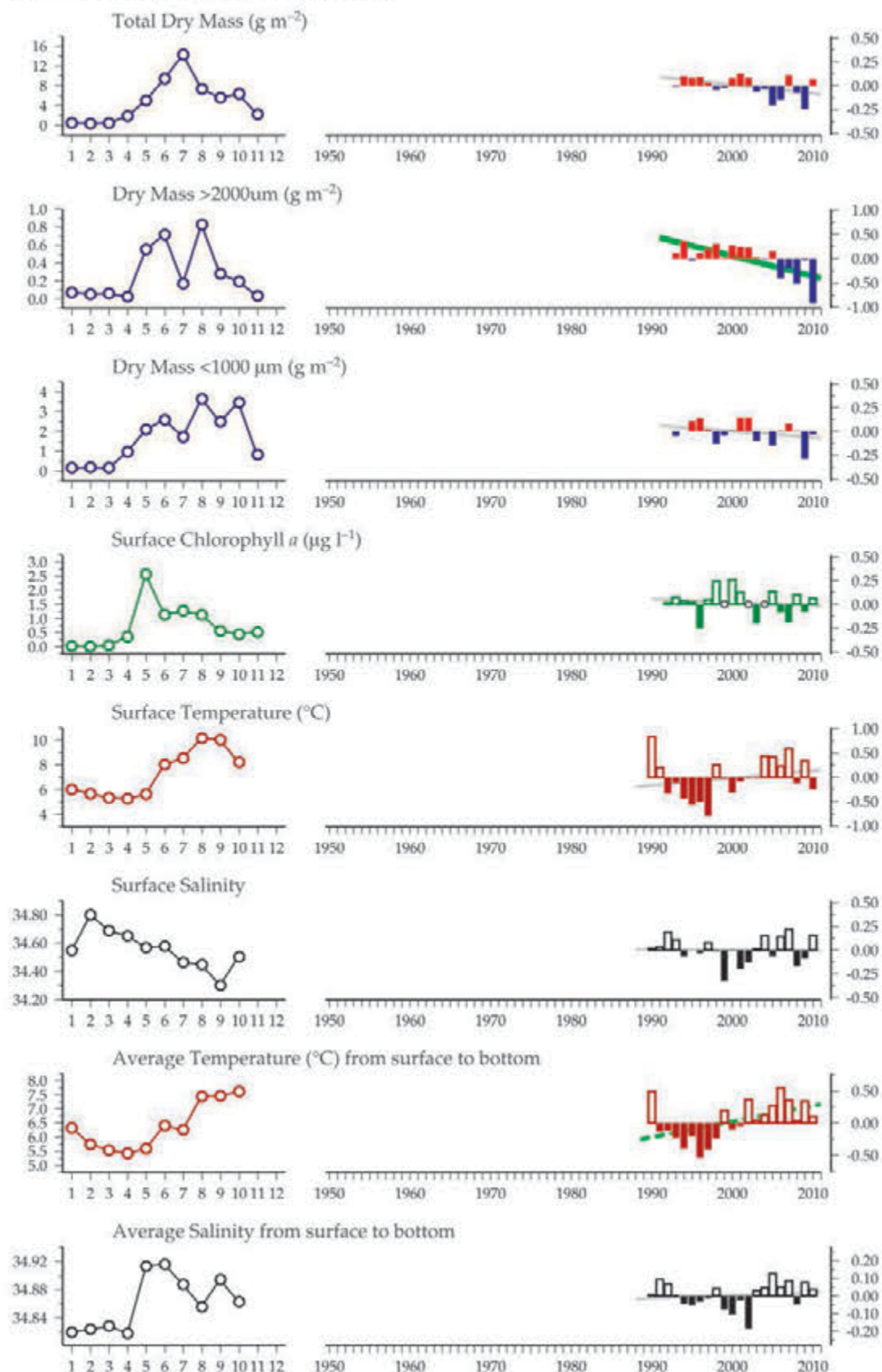
Additional variables are available online at <http://WGZE.net/time-series>.

Figure 5.4.3

Multiple-variable comparison plot (see Section 2.2.2) showing the seasonal and interannual properties of select cosampled variables at the Fugløya-Bjørnøya transect (south) zooplankton monitoring site.

Additional variables are available online at <http://WGZE.net/time-series>.

Fugløya-Bjørnøya Transect (south)



50-year trends in the Fugløya-Bjørnøya (north) / western Barents Sea region

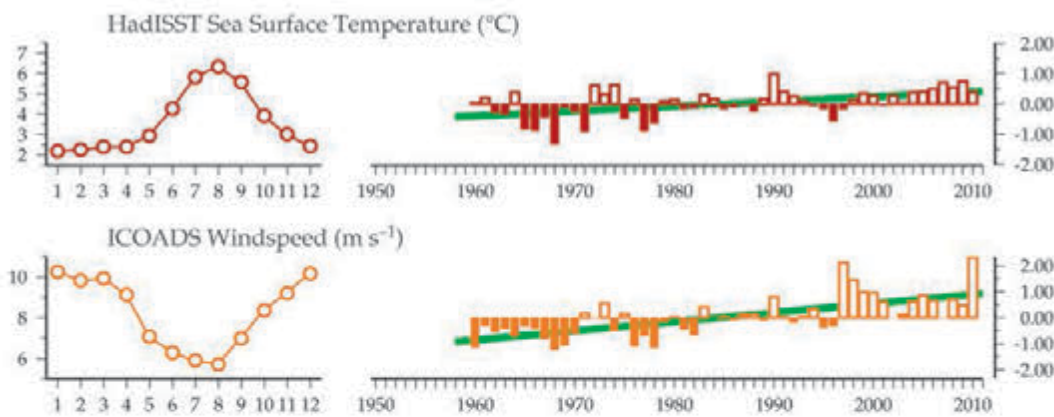
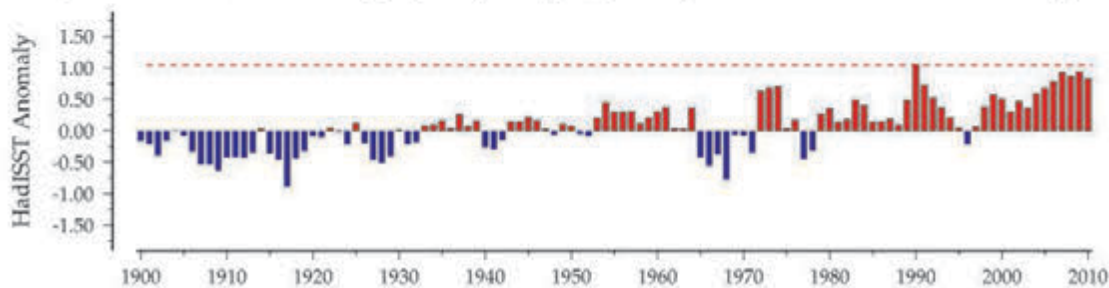
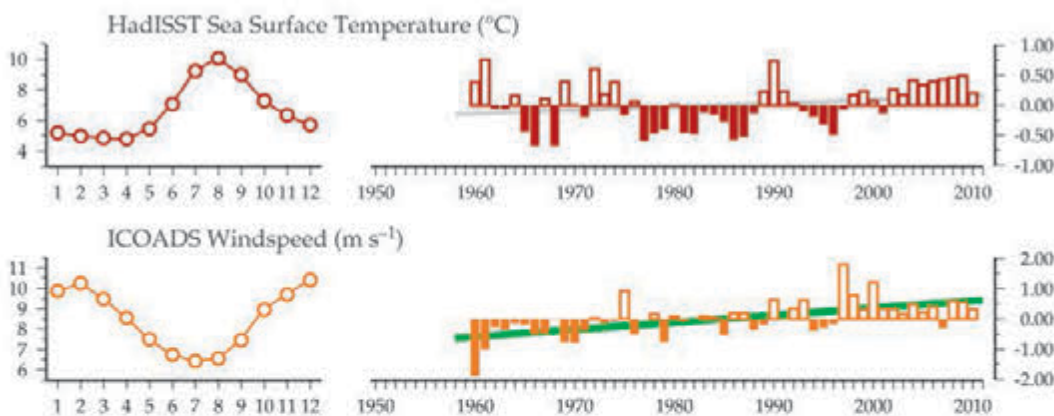


Figure 5.4.4
Regional overview plot
(see Section 2.2.3) showing
long-term sea surface
temperatures and wind
speeds in the general
region surrounding the
northern and southern
Fugløya-Bjørnøya transect
monitoring areas.

100-year trends in the Fugløya-Bjørnøya (north) / western Barents Sea region



50-year trends in the Fugløya-Bjørnøya (south) / western Barents Sea region



100-year trends in the Fugløya-Bjørnøya (south) / western Barents Sea region

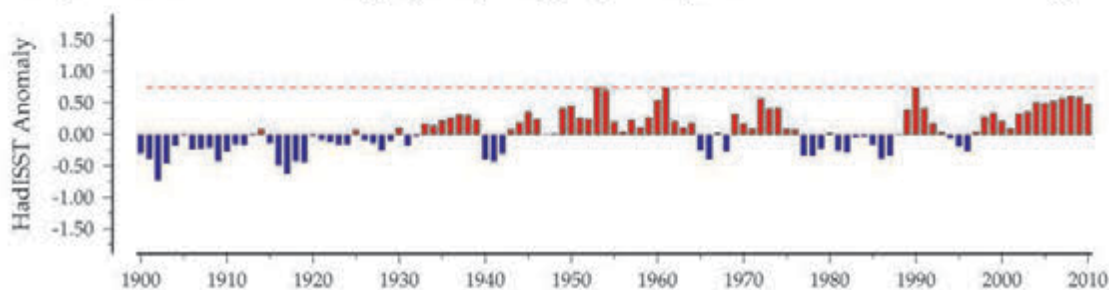
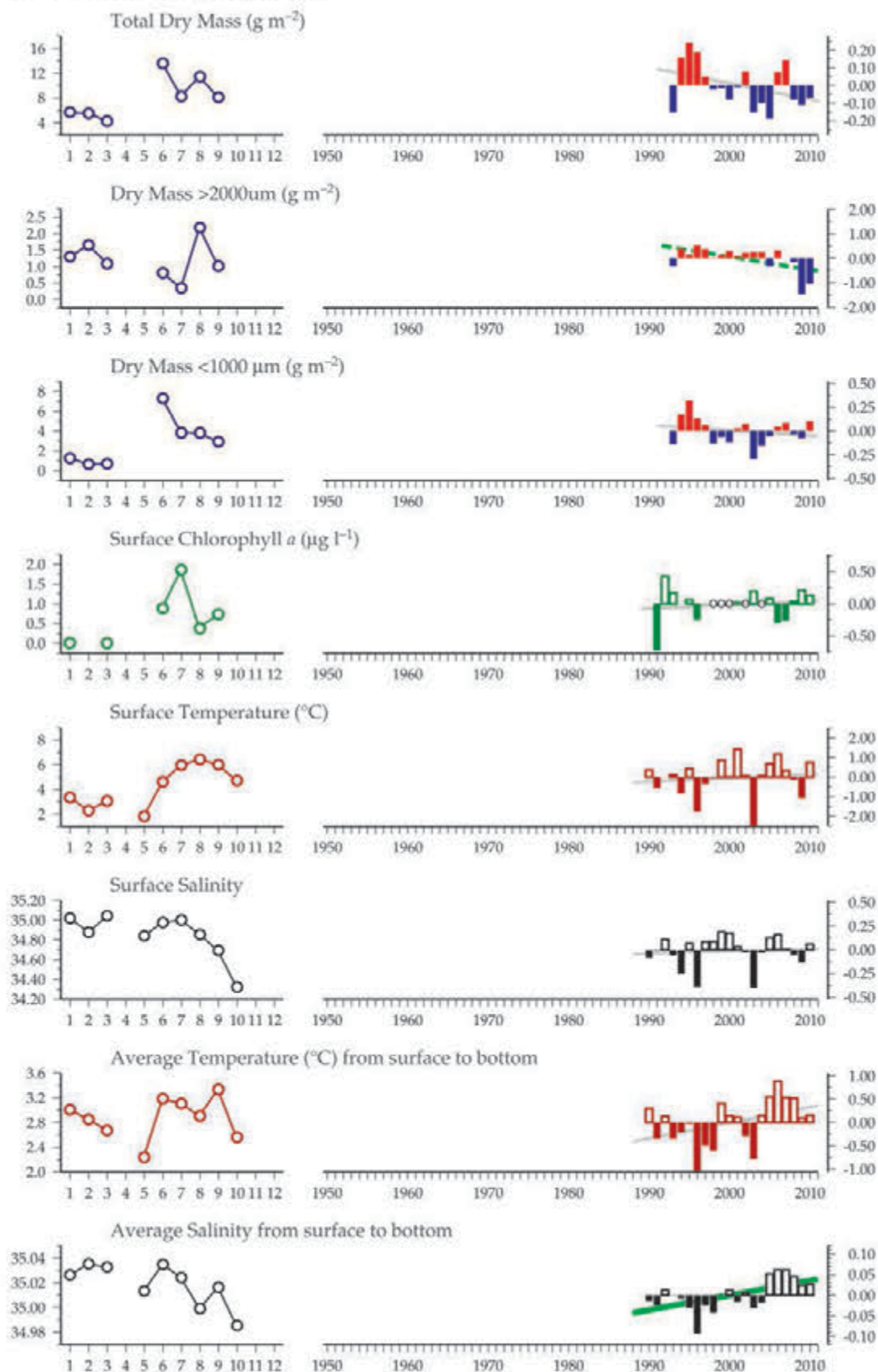


Figure 5.4.5
Multiple-variable comparison plot (see Section 2.2.2) showing the seasonal and interannual properties of select cosampled variables at the Vardø–Nord transect (north) zooplankton monitoring site.

Additional variables are available online at <http://WGZE.net/time-series>.

Vardø–Nord Transect (north)



Vardø-Nord Transect (south)

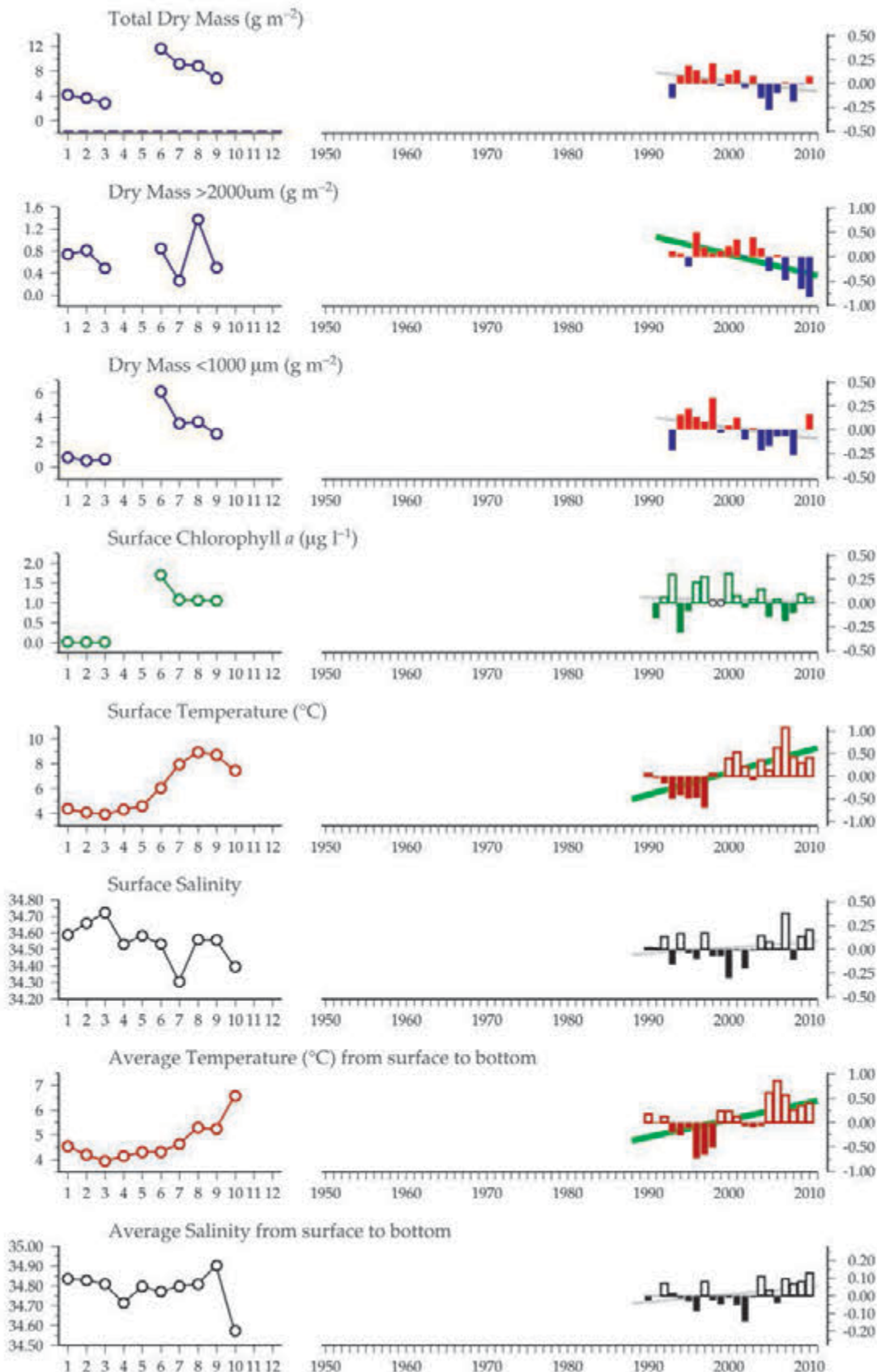
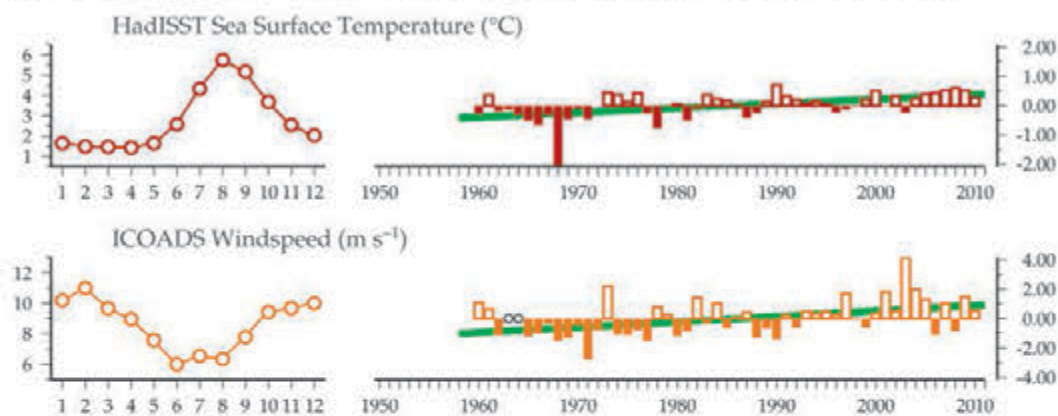


Figure 5.4.6
Multiple-variable comparison plot (see Section 2.2.2) showing the seasonal and interannual properties of select cosampled variables at the Vardø-Nord transect (south) zooplankton monitoring site.

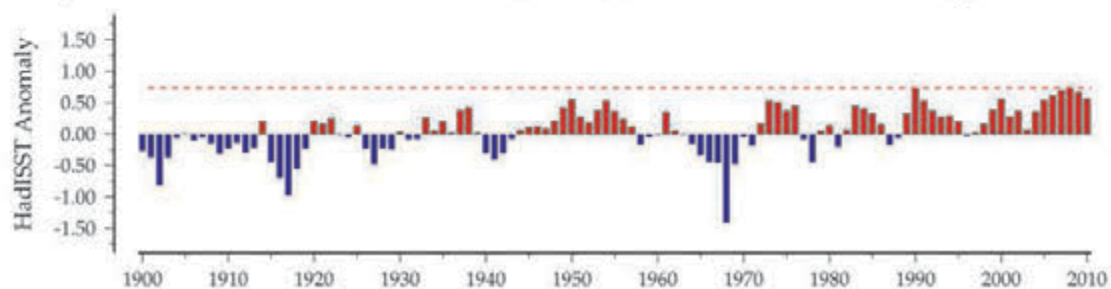
Additional variables are available online at <http://WGZE.net/time-series>.

Figure 5.4.7
Regional overview plot
(see Section 2.2.3) showing
long-term sea surface
temperatures and wind
speeds in the general region
surrounding the northern
and southern Vardø-Nord
transect monitoring areas.

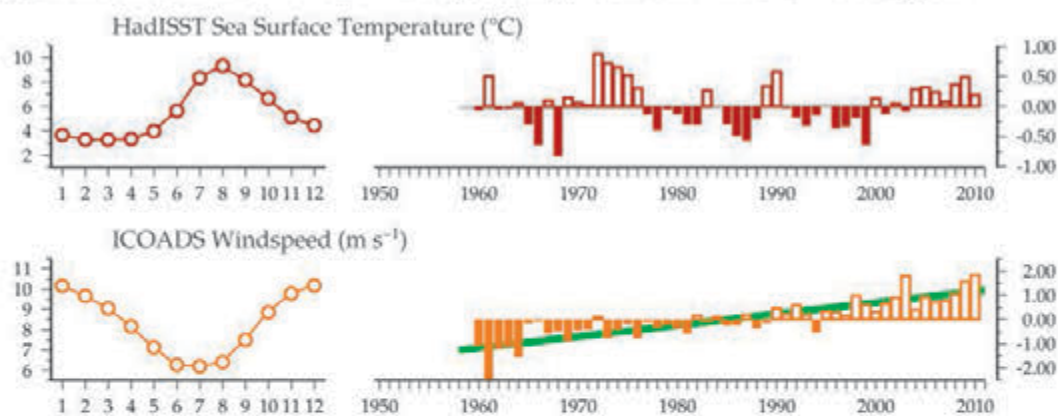
50-year trends in the Vardø-Nord (north) / central Barents Sea region



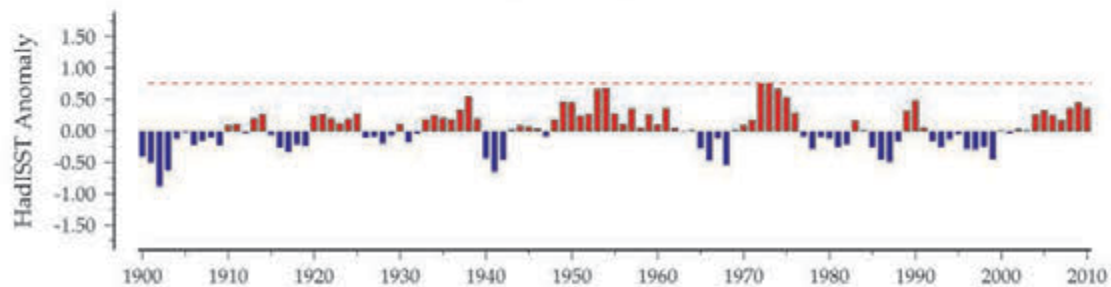
100-year trends in the Vardø-Nord (north) / central Barents Sea region



50-year trends in the Vardø-Nord (south) / central Barents Sea region



100-year trends in the Vardø-Nord (south) / central Barents Sea region





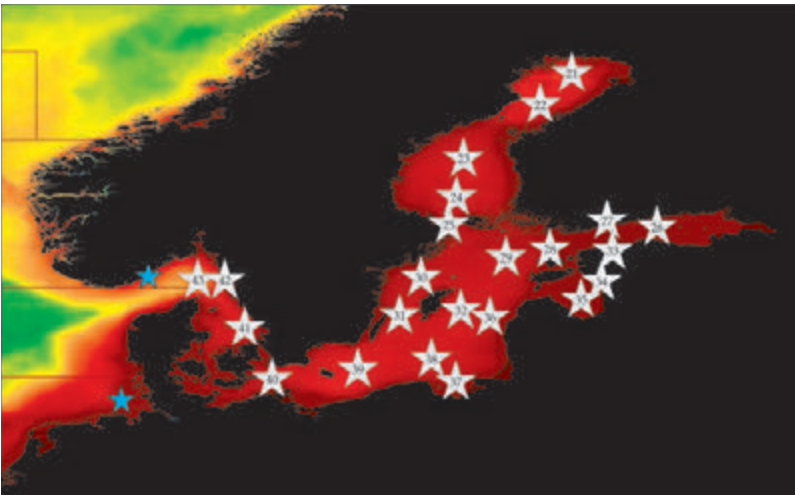
Salpa fusiformis A. Bode (IEO-A Coruña)

6Z OOPLANKTON OF THE BALTIC SEA

Maiju Lehtiniemi, Lutz Postel, Piotr Margonski, Arno Põllumäe, Maria Põllupüü, Mart Simm, Anda Ikauniece, Gunta Rubene, Solvita Strake, Norbert Wasmund, Lars Johan Hansson, and Marie Johansen

Figure 6.0
Locations of Baltic Sea zooplankton monitoring areas (Sites 21–43) plotted on a map of average chlorophyll concentration (see Section 2.3.2).

Blue stars indicate sites discussed in other chapters of this report.



Site ID	Monitoring Site (Region)	Section
2122	SYKE Bothnian Bay (northern Baltic Sea)	6.1
225	SYKE Bothnian Sea (northern Baltic Sea)	6.1
2628	SYKE Gulf of Finland (northern Baltic Sea)	6.1
292	SYKE Northern Baltic Proper (northern Baltic Sea)	6.1
3	Tallinn Bay (Gulf of Finland)	6.2
4	Pärnu Bay (northeast Gulf of Riga)	6.3
5	Station 121 (Gulf of Riga)	6.4
6	Eastern Gotland Basin (central Baltic Sea)	6.5
7	Gdańsk Basin (southern Baltic Proper)	6.6
8	Southern Gotland Basin (southern Baltic Proper)	6.6
9	Bornholm Basin (southern Baltic Sea)	6.6
40	Arkona Basin (southern Baltic Sea)	6.7
41	Anholt East (Kattegat)	6.8
42	Släggö (eastern Skagerrak)	6.8
43	Å17 (eastern Skagerrak)	6.8

The Baltic Sea is a brackish inland sea bounded by the Scandinavian peninsula, mainland Europe, and the Danish islands (Figure 6.0). Average salinity in the Baltic Sea is much lower than that in the North Atlantic and adjacent North Sea because of restricted saline water inflow from the North Sea and freshwater river input and run-off from the surrounding land. There is an estuarine circulation, with an outflow of low-salinity water above the halocline into the North Sea and irregular reverse inflows of higher-salinity deep water from the North Sea. This produces a permanent halocline at ca. 60–80 m depth, which restricts vertical exchange. Owing to seasonality, there is an additional thermocline from late spring until autumn. This strong stratification in the water column, combined with eutrophication and pollution, leads to low oxygen concentrations and even permanent anoxic conditions in some of the Baltic Sea deeper waters. Climate change and decadal-scale variability of these parameters further affect the Baltic Sea's hydrographic characteristics (Feistel *et al.*, 2008).

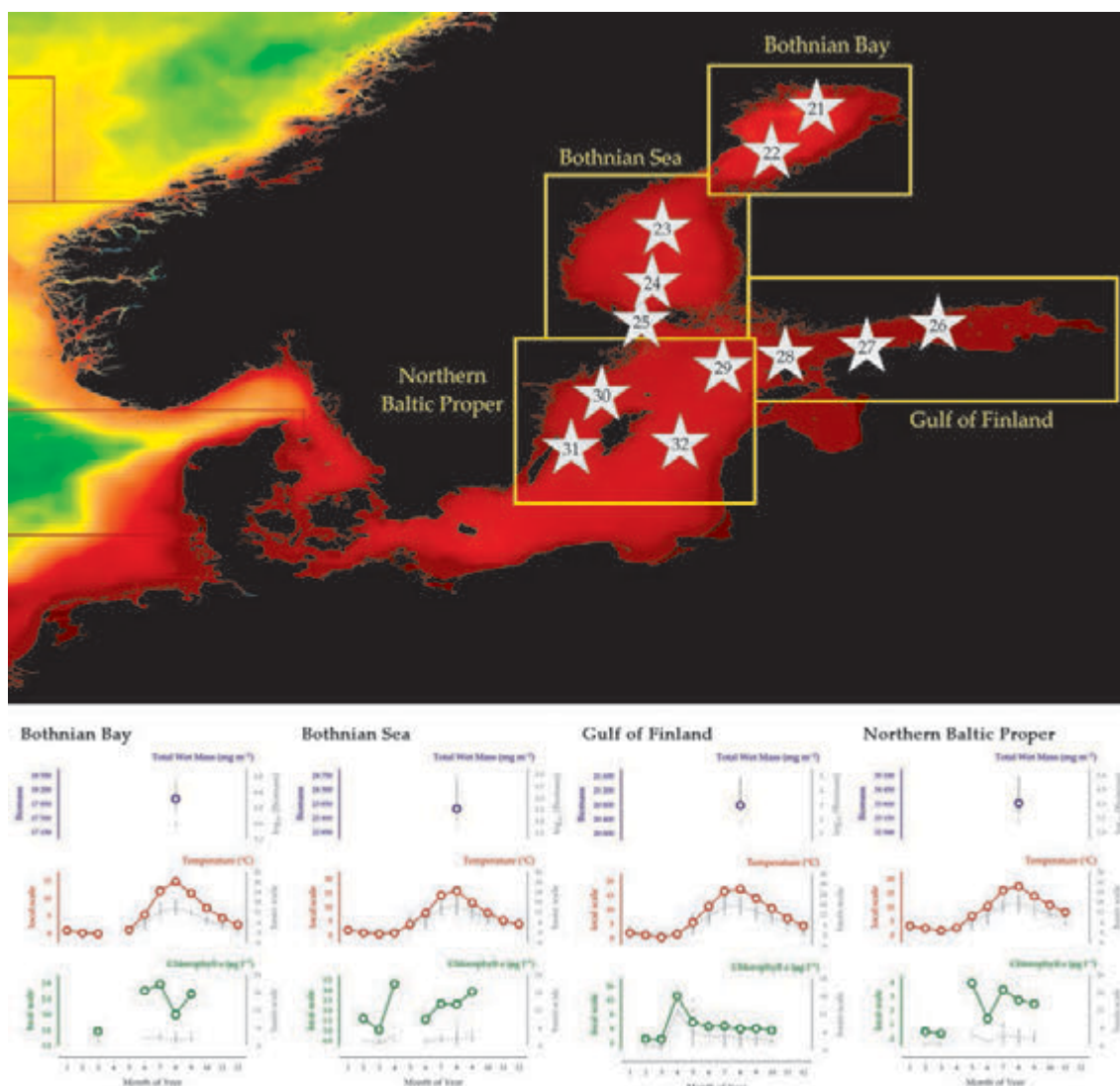
The zooplankton of the Baltic Sea ranges from freshwater-brackish species to North Sea neritic and occasional oceanic species, depending mainly on the distance from the Baltic Sea–North Sea interface. Profound changes in zooplankton species composition have been attributed to changes in the deep-water salinity (e.g. a decline in *Pseudocalanus* spp. since the late 1980s; Möllmann *et al.*, 2000, 2003), changes in temperature (e.g. an increase in *Temora longicornis* and *Acartia* spp. during the 1990s; Möllmann *et al.*, 2000, 2003), and predation pressure (Casini *et al.*, 2008). Changes in the northern and the southern Baltic Sea copepod communities, recently described by Flinkman and Postel (2009), are attributed to changes in temperature, salinity, and degree of eutrophication.

In the eastern Gotland Basin, almost ten years after the last medium-sized deep-water renewal and saltwater influx of 2003, the waters below the halocline have become almost abiotic. Abundance of the marine species *Oithona similis*, an indicator of higher-salinity water, declined to nearly zero as a result of a narrowing of its habitat layer (oxygenated water with suitable salinity) from 160 to 30 m. The general decline in total mesozooplankton abundance across the Baltic since the 1990s continues because of a decrease in many dominant taxa – mostly marine copepods. At the same time, with the decrease in *P. acuspes* abundance throughout the Baltic, other dominant copepod species (mainly *Acartia* spp. and *T. longicornis*) have increased in most of the monitoring regions, and *Calanus* spp. in the westernmost Baltic Sea. The most common invasive zooplankton species (*Mnemiopsis leidyi*, *Cercopagis pengoi*, and *Evadne anonyx*) have not increased in abundance after the first years of introduction but presently have stable populations regulated by salinity and temperature. The invasive cladocerans (*C. pengoi* and *E. anonyx*) are a permanent part of the central and northern Baltic zooplankton during summer months and have formed permanent resting egg banks, which are the basis for the production of new pelagic populations in early summer (Katajisto *et al.*, 2013). The American comb jelly (*M. leidyi*) is observed every year in the southern and western parts of the Baltic with maximum abundance in the autumn (Haraldsson *et al.*, 2013).

6.1 Northern Baltic Sea (Sites 21–32)

Maiju Lehtiniemi

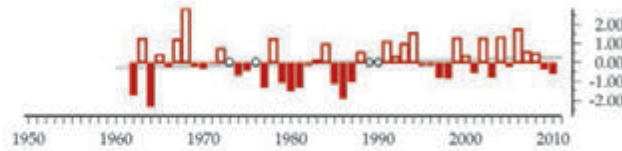
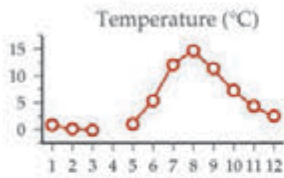
Figure 6.1.1
Location of Finnish Environment Institute (SYKE) monitoring stations in the northern Baltic Sea (Sites 21–32), and their corresponding seasonal summary plots (see Section 2.2.1). The yellow boxes and labels indicate the four subareas described in the report text.



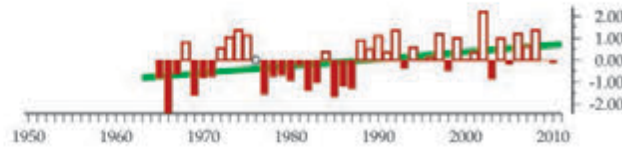
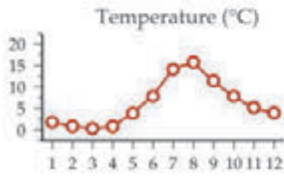
Zooplankton monitoring by the Finnish Environment Institute SYKE [former Finnish Institute of Marine Research (FIMR)] began in 1979 after the Helsinki Commission (HELCOM) initiated cooperative environmental monitoring of the Baltic Sea. Monitoring is divided into four subareas (Figure 6.1.1), based on differing hydrographic environments: Bothnian Bay (sites 21–22), and Bothnian Sea (sites 23–25), Gulf of Finland (sites 26–28), and the Baltic Proper (sites 29–31). Zooplankton samples are collected in August, the peak abundance period, with a WP-2 net (56 cm diameter, 100 µm mesh).

The zooplankton samples are collected from two stations in the Bothnian Bay (“F2”: site 21; “BO3”, site 22), from three stations in the Bothnian Sea (“US5B”, site 23; “SR5”, site 24; “F64”, site 25 located in the Åland Sea, but included in the Bothnian Sea analysis), from three stations in the Gulf of Finland (“LL3a”, site 26; “LL7”, site 27; “LL12”, site 28), and from four stations in the Baltic Proper located within the eastern and northwestern Gotland Basin (“LL17”, site 29; “LL23”, site 30; “BY38”, site 31; “BY15”, site 32).

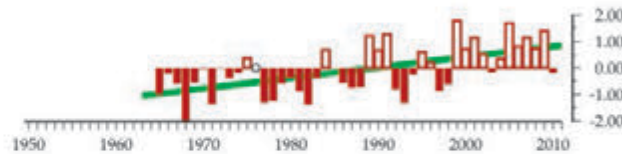
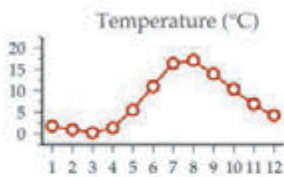
Bothnian Bay



Bothnian Sea



Gulf of Finland



Northern Baltic Proper

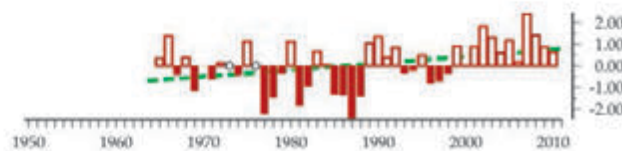
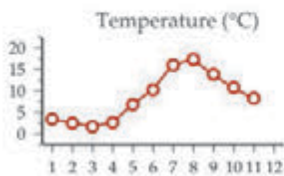
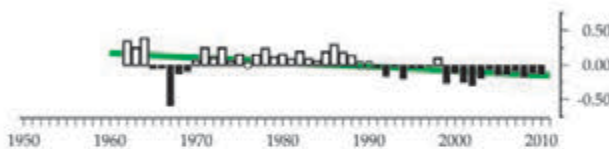
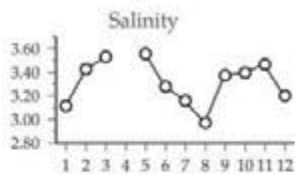
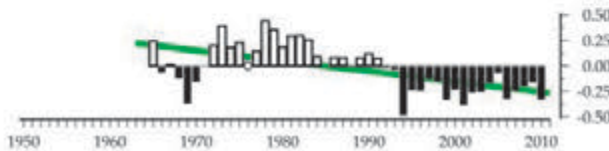
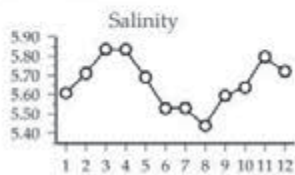


Figure 6.1.2
Multiple-variable comparison plot (see Section 2.2.2) showing the seasonal and interannual properties of surface temperatures within the four northern Baltic Sea monitoring regions.

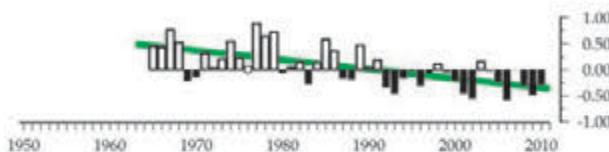
Bothnian Bay



Bothnian Sea



Gulf of Finland



Northern Baltic Proper

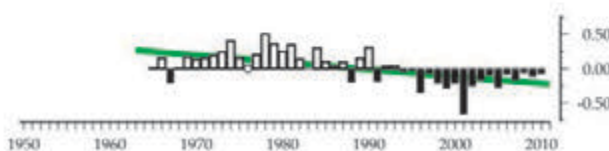
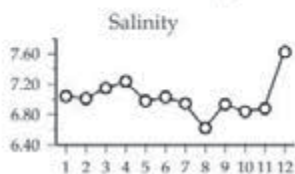


Figure 6.1.3
Multiple-variable comparison plot (see Section 2.2.2) showing the seasonal and interannual properties of surface salinities within the four northern Baltic Sea monitoring regions.

Seasonal and interannual trends in hydrography

Water temperatures are lowest in February–March and warmest in July–August (Figure 6.1.2) in all northern and eastern subbasins. Water temperatures in the Bothnian Bay are generally 1–2°C colder than those in the Bothnian Sea. Both regions have relatively low salinities, ranging from 2 to 4 in the Bothnian Bay (Leppäranta and Myrberg, 2009) and from 4 to 6 in the Bothnian Sea.

The hydrography of the Baltic Proper is characterized by strong stratification, which prevents mixing of the water column. A stable halocline is formed at approximately 70 m depth. Water-column salinity varies from 6 to 8 at the surface to 9–13 in the deeper water (Leppäranta and Myrberg, 2009). Pronounced salinity stratification often leads to oxygen depletion in bottom waters. Only irregular saltwater intrusions from the North Sea ventilate the deep bottom waters of the central Baltic Sea. The hydrography of the Gulf of Finland is similar to the Baltic Proper owing to a direct connection between these basins.

The general Baltic-wide decrease in salinity since mid-1980s is seen in the northern and eastern subbasins (Figure 6.1.3), because of warmer temperatures and increased precipitation and river run-off in the Baltic. The surface salinity in the Gulf of Finland varies from almost freshwater in the eastern parts of the Gulf (LL3a), owing to freshwater discharge from the River Neva, to >6 in the west (LL12). A halocline is formed at 60–80 m depth, preventing mixing of the deeper saltier (5–9) waters with surface layers (Leppäranta and Myrberg, 2009).

Surface temperature has been increasing since the mid-1980s in the Bothnian Sea, Åland Sea, and Gulf of Finland. In the Baltic Proper, sea surface temperature has been higher during the last 10–15 years, but the increasing trend is not as clear as in the Bothnian Sea and Gulf of Finland (Figure 6.1.2). The 100-year HadISST sea surface temperatures (Figure 6.1.11) show the same trends, indicating increasing temperatures in all four regions.

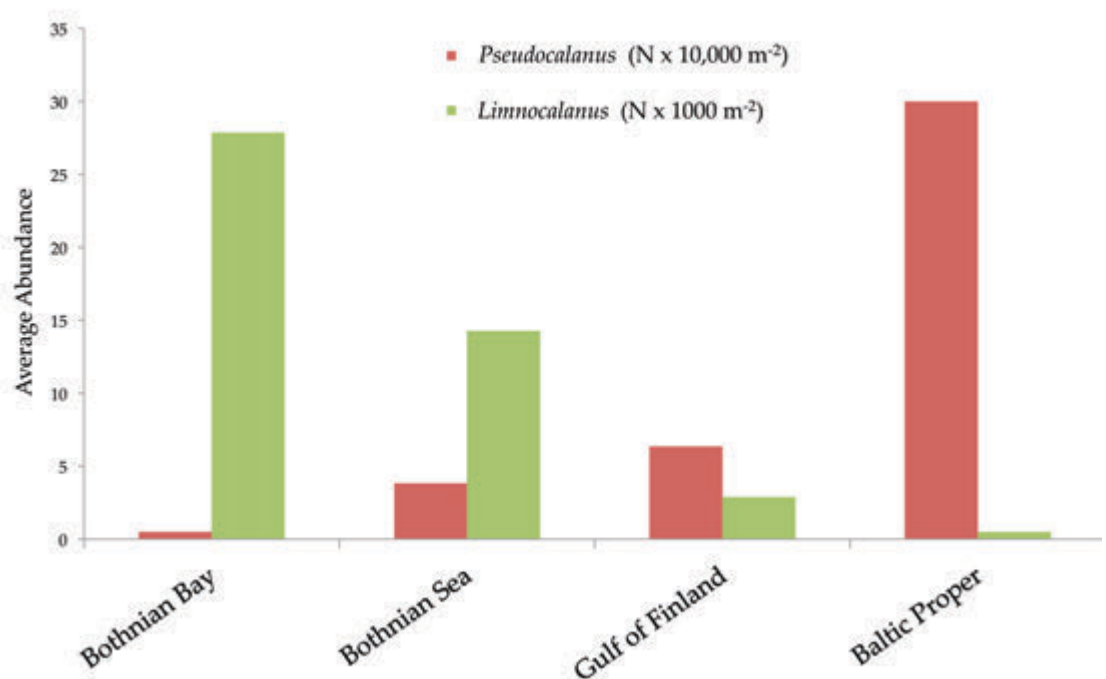
Seasonal and interannual trends in zooplankton

The zooplankton community of the Baltic Sea is a mixture of freshwater, brackish, and marine species. The dominant species are the calanoid copepods *Eurytemora* spp., *Acartia* spp., *Temora longicornis*, *Limnocalanus macrurus*, and the cladocerans *Bosmina (Eubosmina) coregoni* and *Evadne nordmanni*. The differences in salinity between the subbasins influence the zooplankton community structure in each region, with taxa preferring higher salinities (e.g. *Pseudocalanus* spp.) being nearly absent in the relatively lower salinity Bothnian Bay waters, and taxa preferring fresher waters (e.g. *L. macrurus*) being nearly absent in the relatively higher salinity waters of the Baltic Proper (Figure 6.1.4). As a result of these preferences, the overall species composition is changing as both surface and bottom salinities have been decreasing in many regions since the beginning of the sampling programme in 1979.

Figure 6.1.4
Average abundances of two copepods with opposite salinity preferences plotted by northern Baltic Sea regions ordered from relatively low (Bothnian Bay) to higher average salinities (Baltic Proper).

Bothnian Bay salinities average around 3, while Baltic Proper salinities are above 7.

The copepod *Pseudocalanus* prefers higher salinity, while *Limnocalanus* prefers lower-salinity waters.



No large shifts have occurred in the total zooplankton biomass except in the Bothnian Sea, where the biomass has significantly increased (Figure 6.1.5). However, significant changes have occurred in the species composition in many regions. Of the dominant copepods in the northern and eastern Baltic Sea, *Eurytemora* spp. has increased in the Bothnian Sea, Gulf of Finland, and Baltic Proper since the late 1980s, while in the northernmost Bothnian Bay, there has been a slight downward trend (Figure 6.1.6).

The other dominant copepod species, *Acartia* spp. (not shown) has increased in abundance in the Baltic Proper. *L. macrurus* is the largest species of copepods and an important species in the zooplankton communities of the less-saline environments such as the Bothnian Bay, Bothnian Sea, and Gulf of Finland. It is favoured by decreasing salinities and has significantly increased in abundance in the Bothnian Sea (Figure 6.1.7).

Pseudocalanus spp., a copepod genus of marine origin, has been decreasing in biomass over the monitoring period due to decreasing salinities (Flinkman *et al.*, 2007). Another marine copepod, *T. longicornis*, has decreased in the Bothnian Sea, but has strongly increased in the more-saline Baltic Proper (Figure 6.1.8).

The most abundant cladoceran species, *Bosmina* (*Eubosmina*) *coregoni*, has significantly increased from the beginning of the monitoring programme in the Bothnian Sea (Figure 6.1.9). A slight increase can also be seen in the Bothnian Bay. This species favours warm waters and is probably affected by the increasing surface water temperatures. No significant trends can be seen in the abundance of the two other common cladocerans, *E. nordmanni* and *Podon* spp., in any of the subbasins (not shown).

The moon jellyfish *Aurelia aurita* has been very abundant during late summer and early autumn during the last two years after many years of lower abundance. There are no ongoing monitoring programmes on gelatinous zooplankton in the northern and central Baltic Sea, but observations are collected by the public.

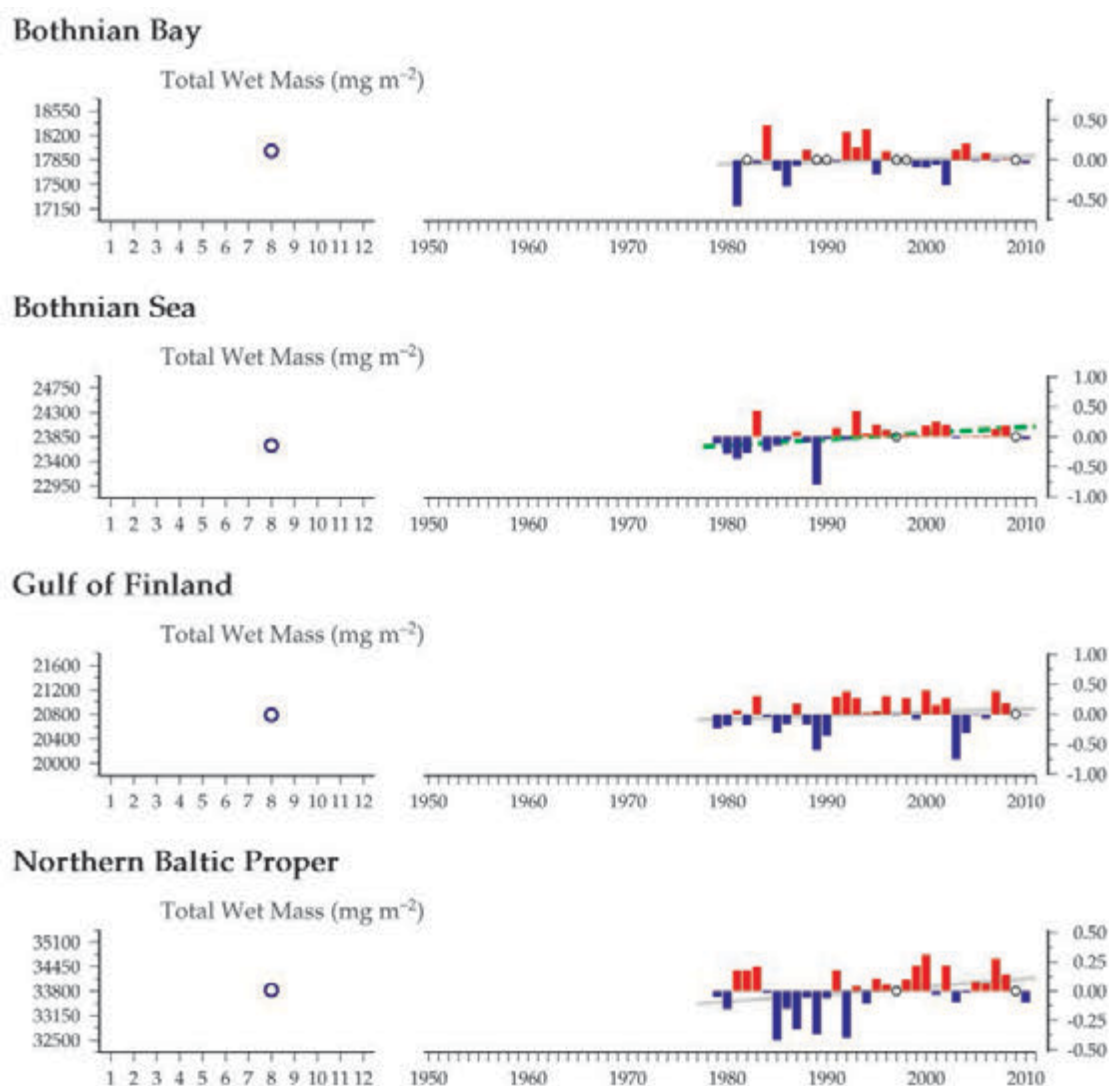


Figure 6.1.5
Multiple-variable comparison plot (see Section 2.2.2) showing the seasonal and interannual properties of total zooplankton wet mass values within the four northern Baltic Sea monitoring regions.

Figure 6.1.6
Multiple-variable comparison plot (see Section 2.2.2) showing the seasonal and interannual properties of *Eurytemora* spp. abundance within the four northern Baltic Sea monitoring regions.

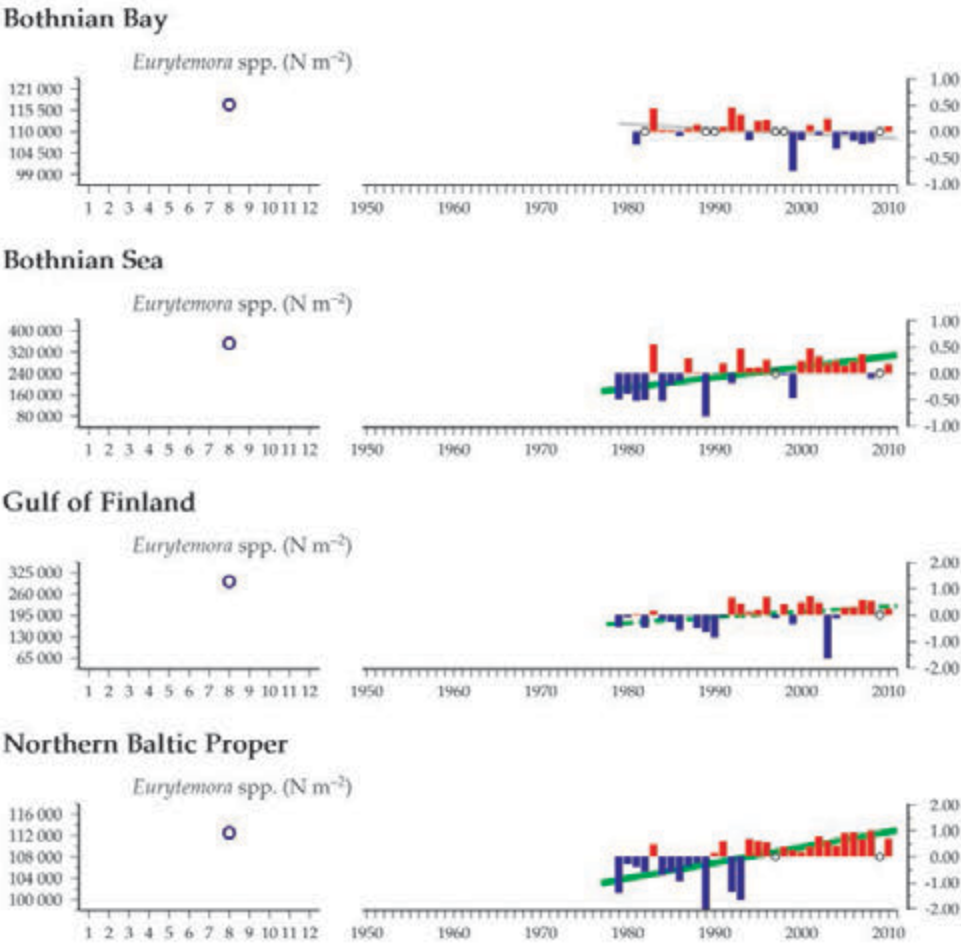
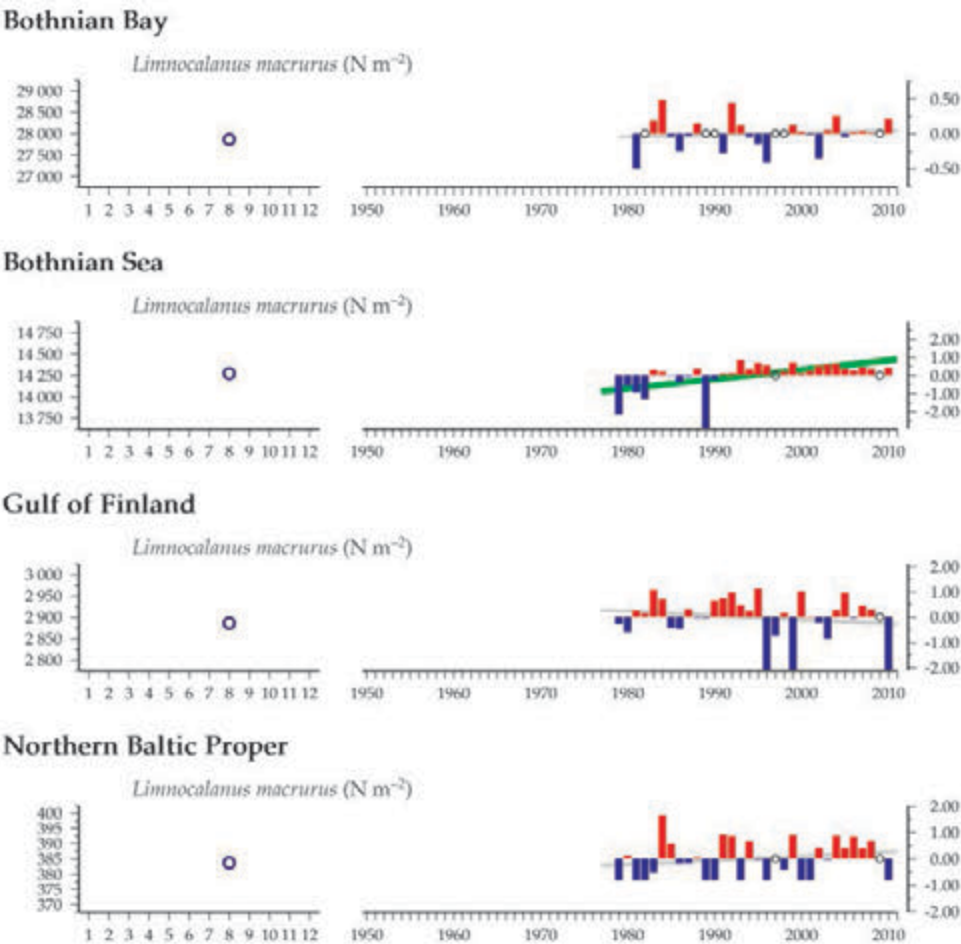
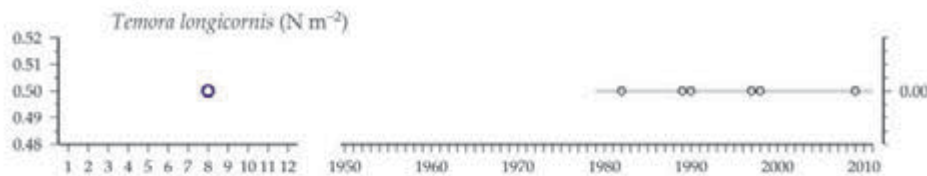


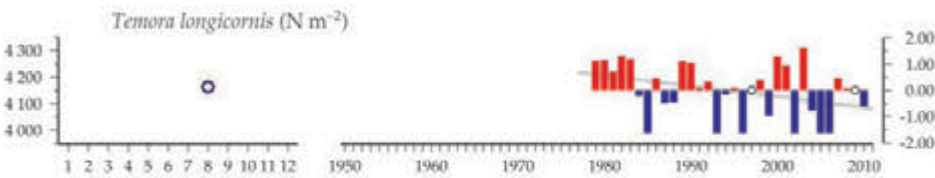
Figure 6.1.7
Multiple-variable comparison plot (see Section 2.2.2) showing the seasonal and interannual properties of *Limnocalanus macrurus* abundance within the four northern Baltic Sea monitoring regions.



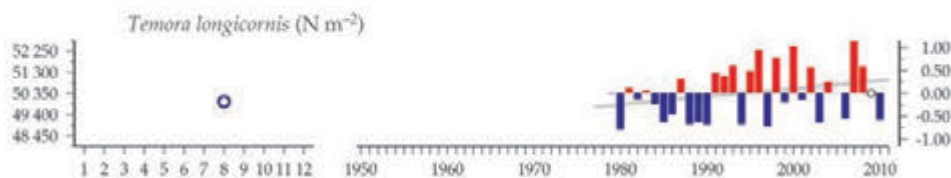
Bothnian Bay



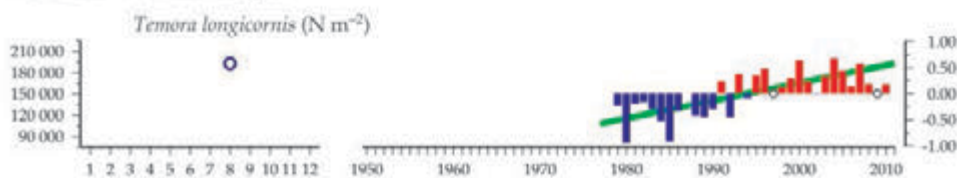
Bothnian Sea



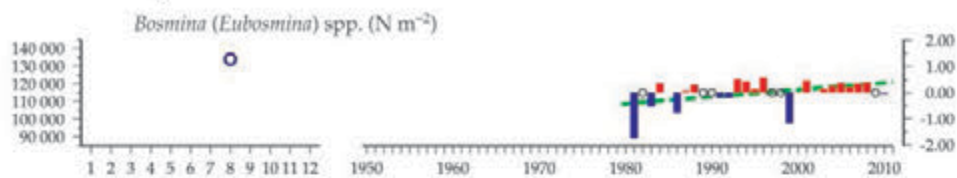
Gulf of Finland



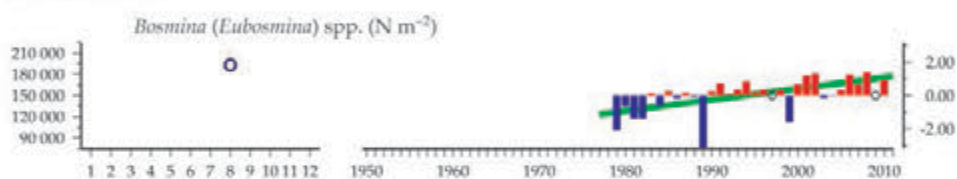
Northern Baltic Proper



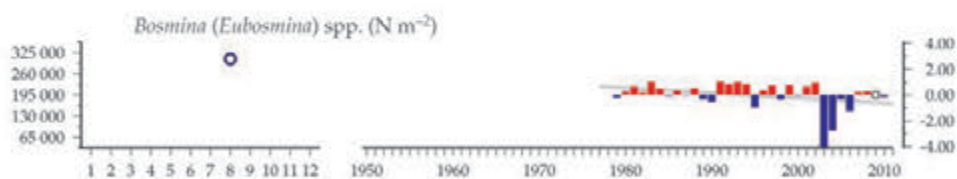
Bothnian Bay



Bothnian Sea



Gulf of Finland



Northern Baltic Proper

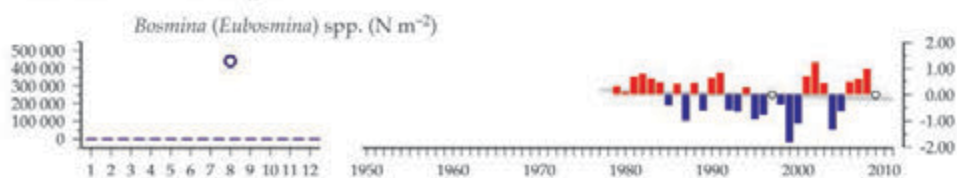


Figure 6.1.8

Multiple-variable comparison plot (see Section 2.2.2) showing the seasonal and interannual properties of *Temora longicornis* abundance within the four northern Baltic Sea monitoring regions.

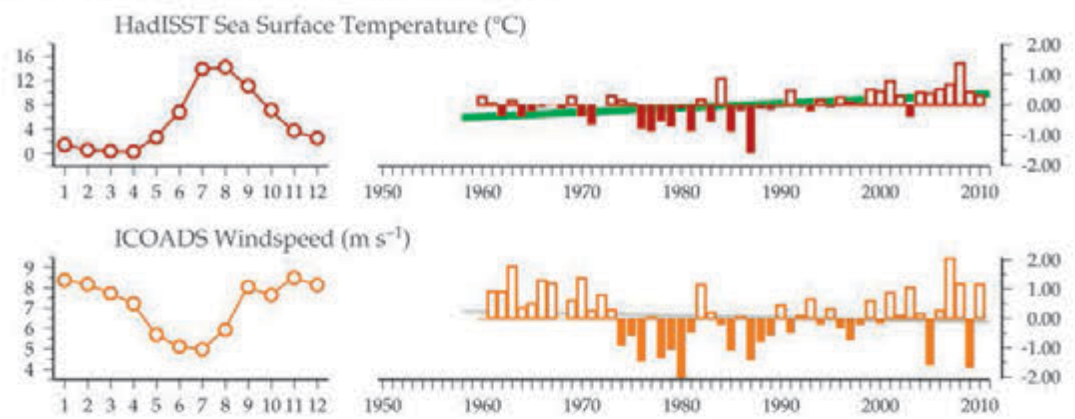
Figure 6.1.9

Multiple-variable comparison plot (see Section 2.2.2) showing the seasonal and interannual properties of *Bosmina (Eubosmina) spp.* abundance within the four northern Baltic Sea monitoring regions.

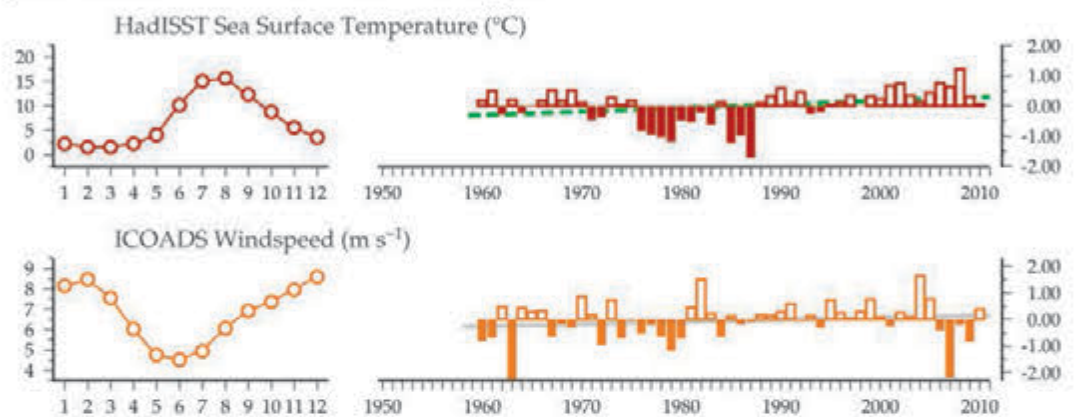
Figure 6.1.10

Regional overview plot
(see Section 2.2.3) showing
long-term sea surface
temperatures and wind
speeds in the general region
surrounding the Northern
Baltic Sea monitoring
areas.

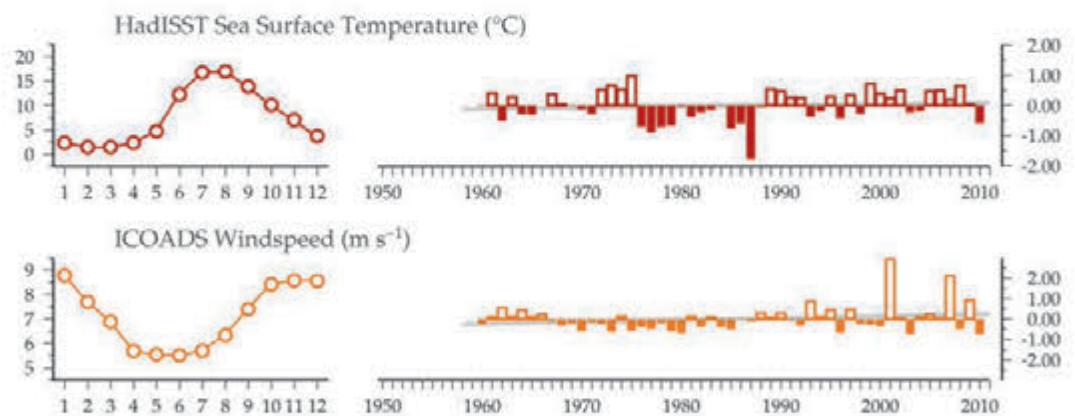
50-year trends in the Bothnian Bay region



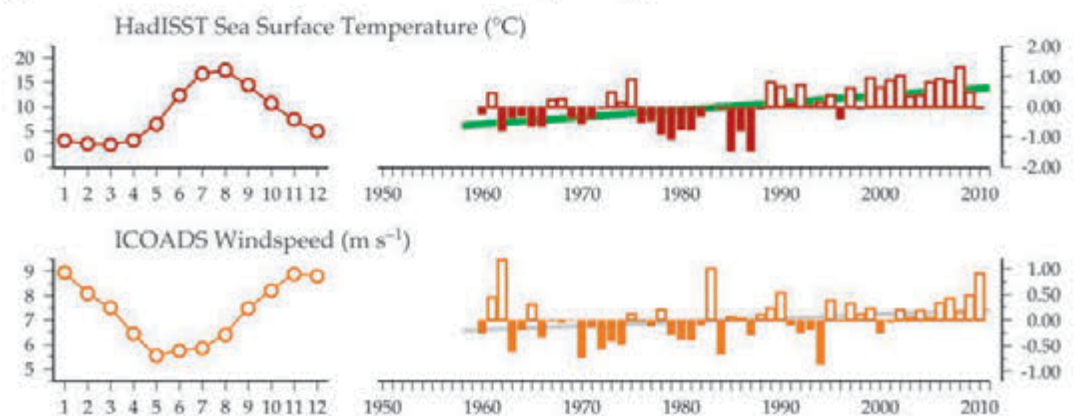
50-year trends in the Bothnian Sea region



50-year trends in the Gulf of Finland region



50-year trends in the northern Baltic Proper region



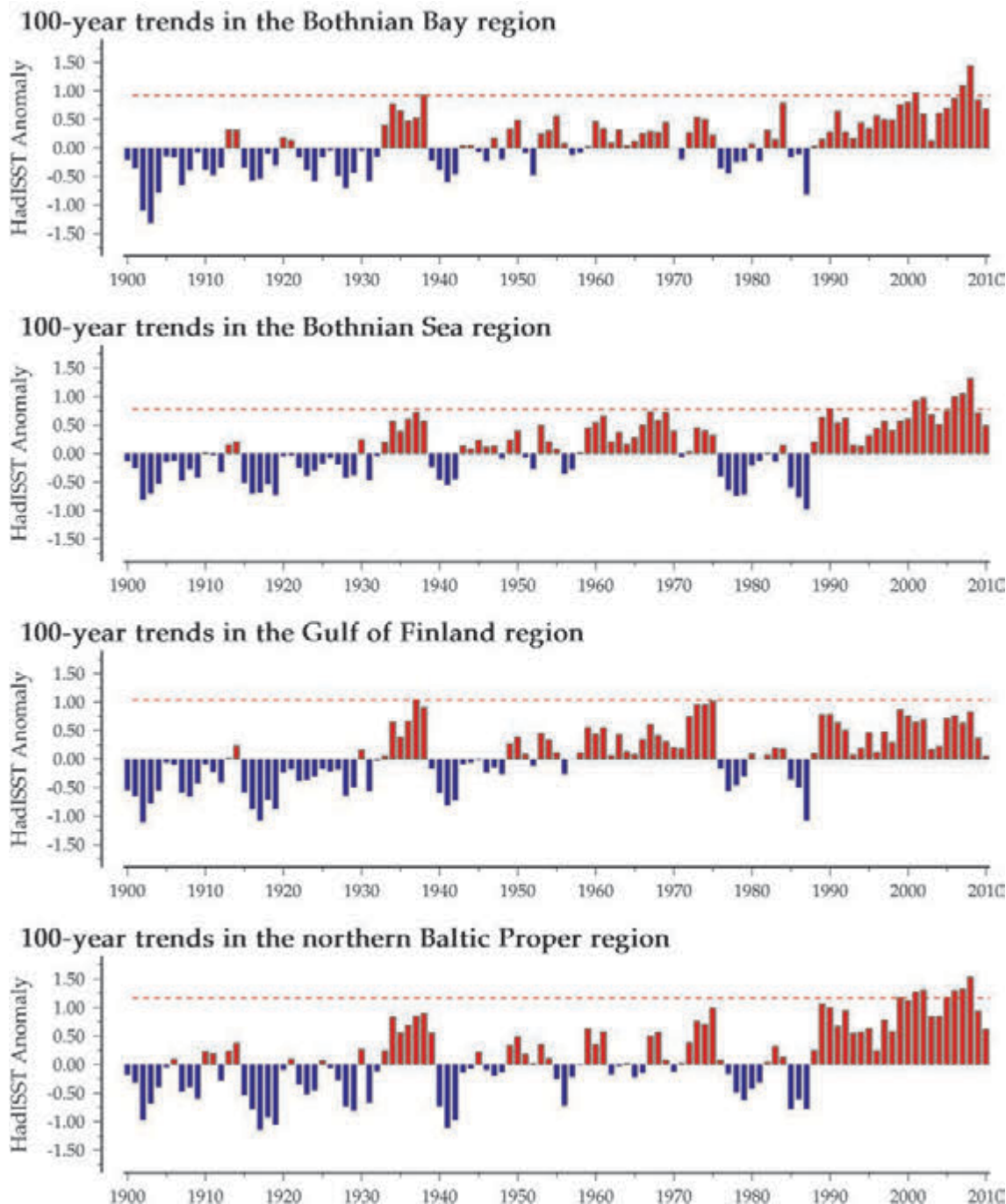


Figure 6.1.11
Regional overview plot
(see Section 2.2.3) showing
100-year sea surface
temperatures in the general
region surrounding
the Northern Baltic Sea
monitoring areas.

6.2 Tallinn Bay (Site 33)

Arno Põllumäe

Figure 6.2.1

Location of the Tallinn Bay monitoring area (Site 33) plotted on a map of average chlorophyll concentration, and its corresponding seasonal summary plot (see Section 2.2.1).



A frequently sampled monitoring station is located in the middle of Tallinn Bay at 59°32.2'N 24°41.3'E (Figure 6.2.1). Tallinn Bay is relatively exposed, and there is good water exchange between it and the open gulf. The maximum depth of the bay is ca. 100 m, whereas the depth of the sampling station is 45 m. Seasonal fluctuations in water temperature occur above 30 m depth, mainly from May to November. During winter, the bay is usually covered with ice, whereas in summer, surface water temperatures as high as 24°C can be observed in July. In the deeper parts of the bay, the temperature is stable throughout the year at 2–5°C. The average salinity at the station is 6, whereas the maximum salinity near the bottom has reached 9.25. The large urban area of Tallinn affects the nutrient status of Tallinn Bay.

Zooplankton have regularly been collected since 1993, using vertical hauls of a Juday plankton net (38 cm diameter, 90–100 mm mesh) up to 12 times a year. Mesozooplankton sample analyses were performed according to guidelines outlined by HELCOM (1988). Phytoplankton, macrozoobenthos, and water chemistry samples are also sampled at the same station with the same frequency.

Zooplankton in the Baltic Sea is typically smaller than in the North Atlantic. The dominant copepod species in Estonian waters are *Eurytemora affinis* and *Acartia bifilosa*, the most abundant cladoceran is *Bosmina* (*Eubosmina*) *coregoni*, and rotifers also constitute a large proportion of the total zooplankton abundance.

Seasonal and interannual trends (Figure 6.2.2)

Maximum copepod abundance is usually observed in late summer, corresponding to the warmest water temperatures (Figure 6.2.2). In years with warmer winters, high abundance may be observed in spring, when a shorter period of ice cover causes more mixing and phosphorus release from the bottom, resulting in higher chlorophyll concentrations in spring and summer. This mechanism may also explain the corresponding increase in chlorophyll with temperature over time and the slight increase in copepod abundance during the same period (Figure 6.2.2). The phytoplankton spring bloom usually occurs in April, but the exact timing depends on ice cover.

The abundance of copepods in Tallinn Bay is positively correlated with HadISST temperature; $r^2 = 0.4$, $p < 0.01$), with higher abundance present through all months during the warmer years. Temperatures in the bay have been above the 100-year average since the 1990s (Figure 6.2.3). Recent studies at species level demonstrate that climatic conditions at some spatial scales play an important role for most mesozooplankton species in the Gulf of Finland. The effect of nutrient loads at local and regional scales is also important (Põllumäe *et al.*, 2009). The dynamics of some local mesozooplankton species (e.g. *B. coregoni*) may also be affected by the recent predatory invader *Cercopagis pengoi* (Põllumäe and Kotta, 2007).

Tallinn Bay, Gulf of Finland

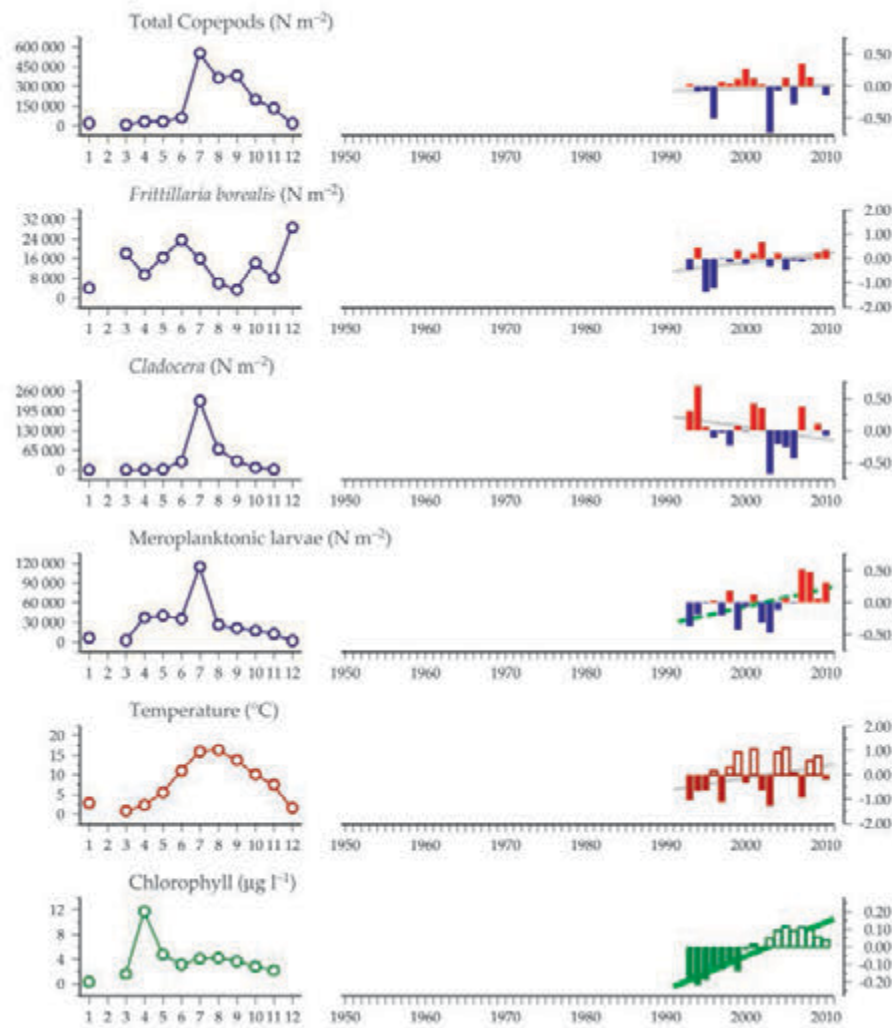


Figure 6.2.2
Multiple-variable comparison plot (see Section 2.2.2) showing the seasonal and interannual properties of select cosampled variables at the Tallinn Bay monitoring area.

Additional variables are available online at: <http://WGZE.net/time-series>.

50-year trends in the Tallinn Bay / Gulf of Finland region

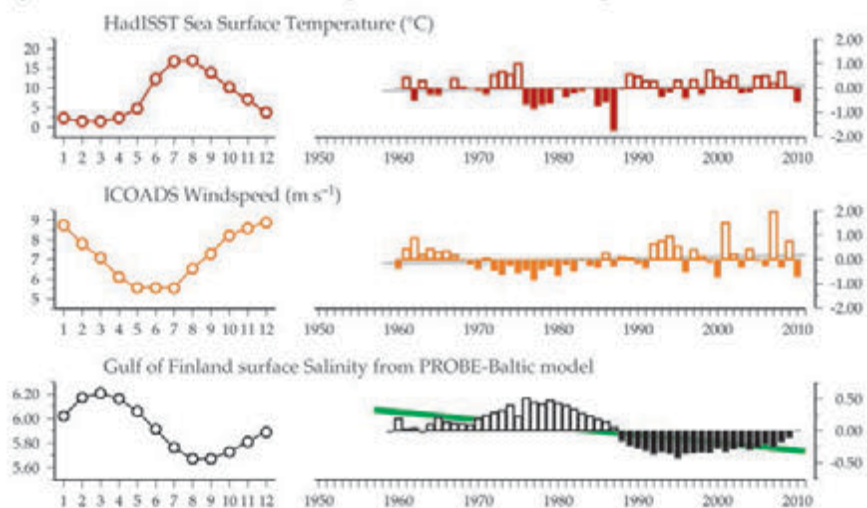
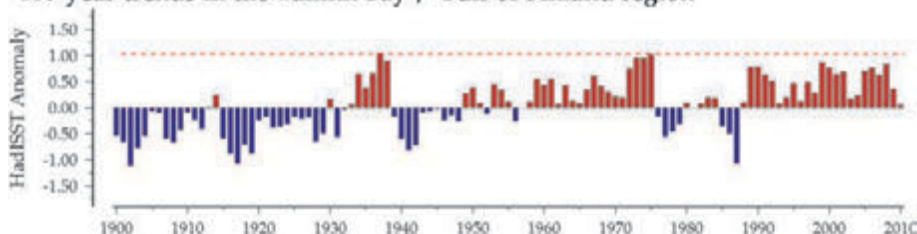


Figure 6.2.3
Regional overview plot (see Section 2.2.3) showing long-term sea surface temperatures, windspeeds, and salinity in the general region surrounding the Tallinn Bay monitoring area.

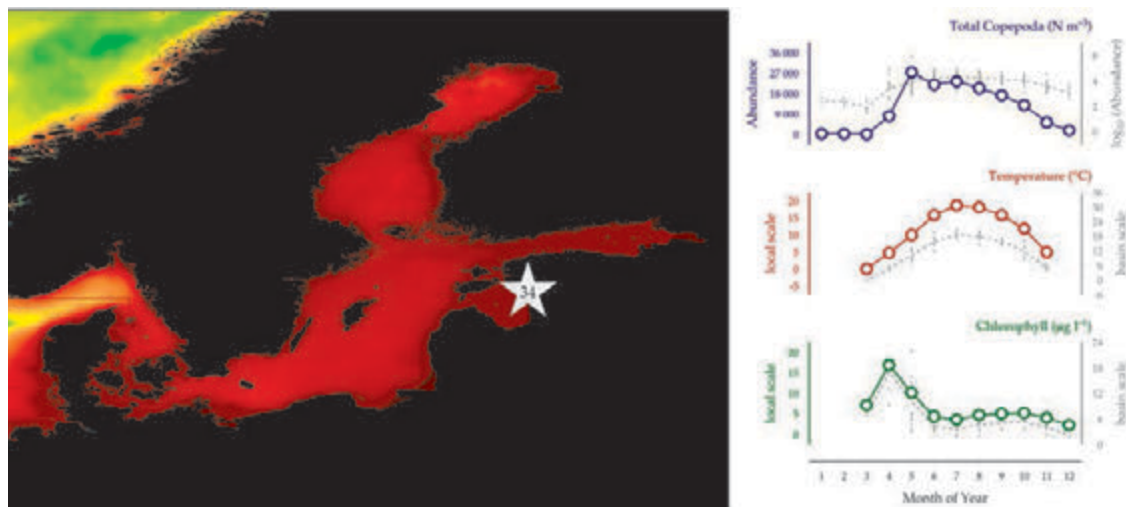
100-year trends in the Tallinn Bay / Gulf of Finland region



6.3 Pärnu Bay (Site 34)

Maria Pöllupüü, Mart Simm, and Arno Põllumäe

Figure 6.3.1
Location of the Pärnu Bay monitoring area (Site 34) plotted on a map of average chlorophyll concentration, and its corresponding seasonal summary plot (see Section 2.2.1).



Pärnu Bay is a shallow, semi-enclosed brackish-water basin located in the northeastern part of the Gulf of Riga and covering approximately 700 km², with a volume of 2 km³. Its maximum depth gradually increases from 7.5 m in the inner part to 23 m in the southwestern part. In most years, Pärnu Bay is covered with ice in winter.

The hydrographic conditions of Pärnu Bay are formed under the complex influence of winter ice conditions, freshwater inputs from the Pärnu River, and water exchange with the open part of the Gulf of Riga. The bay suffers from extensive human pressures (recreation, eutrophication, fishing; Kotta *et al.*, 2008). In summer, surface water temperatures may reach 23°C during July–August. Long-term water temperatures have been warmer than the 100-year average since 1989.

Zooplankton sampling has been carried out since the late 1950s at a monitoring station (10 m depth) located in the middle part of the bay. From 1957 to 1975, sampling started in April–May and was generally performed weekly until the end of October. From 1976 onwards, the sampling period was extended to include all ice-free months. Sampling is performed vertically using a Juday plankton net (0.1 m² mouth opening, 90–100 µm mesh) integrating over the whole water column. Mesozooplankton sample analyses are performed according to guidelines outlined by HELCOM (1988).

Seasonal and interannual trends (Figure 6.3.2)

The zooplankton taxa are represented by brackish-water,

eurythermal, oligothermal, and polythermal species. Rotifers, copepods, cladocerans, and meroplankton dominate the zooplankton communities (Kotta *et al.*, 2009). The diversity of zooplankton in Pärnu Bay is low; two species, *Eurytemora affinis* and *Acartia biflosa*, constitute 99% of the total copepod abundance, and *Bosmina (Eubosmina) coregoni* is the prevailing cladoceran. Peak copepod abundance occurs in the warmer summer months (June–July), after the spring chlorophyll peak and just before the summer temperature maximum (Figure 6.3.2).

Different trends in the long-term abundance of the copepods and cladocerans were observed. In Pärnu Bay, during the period from the late 1950s to the late 1980s, total copepod abundance was generally lower than the long-term average. This period was followed by a rise in both copepod abundance and water temperature from below-average to above-average levels. In contrast to the copepods, cladoceran abundance went from an increasing to a decreasing trend at the beginning of the 1990s. After decreasing rapidly for a few years, it then stabilized at levels considerably lower compared with the earlier period in the middle of the time-series. Over the last few decades, invasions of two additional cladoceran species (*Cercopagis pengoi* and *Evadne anonyx*) of Ponto–Caspian origin have been recorded (Ojaveer and Lumberg, 1995; Pöllupüü *et al.*, 2008). The decrease in native cladoceran abundance coincides with the invasion of the predatory cladoceran *C. pengoi*, which now occurs in large numbers in Pärnu Bay during periods of warm water (Ojaveer *et al.*, 2004; Kotta *et al.*, 2004, 2009).

Pärnu Bay, northeast Gulf of Riga

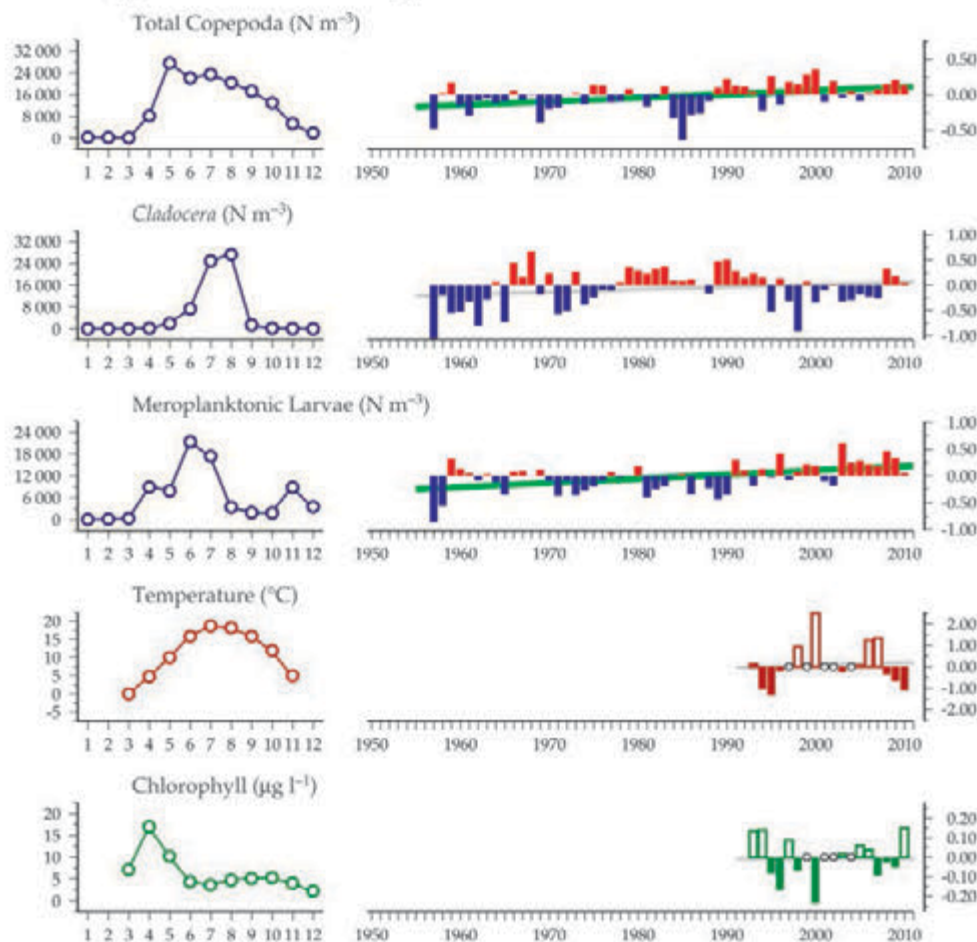


Figure 6.3.2
Multiple-variable comparison plot (see Section 2.2.2) showing the seasonal and interannual properties of select cosampled variables at the Pärnu Bay monitoring area.

Additional variables are available online at: <http://WGZE.net/time-series>.

50-year trends in the Pärnu Bay / northeast Gulf of Riga region

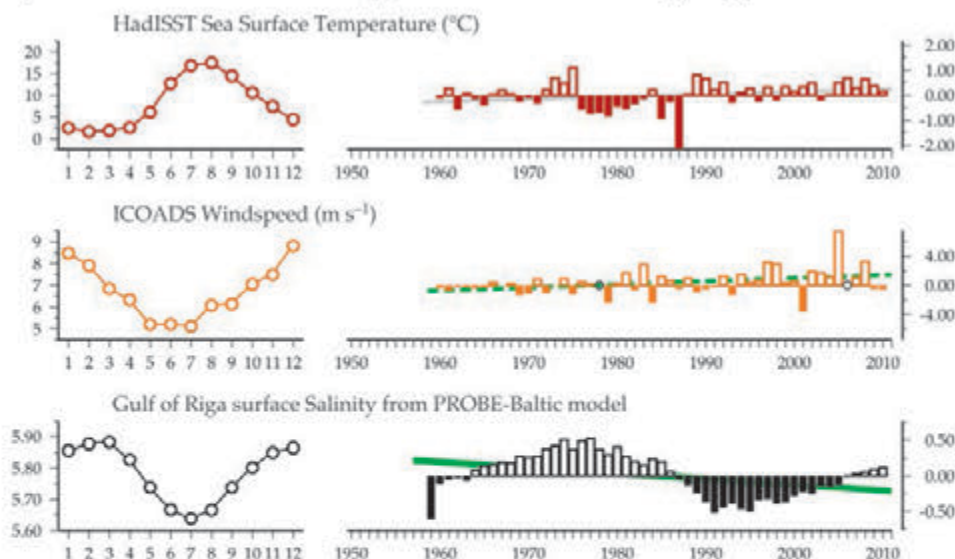
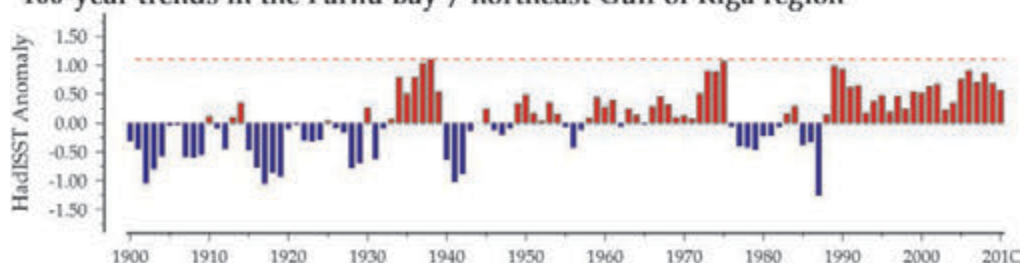


Figure 6.3.3
Regional overview plot (see Section 2.2.3) showing long-term sea surface temperatures, windspeeds, and salinity in the general region surrounding the Pärnu Bay monitoring area.

100-year trends in the Pärnu Bay / northeast Gulf of Riga region



6.4 Station 121 (Site 35)

Anda Ikauniece

Figure 6.4.1

Location of the Station 121 monitoring area (Site 35) plotted on a map of average chlorophyll concentration, and its corresponding seasonal summary plot (see Section 2.2.1).



In the context of the National Monitoring Programme of Latvia, mesozooplankton have been sampled since 1993 as a parameter of aquatic environmental status. Sampling Station 121 is located in the central part of the Gulf of Riga, approximately 50 km from the coast and at a depth of 55 m (Figure 6.3.1). A network of monitoring stations was constructed across the gulf to study the impact of various factors, such as freshwater discharge and general currents. Station 121 represents the central part of the gulf, the deepest of the monitoring stations, which is minimally affected by freshwater and nutrients. Plankton productivity indicators in this area are lower than those of the coastal zones, but species composition does not differ substantially because the whole Gulf is a brackish-water basin, with dominant salinity values of ca. 5.

Zooplankton was sampled with a WP-2 net (56 cm diameter, 100 µm mesh), using vertical hauls from 50 m depth to the surface. Sampling was carried out at least three times a year, reflecting the most productive seasons: spring (May), summer (August), and autumn (October–November).

Seasonal and interannual trends (Figure 6.4.2)

Species diversity in the gulf is low. The total number of zooplankton species does not exceed 40, and there are seldom more than 15 species in any one sample. The zooplankton follows a strong seasonal pattern that is determined by temperature during the first half of the year and by the combined effect of predation and temperature during the second half. Interannual values of zooplankton abundance and biomass are extremely variable, but the seasonal pattern has remained constant throughout the observation period. Copepod abundance and total sample wet mass are lowest from December through April, corresponding to the period of coldest water temperatures. Relatively few species of copepods occur within the monitoring area: *Acartia bifilosa*, *Eurytemora affinis*, and *Limnocalanus macrurus* (the latter

mostly naupliar stages). A steep temperature rise starts in May, causing mass development of rotifers (*Synchaeta* spp.) and copepods. With further temperature increases in June, more species of rotifers (*Keratella* spp.) and cladocerans (*Evadne nordmanni*, *Pleopsis* spp., and *Bosmina longispina*) appear in the zooplankton community. The highest annual abundance and biomass levels are reached in July or early August, with up to 50% of the total biomass comprised of cladocerans, mostly *B. longispina*. Starting in mid-August, predation by herring (*Clupea harengus*), mysids, and the invasive cladoceran *Cercopagis pengoi* affects the total abundance of the zooplankton community. Herring and mysids generally target the copepods, whereas *C. pengoi* preys on the local cladoceran *Bosmina*. Gradual temperature decreases in autumn generally correspond to a reduction in the number of species and abundance values of the community. The autumn species composition resembles that of spring, with the addition of meroplankton, the pelagic larvae of benthic fauna.

Long-term SSTs in the region are fairly variable and agree only partly with smaller-scale on-site measurements for the period after 1993 (Figure 6.4.2 vs. 6.4.3). Still, sea surface temperatures have been warmer than the 100-year average since 1990. There is no clear relationship between temperature and zooplankton within the site, although temperature and salinity changes have been shown to influence zooplankton at other sites within the Baltic. For species inhabiting the Gulf, the range of optimal salinity is wide enough and, therefore, the gradual drop of 1 is not reflected in species composition or abundance of zooplankton. While the total copepod trends show a very slight increase (Figure 6.4.2), Jurgensone *et al.* (2011) report a decline in the summer biomass of two dominant copepod species (*Acartia bifilosa* and *Eurytemora affinis*, not shown) after 1990, even though summer phytoplankton biomass doubled during the same period.

Station 121, Gulf of Riga

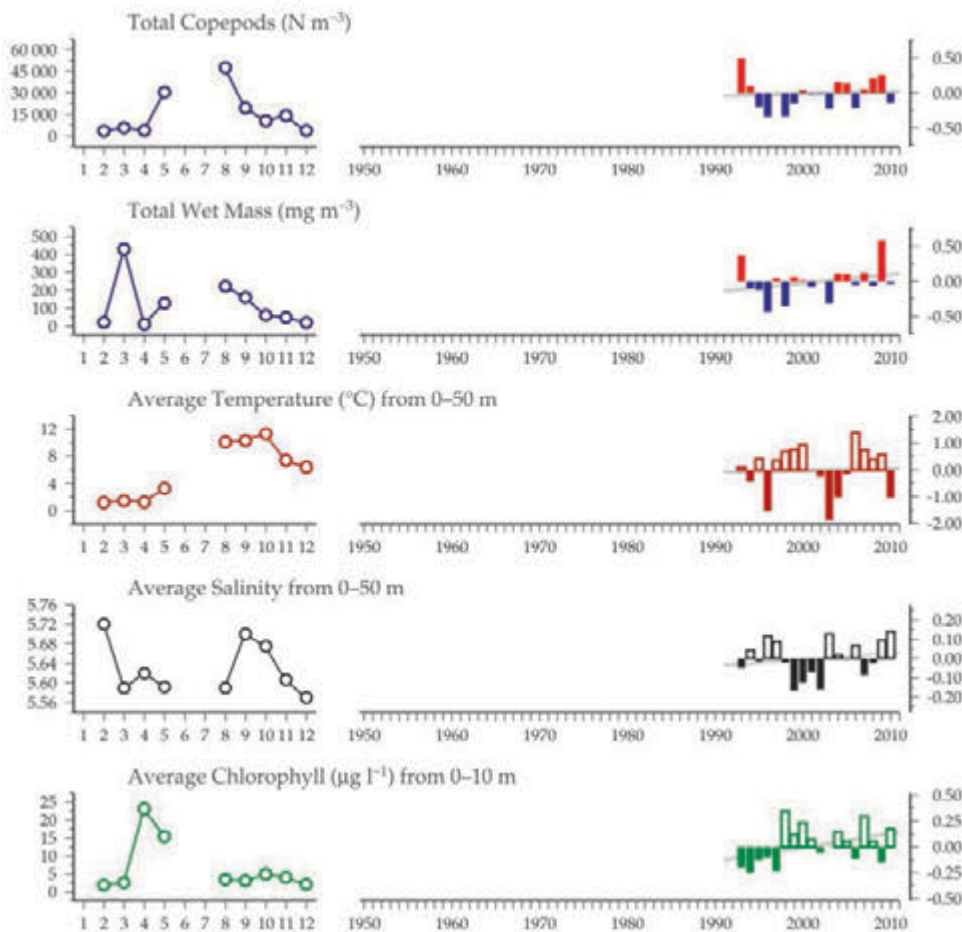


Figure 6.4.2
Multiple-variable comparison plot (see Section 2.2.2) showing the seasonal and interannual properties of select cosampled variables at the Station 121 monitoring area.

Additional variables are available online at: <http://WGZE.net/time-series>.

50-year trends in the Station 121 / Gulf of Riga region

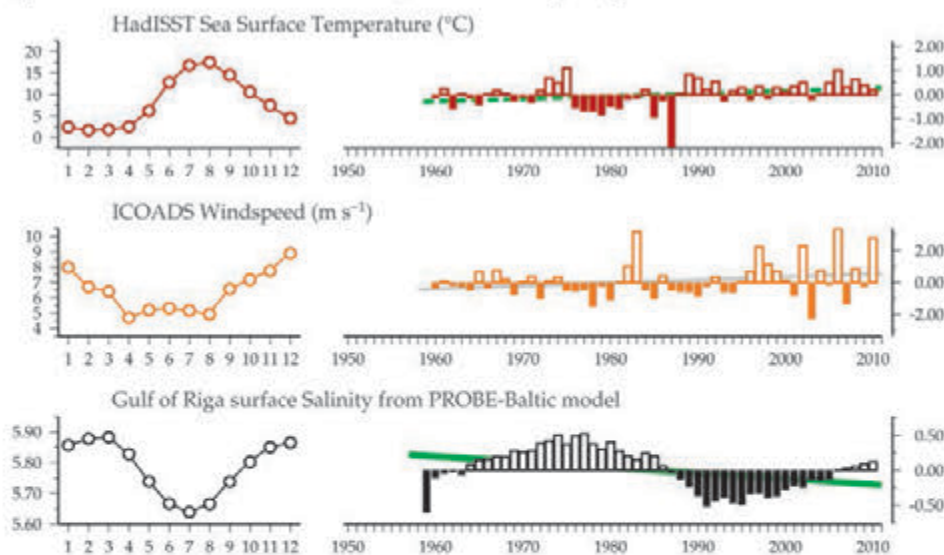
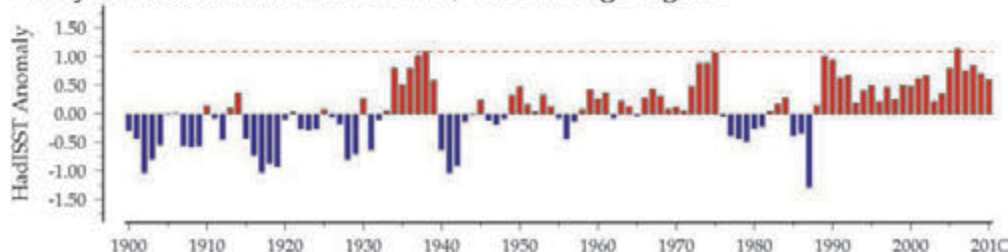


Figure 6.4.3
Regional overview plot (see Section 2.2.3) showing long-term sea surface temperatures, windspeeds, and salinity in the general region surrounding the Station 121 monitoring area.

100-year trends in the Station 121 / Gulf of Riga region



6.5 Eastern Gotland Basin (Site 36)

Gunta Rubene and Solvita Strake

Figure 6.5.1

Location of the Eastern Gotland Basin monitoring area (Site 36) plotted on a map of average chlorophyll concentration, and its corresponding seasonal summary plot (see Section 2.2.1).



The eastern Gotland Basin sampling site is located in the central Baltic Sea, ICES Subdivision 28 (Figure 6.5.1). Zooplankton biomass (wet weight) was sampled using a Juday net (36 cm diameter, 160 µm mesh). Individual hauls were carried out in two vertical steps at each sampling station: the upper water layer with depth of 0–50 m and the bottom layer with full coverage of the water column to a maximum depth of 100 m (results from the 0–100 m samples are presented here). Sampling has been conducted in three seasons—spring (May), summer (August), and autumn (October–November) since 1959.

Climate over the central Baltic Sea area, as described by the North Atlantic Oscillation (NAO) index, shows two distinct periods. During the 1970s and 1980s, the index was mainly in a negative state and mainly positive afterwards (until 2009). This change in the index from negative to positive was mainly associated with more frequent westerly winds, warmer winters, and eventually a warmer climate over the area. A similar time-trend with two different periods is visible for the sea surface water temperature and salinity (Figure 6.5.2).

Seasonal and interannual trends (Figure 6.5.2)

In the central Baltic Sea, the zooplankton biomass is highly seasonal. The lowest biomass is usually at the beginning of the year, and increases rapidly in spring following the seasonal increase in water temperature and chlorophyll. The highest biomass of all copepod species is always found in summer. Cladocerans appear in considerable numbers from spring onwards, with highest biomass in summer (August).

In terms of biomass, the most important copepod species in the central Baltic Sea is *Pseudocalanus* spp., followed by

Temora longicornis, *Acartia* spp., and *Centropages hamatus*. The annual biomass of *Pseudocalanus* spp. was high from 1970 to the late 1980s, but decreased to negative annual anomalies in 1990 and has since remained at low levels. Zooplankton biomass has increased with increasing bottom salinity (not shown), but decreased again in recent years (2010–2012, not shown) following the decrease in bottom salinity. At the same time, an opposite trend was observed for *T. longicornis*, which had low biomass until 1990, followed by high values at the end of the time-series, reaching a maximum in 2008 and 2009. Similarly, *Acartia* spp., which had low annual abundance during the 1980s, increased stepwise during the 1990s (not shown). Increasing water temperatures and decreasing salinity are thought to be the reason for the shift in zooplankton species composition from *Pseudocalanus* spp. to *T. longicornis* and *Acartia* spp. (Möllmann *et al.*, 2005). Although there are few published studies on the long-term trends of phytoplankton, changes in phytoplankton species composition were also observed in the central Baltic Sea. A downward trend was found for diatoms in spring and summer, whereas dinoflagellates generally increased in the Baltic Proper (Wasmund and Uhlig, 2003). Similarly, the species composition of the central Baltic fish community shifted from cod (*Gadus morhua*), which was very abundant during the 1980s, to sprat (*Sprattus sprattus*), which became dominant during the 1990s (Möllmann *et al.*, 2005). Water temperatures in the survey area have been increasing since the 1900s, with some variability, and are currently near the warmest measured in the past century (Figure 6.5.3). Increased precipitation and river run-off have accompanied the warmer temperatures. This directly affects the Baltic and its zooplankton communities by the freshening of the surface waters (Matthäus and Schinke, 1999).

Eastern Gotland Basin, central Baltic Sea

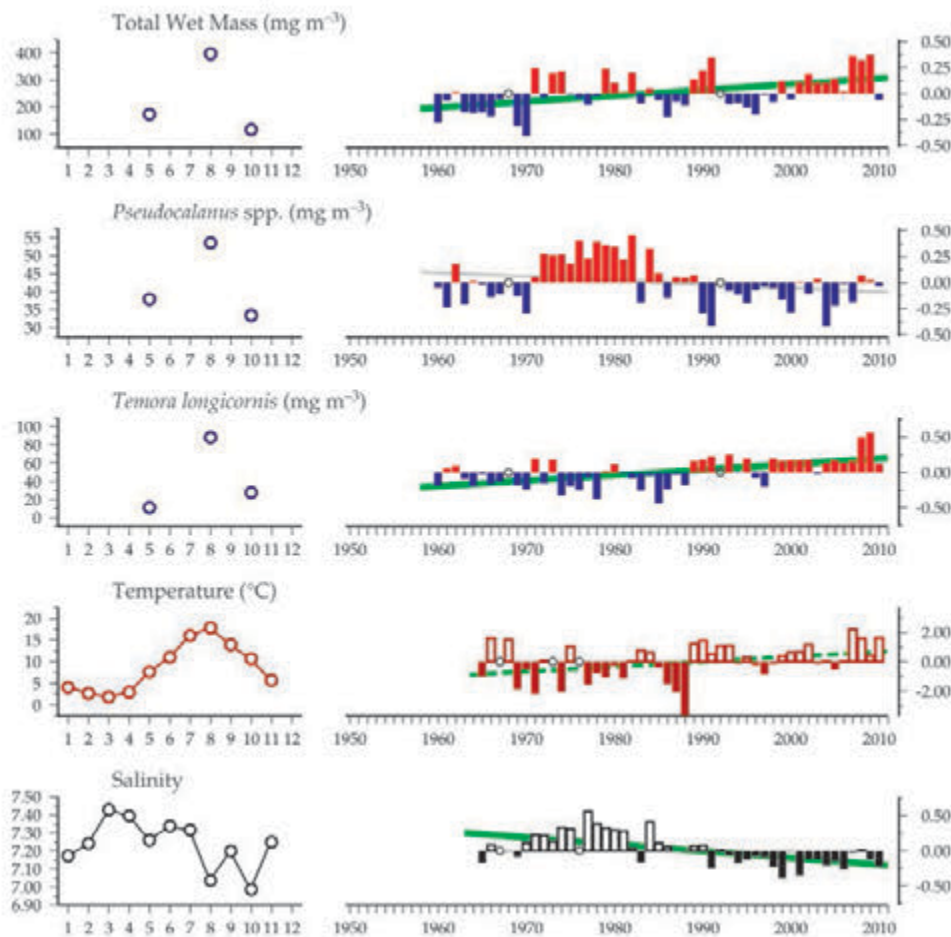


Figure 6.5.2
Multiple-variable comparison plot (see Section 2.2.2) showing the seasonal and interannual properties of select cosampled variables at the Eastern Gotland Basin monitoring area.

Additional variables are available online at: <http://WGZE.net/time-series>.

50-year trends in the Eastern Gotland Basin / central Baltic Sea region

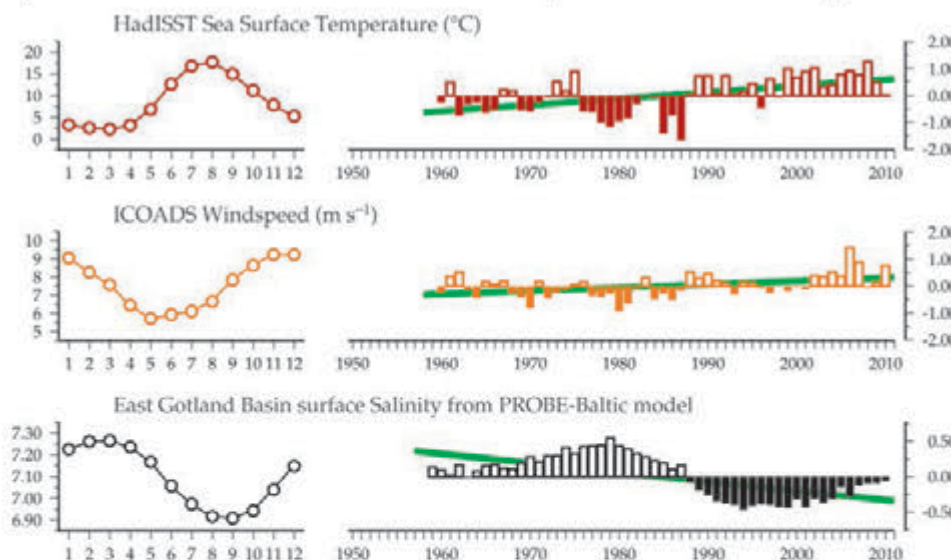
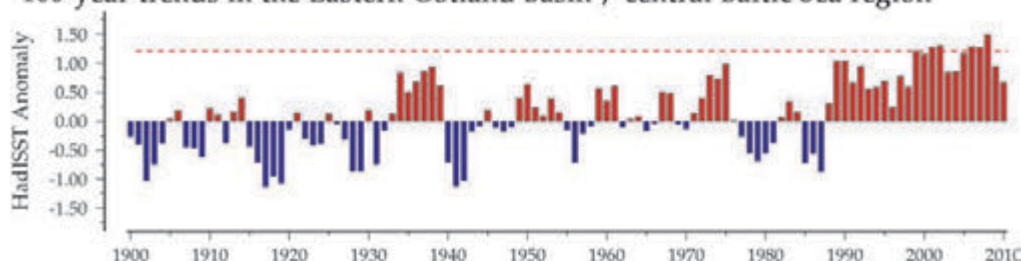


Figure 6.5.3
Regional overview plot (see Section 2.2.3) showing long-term sea surface temperatures, windspeeds, and salinity in the general region surrounding the Eastern Gotland Basin monitoring area.

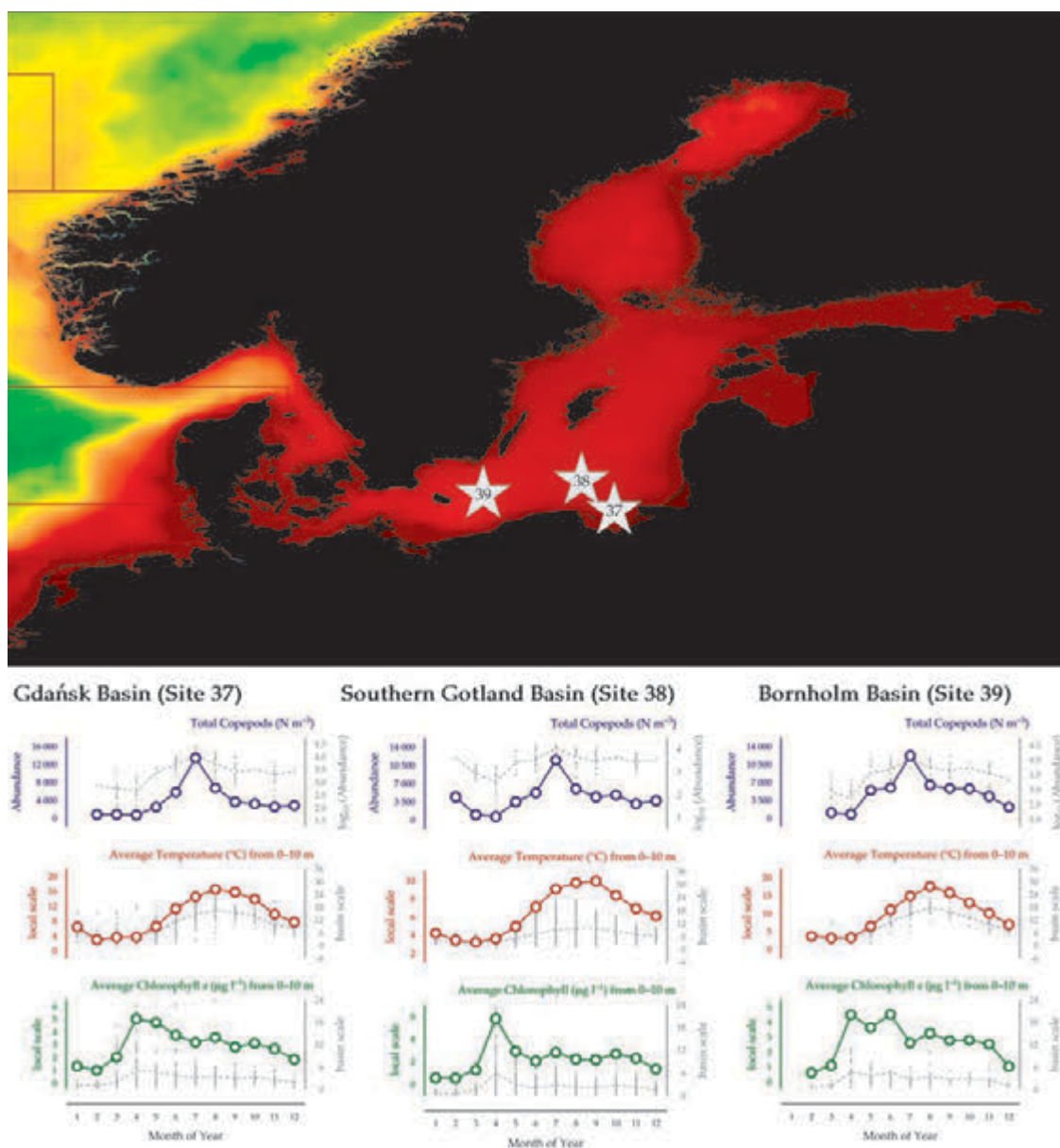
100-year trends in the Eastern Gotland Basin / central Baltic Sea region



6.6 Southern Baltic Proper (Sites 37–39)

Piotr Margonski

Figure 6.6.1
Locations of Polish zoo-
plankton survey areas in
the southern Baltic Proper
(Sites 37–39), and their
corresponding seasonal
summary plot (see Section
2.2.1).



Zooplankton samples are collected within the Baltic Sea HELCOM COMBINE Monitoring Programme. The Maritime Branch of the Institute of Meteorology and Water Management is responsible for collecting the samples along the southern coast of the Baltic Sea (in the Polish EEZ); over the thirty years of monitoring, zooplankton has been analyzed by several experts working in various institutions.

The dataset starts in 1979 with two stations located in the Bornholm Basin (Site 39) and southern Gotland Basin (Site 38). Since 1986, samples have also been taken at the station located in the Gdansk Basin (Site 37). In the same year, the location of the southern Gotland Basin station was shifted.

Samples are taken following the guidelines of the Manual for Marine Monitoring in the COMBINE Programme of

HELCOM (especially Annex C-7: Mesozooplankton), which means that vertical hauls of the WP-2 net with 100 µm mesh size are used. Stratified samples (presented here as an average of the whole water column) were collected in the layers from the bottom to the halocline (included); from the top of the halocline to the thermocline (included); and from the top of the thermocline to the surface. Preservation (4% formaldehyde solution) as well as subsampling and lab analyses are carried out according to the HELCOM guidelines. The frequency of sampling varied in time (3–6 times per year), but spring and summer conditions can be described for each year. Data from years 1998 and 2000–2001 are still missing in the database. In addition, zooplankton samples were not taken at the station located in the Bornholm Basin during the period 2002–2006.

Seasonal and interannual trends (Figures 6.6.2–6.6.6)

In the Gdansk Basin (Figure 6.6.2), a clear trend in the near-surface temperature (positive) and salinity (negative) is evident. Changes in hydrological forcing were, most probably, influencing the decrease in *Pseudocalanus minutus* abundance (a copepod that prefers higher-salinity waters) and increasing presence of other copepods such as *Acartia longiremis* and *Temora longicornis*.

In the Bornholm Basin (Figure 6.6.4), there is an increasing trend in surface temperature, but the pattern in salinity is not so obvious. Nevertheless, since the beginning of the 1990s, mostly negative anomalies in salinity are evident, with a possible reversed trend over the last few years. Positive anomalies in temperature dominated the last decade. Despite the observed year-to-year variation, trends in copepod abundance and biomass are similar to those observed in the Gdansk Basin and the southern Gotland Basin.

In the southern Gotland Basin (Figure 6.6.3), strong year-to-year variation in the abundance of *T. longicornis* and *A. longiremis* has been observed. Here, total copepod abundance is decreasing due to the significant decrease in *P. minutus*.

Long-term surface temperature trends in all three regions present a modest, but consistent increase over the last 50 years (Figure 6.6.5). Within the 100+ year extended time-series, temperatures have been near or above the 100-year maximum (red dashed line, Figure 6.6.6) since the 1990s.

Acknowledgements

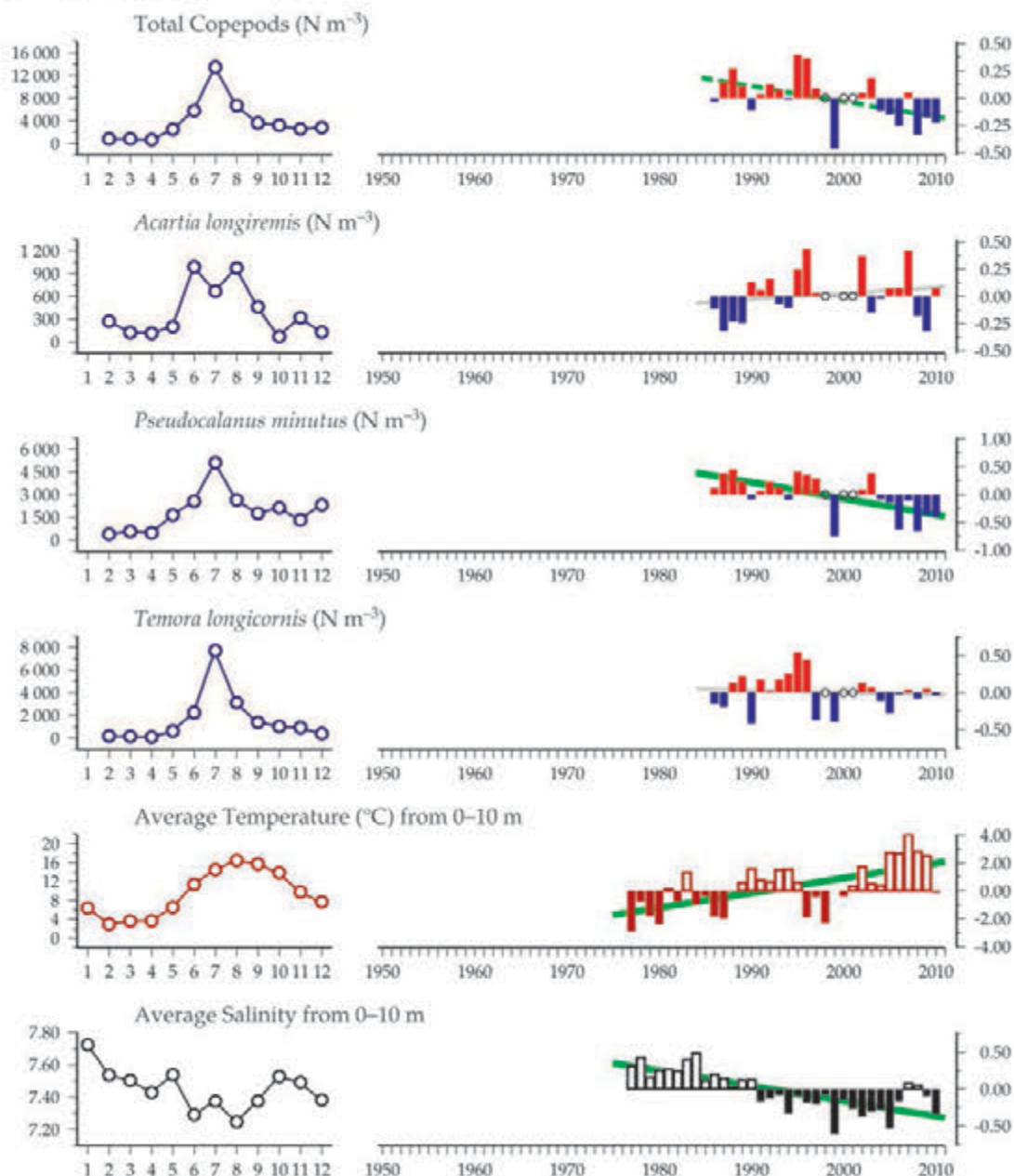
Data were collected within the Polish National Monitoring Programme, and permission to present them was granted by the Chief Inspector of Environmental Protection (<http://www.gios.gov.pl/>).

Figure 6.6.2

Multiple-variable comparison plot (see Section 2.2.2) showing the seasonal and interannual properties of select cosampled variables at the Gdańsk Basin monitoring area.

Additional variables are available online at: <http://WGZE.net/time-series>.

Gdańsk Basin (Site 37)



Southern Gotland Basin (Site 38)

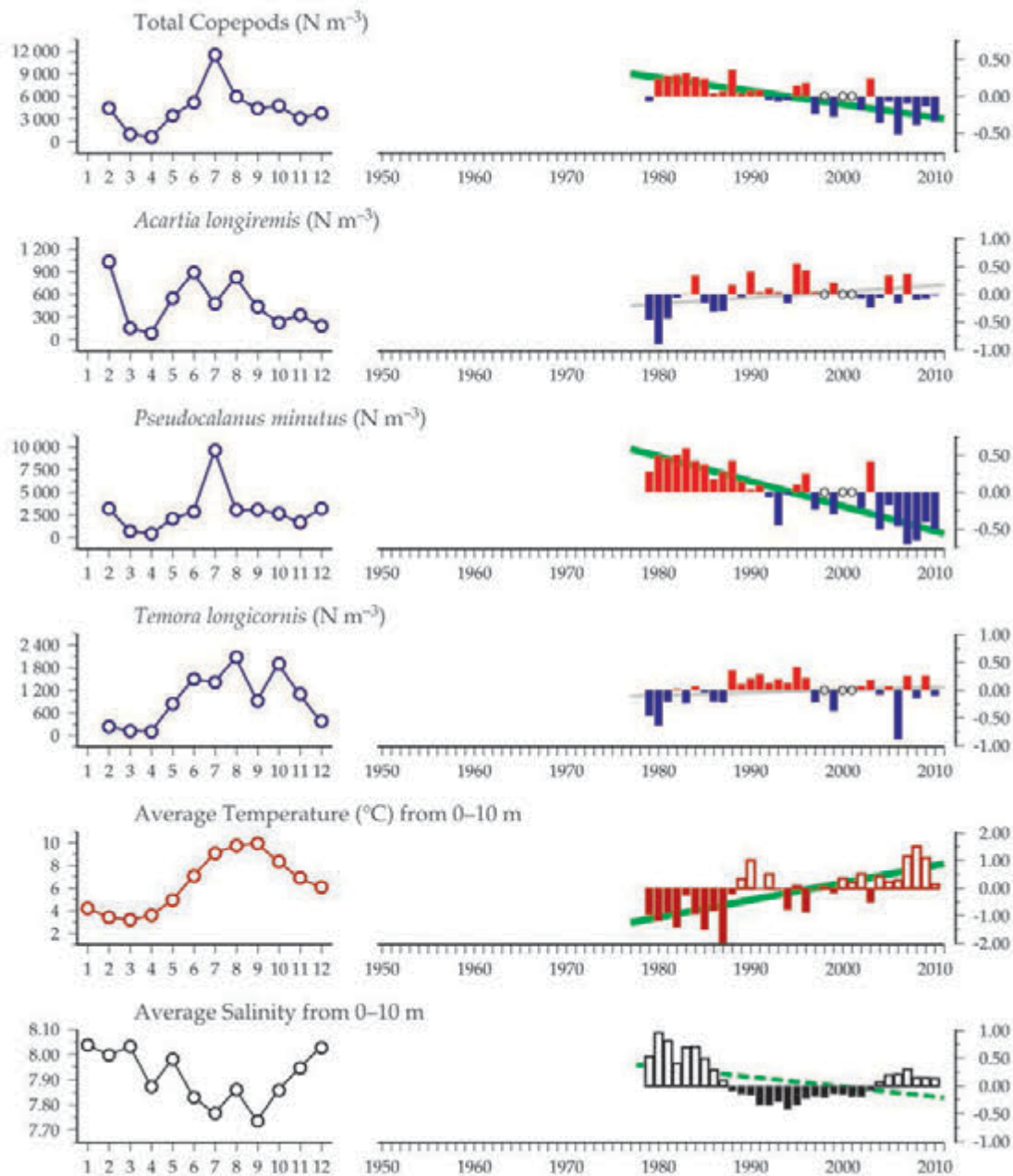
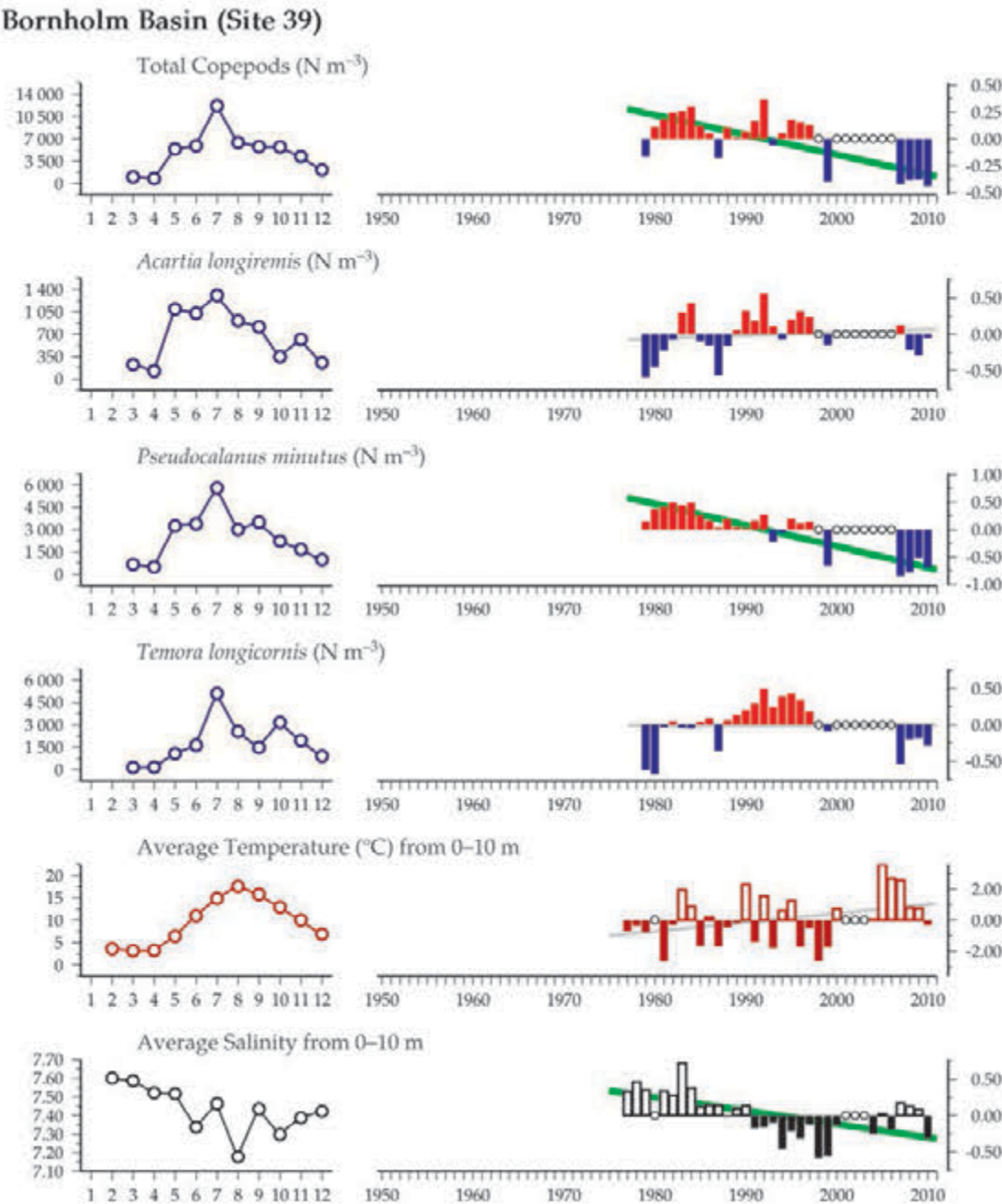


Figure 6.6.3
Multiple-variable comparison plot (see Section 2.2.2) showing the seasonal and interannual properties of select cosampled variables at the southern Gotland Basin monitoring area.

Additional variables are available online at: <http://WGZE.net/time-series>.

Figure 6.6.4
Multiple-variable
comparison plot (see
Section 2.2.2) showing the
seasonal and interannual
properties of select
cosampled variables at the
Bornholm Basin monitoring
area.

Additional variables are
available online at: <http://WGZE.net/time-series>.



50-year trends in the Gdańsk Basin / southern Baltic Proper region

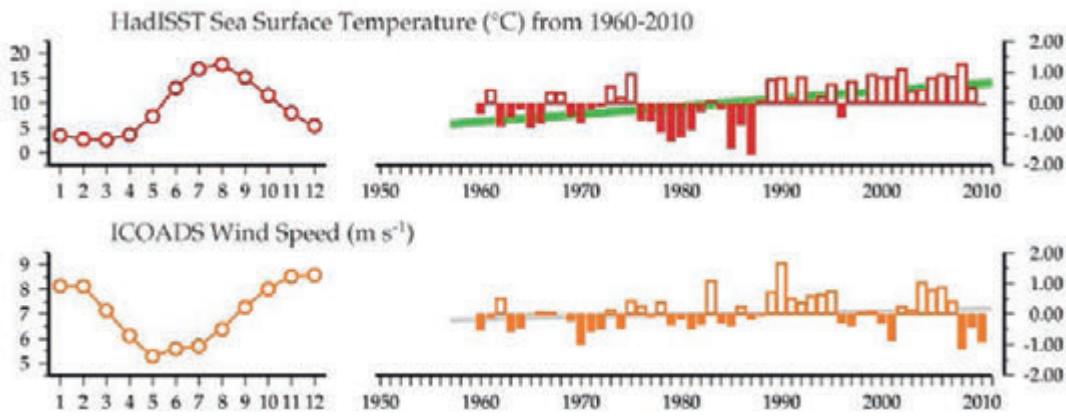
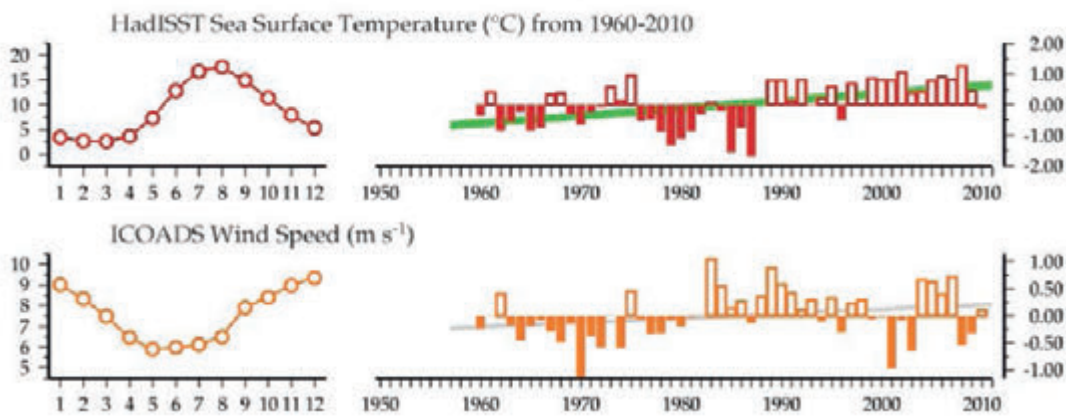


Figure 6.6.5
Regional overview plot
(see Section 2.2.3) showing
long-term sea surface
temperatures and wind
speeds in the general region
surrounding the southern
Baltic Proper monitoring
areas.

50-year trends in the Southern Gotland Basin / southern Baltic Proper region



50-year trends in the Bornholm Basin / southern Baltic Proper region

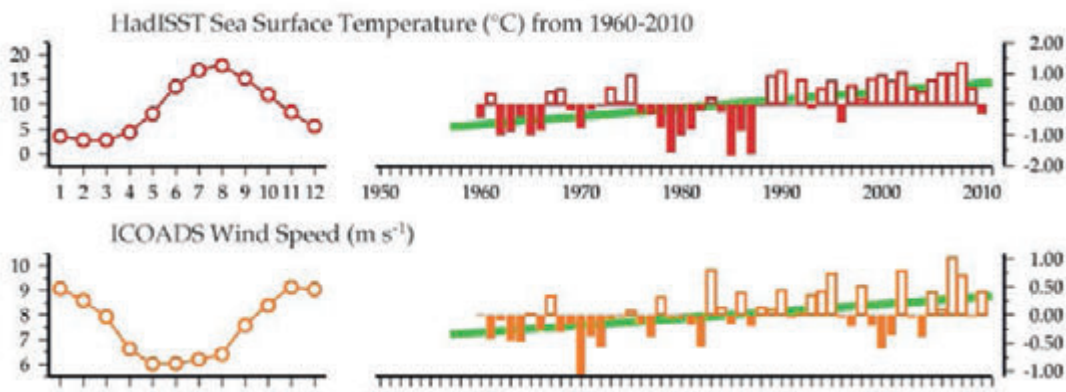
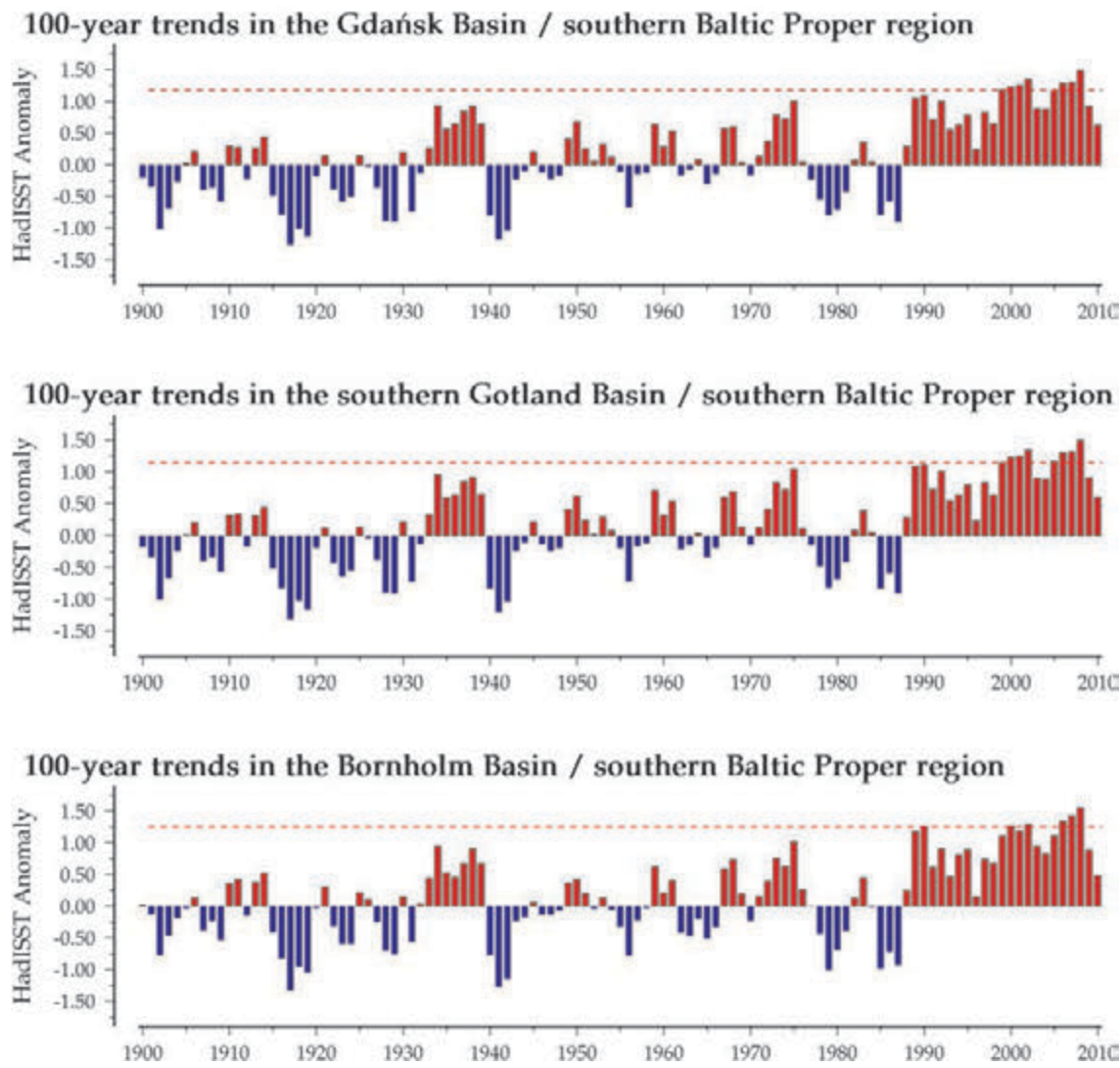


Figure 6.6.6
Regional overview plot
(see Section 2.2.3)
showing 100-year sea
surface temperatures in
the general region
surrounding the Southern
Baltic Proper monitoring
areas.



6.7 Arkona Basin (Site 40)

Lutz Postel and Norbert Wasmund

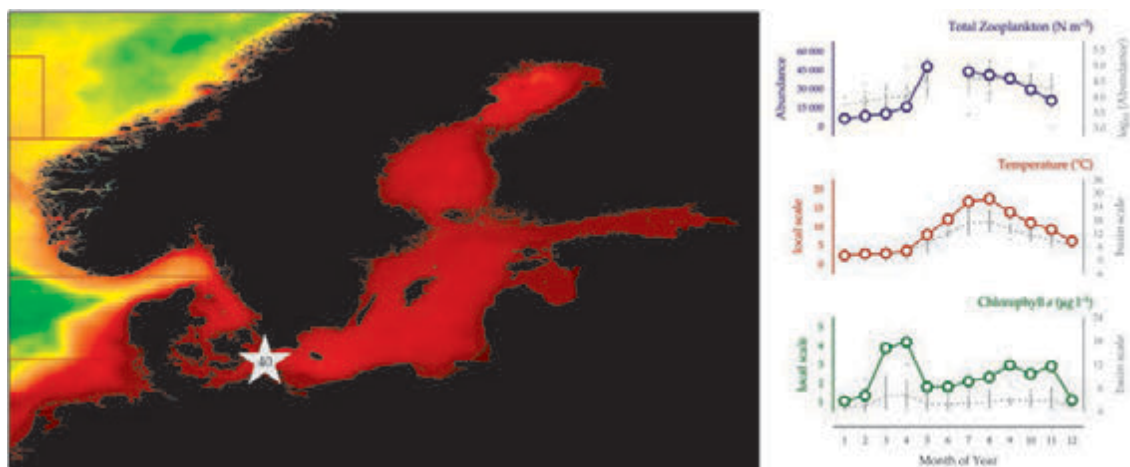


Figure 6.7.1
Location of the Arkona Basin monitoring area (Site 40) plotted on a map of average chlorophyll concentration, and its corresponding seasonal summary plot (see Section 2.2.1).

The Arkona Basin site (54°55'N 13°30'E) is one of six German monitoring stations in the Baltic (Figure 6.7.1). At this site, zooplankton are collected five times a year using a WP-2 net (57 cm diameter, 100 µm mesh) and sampling from the surface to an average depth of 25 m. Although sampling began in 1979, some years have been poorly sampled or completely missed (e.g. 1990 and 1996). Chlorophyll is collected at standard depths and averaged for the 0–10 m layer at three locations surrounding the zooplankton sampling station.

Seasonal and interannual trends (Figure 6.7.2)

Maximum zooplankton abundance occurs in May–August. The mesozooplankton community is dominated by *Acartia* spp. and *Pseudocalanus* spp. nauplii in early spring, followed by meroplanktonic larvae (polychaetes) in March. *Temora longicornis* nauplii and rotifers then dominate during early May, whereas the summer communities are dominated by bivalve larvae. Chlorophyll concentrations at the Arkona Basin site are usually high, with concentrations of more than 2 µg l⁻¹ during most of the year, reaching 6 µg l⁻¹ during the spring bloom.

Mass development of rotifer populations in spring is responsible for the annual peaks in total zooplankton abundance seen in some years (e.g. 1981, 1988, 1997, and 2008), particularly in those springs following a mild winter. During summer, when water temperatures exceed 16°C, the cladoceran *Bosmina* spp. becomes the dominant species.

From a biogeographical point of view, the Arkona Basin and the Mecklenburg Bay zooplankton communities reflect a transition between the dominating marine species assemblage in the western Baltic Sea and the euryhaline and brackish-water taxa in the Baltic Proper (cf. Postel, 2012). Long-term variability is caused by salinity and temperature influences as well as by the trophic interactions and state of the Baltic Sea (Flinkman and Postel, 2009).

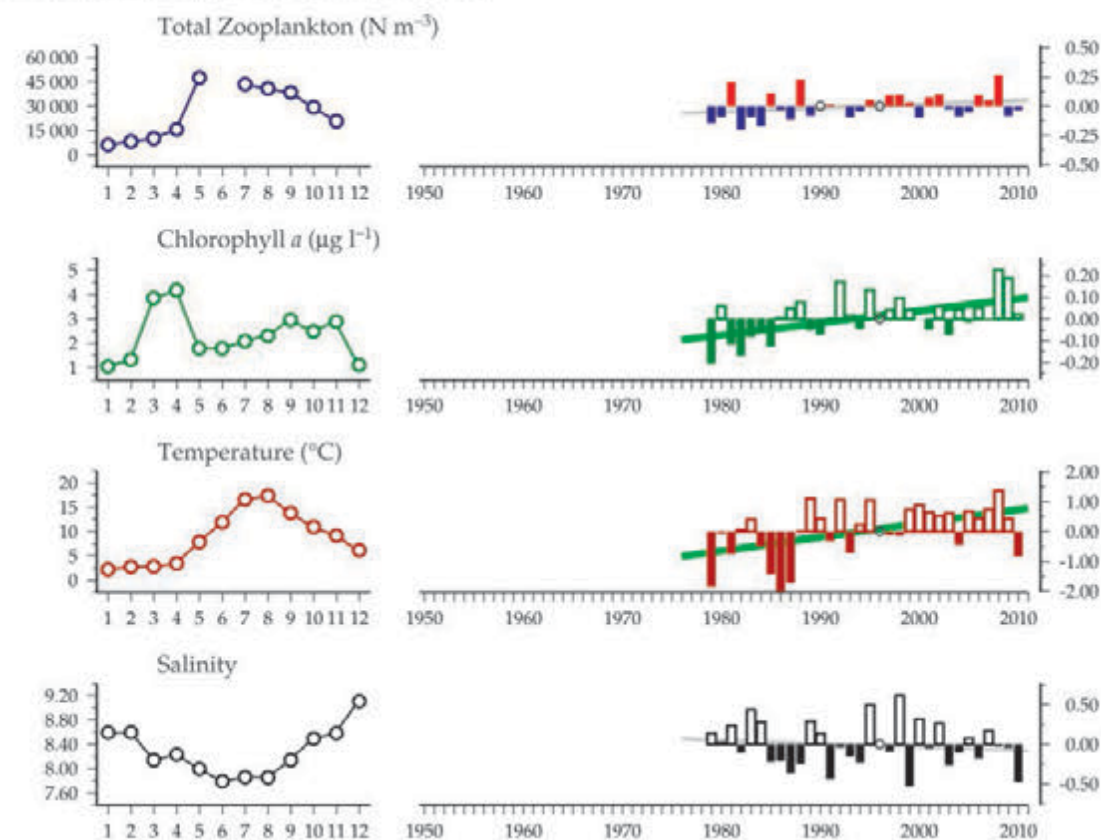
Water temperature and chlorophyll have a significant positive trend, but zooplankton abundance has been varying about the long-term mean with a modest positive trend since the beginning of the time-series in 1979 (Figure 6.7.2). The 100+ year record of regional SST values reveals that, since 1999, this region has experienced a particularly warm period, with temperatures frequently higher than the 100-year maximum observed prior to 2000 (Figure 6.7.3, red dashed line).

Figure 6.7.2

Multiple-variable comparison plot (see Section 2.2.2) showing the seasonal and interannual properties of select cosampled variables at the Arkona Basin monitoring area.

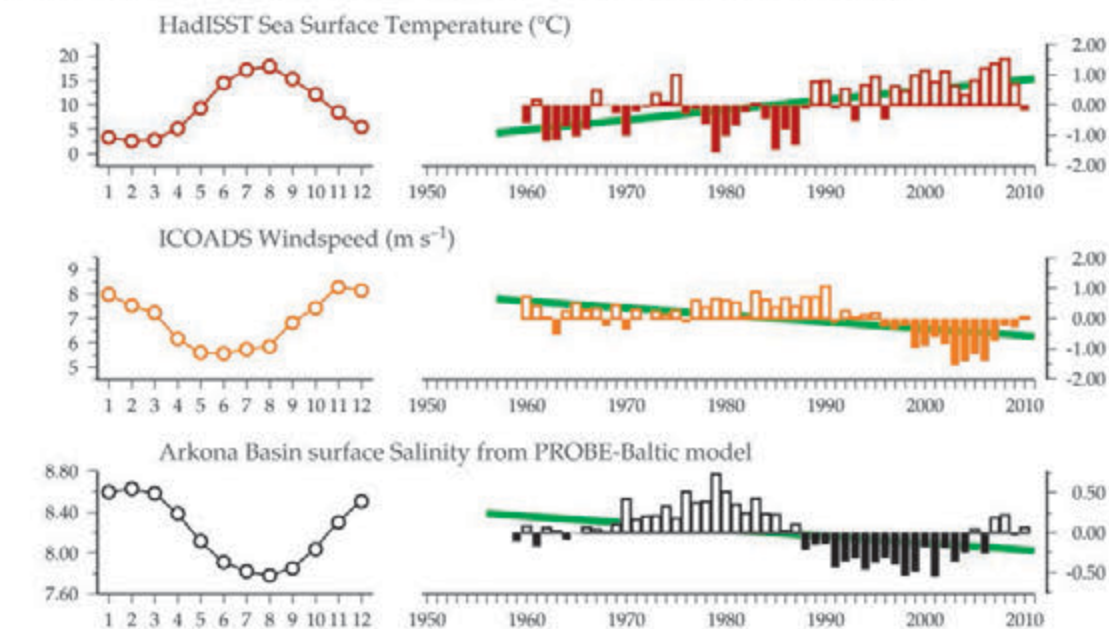
Additional variables are available online at: <http://WGZE.net/time-series>.

Arkona Basin, southern Baltic Sea

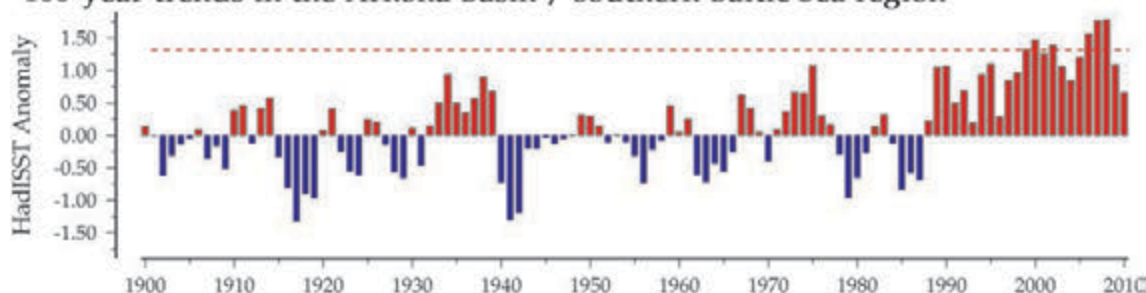
**Figure 6.7.3**

Regional overview plot (see Section 2.2.3) showing long-term sea surface temperatures, windspeeds, and salinity in the general region surrounding the Arkona Basin monitoring area.

50-year trends in the Arkona Basin / southern Baltic Sea region



100-year trends in the Arkona Basin / southern Baltic Sea region



6.8 Kattegat and Skagerrak (Sites 41–43)

Lars Johan Hansson and Marie Johansen

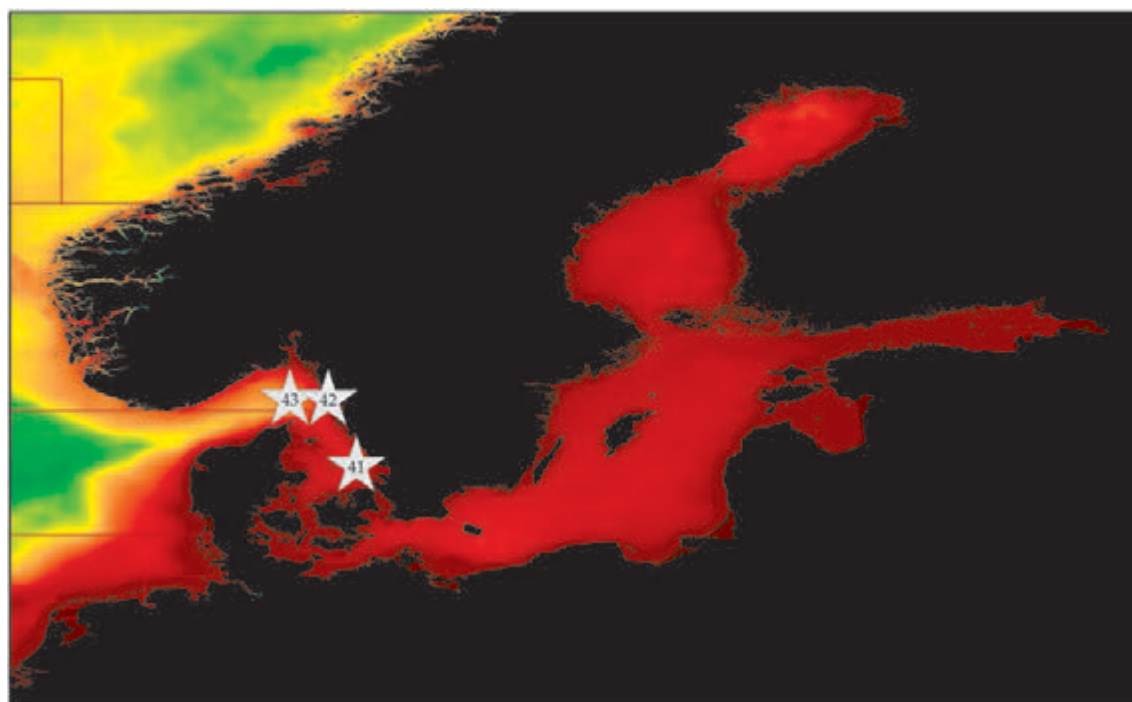
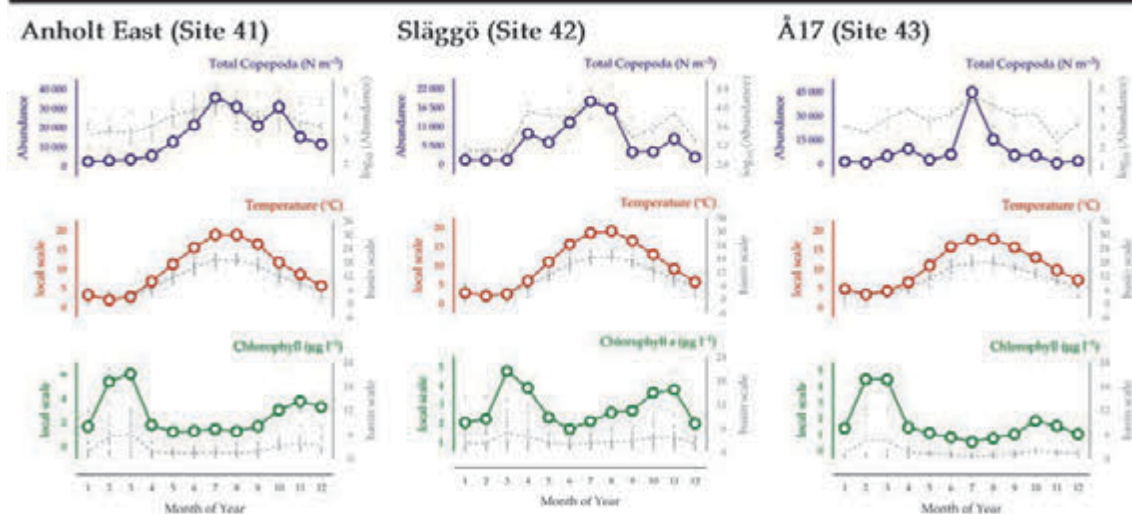


Figure 6.8.1
Locations of the Swedish Meteorological and Hydrological Institute (SMHI) survey areas in the Kattegat and Skagerrak region (Sites 41–43), and their corresponding seasonal summary plot (see Section 2.2.1).



The Kattegat is the transition area between the Baltic and North seas. It is included as part of the Baltic Sea in the HELCOM Convention area, but also as part of the North Sea in the OSPAR Convention. The mean depth is only ca. 20 m, and half the area has a depth of < 25 m (Fonselius, 1995), although the maximum depth exceeds 90 m at the northern Skagerrak boundary. Close to the Swedish coastline, it has a connection with Skagerrak deep water through a deeper channel with elongated basins that run in a mainly north–south direction. The Kattegat has a strong halocline, with an average salinity of around 23 in the upper part (0–15 m) and ca. 32–33 in the deep water (below 60–80 m; Dyrssen, 1993). Surface water generally comes from the low saline Baltic Proper

via the Danish straits, whereas the North Sea delivers deeper, more saline waters from the north. The Baltic outflow from the Danish straits coalesces in the eastern Kattegat to form the north-flowing Baltic Current. At the northern limit of the Kattegat, North Sea water from the Jutland Coastal Current splits, with some flowing as a bottom current into the Kattegat, whereas the remainder eventually combines with the Baltic Current, which is further augmented by significant freshwater outflows as it becomes the Norwegian Coastal Current in the Skagerrak. The Kattegat, thereby, forms a hydrographic transition zone between the Baltic Sea and the North Sea, with a substantially higher salinity range (and variability) than in nearby sea areas.

In the frame of the international monitoring programme of the Helsinki Commission (HELCOM), two stations are sampled by SMHI (Swedish Meteorological and Hydrological Institute) in the Kattegat; Anholt East (Site 41, 56°40'N 12°07'E) and N14 Falkenberg (56°56.40'N 12°12.7'E); and two stations are sampled in the Skagerrak Släggö (Site 42, 58°15.5'N 11°26'E) and Å17 (Site 43, 58°16.5'N 10°30.8'E). Of these four stations, N14 Falkenberg has only been sampled for a couple of years and is not included in the map or figures.

Sampling and sample processing are conducted according to the HELCOM COMBINE manual for zooplankton (HELCOM, 2010). Zooplankton are sampled using a WP-2 net with 180 µm mesh towed from 25 m to the surface. Formalin-preserved samples are often split into smaller fractions during analysis. All individuals are taxonomically identified to the lowest possible level, but are presented as genus in the graphs. This report will focus on the copepods as they constitute the most common group of zooplankton found in the samples and are an important link between autotrophic plankton and fish.

Seasonal and interannual trends (Figure 6.8.2)

Across all of the sites, total copepod abundance is low until around April when it increases at a near-constant rate to its maximum level during summer (see Figure 6.8.1, lower panel). This seasonal maximum is followed by a strong decrease to low winter abundance. This

overall development correlates well with sea surface temperature. Seasonal patterns and the magnitude of temperatures across the three sites were comparable. Chlorophyll concentrations exhibited a large March peak, followed by a significantly smaller October/November peak.

An examination of interannual trends was only possible within the longer running Anholt East site. From 1998 to 2010, there was an overall decrease in total copepods, with the greatest decrease starting around 2004–2005. This abrupt 2004–2005 shift is evident in most of the copepod species, especially within the genera *Centropages*, *Oithona*, and *Paracalanus*, all of which have had a constant downward trend over the sampling period. In contrast, the large copepod genus *Calanus*, whose abundance was quite low in the Kattegat area, shows a steady increase over the data period. While clear trends were present in most of the copepod species at Anholt East, trends in the underlying hydrographic and phytoplankton data were inconclusive (see the ICES Phytoplankton and Microbial Plankton Status Report, O'Brien *et al.*, 2012), attributed to both the relative shortness of the time-series along with the dynamic hydrographic conditions of the region. Looking at longer-term time-series products and model output from the larger Kattegat region (see Figure 6.8.3), the 1998–2010 trends in the Anholt East copepods fall cleanly within a period of increasing water temperatures, surface winds, and salinity.

Figure 6.8.2.
Multiple-variable comparison plot (see Section 2.2.2) showing the seasonal and interannual properties of select cosampled variables at the Anholt East (Site 41) monitoring area.

Additional variables are available online at: <http://WGZE.net/time-series>.

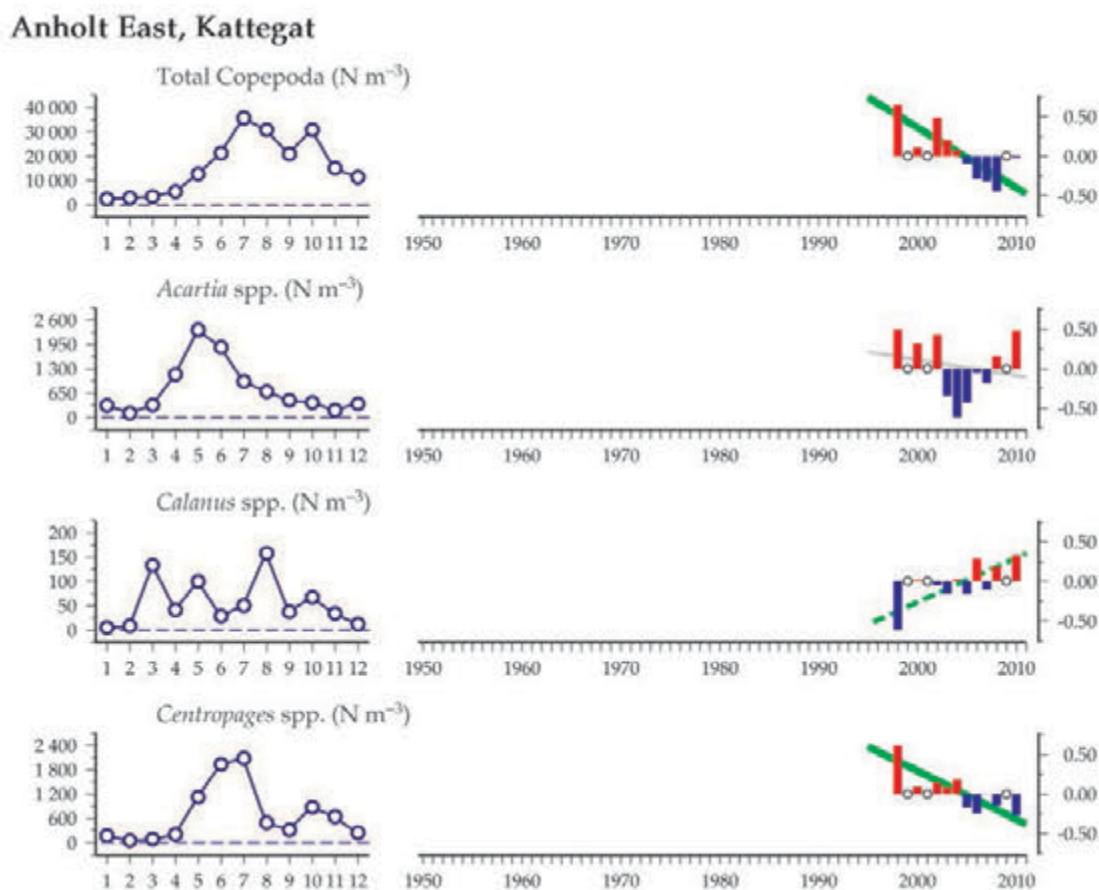


Figure 6.8.2
continued

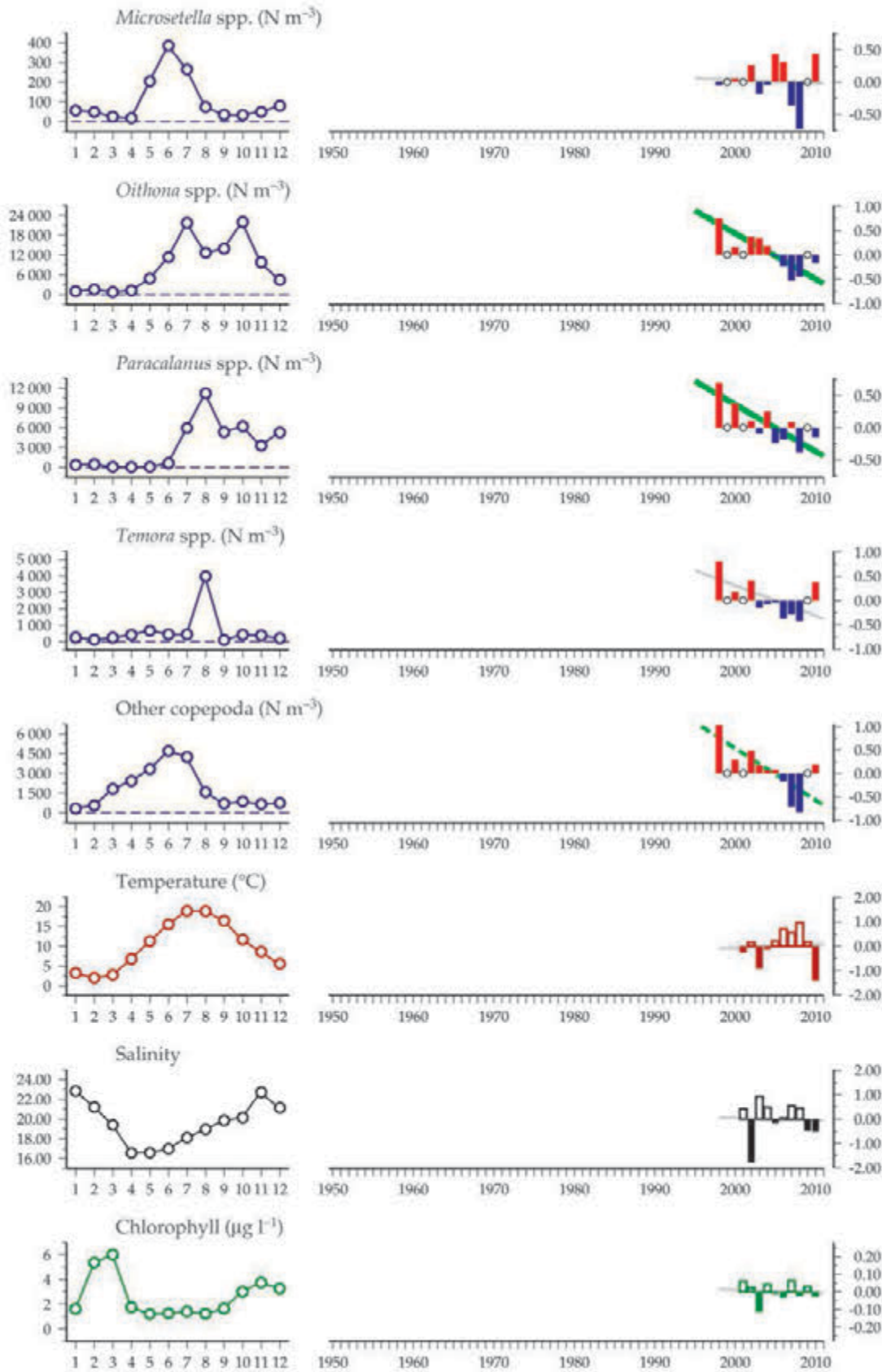
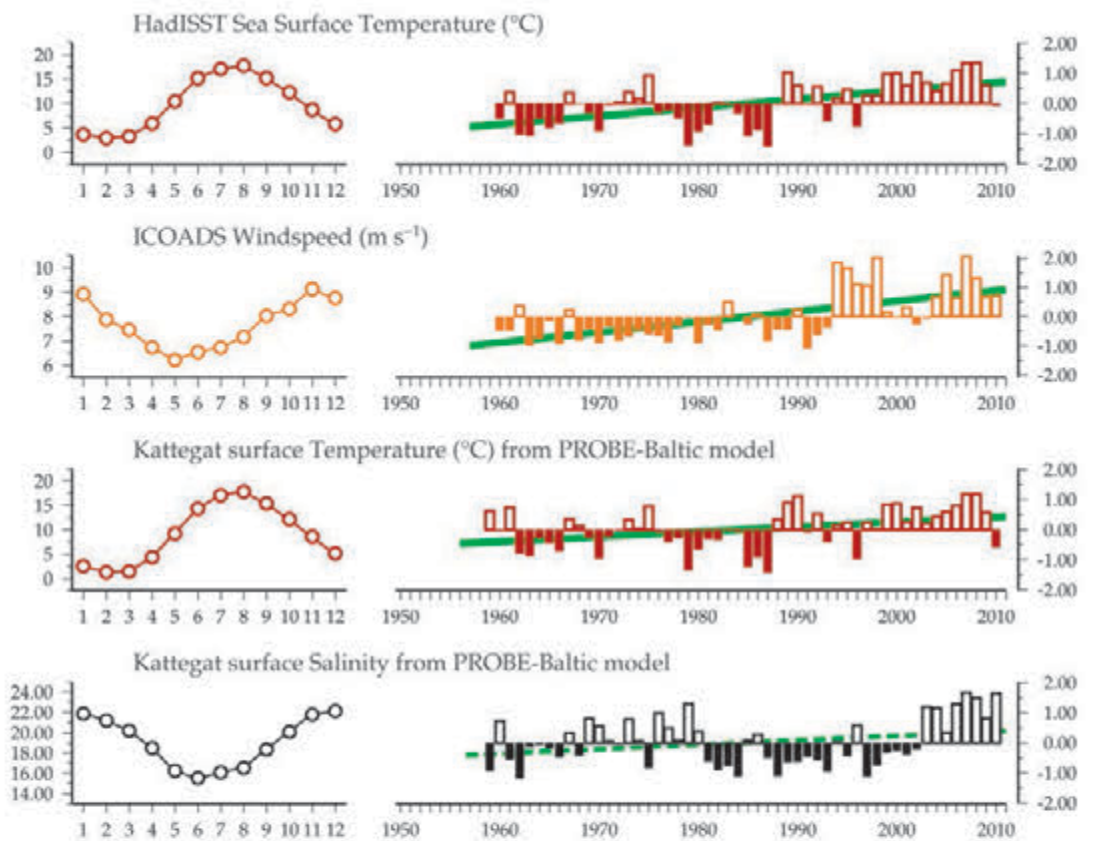
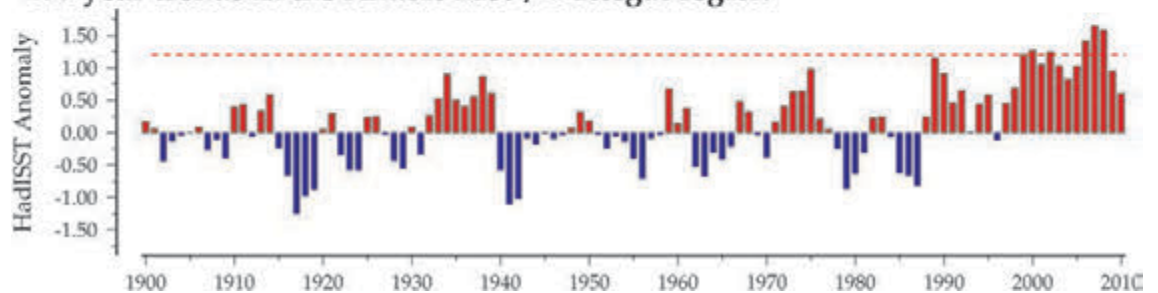


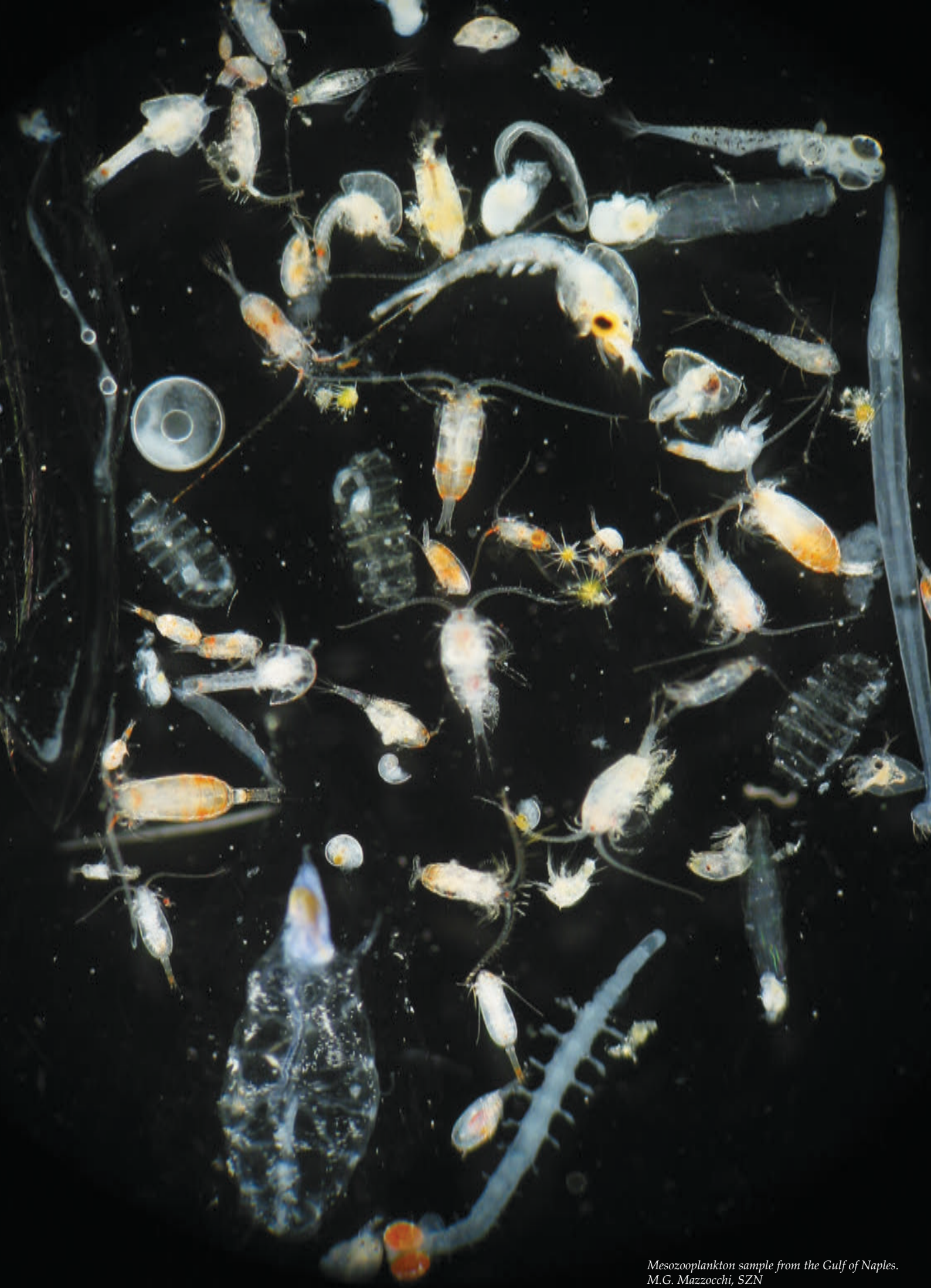
Figure 6.8.3
Regional overview plot
(see Section 2.2.3) showing
long-term sea surface
temperatures, windspeeds,
and salinity in the general
region surrounding the
Anholt East monitoring
area.

50-year trends in the Anholt East / Kattegat region



100-year trends in the Anholt East / Kattegat region





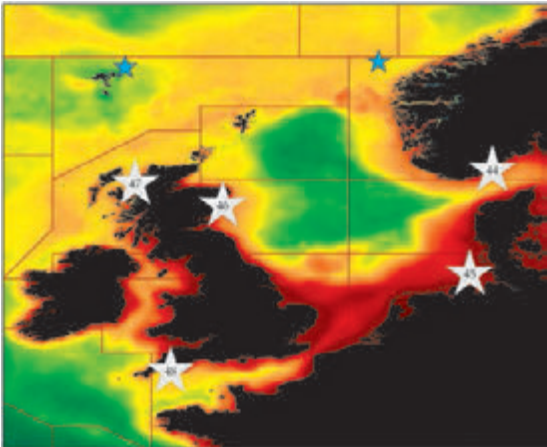
*Mesozooplankton sample from the Gulf of Naples.
M.G. Mazzocchi, SZN*

7Z OOPLANKTON OF THE NORTH SEA AND ENGLISH CHANNEL

Tone Falkenhaug, Lena Omli, Maarten Boersma, Jasmin Renz, Kathryn Cook, Angus Atkinson, Elaine Fileman, Claire Widdicombe, Rachel Harmer, Andrea McEvoy, Roger Harris, Tim Smyth, and Steve Hay

Figure 7
Locations of the North Sea and English Channel survey areas (Sites 44–48) plotted on a map of average chlorophyll concentration (see Section 2.3.2).

Blue stars indicate sites discussed in other chapters of this report.



Site ID	Monitoring Site (Region)	Section
44	Arendal Station 2 (northern Skagerrak)	7.1
45	Helgoland Roads (southeastern North Sea)	7.2
46	Stonehaven (northwestern North Sea)	7.3
47	Loch Ewe (Scottish west coast)	7.4
48	Plymouth L4 (western English Channel)	7.5

The North Sea and English Channel (Figure 6.1) are classified by Longhurst (1998) as part of the Northeast Atlantic Shelf Province (NASP). This extends from northern Spain to Denmark and is separated from the Atlantic Subarctic Region by the Faroe–Shetland Channel and the Norwegian Trench. The NASP follows the classic seasonal pattern for temperate regions: well-mixed conditions in winter, when nutrients are replenished and light is limited; a strong spring bloom, becoming nutrient-limited as summer stratification sets in; and a more or less pronounced secondary bloom during autumn, as increased mixing breaks down the thermocline to release nutrient supplies. This general pattern is often broken up by locally strong tidal and shelf fronts (Pingree and Griffiths, 1978), where primary and secondary production is often enhanced, and may lead to subsurface blooms, at times extensive. The zooplankton in the shelf areas of the region is a characteristic mixture of neritic species, with strong seasonal components of benthic larvae (meroplankton; Beaugrand *et al.*, 2002a, 2002b; Vezzulli and Reid, 2003) and occasional and temporary influxes of oceanic species. Several of the common neritic species overwinter as resting stages, whereas other holoplankton species remain more or less active all year. There are also substantial problems with harmful algal blooms, alien-species introductions, and local areas with evidence of eutrophication, all influencing the zooplankton ecology in the region.

The north-flowing Continental Slope Current in the west, flowing off the Iberian Peninsula, carries oceanic plankton communities (Lusitanian fauna) that become entrained to

varying degrees into the coastal seas. Evidence suggests a strengthening of this influx in recent years. These mixed coastal and oceanic waters form influxes into the Bay of Biscay, the Celtic and Irish seas, and through the English Channel into the shallow southern North Sea, where the flow is eastward along the continental margin. These mixed waters and plankton are also carried into the Irish and Scottish western shelf seas and form major inflows into the deeper basin of the northern North Sea via the Fair Isle inflow and inflows east of the Shetland Isles. The northern North Sea is a fairly deep basin, which shelves in the west to the Scottish mainland and northern islands, with the deep Norwegian Trench in the east shelving into the fjordic coast of Norway. The deeper northern basin shallows distinctly into the central and southern North Sea, where prominent topographic features are Dogger Bank in the west, and the Skagerrak and entrance to the Baltic Sea in the east. The residual North Sea circulation is cyclonic, with inputs from the surface outflow of the low-salinity Baltic Sea in the east and from major rivers and coastal estuaries. The whole empties northwards along the Norwegian coast, following the Norwegian Trench northwards into the Norwegian Sea.

Surrounded by active and prosperous countries, this maritime region provides a wide range of ecosystem services (e.g. fish and shellfish harvests, energy production, transport, and tourism) and, historically, is perhaps the most studied marine area on earth. In addition to the venerable and comprehensive monthly series of Continuous Plankton Recorder (CPR) surveys

(conducted since before 1948), there are significant coastal time-series of plankton collections and environmental data. The main time-series that sample zooplankton are: Helgoland Roads (German Bight; since 1975), Plymouth L4 (western English Channel; since 1988), Dove (western central North Sea; since the mid-1970s), Stonehaven (northwestern North Sea; since 1997), Arendal (eastern central North Sea; since 1994), and the new Loch Ewe station (northwest Scotland; since 2002).

Analysis of plankton, fisheries, oceanographic, and meteorological data in recent years, particularly data related to the CPR survey, demonstrates that the region has been subject to a series of regime shifts and changes associated with changes in the climate and global-ocean systems (Reid and Edwards, 2001a, 2001b; Edwards *et al.*, 2002; Beaugrand and Reid, 2003; Beaugrand *et al.*, 2003; Alheit *et al.*, 2005; Alvarez-Fernandez *et al.*, 2012; Llope *et al.*, 2012). These changes in water-mass fluxes and properties, such as temperatures, mixing depths, and seasonal stratification, have seen corresponding shifts in diversity, niche ranges, and phenology of species and communities (Lindley and Batten, 2002; Lindley and Reid, 2002). Such changes have also been seen in fish, and, in general, they mirror the often less dramatic climate effects on terrestrial ecosystems and species.

The combination of climate change and overfishing in the North Sea has seen shifts in the patterns of foodweb fluxes and productivity in recent years. Changes in plankton production, biodiversity, species distribution, community composition, and phenology are related to effects on fish and other species. Changes in the structure and functioning of the pelagic foodweb will also affect the carbon cycle and the rate of downward transport of carbon to the adjacent deep ocean (North Sea continental carbon pump; Beaugrand *et al.*, 2010).

Most of these changes are correlated with shifts in climate indices, such as the North Atlantic Oscillation (NAO), particularly with northern hemisphere temperature, which has been increasing for >30 years and warming the European continental shelf surface waters. Many plankton and fish species have demonstrated northward shifts in distributions in the Northeast Atlantic region (some by >1000 km) over the past 50 years (Edwards *et al.*, 2001, 2002; Reid and Edwards, 2001a; Beaugrand, 2003; Beaugrand *et al.*, 2002b; Beaugrand and Reid, 2003; Brander *et al.*, 2003; Edwards and Richardson, 2004; Genner *et al.*, 2004; Richardson and Schoeman, 2004; Southward *et al.*, 2004; Alheit *et al.*, 2005; Brander, 2005; Heath, 2005; Leterme *et al.*, 2008).

Some examples include 40 years of declining abundance and northward retreat of the northern boreal copepod *Calanus finmarchicus*, with simultaneous increase in its southern temperate congener *Calanus helgolandicus*. Since the 1960s, the previously dominant biomass of *C. finmarchicus* in the North Sea, declined by 70% as the 10°C isotherm moved northwards by more than 21 km year⁻¹ (Helaouët and Beaugrand, 2007). Seasonal and interannual changes in the relative abundance of meroplankton larvae of benthic invertebrates have been observed (Kirby and Lindley, 2005). There have been indications

of increased jellyfish abundance (Lynam *et al.*, 2005; Attrill *et al.*, 2007), with notable increases and incursions of the oceanic scyphozoan *Pelagia noctiluca* into western shelf areas, causing mortalities in farmed salmon (*Salmo salar*) (Licandro *et al.*, 2010). Some species, such as the dinoflagellate *Ceratium*, have demonstrated dramatically reduced abundance in recent years (Edwards *et al.*, 2009). Appearances of “alien” species have been noted, such as the voracious ctenophore *Mnemiopsis leidyi* (Oliveira, 2007) and the cladoceran *Penilia avirostris* (Johns *et al.*, 2005) in the Baltic Sea and in northern European coastal waters, from Dutch waters to as far north as southern Norway.

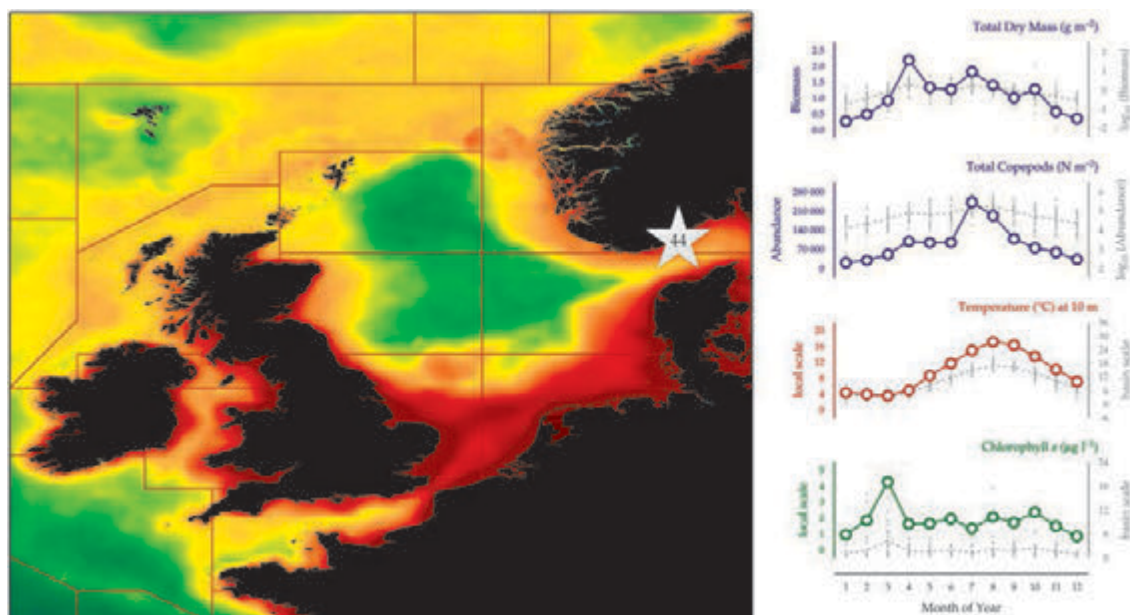
Species declines, losses, shifts, introductions, and an increased presence of invertebrate predators are occurring in the North Sea. These changes influence recruitment, mortality, and resource supply to the benthos and to higher predators such as pelagic and demersal fish, seabirds, and mammals (Lindley *et al.*, 2002; Heath, 2005; Frederiksen *et al.*, 2006). Changes affect and propagate through foodwebs, with potentially critical mismatches between predators and prey (Burthe *et al.*, 2012). Brander (2005) has demonstrated that declining cod (*Gadus morhua*) populations, while affected by fishing pressure, may also be responding to changes in availability of zooplankton food for their larvae. Although these climate-related changes form a general pattern in the Northeast Atlantic, there are regional differences, with the southern North Sea warming faster than the deeper northern basin. There is variability among species in their sensitivities, adaptive capabilities, and responses. It is becoming increasingly evident that future changes in plankton populations will affect ecosystem services ranging from biogeochemical cycles to the survival and production of fish, birds, and mammals.

The winter NAO index has been in a low negative phase during the last couple of years, contributing to cold winters in northern Europe during 2009/2010 and 2010/2011. Negative temperature anomalies were observed on all the monitoring sites in this region in 2010, which was reflected in the zooplankton composition at some sites. Although many changes in North Sea zooplankton are correlated with the NAO index and temperature, different and sometimes opposite trends in zooplankton interannual fluctuation have been observed at the monitoring sites in this region, and the variations do not always correlate with trends in the CPR data. This may be explained by different sampling methods, but also suggests that local conditions modify the relationship between climatic conditions and the year-to-year fluctuations of zooplankton.

7.1 Arendal Station 2 (Site 44)

Tone Falkenhaug and Lena Omli

Figure 7.1.1
Location of the Arendal Station monitoring area (Site 44) plotted on a map of average chlorophyll concentration, and its corresponding seasonal summary plot (see Section 2.2.1).



The Arendal sampling site (northern Skagerrak) is located at 58°23'N 8°49'E, approximately 1 nautical mile offshore from the Flødevigen Research Station (Norwegian Institute of Marine Research, IMR) off southern Norway (Figure 7.1.1). The water depth at the site is 105 m. Sampling for hydrographic parameters and abundance of phytoplankton and zooplankton (biomass and species) has been carried out twice a month since January 1994. The sampling programme is part of the Norwegian Coastal Long-term Monitoring Programme of Environmental Quality. The objective of the programme is to monitor the environmental status in coastal waters and to document changes in the plankton communities.

Zooplankton is sampled fortnightly with a WP-2 net (56 cm diameter, 180 μm mesh) towed vertically from a depth of 50 m to the surface. Each sample is split in half, providing data on both species composition–abundance and biomass. During the first period of the time-series (1994–1999), copepods were identified into three main taxonomic groups (*Calanus* spp., other calanoid copepods, and cyclopoid copepods). From 2000 onwards, all copepods are identified to species or genus level.

Seasonal and interannual trends (Figure 7.1.2)

The Arendal sampling site is influenced by relatively fresh coastal waters (25–32 psu) in the upper 30 m and by saltier Skagerrak water (32–35 psu) in the greater depths. Water movement is generally westward and is caused by the coastal current bringing low-salinity water from the Baltic Sea and Kattegat. The site is also influenced by Atlantic water (>35 psu) advected from the Norwegian Sea into the Skagerrak Deep during winter. Together, these influxes

create a relatively large seasonal cycle in salinity (Figure 7.1.2). The seasonal minimum temperature in the surface layer generally occurs in February (2°C) and the maximum in August (>20°C). At 75 m, the variation is less pronounced (minimum 4°C in February–March to maximum 14°C in August–September). Although the water column is mixed throughout winter, increased freshwater run-off causes a strong halocline to appear from February/March to June. A spring bloom usually occurs in April–March, dominated by diatoms. Chlorophyll values are generally low during summer (May–August), followed by an autumn bloom of dinoflagellates in August–September. In summer, the water remains stratified because of surface heating. During the past 20 years, a trend towards higher temperatures has been observed in the Skagerrak, both in surface and deeper layers. Since 2001, water temperatures in the region have been higher than those seen in the past 100 years (Figure 7.1.4). About 70% of the water entering the North Sea is assumed to pass through the Skagerrak before it leaves the North Sea, and thus many of the hydrographic events taking place in the North Sea will be reflected in this area.

At the Arendal site, the zooplankton biomass is dominated by copepods. The seasonal maximum in zooplankton biomass generally occurs in April–May (Figure 7.1.2), with a secondary, smaller peak occurring in July–August. The annual spring peak in zooplankton biomass is dominated by *Calanus finmarchicus*, whereas the secondary peak (July–August) is dominated by smaller copepods (*Para-* and *Pseudocalanus*, *Oithona*, *Acartia*, *Temora*). The important common copepod genus, *Calanus*, is represented by three species at the Arendal sampling site: *C. finmarchicus*, *C. helgolandicus*, and *C. hyperboreus*.

C. finmarchicus is the most abundant species during spring. This species overwinters in the Skagerrak Deep (Norwegian Trench, 20 nautical miles farther offshore from this station). Interannual variability in overwinter survival and advection is likely to affect the population dynamics. *C. helgolandicus* generally occurs in smaller numbers than *C. finmarchicus*, although the proportion of *C. helgolandicus* increases from spring (< 10%) to autumn (>80%). *C. hyperboreus* is rarely observed in spring (March–April) and is associated with the influx of Atlantic water from the Norwegian Sea.

Large interannual differences can be seen in the observed biomass of zooplankton, with maximum values in 2003 and minimum values in 1998. A general increase in biomass and copepod abundance was observed from 1998 to 2003, but a lesser abundance overall was observed in 2004–2010 (Figure 7.1.2). Values for the monthly mean copepod abundance by year reveal that years with negative annual anomaly (2004–2010) are characterized by low abundance of copepods in the late summer peak (July–August). This is mainly caused by the reduced abundance of the copepods *Oithona* spp. and the *Para-* and *Pseudocalanus* spp. in the period 2004–2010 (Figures 7.1.2 and 7.1.3).

The CPR standard area nearest to the Arendal site is B1. The CPR copepod data correspond well with the observed interannual trend in total copepods on Arendal, with positive anomalies in 1999–2003, and low or negative anomalies prior to and after this period. In 2010, however, the annual total copepod abundance in the CPR data was above average, which is in contrast with the observed copepod abundance at Arendal, which has been below average since 2006.

The invasive ctenophore species *Mnemiopsis leidyi* was observed in Skagerrak for the first time in 2006. During 2007–2009, the species occurred in high densities at Arendal Station 2 in late summer–autumn, but with lower abundance in 2010 and few observations in 2011–2012. The seasonal peak of *M. leidyi* coincides with maximum temperatures in the surface water (>20°C), which occur after the seasonal maximum in zooplankton abundance.

Arendal Station 2, northern Skagerrak

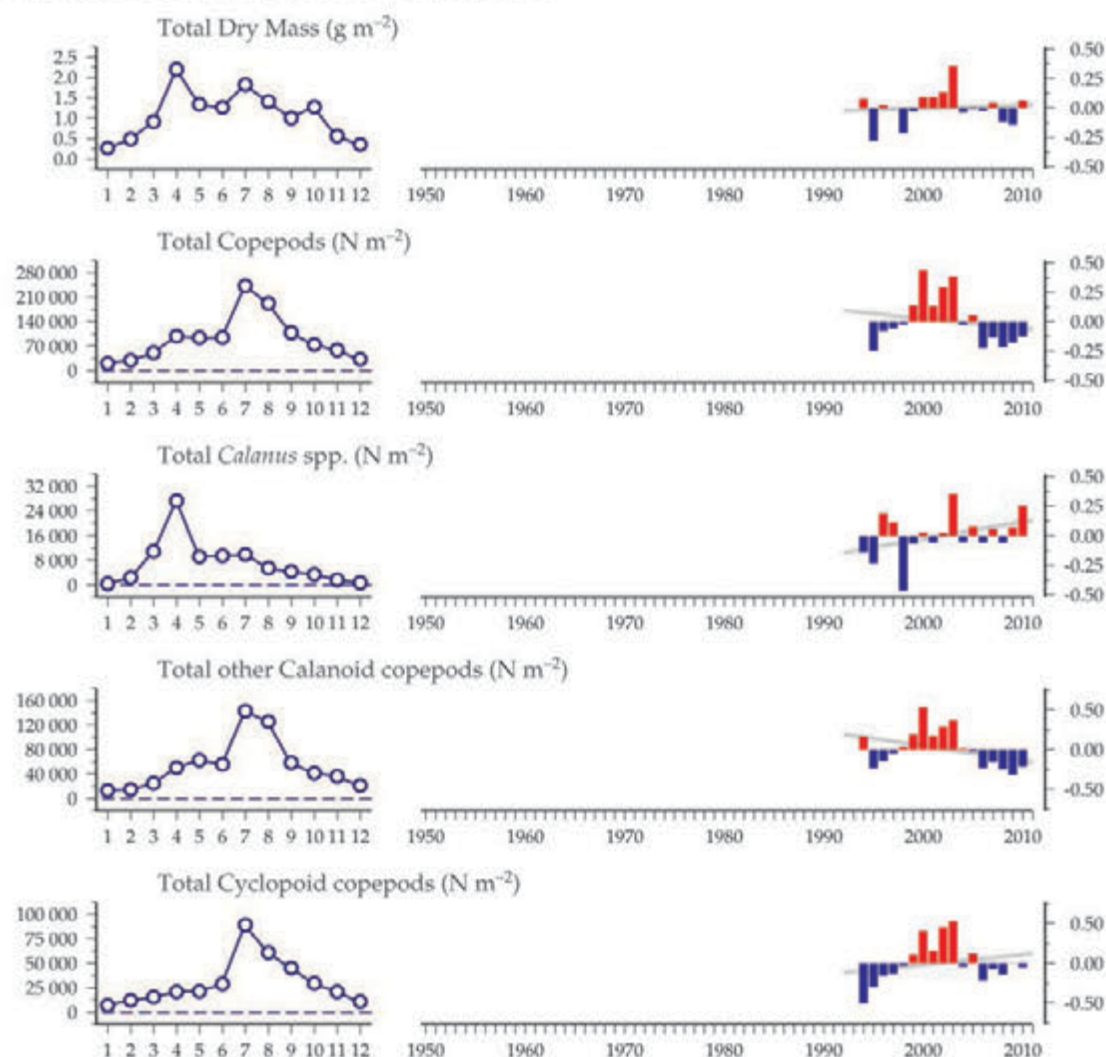
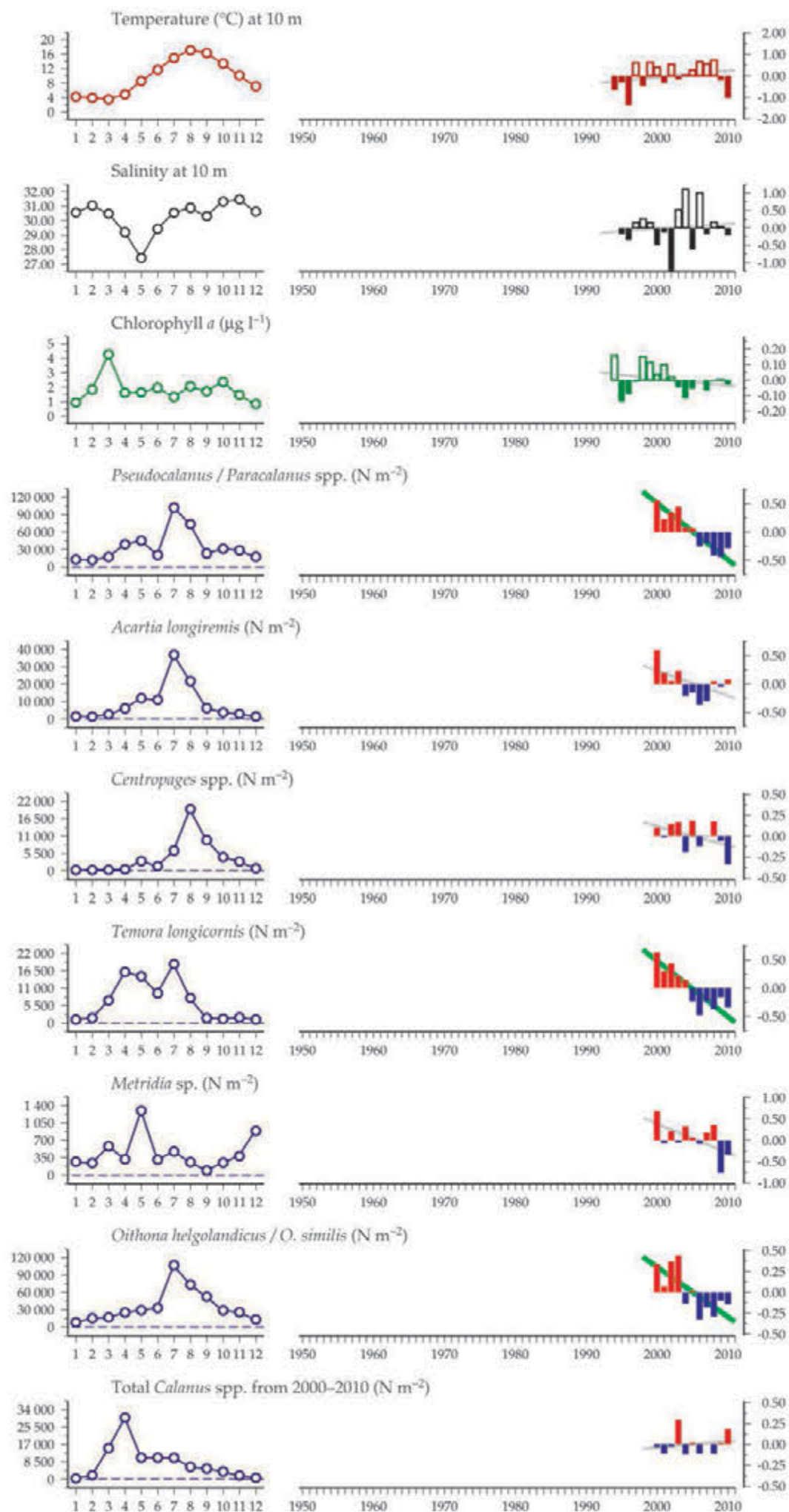


Figure 7.1.2
Multiple-variable comparison plot (see Section 2.2.2) showing the seasonal and interannual properties of select cosampled variables at the Arendal Station 2 monitoring area.

Additional variables are available online at: <http://WGZE.net/time-series>.

Figure 7.1.2
continued

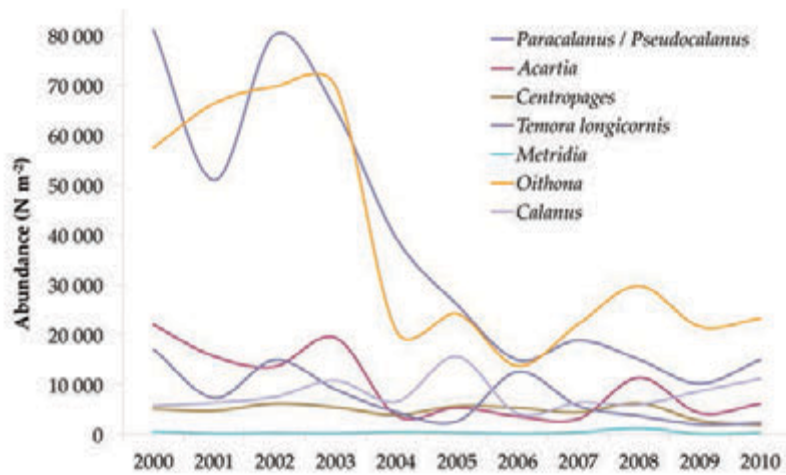


Figure 7.1.3
Annual average abundance
of eight major copepod
genera at Arendal Station 2.

50-year trends in the Arendal Station / northern Skagerrak region

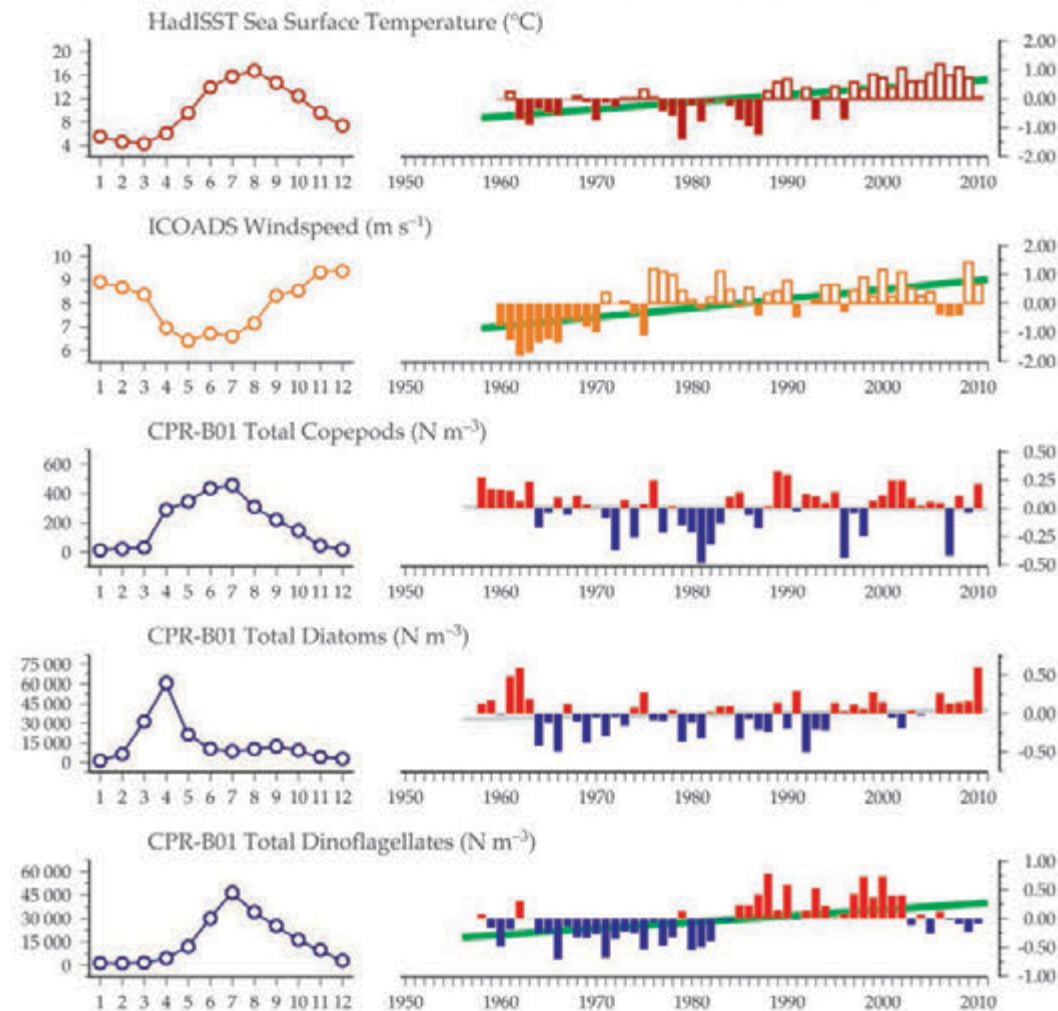
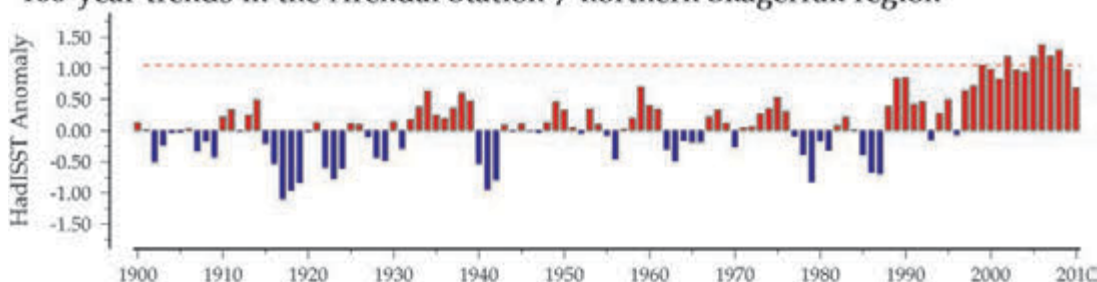


Figure 7.1.4
Regional overview plot
(see Section 2.2.3) showing
long-term sea surface
temperatures and wind
speeds in the general region
surrounding the Arendal
Station monitoring area,
along with data from
the adjacent CPR B01
Standard Area.

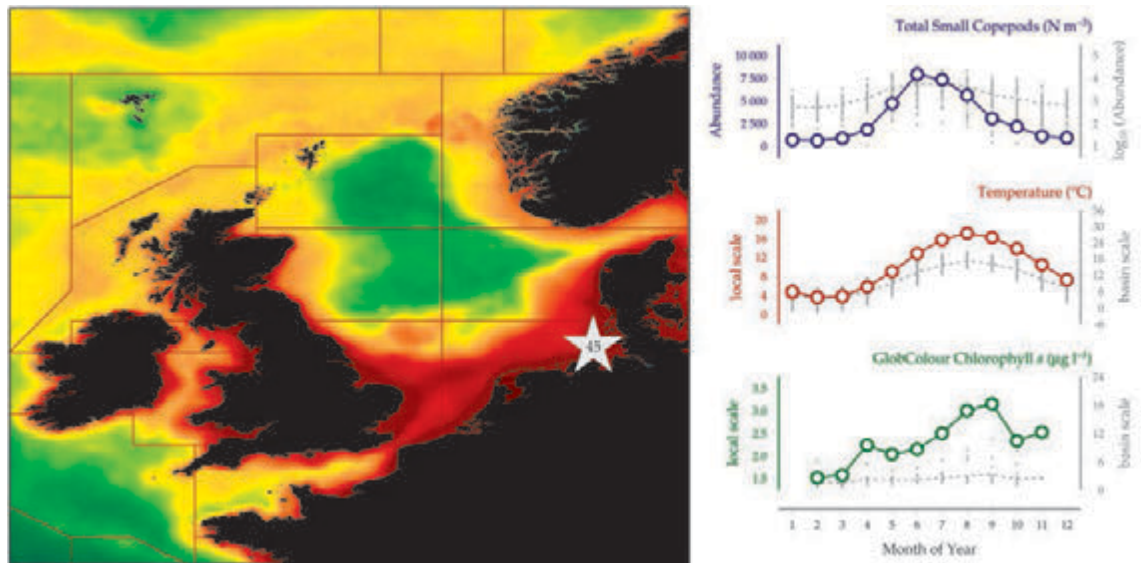
100-year trends in the Arendal Station / northern Skagerrak region



7.2 Helgoland Roads (Site 45)

Maarten Boersma and Jasmin Renz

Figure 7.2.1
Location of the Helgoland Roads monitoring area (Site 45) plotted on a map of average chlorophyll concentration, and its corresponding seasonal summary plot (see Section 2.2.1).



The island of Helgoland is located in the German Bight, approximately 60 km off the German mainland (Figure 7.2.1). The Helgoland Roads time-series is one of the richest temporal marine datasets available. It includes daily surface water sampling from 1962 until the present, resulting in a pelagic dataset comprising phytoplankton species counts, salinity, transparency (Secchi-disc depth), and macronutrient concentrations. The phytoplankton time-series was merged with the Helgoland Roads zooplankton time-series, which was started in 1974. Sampling and analysis are now carried out by the Alfred Wegener Institute for Polar- and Marine Research and the German Centre for Marine Biodiversity. Every Monday, Wednesday, and Friday, two oblique plankton net samples (150 µm, 500 µm) are collected from the monitoring site (54°11'18"N 7°54'E). From each sample, almost 400 taxonomic entities of holoplankton and meroplankton (e.g. larvae from benthic organisms and fish larvae) are identified and counted, making the Helgoland Roads time-series one of the finest zooplankton series both in taxonomic resolution as well as in temporal sampling resolution.

The purpose of the Helgoland Roads programme was and is to document high-frequency plankton population dynamics in order to detect variability and regularities in distributions, with the ultimate aim being to differentiate between different signals (natural variability and anthropogenically induced climate change). A wealth of publications is available from the site, using several analytical techniques (e.g. Heyen *et al.*, 1998; Greve *et al.*, 2001, 2004; Bonnet *et al.*, 2005, 2007; Boersma *et al.*, 2007; Malzahn and Boersma, 2007; Wiltshire *et al.*, 2008; Schlüter *et al.*, 2010).

Seasonal and interannual trends (Figure 7.2.2)

At the Helgoland Roads sampling site, small calanoid copepods, mostly *Acartia clausi*, *Temora longicornis*, and *Para-/Pseudocalanus* spp. represent a significant fraction of the total zooplankton population. Seasonal and interannual variability in the small copepods is large both in timing as well as in magnitude. Maximum densities of the small copepods can be found in mid-summer in most years and the 37-year time-series shows clear decadal variability. Starting with a negative phase at the beginning of the time-series (1975), copepod abundance increased steadily and was consistently higher than average during much of the 1980s. After a period of transition (1990–1997), copepod density decreased and remains now in a negative phase where abundance is consistently getting lower. Looking at monthly mean copepod abundance by year and the corresponding monthly anomalies, years with strong positive annual anomalies (e.g. 1983–1990) were characterized by an extended period of high abundance in mid-summer, whereas years with strong negative annual anomalies (e.g. 2006–2010) had both a shorter period and lower maximum abundance during mid-summer. In general, years with a strong positive annual anomaly correspond to positive monthly anomalies for every month in that year, with the opposite also true for years with strong negative annual anomaly. The extent of the peak abundance of these species each year is, therefore, most likely influenced by the copepod population density present through the winter months and leading up to the summer peak.

The only copepod species showing a different pattern is *Oithona* spp. (see Figure 7.2.2). This smaller, cyclopoid species usually occurs later in the season, and its abundance increased more or less steadily over the time-period from the late 1980s until 2008.

Looking at causal agents for changes within the copepod community, the general trend of negative anomalies in copepod abundance over the last century was accompanied by positive anomalies in sea surface temperature in the Helgoland region and positive anomalies in diatom and dinoflagellate concentrations (Wiltshire *et al.*, 2008; O'Brien *et al.*, 2012). Furthermore, a general shift in the size structure within the diatom community towards larger diatoms (Kraberg *et al.*, 2011) could be observed. It is, therefore, unclear whether the decreasing abundance of calanoids and concurrent increase in *Oithona* spp. is caused directly by internal physiological responses to the increasing temperature or indirectly by changes in predation and food, since e.g. *Oithona* spp., which has a different dietary preference and

is considered to have a more omnivorous feeding mode, is the only copepod increasing in abundance. Further research is, therefore, needed to identify those factors responsible for changes within the different copepod populations.

The nearest CPR Standard Area to Helgoland Roads is "D1". The relationship between water temperature and CPR copepod abundance was variable, switching from positive to negative throughout periods in the time-series. Like the Helgoland Roads data, the CPR data have also clearly entered a phase of negative and decreasing annual anomalies since 1988. Comparing Helgoland Roads to the CPR data, there seems to be a time-lagged synchrony in copepod abundance, with the Helgoland Roads abundance anomalies leading the CPR anomalies by 3–5 years. Water temperature increases around the shallow Helgoland Roads site have been more dramatic than in the North Sea as a whole, possibly causing changes in the copepod population to occur faster than those sampled in the larger water body within the CPR standard area.

Helgoland Roads, southeastern North Sea

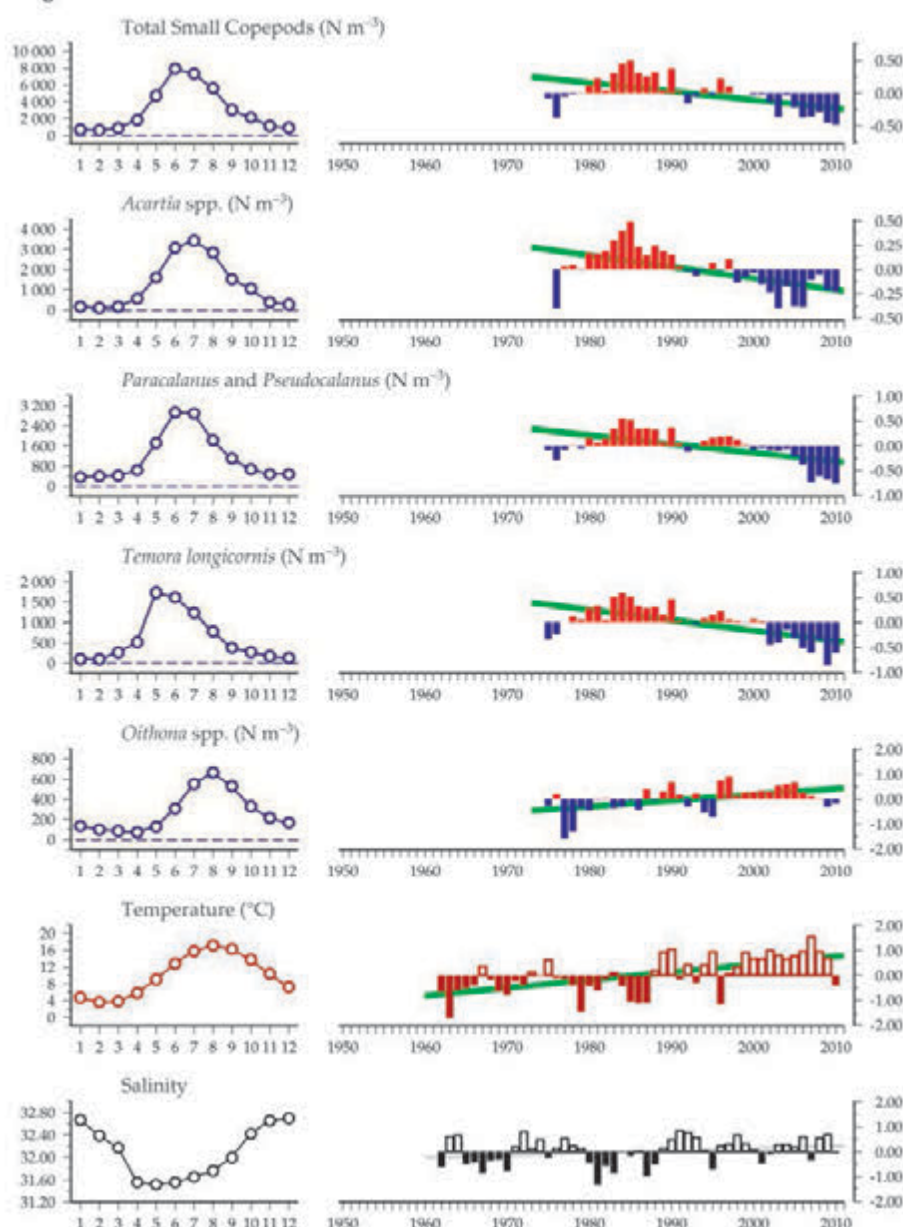
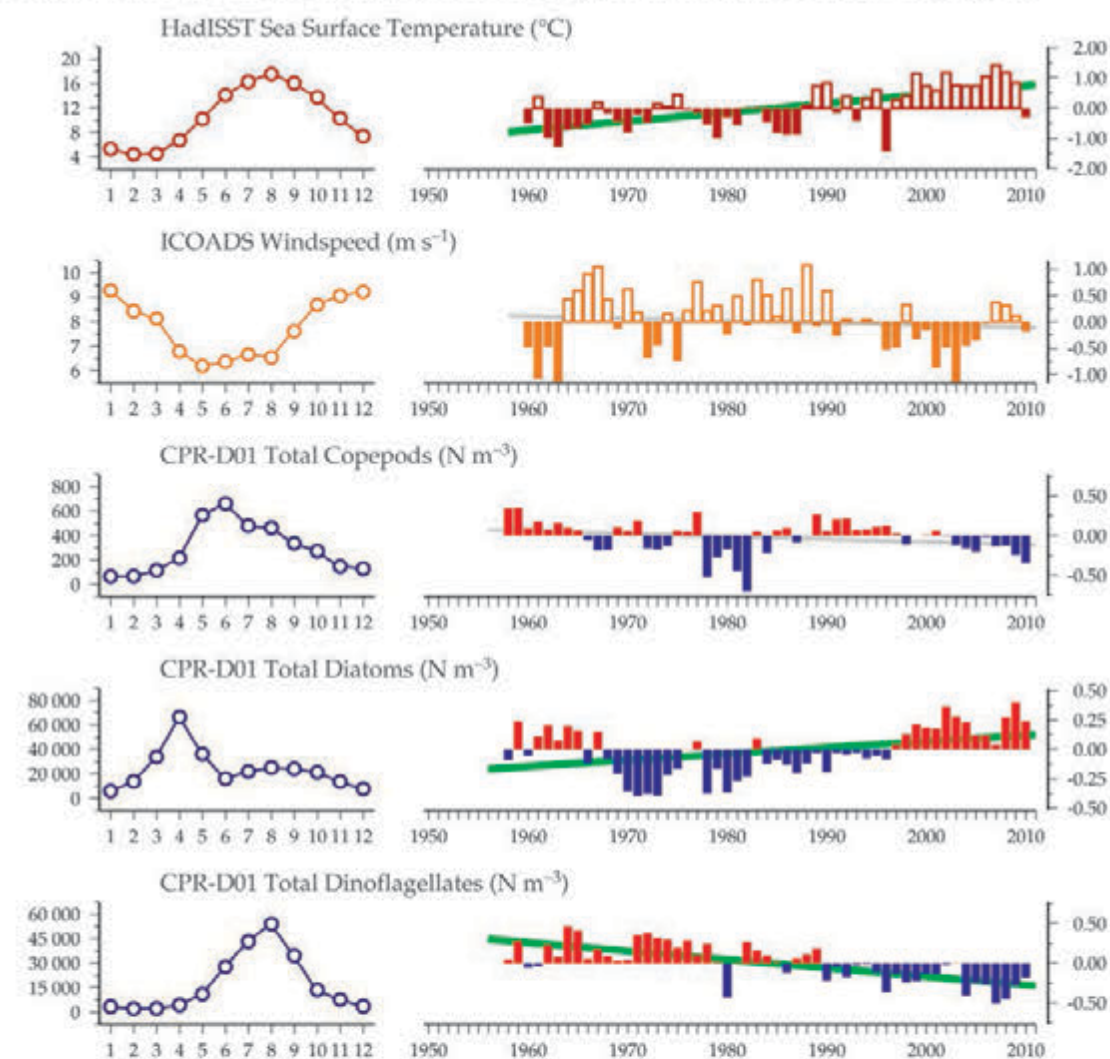


Figure 7.2.2
Multiple-variable comparison plot (see Section 2.2.2) showing the seasonal and interannual properties of select cosampled variables at the Helgoland Roads monitoring area.

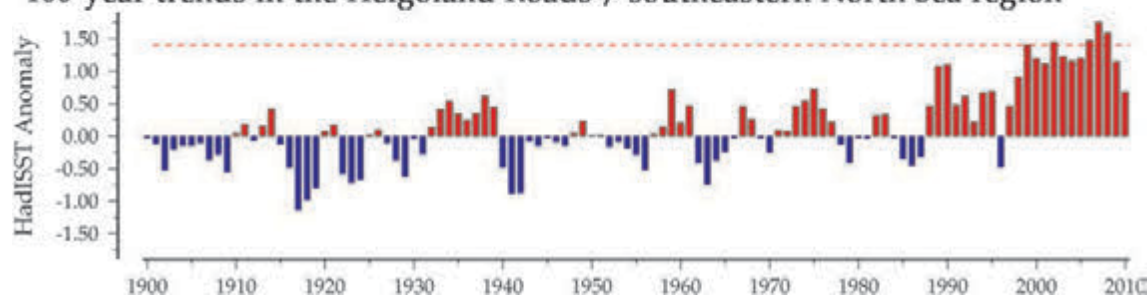
Additional variables are available online at: <http://WGZE.net/time-series>.

Figure 7.2.3
Regional overview plot
(see Section 2.2.3) showing
long-term sea surface
temperatures and wind
speeds in the general region
surrounding the Helgoland
Roads monitoring area,
along with data from
the adjacent CPR D01
Standard Area.

50-year trends in the Helgoland Roads / southeastern North Sea region

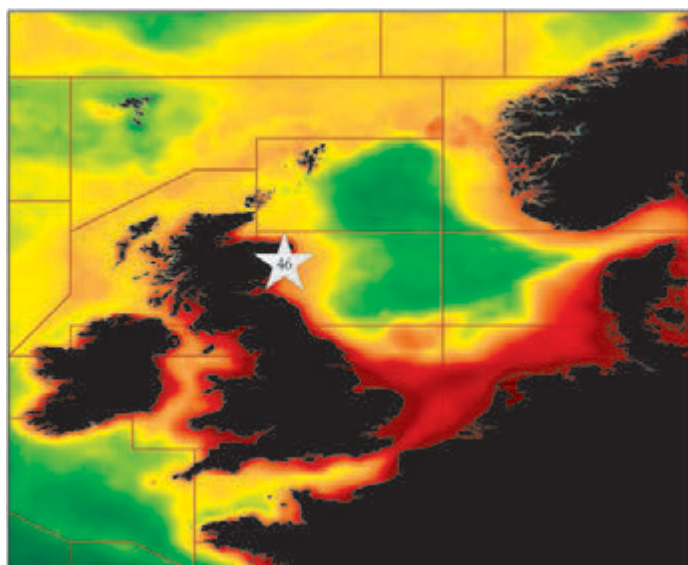


100-year trends in the Helgoland Roads / southeastern North Sea region



7.3 Stonehaven (Site 46)

Kathryn Cook



The Marine Scotland Stonehaven sampling site is located at 56°57.80'N 02°06.20'W (Figure 7.3.1), approximately 5 km offshore from Stonehaven, a small town 28 km south of Aberdeen, Scotland, in a water depth of 50 m. Since January 1997, samples for the determination of surface and near-seabed hydrographic parameters and concentrations of inorganic chemical nutrients have been taken using water bottles and reversing digital thermometers, and integrated (0–10 m) phytoplankton and chlorophyll samples have been collected using a Lund tube (see Lund and Talling, 1957). Mesozooplankton samples (200 µm mesh) were collected by a vertical deployment of a 30 cm diameter Bongo net until 10 March 1999, after which time these samples have been collected by vertical deployment of a 40 cm diameter Bongo net. Since 1999, detailed taxonomic analysis has been carried out on the mesozooplankton and phytoplankton samples. Fine-mesh zooplankton samples (95 µm mesh from 1997 to April 2001, then 68 µm mesh to the present) have also been collected using a bongo net, but these are currently archived and not analysed because of the limited availability of trained staff. Macrozooplankton (350 µm mesh) is sampled using a 1 m ringnet deployed with a double oblique tow at 2 knots. These samples are also archived, although a current project is analysing these macroplankton samples using a ZooScan system and automated species-group recognition. Other short-term sampling at the site is done in support of a variety of time-limited research projects that study aspects of the coastal species or ecology in more detail. The objective of the time-series is to establish a monitoring base for assessing the status of the Scottish coastal ecosystem and to gauge responses to climate change. Some of these data are available online at <https://sites.google.com/site/mssmonitoring/home>.

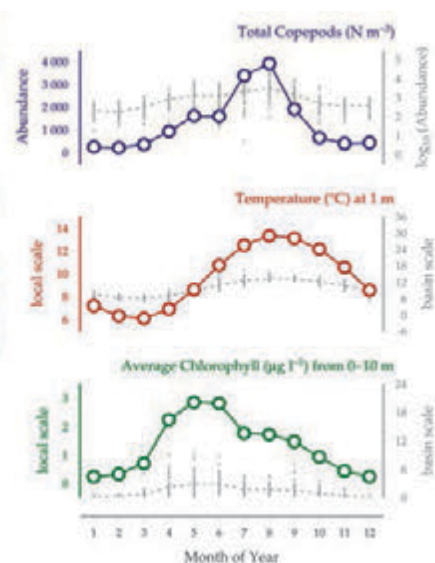


Figure 7.3.1
Location of the Stonehaven monitoring area (Site 46) plotted on a map of average chlorophyll concentration, and its corresponding seasonal summary plot (see Section 2.2.1).

Seasonal and interannual trends (Figure 7.3.2)

The origins of the water passing down the Scottish east coast lie mainly north and west of Scotland and are a variable mix of coastal and oceanic Atlantic waters. Water movement is generally southerly, with fairly strong tidal currents and a local tidal excursion of about 10 km. The water column at the sampling site remains well mixed throughout much of the year, with the exception of summer and early autumn, when surface heating and calm weather can cause temporary thermoclines to appear. Occasional haloclines are transient and depend largely on periods of extensive river and land run-off to surface layers in the coastal area. The seasonal minimum temperature of about 6°C generally occurs in late February to early March and rises to about 12–14°C in August. Throughout late summer and autumn, the increased salinity measured at Stonehaven indicates a variable, but often significant, increase in the proportion of Atlantic water passing the site. Comparison of the results with archive regional data on temperature, salinity, nutrients, and chlorophyll *a* indicates that the site provides a reliable index of the state of wider Scottish coastal waters (Heath *et al.*, 1999).

At the Stonehaven site, seasonal cycles are evident in all of the measured variables. The concentration of nitrate, a vital nutrient for phytoplankton growth, falls as chlorophyll increases with the onset of the spring phytoplankton bloom in March–April. Zooplankton, in turn, feed on phytoplankton and on each other and increase in abundance after the spring phytoplankton bloom. Throughout summer, phytoplankton growth relies on regenerated nitrate and ammonia supplied by microbial action and zooplankton excretion. After a late summer peak in August–September, which coincides with the highest

water temperature, zooplankton abundance declines as food becomes scarce because phytoplankton growth is light and temperature limited. The nitrate concentration then begins to rise as it is replenished during winter by resuspension from the sediment due to storm action and increased river and land run-off. In order to survive winter, some species such as the large copepod genus *Calanus* and euphausiids build up oil reserves, whereas others rely on resting eggs or simply survive on whatever they find to eat through winter (e.g. the copepod *Oithona* spp.). Some species (e.g. the copepod *Calanus finmarchicus*, Figure 7.3.2) are not resident at Stonehaven throughout winter, but are reseeded each year by the influx of waters from the north or from areas south and west of Scotland.

Although the patterns are broadly consistent, the dynamics of seasonal cycles vary between years for both the environmental and species components of the ecosystem. Temperature has generally been higher than average since 2003, although 2010 was a cold year, whereas salinity appears to have been decreasing during this time. There are no obvious patterns in the annual concentration of nitrate, but chlorophyll has been higher than average since 2005. Overall, copepod abundance increased between 1997 and 2003, and since has fluctuated around the long-term average. This is in contrast to the decreasing trend seen in the offshore CPR data from the region (Figure 7.3.3), particularly since 2005. 2010 was a year of lower-than-average copepod abundance at the Stonehaven site, but higher-than-average copepod abundance in the CPR data. The causes of this discrepancy are not understood, but it is probably

the result of differences in sampling methods and in the hydrographic influences at the nearshore Stonehaven station, compared with the much wider and offshore region encompassed by the adjacent CPR survey tracks. It is notable that anomalies in the interannual abundance of the arrow worms (Chaetognatha), which feed on copepods and their larvae, follow interannual patterns similar to those of their main prey at Stonehaven (Figure 7.3.2). However, this is not seen in the abundance of the cnidarians, also predators of copepods, at Stonehaven which have decreased since 2006.

The important copepod genus *Calanus* is represented by two species in Scottish seas: *C. finmarchicus* and *C. helgolandicus*. The Arctic–boreal *C. finmarchicus* has a spring influx arising from the winter diapause in deeper waters off the edge of the continental shelf. Historically, *C. finmarchicus* has been the dominant *Calanus* species in the northern North Sea, providing food for many fish larvae in spring. However, in recent decades, the proportion of the more southerly *C. helgolandicus*, generally most productive in summer and autumn, has increased rapidly (Beaugrand, 2009), so that it is now approximately tenfold more abundant than *C. finmarchicus*. At Stonehaven, the pattern in annual abundance anomalies has been the same for both *Calanus* species: abundance has increased between 1997 and 2008, and 2009–2010 have been years of lower abundance. A similar pattern is also seen in the *Oithonidae* spp. copepod.

Figure 7.3.2
Multiple-variable
comparison plot (see
Section 2.2.2) showing the
seasonal and interannual
properties of select
cosampled variables at the
Stonehaven monitoring
area.

Additional variables are
available online at: <http://WGZE.net/time-series>.

Stonehaven, northwestern North Sea

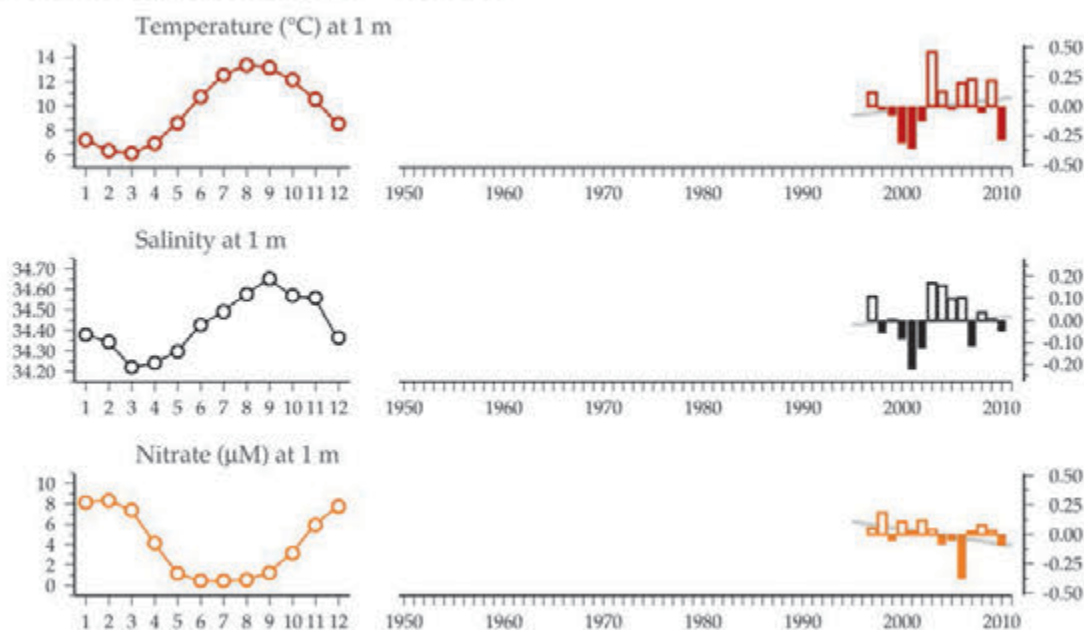


Figure 7.3.2
continued

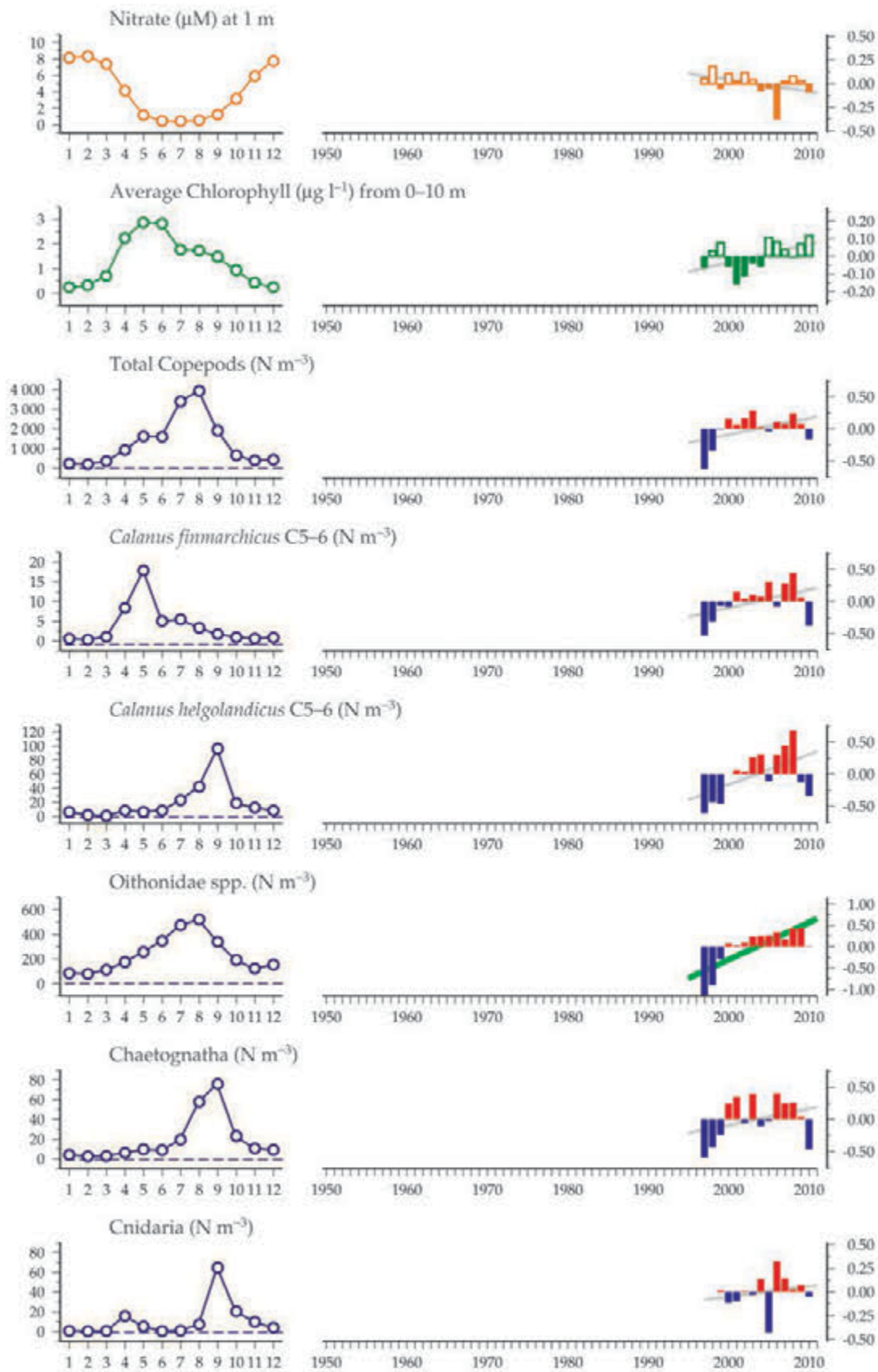
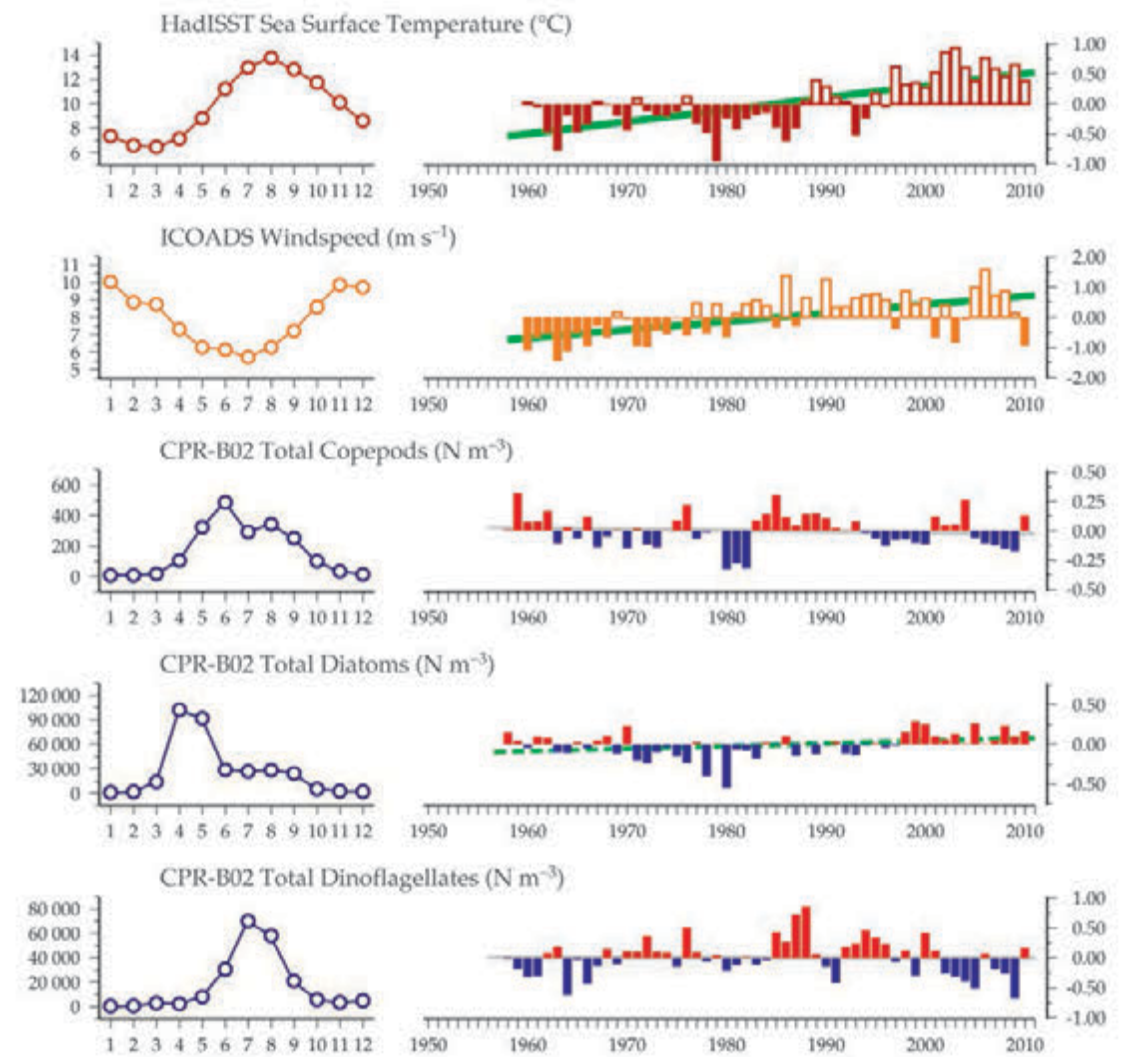
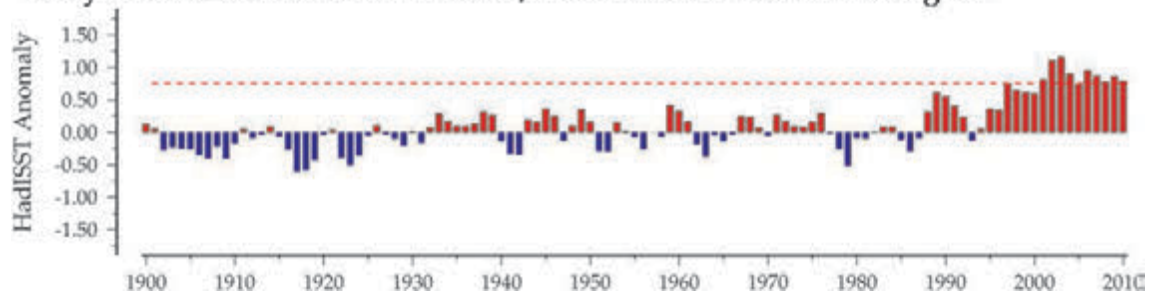


Figure 7.3.3
Regional overview
plot (see Section 2.2.3)
showing long-term sea
surface temperatures and
windspeeds in the general
region surrounding the
Stonehaven monitoring
area, along with data from
the adjacent CPR B02
Standard Area.

50-year trends in the Stonehaven / northwestern North Sea region



100-year trends in the Stonehaven / northwestern North Sea region

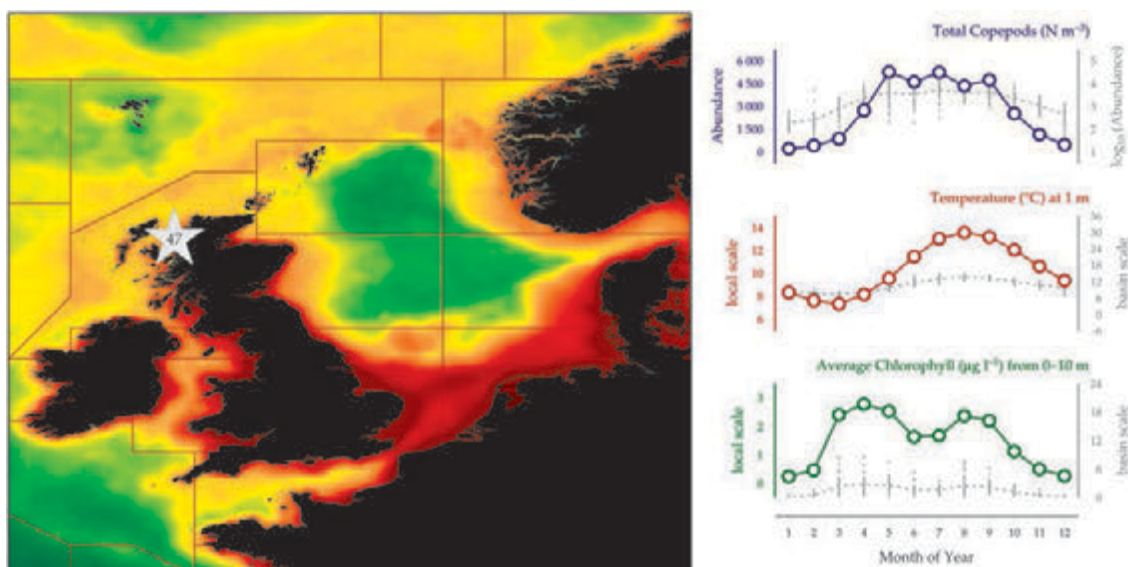


7.4 Loch Ewe (Site 47)

Kathryn Cook

Figure 7.4.1

Location of the Loch Ewe monitoring area (Site 47) plotted on a map of average chlorophyll concentration, and its corresponding seasonal summary plot (see Section 2.2.1).



The Marine Scotland Loch Ewe sampling site is located at 57°50.99'N 05°38.97'W (Figure 7.4.1) approximately 0.5 km offshore in a Scottish west coast sea loch in a water depth of 35–40 m. To the north, the loch opens into the Scottish coastal sea basin of the North Minch and then to the open eastern Atlantic. Sampling, which began in April 2002, is similar to that at the Stonehaven site and is also carried out weekly. Samples for the determination of surface and near-seabed hydrographic parameters and concentrations of inorganic chemical nutrients are taken using water bottles and reversing digital thermometers, and integrated (0–10 m) phytoplankton and chlorophyll samples have been collected using a Lund tube. Mesozooplankton samples (200 µm mesh) are collected by the vertical deployment of a 40 cm diameter bongo net. Detailed taxonomic analysis is carried out on the mesozooplankton and phytoplankton samples. Fine-mesh zooplankton samples (68 µm mesh) are also collected using a bongo net, but these are currently archived and not analysed because of the limited availability of trained staff. Other short-term sampling at the site is done in support of a variety of time-limited research projects that study aspects of the coastal species or ecology in more detail. The objective of the time-series is to establish a monitoring base for assessing the status of the Scottish coastal ecosystem and to gauge responses to climate change. Although this time-series is too short for full statistical analysis of interannual patterns, it already provides data on seasonality and can be compared with other longer-term monitoring data. Some of these data are available online at <https://sites.google.com/site/mssmonitoring/home>.

Seasonal and interannual trends (Figure 7.4.2)

Water movement in this fjordic loch is complex and strongly influenced by wind and tide. The loch faces north and has quite strong tidal currents, with variable exchange with the coastal sea of the North Minch. The origins of the water that exchanges into the loch are not simply the Scottish Coastal Current waters that flow north along the Scottish west coast shelf. The North Minch is affected by influxes of oceanic Atlantic water from the northwest, particularly into the deeper basin. When strong, this influx may influence exchange between the loch and the adjacent coastal waters, varying the environment, sometimes quite suddenly, and thus affecting the composition of flora and fauna in the loch. The diversity of zooplankton species is higher at Loch Ewe compared to Stonehaven on the east coast of Scotland, owing to the more direct influence of waters and communities of southern origin. Most of the water column at the Loch Ewe site is well mixed throughout the year, although in summer and early autumn, surface heating and calm weather can cause temporary thermoclines to appear. The seasonal minimum temperature of about 8°C generally occurs in mid-March and rises to about 12–14°C in August–September. Winter temperatures in the loch are generally about 1.5°C higher than in the exposed North Sea site at Stonehaven on the Scottish east coast. It is also noticeable that the sea cools more slowly through autumn and winter in this semi-enclosed loch than at the Stonehaven site. As the Loch Ewe site lies in a semi-enclosed sea loch, it is affected by river and land run-off, which is reflected in the surface water as lower salinities, particularly in autumn–winter, when freshwater inputs are high.

Seasonal cycles, very similar to those seen at the Stonehaven site, are evident in all of the measured variables (Figure 7.4.2). The concentration of nitrate, a vital nutrient for phytoplankton growth, falls as chlorophyll increases with the onset of the spring phytoplankton bloom in March–April. Zooplankton, in turn, feed on phytoplankton and on each other and increase in abundance after the spring phytoplankton bloom (see Figure 7.4.1, right subpanel). Throughout summer, phytoplankton growth relies on regenerated nitrate and ammonia supplied by microbial action and zooplankton excretion. After a late-summer peak in August–September, which coincides with the highest water temperature, zooplankton abundance declines as food becomes scarce because phytoplankton growth is light and temperature limited. The nitrate concentration then begins to rise as it is replenished during winter by resuspension from the sediment due to storm action and increased river and land run-off. In order to survive winter, some species, such as the large copepod genus *Calanus* and euphausiids build up oil reserves, whereas others rely on resting eggs or simply survive on whatever they find to eat through winter (e.g. the copepod *Oithonidae* spp.). Some species (e.g. the copepod *Calanus finmarchicus*, Figure 7.4.2) are not resident in Loch Ewe throughout winter, but are reseeded each year by the influx of waters from the north or from areas south and west of Scotland.

Although the patterns are broadly consistent, the dynamics of seasonal cycles vary between years for both the environmental and species components of the ecosystem. Temperature has generally been slightly higher than average since monitoring began in 2002, although 2010 was a cold year. Salinity appeared to be decreasing between 2002 and 2007, but in 2010, salinity was higher than the long-term average. The concentration of nitrate has been increasing since 2002, although in 2010, nitrate concentration was much lower than in 2009, but there are no obvious patterns in the annual concentration of chlorophyll. Overall, copepod abundance has been fluctuating around the long-term average since monitoring began, although 2009 had the lowest copepod abundance and 2010 had the highest copepod abundance. 2010 also saw the highest abundance of *Oithonidae* copepods since the beginning of the time-series. This is in contrast to the decreasing trend seen in the offshore CPR data from the region (Figure 7.4.3) during this time-period. However, copepod abundance was much higher in 2010 compared to 2009 in both datasets. As at Stonehaven, the causes of this discrepancy are not understood, but it is probably the result of differences in sampling methods and in the hydrographic influences at the semi-enclosed Loch Ewe station, compared with the much wider and offshore region encompassed by the adjacent CPR survey tracks. In contrast to the Stonehaven site, interannual abundance of the arrow

worms (*Chaetognatha*), which feed on copepods and their larvae, do not follow interannual patterns similar to those of their main prey (Figure 7.4.2). In fact, the abundance of *Chaetognatha* has been decreasing since 2005. The abundance of cnidarians, also predators of copepods, at Loch Ewe does not show the decrease since 2006 seen at Stonehaven. 2003 was a year of high cnidarian abundance, but values have since fluctuated around the long-term mean.

At Loch Ewe, as at Stonehaven, the important copepod genus *Calanus* is represented by two species: *C. finmarchicus* and *C. helgolandicus*. The Arctic–boreal *C. finmarchicus* has a spring influx arising from the winter diapause in deeper waters off the edge of the continental shelf, and the species provides food for many fish larvae in spring. However, in recent decades, the proportion of the more southerly *C. helgolandicus*, generally most productive in summer and autumn, has increased rapidly (Beaugrand, 2009) so that it is now approximately tenfold more abundant than *C. finmarchicus*. At Loch Ewe, as at Stonehaven, the pattern in annual abundance anomalies has been the same for both *Calanus* species: abundance has increased between 2002 and 2008, and 2009–2010 have been years of lower abundance (Figure 7.4.2).

Loch Ewe, Scottish west coast

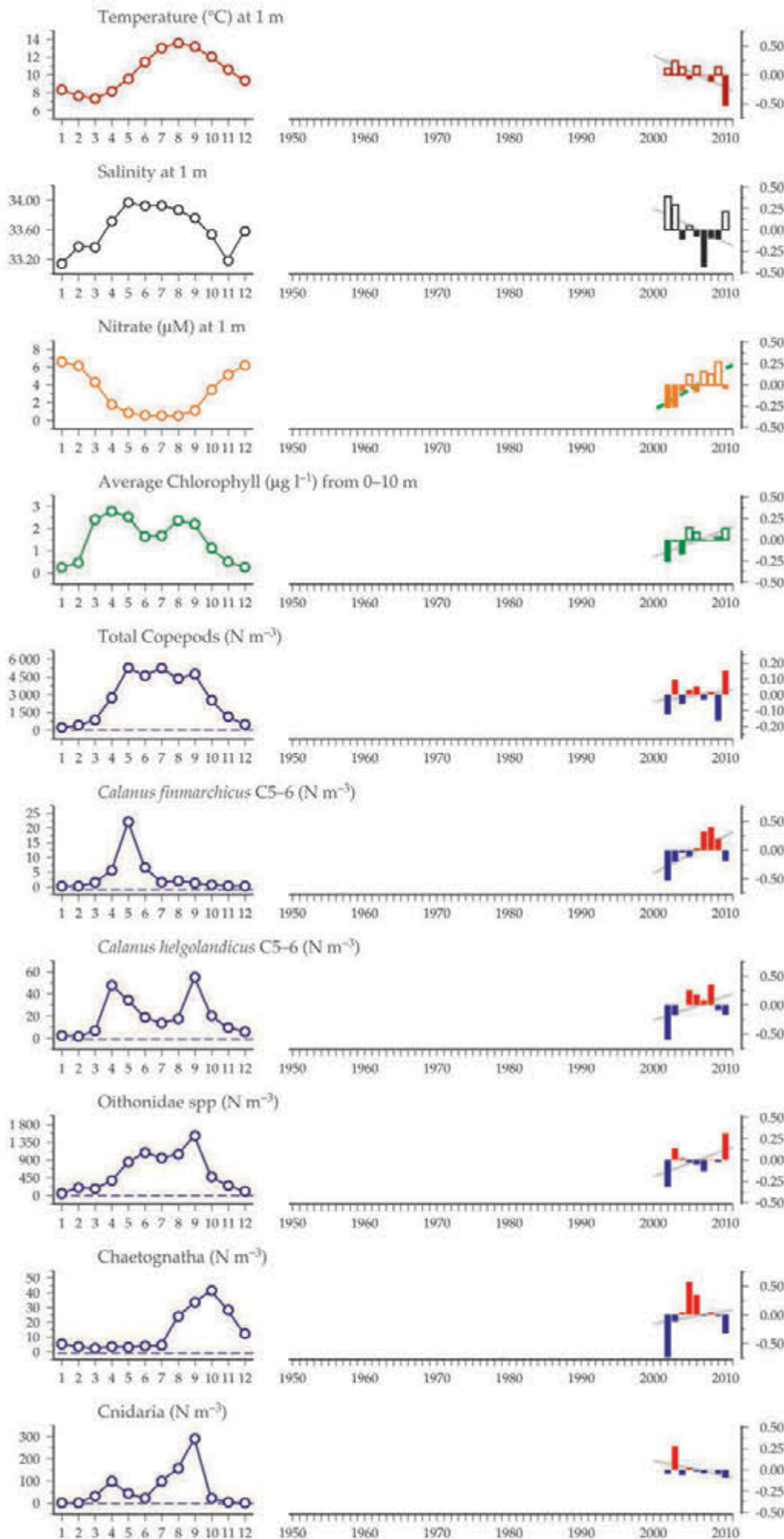
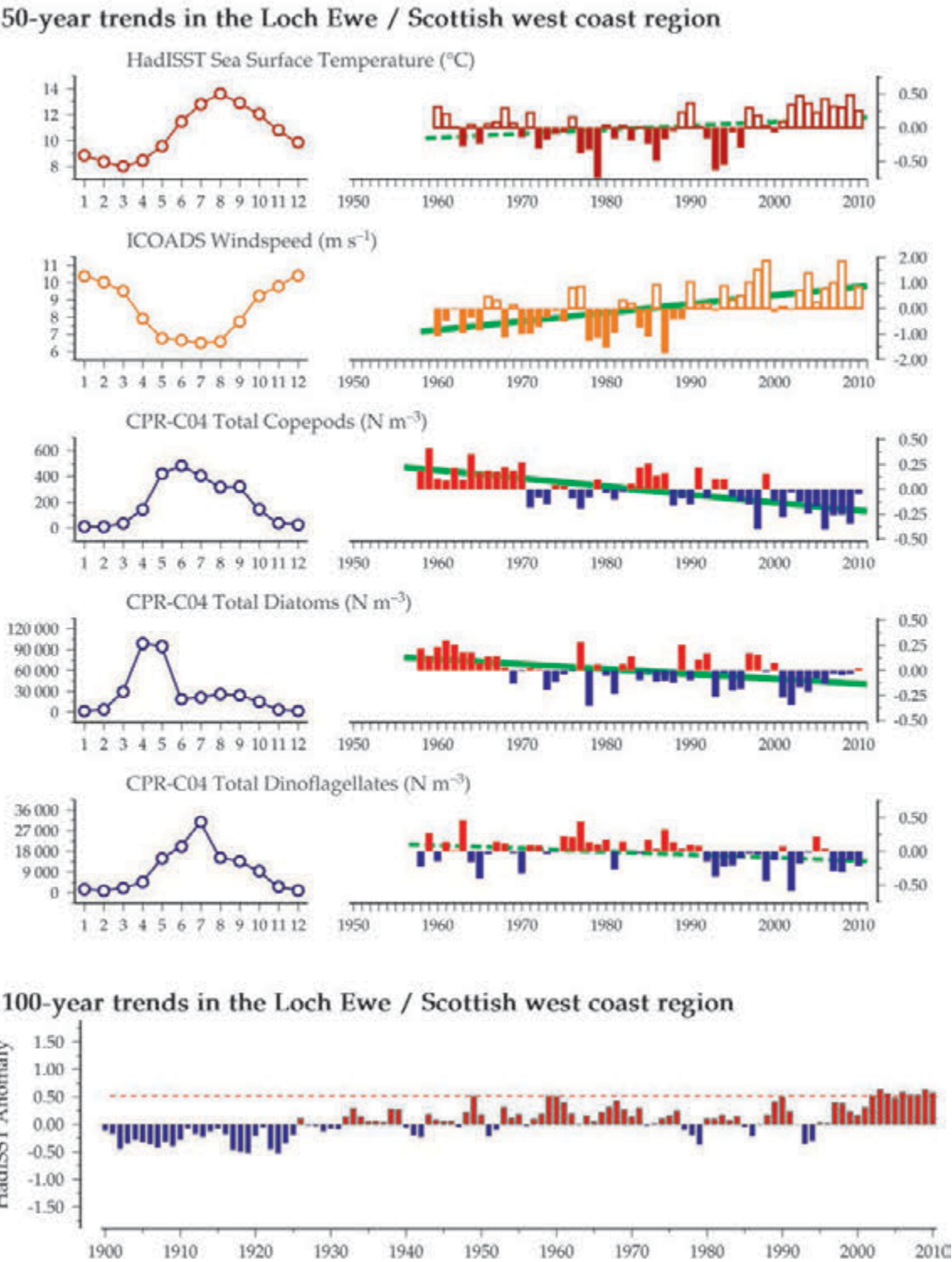


Figure 7.4.2
Multiple-variable comparison plot (see Section 2.2.2) showing the seasonal and interannual properties of select cosampled variables at the Loch Ewe monitoring area.

Additional variables are available online at: <http://WGZE.net/time-series>.

Figure 7.4.3
Regional overview
plot (see Section 2.2.3)
showing long-term sea
surface temperatures and
windspeeds in the general
region surrounding the
Loch Ewe monitoring area.



7.5 Plymouth L4 (Site 48)

Angus Atkinson, Elaine Fileman, Claire Widdicombe, Rachel Harmer, Andrea McEvoy, Roger Harris, and Tim Smyth

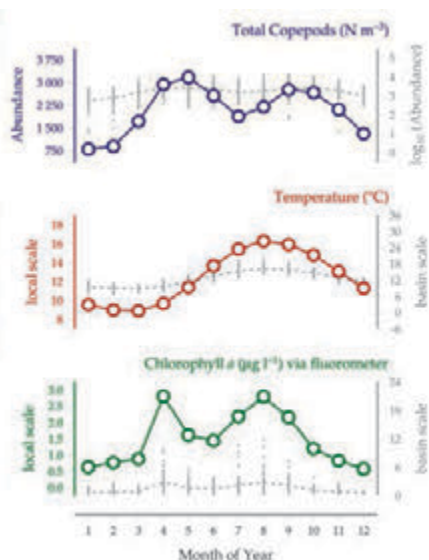
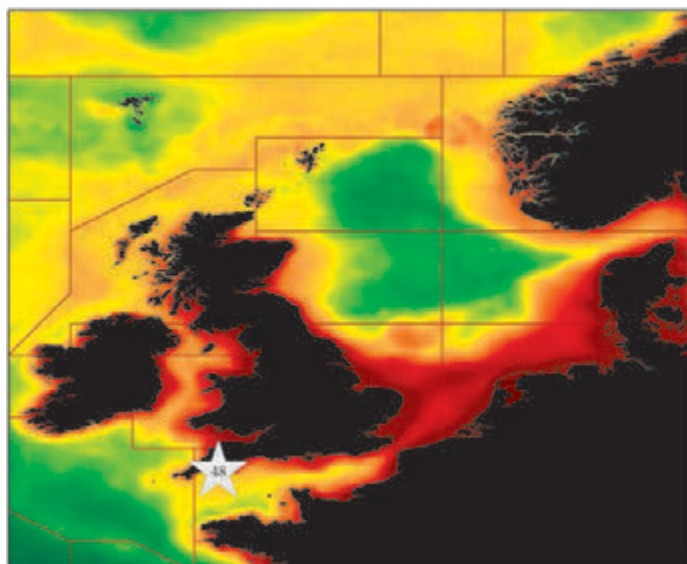


Figure 7.5.1
Location of the Plymouth L4 monitoring area (Site 48) plotted on a map of average chlorophyll concentration, and its corresponding seasonal summary plot (see Section 2.2.1).

The zooplankton time-series at Plymouth Station L4 (50°15'N 4°13'W) in the western English Channel is ongoing, with weekly sampling by Plymouth Marine Laboratory (PML) since 1988 (Harris, 2010; see <http://www.westernchannelobservatory.org.uk/>). Samples are usually taken every Monday morning at the site ~16 km southwest of Plymouth (Figure 7.5.1). Two replicate tows are made using a WP-2 net (56 cm diameter, 200 µm mesh) towed vertically from the seabed at ca. 50 m depth to the surface.

Mesozooplankton are identified and counted from catch fractions. For some taxa, particularly copepods such as *Calanus helgolandicus*, identification is to species level, with additional information on sex and life stages. Sea surface temperature (SST) has been measured since 1988 using a mercury-in-glass thermometer immersed in an aluminium bucket of water collected at the surface. Since 2002, water-column profiles have been recorded with a conductivity–temperature–depth (CTD) instrument, providing temperature, salinity, and fluorescence data. Water samples collected from a depth of 10 m with a Niskin bottle have been analysed since 1992 to determine abundance and to estimate carbon biomass of phytoplankton and microzooplankton. Organisms are counted and identified to genus or species level using inverted microscopy. At the same time, chlorophyll a triplicate measurements are made using a Turner fluorometer after filtering and extraction of sea surface water samples. Nutrient data (nitrate, nitrite, phosphate, and silicate) are also available from 2000 onwards. All L4 samples are analysed at PML, and the data are available through Pangaea, BODC, and the above Western Channel Observatory website.

Seasonal and interannual trends (Figure 7.5.2)

In line with observations around the UK shelf seas, the western English Channel has warmed by ~0.6°C per decade over the past 20 years. The greatest temperature rises followed a period of reduced wind speeds and enhanced surface solar irradiation in recent years (Smyth *et al.*, 2010). Set in this context, Station L4 is continually affected by the tide, which is associated with an interplay of regular estuarine outflow from Plymouth Sound and oceanic waters coming in with the dominating southwesterly winds. The water column is weakly stratified from mid-April to September and mixed during winter (Pingree and Griffiths, 1978); the minimum and maximum surface temperatures occur in March (9.1°C) and August (16.4°C), respectively. The seasonal cycle of the phytoplankton community is characterized by spring diatom and autumn dinoflagellate blooms, but there is high interannual variability in abundance and floristic composition (Widdicombe *et al.*, 2010).

Trends in total microzooplankton seasonal abundance show a transition from low abundance in winter months to a peak in summer, the timing of which has varied. Between 1992 and 2005, the peak in average monthly microzooplankton abundance varied from June to August, whereas since 2006, the peak in average abundance has occurred in May. Heterotrophic dinoflagellates are most abundant from May to September, and in the last decade, there have been a number of positive abundance anomalies for this group. The ciliate community is dominated by the genus *Strombidium* and *Myrionecta rubra* (Fileman *et al.*, 2010; Widdicombe *et al.*, 2010), and over the last decade, ciliates have shown a number of negative abundance anomalies.

The seasonal cycle of mesozooplankton abundance is characterized by high values from April right through to October (Figure 7.5.2). It then decreases, and the lowest values, in January–February, correspond to the lowest values in chlorophyll *a* and phytoplankton abundance. The mesozooplankton community at L4 is dominated by copepods, which typically form around 90% of the total during winter. In summer, this percentage drops to ~50% when meroplanktonic larvae and non-crustacean groups peak strongly (Eloire *et al.*, 2010). Meroplankton larvae play an important role at L4 right through the productive season. Cirripedes are particularly abundant in March and April (see Figure 7.5.2; see also Highfield *et al.*, 2010). By contrast, other groups, such as echinoderms, bivalves, and gastropods, reach maximum abundance in late summer or autumn. The non-crustacean holoplankton component is also significant and functionally diverse at L4, with appendicularians, chaetognaths, siphonophores, and medusae showing pronounced peaks, often during late summer.

Over the 23-year sampling period, trends in total mesozooplankton reflect those of the dominant component, the copepods. These typically show an irregular pattern often of 2–5-year periods of successive negative and positive anomalies (Figure 7.5.2, right subfigures). Interleaving periods of negative and positive anomalies are also seen in the CPR data for the corresponding area (Figure 7.5.3). However, these do not relate clearly to cycles seen at L4, suggesting either local conditions (L4 is a relatively inshore site) or effects of the

different sampling method. More detailed investigations of relationships between phyto- and zooplankton phenological patterns are needed to understand predator–prey relationships and their impact on abundance variability (Mackas *et al.*, 2012).

The last several years of data seem to reflect a period of positive abundance anomalies for most of the mesozooplankton taxa. As a group, the copepods have increased, as have the non-crustacean holoplankton (e.g. chaetognaths, siphonophores, medusae, appendicularians) and fish eggs and larvae. Most of the meroplanktonic taxa have shown a recent increasing trend (e.g. echinoderms, polychaetes, bivalves, gastropods, decapods), but this is not universal (e.g. cirripede nauplii). Further, the timing of the progression from negative towards the recent positive anomalies varies. This occurs earlier for some taxa (e.g. fish eggs and larvae, echinoderms) than others (e.g. copepods, bivalves, gastropods). While the 23 years of data may be too short to reveal firm evidence of multidecadal or longer-term trends, the fine-resolution weekly sampling of zooplankton, phytoplankton, and nutrients at L4 captures well the complex variation in phenology as well as interannual and subdecadal periodicity.

Figure 7.5.2
Multiple-variable
comparison plot (see
Section 2.2.2) showing the
seasonal and interannual
properties of select
cosampled variables at the
Plymouth L4 monitoring
area.

Additional variables are
available online at: <http://WGZE.net/time-series>.

Plymouth L4, western English Channel

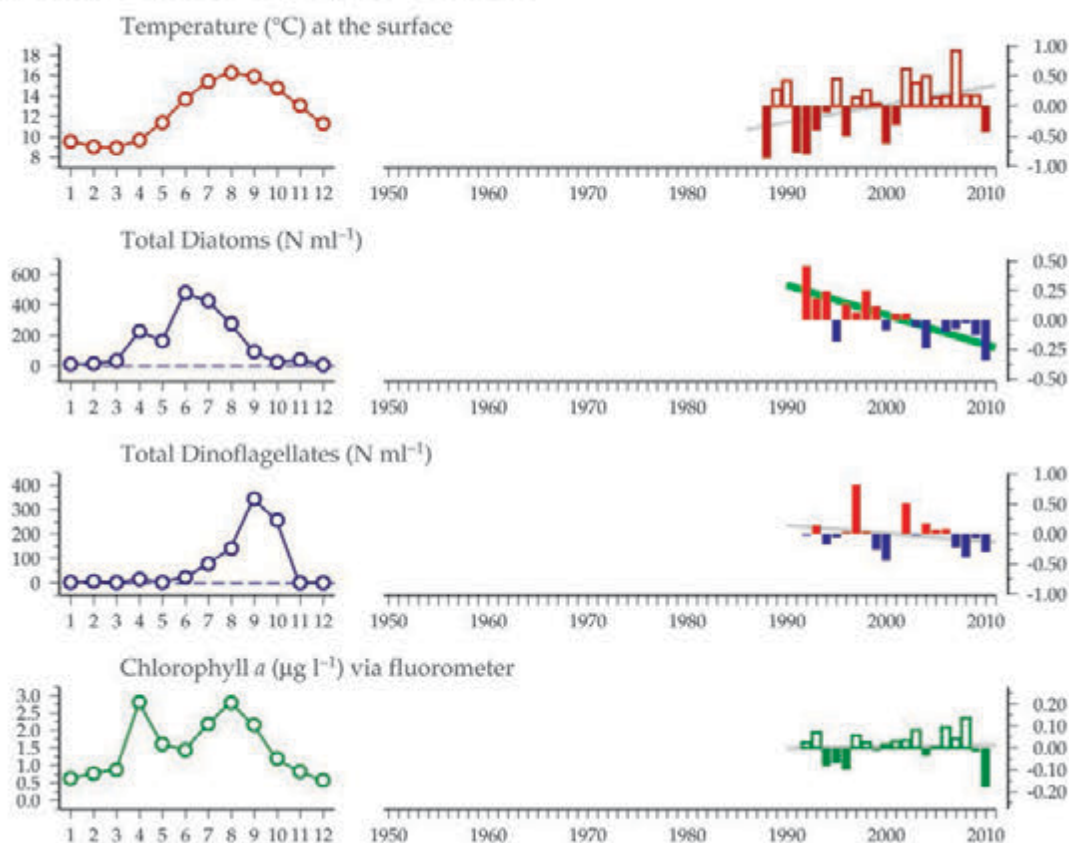


Figure 7.5.2
continued

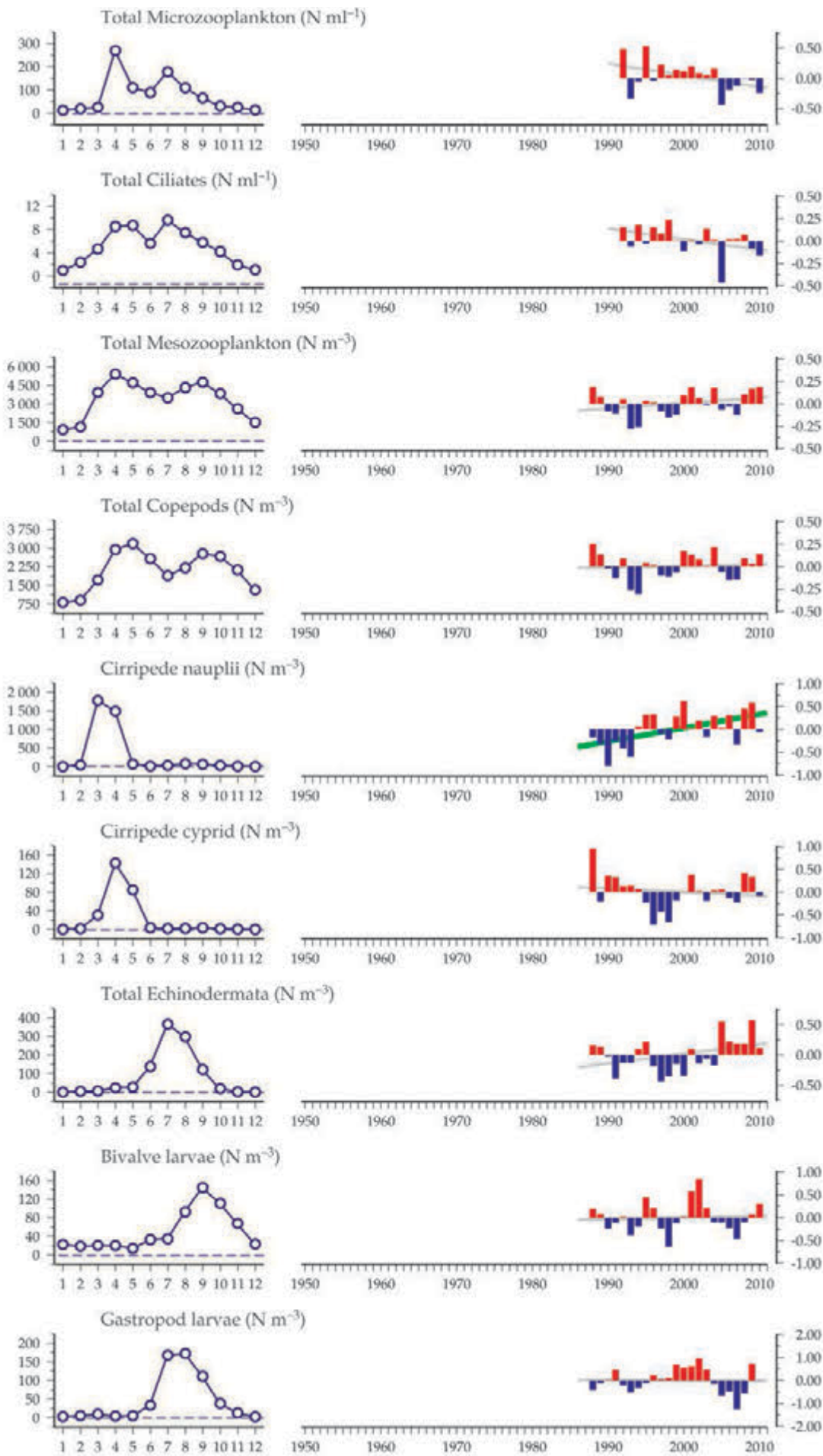
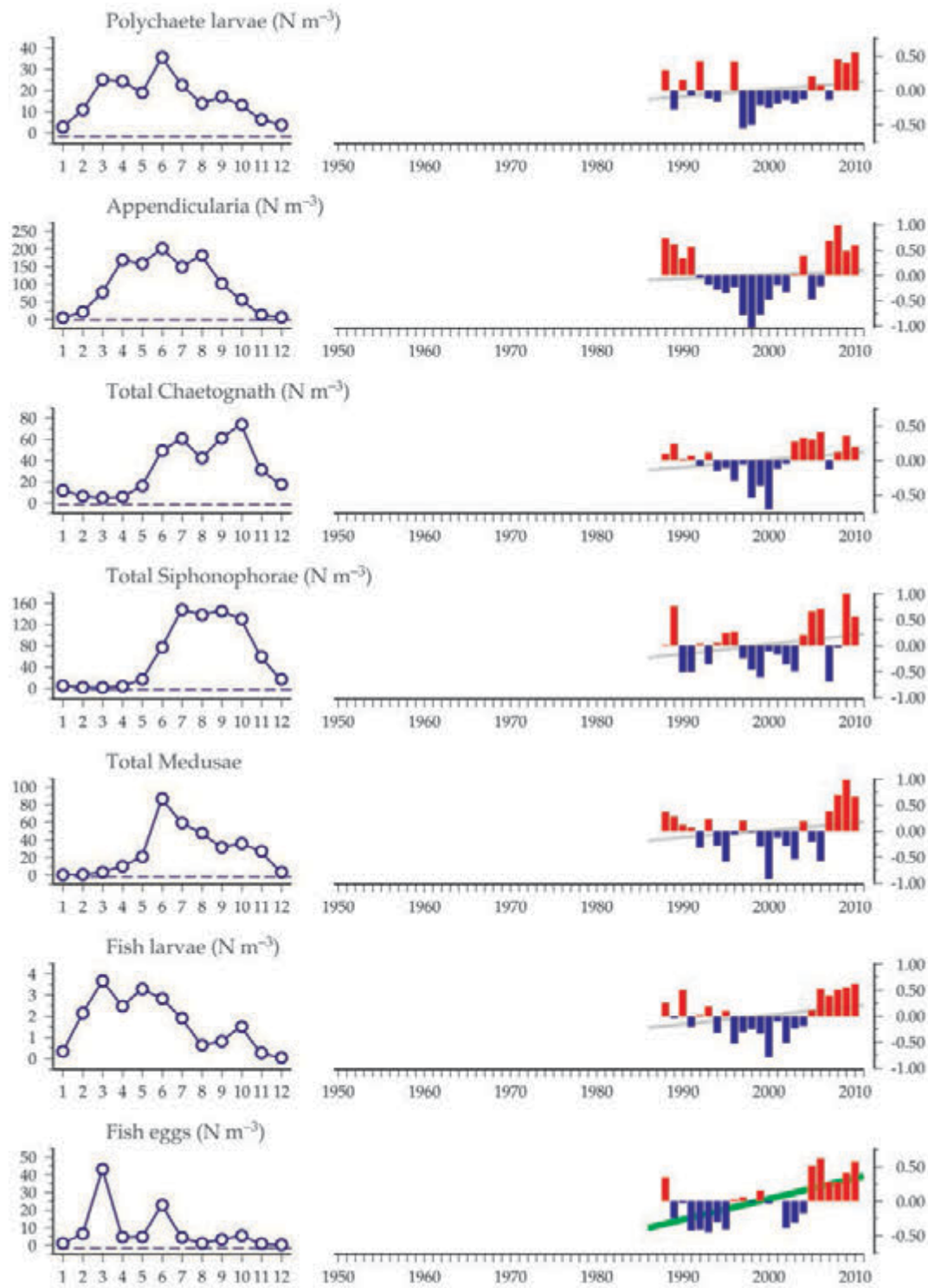


Figure 7.5.2
continued



50-year trends in the Plymouth L4 / western English Channel region

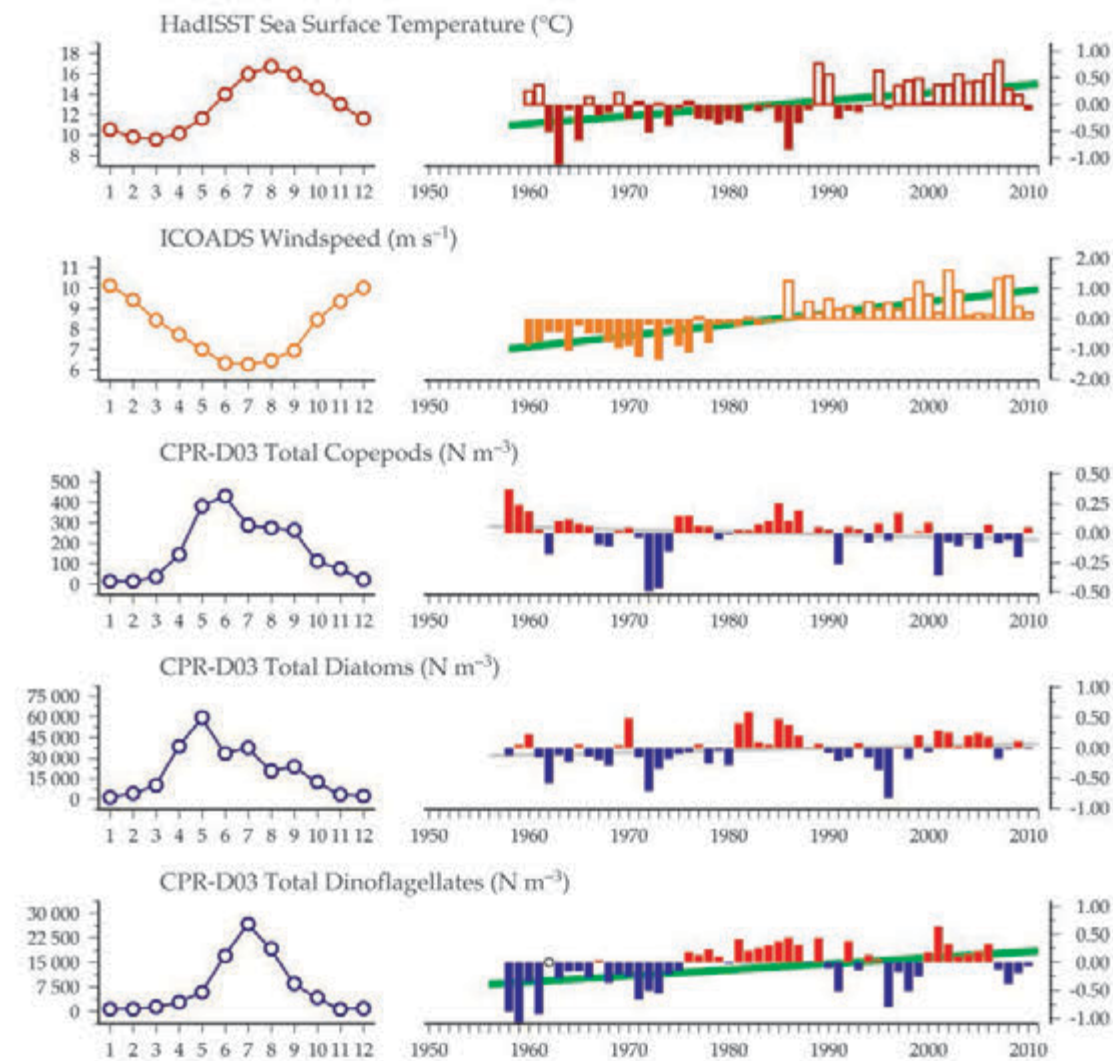
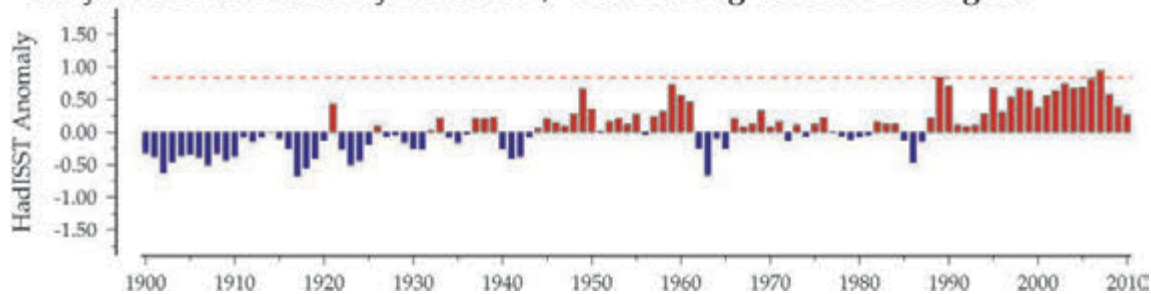


Figure 7.5.3
Regional overview
plot (see Section 2.2.3)
showing long-term sea
surface temperatures and
windspeeds in the general
region surrounding the
Plymouth L4 monitoring
area, along with data from
the adjacent CPR D03
Standard Area.

100-year trends in the Plymouth L4 / western English Channel region



8 ZOOPLANKTON OF THE BAY OF BISCAY AND WESTERN IBERIAN SHELF

Antonio Bode, Juan Bueno, Ángel López-Urrutia, Fernando Villate, Ibon Uriarte, Arantza Iriarte, M.Teresa Alvarez-Ossorio, Ana Miranda, Gerardo Casas, Antonina dos Santos, A. Miguel P. Santos, Maria Alexandra Chícharo, Joana Cruz, Radhouan Ben-Hamadou, and Luis Chícharo

Figure 8.0
Locations of the Bay of Biscay and western Iberian Shelf survey areas (Sites 49–55) plotted on a map of average chlorophyll concentration (see Section 2.3.2).



Site ID	Monitoring Site (Region)	Section
49	Bilbao and Urdaibai Estuaries (inner Bay of Biscay)	81
50	RADIALES Santander Transect (southern Bay of Biscay)	82
51	RADIALES Gijón/Xixón Transect (southwestern Bay of Biscay)	83
52	RADIALES A Coruña Transect (northwest Iberian Shelf)	84
53	RADIALES Vigo Transect (northwest Iberian Shelf)	85
54	Cascais Bay (southwestern Iberian Peninsula)	86
55	Guadiana Lower Estuary (southern Iberian Peninsula)	87

The oceanography of the north and northwest coasts of the Iberian Peninsula is a transition zone between two distinct regimes. On the northern coast (Cantabrian Sea, southern Bay of Biscay), it fits the classical pattern of temperate seas, with a period of water-column stratification in summer and relatively strong mixing during winter (Lavín *et al.*, 2006). On the western coast (Galicia and Portugal coasts), it is under the influence of the Canary–North African upwelling, characterized by a succession of nutrient inputs during most of spring and summer due to northern and northeastern winds (Aristegui *et al.*, 2006). This region is an ideal ecological study area, owing to the gradient of environmental changes found from south to north (western coast) and from west to east (Cantabrian Sea). These gradual changes are clearly reflected in the plankton community. An example of these environmental gradients is the influence of the upwelling events characteristic of the coasts of Portugal and Galicia during spring and summer. These events break the stratified upper layers of the water column, and their influence can be noticed along the Cantabrian Sea, with an eastward decreasing intensity (Valdés *et al.*, 2007; Cabal *et al.*, 2008; Bode *et al.*, 2012). The region is also affected by a saline, warm slope current flowing poleward during autumn and winter, the Portugal Coastal Counter Current (PCCC; Álvarez-Salgado *et al.*, 2003), also known as the Iberian Poleward Current (IPC). This current drives warm saline water from the Portuguese continental shelf first northwards and then eastwards, and follows the Galician coast to reach the Cantabrian Sea, usually during December (González-Nuevo and Nogueira, 2005; Lavín *et al.*, 2006). Other important hydrographic features influencing zooplankton assemblages include: (i) slope-water anticyclonic eddies in offshore waters of the Bay of Biscay (Pingree and Le Cann, 1993; Fernández *et al.*, 2004); (ii) the separation between Eastern North Atlantic Central Water (ENACW) of subtropical and subpolar origin by a persistent frontal structure at the subsurface off Cape Fisterra (Aristegui *et al.*, 2006); and (iii) other mesoscale features such as upwelling filaments, fronts, and eddies off southwest Iberia (Lafuente and Ruiz, 2007; Relvas *et al.*, 2007).

The southwest region of the Iberian Peninsula carries many of the same hydrographic features described for the northwest Iberian coast, most notably upwelling events during spring and summer, with additional influences of buoyant river plumes (Peliz *et al.*, 2002). The seasonal plankton cycle in this region does not follow the classical pattern for temperate seas. The local pattern is transitional between temperate and tropical patterns, presenting fairly constant values almost year-round. The factors that contribute to this pattern are probably related to the location of the area, which is in an upwelling shadow (Moita *et al.*, 2003) that is considered to give some stability during upwelling-favourable winds, as well as being subject to the influence of the Tejo River estuary. The most southern region of the Iberian Peninsula, the Guadiana site, is under the influence of Mediterranean climate, and the zooplankton reflect not only the transitional location, but also the role of river flow and climate variability typical of this region.

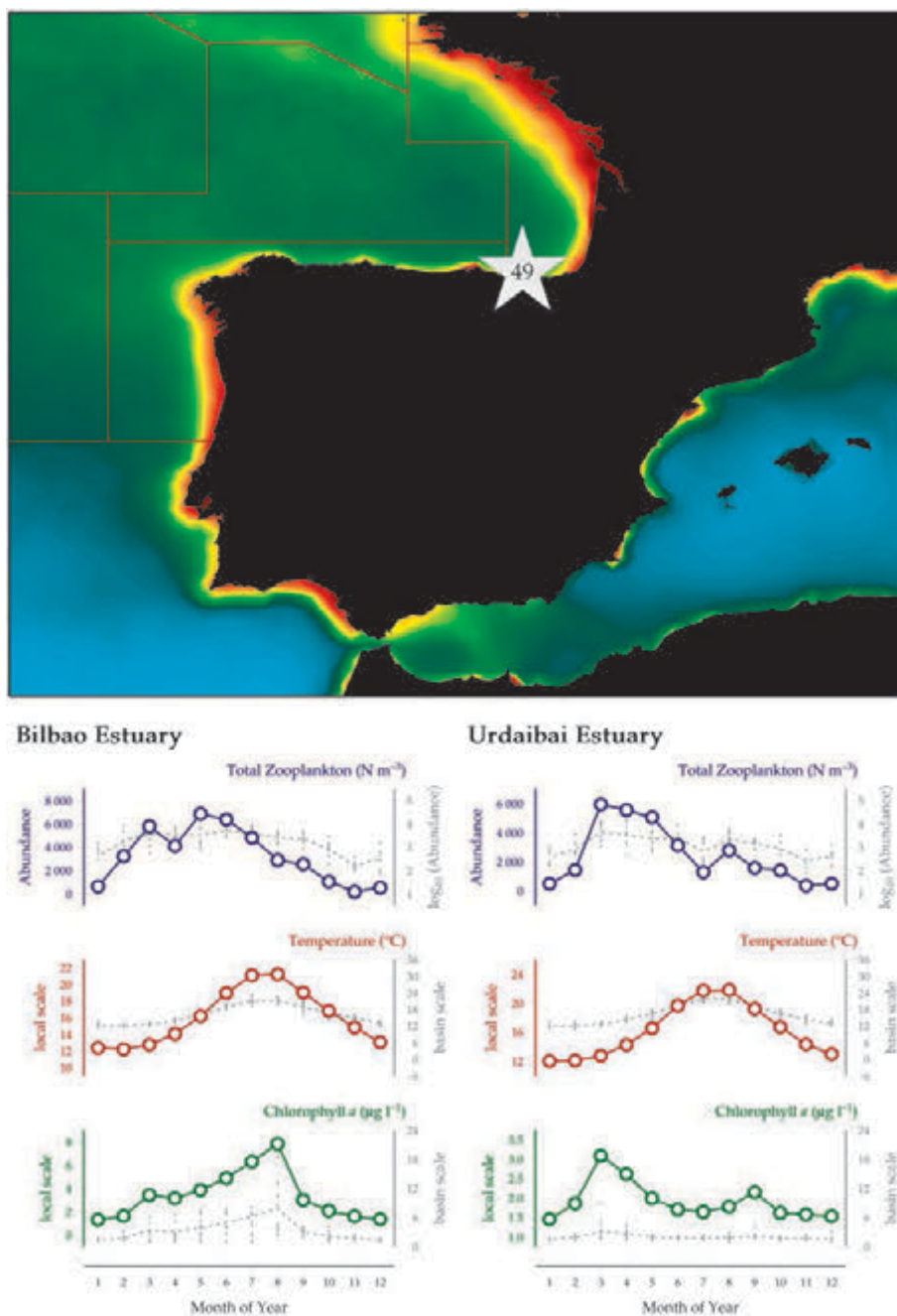
Decadal variability in ocean–climatic observations includes a generalized sea surface warming, shallowing of the summer coastal thermocline depth, weakening of the upwelling intensity during most of the year along the western Iberian coast, and intensification in upwelling intensity during peak summer along the southwestern Iberian coast (Lemos and Sansó, 2006; Álvarez *et al.*, 2008; Relvas *et al.*, 2009; Pardo *et al.*, 2011; Santos *et al.*, 2011).

Time-series data on zooplankton are available for seven sites distributed along the continental shelf of this region, with reasonably good coverage of the southern Bay of Biscay (Figure 8.0). Available sites include several relatively confined coastal ecosystems at the land–ocean interface, as the Nervión and Urdaibai estuaries, the Cascais Bay, and the Guadiana estuary.

8.1 Bilbao and Urdaibai Estuaries (Site 49)

Fernando Villate, Ibon Uriarte, and Arantza Iriarte

Figure 8.1.1
Location of the Bilbao/Urdaibai Estuary monitoring area (Site 49) plotted on a map of average chlorophyll concentration, and its corresponding seasonal summary plot (see Section 2.2.1).



The Bilbao and Urdaibai estuary time-series have been obtained with a monitoring programme initiated in 1997 by the Zooplankton Ecology Group of the University of the Basque Country in the contrasting estuaries of Bilbao and Urdaibai, in order to analyse the effect of climate change and local human activities on the plankton ecosystem of the estuaries of the Basque coast (inner Bay of Biscay). Surveys are carried out monthly at stations 35, 34 (Bilbao), 33, 30, and 26 (Urdaibai) to obtain vertical profiles of temperature, salinity, and dissolved oxygen, and to take samples for chlorophyll *a* determination and zooplankton analysis at

mid-depth below the halocline. Water samples are obtained with Niskin bottles, and zooplankton are sampled by horizontal hauls with 200 μm plankton nets. (At the time of this report, only zooplankton samples through the end of 2005 were analysed.)

The Bilbao Estuary (43°23'N 3°W) is a shallow, mesomacrotidal system surrounded by the most urbanized and industrialized area of the Basque coast. The present estuary is a morphologically modified system constituted by a narrow (50–150 m) man-made channel ca. 15 km in length and 2–9 m in depth that becomes a wider (ca. 3.8 km) and deeper (10–25 m) embayment with port developments at the lower end. Most of the estuary shows noticeable water-column stratification, and a permanent salt wedge exists in the bottom layer where salinity is usually ≥ 30 . The water column is partially mixed in the outer estuary, partially mixed-to-stratified in the intermediate zone, and stratified in the inner estuary.

The Urdaibai Estuary (43°22'N 2°43'W), also called the Mundaka Estuary, is also a shallow, mesomacrotidal system, which has high natural values and constitutes the core of the Urdaibai Biosphere Reserve. It is a short (12.5 km) estuary, with a mean depth of 3 m. The main channel is bordered by saltmarshes at its upper (ca. 15 m wide) and middle reaches and by relatively extensive intertidal flats (mainly sandy) and sandy beaches at its lower reaches (ca. 1 km wide). The watershed area is relatively small in relation to the estuarine basin, and river inputs are usually low in relation to the tidal prism. As a consequence, most of the estuary is marine-dominated, with high-salinity waters in the outer half and a stronger decreasing axial gradient of salinity towards the head at high water.

Seasonal and interannual trends in the Bilbao Estuary (Figure 8.1.2)

Here, we only report the results from a single station in the marine zone of the Bilbao Estuary (WGS84/ETRS89: 43.3487°N 3.0283°W). In this zone, the seasonal cycle of temperature generally reaches a minimum (12–13°C) in January–February and a maximum (21–22°C) in July–August. Interannual variability of temperature from 1997 to 2010 shows that the 2003–2006 period was warmer than previous and later years in the series, which is in agreement with the pattern observed for the same period in the HadISST sea surface temperature series and in the long-term sea surface temperatures in the region surrounding the Bilbao Estuary, as shown in Figure 8.1.4. The annual cycle of chlorophyll *a* is unimodal, with summer (July–August) maximum and winter minimum, owing to the fact that the sampling station is a nearshore coastal site with relatively high influence of anthropogenic nutrient discharges (Iriarte *et al.*, 2010). The interannual variability of chlorophyll *a* during the period 1997–2008 did not show clear trends.

During the 1997–2005 period, total mesozooplankton, copepods, siphonophores, appendicularians, gastropod larvae, and bivalve larvae were more abundant during the spring–summer period, whereas hydromedusae, chaetognaths, cirriped larvae, and bivalve larvae peaked in summer, and cladocerans in spring. Among the strongly seasonal groups, *Noctiluca* showed maxima in summer and doliolids in late summer–early autumn. Interannual variability showed increasing trends of abundance throughout 1997–2005 for copepods, mollusc (gastropod and bivalve) larvae, and decapod larvae, and decreasing trends for hydromedusae. The other taxa showed either

no clear or statistically non-significant trends. The positive and negative trends of abundance observed for several taxonomic categories coincide with the general increase of temperature during the same period, but the relationships are not significant. The addition of new zooplankton data to the time-series will be necessary to confirm zooplankton–temperature relationships at a medium-term time-scale. Preliminary analysis of the dynamics of copepod species in relation to environmental variables indicates that interannual variability of the dominant *Acartia* species in the lower salinity zones of the Bilbao Estuary is associated with temperature directly or indirectly via the effect of temperature on dissolved oxygen (Aravena *et al.*, 2009; Iriarte *et al.*, 2010).

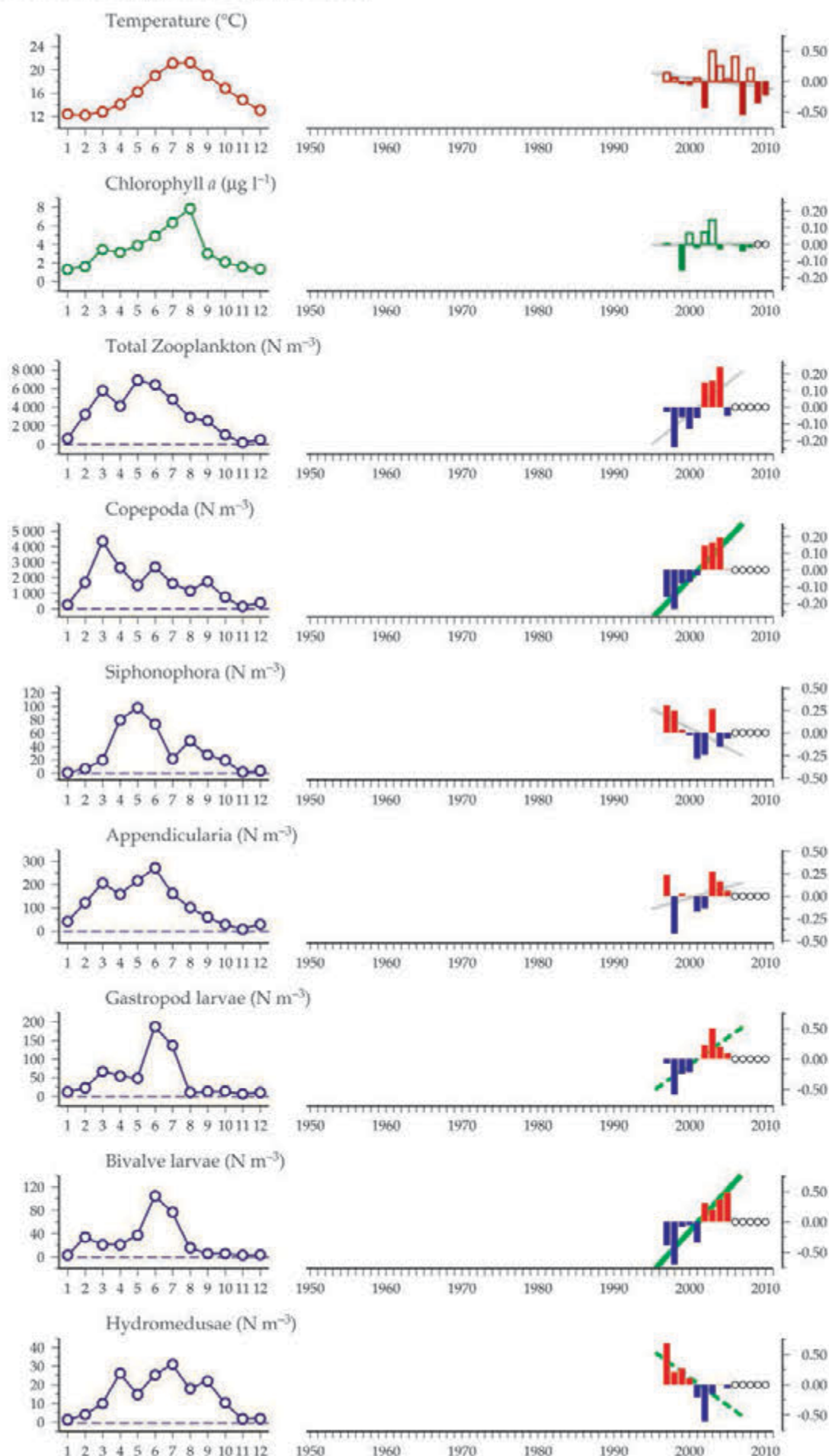
Seasonal and interannual trends in the Urdaibai Estuary (Figure 8.1.3)

In this summary, we only report the results of the marine zone of this estuary at the salinity site of 35 (WGS84/ETRS89: 43.4048°N 2.6964°W). In this zone, temperature generally ranges from 12 to 13°C in winter (January–February) to 21–22°C in summer (July–August). The 2003–2006 period was warmer than the previous and later years in the 1997–2010 series (Figure 8.1.3), which is in agreement with that reported for the Bilbao Estuary. However, unlike the unimodal pattern observed in the marine zone of the Bilbao Estuary, the annual cycle of chlorophyll *a* is bimodal in the marine zone of the Urdaibai Estuary, with a major peak in early spring (March–April) and a secondary peak in late summer–early autumn (August–September). The summer decrease is attributed to nutrient limitation (Villate *et al.*, 2008). Interannual variation did not show a clear trend during the 1997–2008 period. Bimodal patterns of abundance with peaks in spring–early summer and late summer–early autumn were also observed in total mesozooplankton and several groups within them (e.g. copepods, hydromedusae, siphonophores, cladocerans, and bivalve larvae). A spring maximum without clear later secondary peaks was observed in appendicularians. Chaetognaths and gastropod larvae were more abundant in summer, and doliolids occurred almost exclusively in late summer–early autumn. During the 1997–2005 period, increasing trends in abundance were observed for total mesozooplankton, copepods, appendicularians, and mollusc (gastropod and bivalve) larvae, and decreasing trends for cnidarians (both hydromedusae and siphonophores). These trends do not show a clear relationship with temperature, but as in the Bilbao Estuary, the addition of new zooplankton data may clarify the zooplankton–temperature relationships at a medium-term time-scale in the Urdaibai Estuary. The results of the analysis of the chlorophyll *a*–temperature relationship (Villate *et al.*, 2008) suggest that the effect of temperature driving interannual changes in planktonic variables decreases drastically seaward along this estuary.

Figure 8.1.2
Multiple-variable
comparison plot (see
Section 2.2.2) showing the
seasonal and interannual
properties of select
cosampled variables at the
Bilbao Estuary monitoring
area.

Additional variables are
available online at: <http://WGZE.net/time-series>.

Bilbao Estuary, inner Bay of Biscay



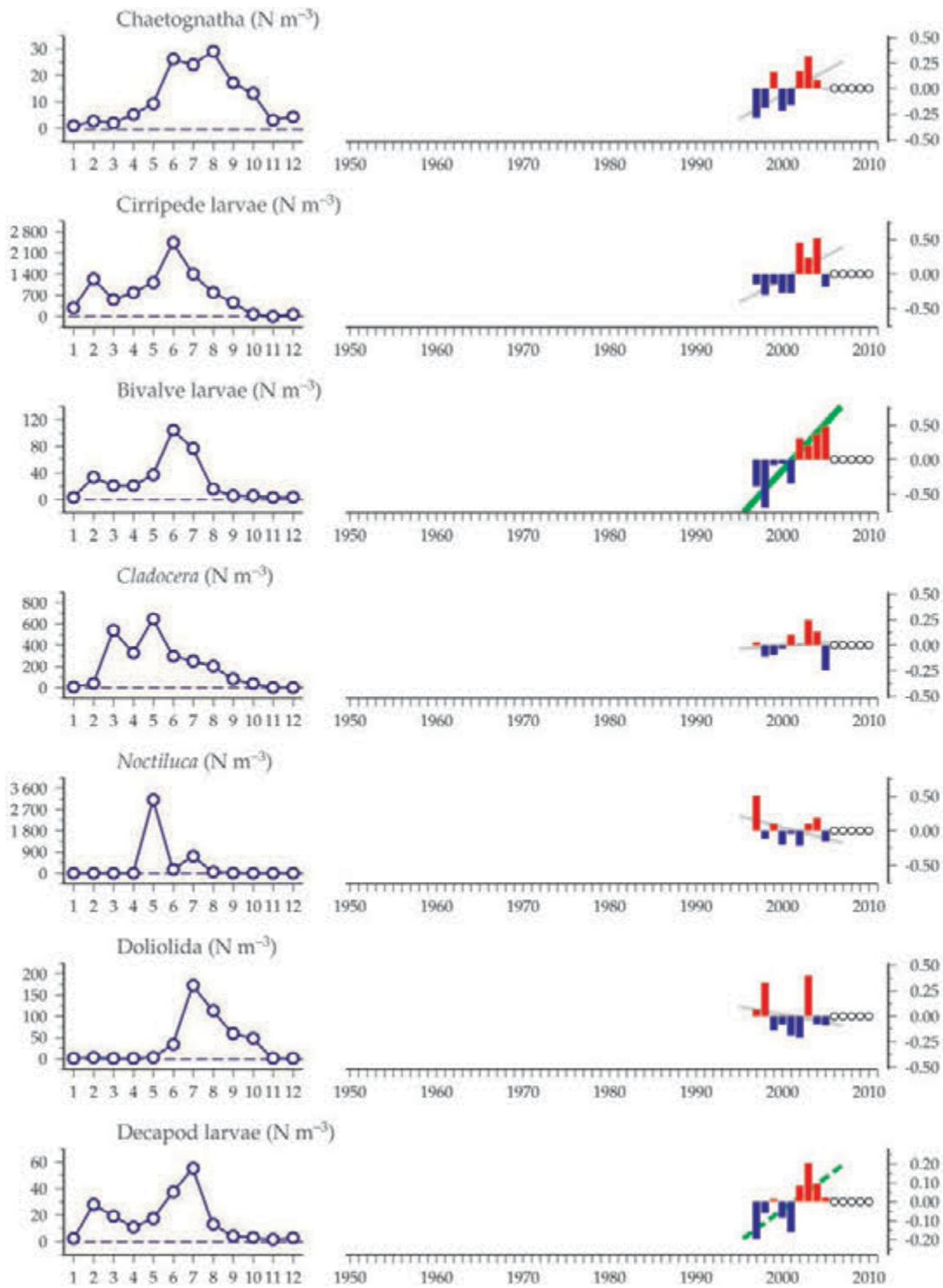
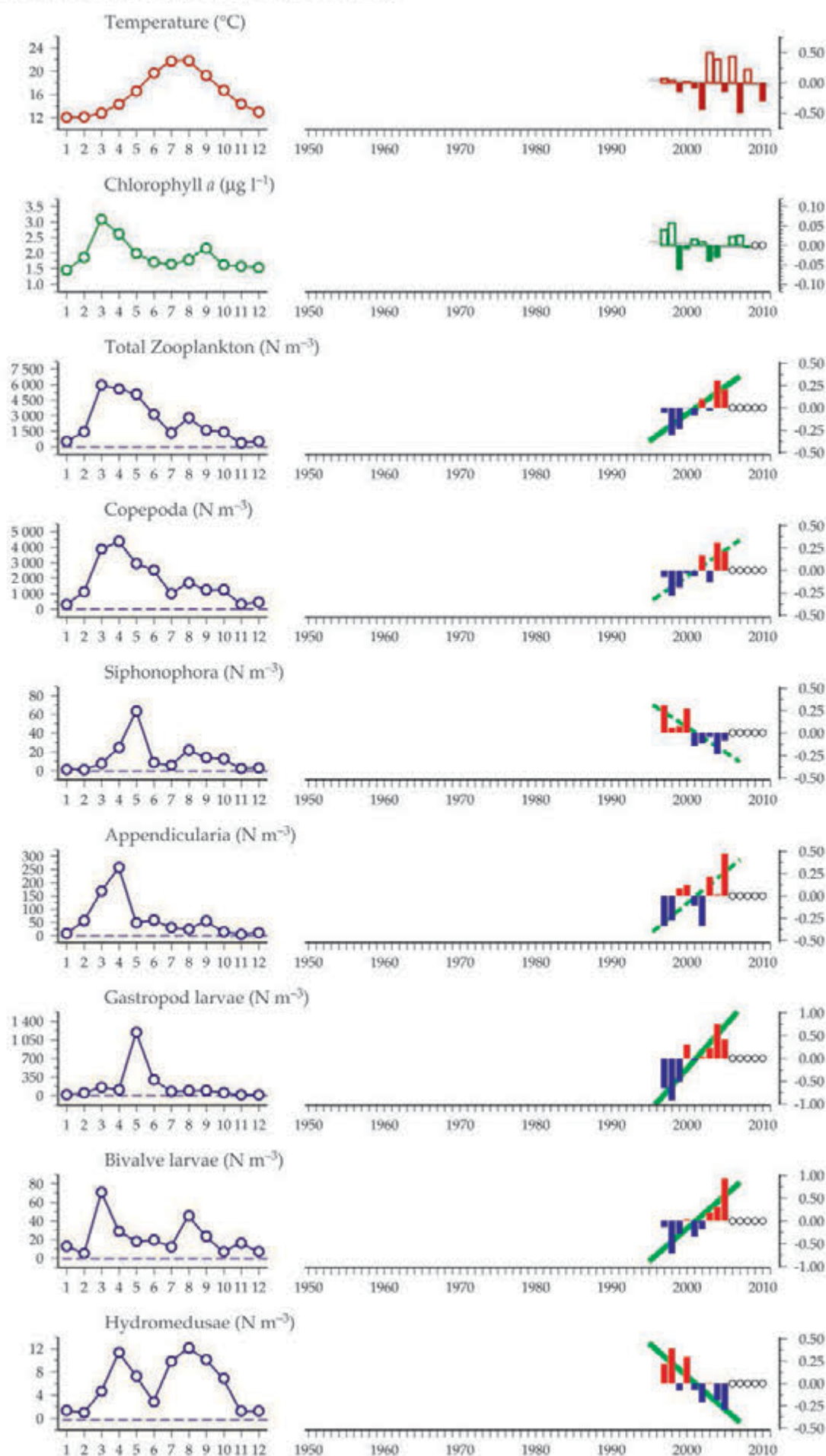


Figure 8.1.2
continued

Figure 8.1.3
Multiple-variable
comparison plot (see
Section 2.2.2) showing the
seasonal and interannual
properties of select
cosampled variables at
the Urdaibai Estuary
monitoring area.

Additional variables are
available online at: <http://WGZE.net/time-series>.

Urdaibai Estuary, inner Bay of Biscay



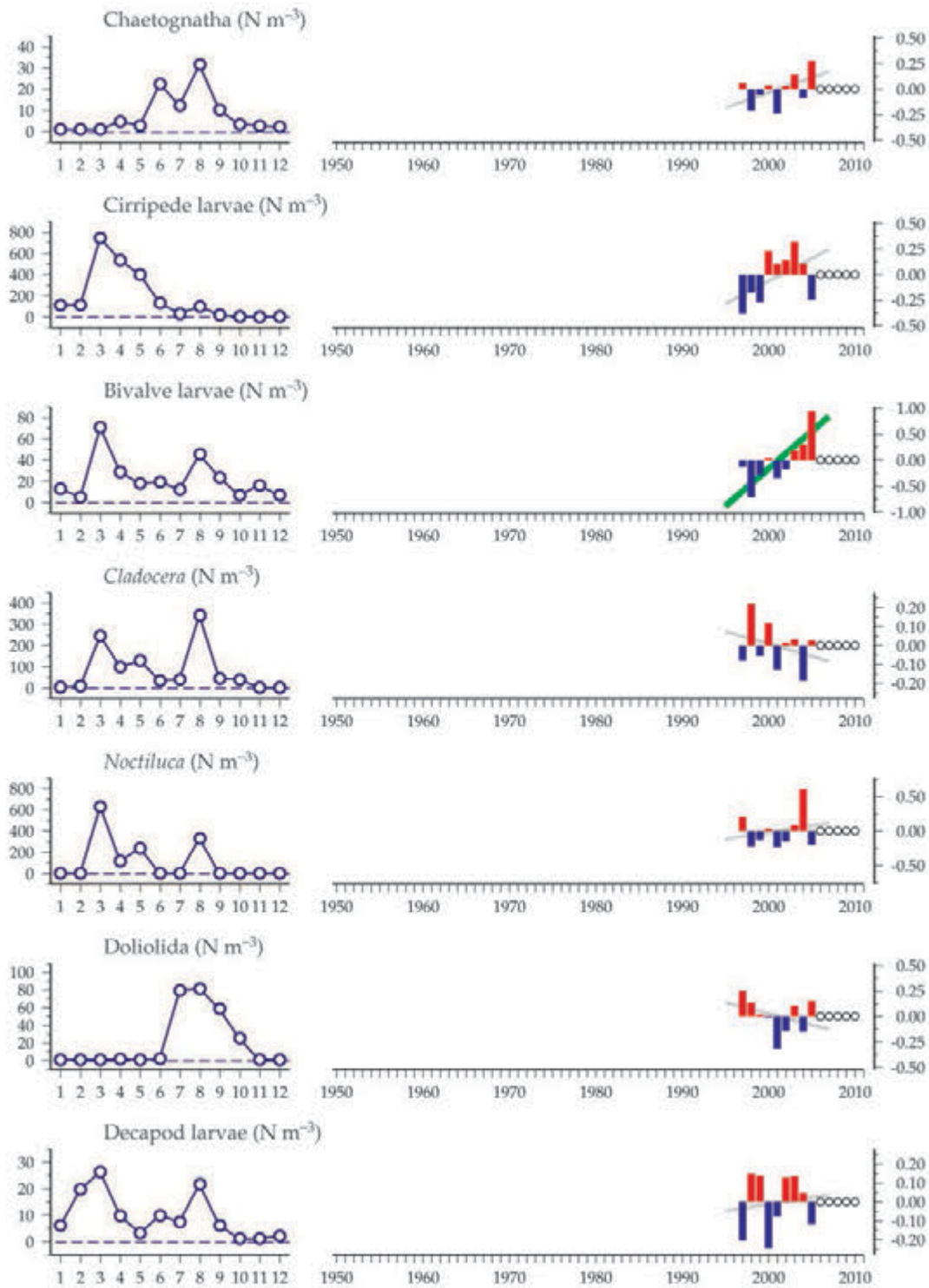
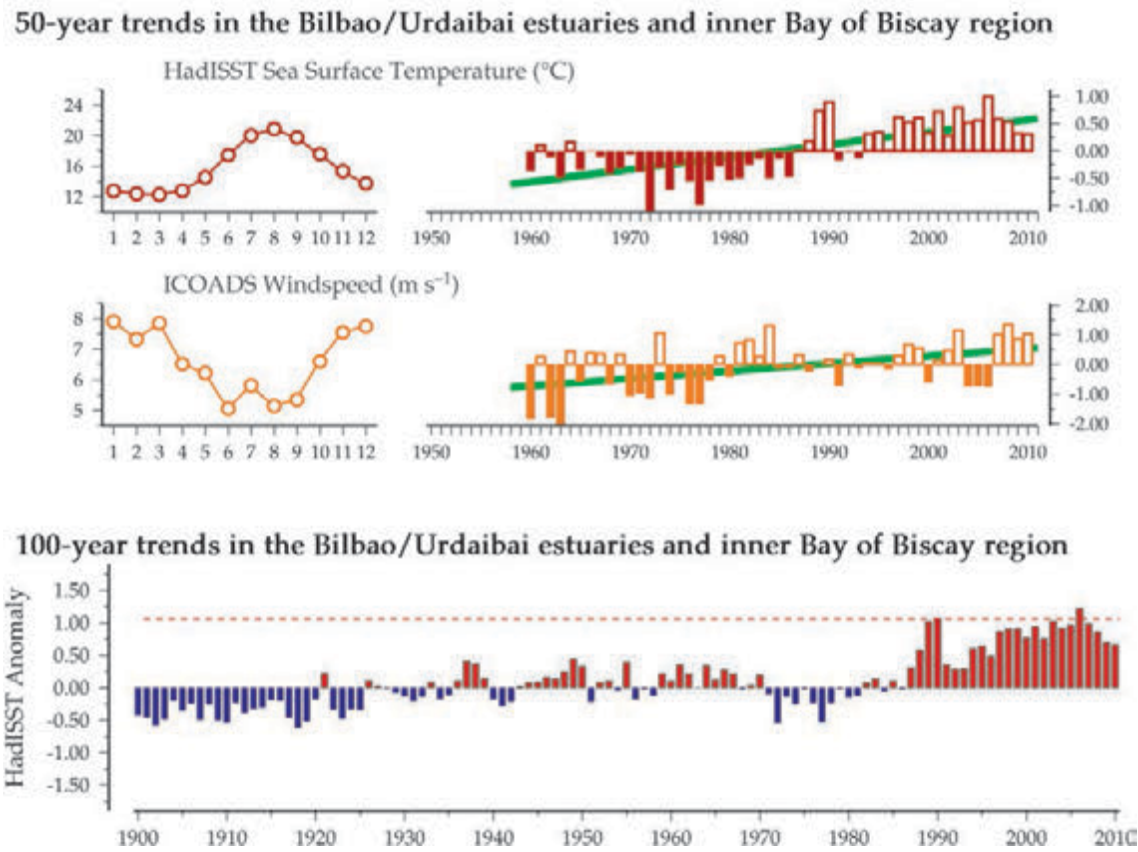


Figure 8.1.3
continued

Figure 8.1.4
Regional overview
plot (see Section 2.2.3)
showing long-term sea
surface temperatures and
windspeeds in the general
region surrounding the
Bilbao/Urdaibai Estuary
monitoring area.



8.2 RADIALES Santander Transect (Site 50)

Juan Bueno and Ángel López-Urrutia

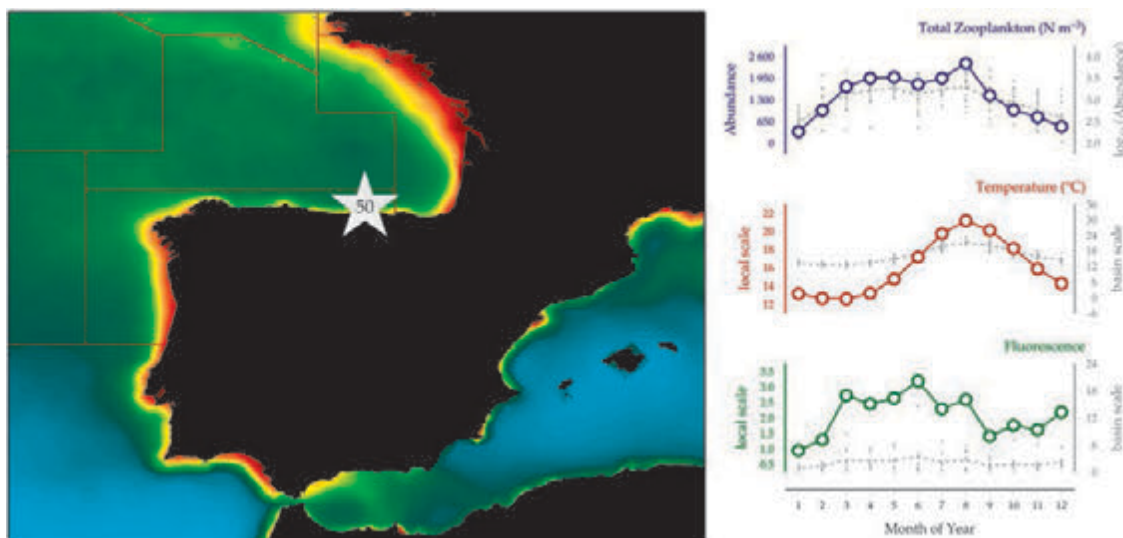


Figure 8.2.1
Location of the Santander transect monitoring area (Site 50) plotted on a map of average chlorophyll concentration, and its corresponding seasonal summary plot (see Section 2.2.1).

The transect off Santander (Figure 8.2.1) has been surveyed since 1992 in the framework of the project RADIALES of the Instituto Español de Oceanografía. This transect is carried out each month on board the RV “José de Rioja” and consists of four stations, although only the data from Station 4 (110 m deep, 43°34.4’N 3°47.0’W) is used for this report.

Zooplankton are sampled at each station by means of oblique tows from 50 m depth, using a Juday–Bogorov net of 50 cm mouth diameter and 250 µm mesh. Once on board, the samples are immediately preserved in 4% formalin in sodium-borate-buffered seawater and transported to the laboratory, where they are analysed by specialists for taxonomy and biomass. To estimate the total zooplankton dry weight, the samples are rinsed with 0.2 µm filtered seawater and put on a pre-combusted (24 h at 450°C) Whatman GF/A filter of known weight. Then, both the sample and the GF/A filter are dried at 60°C for 24 h. Finally, the total dry weight of the sample is obtained using a high-precision Sartorius microbalance.

Seasonal and interannual trends (Figure 8.2.2)

Total zooplankton biomass and abundance show the highest annual values from March to August. Zooplankton abundance is quite constant during this period, but there is a small drop in the central months, indicating a possible bimodal cycle, similar to that observed in the survey off Gijón. Although there is no clear trend in the zooplankton abundance or biomass during the years of sampling at Santander, there seems to be a low-frequency (5–6 years) cycle of high–low zooplankton abundance (Figure 8.2.2). This cycle also can be perceived in the data from the Continuous Plankton Recorder (CPR) from the adjacent CPR standard area E4 (Figure 8.2.3).

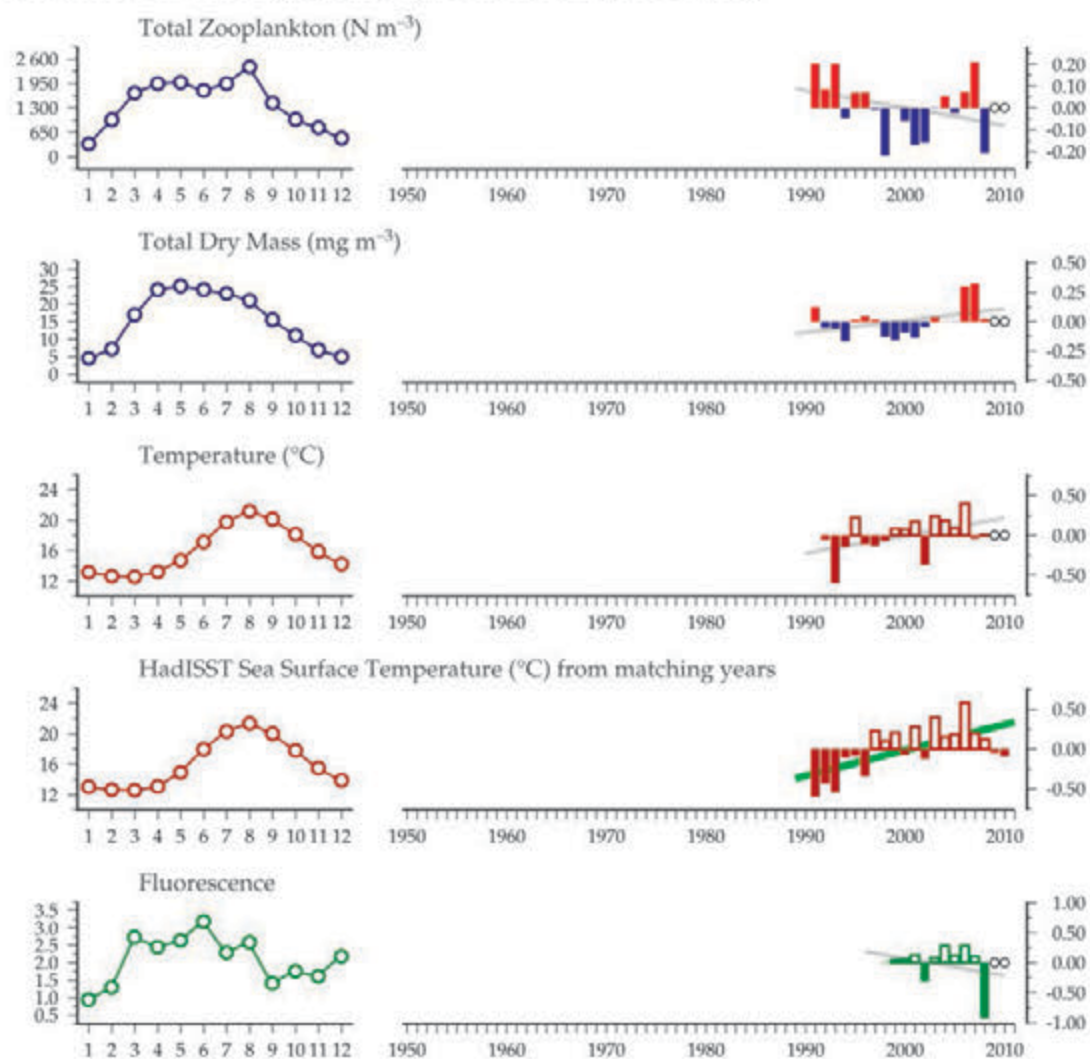
Temperature data from the 20 years sampling off Santander show a clear upward trend (Figure 8.2.2), supported by the data from the past 100 years (Figure 8.2.3). Similarly, copepod abundance in the CPR show a decreasing long-term trend (Figure 8.2.3), related to the decreasing trend in total abundance of diatoms and dinoflagellates.

The occurrence of warm-water-adapted marine species and the decrease in the abundance of species from upwelling zones in the Cantabrian Sea (Bode *et al.*, 2009) has been linked to the overall pattern of increasing temperature as well as to the transport by hydrological features such as the Iberian Poleward Current (IPC), a shelf-edge current flowing northward along the coast of southern Spain and Portugal during winter. Upwelling events are highly variable along the north coast of Spain in intensity and frequency. According to Lavín *et al.* (1998), stratification of the water column off Santander is now stronger and lasts longer than at the beginning of the monitoring survey. The increase in stratification of the water column leads to more oligotrophic conditions, which reinforces the microbial loop, but can also be viewed as a cause of the drop in zooplankton biomass (Valdés and Moral, 1998; Valdés *et al.*, 2007).

Figure 8.2.2
Multiple-variable
comparison plot (see
Section 2.2.2) showing the
seasonal and interannual
properties of select
cosampled variables at
the Santander transect
monitoring area.

Additional variables are
available online at: <http://WGZE.net/time-series>.

Santander Transect (Station 4), southern Bay of Biscay



50-year trends in the Santander Transect / southern Bay of Biscay region

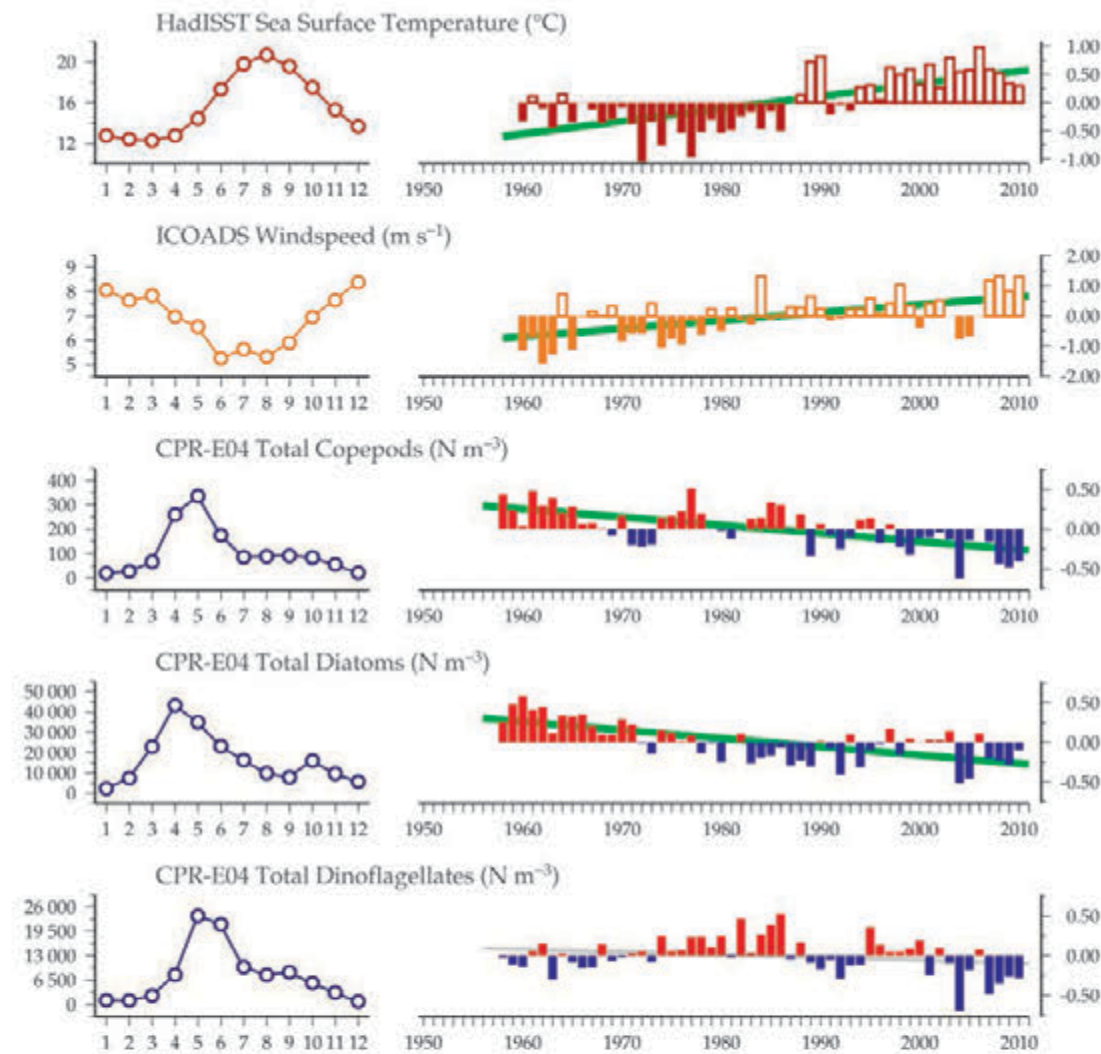
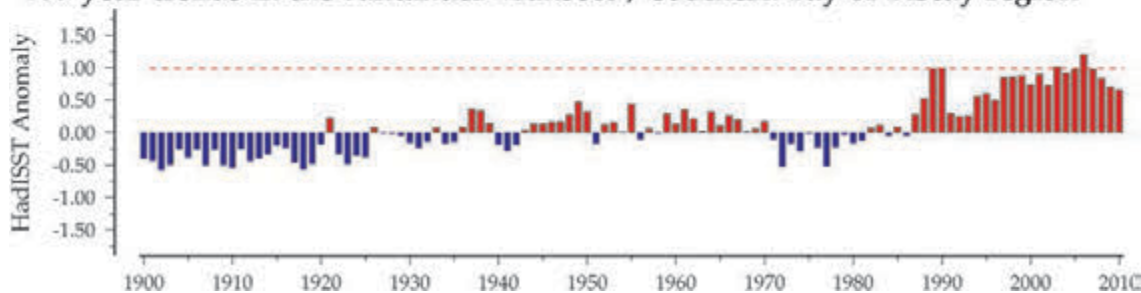


Figure 8.2.3
Regional overview plot
(see Section 2.2.3) showing
long-term sea surface
temperatures and wind
speeds in the general region
surrounding the Santander
transect monitoring area,
along with data from
the adjacent CPR E04
Standard Area.

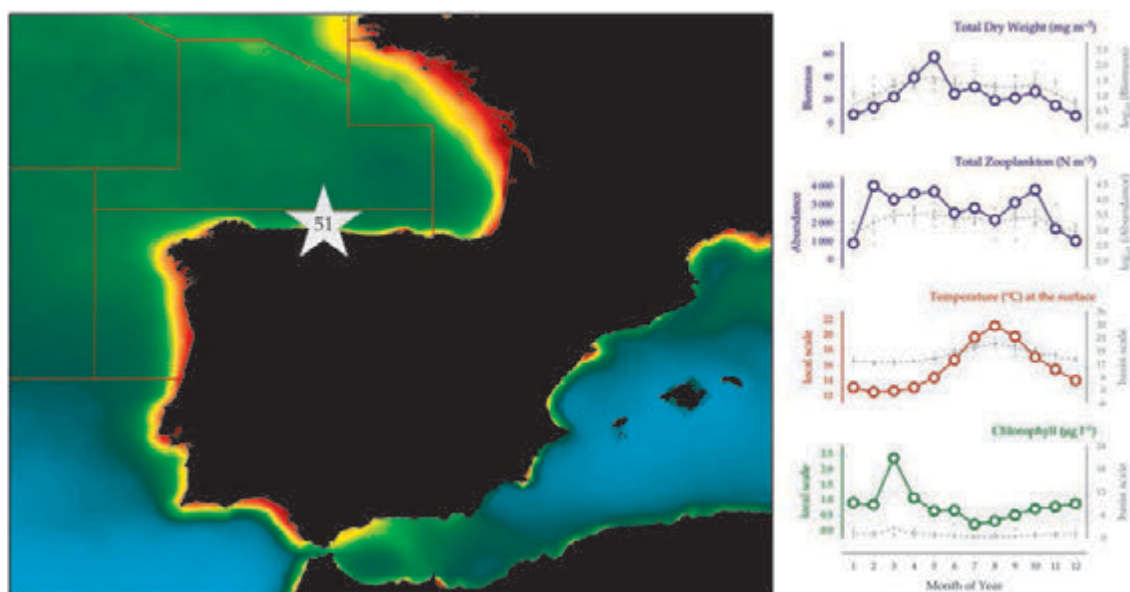
100-year trends in the Santander Transect / southern Bay of Biscay region



8.3 RADIALES Gijón/Xixón Transect (Site 51)

Juan Bueno and Ángel López-Urrutia

Figure 8.3.1
Location of the Gijón/
Xixón Transect monitoring
area (Site 51) plotted on a
map of average chlorophyll
concentration, and its
corresponding seasonal
summary plot (see Section
2.2.1).



The monthly transect off Gijón (Figure 8.3.1) has been carried out since 2001 as part of the temporal data-series project RADIALES (Insitituto Español de Oceanografía; <http://www.seriestemporales-ieo.com>). The survey consists of three sampling stations, of which previous zooplankton reports have considered the most oceanic Station 3. However, in order to homogenize the origin of the data for both zooplankton and phytoplankton status reports, we will consider Station 2 (43°40.05'N 05°34.91'W, 109 m depth) in this report.

This survey is carried out on board the 15.80 m long RV “José de Rioja”. Zooplankton samples are collected monthly by means of a triple WP-2 net (38 cm diameter, 200 µm) in vertical hauls from 100 m depth to the surface and immediately preserved with 4% formalin in sodium-borate-buffered seawater for posterior laboratory analysis. Once in the laboratory at the Oceanographic Center of Gijón, the protocol for zooplankton dry weight measurement starts by separating the samples into three size classes (200–500, 500–1000, and >1000 µm) using sieve cups equipped with Nitex screens. The samples are rinsed with 0.2 µm filtered seawater and dried at 60°C on preweighted, precombusted (450°C, 24 h) Wathman GF/A filters. The total dry weight is measured after 24 h.

The Bay of Biscay is located in the subtemperate part of the eastern North Atlantic, and the hydrographic conditions along the Gijón survey are characterized by a marked seasonality reflected in the cycle of stratification-mixing. In the southern Bay of Biscay, the most remarkable hydrographic feature is the occurrence of the warm and saline Iberian Poleward Current (IPC) during winter. The pattern of upwelling events in the area is driven by the winds in spring and also is dependent on the topography of the coast (Botas *et al.*, 1990).

Seasonal and interannual trends (Figure 8.3.2)

The annual pattern of zooplankton abundance is characterized by minimum values in winter (November–January) and peaks in spring and late summer. This pattern is also observed for zooplankton biomass. This finding is consistent with the observations in previous years at Station 3, and it seems to be related to the spring bloom of phytoplankton. Furthermore, the relative short duration of sampling off Gijón makes it difficult to infer any long-term trend in zooplankton abundance, although a low-frequency pattern (5–6 years) can be perceived in the data from the adjacent Continuous Plankton Recorder standard area E4 (Figure 8.3.3), with a clear overall decreasing trend in abundance of copepods that is also observed in total diatom abundance. While the peak in phytoplankton biomass occurs in March on this transect, the abundance peak of zooplankton seems to occur two months later. Given that zooplankton abundance remains constant during these months, the increase in biomass is likely caused by zooplankton growth and development.

Gijón/Xixón Transect (Station 2), southwestern Bay of Biscay

Figure 8.3.2
Multiple-variable
comparison plot (see
Section 2.2.2) showing the
seasonal and interannual
properties of select
cosampled variables at
the Gijón/Xixón Transect
monitoring area.

Additional variables are
available online at: <http://WGZE.net/time-series>.

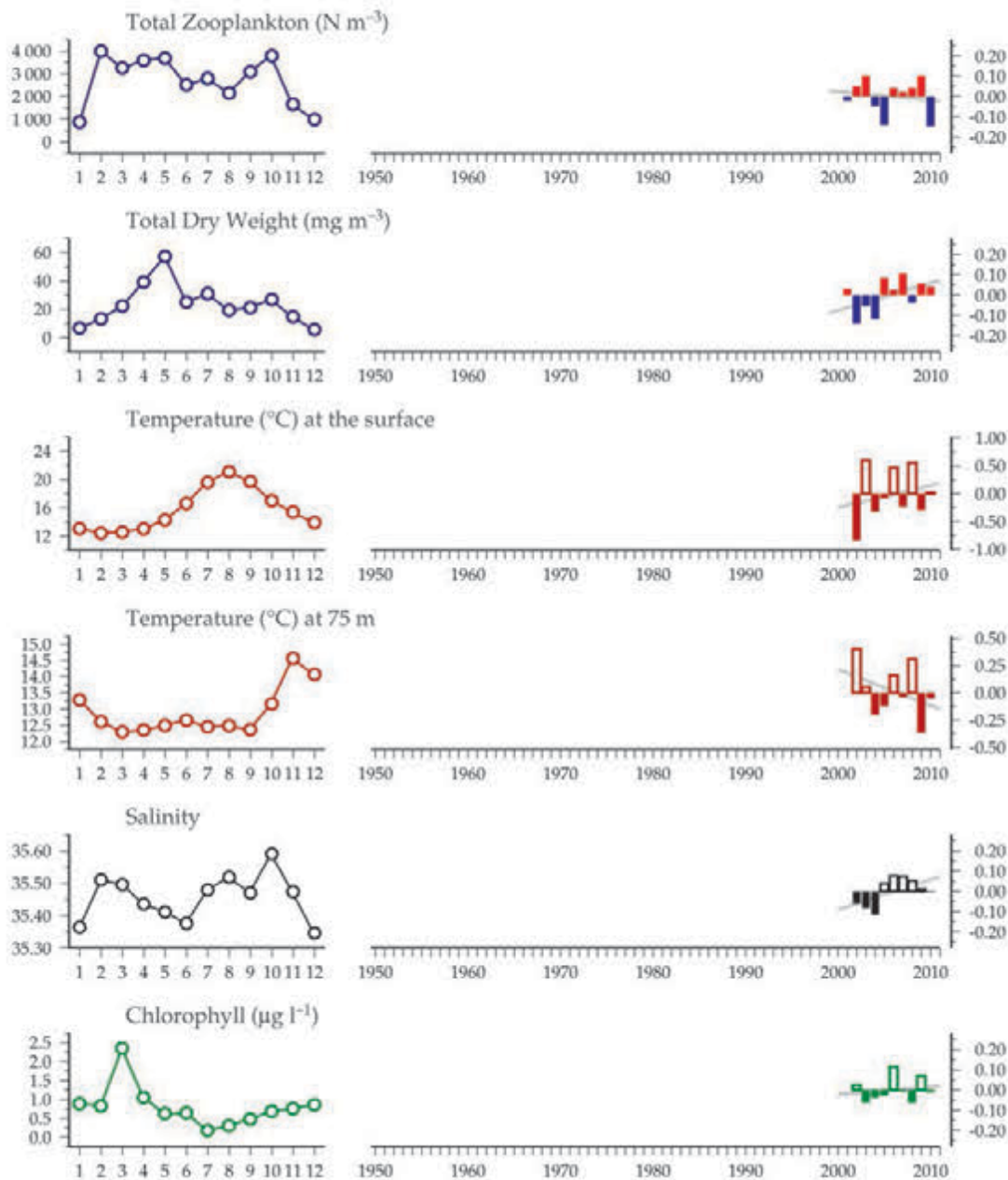
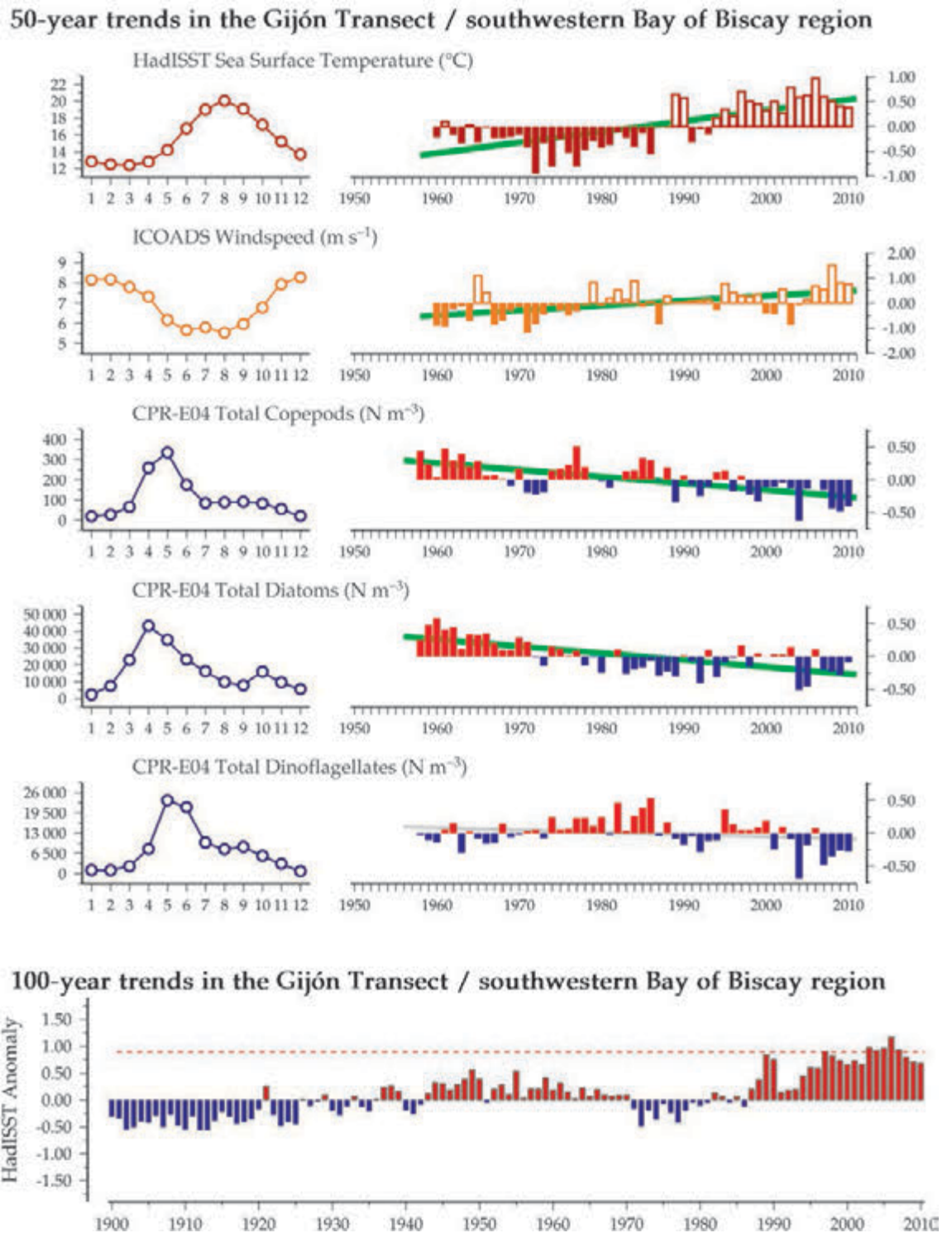


Figure 8.3.3
Regional overview
plot (see Section 2.2.3)
showing long-term sea
surface temperatures and
windspeeds in the general
region surrounding the
Gijón/Xixón Transect
monitoring area, along with
data from the adjacent CPR
E04 Standard Area.



8.4 RADIALES A Coruña Transect (Site 52)

M. Teresa Alvarez-Ossorio and Antonio Bode

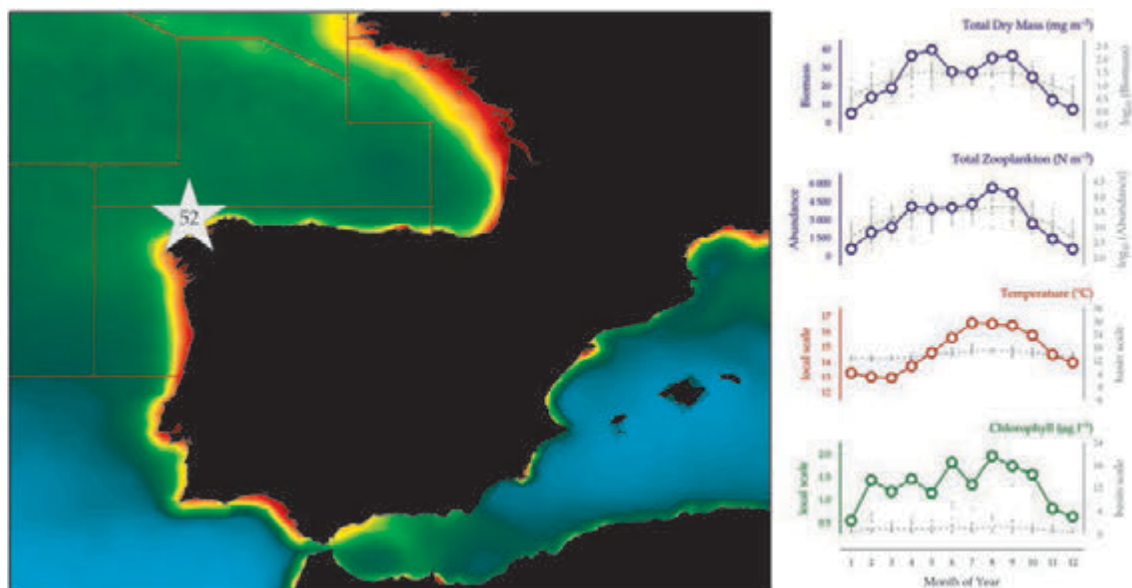


Figure 8.4.1
Location of the A Coruña Transect monitoring area (Site 52) plotted on a map of average chlorophyll concentration, and its corresponding seasonal summary plot (see Section 2.2.1).

The A Coruña transect is part of the time-series project RADIALES of the Instituto Español de Oceanografía (<http://www.seriestemporales-ieo.com>). Station 2, used for this summary, is located off the northwest Iberian coast at 43°25.3'N 8°26.2'W (Figure 8.4.1). Zooplankton samples are collected from 65 m to the surface (oblique hauls) on a monthly basis with a Juday–Bogorov net (0.5 m diameter, 200 µm mesh). Samples are preserved in 4% formalin in sodium-borate-buffered seawater and then examined in the laboratory for identification and counting of mesozooplankton by the rarefaction method (Omori and Ikeda, 1984). Biomass is calculated as dry weight (Lovegrove, 1962) of samples filtered upon arrival at the laboratory.

In the coastal region off Galicia (northwest Spain), the classical pattern of seasonal stratification of the water column in temperate regions is masked by upwelling events from April to September. These upwelling events provide zooplankton populations with favourable conditions for development in summer, which is the opposite of what occurs in other temperate seas in this season of the year. Nevertheless, upwelling is highly variable in intensity and frequency, demonstrating substantial year-to-year variability.

Seasonal and interannual trends (Figure 8.4.2)

The seasonal cycle in zooplankton biomass is characterized by high values from April to September, with a slight reduction in biomass from June to August, resulting in a modest bimodal seasonal cycle. Both biomass and

abundance demonstrate an overall increasing trend since 1989, although small decreases in biomass were observed in 2000 and 2006. The abundance of juvenile copepods increased significantly for some species (e.g. *Acartia clausi*, *Calanus helgolandicus*), while there were no significant trends for adults in most species. The increasing trends in copepods followed an increasing trend in surface-water temperature and chlorophyll measured at the same station (Bode *et al.*, 2011).

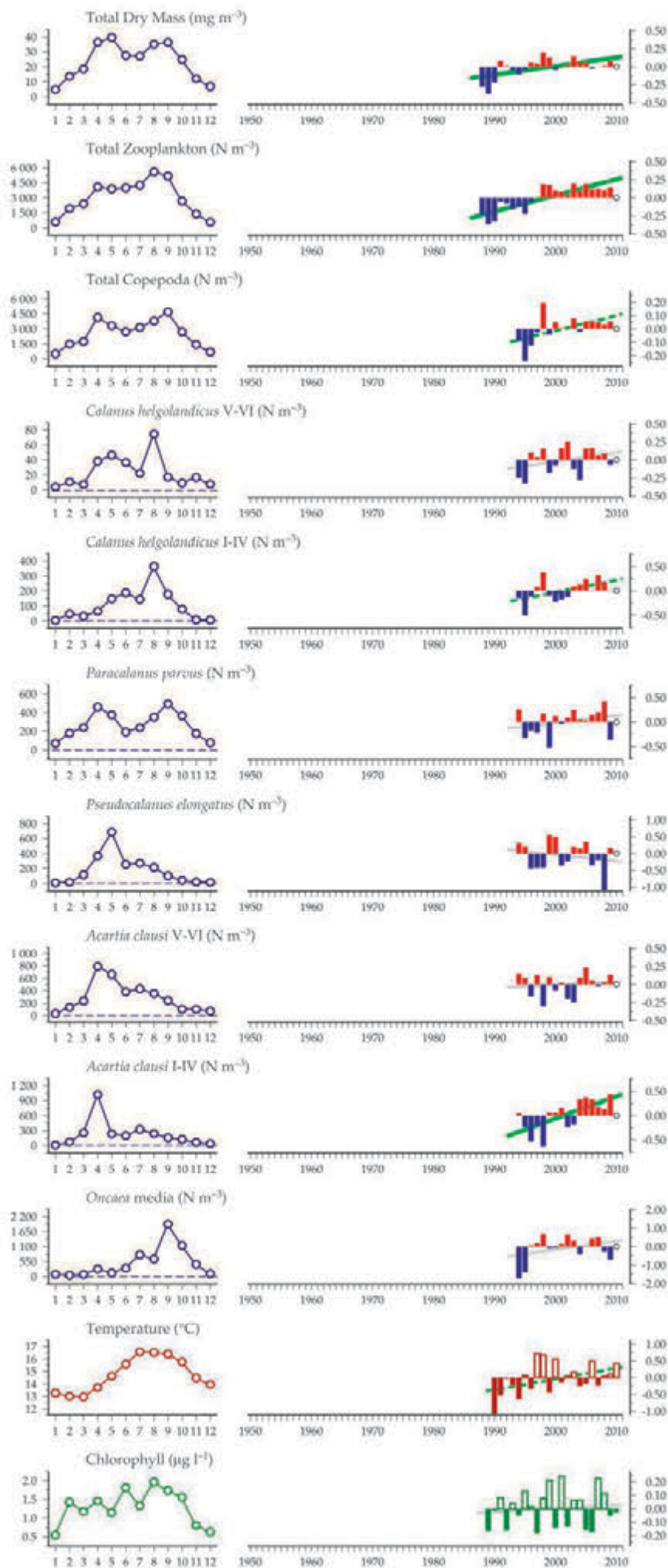
In situ temperature and Reynolds SST reveal an increasing trend of 1°C during the 20 years of the time-series. To further investigate both temperature and zooplankton trends at the site, data were compared with long-term data from CPR and Reynolds SST. Although the increasing trend in SST is also evident in the longer record, with SST increasing almost 1°C during the last half century, the increase in zooplankton abundance recorded at A Coruña during the last 20 years corresponds to a period of low copepod abundance in CPR standard area “F4” (see Figure 8.4.3). Although the abundance recorded by the CPR during the last 10 years in this area features negative anomalies, there is an increasing trend in the CPR data (i.e. moving from negative to positive), suggesting that the increasing trend observed off A Coruña may be a recovery from a period of low abundance (Bode *et al.*, 2009). Nevertheless, the CPR series contains only surface plankton data from outer shelf or oceanic waters and, although related, cannot be directly compared with coastal series even in the same region (Bode *et al.*, 2012).

Figure 8.4.2

Multiple-variable comparison plot (see Section 2.2.2) showing the seasonal and interannual properties of select cosampled variables at the A Coruña Transect monitoring area.

Additional variables are available online at: <http://WGZE.net/time-series>.

A Coruña Transect (Station 2), northwest Iberian Shelf



50-year trends in the A Coruña Transect / northwest Iberian Shelf region

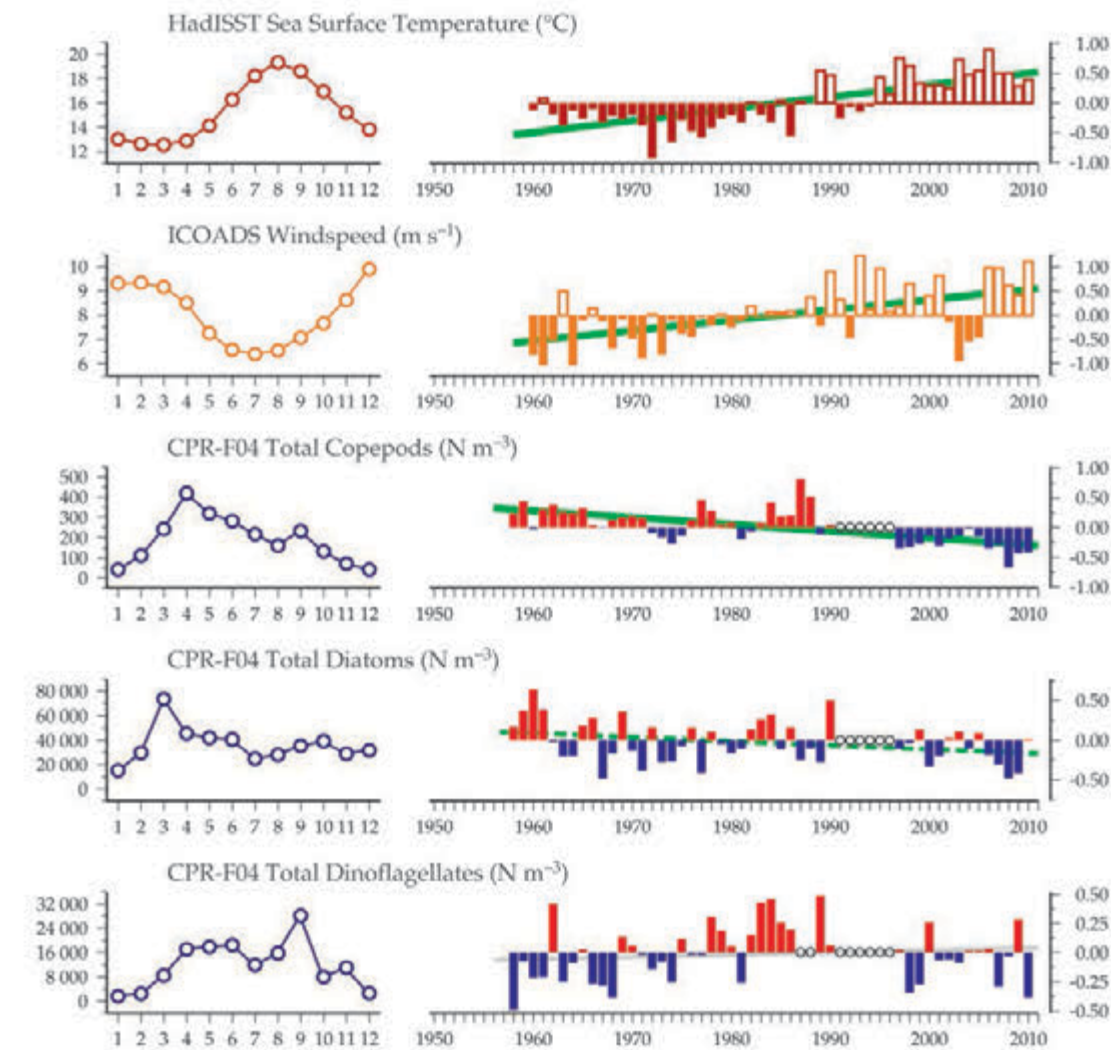
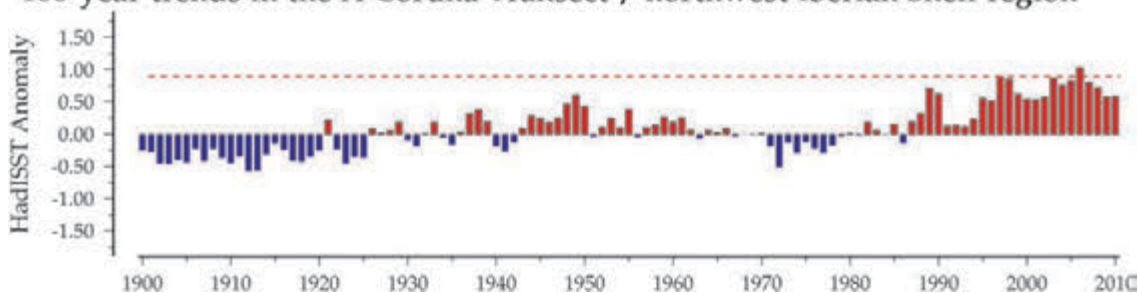


Figure 8.4.3
Regional overview plot (see Section 2.2.3) showing long-term sea surface temperatures and windspeeds in the general region surrounding the A Coruña Transect monitoring area, along with data from the adjacent CPR F04 Standard Area.

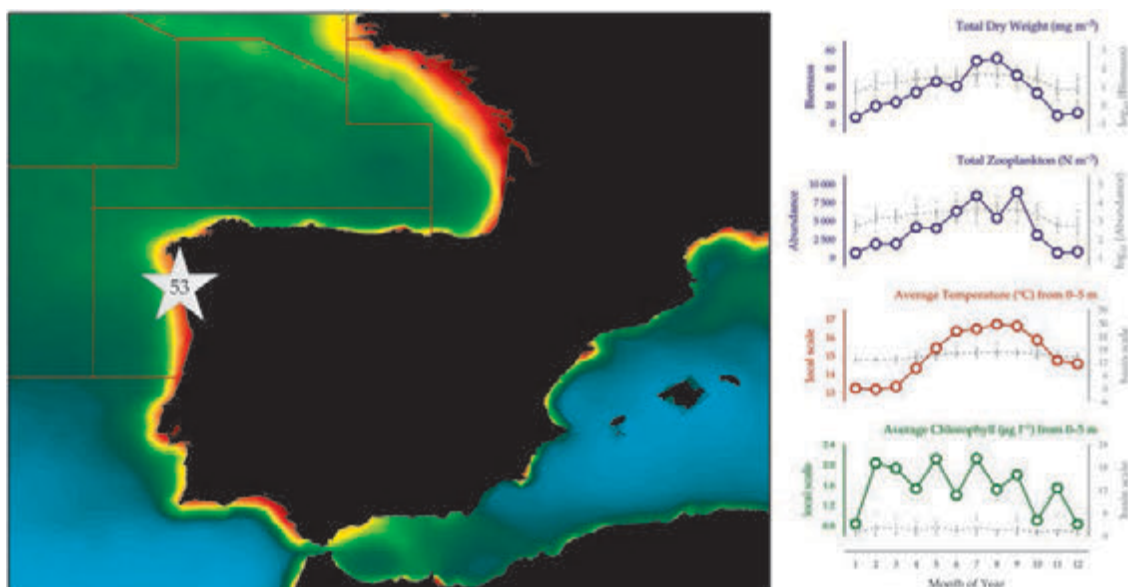
100-year trends in the A Coruña Transect / northwest Iberian Shelf region



8.5 RADIALES Vigo Transect (Site 53)

Ana Miranda, Gerardo Casa, and Antonio Bode

Figure 8.5.1
Location of the RADIALES Vigo survey area (Site 53), plotted on a map of average chlorophyll concentration, and their corresponding seasonal summary plot (see Section 2.2.1).



The Vigo transect has been sampled since 1987 as part of the time-series project RADIALES of the Instituto Español de Oceanografía (<http://www.seriestemporales-ieo.com>). Station 3 of the Vigo transect, which was used for this summary, is located off the northwest Iberian coast at 42.1417°N 8.9533°W. Zooplankton samples are collected from 50 m to the surface (oblique hauls) on a monthly basis with a Juday–Bogorov net (0.5 m diameter, 200 µm mesh). Samples are preserved in 4% formalin in sodium-borate-buffered seawater and then examined in the laboratory for identification and counting of mesozooplankton by the rarefaction method (Omori and Ikeda, 1984). Biomass is calculated as dry weight (Lovegrove, 1962) of samples filtered upon arrival at the laboratory.

In the coastal region off Galicia (northwest Spain), the classical pattern of seasonal stratification of the water column in temperate regions is masked by upwelling events from April to September. These upwelling events provide zooplankton populations with favourable conditions for development in summer, which is the opposite of what occurs in other temperate seas in this season of the year. Nevertheless, upwelling is highly variable in intensity and frequency, demonstrating substantial year-to-year variability.

Seasonal and interannual trends (Figure 8.5.2)

The seasonal cycle of zooplankton biomass is characterized by high values from April to October, with a slight reduction in June and August and a clear reduction in winter. In contrast with the series in A Coruña, the zooplankton at Vigo shows a single late summer biomass and abundance peak. Interannual biomass anomalies reveal an increasing

trend, following a period of low biomass observed in the period 1994–2001. Copepod species typical of warm waters (e.g. *Temora stylifera*) appeared in relatively large numbers during warmer periods (e.g. 1997–1998, 2001–2002, and 2009), while other species decreased in the five years prior to 2010 (e.g. *Calanoides carinatus*, *Acartia clausi*).

In situ temperature decreased over the 21 years of the time-series, in contrast with regional averages at nearby locations (e.g. A Coruña). To investigate longer-term trends in both temperature and zooplankton at the site, data were compared with long-term data from CPR and SST records (Figure 8.5.3). Long-term temperatures in the region reveal an increase of almost 1°C in SST during the last half century. As described for the A Coruña series, the increase in zooplankton biomass and abundance recorded at Vigo during the past 15 years is not reflected in the period of below-average copepod abundance in CPR standard area F4, due to local upwelling conditions near the coast and to the differences in the waters sampled by each series (Bode *et al.*, 2012).

Vigo Transect (Station 3), northwest Iberian Shelf

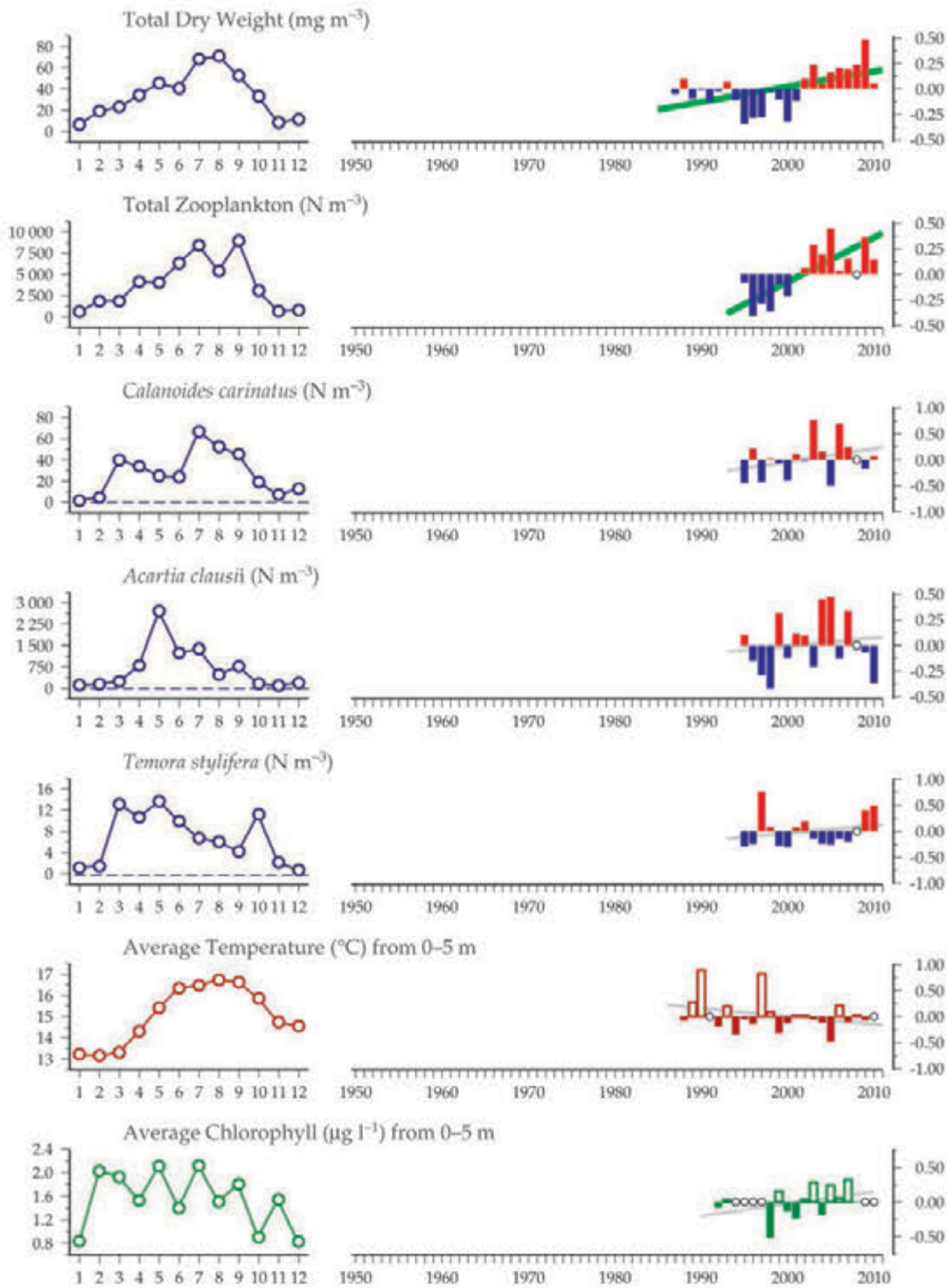


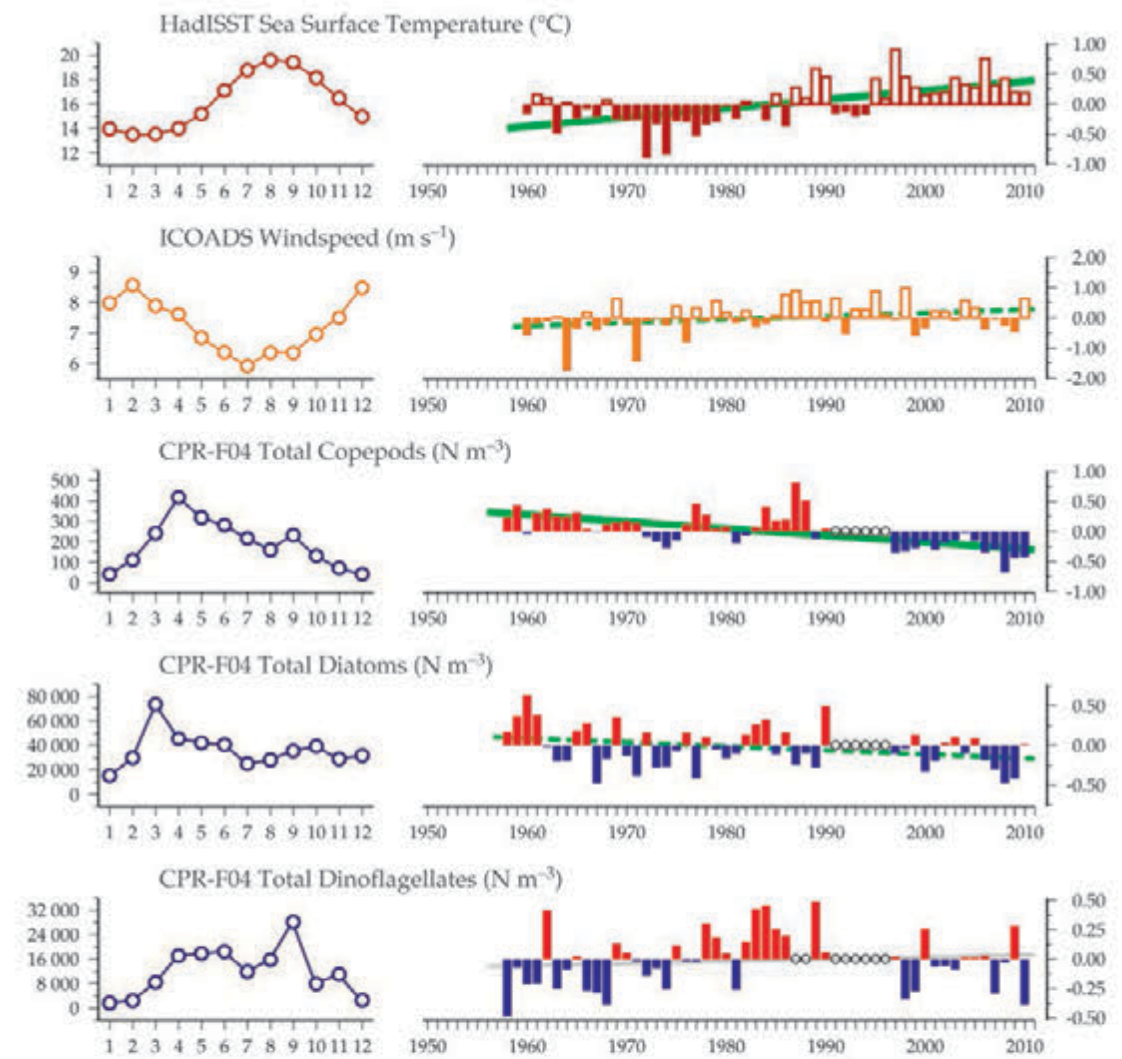
Figure 8.5.2
Multiple-variable
comparison plot (see
Section 2.2.2) showing the
seasonal and interannual
properties of select
cosampled variables at the
Vigo Transect monitoring
area.

Additional variables are
available online at: <http://WGZE.net/time-series>.

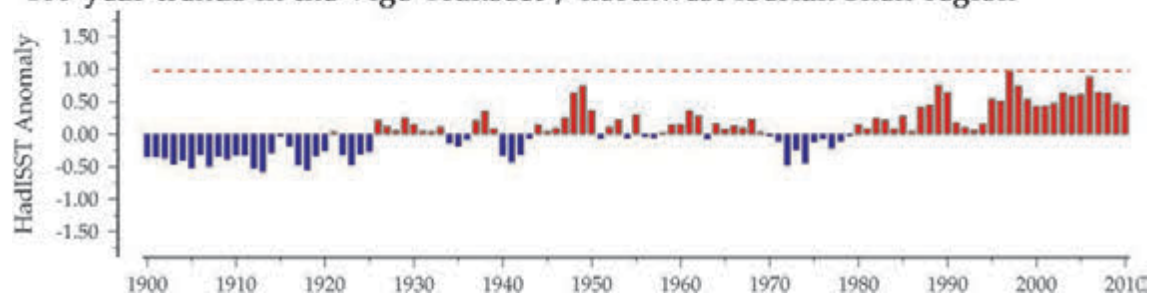
Figure 8.5.3

Regional overview plot
(see Section 2.2.3) showing
long-term sea surface
temperatures and wind
speeds in the general region
surrounding the Vigo
Transect monitoring area,
along with data from the
adjacent CPR F04 Standard
Area.

50-year trends in the Vigo Transect / northwest Iberian Shelf region



100-year trends in the Vigo Transect / northwest Iberian Shelf region



8.6 Cascais Bay (Site 54)

Antonina dos Santos and A. Miguel P. Santos

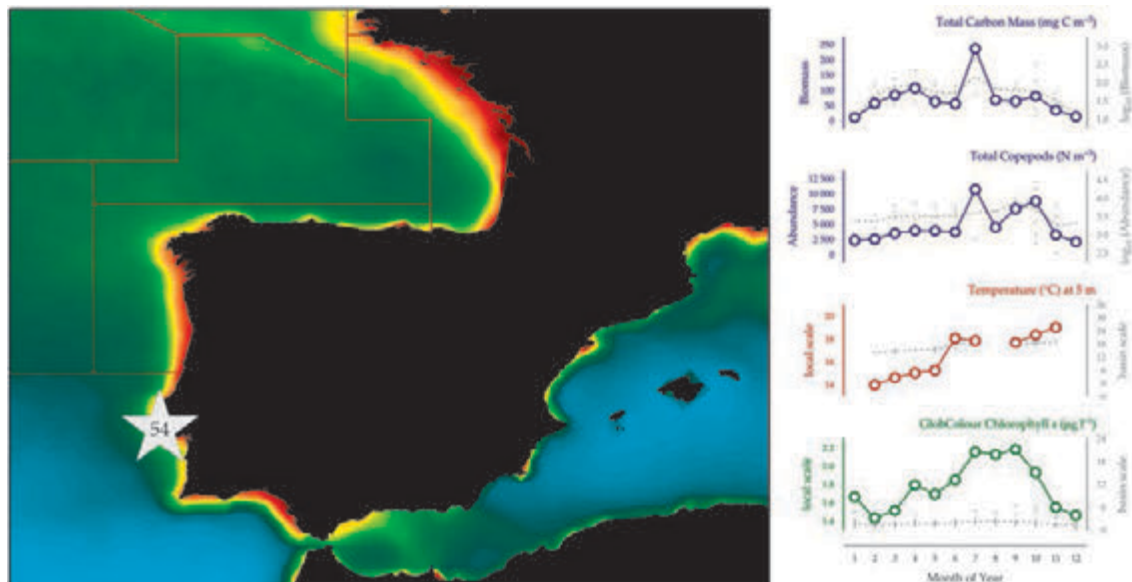


Figure 8.6.1
Location of the Cascais Bay monitoring area (Site 54) plotted on a map of average chlorophyll concentration, and its corresponding seasonal summary plot (see Section 2.2.1).

The Cascais monitoring site is a station of the time-series CASCAIS-WATCH, the oceanographic observation programme of the Oceanography and Plankton Group of the Instituto Português do Mar e da Atmosfera (IPMA), former Instituto Nacional de Recursos Biológicos. The station is located off Cascais Bay, outside the Tagus River estuary at 38°40'N 09°26.2'W and approximately 4 km offshore from Cascais, a town 40 km west of Lisbon, in a water depth of around 38 m. The hydrography of the bay is influenced by coastal morphology, the bottom topography (submarine canyons of Lisbon and Setúbal), and the discharge of freshwater from the Tagus River (Ribeiro and Amorim, 2008).

Zooplankton samples are collected from 30 m to the surface (oblique hauls) on a monthly basis with a WP2 net (50 cm diameter, 200 µm mesh). Samples are divided into two with a Folsom plankton splitter: one half is preserved in 4% borax-buffered formalin in seawater and later examined for identification and counting of mesozooplankton. The other half is lyophilized and weighed for biomass determination. During the first four years of sampling (2005–2008), neuston samples were also taken with a rectangular net with a mouth

opening of 0.2 × 1.0 m and 200 µm mesh size, towed horizontally at the surface for 3 min. The samples were preserved and stored for later analysis. During the first year of sampling, *Calanus helgolandicus* egg production was determined whenever possible. After the first year of sampling and having concluded that *Acartia* spp. was the most abundant copepod present in the samples, egg production measurements were started for this taxon and stopped for *C. helgolandicus*. Besides zooplankton monitoring, temperature, salinity, and chlorophyll *a* are measured with a CTD fluorometer.

The Cascais site is thought to be under the influence of the Eastern North Atlantic Upwelling System in spring and summer. This seasonal upwelling is responsible for the high phytoplankton production that promotes stable zooplankton abundance through the year (Santos *et al.*, 2007). *In situ* temperatures at Cascais demonstrate a two-tier seasonal pattern, usually < 16°C during winter and spring, and ≥18°C in June–November. This pattern is attributed to the station being located in an upwelling shadow (Moita *et al.*, 2003), where winds favourable to upwelling can promote local water stratification and stability.

Seasonal and interannual trends (Figure 8.6.2)

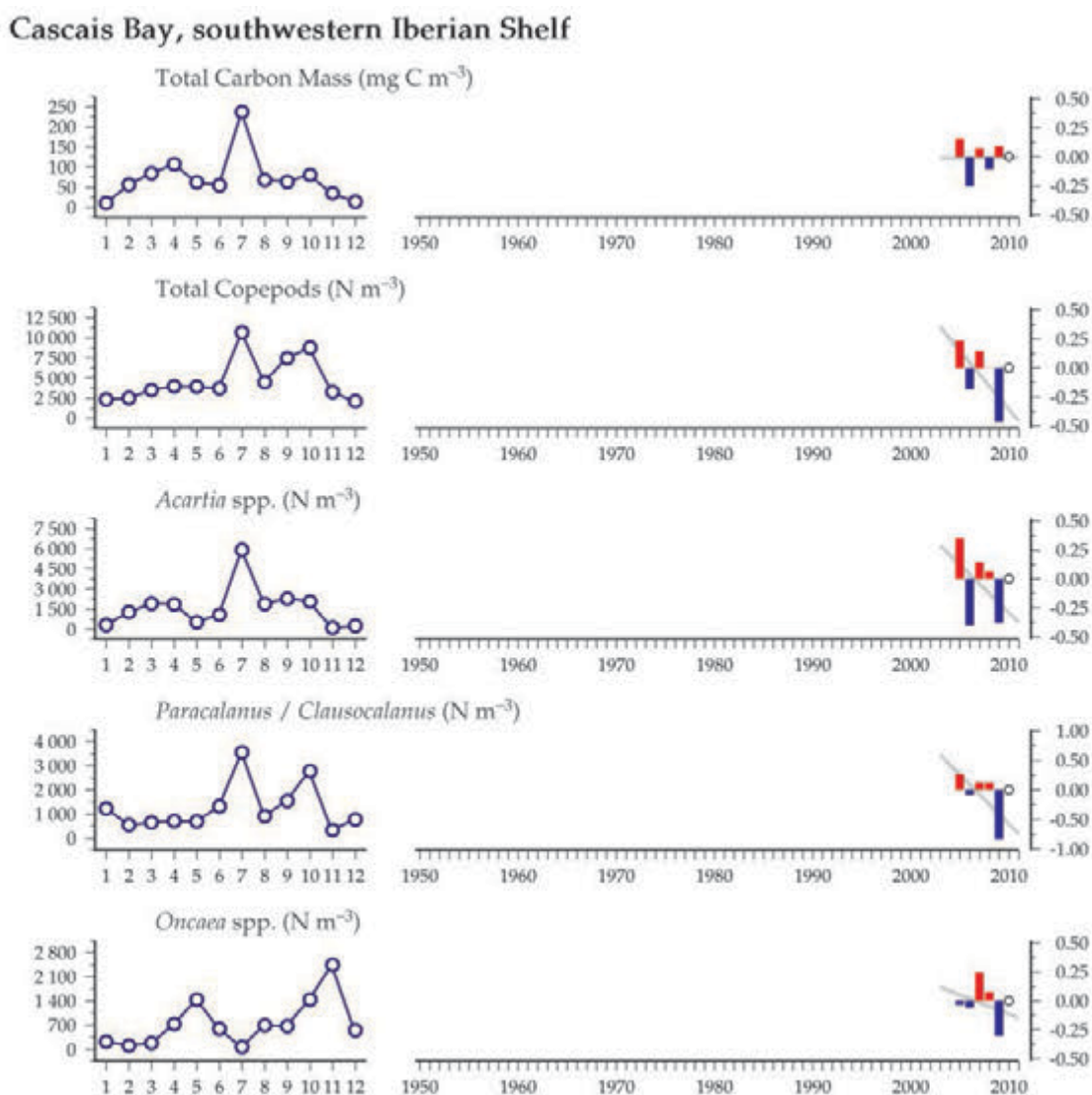
The seasonal cycle of zooplankton biomass is characterized by a bimodal pattern, as observed at sites 52 and 53 to the north, with peak biomass in April and August. Copepod abundance remains high throughout the season, with highest abundance from August through November. The observed bimodal pattern is caused by seasonal upwelling in the area. Copepods at Cascais Bay are mainly represented by the genera *Acartia*, *Paracalanus*, *Oncaea*, and *Oithona*. Other species (*Temora stylifera*, *T. longicornis*, and *Centropages* spp.) are also important, but occur later in the season, which explains the high copepod abundance late in the year. The short length of this time-series limits its interannual analysis. Total copepod abundance and *in situ* temperature interannual anomalies oscillate together and result in a significant negative correlation ($r^2 = 0.7848$). Total copepod abundance has been decreasing in the last two years of sampling, mainly caused by a reduction in the three most abundant genera: *Acartia*, *Paracalanus*, and *Oithona*. The trends in these species are positively correlated. Following the decrease in abundance of copepods, bivalve

veligers have become more abundant in the area, being the most abundant taxa in 2009, representing 26.2% of total zooplankton in that year. Veliger abundance follows the increasing abundance of the invasive species *Ruditapes philippinarum* in the Tagus estuary since its establishment 10 years ago. This clam now supports a local fishery (Garaulet, 2011). The decrease in copepod abundance at this site (54) follows the trends shown at site 53 Vigo (north of Cascais site) where the copepods *A. clausi* and *Calanoides carinatus* have been decreasing. However, additional data are necessary to better understand this shift in species abundance at the Cascais site and the relationship with the temperature increase over the past 30 years (Figure 8.6.3). Also, identification of the bivalve veligers to lower taxonomic levels is necessary in order to understand the importance of introduced species in the area.

The long-term temperature record for this region (Figure 8.6.3) demonstrates that SSTs are currently at the high end of those seen in the past 100 years.

Figure 8.6.2
Multiple-variable
comparison plot (see
Section 2.2.2) showing the
seasonal and interannual
properties of select
cosampled variables at the
Cascais Bay monitoring
area.

Additional variables are
available online at: <http://WGZE.net/time-series>.



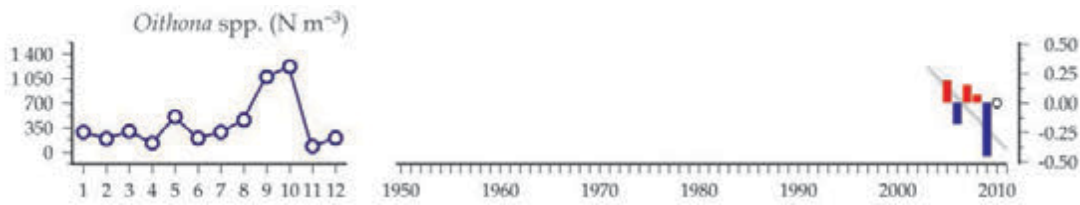


Figure 8.6.2
continued

50-year trends in the Cascais Bay, southwestern Iberian Shelf region

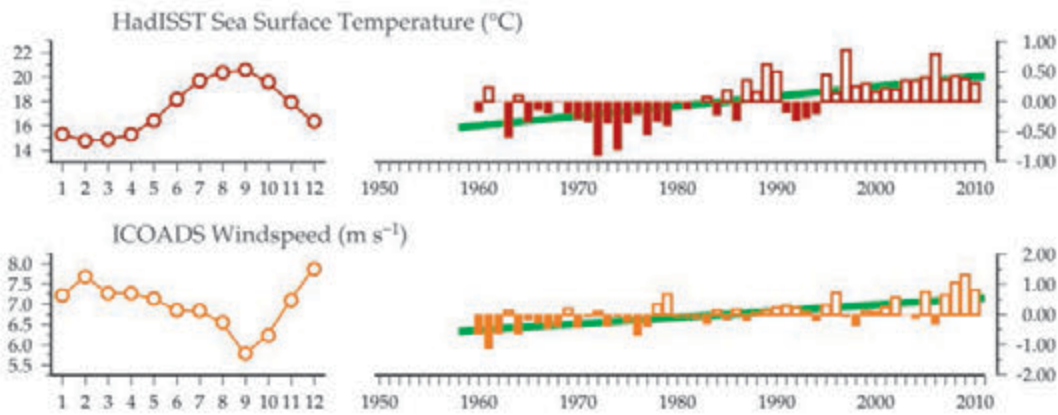
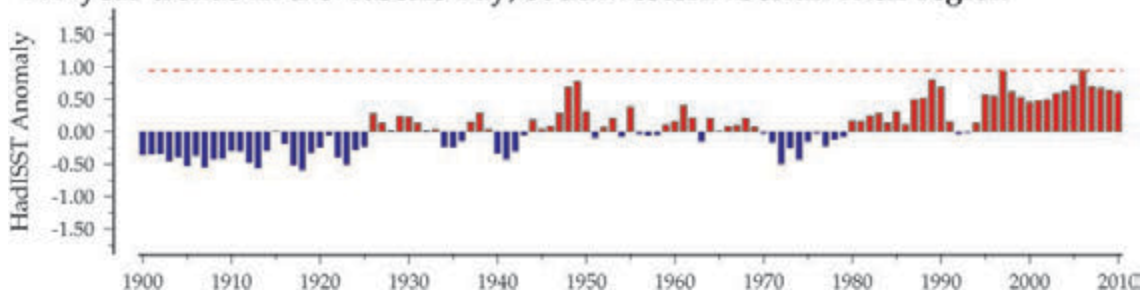


Figure 8.6.3
Regional overview
plot (see Section 2.2.3)
showing long-term sea
surface temperatures and
windspeeds in the general
region surrounding the
Cascais Bay monitoring
area.

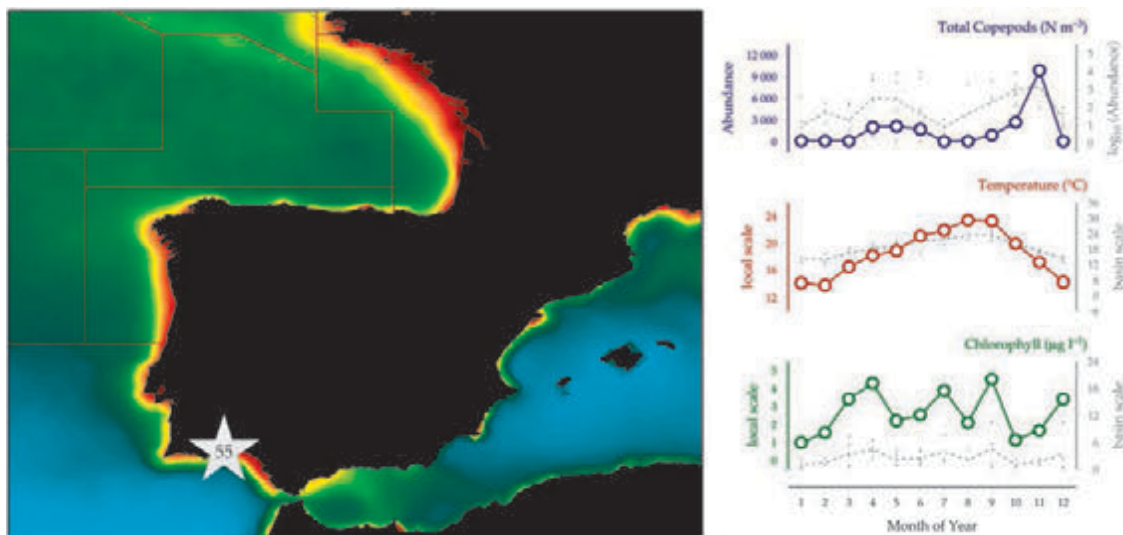
100-year trends in the Cascais Bay, southwestern Iberian Shelf region



8.7 Guadiana Lower Estuary (Site 55)

*Maria Alexandra Chícharo, Joana Cruz,
Radhouan Ben-Hamadou, and Luis Chícharo*

Figure 8.7.1
Location of the Guadiana Lower Estuary monitoring area (Site 55) plotted on a map of average chlorophyll concentration, and its corresponding seasonal summary plot (see Section 2.2.1).



The Guadiana Lower Estuary sampling site is located between 37°13'15.03"N 007°24'49.86"W and 37°07'44.04"N 007°24'06.36"W, and includes two sampling stations, one in the estuary mouth and one in the plume (stations G1 and G2, respectively), in a water depth ranging from 5 to 30 m.

The Guadiana site is a mesotidal estuary with an average tidal amplitude of 2 m, ranging from partially stratified to well-mixed. It has an average depth of 6.5 m and an area of 22 km². It can be divided into three subareas: upper, middle, and lower estuary (Chícharo *et al.*, 2001). The lower estuarine area is influenced by extensive saltmarsh areas, and the salinity is usually above 20.

The Guadiana Estuary is located in the Northeast Atlantic, but is under the influence of the Mediterranean climate. Natural river inflows typically vary markedly, within and between years, as a result of seasonal and annual fluctuations in rainfall. In addition to this natural variation in freshwater discharge into the estuary, extensive urban and agricultural development in the Guadiana River basin (fourth largest river basin in the Iberian Peninsula; 67 480 km²) mainly since the 1950s, led to the construction of hundreds of dams. Recent construction of the large Alqueva Dam, begun in 1999 and completed in 2002, further increased freshwater flow regulation, and according to an international agreement between Portugal and Spain, the average daily flow in lower riverine areas cannot be lower than 2 m³ s⁻¹ (Chícharo *et al.*, 2006). As a consequence, the Guadiana Estuary shifts between being freshwater-dominated during winter and flood periods, and being influenced by marine waters during the rest of

the year. The Guadiana Estuary is also influenced by weak upwelling events (Morais *et al.*, 2009).

Sampling at the site is done in support of a variety of time-limited research projects. Zooplankton monitoring in the lower Guadiana Estuary began in 1997 and was motivated by the need for a reference description of communities before the finalization of the construction of the Alqueva Dam. Physical-chemical variables (e.g. temperature, salinity, *in situ* chlorophyll), and zooplankton abundance and composition were monitored at different stations of the estuary and seasons.

Zooplankton samples are collected using a WP2 net (40 cm diameter, 200 µm mesh) and a flowmetre towed horizontally. Samples are preserved in 4% borax-buffered formalin in seawater. Since 1997, detailed taxonomic analysis has been carried out on the mesozooplankton samples every month or every 2–3 months, depending on the supporting project aims. In 2003, 2004, and 2005, no sampling occurred due to the absence of supporting funding. Data presented here are average monthly values collected at two stations just below the surface (ca. 0.5 m). Temperature and salinity are determined with YSI CTD 6600 or a multiparameter probe (PRO YSI). Chlorophyll *a* concentration, used as a proxy for phytoplankton biomass, is analyzed using an *in situ* fluorimetric method (Turner 10 AU), and periodically corrected with a spectrophotometric method after GF/F sample filtration and acetone extraction. Abundance of major zooplankton groups is estimated using binocular microscopy.

Seasonal and interannual trends (Figure 8.7.2)

The seasonal minimum temperature of ca. 13°C generally occurs in late February–early March and rises to 25°C in August–September. Total zooplankton has low seasonal variability and tends to be higher in spring/summer and autumn than in winter. Cladocerans and copepods tend to mirror the total zooplankton, but gelatinous organisms like appendicularians and hydromedusae also contribute to summer mesozooplankton density. Zooplankton seasonal patterns follow the phytoplankton proxy chlorophyll *a*, with maxima usually occurring between March and October. The most abundant invertebrate meroplankton exhibits maxima in summer and include decapods and molluscs, while fish eggs and larvae are also represented in spring and autumn months.

The HadISST temperatures time-series in the Guadiana Estuary area from 1950 indicates that sea temperature around the site has increased. Interannual variability in salinity and freshwater input show some increases in salinity and decreases in freshwater inflow, which may be explained by regulation of river flow by dams in the Guadiana catchment and or NAO-influenced precipitation levels.

The Guadiana Estuary has been recently invaded by the jellyfish, *Blackfordia virginica* (Chícharo *et al.*, 2009). An increasing trend in density of hydromedusae has been found, probably related to this invasion. Studies such as those of Molinero *et al.* (2005) note that warmer water temperatures (and subsequent water-column stability) tend to favour higher jellyfish abundance. This was explained by modified flow regimes that encourage invasions of estuarine areas (Bunn and Arthington, 2002). In addition, several studies have demonstrated that the large climatic signals, such as the North Atlantic Oscillation (NAO), could affect the zooplankton communities and structures (Molinero *et al.*, 2005).

Cladocerans are mainly represented by *Penilia* and *Podon* in recent years. In previous years, before intense dam regulation of the flow in 1997/1998, strong freshwater pulses occurred, and the brackish and freshwater cladocerans *Bosmina longirostris* and *Ceriodaphnia* spp. were more important in the lower estuary. A decrease in Insecta larvae and Mysidacea density (mostly *Mesopodopsis slabberi*) was also observed and was associated with the reduction in freshwater habitat, which more recently is restricted to the upper estuarine areas (Chícharo *et al.*, 2001). According to results from the Associated Phytoplankton time-series (Guadiana) in the upper estuarine area (Barbosa *et al.*, 2010), phytoplankton abundance displayed a significant interannual decline over the period 1996–2010, which can be linked to increased water retention by the Alqueva Dam. This has led to interannual decreases not only in turbidity, but also in nutrient inputs, thus promoting a shift from persistent light limitation towards a more nutrient limited mode.

In the lower Guadiana Estuary, copepod density, mainly represented by the genera *Acartia* and *Paracalanus*, has increased lasting recent years (Figure 8.7.2). This is in contrast to the decreasing trend seen in northwest Iberia (Cascais station) and the offshore (open-water) CPR data from the same region. Nevertheless, the nearby Mediterranean stations Malaga (Mar de Alboran) and Baleares also show increasing trends of copepods in recent years. Water temperatures are often related to the NAO; however, currently any relationship between water temperature and zooplankton abundance is inconclusive.

Temporal changes in the zooplankton community in the Guadiana area demonstrate positive anomalies for some taxa and negative anomalies for other taxa, which may be related to changes in water temperature and the NAO winter index. However, interpretations must be formed carefully because there is more complexity in reality than is evident in the samples. There is a need for the future employment of more integrated and multidisciplinary approaches based on continuous monitoring of mesozooplankton in order to increase our understanding of estuarine ecosystems. The Guadiana Estuary is classified as highly sensitive to climate change and is currently considered one of the best preserved and most vulnerable estuaries of the Iberian Peninsula.

Acknowledgement

This work was supported by a number of projects funded by the European Union and Portuguese Foundation of Science and Technology (FCT), namely: Characterization of the Guadiana estuary ecosystem as a baseline to evaluate environmental changes, EU-INTERREG II, contract Nr 15/REGII/6/96; Estuarine zone management for control of eutrophication, toxic blooms, invasive species and conservation of biodiversity-Guadiana Demosite in Ecohydrology 2005–2008, contract No. 450.003.9232 UNESCO Paris; Development and harmonization of new indicators, methodologies and strategies common for Portugal and Spain for the application of the Water Frame Directive to transitional and coastal water mass in the Guadiana, 0252_DIMEAGUA_5_P 2009-2012, EU-INTERREG; Effects on river flow changes on the fish communities of the Douro, Tagus and Guadiana estuaries, Ecological and socio-economic predictions, ERIC, PDCTM/C/MAR/15263/1999; Nutritional condition of larval fish in two marine protected areas of the South of Portugal, Ria Formosa and Guadiana estuary, GUADIRIA, POCI/BIA-BDE/59200/2004 and; Vital rates of pelagic fish larvae, VITAL, PTDC/MAR/111304/2009.

We are grateful to Ana Faria, David Piló, Isabel Gaspar, Isabel Gouveia, Luis Cristovão, João Encarnação, Pedro Morais, Pedro Range, Renata Gonçalves, Rita Pereira, Susana Ferreira, Tania Leitão, Teja Muha, and Vanessa Neves for their support during fieldwork and for helping in the sorting and identification of mesozooplankton.

Figure 8.7.2
Multiple-variable
comparison plot (see
Section 2.2.2) showing the
seasonal and interannual
properties of select
cosampled variables at the
Guadiana Lower Estuary
monitoring area.

Additional variables are
available online at: <http://WGZE.net/time-series>.

Guadiana lower Estuary, southern Iberian Peninsula

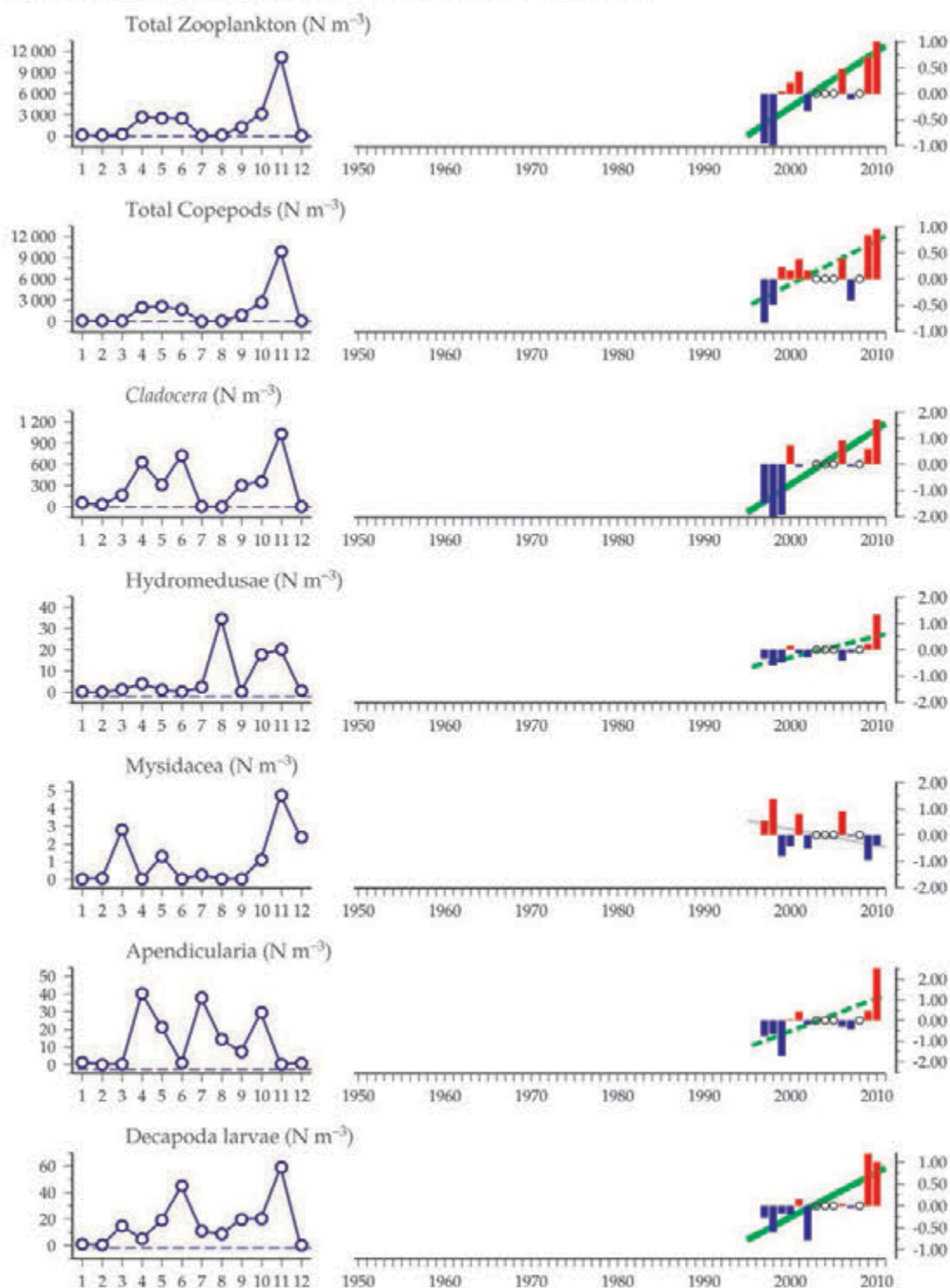


Figure 8.7.2
continued

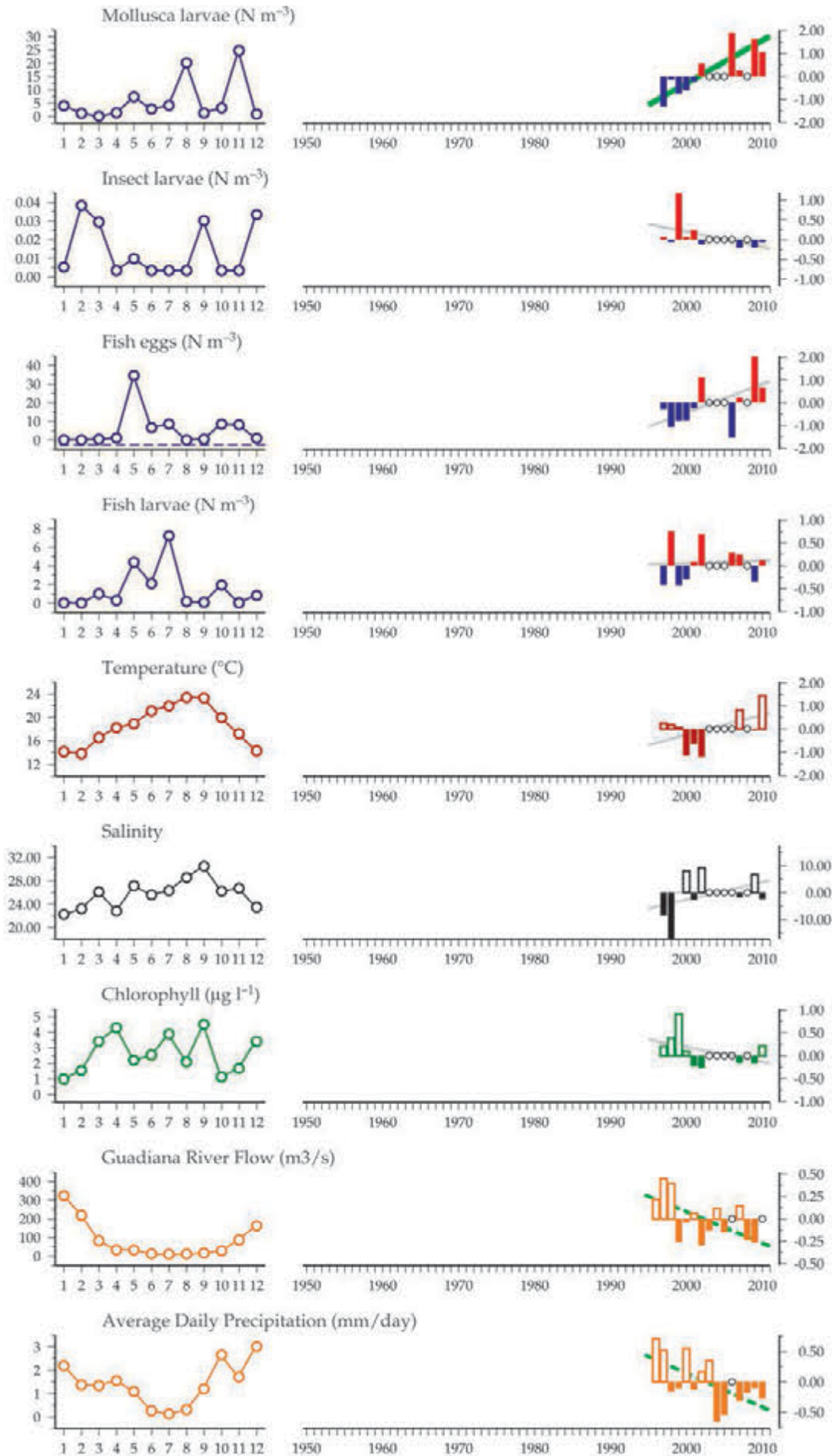
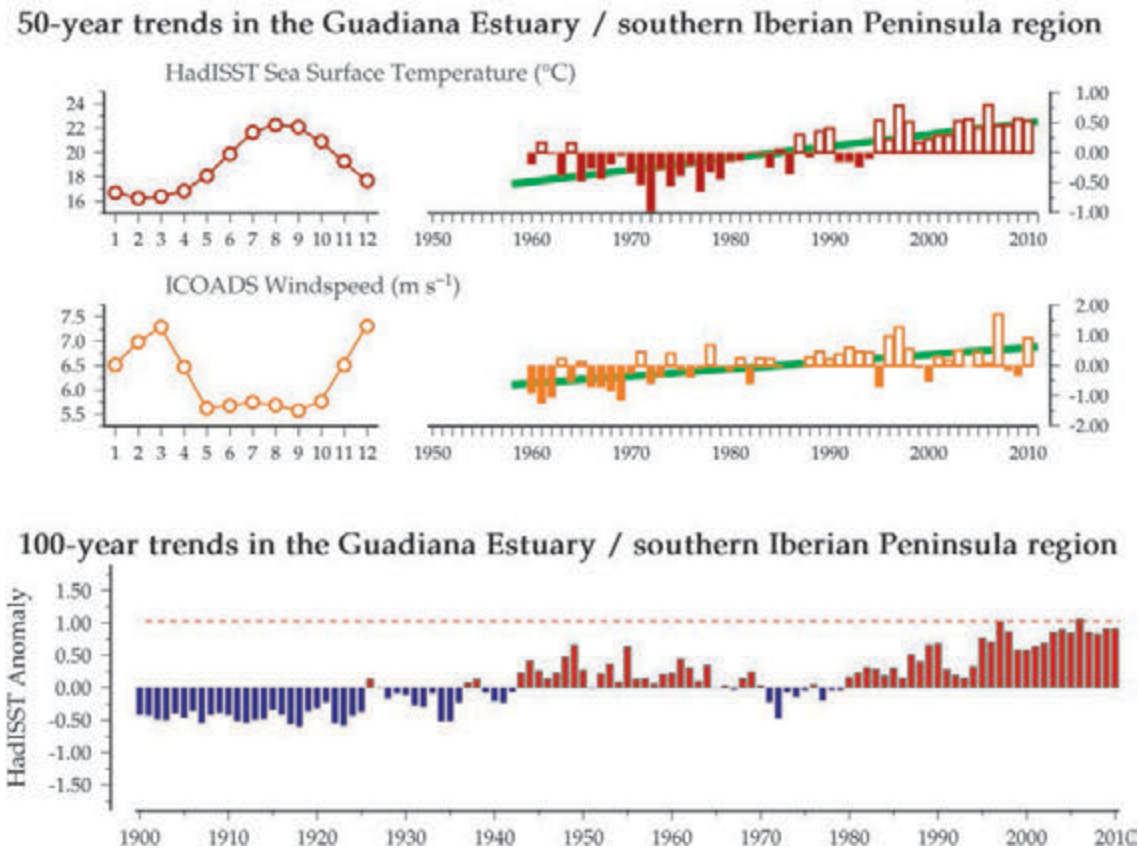


Figure 8.7.3
Regional overview plot
(see Section 2.2.3) showing
long-term sea surface
temperatures and wind
speeds in the general region
surrounding the Guadiana
Lower Estuary monitoring
area.





*The ctenophore Mniemiopsis leidyi in the bay of
Villefranche sur Mer. – Fabien Lombard, Université
Pierre et Marie Curie (IPMC)*

9Z OOPLANKTON OF THE M DITERRANEAN SEA

Lidia Yebra, Jesús M. Mercado, Dolores Cortés, Sébastien Putzeys, Maria Luz Fernández de Puellas, Lars Stemmann, Gabriel Gorsky, Maria Grazia Mazzocchi, Iole Di Capua, Valentina Tirelli, Alessanda de Olazabal, Serena Fonda-Umani, Olja Vidjak, Ioanna Siokou-Frangou, Soultana Zervoudaki, and Epaminondas Christou

Figure 9.0
Locations of Mediterranean Sea survey areas (Sites 56–62) plotted on a map of average chlorophyll concentration (see Section 2.3.2).



5	Málaga Bay (Alborán Sea)	9.1
5	Baleares Station (Mallorca Channel)	9.2
8	Villefranche Point B (Cote d'Azur)	9.3
9	Gulf of Naples LTER-MC (Gulf of Naples)	9.4
60	Gulf of Trieste LTER (northern Adriatic Sea)	9.5
61	Stončica (central Adriatic Sea)	9.6
62	Saronikos S11 (Aegean Sea)	9.7

The Mediterranean Sea is an oligotrophic basin (except the northwestern and Alboran Sea regions), where the nutrient balance is maintained by water exchange through the Strait of Gibraltar and the Bosphorus, together with terrestrial and atmospheric inputs (Gómez *et al.*, 2000; Béthoux *et al.*, 2002; Dafner *et al.*, 2003; Markaki *et al.*, 2010). The seasonal cycles of primary and secondary production are driven by physical processes that affect the stability of the upper layers of the water column and the supply of nutrients from the deeper layers into the photic zone.

Changes observed in the thermohaline characteristics and in some circulation patterns in the Mediterranean are likely related to meteorological events and climatic factors (Roether *et al.*, 1996; Béthoux *et al.*, 1998; Malanotte-Rizzoli *et al.*, 1999; Tsimplis *et al.*, 2006) and might be causing important imbalances in the structure (biodiversity) and functioning (energy and matter fluxes) of marine ecosystems. Molinero *et al.* (2005), Garcia-Comas *et al.* (2011), and Vandromme *et al.* (2011) have observed that interannual variability of the zooplankton communities in the northwest Mediterranean Sea may be linked to large-scale atmospheric changes. It is suggested that the long-term changes in zooplankton might be caused by successive periods of drought, for which a long-term trend has not yet been shown. Civitarese *et al.* (2010) suggested that changes in the biodiversity and structure of plankton in the eastern Mediterranean (Adriatic and Ionian seas) may be related to the Bimodal Oscillation System (BiOS) mechanism that changes the circulation of the North Ionian Gyre (NIG) from cyclonic to anticyclonic, and vice versa, on a decadal time-scale.

Several Mediterranean zooplankton time-series have recently been included in regional and global comparisons, which focused, respectively, on seasonal and long-term variability of major taxonomic groups (Berline *et al.*, 2012) and changes in species phenology (Mackas *et al.*, 2012). On the regional scale, Berline *et al.* (2012) found no significant correlations between climate indices (e.g. NAO, EA, EA/WR, AO, NHT, SCA) that are linked to Mediterranean climate and local temperature or zooplankton abundance and taxonomic composition, nor between stations for zooplankton abundance. This suggests that, for these coastal stations, local drivers (climatic, anthropogenic) are dominant or that the time-series are not long enough to reveal interannual variability associated with change in climate indices. However, in the Balearic Sea, decadal changes were observed in zooplankton abundance related to seawater temperature recorded during strong anomalies in the North Atlantic climate (>1 s.d.). Although the period analyzed could be short for investigating climate effects on marine ecosystem, the statistical results were consistent enough to emphasize the North Atlantic's climate effect on the zooplankton community around the Balearic Islands (Fernandez de Puellas and Molinero, 2008). More recently, the same authors found increasing zooplankton variance unveiling hydroclimate modifications, suggesting an impending ecological shift around 1999 (Fernandez de Puellas and Molinero, 2013). In addition, Conversi *et al.* (2010), analyzing and reviewing long-term records of copepod and zooplankton abundance in the Gulf of Trieste and the Bay of Villefranche-sur-mer, respectively, red tides and mucilage events in the North Adriatic Sea as well as

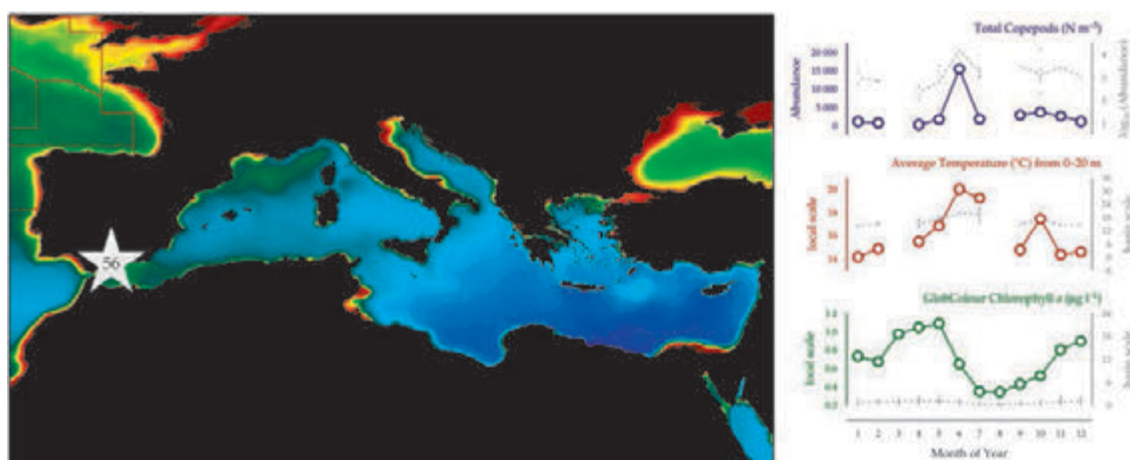
Mediterranean hydroclimate variables, found that all point to a synchronous change in the late 1980s. They concluded that this Mediterranean shift is part of a large-scale change in the Northern Hemisphere. Mozetič *et al.* (2012) analyzed abiotic parameters and plankton community structure in the Gulf of Trieste in the period 1989–2009 and reported a regime shift in zooplankton biomass, which was observed as an abrupt decrease in 2004. The authors suggested that the observed zooplankton dynamics were mainly linked to bottom-up control drivers during periods when the classical food chain prevails, while the increasing abundance of jellyfish from 2003 to 2004 (Kogovšek *et al.*, 2010) supported a top-down control. On a global scale, Mackas *et al.* (2012) found that one of the most striking results from the Mediterranean zooplankton data is that the “earlier when warmer” response in phenology seen in most of the Atlantic and Pacific time-series is less frequent in the Mediterranean and is replaced in several target species by a strong “later when warmer” pattern (e.g. in Villefranche, Gulf of Trieste, and Gulf of Naples).

In this report, a new site is provided in the Alboran Sea, the western-most basin of the Mediterranean. It is an area with very complex hydrodynamic forces and connects the Atlantic and the Mediterranean. It is characterized by the presence of a surface layer of nutrient-poor Atlantic water (SAW) entering through the Strait of Gibraltar and a nutrient-rich layer of Mediterranean water (MW), which flows out below the SAW (Minas *et al.*, 1991; Ramírez *et al.*, 2005). Episodically, the MW reaches the surface layer and promotes phytoplankton growth and the accumulation of chlorophyll *a* (Minas *et al.*, 1991; Rodríguez *et al.*, 1997; García-Górriz and Carr, 2001). The intensity of the upwelling varies seasonally due to the thermal stratification cycle (Mercado *et al.*, 2005, 2007) and the changes in the inflow and outflow through the Strait of Gibraltar (García-Lafuente *et al.*, 2000; Gómez *et al.*, 2000). In addition to the upwelling associated with the geostrophic front, upwelling events induced by westerlies are very frequent along the Spanish coast (Sarhan *et al.*, 2000). These upwelling events lead to high production in the western Alboran Sea, in contrast to the more oligotrophic eastern parts of the Mediterranean. The study of the time-series available in the region reveals that both chlorophyll *a* and phytoplankton communities present interannual variability patterns, with maxima every 4–5 years (Mercado *et al.*, 2012).

9.1 Málaga Bay (Site 56)

Lidia Yebra, Jesús M. Mercado, Dolores Cortés, and Sébastien Putzeys

Figure 9.1.1
Location of the Málaga Bay monitoring area (Site 56) plotted on a map of average chlorophyll concentration, and its corresponding seasonal summary plot (see Section 2.2.1).



Málaga Bay was sampled from 1992 to 2000 as part of the ECOMÁLAGA time-series operated by the Instituto Español de Oceanografía (IEO). In 2010, sampling at Station MA2 of the Málaga transect was restarted. Station MA2 is located within the Bay of Málaga (36°41.76'N 4°24.35'W) in the northwest Alboran Sea, with a bottom depth of 28 m (Figure 9.1.1).

Zooplankton samples were collected on a quarterly basis from near-bottom to the surface using a bongo net (40 cm diameter, 200 µm mesh). Once on board, samples were preserved in 100 ml plastic jars with 4% buffered formalin-seawater solution (pH 7.0) for abundance and taxonomic composition analyses. Abundance counts and taxonomic identification were done with a binocular macroscope (Zeiss, Stemi SV11). Prior to the analyses, samples were stained with Rose Bengal to facilitate identification of gelatinous plankton. A Seabird25 CTD was used to obtain *in situ* profiles of temperature and salinity.

Seasonal and interannual trends (Figure 9.1.2)

The northwest region of the Alboran Sea presents high variability in hydrological as well as physical and chemical conditions. This is due to the presence of an anticyclonic gyre formed by the jet of Atlantic water that enters the Mediterranean through the Strait of Gibraltar. The Atlantic jet circulation affects the open waters. However, within the shelf, local currents are defined by winds. In the northwest section of the jet, divergence areas appear between Gibraltar and the Bay of Málaga, associated with westerly wind-induced upwelling events. In this frontal area, increases in nutrients and plankton have been detected.

The peculiar oceanographic conditions generate an annual zooplankton cycle different from nearby areas, with communities typical from upwelling zones and warm waters, with predominant neritic species dominated by copepods. Maximum zooplankton abundance was observed in summer and autumn, while minimum zooplankton abundance was observed in winter. Copepods were the most abundant group in spring, autumn, and winter, while in summer, cladocerans were the dominant group. Interannually, an increasing trend was recorded from 1994 to 2000 in total copepod density, although mesozooplankton density showed a decreasing trend. However, this trend in total zooplankton seems to have changed in 2010. In spite of the interannual variations, the different phases of the annual cycle and the occurrence of several plankton species were remarkably regular.

In the Bay of Málaga, water temperatures in the top 20 m have been increasing since 1992 (Figure 9.1.2). However, no correlation has been found between copepod abundance and hydrological parameters (temperature and salinity).

Málaga Bay, Alborán Sea

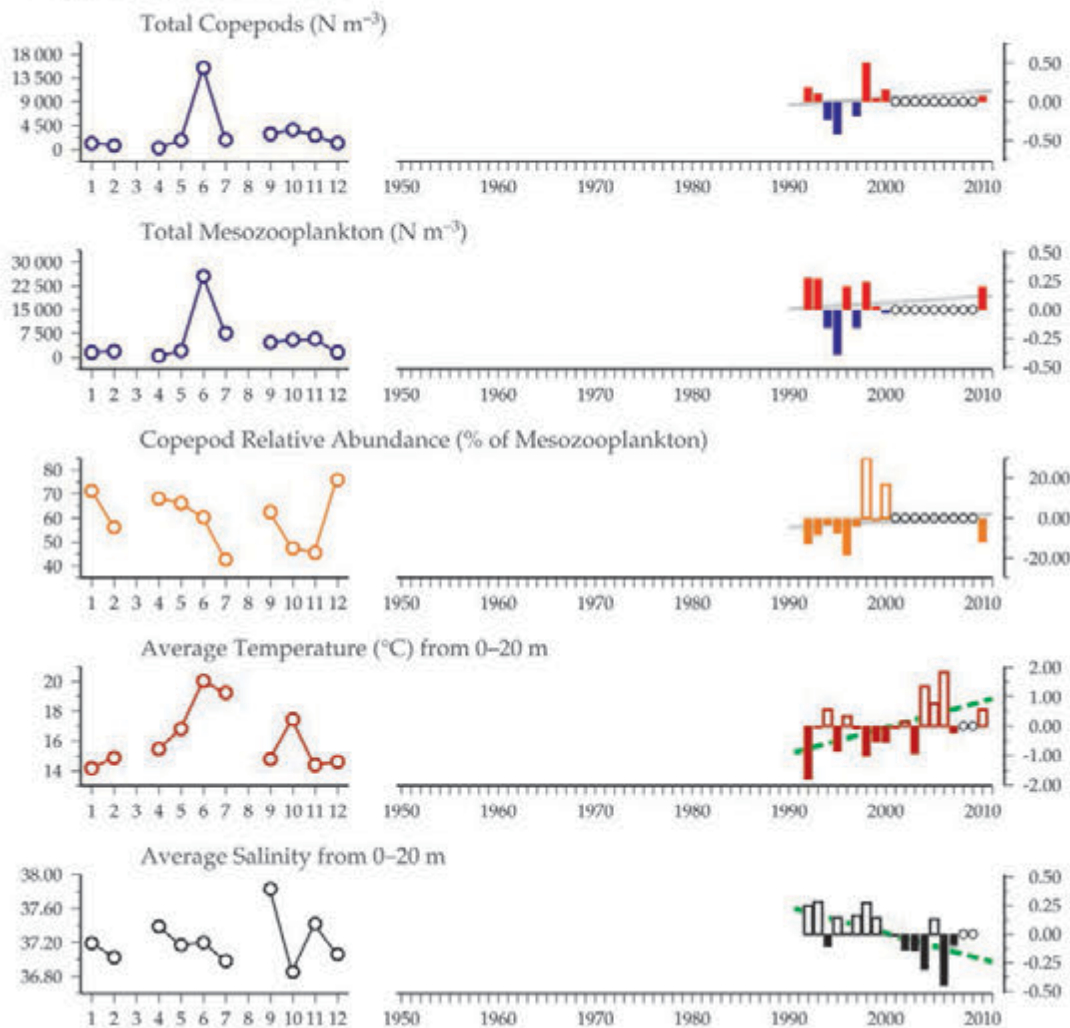


Figure 9.1.2
Multiple-variable comparison plot (see Section 2.2.2) showing the seasonal and interannual properties of select cosampled variables at the Málaga Bay monitoring area.

Additional variables are available online at: <http://WGZE.net/time-series>.

50-year trends in the Málaga Bay / Alborán Sea region

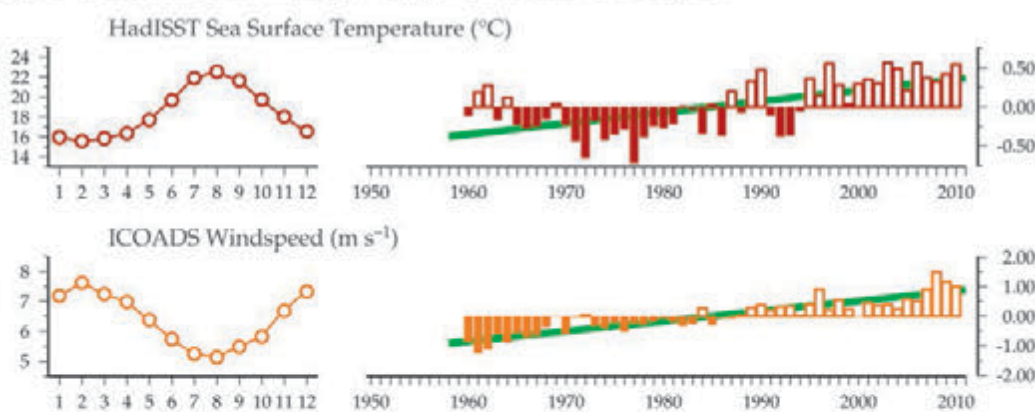
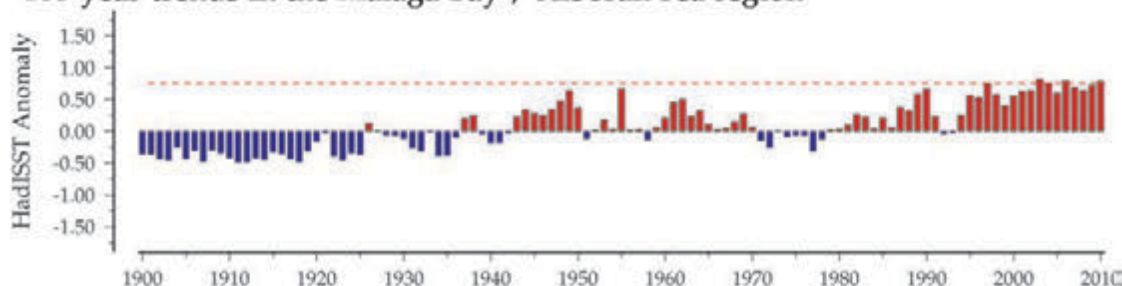


Figure 9.1.3
Regional overview plot (see Section 2.2.3) showing long-term sea surface temperatures and windspeeds in the general region surrounding the Málaga Bay monitoring area.

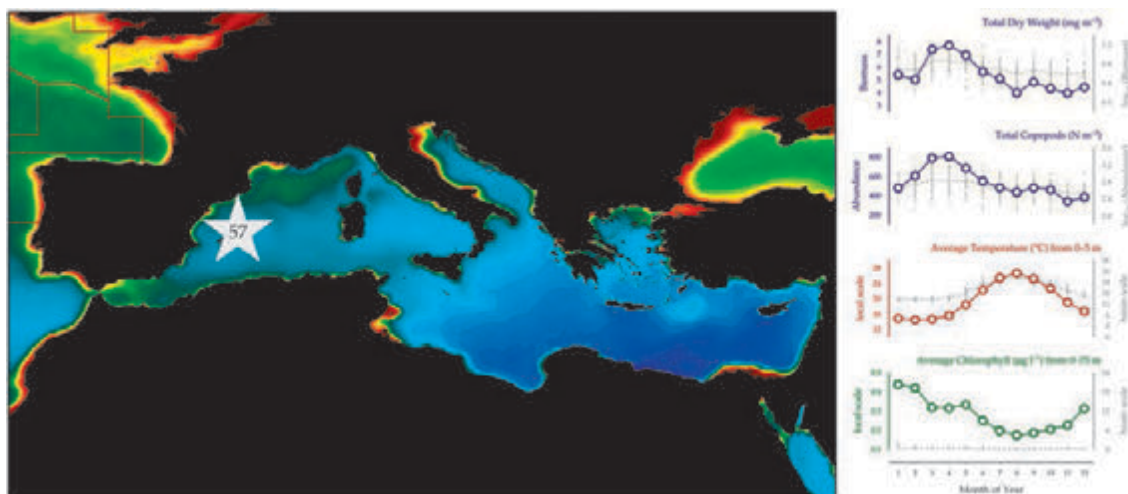
100-year trends in the Málaga Bay / Alborán Sea region



9.2 Balears Station (Site 57)

Maria Luz Fernández de Puelles

Figure 9.2.1
Location of the Balears Station monitoring area (Site 57) plotted on a map of average chlorophyll concentration, and its corresponding seasonal summary plot (see Section 2.2.1).



The Balearic sampling site is located southwest of the island of Mallorca at 39°29'N 2°25'E and has a bottom depth of 77 m (Figure 9.2.1). Beginning in 1994, sampling of the station took place every 10 d until December 2005, after which it has been sampled seasonally four times a year. Zooplankton are sampled by means of oblique hauls from a depth of 75 m to the surface with a bongo net (40 cm diameter, 250 µm mesh). A full description of the methodology is given in Fernández de Puelles *et al.* (2007).

The Balearic Sea is characterized by complex mesoscale features resulting from the interaction between the saline and colder northern waters of the western Mediterranean and the southern, less-saline, and warmer water from the Alboran Sea. This ecologically important region encompasses major spawning areas of pelagic fish, possibly owing to an “island stirring” effect that may produce concentrated plankton biomass around the islands. Overall, the annual circulation pattern consists of cool, south-flowing waters of northern origin during the first part of the year, changing to warm, north-flowing waters of Atlantic origin in the second part. Circulation within the region becomes very complex because of the permanent mesoscale activity and the north Balearic front (Pinot *et al.*, 2002). Depending on the influence of these hydrographic structures, the region can undergo mixing or incursions of different water masses, forming frontal systems or eddies that drive the planktonic community dynamics (Fernández de Puelles *et al.*, 2004a, 2004b, 2007, 2009).

Seasonal and interannual trends (Figures 9.2.2–9.2.3)

Chlorophyll concentrations are highest from December through February (Figure 9.2.2) before the onset of warmer water temperatures and stratification. Seasonal temperature cycles indicate a mixing period during colder months and a stratification period from June to October. Mean surface water temperatures have a seasonal difference of up to 14°C, with a winter minimum of ca. 13°C and a summer maximum as high as 27°C. At a depth of 75 m, this seasonal difference is only 3°C: from 13°C (in March) to 16°C (in October). In general, this area has low nutrient concentrations and low primary production because of the development of the thermocline, which acts as a barrier to the supply of nutrients to the photic layer.

Zooplankton biomass (total dry weight; Figure 9.2.2) demonstrates a seasonal pattern, with higher mean biomass in the first half of the year (maximum in April) and lower biomass in the second half of the year (minimum in August). The Balearic area is characterized by the presence of relatively small-sized organisms. Large gelatinous zooplankton did not appear in great quantities in the samples. The zooplankton peak in March was related to a period of vertical mixing, when the cold, dense, nutrient-rich waters reach the surface, a widespread event in the Mediterranean. This early-spring zooplankton maximum seems to occur yearly in response to the previous winter phytoplankton bloom. During spring, when the thermocline is developing, the inputs of offshore waters and the proximity of frontal systems usually enhance zooplankton abundance.

Copepods were the most abundant and perennial group in the zooplankton samples (56% of the total). Other important groups were gelatinous zooplankton (23%, consisting primarily of 17% appendicularians, 5% doliolids, and 1% salps), cladocerans (10%), and meroplankton (4%). In addition, siphonophores (3%), chaetognaths (2%), ostracods (1%), and pteropods (1%) were also found in the area. More than 80 copepod species were identified during the entire study period, ten of which accounted for 60% of the total. The group of *Clausocalanus* was the most abundant (*C. arcuicornis*, *C. furcatus*, *C. pergens*, and *C. paululus*; 27%), followed by *Oithona* spp. (25%). Some species had very low abundance during short periods, such as *Calanus helgolandicus* in winter or *Acartia danae* in late summer.

The SSTs in the region have been above the 100-year average since 1985 and, since 2000, have often been the warmest seen in the region for the past 100 years (Figure 9.2.3). Although no significant zooplankton biomass decrease was observed during this time-series, a correlation of copepods with temperature (negative) and salinity (positive) indicated their direct relationship with the presence of the different surface water masses; when colder and saltier Mediterranean waters prevailed in the area, higher zooplankton biomass values were observed.

Although factors other than temperature and salinity could contribute to the plankton pattern observed, the recognition of large-scale dependence on the physical environment is a first and necessary step towards understanding zooplankton distributions in the western Mediterranean.

Baleares Station, Mallorca Channel

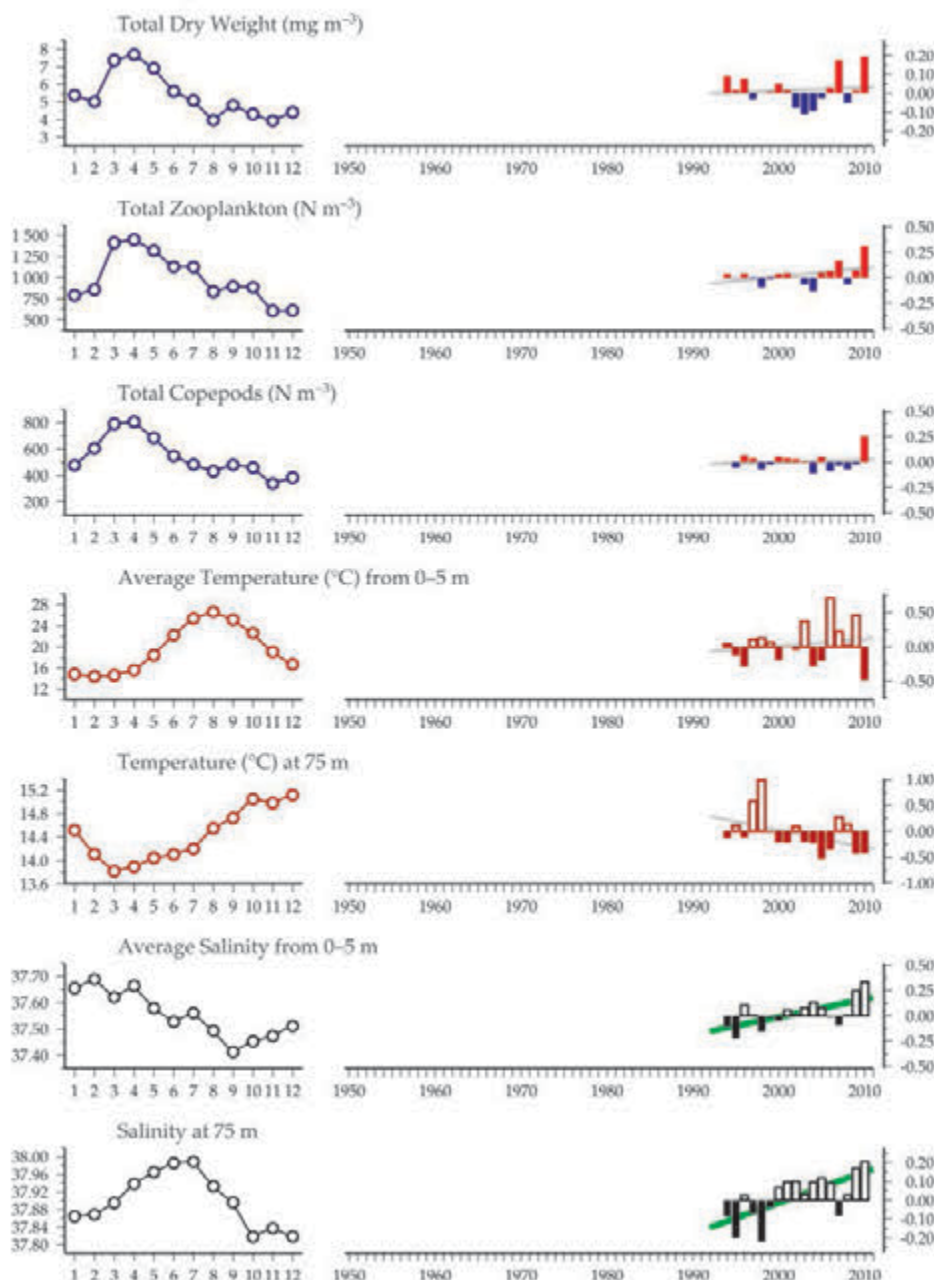
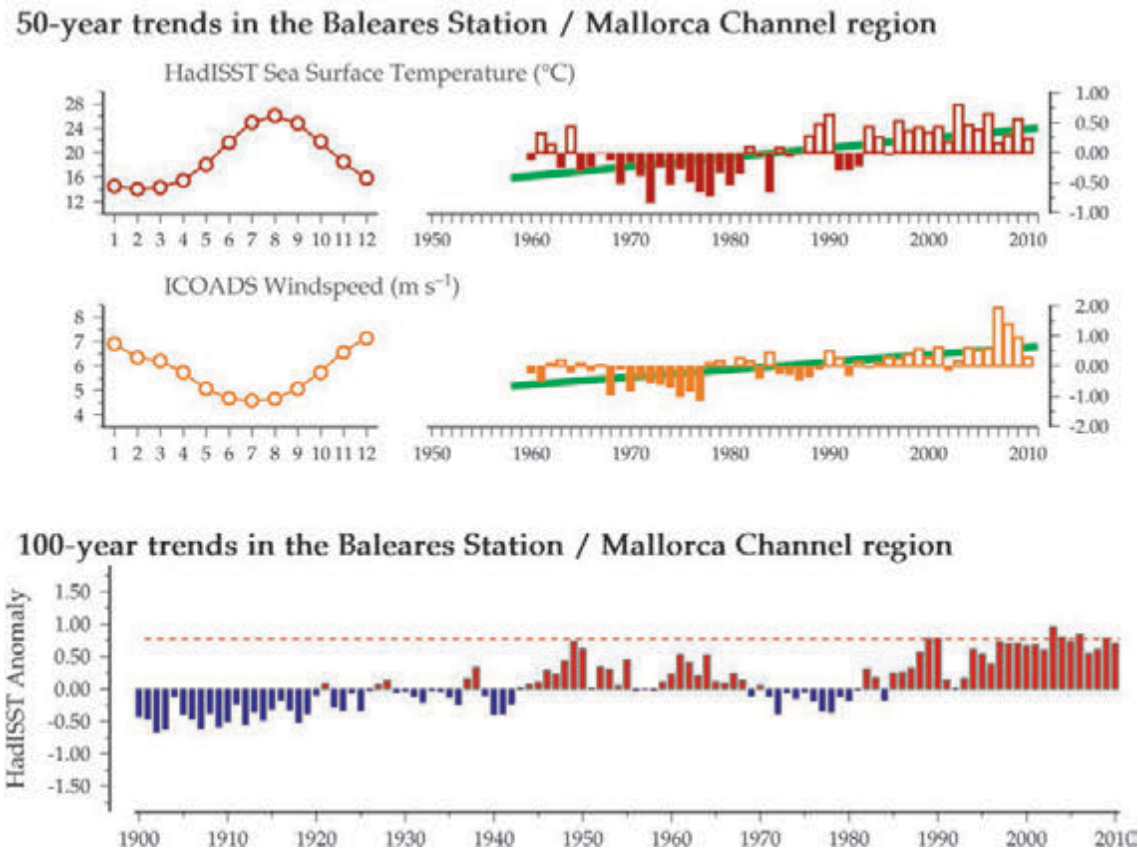


Figure 9.2.2
Multiple-variable comparison plot (see Section 2.2.2) showing the seasonal and interannual properties of select cosampled variables at the Baleares Station monitoring area.

Additional variables are available online at: <http://WGZE.net/time-series>.

Figure 9.2.3
Regional overview
plot (see Section 2.2.3)
showing long-term sea
surface temperatures and
windspeeds in the general
region surrounding the
Balears Station monitoring
area.



9.3 Villefranche Point B (Site 58)

Lars Stemmann and Gabriel Gorsky

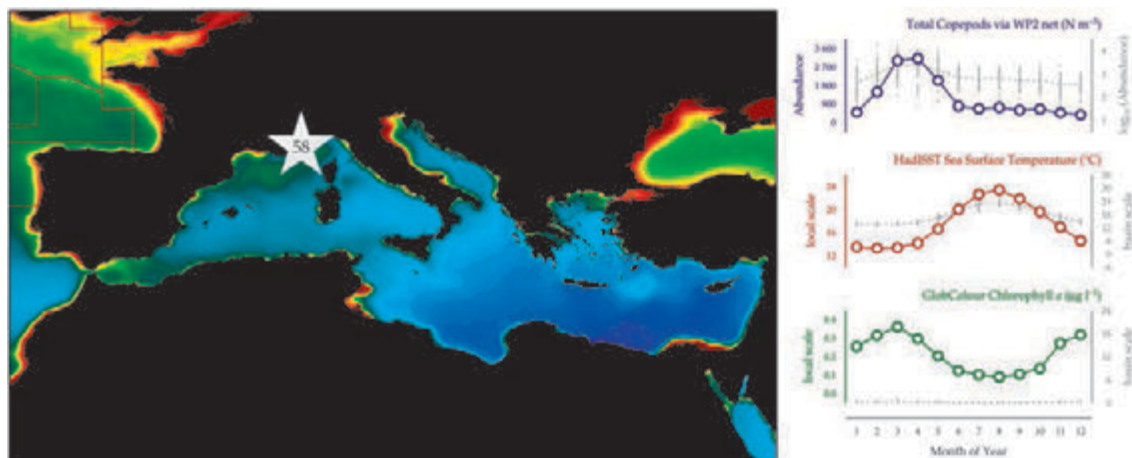


Figure 9.3.1
Location of the Villefranche Point B monitoring area (Site 58) plotted on a map of average chlorophyll concentration, and its corresponding seasonal summary plot (see Section 2.2.1).

The Villefranche Point B dataset consists of more than 46 years of samples collected daily off Villefranche at 43°41N 07°19E (Figure 9.3.1). Samples were collected by a vertical tow from bottom to surface (75–0 m), using a Juday–Bogorov net (1996–2003 and 2009–2013, 330 µm mesh) and WP2 net (1995–2013, 200 µm mesh). Copepod abundance was counted from ongoing and historical samples using the wet-bed image scanning technique of ZooScan (Gorsky *et al.*, 2010; Vandromme *et al.*, 2012). Zooplankton sample analysis is performed by the RADEZOO service at the Oceanologic Observatory of Villefranche-sur-Mer. Only total copepod abundance is reported here. Other taxa are counted. A complete list of taxa is available online at <http://www.obs-vlfr.fr/Rade/RadeZoo>.

Seasonal and interannual trends (Figures 9.3.2–9.3.3)

Seasonal copepod abundance is highest shortly after the well-mixed winter period, followed by a general decline in abundance as the water warms and stratifies. At longer time-scales, copepod abundance decreased with rising water temperatures and increasing stratification seen in the 1990s (Garcia Comas *et al.*, 2011). After 2000, copepod and mesozooplankton abundance again reached the

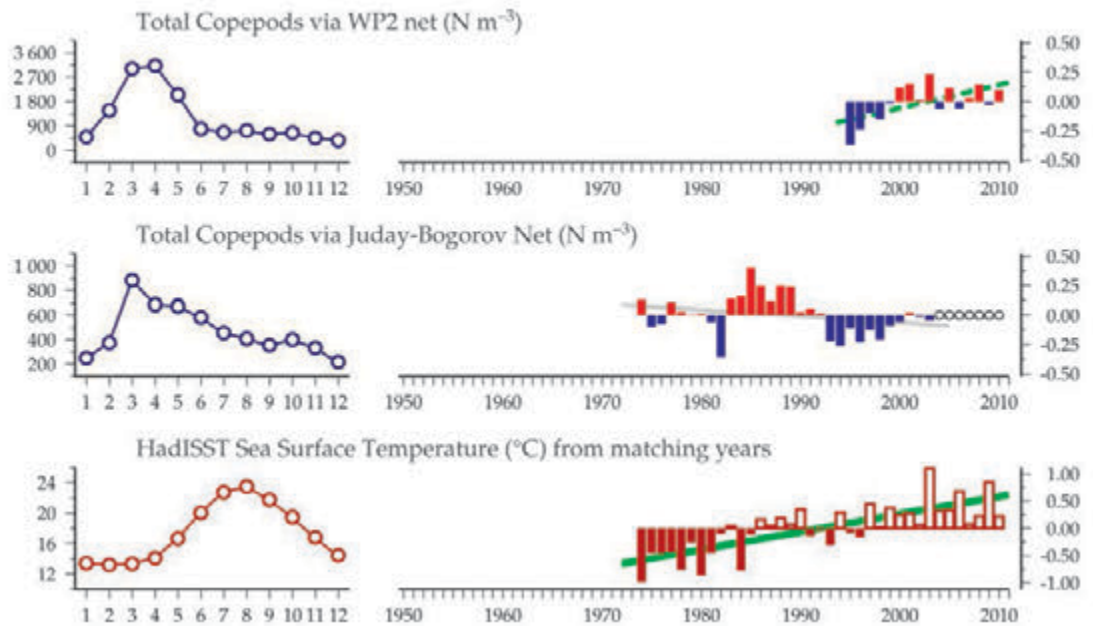
values of the 1980s (Vandrome *et al.*, 2011). The oscillating pattern of zooplankton abundance is related to climatic variability and the occurrence of “dry years”. During these years (1980s and after 2000), less precipitation and cloud coverage during winter trigger higher salinities and lower temperature, causing the surface layer to mix deeper. As a result, surface nutrient concentration is enhanced, promoting strong blooms and zooplankton development (Garcia-Comas *et al.*, 2011; Vandromme *et al.*, 2011). For this reason, zooplankton concentrations remain high in spite of warming water temperatures and earlier stratification.

Figure 9.3.2

Multiple-variable comparison plot (see Section 2.2.2) showing the seasonal and interannual properties of select cosampled variables at the Villefranche Point B monitoring area.

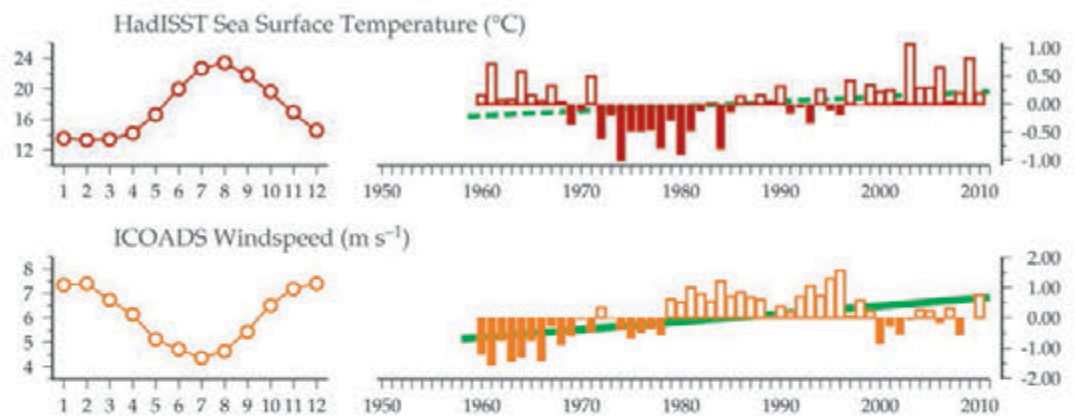
Additional variables are available online at: <http://WGZE.net/time-series>.

Villefranche Point B, Cote d'Azur

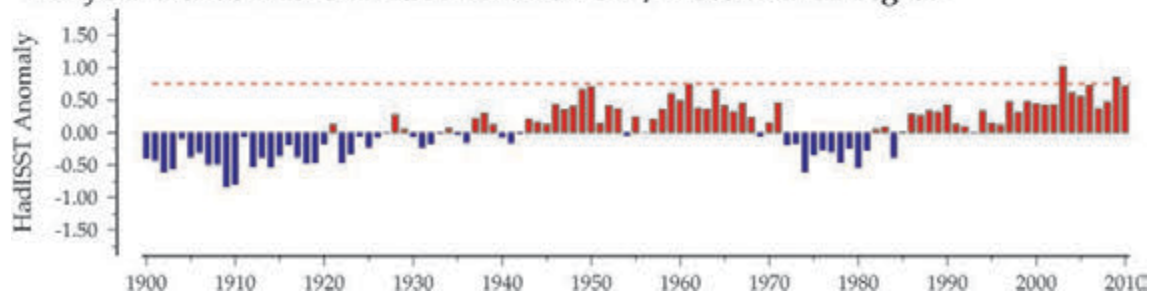
**Figure 9.3.3**

Regional overview plot (see Section 2.2.3) showing long-term sea surface temperatures and windspeeds in the general region surrounding the Villefranche Point B monitoring area.

50-year trends in the Villefranche Point B / Cote d'Azur region



100-year trends in the Villefranche Point B / Cote d'Azur region



9.4 Gulf of Naples LTER-MC (Site 59)

Maria Grazia Mazzocchi and Iole Di Capua

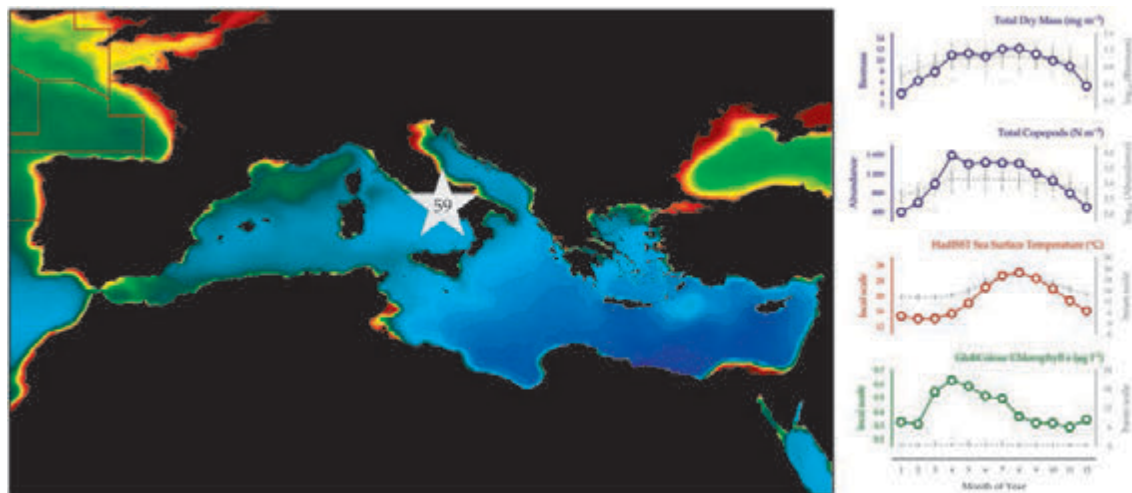


Figure 9.4.1
Location of the Gulf of Naples LTER-MC monitoring area (Site 59) plotted on a map of average chlorophyll concentration, and its corresponding seasonal summary plot (see Section 2.2.1).

The Gulf of Naples, located in the Tyrrhenian Sea at the border between the central and southern regions of the western Mediterranean, has been a study site for investigations on zooplankton taxonomy and distribution since the 19th century (Giesbrecht, 1893 [“1892”]). However, it is only regular sampling, begun in 1984 for the MareChiara time-series, which has started to unveil aspects of zooplankton temporal evolution and recurrences in this typical Mediterranean embayment (Mazzocchi and Ribera d’Alcalà, 1995). This long-term time-series focuses on characterizing the structure of plankton communities in terms of standing stocks and species composition and on following their variability at different temporal scales in relation to environmental conditions. In 2006, the MareChiara site joined the European (www.lter-europe.net) and international (www.ilternet.edu) networks of Long-Term Ecological Research as LTER-MC.

The sampling site is located ca. 3 km from the coastline near the 75 m isobath (40°48.5’N 14°15’E) and at the boundary between two subsystems whose exchanges are very dynamic: the coastal eutrophic area, influenced by land run-off from a very densely populated region, and the offshore oligotrophic area, similar to the open Tyrrhenian waters (Figure 9.4.1). Sampling has been ongoing since January 1984, with a major interruption from January 1991 to February 1995. Sampling frequency was fortnightly until 1990 and weekly from 1995 to present (Ribera d’Alcalà *et al.*, 2004). Zooplankton samples were collected with two successive vertical tows from a depth of 50 m to the surface with a Nansen net (113 cm diameter, 200 µm mesh). One fresh sample was processed for biomass measurements as dry mass; the other sample was fixed with buffered

formalin (2–4% final concentration) for the determination of species composition and abundance.

Seasonal and interannual trends (Figure 9.4.2)

The water column at the site is thoroughly mixed from December to March and stratified during the rest of the year. The annual cycle of depth-integrated temperature (not shown) is characterized by lowest values in March (~14°C) and highest values in September–October (~20°C). Temperature, salinity, and chlorophyll demonstrate high interannual variability. Significant trends during the period 1984–2006 have been recorded in the increasing summer temperatures and in the decreasing annual chlorophyll *a* concentrations (Zingone *et al.*, 2010; Mazzocchi *et al.*, 2012).

The zooplankton community is numerically dominated by copepods, followed by cladocerans, tunicates (mainly appendicularians), meroplankton (mainly decapod larvae), cnidarians, chaetognaths, and ostracods. A few other taxonomic groups (e.g. amphipods, pteropods, fish eggs and larvae) were much less abundant and frequent, thus contributing with negligible percentages (< 0.1%) to total zooplankton abundance. Five robust zooplankton associations were identified with well-defined composition and abundance, which had long-term persistence and likely reflected different modes of community functioning (Mazzocchi *et al.*, 2011). The temporal course of these associations was largely shaped by strong seasonal forcing comprising both physical and biological (e.g. trophic) signals.

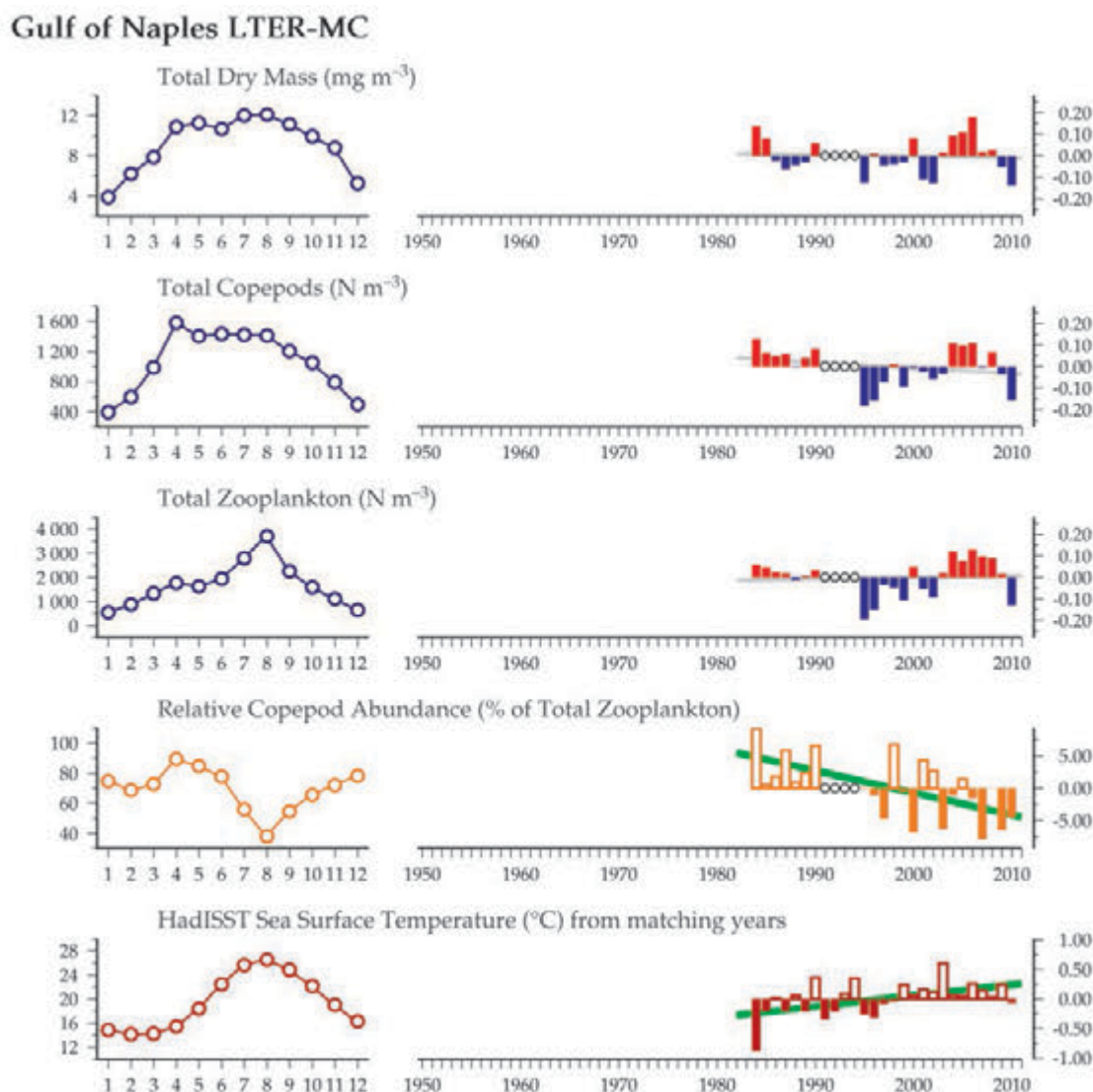
Copepod assemblages were highly diversified, with 136 identified species. Abundance and species composition changed throughout the year, acquiring a strong seasonal signature, with spring and summer peaks and winter lows (Mazzocchi *et al.*, 2012). Four abundant species peaked in succession: *Acartia clausi* and *Centropages typicus* in spring–early summer, *Paracalanus parvus* in full summer–early autumn, and *Temora stylifera* in late summer–autumn. In late autumn–winter, copepod assemblages were more diversified than in the rest of the year. The most common genera in this season were the small calanoids *Clausocalanus*, *Calocalanus*, *Ctenocalanus vanus*, and the cyclopoids *Oithona*, oncaeids, and corycaeids. The winter–early spring copepod assemblages were further enriched by the regular, although numerically negligible, occurrence of large calanoid species (>1.5 mm total length), which thrive in offshore deeper waters (mainly *Nannocalanus minor*, *Candacia* spp., and *Pleuromamma* spp.). The occurrence of *Calanus helgolandicus*, *Neocalanus gracilis*, *Mesocalanus tenuicornis*, *C. violaceus*, as well as various species belonging to Aetideidae, Eucalanidae, Euchaeta, Haloptilus, Heterorhabdus, Lucicutia, and Scolecithricella was generally negligible in quantity and scattered in time.

A few indications suggest that this station might have acquired fewer coastal characteristics (e.g. decreasing chlorophyll *a* concentrations) from 1984 to 2006, but the signals from the copepod assemblages appeared only in rare species (Mazzocchi *et al.*, 2012). A significant increase was observed in the occurrence of some calanoids from open sea (e.g. *N. gracilis*, *Scolecithricella* spp.), while a few species typical of confined areas disappeared (e.g. *A. margalefi*, *Paracartia latisetosa*).

Overall, at this site in 1984–2006, a significant resilience appeared in the whole community structure and in the seasonal cycle of the bulk copepod assemblages, indicating some stable characters in zooplankton thriving in highly variable coastal conditions (Mazzocchi *et al.*, 2011, 2012). After 2006, the relative importance of copepods in the total zooplankton showed a decreasing trend (Figure 9.4.2), especially due to reduced summer abundance, in conjunction with a marked increase of cladocerans (not shown).

Figure 9.4.2
Multiple-variable comparison plot (see Section 2.2.2) showing the seasonal and interannual properties of select cosampled variables at the Gulf of Naples LTER-MC monitoring area.

Additional variables are available online at: <http://WGZE.net/time-series>.



50-year trends in the Gulf of Naples / Tyrrhenian Sea region

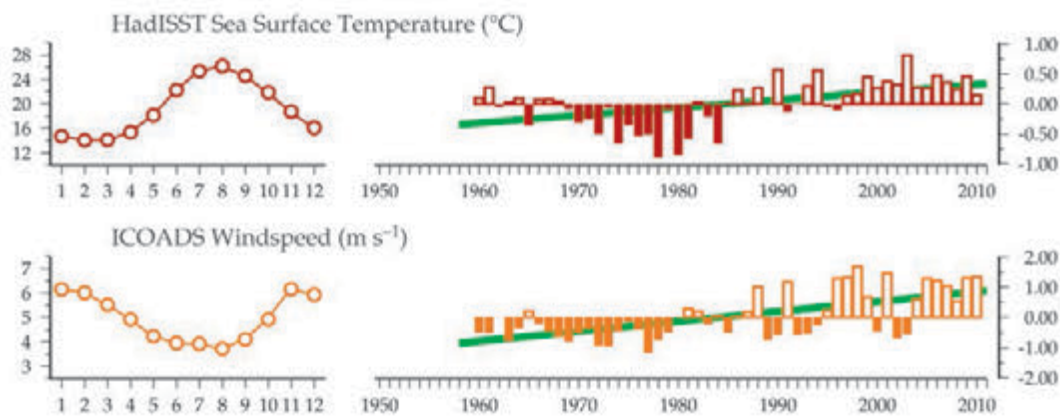
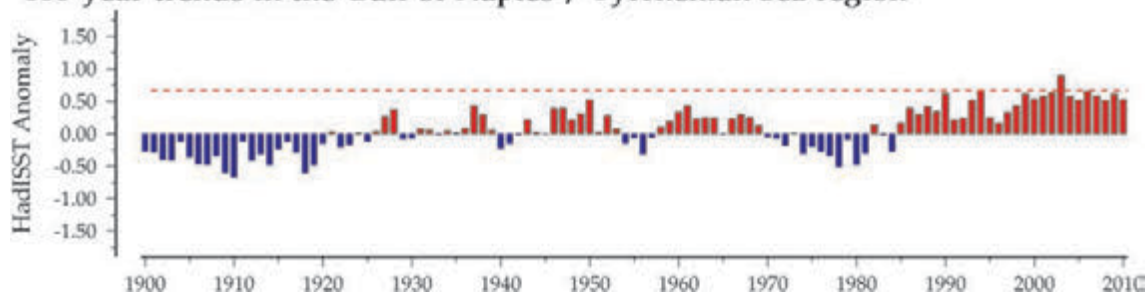


Figure 9.4.3
Regional overview plot (see Section 2.2.3) showing long-term sea surface temperatures and wind speeds in the general region surrounding the Gulf of Naples LTER-MC monitoring area.

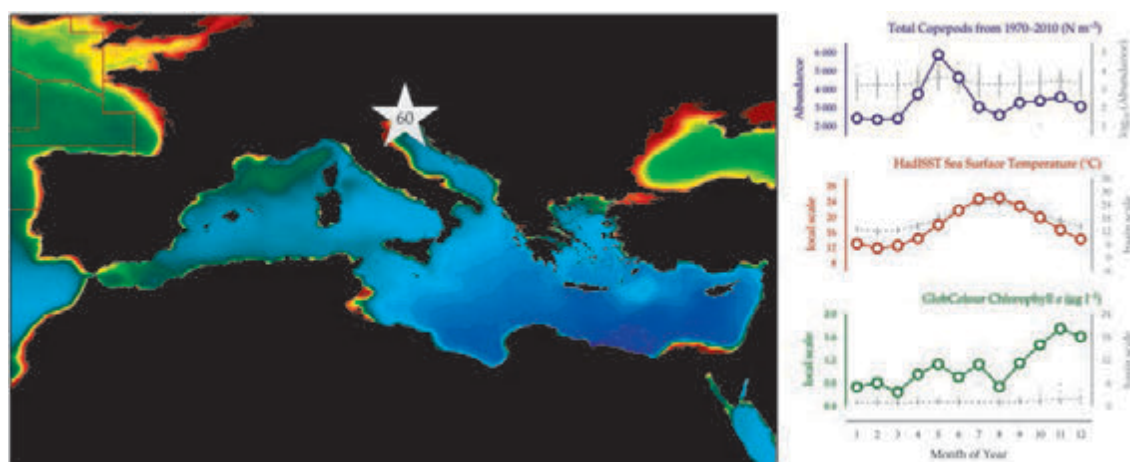
100-year trends in the Gulf of Naples / Tyrrhenian Sea region



9.5 Gulf of Trieste (Site 60)

Valentina Tirelli, Alessandra de Olazabal, and Serena Fonda-Umani

Figure 9.5.1
Location of the Gulf of Trieste monitoring area (Site 60) plotted on a map of average chlorophyll concentration, and its corresponding seasonal summary plot (see Section 2.2.1).



The Gulf of Trieste, located in the northernmost part of the Adriatic Sea (Figure 9.5.1), is a semi-enclosed coastal area, with a maximum depth of less than 25 m. It is characterized by large and variable freshwater input.

Marine biological studies in the Gulf of Trieste began in the late 1800s, and it was in Trieste that the first biological research station in the Adriatic Sea, the Zoological Station of Trieste, was founded in 1875. Zooplankton and particularly jellyfish, ctenophores, cladocerans, and copepods were the principal subjects of investigations [Notable among many others are the studies by Steuer (1902)]. During the First World War, biological research was interrupted, and the Zoological Station was closed. In the 1960s, marine research in Trieste was resumed, and in the early 1970s, studies on the zooplankton community started again. In 1986, a regular monthly sampling for biological (phytoplankton and zooplankton in several size classes), hydrological, and chemical analysis began. Since 1994, the set of measured parameters has progressively increased, including smaller size classes such as nanoplankton, picoplankton, viruses, and several physiological processes (for more information about the activity, see the website: <http://nettuno.ogs.trieste.it/ilter/BIO>). In 2006, the time-series station C1 was formally included in the Italian network of long-term ecological research sites (LTER-Italy) as part of the northern Adriatic LTER site (I-LTER; <http://www.ilternet.edu>).

Sampling at the time-series station C1, initiated by the University of Trieste, was later taken over by the Laboratory of Marine Biology of Trieste after its formal establishment in December 1979 and, since October 2005, by the Department of Oceanography (OCE) of the Istituto Nazionale di Oceanografia e Geofisica Sperimentale (OGS) of Trieste.

Zooplankton are collected by vertical hauls from 15 m to the surface using a WP2 net (56 cm diameter, 200 mm mesh). Half of the sample is processed for biomass measurements as dry mass; the other half is fixed with buffered formalin (2–4% final concentration) for the determination of species composition and abundance. Sampling has been ongoing since April 1970, with a major interruption from January 1981 to February 1986, inclusive. Sampling frequency is monthly, but was fortnightly during a few months of 1980 and the years 2002–2004.

While the mesozooplankton taxonomic list of the Gulf of Trieste is composed of 127 taxa, the mesozooplankton community is characterized by a small number of coastal and estuarine species, which can exhibit high dominance.

Seasonal and interannual trends (Figure 9.5.2)

Copepods represented on average more than 60% of the total annual zooplankton during 2006–2011, with higher values during the cold months, when they frequently represented more than 90% of the total zooplankton abundance. Despite the importance of copepods, the values for the ten most-abundant taxa (Table 9.5.1) showed the cladoceran *Penilia avirostris* as the dominant species, with a percentage more than double that of the second most-abundant taxa, the copepod *Acartia clausi*. Copepods of the genus *Paracalanus*, *Oncaea*, and *Oithona* occupy the next four positions, and the list is completed by Gastropoda larvae, *Siphonophora*, and *Ophiuroidea plutei*.

		Annual average (all months) from 2006–2011	
Rank	Taxa	% of mean abundance	Mean abundance (N m ⁻³)
1	<i>Penilia avirostris</i>	26,4	25 455
2	<i>Acartia clausi</i> + <i>Acartia</i> juv.	12,3	11 819
3	<i>Paracalanus</i> juv.	7,2	6 932
4	<i>Oncaea</i> spp.	5,7	5 504
5	<i>Oithona</i> juv.	4,1	3 965
6	<i>Paracalanus parvus</i>	4,0	3 825
7	Gastropoda larvae	3,6	3 434
8	Copepoditi Calanoida	3,2	3 095
9	Siphonophora sp. indet.	2,9	2 768
10	Ophiuroidea plutei	2,3	2 207
Total mean abundance of “Top Ten Taxa”			69 005
Total mean abundance of entire zooplankton sample			96 270
% of entire zooplankton sample represented by “Top Ten Taxa”		71,7	

Table 9.5.1

Average abundance and relative dominance (percentage of the total zooplankton collected) of the top ten most abundant taxa collected in the Gulf of Trieste throughout the entire year (all months) in the period 2006–2011.

Cladocerans are only present in the Gulf of Trieste during summer, generally from June to October (Piontkovski *et al.*, 2012). In this period, their abundance largely exceeds that of copepods. In summer (June–October) of 2006–2011, *P. avirostris* alone constituted 38% of the total zooplankton (Table 9.5.2). The ten dominant species were very similar

to those observed for the entire year (Table 9.5.1), with only few changes in the rank order, the appearance of bivalve larvae, another taxa that typically shows maximal abundance during summer, and the absence of the genus *Oithona*.

		Annual average (all months) from 2006–2011	
Rank	Taxa	% of mean abundance	Mean abundance (N m ⁻³)
1	<i>Penilia avirostris</i>	37,9	25 335
2	<i>Acartia clausi</i> + <i>Acartia</i> juv.	9,3	6 189
3	<i>Paracalanus</i> juv.	7,3	4 898
4	<i>Paracalanus parvus</i>	4,3	2 841
5	<i>Oncaea</i> spp.	3,8	2 569
6	Gastropoda larve	3,4	2 273
7	Siphonophora sp. indet.	3,2	2 165
8	Ophiuroidea plutei	2,9	1 953
9	Bivalvia larvae indet.	2,3	1 511
10	Calanoida copepodites	2,3	1 507
Total mean abundance of entire zooplankton sample			51 242
% of entire zooplankton sample represented by “Top Ten Taxa”		71,2	66 792

Table 9.5.2

Average abundance and relative dominance (percentage of the total zooplankton collected) of the top ten most abundant taxa collected in the Gulf of Trieste during the summer months (June–October) in the period 2006–2011.

The situation completely changes when summer months are excluded from the analysis. In fact, considering only the months January, February, March, April, May, November, and December, Cladocerans disappear from the list of ten dominant species, which almost totally consists of copepods. The only non-copepod taxa

present are Oikopleura and Doliolum. Moreover, all the meroplanktonic taxa, characterizing the summer period, but initially present also in Table 9.3d disappear.

Table 9.5.3
Average abundance and relative dominance (percentage of the total zooplankton collected) of the top ten most abundant taxa collected in the Gulf of Trieste during the non-summer months (November–May) in the period 2006–2011.

Annual average (all months) from 2006–2011			
Rank	Taxa	% of mean abundance	Mean abundance (N m ⁻³)
1	<i>Acartia clausi</i> + <i>Acartia</i> juv.	18,9	378
2	<i>Oithona</i> juv.	10,5	293
3	<i>Oncaea</i> spp.	9,9	2773
4	<i>Paracalanus</i> juv.	7,1	1977
5	Calanoida copepodites	5,6	159
6	<i>Oithona similis</i>	4,8	135
7	<i>Oikopleura</i> spp.	4,0	1112
8	<i>Paracalanus parvus</i>	3,8	103
9	<i>Doliolum denticulatum</i>	3,6	1017
10	<i>Temora longicornis</i>	3,0	8
	Total mean abundance of entire zooplankton sample		19904
	% of entire zooplankton sample represented by "Top Ten Taxa"	76,7	27960

In 2011, the arrival of the Asian egg-carrying copepod *Pseudodiaptomus marinus* (de Olazábal and Tirelli, 2011) was reported in the North Adriatic Sea (Mediterranean Sea). This species was recorded for the first time in two different areas, one of which is in the Gulf of Trieste, very close to Station C1. Its introduction was probably due to human activity linked to vessel traffic or aquaculture.

Over the more than 80-year time-series, a regular peak in total copepod abundance was present in May (Figure 9.5) , with a smaller second peak in November. Since 1980 (Conversi *et al.*, 2009, 2010), a significant increase in

temperature (particularly in summer and autumn) was observed, as well as a general increase in total copepod abundance (Figure 9.5) . Sea surface temperatures in the region have been above the 100-year average since 1980 and, since 2000, have often been the warmest seen for the past 100 years (Figure 9.5) .

Gulf of Trieste, northern Adriatic Sea

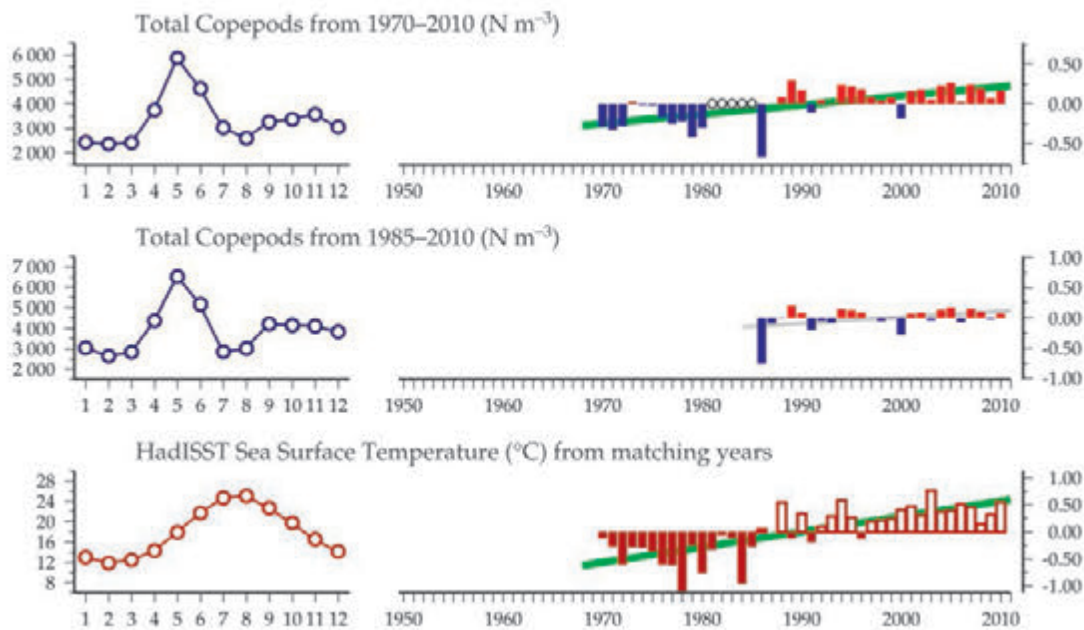


Fig 9.5.2
Multiple-variable comparison plot (see Section 2.2.2) showing the seasonal and interannual properties of select cosampled variables at the Gulf of Trieste monitoring area.

Additional variables are available online at: <http://WGZE.net/time-series>.

50-year trends in the Gulf of Trieste / northern Adriatic Sea region

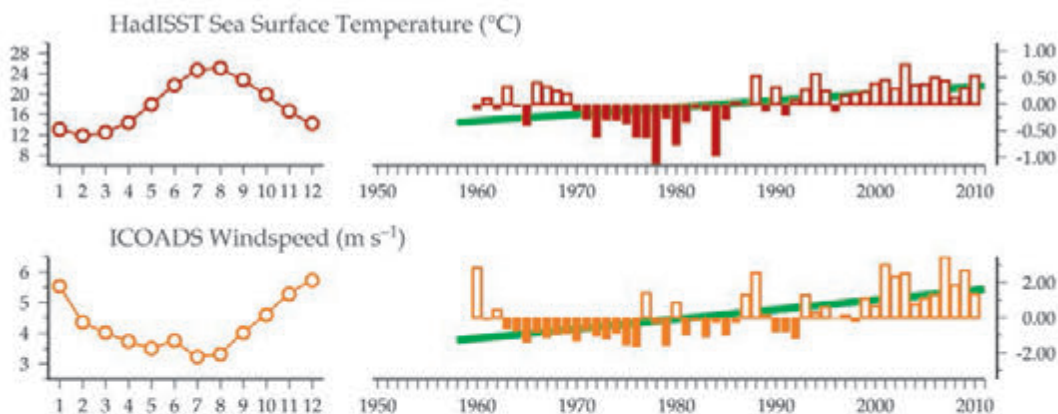
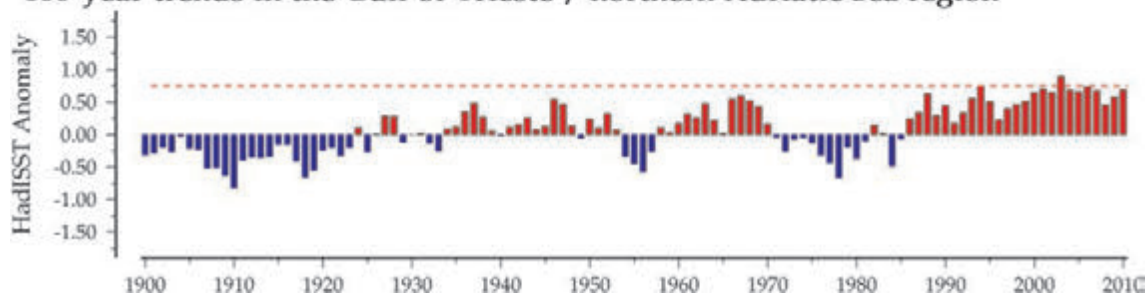


Fig 9.5.3
Regional overview plot (see Section 2.2.3) showing long-term sea surface temperatures and wind speeds in the general region surrounding the Gulf of Trieste monitoring area.

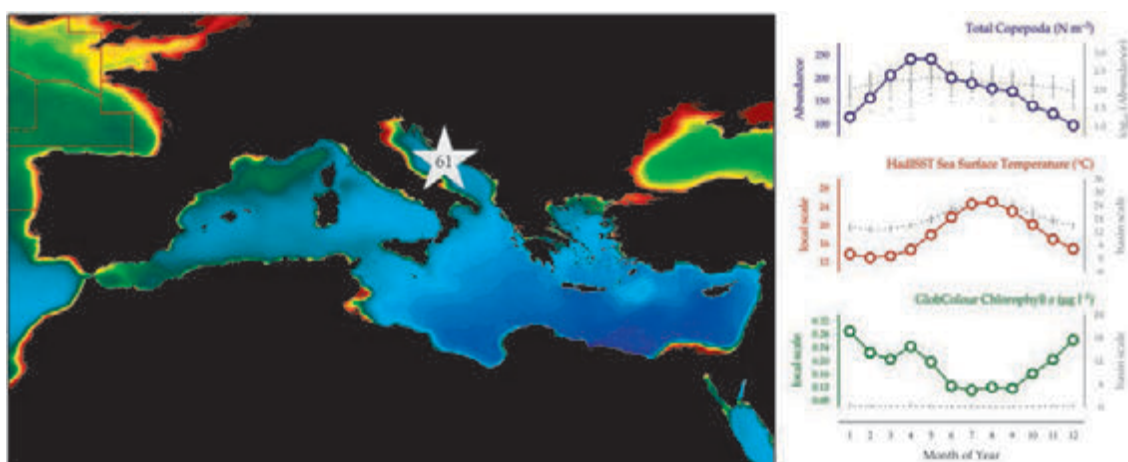
100-year trends in the Gulf of Trieste / northern Adriatic Sea region



9.6 Stončica (Site 61)

Olja Vidjak

Figure 9.6.1
Location of the Stončica monitoring area (Site 61) plotted on a map of average chlorophyll concentration, and its corresponding seasonal summary plot (see Section 2.2.1).



The offshore station of Stončica is located at 43°02'38"N 16°17'7"E in the central Adriatic Sea (Figure 9.6.1) at a maximum depth of 107 m and with a detrital and slightly muddy bottom. The annual dynamics of the surface temperature are characterized by a peak in August and minimum in March (Figure 9.6.1). Based on long-term monitoring of the chemical and biological parameters, the area is designated as an oligotrophic open sea, characterized by high transparency and decreased phytoplankton and zooplankton abundance, compared with the more productive coastal areas around the central Adriatic. The station is strongly influenced by the incoming Mediterranean water masses known as the Levantine Intermediate Water (LIW).

Regular zooplankton sampling at this permanent monitoring site began in 1959 and was performed at approximately monthly intervals using a Hensen net (73 cm diameter, 330 µm mesh) towed vertically from near-bottom to the surface (100–0 m). Special emphasis was placed on copepods, because they are generally the most important net zooplankton component and are significant prey to the commercially important planktivorous fish. Approximately 90 copepod species have been registered in this area, where, apart from the open-sea species, the surface waters also host many neritic copepods. These are distributed either from the shallow northern Adriatic area via south-flowing surface currents during summer or through the spreading of coastal waters towards the open sea.

The same sampling methodology was consistent until 1991; during 1991–1994, the sampling programme was interrupted. In January 1995, the programme was resumed regularly until 2004. From the end of the 1990s, the research interests within the Institute shifted towards the role of smaller fractions of the zooplankton, such as tintinnids, radiolarians, copepod developmental stages, and small copepod species. Consequently, samplings with finer plankton nets are currently performed regularly at this site.

Seasonal and interannual trends (Figure 9.6.2)

Long-term zooplankton data from Stončica have been analysed in several papers (Regner, 1981, 1985, 1991; Baranović *et al.*, 1993; Šolić *et al.*, 1997; Berline *et al.*, 2012). The analyses of copepod abundance identified the dominant seasonal pattern, with the appearance of a strong peak in April (Figure 9.6.2); on an interannual scale, a slight decrease in abundance was observed after the 1980s.

Stončica, central Adriatic Sea

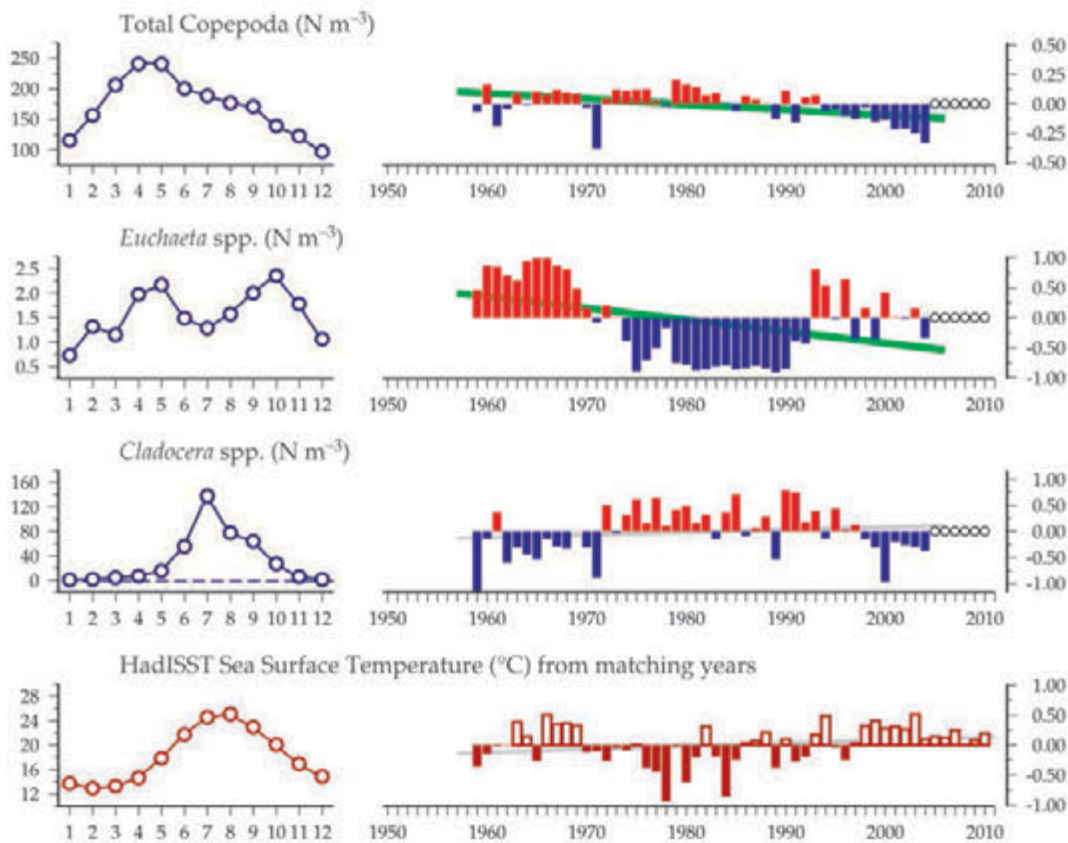


Figure 9.6.2
Multiple-variable comparison plot (see Section 2.2.2) showing the seasonal and interannual properties of select cosampled variables at the Stončica monitoring area.

Additional variables are available online at: <http://WGZE.net/time-series>.

50-year trends in the Stončica / central Adriatic Sea region

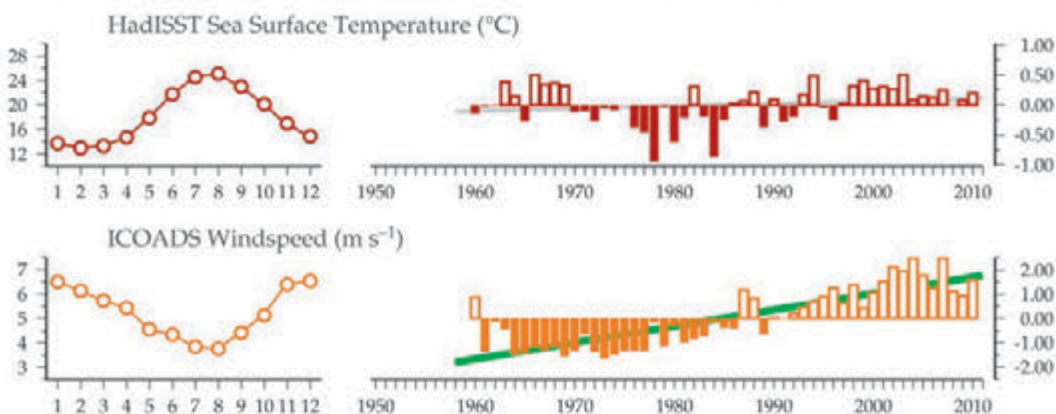
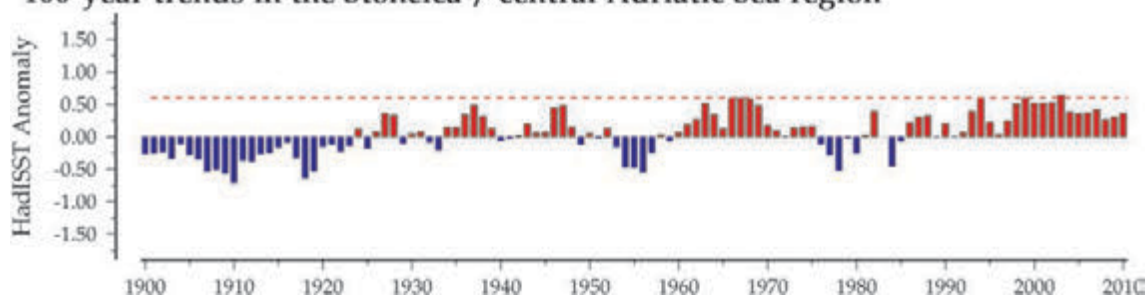


Figure 9.6.3
Regional overview plot (see Section 2.2.3) showing long-term sea surface temperatures and windspeeds in the general region surrounding the Stončica monitoring area.

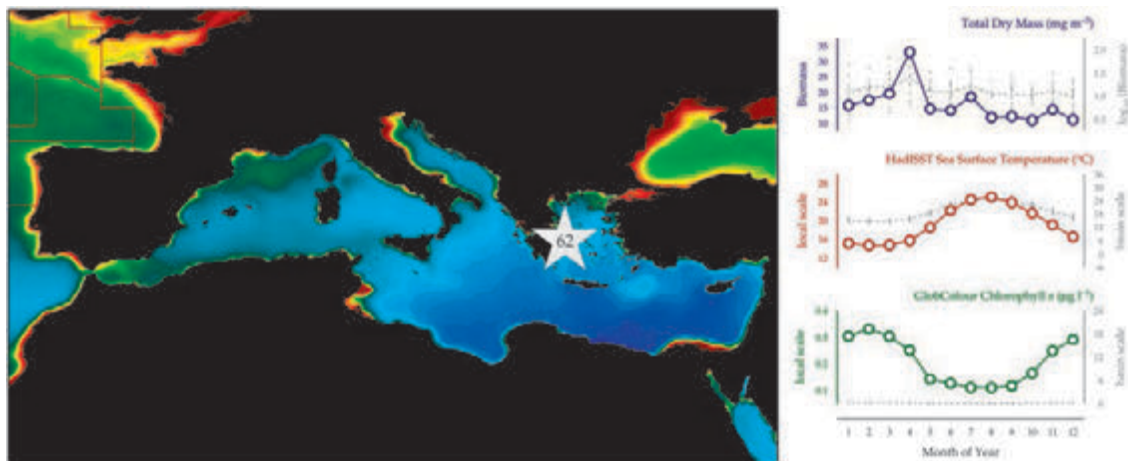
100-year trends in the Stončica / central Adriatic Sea region



9.7 Saronikos S11 (Site 62)

Ioanna Siokou-Frangou, Soultana Zervoudaki, and Epaminondas Christou

Figure 9.7.1
Location of the Saronikos S11 monitoring area (Site 62) plotted on a map of average chlorophyll concentration, and its corresponding seasonal summary plot (see Section 2.2.1).



Saronikos Station 11 (Saronikos S11) is located in the Saronikos Gulf at 37°52.36'N 23°38.30'E (Figure 9.7.1), with a bottom depth of 78 m. Zooplankton were sampled with a WP2 net (56 cm diameter, 200 µm mesh) from a depth of 75 m to the surface. Monitoring of zooplankton and abiotic parameters began in 1987, with variable (monthly or seasonal) sampling frequency and periodic gaps.

Seasonal and interannual trends (Figure 9.7.2)

Zooplankton biomass (total dry mass) was highest during the well-mixed winter period, with maxima in April, followed by a general decline accompanying increasing water temperatures and stratification. Saronikos S11 surface temperature peaks in August and has a minimum in February–March. Salinity ranges between 38 and 39, depending on the variable inflow of Aegean water (Kontoyiannis *et al.*, 2005).

Saronikos S11 is located 7 km from the Athens domestic sewage outfall. Prior to 1994, untreated wastewater was disposed at the sea surface. In 1994, primary-treated wastewater was disposed at a depth of 60 m, below the seasonal thermocline. Since 2004, this wastewater has been further treated in order to eliminate its organic load and to

greatly reduce its nutrient content. In spite of additional treatment, nutrient concentrations increased during the period 1987–2004, related to an increase in sewage volume. During this period, phytoplankton biomass decreased until 2002, probably because of the availability of nutrients at depth after 1994 and the competition with bacteria (Siokou-Frangou *et al.*, 2007; Zeri *et al.*, 2009). In contrast, zooplankton biomass revealed a clear increasing trend from 1987 to 2003, followed by a gradual decrease trend until 2009 (Figure 9.7.2). Zooplankton biomass seemed to recover in 2010.

Despite an apparent covariability of seawater temperature and zooplankton biomass anomalies, no correlation was found between climate indices and zooplankton groups (Berline *et al.*, 2012). Nevertheless, investigation at the species level could provide more information for the study area. The combination of several driving forces affecting the area and the lack of data makes the investigation of zooplankton variability quite difficult. Continuation of the monitoring without gaps and greater stability obtained in anthropogenic factors could permit a better understanding of zooplankton dynamics in the future.

Saronikos S11, Aegean Sea

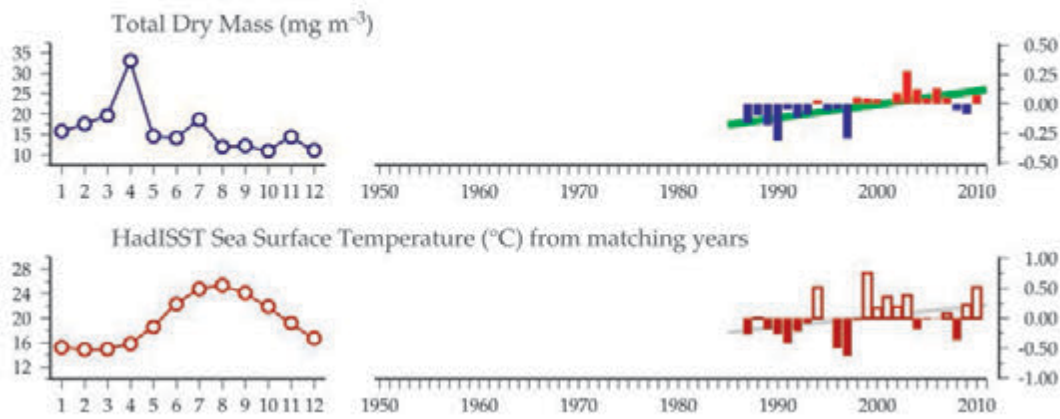


Figure 9.7.2
Multiple-variable comparison plot (see Section 2.2.2) showing the seasonal and interannual properties of select cosampled variables at the Saronikos S11 monitoring area.

Additional variables are available online at: <http://WGZE.net/time-series>.

50-year trends in the Saronikos S11 / Aegean Sea region

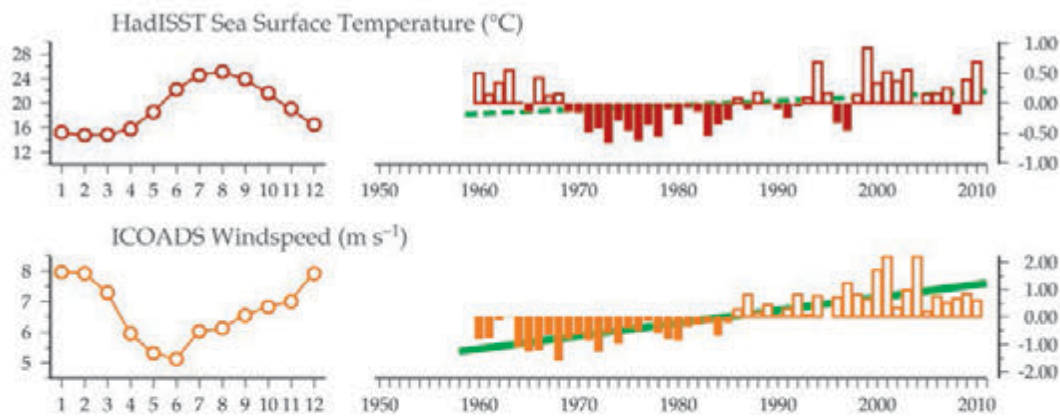
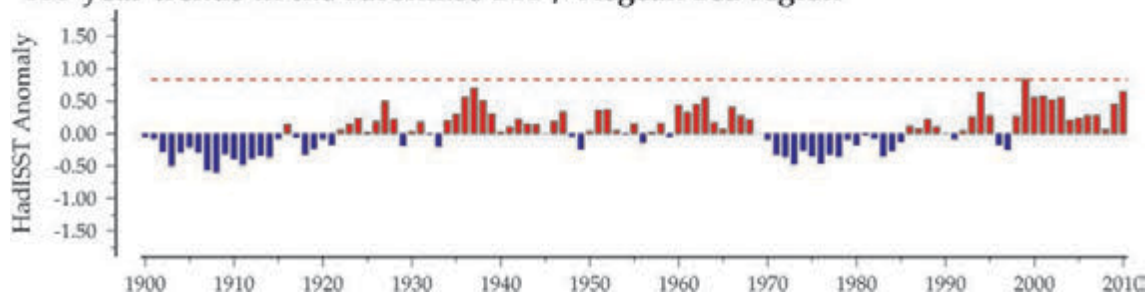


Figure 9.7.3
Regional overview plot (see Section 2.2.3) showing long-term sea surface temperatures and windspeeds in the general region surrounding the Saronikos S11 monitoring area.

100-year trends in the Saronikos S11 / Aegean Sea region

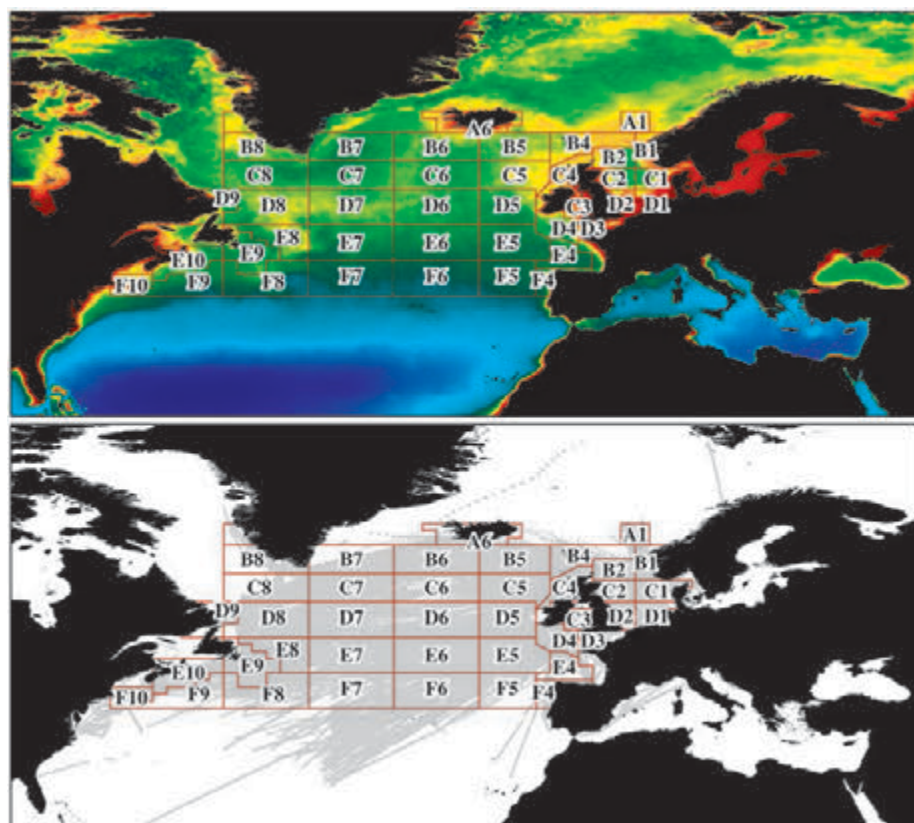


10. ZOOPLANKTON OF THE NORTH ATLANTIC BASIN

Priscilla Licandro, Claudia Castellani, Martin Edwards, and Rowena Stern

Figure 10.1

Locations of Continuous Plankton Recorder (CPR) standard areas (outlined in red). The top panel shows these areas on a map of average chlorophyll concentrations (see Section 2.3.2). The bottom panel shows the CPR transect and sampling coverage (grey dots) available within each of these areas.



The CPR survey is a long-term subsurface marine plankton monitoring programme consisting of a network of CPR transects towed monthly across the major geographical regions of the North Atlantic. It has been operated by the Sir Alister Hardy Foundation for Ocean Science (SAHFOS; <http://www.SAHFOS.org>) in the North Sea since 1931, with some standard routes existing with virtually unbroken monthly coverage back to 1946.

The CPR instrument is towed just below the surface behind volunteer-operated vessels (ships of opportunity), sampling plankton onto a moving 270 μ m band of net silk as the vessel and CPR unit traverse the North Atlantic and/or North Sea. Within the CPR instrument, the net silk and its captured plankton are preserved in formalin until they are returned to the SAHFOS laboratory. During processing, the net silk is divided into sections representing 10 nautical miles of towing, and each section, which represents ~ 3 m³ of filtered seawater, is analysed for plankton composition and abundance and other routine analyses including the estimation of the greenness of the silk (i.e. Phytoplankton Colour Index, PCI). The identification of up to 500 different phytoplankton and zooplankton taxa is part of

the analysis (Warner and Hays, 1994). The greenness of the silk is determined by the chloroplasts of unbroken and broken cells as well as small, unarmoured flagellates, which tend to disintegrate on contact with the net. Direct comparisons between the phytoplankton colour index and other chlorophyll *a* estimates, including SeaWiFS satellite estimates, indicate strong positive correlations (Batten *et al.*, 2003; Raitso *et al.*, 2005). The PCI, thereby, is considered a good index of total phytoplankton biomass.

The North Atlantic CPR database contains more than 5 million plankton observations analysed from more than 200 000 silk sections. By representing the midpoint of each silk section with a grey dot, the spatial coverage of the North Atlantic area of the CPR survey is shown in Figure 10.1. For the purpose of the assessment in this report, the North Atlantic basin has been geographically subdivided into different spatial regions (Figure 10.1; red boxes). The forty geographical regions shown in the figures are known as CPR standard areas and are referenced by their alphanumeric identifiers (e.g. “B2”, “D8”).

The CPR data from the standard areas were processed using standard report methods (see Section 2.1) as applied to the other plankton time-series presented in this report. For the purpose of viewing the long-term CPR trends in a spatial context, the standard report graphics (see Section 2.2) were truncated into the graphical forms described in Figure 10.2 and used in the “Spatial Trends Plots” of this section (Figures 10.3–10.8).

Basin-scale trends in zooplankton

In inshore and offshore waters of the Northeast Atlantic, total copepod abundance (Figure 10.3) has been significantly decreasing since the beginning of the time-series ($p < 0.05$). A similar trend was also observed in the central part of the western North Sea (e.g. C2 and D2), while in the western North Atlantic, copepod abundance has remained relatively stable.

To understand long-term changes in zooplankton populations, it is essential to consider the changes occurring in the lower trophic levels and in the regional marine environment. Indices of phytoplankton, such as the PCI and the sum of the abundance of all counted diatoms and dinoflagellates, help to represent the general functional response of phytoplankton to the changing environment. Sea surface temperature (SST) is considered to be a good proxy for hydroclimatic variability.

Overall, Figures 10.4 and 10.5 show a general increase in SST and PCI along the western and eastern boundaries. It is worth noting that phytoplankton biomass (based on PCI) mainly increased in the Northeast Atlantic and around the Newfoundland Shelf, where the increase in temperature was particularly significant ($p < 0.01$). In contrast Figures 10.3 and 10.6–10.8 show a clear west–east difference in the decadal trends of total copepods, diatoms, dinoflagellates, and tintinnids. In the western North Atlantic, diatoms, dinoflagellates, and tintinnids have increased, whereas copepod abundance has remained more or less the same. In contrast, in the eastern North Atlantic, diatoms, dinoflagellates, and copepods have generally decreased. Hence, the basin-wide trend increase in PCI suggests that the phytoplankton increase in the eastern Atlantic may be due to an increase in small photosynthetic organisms such as flagellates, which are less nutritious than diatoms and dinoflagellates for copepods. Thus, the observed decadal decline in copepod abundance appears to be driven by a decline in prey availability in the eastern North Atlantic (Figures 10.6–10.8) compared to the western North Atlantic. Although the basin-scale increase in SST alone cannot explain the difference in total copepod abundance between the western and eastern North Atlantic, temperature does exert an important effect on copepod physiology and metabolic rates. Hence, it is possible that the SST increase also contributed to the decline in total copepod abundance, particularly in the eastern Atlantic, where copepods might have been more food-deprived.

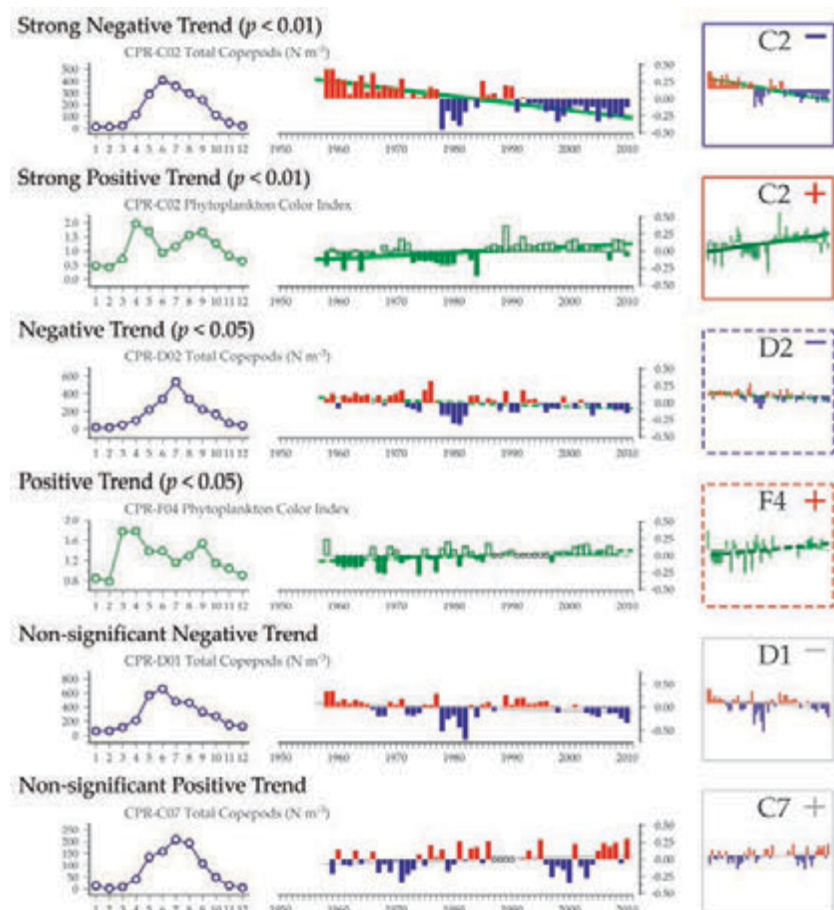


Figure 10.2
Examples of CPR standard area data shown in the standard report plot format (left column, see Section 2.2.2) and their corresponding truncated forms (right column) as presented in the “Spatial Trends Plots” shown later in this section.

The truncated form incorporates the standard annual anomaly trend representation (e.g. the green and grey slope lines) as described in Section 2.2. Positive significant trends ($p < 0.01$ or $p < 0.05$) are indicated with a red box outline, negative significant trends are indicated with blue box outline. Solid box outlines indicate $p < 0.01$, dashed boxed outlines indicate $p < 0.05$. Non-significant trends are outlined in grey. Trend directions (“+”, “-”) are also indicated in all cases.

Total Copepods

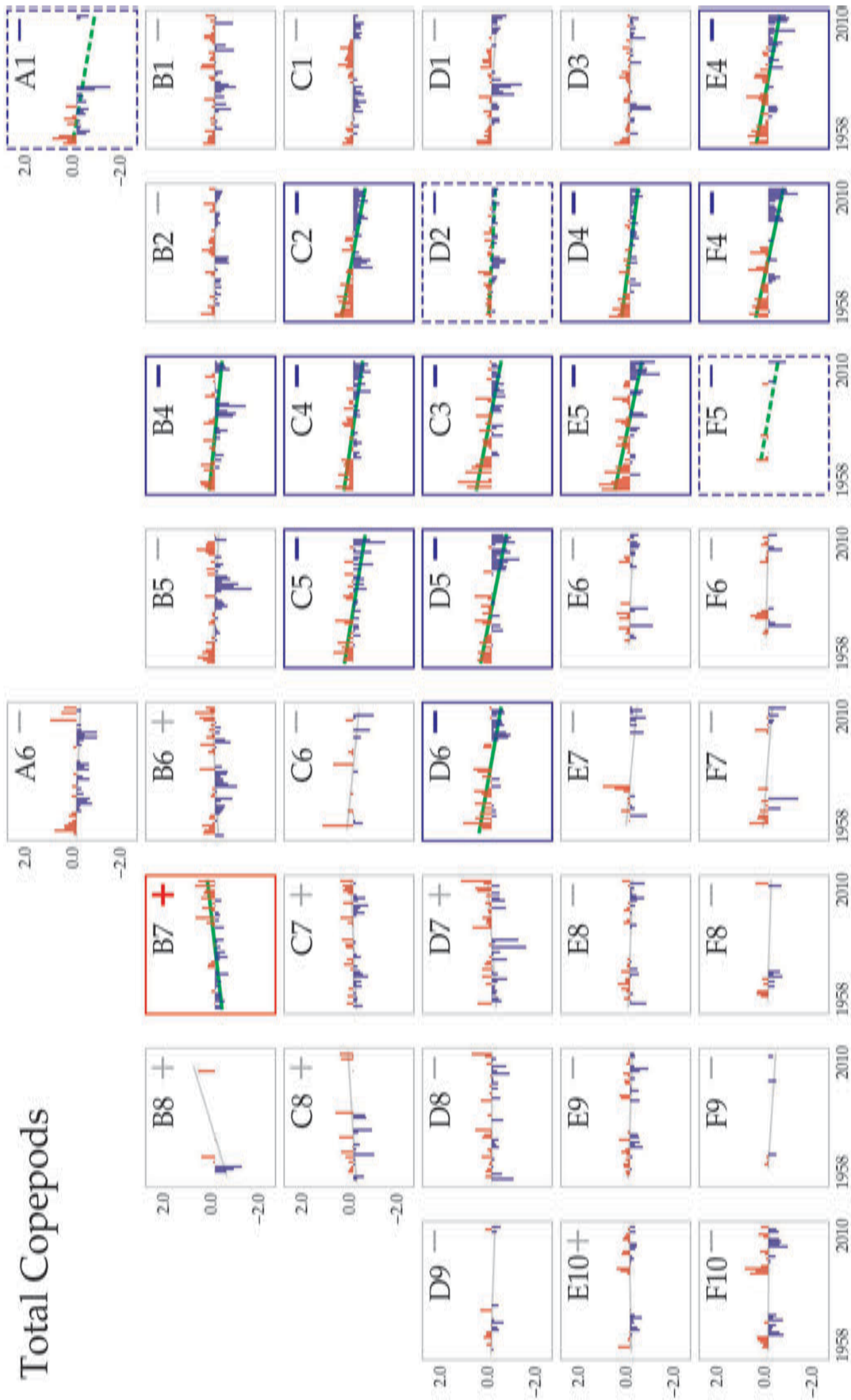


Figure 10.3
Spatio-temporal trends plot for Total Copepods time-series in the CPR standard areas of the North Atlantic Basin, based on data from 1958 to 2010.

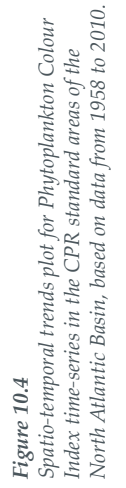




Figure 10.5
Spatio-temporal trends plot for Sea Surface Temperature
time-series in the CPR standard areas of the North Atlantic
Basin, based on data from 1958 to 2010.

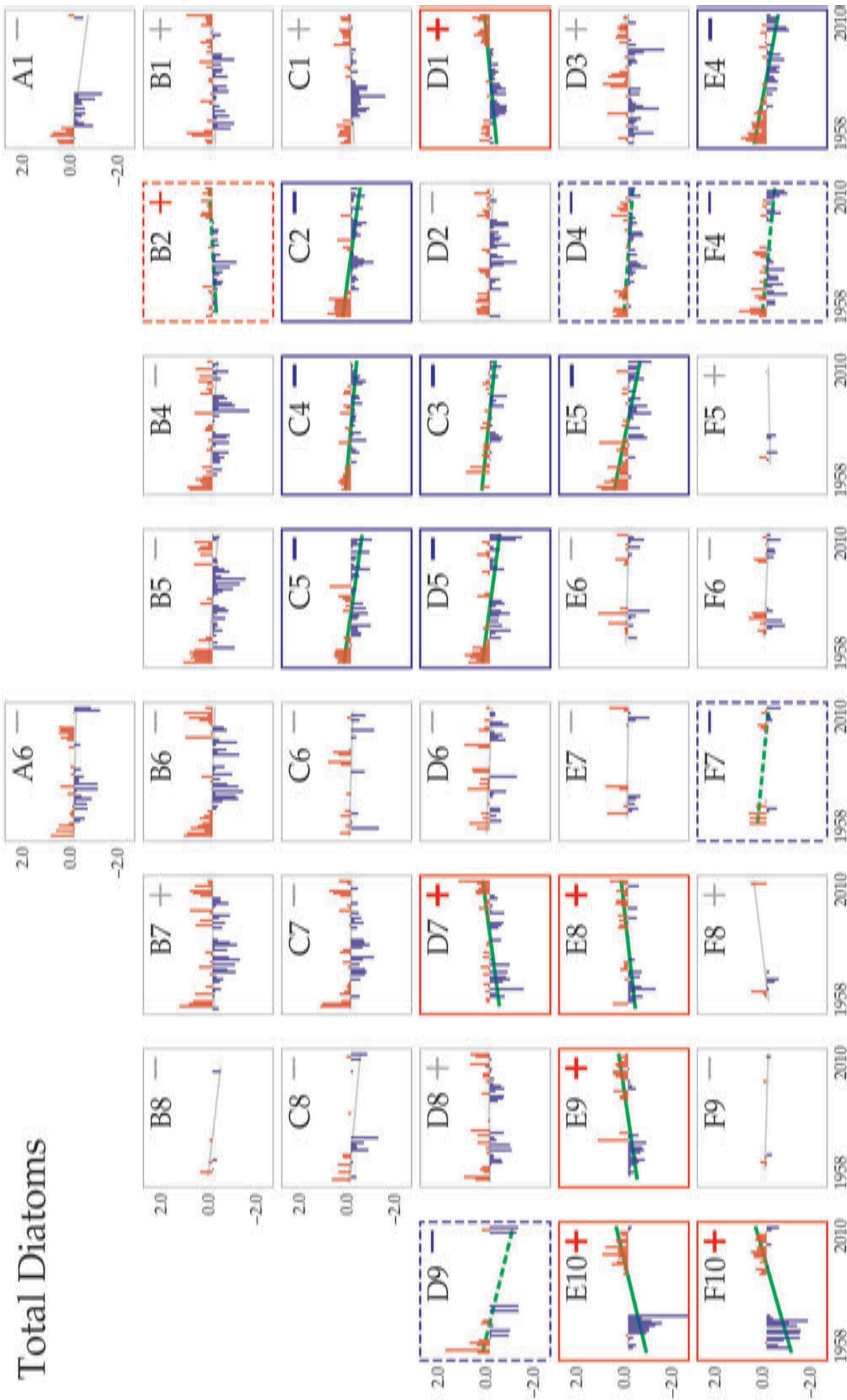


Figure 10.6
Spatio-temporal trends plot for Total Diatoms time-series in the CPR
standard areas of the North Atlantic Basin, based on data from 1958 to
2010. (Adapted from O'Brien et al., 2012.)

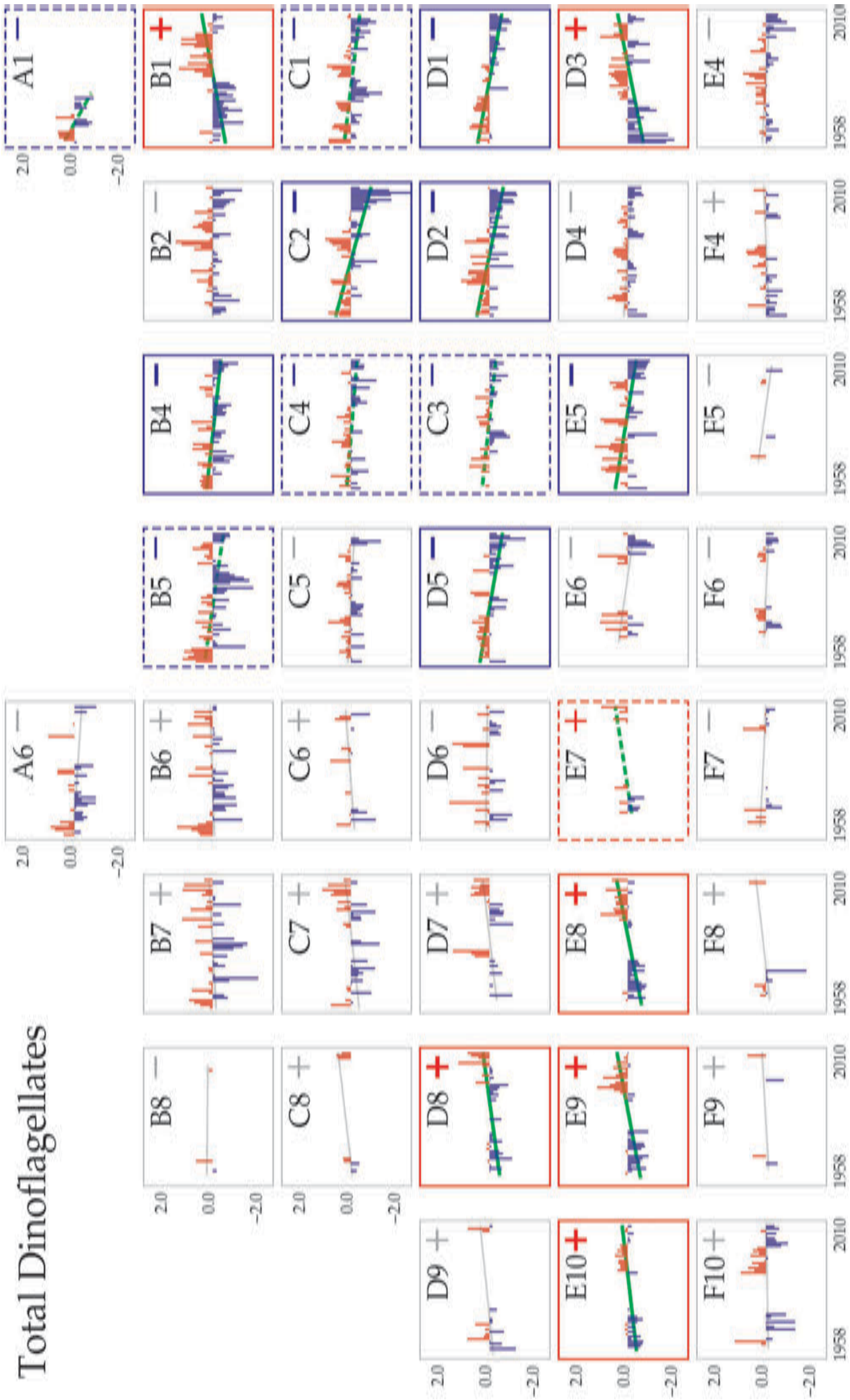


Figure 10.7
Spatio-temporal trends plot for Total Dinoflagellates time-series in the
CPR standard areas of the North Atlantic Basin, based on data from
1958 to 2010. (Adapted from O'Brien et al., 2012.)

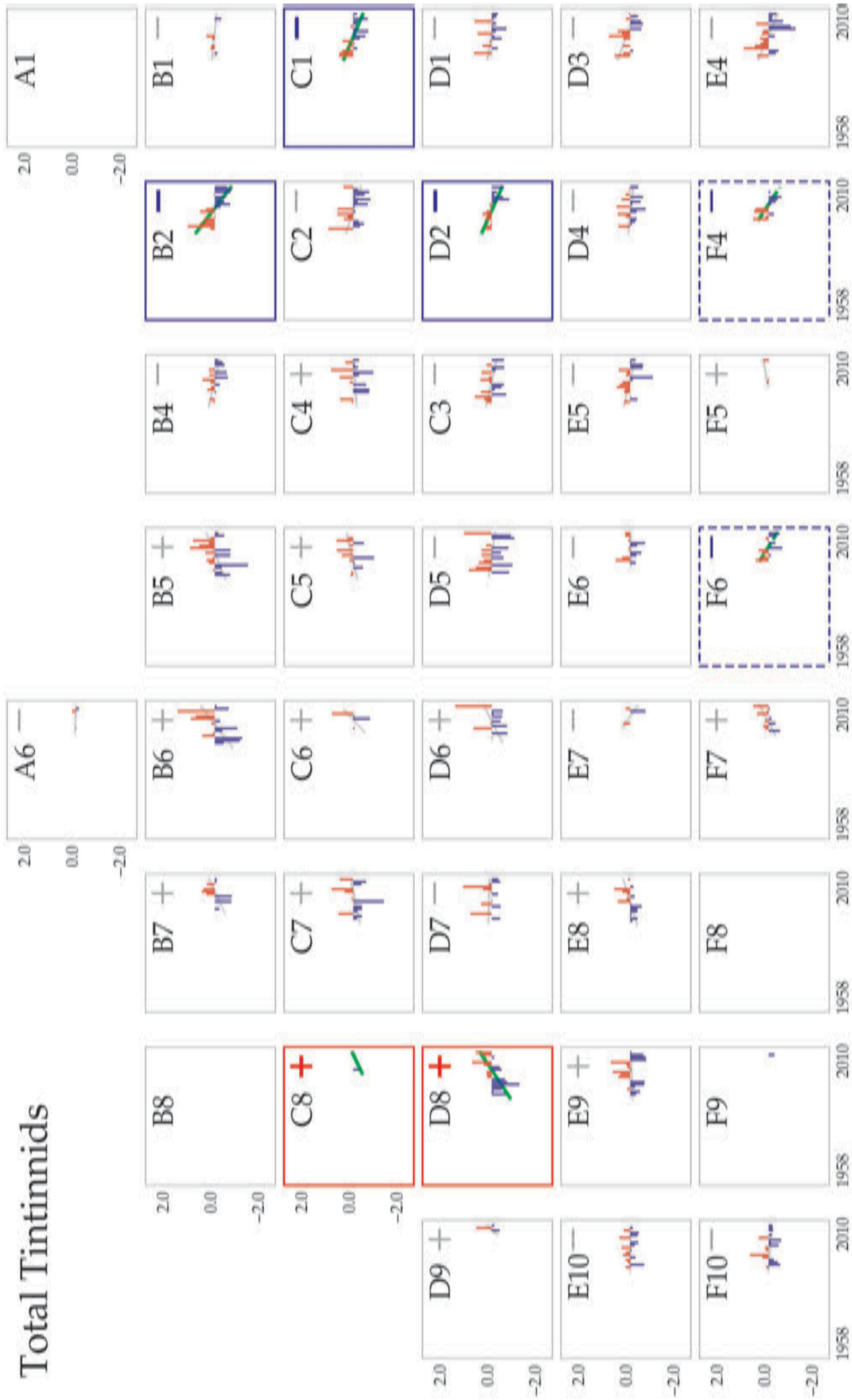


Figure 10.8
Spatio-temporal trends plot for Total Tintinnids time-series in the CPR
standard areas of the North Atlantic Basin, based on data from
1993 to 2010. (Adapted from O'Brien et al., 2012.)

11. REFERENCES

- Alheit, J., Möllmann, C., Dutz, J., Kornilovs, G., Loewe, P., Mohrholz, V., and Wasmund, N. 2005. Synchronous ecological regime shifts in the central Baltic and the North Sea in the late 1980s. *ICES Journal of Marine Science*, 62: 1205–1215.
- Alvarez-Salgado, X. A., Figueiras, F. G., Pérez, F. F., Groom, S., Nogueira, E., Borges, A. V., Chou, L., *et al.* 2003. The Portugal coastal counter current off NW Spain: new insights on its biogeochemical variability. *Progress in Oceanography*, 56(2): 281–321.
- Alvarez, I., Gómez-Gesteira, M., De Castro, M., and Dias, J. M., 2008. Spatiotemporal evolution of upwelling regime along the western coast of the Iberian Peninsula. *Journal of Geophysical Research*, 113(C07020): doi:10.1029/2008JC004744.
- Aravena, G., Villate, F., Uriarte, I., Iriarte, A., and Ibáñez, B. 2009. Response of *Acartia* populations to environmental variability and effects of invasive congeners in the estuary of Bilbao, Bay of Biscay. *Estuarine, Coastal and Shelf Science*, 83: 621–628.
- Arístegui, J., Alvarez-Salgado, X. A., Barton, E. D., Figueiras, F. G., Hernández-León, S., Roy, C., and Santos, A. M. P. 2006. Chapter 23. Oceanography and fisheries of the Canary Current/Iberian region of the Eastern North Atlantic (18a, E). *In* The Global Coastal Ocean: Interdisciplinary Regional Studies and Syntheses. The Sea: Ideas and Observations on Progress in the Study of the Seas, pp. 877–931. Ed. by A. R. Robinson and K. Brink. Harvard University Press, Boston.
- Astthorsson, O. S., and Gislason, A. 1998. Environmental conditions, zooplankton, and capelin in the waters north of Iceland. *ICES Journal of Marine Science*, 55: 808–810.
- Astthorsson, O. S., and Vilhjálmsson, H. 2002. Iceland Shelf LME: decadal assessment and resource. *In* Large Marine Ecosystems of the North Atlantic: Changing States and Sustainability, pp. 219–243. Ed. by K. Sherman and H. R. Skjoldal. Elsevier, Amsterdam. 449 pp.
- Attrill, M., Wright, J., and Edwards, M. 2007. Climate-related increases in jellyfish frequency suggest a more gelatinous future for the North Sea. *Limnology and Oceanography*, 52: 480–485.
- Bagøien, E., Melle, W., and Kaartvedt, S. 2012. Seasonal development of mixed layer depths, nutrients, chlorophyll and *Calanus finmarchicus* in the Norwegian Sea – A basin-scale habitat comparison. *Progress in Oceanography*, 103: 58–79.
- Baranović, A., Šolić, M., and Krstulović, N. 1993. Temporal fluctuations of zooplankton and bacteria in the middle Adriatic Sea. *Marine Ecology Progress Series*, 92: 65–75.
- Barbosa, A. B., Domingues, R. B., and Galvão, H. M. 2010. Environmental forcing of phytoplankton in a semi-arid estuary (Guadiana estuary, south-western Iberia): a decadal study of climatic and anthropogenic influences. *Estuaries and Coasts*, 33(2): 324–341.
- Beaugrand, G. 2003. Long-term changes in copepod abundance and diversity in the northeast Atlantic in relation to fluctuations in the hydroclimatic environment. *Fisheries Oceanography*, 12: 270–283.
- Beaugrand, G. 2005. Monitoring pelagic ecosystems using plankton indicators. *ICES Journal of Marine Science*, 62: 333–338.
- Beaugrand, G. 2009. Decadal changes in climate and ecosystems in the North Atlantic Ocean and adjacent seas. *Deep-Sea Research II*, 56(8–10): 656–673.
- Beaugrand, G., and Reid, P. C. 2003. Long-term changes in phytoplankton, zooplankton and salmon related to climate. *Global Change Biology*, 9: 801–817.
- Beaugrand, G., Ibáñez, F., Lindley, J. A., and Reid, P. C. 2002a. Diversity of calanoid copepods in the North Atlantic and adjacent seas: species associations and biogeography. *Marine Ecology Progress Series*, 232: 179–195.
- Beaugrand, G., Reid, P. C., Ibanez, F., Lindley, J. A., and Edwards, M. 2002b. Reorganisation of North Atlantic marine copepod biodiversity and climate. *Science*, 296: 1692–1694.
- Beaugrand, G., Edwards, M., and Legendre, L. 2010. Marine biodiversity, ecosystem functioning and carbon cycles. *Proceedings of the National Academy of Sciences of the United States of America*, 107(22): 10120–10124. doi:10.1073/pnas.0913855107.
- Berline, L., Siokou-Frangou, I., Marasović, I., Vidjak, O., Fernández de Puellas, M. L., Mazzocchi, M. G., Assimakopoulou, G., *et al.* 2012. Intercomparison of six Mediterranean zooplankton time series. *Progress in Oceanography*, 97–100: 76–91. doi: t10.1016/j.pocean.2011.11.011.
- Béthoux, J. P., Durrieu de Madron, X., Nyffeler, F., and Taillez, D. 2002. Deep water in the western Mediterranean: peculiar 1999 and 2000 characteristics, shelf formation hypothesis, variability since 1970 and geochemical inferences. *Journal of Marine Systems*, 33–34: 117–131.

- Béthoux, J. P., Gentili, B., and Tailliez, D. 1998. Warming and freshwater budget change in the Mediterranean since the 1940s, their possible relation to the greenhouse effect. *Geophysical Research Letters*, 25: 1023–1026.
- Bode, A., Alvarez-Ossorio, M. T., Cabanas, J. M., Miranda, A., and Varela, M. 2009. Recent trends in plankton and upwelling intensity off Galicia (NW Spain). *Progress in Oceanography*, 83: 342–350.
- Bode, A., Alvarez-Ossorio, M. T., Miranda, A., López-Urrutia, A., and Valdés, L. 2012. Comparing copepod time-series in the north of Spain: spatial autocorrelation of community composition. *Progress in Oceanography*, 97–100: 108–119.
- Bode, A., Anadón, R., Morán, X. A. G., Nogueira, E., Teira, E., and Varela, M. 2011. Decadal variability in chlorophyll and primary production off NW Spain. *Climate Research*, 48: 293–305.
- Boersma, M., Malzahn, A. M., Greve, W., and Javidpour, J. 2007. The first occurrence of the ctenophore *Mnemiopsis leidyi* in the North Sea. *Helgoland Marine Research*, 61: 153–155.
- Bonnet, D., Harris, R., Lopez-Urrutia, A., Halsband-Lenk, C., Greve, W., Valdes, L., Hirche, H.-J., *et al.* 2007. Comparative seasonal dynamics of *Centropages typicus* at seven coastal monitoring stations in the North Sea, English Channel and Bay of Biscay. *Progress in Oceanography*, 72: 233–248.
- Bonnet, D., Richardson, A., Harris, R. P., Hirst, A. G., Beaugrand, G., Edwards, M., Ceballos, S., *et al.* 2005. An overview of *Calanus helgolandicus* ecology in European waters. *Progress in Oceanography*, 65: 1–53.
- Botas, J. A., Bode, A., Fernández, E., and Anadón, R. 1990. A persistent upwelling off the Central Cantabrian coast (Bay of Biscay). *Estuarine, Coastal and Shelf Science*, 30: 185–199.
- Brander, K. 2005. Cod recruitment is strongly affected by climate when stock biomass is low. *ICES Journal of Marine Science*, 62: 339–343.
- Brander, K. M., Dickson, R. R., and Edwards, M. 2003. Use of Continuous Plankton Recorder information in support of marine management: applications in fisheries, environmental protection, and in the study of ecosystem response to environmental change. *Progress in Oceanography*, 58: 175–191.
- Broms, C., and Melle, W. 2007. Seasonal development of *Calanus finmarchicus* in relation to phytoplankton bloom dynamics in the Norwegian Sea. *Deep-Sea Research (Part II, Topical Studies in Oceanography)*, 54(23–26): 2760–2775.
- Broms, C., Melle, W., and Kaartvedt, S. 2009. Oceanic distribution and life cycle of *Calanus* species in the Norwegian Sea and adjacent waters. *Deep-Sea Research II*, 56: 1910–1921.
- Bunn, S., and Arthington, A. 2002. Basic principles and ecological consequences of altered flow regimes for aquatic biodiversity. *Environmental Management*, 30(4): 492–507.
- Burthe, S., Daunt, F. H. J., Butler, A., Elston, D., Frederiksen, M., Johns, D. G., Thackeray, S. J., and Wanless, S., 2012. Phenological trends and trophic mismatch across multiple levels of a North Sea pelagic food web. *Marine Ecology Progress Series*, 454: 119–133.
- Cabal, J., González-Nuevo, G., and Nogueira, E. 2008. Mesozooplankton species distribution in the NW and N Iberian shelf during spring 2004: relationship with frontal structures. *Journal of Marine Systems*, 72: 282–297.
- Casini, M., Lövgren, J., Hjelm, J., Cardinale, M., Molinero, J. C., and Kornilovs, G. 2008. Multi-level trophic cascades in a heavily exploited open marine ecosystem. *Proceedings of the Royal Society B*, 275: 1793–1801.
- Chícharo, M. A., Chícharo, L., Galvão, H., Barbosa, A., Marques, H., Andrade, J. P., Esteves, E., *et al.* 2001. Status of the Guadiana estuary (South Portugal) during 1996–1998: an ecohydrological approach. *Aquatic Ecosystem Health and Management*, 4: 73–90.
- Chícharo, L., Chícharo, M. A., and Ben-Hamadou, R. 2006. Use of a hydrotechnical infrastructure (Alqueva Dam) to regulate planktonic assemblages in the Guadiana estuary: basis for sustainable water and ecosystem services management. *Estuarine Coastal and Shelf Science*, 70 (1–2): 3–18.
- Civitarese, G., Gačić, M., Lipizer, M., and Eusebi Borzelli, G. L. 2010. On the impact of the Bimodal Oscillating System (BiOS) on the biogeochemistry and biology of the Adriatic and Ionian Seas (Eastern Mediterranean). *Biogeosciences*, 7: 3987–3997.
- Conover, R. J. 1988. Comparative life histories in the genera *Calanus* and *Neocalanus* in high latitudes of the Northern Hemisphere. *Hydrobiologia*, 167/168: 127–142.
- Conversi, A., Fonda-Umani, S., Peluso, T., Molinero, J. C., and Edwards, E. 2010. The Mediterranean Sea regime shift at the end of the 1980s, and its links to other European basins. *PloS One*, 5: 1–15.
- Conversi, A., Peluso, T., and Fonda-Umani, S. 2009. The Gulf of Trieste: a changing ecosystem. *Journal of Geophysical Research*, 114, C03S90, doi:10.1029/2008JC004763.
- Cox, J. L., and Wiebe, P. H. 1979. Origins of plankton in the Middle Atlantic Bight. *Estuarine and Coastal Marine Science*, 9: 509–527.
- Dafner, E. V., Boscolo, R., and Bryden, H. L. 2003. The N:Si:P molar ratio in the Strait of Gibraltar. *Geophysical Research Letters*, 30(10): 13.1–13.4.

- de Lafontaine, Y., Demers, S., and Runge, J. 1991. Pelagic food web interactions and productivity in the Gulf of St Lawrence: a perspective. *In* The Gulf of St Lawrence: Small Ocean or Big Estuary? pp. 99–123. Ed. by J-C. Theriault. Canadian Special Publication of Fisheries and Aquatic Sciences, 113. 359 pp.
- de Olazabal, A., and Tirelli, V. 2011. First record of the egg-carrying calanoid copepod *Pseudodiaptomus marinus* Sato, 1913 in the Adriatic Sea. *Marine Biodiversity Records*, Vol. 4; e85; 2011. doi: 10.1017/S1755267211000935.
- Dyrssen, D. 1993. The Baltic-Kattegat-Skagerrak Estuarine System. *Estuaries*, 16: 448–452.
- Ecosystem Assessment Program. 2009. Ecosystem Assessment Report for the Northeast US Continental Shelf Large Marine Ecosystem. US Department of Commerce, Northeast Fisheries Science Center Reference Document 09–11. 34 pp.
- Edwards, M., Beaugrand, G., John, A. W. G., Johns, D. G., Licandro, P., McQuatters-Gollop, A., and Reid, P. C. 2009. Ecological Status Report: results from the CPR survey 2007/2008. SAHFOS Technical Report, 6: 1–12.
- Edwards, M., and Richardson, A. J. 2004. Impact of climate change on marine pelagic phenology and trophic mismatch. *Nature*, 430: 881–884.
- Eloire, D., Somerfield, P. J., Conway, D. V. P., Halsband-Lenk, C., Harris, R. P., and Bonnet, D. 2010. Temporal variability and community composition of zooplankton at station L4 in the Western Channel: 20 years of sampling. *Journal of Plankton Research*, 32: 657–679.
- Feistel, R., Nausch, G., and Wasmund, N. (Eds). 2008. State and Evolution of the Baltic Sea 1952–2005: A Detailed 50-year Survey of Methodology and Climate, Physics, Chemistry, Biology and Marine Environment. John Wiley and Sons, Hoboken, NJ. 703 pp.
- Fernández, E., Álvarez, F., Anadón, R., Barquero, S., Bode, A., García, A., García-Soto, C., *et al.* 2004. The spatial distribution of plankton communities in a Slope Water anticyclonic Oceanic eDDY (SWODDY) in the Southern Bay of Biscay. *Journal of the Marine Biological Association of the United Kingdom*, 84: 501–517.
- Fernández de Puellas, M. L., Alemany, F., and Jansa, J. 2007. Zooplankton time-series in the Balearic Sea (Western Mediterranean): variability during the decade 1994–2003. *Progress in Oceanography*, 74: 329–354.
- Fernández de Puellas, M. L., and Molinero, J. C. 2008. Decadal changes in hydrographic and ecological time-series in the Balearic Sea (Western Mediterranean), identifying links between climate and zooplankton. *ICES Journal of Marine Science*, 65(3): 311–318.
- Fernández de Puellas, M. L. and Molinero, J. C. 2013. Increasing zooplankton variance in the late 1990s unveils hydroclimate modifications in the Balearic Sea, Western Mediterranean. *Marine Environmental Research*, 86: 76–80.
- Fernández de Puellas, M. L., Morillas, A., Lopez-Urrutia, A., and Molinero, J. C. 2009. Seasonal and interannual variability of copepod abundance in the Balearic region (Western Mediterranean) as indicator of basin scale hydrological changes. *Hydrobiologia*, 617: 3–16.
- Fernández de Puellas, M. L., Valencia, J., Jansá, J., and Morillas, A. 2004b. Hydrographical characteristics and zooplankton distribution in the Mallorca Channel (Western Mediterranean). *ICES Journal of Marine Science*, 61: 654–666.
- Fernández de Puellas, M. L., Valencia, J., and Vicente, L. 2004a. Zooplankton variability and climatic anomalies from 1994 to 2001 in the Balearic Sea (Western Mediterranean). *ICES Journal of Marine Science*, 61: 492–500.
- Fileman, E., Petropavlovsky, A., and Harris, R. 2010. Grazing by the copepods *Calanus helgolandicus* and *Acartia clausi* on the protozooplankton community station L4 in the Western English Channel. *Journal of Plankton Research*, 32: 709–724.
- Flinkman, J., Paakkonen, J-P., Saesmaa, S., and Bruun, J-E. 2007. Zooplankton time-series 1979–2005 in the Baltic Sea – life in a vice of bottom-up and top-down forces in 2007. *In* FIMR Monitoring of the Baltic Sea Environment: Annual Report 2006, pp. 73–86. Ed. by R. Olsonen. MERI (Report Series of the Finnish Institute of Marine Research), 59.
- Flinkman, J., and Postel, L. 2009. Zooplankton communities. *In* Biodiversity in the Baltic Sea. An Integrated Thematic Assessment on Biodiversity and Nature Conservation in the Baltic Sea, pp. 43–46. Ed. by U. Zweifel and M. Laamanen. Baltic Sea Environment Proceedings, 116B. 188 pp.
- Fonselius, S. 1995. Västerhavet och Östersjöns Oceanografi. SMHI Västra Frölunda. 200 pp.
- Frajka-Williams, E., and Rhines, P. B. 2010. Physical controls and interannual variability of the Labrador Sea spring phytoplankton bloom in distinct regions. *Deep-Sea Research I*, 57: 541–552.
- Frederiksen, M., Edwards, M., Richardson, A. J., Halliday, N. C., and Wanless, S. 2006. From plankton to top predators: bottom-up control of a marine food web across four trophic levels. *Journal of Animal Ecology*, 75: 1259–1268.

- Garaulet, L. L. 2011. Estabelecimento do bivalve exótico *Ruditapes philippinarum* (Adams & Reeve, 1850) no estuário do Tejo: caracterização da população actual e análise comparativa com a congénere nativa *Ruditapes decussatus* (Linnaeus, 1758) e macrofauna bentónica acompanhante. Msc. Thesis. University of Lisbon. 77 pp.
- Garcia-Comas, C., Stemmann, L., Ibanez, F., Berline, L., Mazzocchi, M. G., Gasparini, S., Picheral, M., *et al.* 2011. Zooplankton long-term changes in the NW Mediterranean Sea: Decadal periodicity forced by winter hydrographic conditions related to large-scale atmospheric changes? *Journal of Marine Systems*, 87(3–4): 216–226.
- García-Gorrioz, E., and Carr, M. E. 2001. Physical control of phytoplankton distributions in the Alboran Sea: a numerical and satellite approach. *Journal of Geophysical Research*, 106: 16 795–16 805.
- García-Lafuente, J., Vargas, J. M., Candela, J., Bascheck, B., Plaza, F., and Sarchan, T. 2000. The tide at the eastern section of the Strait of Gibraltar. *Journal of Geophysical Research*, 105(C6): 14197–14213.
- Genner, M. J., Sims, D. W., Wearmouth, V. J., Southall, E. J., Southward, A. J., Henderson, P. A., and Hawkins, S. J. 2004. Regional climatic warming drives long-term community changes of British marine fish. *Proceedings of the Royal Society B*, 271: 655–661.
- Giesbrecht, W. 1893 [“1892”]. Systematik und Faunistik des pelagischen Copepoden des Golfes von Neapel und der angrenzenden Meeres-Abschnitte. *Fauna und Flora des Golfes von Neapel*, 19: 1–831.
- Gislason, A., Petursdottir, H., Astthorsson, O. S., Gudmundsson, K., and Valdimarsson, H. 2009. Interannual variability in abundance and community structure of zooplankton south and north of Iceland in relation to environmental conditions in spring 1990–2007. *Journal of Plankton Research*, 31: 541–551.
- Gómez, F., Echevarría, F., García, C. M., Prieto, L., Ruiz, J., Reul, A., and Jiménez-Gómez, F. 2000. Microplankton distribution in the Strait of Gibraltar: coupling between organisms and hydrodynamic structures. *Journal of Plankton Research*, 22(4): 603–617.
- González-Nuevo, G., and Nogueira, E. 2005. Intrusions of warm and salty waters onto the NW and N Iberian shelf in early spring and its relationship to climate variability. *Journal of Atmospheric and Ocean Science*, 10(4): 361–375.
- Gorsky, G., Ohman, M. D., Picheral, M., Gasparini, S., Stemmann, L., Romagnan, J. B., Cawood, A., *et al.* 2010. Digital zooplankton image analysis using the ZooScan integrated system. *Journal of Plankton Research*, 32(3): 285–303.
- Greene, C. H., and Pershing, A. J. 2003. The flip-side of the North Atlantic Oscillation and modal shifts in slope-water circulation patterns. *Limnology and Oceanography*, 48: 319–322.
- Greve, W., Lange, U., Reiners, F., and Nast, J. 2001. Predicting the seasonality of North Sea zooplankton *In* Burning issues of North Sea ecology, The 14th International Senckenberg Conference “North Sea 2000”, Wilhelmshaven, Germany, 8–12 May 2000, pp. 263–268. Ed. by I. Kröncke, M. Türkay, and J. Sündermann. *Senckenbergiana Maritima*, 31(2). 273 pp.
- Greve, W., Reiners, F., Nast, J., and Hoffmann, S. 2004. Helgoland Roads time-series meso- and macrozooplankton 1975 to 2004: lessons from 30 years of single spot high frequency sampling at the only offshore island of the North Sea. *Helgoland Marine Research*, 58: 274–288.
- Haraldsson, M., Jaspers, C., Tiselius, P., Aksnes, D. G., Andersen, T., and Titelman, J. 2013. Environmental constraints of the invasive *Mnemiopsis leidyi* in Scandinavian waters. *Limnology and Oceanography*, 58: 37–48.
- Harris, R. P. 2010. The L4 time-series: the first 20 years. *Journal of Plankton Research*, 32: 577–583.
- Harrison, G., Johnson, C., Head, E., Spry, J., Pauley, K., Maass, H., Kennedy, M., *et al.* 2009. Optical, chemical, and biological oceanographic conditions in the Maritimes Region in 2008. Canadian Science Advisory Secretariat Research Document 2009/054. 55 pp.
- Harvey, M., and Devine, L. 2009. Oceanographic conditions in the Estuary and the Gulf of St Lawrence during 2008: zooplankton. Canadian Science Advisory Secretariat Research Document 2009/083. 54 pp.
- Head, E. J. H., Brickman, D., and Harris, L. R. 2005. An exceptional haddock year class and unusual environmental conditions on the Scotian Shelf in 1999. *Journal of Plankton Research*, 27: 597–602.
- Head, E. J. H., Harris, L. R., and Campbell, R. W. 2000. Investigations on the ecology of *Calanus* spp. in the Labrador Sea. I. Relationship between the phytoplankton bloom and reproduction and development of *Calanus finmarchicus* in spring. *Marine Ecology Progress Series*, 193: 53–73.
- Head, E. J. H., Harris, L. R., and Yashayaev, I. 2003. Distributions of *Calanus* spp. and other mesozooplankton in the Labrador Sea in relation to hydrography in spring and early summer (1995–2000). *Progress in Oceanography*, 59: 1–30.
- Head, E. J. H., Melle, W., Pepin, P., Bagøien, E., and Broms, C. 2013. On the ecology of *Calanus finmarchicus* in the Subarctic North Atlantic: a comparison of population dynamics and environmental conditions in areas of the Labrador Sea-Labrador/Newfoundland shelf and Norwegian Sea Atlantic and Coastal waters. *Progress in Oceanography*. 114:46-63. Doi: 10.1016/j.pocean.2013.05.004.

- Head, E. J. H., and Sameoto, D. D. 2007. Interdecadal variability in zooplankton and phytoplankton abundance on the Newfoundland and Scotian shelves. *Deep-Sea Research II*, 54: 2686–2701.
- Heath, M. R. 2005. Changes in the structure and function of the North Sea fish foodweb, 1973–2000, and the impacts of fishing and climate. *ICES Journal of Marine Science*, 62: 847–868.
- Heath, M. R., Adams, R. D., Brown, F., Dunn, J., Fraser, S., Hay, S. J., Kelly, M. C., *et al.* 1999. Plankton monitoring off the east coast of Scotland in 1997 and 1998. Fisheries Research Services Report, No 13/99.
- Heath, M. R., Rasmussen, J., Ahmed, Y., Allen, J., Anderson, C. I. H., Brierly, A. S., Brown, L., *et al.* 2008. Spatial demography of *Calanus finmarchicus* in the Irminger Sea. *Progress in Oceanography*, 76: 39–88.
- Helaouët, P., and Beaugrand, G. 2007. Macroecology of *Calanus finmarchicus* and *C. helgolandicus* in the North Atlantic Ocean and adjacent seas. *Marine Ecology Progress Series*, 345: 147–165.
- HELCOM. 1988. Guidelines for the Baltic Monitoring Programme for the Third Stage. Baltic Sea Environment Proceedings, 27D. 161 pp.
- HELCOM. 2010. Manual for marine monitoring in the COMBINE programme of HELCOM, Part C. – Internet, updated 2010: http://www.helcom.fi/groups/monas/CombineManual/AnnexesC/en_GB/.
- Heyen, H., Fock, H., and Greve, W. 1998. Detecting relationships between the interannual variability in ecological time-series and climate using a multivariate statistical approach; a case study on Helgoland Roads zooplankton. *Climate Research*, 10: 179–191.
- Highfield, J., Eloire, D., Conway, D. V. P., Lindeque, P. K., Attrill, M. J., and Somerfield, P. J. 2010. Seasonal dynamics of meroplankton assemblages at station L4. *Journal of Plankton Research*, 32: 681–691.
- Hinder, S. L., Hays, G. C., Edwards, M., Roberts, E. C., Walne, A. W., and Gravenor, M. B. 2012. Changes in marine dinoflagellates and diatom abundance under climate change. *Nature Climate Change*, 12: 1–5.
- Hughes, S. L., Holliday, N. P., and Beszcznska-Möller, A. (Eds). 2011. ICES Report on Ocean Climate 2010. ICES Cooperative Research Report No. 309. 69 pp.
- Iriarte, A., Aravena, G., Villate, F., Uriarte, I., Ibáñez, B., Llope, M., and Stenseth, N. C. 2010. Dissolved oxygen in contrasting estuaries of the Bay of Biscay: effects of temperature, river discharge and chlorophyll. *Marine Ecology Progress Series*, 418: 57–71.
- Iselin, C. O'D. 1936. A study of the circulation of the western North Atlantic. *Papers in Physical Oceanography and Meteorology*, 4(4): 1–101.
- Ji, R., Davis, C. S., Chen, C., Townsend, D. W., Mountain, D. G., and Beardsley, R. C. 2008. Modeling the influence of low-salinity water inflow on winter–spring phytoplankton dynamics in the Nova Scotian Shelf–Gulf of Maine region. *Journal of Plankton Research*, 30: 1399–1416.
- Johns, D. G., Edwards, M., and Batten, S. D. 2001. Arctic boreal plankton species in the Northwest Atlantic. *Canadian Journal of Fisheries and Aquatic Sciences*, 58(11): 2121–2124.
- Johns, D. G., Edwards, M., John, A. W. G., and Greve, W. 2005. Increasing prevalence of the marine cladoceran *Penilia avirostris* (Dana, 1852) in the North Sea. *Helgoland Marine Research*, 59: 214–218.
- Jurgensone, I., Carstensen, J., Ikauniece, A., and Kalveka, B. 2011. Long-term changes and controlling factors of phytoplankton community in the Gulf of Riga (Baltic Sea). *Estuaries and Coasts*, 34: 1205–1219.
- Kane, J. 2007. Zooplankton abundance trends on Georges Bank, 1977–2004. *ICES Journal of Marine Science*, 64: 909–919.
- Katajisto, T., Karjala, L., and Lehtiniemi, M. 2013. Fifteen years after invasion: egg bank of the predatory cladoceran *Cercopagis pengoi* in the Baltic Sea. *Marine Ecology Progress Series*, 482: 81–91. doi: 10.3354/meps10266.
- Kirby, R. R., and Lindley, J. A. 2005. Molecular analysis of Continuous Plankton Recorder samples, an examination of echinoderm larvae in the North Sea. *Journal of the Marine Biological Association of the UK*, 85: 451–459.
- Kogovšek, T., Bogunovič, B., and Malej, A. 2010. Recurrence of bloom-forming scyphomedusae: wavelet analysis of 200-years time-series. *Hydrobiologia*, 645(1): 81–96.
- Kontoyiannis, H., Krestenitis, I., Petyhakis, G., and Tsiartsis, G. 2005. Coastal areas: Circulation and hydrological features. *In State of the Hellenic Marine Environment*, pp. 95–104. Ed. by E. Papathanassiou and A. Zenetos. Hellenic Centre for Marine Research, Athens. 358 pp.
- Kotta, J., Kotta, I., Simm, M., and Põllupüü, M. 2009. Separate and interactive effects of eutrophication and climate variables on the ecosystem elements of the Gulf of Riga. *Estuarine, Coastal and Shelf Science*, 84: 509–518.
- Kotta, J., Lauringson, V., Martin, G., Simm, M., Kotta, I., Herkül, K., and Ojaveer, H. 2008. Gulf of Riga and Pärnu Bay. *In Ecology of Baltic Coastal Waters*, pp. 217–243. Ed. by U. Schiewer. Ecological Studies No. 197, Springer, Berlin. 428 pp.
- Kotta, J., Simm, M., Kotta, I., Kanošina, I., Kallaste, K., and Raid, T. 2004. Factors controlling long-term changes of the eutrophicated ecosystem of Pärnu Bay, Gulf of Riga. *Hydrobiologia*, 514: 259–268.

- Kraberg, A. C., Carstens, K., Peters, S., Tilly, K., and Wiltshire, K. H. 2011. The diatom *Mediopyxis helysia* Kühn, Hargreaves and Halliger, 2006 at Helgoland Roads: a success story? Helgoland Marine Research, doi: 10.1007/s10152-10011-1 0277-10159.
- Lafuente, J. G., and Ruiz, J. 2007. The Gulf of Cádiz pelagic ecosystem: a review. Progress in Oceanography, 74: 228–251.
- Lavín, A., Valdeś, L., Gil, J., and Moral, M. 1998. Seasonal and inter-annual variability in properties of surface water off Santander, Bay of Biscay, 1991–1995. Oceanologica Acta, 21: 179–190.
- Lavín, A., Valdes, L., Sanchez, F., Abaunza, P., Forest, A., Boucher, A., Lazure, P., *et al.* 2006. The Bay of Biscay: The encountering of the ocean and the shelf (18b, E). In The Sea, Volume 14, pp. 933–1001. Ed. by A. R. Robinson and K. H. Brink. Harvard University Press, Boston.
- Lemos, R. T., and Sanso, B. 2006. Spatio-temporal variability of ocean temperature in the Portugal Current System. Journal of Geophysical Research, 111: doi:10.1029/2005JC003051.
- Leppäranta, M., and Myrberg, K. 2009. Physical Oceanography of the Baltic Sea. Springer, Berlin. 378 pp.
- Leterme, S. C., Pingree, R. D., Skogen, M. D., Seuront, L., Reid, P. C., and Attrill, M. J. 2008. Decadal fluctuations in North Atlantic water inflow in the North Sea between 1958–2003: impacts on temperature and phytoplankton populations. Oceanologia, 50: 59–72.
- Li, W. K. W., Harrison, W. G., and Head, E. J. H. 2006. Multiyear trends in plankton show coherent sign switching. Science, 311: 1157–1160.
- Licandro, P., Conway, D. V. P., Daly Yahia, M. N., Fernandez de Puelles, M. L., Gasparini, S., Hecq, J. H., Tranter, P., *et al.* 2010. A blooming jellyfish in the northeast Atlantic and Mediterranean. Biology Letters. doi:10-1098/rsbl.2010-0150.
- Licandro, P., Head, E., Gislason, A., Benfield, M. C., Harvey, M., Margonski, P., and Silke, J. 2011. Overview of trends in plankton communities. In ICES Status Report on Climate Change in the North Atlantic, pp. 103–122. Ed. by P. C. Reid and L. Valdés. ICES Cooperative Research Report No. 310. 262 pp.
- Lindley, J. A., Reid, P. C., and Brander, K. M. 2002. Inverse relationship between cod recruitment in the North Sea and young fish in the Continuous Plankton Recorder survey. Scientia Marina, 67 (Suppl. 1): 191–200.
- Llope, M., Licandro, P., Chan, K.-S., and Stenseth, N. C. 2012. Spatial variability of the plankton trophic interaction in the North Sea: a new feature after the early 1970s. Global Change Biology, 18: 106–117.
- Loder, J. W., Gawarkiewicz, G., and Petrie, B. 1998. The coastal ocean of northeastern North America (Cape Hatteras to Hudson trait). In The Sea: Ideas and Observations on Progress in the Study of the Seas. Vol. 11: The Global Coastal Ocean: Regional Studies and Syntheses, pp. 105–133. Ed. by A. Robinson and K. Brink. John Wiley and Sons, Toronto. 1062 pp.
- Longhurst, A. R. 1998. Ecological Geography of the Sea, 2nd edition. Academic Press, San Diego. 398 pp.
- Lovegrove, T. 1962. The effect of various factors on dry weight values. Rapports et Procès-Verbaux des Réunions du Conseil International pour l'Exploration de la Mer, 153: 86–91.
- Lund, J. W. G., and Talling, J. F. 1957. Botanical limnological methods with special reference to the algae. Botanical Review, 23, 489–583.
- Lynam, C. P., Hay, S. J., and Brierley, A. S. 2005. Jellyfish abundance and climatic variation: contrasting responses in oceanographically distinct regions of the North Sea, and possible implications for fisheries. Journal of Marine Biological Association of the UK, 85: 435–450.
- Mackas, D. L., Greve, W., Edwards, M., Chiba, S., Tadokoro, K., Eloire, D., Mazzocchi, M. G., *et al.* 2012. Changing zooplankton seasonality in a changing ocean: comparing time series of zooplankton phenology. Progress in Oceanography, 97–100: 31–62.
- Mackas, D. L., Thomson, R. E., and Galbraith, M. 2001. Covariation of zooplankton community changes and oceanographic conditions on the British Columbia continental margin, 1995–1998. Canadian Journal of Fisheries and Aquatic Sciences, 58: 1–18.
- Madin, L. P., Horgan, E. F., and Steinberg, D. K. 2001. Zooplankton at the Bermuda Atlantic Time-series Study (BATS) station: Seasonal and interannual variation in biomass 1994–1998. Deep-Sea Research II, 48: 2063–2082.
- Malanotte-Rizzoli, P., Manca, B. B., Ribera d'Alcalà, M., Theocharis, A., Brenner, S., Budillon, G., and Ozsoy, E. 1999. The eastern Mediterranean in the 80s and in the 90s: the big transition in the intermediate and deep circulations. Dynamics of Atmospheres and Oceans, 29: 365–395.
- Malzahn, A. M., and Boersma, M. 2007. Year-to-year variation in larval fish assemblages of the Southern North Sea. Helgoland Marine Research, 61: 117–126.
- Maps, F., Zakardjian, B., Plourde, S., and Saucier, F. J. 2011. Modeling the interactions between the seasonal and diel migration behaviors of *Calanus finmarchicus* and the circulation in the Gulf of St. Lawrence (Canada). Journal of Marine Systems, 88: 183–202. doi: 10.1016/j.jmarsys.2011.04.004.

- Markaki, Z., Loýe-Pilot, M. D., Violaki, K., Benyahya, L., and Mihalopoulos, N. 2010. Variability of atmospheric deposition of dissolved nitrogen and phosphorus in the Mediterranean and possible link to the anomalous seawater N/P ratio. *Marine Chemistry*, 120: 189–196.
- Matthäus, W., and Schinke, H. 1999. The influence of river runoff on deep water conditions of the Baltic Sea. *Hydrobiologia*, 393: 1–10.
- Mazzocchi, M. G., and Ribera d'Alcalà, M. 1995. Recurrent patterns in zooplankton structure and succession in a variable coastal environment. *ICES Journal of Marine Science*, 52: 679–691.
- Mazzocchi, M. G., Dubroca, L., Garcia-Comas, C., Di Capua, I., and Ribera d'Alcalà, M. 2012. Stability and resilience in coastal copepod assemblages: The case of the Mediterranean long-term ecological research at stn MC (LTER-MC). *Progress in Oceanography*, 97–100: 135–151.
- Mazzocchi, M. G., Licandro, P., Dubroca, L., Di Capua, I., and Saggiomo, V. 2011. Zooplankton associations in a Mediterranean long-term time-series. *Journal of Plankton Research*, 33: 1163–1181.
- Melle, V., Ellertsen, B., and Skjoldal, H. R. 2004. Zooplankton: the link to higher trophic levels. In *The Norwegian Sea Ecosystem*, pp. 137–202. Ed. by H. R. Skjoldal. Tapir Academic Press, Trondheim.
- Mercado, J. M., Cortés, D., García, A., and Ramírez, T. 2007. Seasonal and inter-annual changes in the planktonic communities of the northwest Alborán Sea (Mediterranean Sea). *Progress in Oceanography*, 74: 273–293.
- Mercado, J. M., Cortés, D., Ramírez, T., and Gómez, F. 2012. Decadal weakening of the wind-induced upwelling reduces the impact of nutrient pollution in the Bay of Málaga (western Mediterranean Sea). *Hydrobiologia*, 680(1): 91–107.
- Mercado, J. M., Ramírez, T., Cortés, D., Sebastián, M., and Vargas-Yáñez, M. 2005. Seasonal and inter-annual variability of the phytoplankton communities in an upwelling area of the Alborán Sea (SW Mediterranean Sea). *Scientia Marina*, 69(4): 451–465.
- Minas, H. J., Coste, B., and Le Corre, P. 1991. Biological and geochemical signatures associated with the water circulation through the Strait of Gibraltar and in the western Alborán Sea. *Journal of Geophysical Research*, 96(C5): 8755–8771.
- Moita, M. Y., Oliveira, P. B., Mendes, J. C., and Palma, A. S. 2003. Distribution of chlorophyll *a* and *Gymnodinium catenatum* associated with coastal upwelling plumes off central Portugal. *Acta Oecologica*, 24(S1): S125–S132.
- Molinero, J. C., Ibanez, F., Nival, P., Buecher, E., and Souissi, S. 2005. The North Atlantic climate and the northwestern Mediterranean plankton variability. *Limnology and Oceanography*, 50: 1213–1220.
- Möllmann, C., Kornilovs, G., Fetter, M., and Köster, F. W. 2005. Climate, zooplankton, and pelagic fish growth in the central Baltic Sea. *ICES Journal of Marine Science*, 62: 1270–1280.
- Möllmann, C., Kornilovs, G., Fetter, M., Köster, F. W., and Hinrichsen, H. H. 2003. The marine copepod, *Pseudocalanus elongatus*, as a mediator between climate variability and fisheries in the central Baltic Sea. *Fisheries Oceanography*, 12: 360–368.
- Möllmann, C., Kornilovs, G., and Sidrevics, L. 2000. Long-term dynamics of the main mesozooplankton species in the central Baltic Sea. *Journal of Plankton Research*, 22: 2015–2038.
- Morais P, Chicharo, M.A., Chicharo, L. 2009. Changes in a temperate estuary during the filling of the biggest European dam. *Science of the Total Environment*, 407: 2245–2259.
- Mountain, D. G. 2004. Variability of the water properties in NAFO Subareas 5 and 6 during the 1990s. *Journal of Northwest Atlantic Fishery Science*, 34: 103–112.
- Mozetič, P., Francé, J., Kogovšek, T., Talaber, I., and Malej, A. 2012. Plankton trends and community changes in a coastal sea (northern Adriatic): Bottom-up vs. top-down control in relation to environmental drivers. *Estuarine, Coastal and Shelf Science*, 115: 138–148.
- O'Brien, T. D., Li, W. K. W., and Morán, X. A. G. 2012. ICES Phytoplankton and Microbial Plankton Status Report 2009/2010. ICES Cooperative Research Report No. 313. 196 pp.
- Oliveira, O. M. P. 2007. The presence of the ctenophore *Mnemiopsis leidyi* in the Oslofjorden and considerations on the initial invasion pathways to the North and Baltic Seas. *Aquatic Invasions*, 2: 185–189.
- Ojaveer, H., and Lumberg, A. 1995. On the role of *Cercopagis* (*Cercopagis*) *pengoi* (Ostroumov) in Pärnu Bay and the NE part of the Gulf of Riga ecosystem. *Proceedings of the Estonian Academy of Sciences*, 5: 20–25.
- Ojaveer, H., Simm, M., and Lankov, A. 2004. Population dynamics and ecological impact of the non-indigenous *Cercopagis pengoi* in the Gulf of Riga (Baltic Sea). *Hydrobiologia*, 522: 261–269.
- Omori, M., and Ikeda, T. 1984. *Methods in Marine Zooplankton Ecology*. John Wiley & Sons, Inc., Toronto. 332 pp.
- Omstedt, A. 2011. *Guide to Process Based Modeling of Lakes and Coastal Seas*. Springer-Verlag Berlin Heidelberg. 258 pp. doi: 10.1007/978 3 642 17728 6.
- Ouellet, M., Petrie, B., and Chassé, J. 2003. Temporal and spatial scales of sea-surface temperature variability in Canadian Atlantic waters. *Canadian Technical Report of Hydrography and Ocean Sciences*, 228. 30 pp.

- Pardo, P. C., Padin, X. A., Gilcoto, M., Farina-Busto, L., and Pérez, F. F. 2011. Evolution of upwelling systems coupled to the long-term variability in sea surface temperature and Ekman transport. *Climate Research*, 48: 231–246.
- Peliz, A., Rosa, T. L., Santos, A. M. P., and Pissarra, J. L. 2002. Fronts, jets, and counter-flows in the Western Iberian upwelling system. *Journal of Marine Systems*, 35: 61–77.
- Pershing, A. J., Greene, C. H., Jossi, J. W., O'Brien, L., Brodziak, J. K.T., and Bailey, B. A. 2005. Interdecadal variability in the Gulf of Maine zooplankton community, with potential impacts on fish recruitment. *ICES Journal of Marine Science*, 62: 1511–1523.
- Pingree, R. D., and Le Cann, B. 1993. Three anticyclonic Slope Water eDDIES (SWODDIES) in the Southern Bay of Biscay in 1990. *Deep-Sea Research II*, 39: 1147–1175.
- Pingree, R. D., and Griffiths, D. K. 1978. Tidal fronts on the shelf seas around the British Isles. *Journal of Geophysical Research*, 83: 4615–4622.
- Pinot J. M., Lopez-Jurado J. L., and Riera M. 2002. The CANALES experiment (1996–1998), interannual, seasonal, and mesoscale variability of the circulation in the Balearic Channels. *Progress in Oceanography*, 55: 335–370.
- Piontkovski, S. A., Fonda-Umani, S., de Olazabal, A., and Gubanova, A. D. 2012. *Penilia avirostris*: regional and global patterns of seasonal cycles. *International Journal of Oceans and Oceanography*, 6(1): 9–25.
- Platt, T., Fuentes-Yaco, C., and Frank, K. T. 2003. Spring algal bloom and larval fish survival. *Nature*, 423: 398–399.
- Plourde, S., Dodson, J. J., Runge, J. A., and Therriault, J.-C. 2002. Spatial and temporal variations in copepod community structure in the lower St. Lawrence Estuary, Canada. *Marine Ecology Progress Series*, 230: 221–224.
- Plourde, S., Joly, P., Runge, J. A., Dodson, J. D., and Zakardjian, B. 2003. Life cycle of *Calanus hyperboreus* in the lower St. Lawrence Estuary: is it coupled to local environmental conditions? *Marine Ecology Progress Series*, 255: 219–233.
- Plourde, S., Joly, P., Runge, J. A., Zakardjian, B., and Dodson, J. J. 2001. Life cycle of *Calanus finmarchicus* in the lower St. Lawrence Estuary: imprint of circulation and late phytoplankton bloom. *Canadian Journal of Fisheries and Aquatic Sciences*, 58: 647–658.
- Pöllumäe, A., and Kotta, J. 2007. Factors describing the distribution of the zooplankton community in the Gulf of Finland in the context of interactions between native and introduced predatory cladocerans. *Oceanologia*, 49: 277–290.
- Pöllumäe, A., Kotta, J., and Leisk, Ü. 2009. Scale-dependent effects of nutrient loads and climatic conditions on benthic and pelagic communities in the Gulf of Finland. *Marine Ecology*, 30: 20–32.
- Pöllupüü, M., Simm, M., Pöllumäe, A., and Ojaveer, H. 2008. Successful establishment of the Ponto–Caspian alien cladoceran *Evadne anonyx* G. O. Sars 1897 in low-salinity environment in the Baltic Sea. *Journal of Plankton Research*, 30: 777–782.
- Postel, L. 2012. Mesozooplankton diversity, reproduction modes, and potential invasibility in the Baltic Sea. In *Proceedings of the 1st International Workshop on Blooms and Invasions of Marine Species*, Sète, France, 21–23 June 2011. Ed. by D. Bonnet, F. Carcaillet, J. Klein, and M. Laabir. *Cahiers de Biologie Marine*, 53(3): 327–336.
- Ramírez, T., Cortés, D., Mercado, J. M., Vargas-Yañez, M., Sebastián, M., and Liger, E. 2005. Seasonal dynamics of inorganic nutrients and phytoplankton biomass in the NW Alboran Sea. *Estuarine, Coastal and Shelf Science*, 65: 654–670.
- Regner, D. 1981. The changes in seasonal oscillations of copepods in the central Adriatic. *Rapport Commission International pour l'exploration scientifique de la Mer Méditerranée*, 27(7): 177–179.
- Regner, D. 1985. Seasonal and multiannual dynamics of copepods in the middle Adriatic. *Acta Adriatica*, 26(2): 11–99.
- Regner, D. 1991. Long-term investigations of copepods (zooplankton) in the coastal waters of the eastern Middle Adriatic. *Acta Adriatica*, 32(2): 631–740.
- Reid, P. C., and Edwards, M. 2001a. Plankton and climate. In *Encyclopaedia of Ocean Sciences*, pp. 2194–2200. Ed. by J. H. Steele, S. A. Thorpe, and K. K. Turekian. Academic Press, New York, NY. 3399 pp.
- Reid, P. C., and Edwards, M. 2001b. Long-term changes in the pelagos, benthos and fisheries of the North Sea. *Senckenbergiana Maritima*, 31: 107–115.
- Relvas, P., Luis, J., and Santos, A. M. P. 2009. Importance of the mesoscale in the decadal changes observed in the northern Canary upwelling system. *Geophysical Research Letters*, 36, L22601, doi: 10.1029/2009GL040504.
- Relvas, P., Barton, E. D., Dubert, J., Oliveira, P. B., Peliz, A., da Silva, J. C. B., and Santos, A. M. P. 2007. Physical oceanography of the western Iberia ecosystem: Latest views and challenges. *Progress in Oceanography*, 74: 149–173.
- Ribeiro, S., and Amorim, A. 2008. Environmental drivers of temporal succession in recent dinoflagellate cyst assemblages from a coastal site in the North-East Atlantic (Lisbon Bay, Portugal). *Marine Micropaleontology*, 68: 156–178.
- Ribera d'Alcalà, M., Conversano, F., Corato, F., Licandro, P., Mangoni, O., Marino, D., Mazzocchi, M. G., et al. 2004. Seasonal patterns in plankton communities in a pluriannual time series at a coastal Mediterranean site (Gulf of Naples): an attempt to discern recurrences and trends. *Scientia Marina*, 68 (Suppl. 1): 65–83.

- Richardson, A. J., and Schoeman, D. S. 2004. Climate impact on plankton ecosystems in the Northeast Atlantic. *Science*, 305: 1609–1612.
- Rodriguez, L., Marin, V. A., Farias, M., and Oyarce, E. 1991. Identification of an upwelling zone by remote sensing and *in situ* measurements, Mejilones del Sur Bay (Antofagasta-Chile). *Scientia Marina*, 55: 467–473.
- Roether, W., Manca, B., Klein, B., Bregant, D., Georgopoulos, D., Beitzel, V., Kovacevic, V., *et al.* 1996. Recent changes in Eastern Mediterranean deep waters. *Science*, 271: 333–335.
- Roy, S., Silverberg, N., Romero, N., Deibel, D., Klein, B., Savenkoff, C., Vezina, A. F., *et al.* 2000. Importance of mesozooplankton feeding for the downward flux of biogenic carbon in the Gulf of St Lawrence (Canada). *Deep-Sea Research Part II*, 47: 519–544.
- Santos, F., Gómez-Gesteira, M., deCastro, M., and Álvarez, I., 2011. Upwelling along the western coast of the Iberian Peninsula: dependence of trends on fitting strategy. *Climate Research*, 48: 213–218.
- Santos, A. M. P., Chícharo, A., dos Santos, A., Moita, T., Oliveira, P. B., Peliz, A., and Ré, P. 2007. Physical-biological interactions in the life history of small pelagic fish in the Western Iberia Upwelling Ecosystem. *Progress in Oceanography*, 74: 192–209.
- Sarhan, T., García Lafuente, J., Vargas, M., Vargas, J. M., and Plaza, F. 2000. Upwelling mechanisms in the northwestern Alborán Sea. *Journal of Marine Systems*, 23: 317–331.
- Saucier, F. J., Roy, F., Gilbert, D., Pellerin, P., and Ritchie, H. 2003. Modeling the formation and circulation processes of water masses and sea ice in the Gulf of St. Lawrence, Canada. *Journal of Geophysical Research*, 108, 3269, doi:10.1029/2000JC000686, C8.
- Schlüter, M. H., Merico, A., Reginatto, M., Boersma, M., Wiltshire, K. H., and Greve, W. 2010. Phenological shifts of three interacting zooplankton groups in relation to climate change. *Global Change Biology*, 16: 3144–3153.
- Siokou-Frangou, I., Assimakopoulou, G., Christou, E., Kontoyiannis, H., Pagou, K., Pavlidou, A., and Zervoudaki, S. 2007. Long-term mesozooplankton variability in a Mediterranean coastal area, as influenced by trophic relationships and climate. *In Human and Climate Forcing of Zooplankton Populations*, p. 61. 4th International Zooplankton Production Symposium, Hiroshima, Japan, 28 May–1 June 2007. North Pacific Marine Science Organization. 281 pp.
- Smyth, T. J., Fishwick, J. R., AL Moosawi, L., Cummings, D. G., Harris, C., Kitidis, V., Rees, A., *et al.* 2010. A broad spatio-temporal view of the Western English Channel observatory. *Journal of Plankton Research*, 32: 585–601.
- Šolić, M., Krstulović, N., Marasović, I., Baranović, A., Pucher-Petković, T., and Vučetić, T. 1997. Analysis of time series of planktonic communities in the Adriatic Sea: distinguishing between natural and man-induced changes. *Oceanologica Acta*, 20(1): 131–143.
- Southward, A. J., Langmead, O., Hardman-Mountford, N. J., Aiken, J., Boalch, G. T., Dando, P. R., Genner, M. J., *et al.* 2004. Long-Term Oceanographic and Ecological Research in the Western English Channel. *Advances in Marine Biology*, 47: 1–105.
- Steinberg, D. K., Lomas, M. W., and Cope, J. S. 2012. Long-term increase in mesozooplankton biomass in the Sargasso Sea: Linkage to climate and implications for food web dynamics and biogeochemical cycling. *Global Biogeochemical Cycles*, 26, GB1004, doi:10.1029/2010GB004026.
- Steinberg, D. K., Carlson, C. A., Bates, N. R., Goldthwait, S. A., Madin, L. P., and Michaels, A. F. 2000. Zooplankton vertical migration and the active transport of dissolved organic and inorganic carbon in the Sargasso Sea. *Deep-Sea Research I*, 47: 137–158.
- Steuer, A. 1902. Beobachtungen ilber das Plankton des Triester Golfes im Jahre 1901. *Zoologischer Anzeiger*, 25(671): 369–372.
- Tsimplis, M., Zervakis, V., Josey, S., Peneva, E., Struglia, M. V., Stanev, E., Lionello, P., *et al.* 2006. Changes in the oceanography of the Mediterranean Sea and their link to climate variability. *In Mediterranean Climate Variability*, pp. 228–282. Ed. by P. Lionello, P. Malanotte-Rizzoli, and R. Boscolo. Elsevier, Amsterdam.
- Wu, Y., Peterson, I. K., Tang, C. C. L., Platt, T., Sathyendranath, D., and Fuentes-Yaco, C. 2007. The impact of sea ice on the initiation of the spring bloom on the Newfoundland and Labrador Shelves. *Journal of Plankton Research*, 29: 509–514.
- Valdés, L., López-Urrutia, A., Cabal, J., Alvarez-Ossorio, M., Bode, A., Miranda, A., Cabanas, M., *et al.* 2007. A decade of sampling in the Bay of Biscay: What are the zooplankton time series telling us? *Progress in Oceanography*, 74: 98–114.
- Valdés, L., and Moral, M. 1998. Time-series analysis of copepod diversity and species richness in the Sourthern Bay of Biscay (Santander; Spain) and their relationships with environmental conditions. *ICES Journal of Marine Science*, 55: 783–792.
- Vandromme, P., Stemmann, L., Berline, L., Gasparini, S., Mousseau, L., Prejger, F., Passafiume, O., *et al.* 2011. Inter-annual fluctuations of zooplankton communities in the Bay of Villefranche-sur-mer from 1995 to 2005 (Northern Ligurian Sea, France). *Biogeosciences*, 8: 3143–3158, doi:10.5194/bg 8 3143 2011.

Vandromme, P., Stemmann, L., Garcia-Comas, C., Berline, L., Sun, X., and Gorsky, G. 2012. Assessing biases in computing size spectra of automatically classified zooplankton from imaging systems: A case study with the ZooScan integrated system. *Methods in Oceanography*, doi:10.1016/j.mio.2012.06.001.

Villate, F., Aravena, G., Iriarte, A., and Uriarte, I. 2008. Axial variability in the relationship of chlorophyll *a* with climatic factors and the North Atlantic Oscillation in a Basque coast estuary, Bay of Biscay (1997–2006). *Journal of Plankton Research*, 30: 1041–1049.

Vezzulli, L., and Reid, P. C. 2003. The CPR survey (1948–1997): a gridded database browser of plankton abundance in the North Sea. *Progress in Oceanography*, 58: 327–336.

Wasmund, N., and Uhlig, S. 2003. Phytoplankton trends in the Baltic Sea. *ICES Journal of Marine Science*, 60: 177–186.

Widdicombe, C. E., Eloire, D., Harbour, D., Harris, R. P., and Somerfield, P. J. 2010. Long-term phytoplankton community dynamics in the Western English Channel. *Journal of Plankton Research*, 32: 643–655.

Wiltshire, K. H., Malzahn, A. M., Wirtz, K., Greve, W., Janisch, S., Mangelsdorf, P., Manly, B. F. J., *et al.* 2008. Resilience of North Sea phytoplankton spring blooms dynamics: an analysis of long-term data at Helgoland Roads. *Limnology and Oceanography*, 53: 1294–1302.

Zeri, C., Kontoyiannis, H., and Giannakourou, A. 2009. Distribution, fluxes and bacterial consumption of total organic carbon in a populated Mediterranean Gulf. *Continental Shelf Research*, 29: 886–895.

Zingone, A., Dubroca, L., Iudicone, D., Margiotta, F., Corato, F., Ribera d'Alcalà, M., Saggiomo, V. and Sarno, D., 2010. Coastal phytoplankton do not rest in winter. *Estuaries and Coasts*, 33: 342–361.

25

ITEM DATA: TIME-SERIES

SAMPLING CHARACTERISTICS AND

CONTACT INFORMATION

Ocean Region	Northwest Atlantic Shelf							
Country	United States of America				Canada			USA
Sampling / Monitoring Programme	NEFSC Ecosystem Monitoring Program				Atlantic Zone Monitoring Program (AZMP)			Bermuda Atlantic Time-series Study (BATS)
Report Section	Section 1				Section 2	Section 3	Section 4	Section 5
Sampling Site Name	MAB	SNE	GOM	GB	Prince 5	Halifax Line 2	Anticosti Gyre and Gaspar Current	BATS
WGZE Site Number	1	2	3	4	5	6	7	8
Sampling Location	Mid-Atlantic Bight (MAB)	Southern New England (SNE)	Gulf of Maine (GOM)	Georges Bank (GB)	Bay of Fundy	Scotian Shelf	Gulf of St. Lawrence	Sargasso Sea
Sampling Duration	1977 - present				1999 - present			1994 - present
Sampling Frequency	Cross-monthly surveys, six times per year				Monthly / Biweekly / Weekly			Monthly / Biweekly
Sampling Gear (diameter)	Bongo Net (60 cm)				Ring Net (75 m)			Rectangle net (80 m x 120 cm)
Sampling Mesh (µm)	300 µm				200 µm			202 µm
Sampling Depth (m)	0 to 200 (or bottom)				0 to bottom			0 to 200
Contact Person	Jon Hare				Catherine Johnson		Stephane Plourde	Deborah Steinberg
Contact's Email Address	Jon.Hare@noaa.gov				Catherine.Johnson@dfo-mpo.gc.ca		Stephane.Plourde@dfo-mpo.gc.ca	DebbieS@vims.edu
Associated Persons					Erica Head		Michel Harvey	
Associated Institutions	US National Marine Fisheries Service (NMFS), Northeast Fisheries Science Center (NEFSC)				Bedford Institute of Oceanography, Department of Fisheries and Oceans (DFO), Fisheries and Oceans Canada,		Department of Fisheries and Oceans (DFO), Fisheries and Oceans Canada	Bermuda Institute of Ocean Sciences (BIOS)



Sapphirina angusta (female). M.T. Alvarez-Ossorio
& A. Bode (IEO A Coruña)

Ocean Region	Labrador Sea					
Country	Canada					
Sampling / Monitoring Programme	AZMP	Atlantic Zone Off-Shelf Monitoring Program (AZOMP), Atlantic Repeat Hydrography Line 7 (AR7W)				
Report Section	Section 4.1	Section 4.2				
Sampling Site Name	Station 27	AR7W Zone 1	AR7W Zone 2	AR7W Zone 3	AR7W Zone 4	AR7W Zone 5
WGZE Site Number	9	10	11	12	13	14
Sampling Location	Newfoundland Shelf	Labrador Shelf	Labrador Slope	Central Labrador Sea	Eastern Labrador Sea	Greenland Shelf
Sampling Duration	1999 - present	1996 - present				
Sampling Frequency	Monthly / Biweekly	Annually (Late May)				
Sampling Gear (diameter)	Ring Net (75 m)	Ring net (diameter 0.75m)				
Sampling Mesh (µm)	200 µm	202 µm				
Sampling Depth (m)	0 to bottom	0-100 m (vertical)				
Contact Person	Pierre Pepin	Erica Head				
Contact's Email Address	Pierre.Pepin@dfo-mpo.gc.ca	Erica.Head@dfo-mpo.gc.ca				
Associated Persons						
Associated Institutions	Fisheries and Oceans Canada (DFO), Northwest Atlantic Fisheries Centre	Department of Fisheries and Oceans (DFO), Fisheries and Oceans Canada, Bedford Institute of Oceanography				

Ocean Region	Nordic and Barents seas					
Country	Iceland		Faroe Islands	Norway		
Sampling / Monitoring Programme	Icelandic Spring Cruise		Faroe Marine Research Institute (FAMRI)	IMR-Bergen		
Report Section	Section 51		Section 52	Section 53	Section 54	
Sampling Site Name	Selvogsbanki Transect	Siglunes Transect	Faroe Shelf and Northern Transect	Svinøy Transect	Fugløya-Bjørnøya Transect	Vardø-Nord Transect
WGZE Site Number	15	16	17	18	19	20
Sampling Location	South Iceland	North Iceland	Southern Norwegian Sea (Faroe Islands)	Norwegian Sea	Western Barents Sea	Central Barents Sea
Sampling Duration	1971 - present	1961 - present	1990 - present	1996 - present	1994 - present	
Sampling Frequency	Annually (May-June)		Annually (late May)	4 - 6 times per year	3 - 6 times per year	3 - 4 times per year
Sampling Gear (diameter)	1971-1991: Hensen Net; 1992-present: WP-2 Net		1990-1991: Hensen Net; 1992-present: WP-2 Net	WP-2 Net (5 cm)		
Sampling Mesh (µm)	200 µm		200 µm	100 µm		
Sampling Depth (m)	0 to 6		0 to 6	0 to 200	0 to 100 and 0 to bottom	
Contact Person	Astthor Gislason		Eilif Gaard	Webjørn Melle	Padmini Dalpadado	
Contact's Email Address	astthor@hafro.is		eilifg@hav.fo	webjorn@imr.no	Padmini.Dalpadado@imr.no	
Associated Persons	Hildur Petursdottir		Høgne Debes	Cecilie Broms		
Associated Institutions	Marine Research Institute (MRI)		Faroe Marine Research Institute (FAMRI)	Institute of Marine Research (IMR)	Institute of Marine Research (IMR)	

Ocean Region	Baltic Sea							
Country	Finland				Estonia		Latvia	
Sampling / Monitoring Programme	Finnish Environment Institute SYKE / HELCOM Monitoring				HELCOM Monitoring		National monitoring programme of Latvia	Latvian National Program for Collection of Fisheries Data
Report Section	Section 6.1				Section 6.2	Section 6.3	Section 6.4	Section 6.5
Sampling Site Name	Bothnian Bay	Bothnian Sea	Gulf of Finland	The Baltic Proper	Tallinn Bay	Pärnu Bay	Station 121	Eastern Gotland Basin
WGZE Site Number	21 - 22	23 - 25	26 - 28	29 - 3	3	4	5	6
Sampling Location	Northern Baltic Sea	Northern Baltic Sea	Gulf of Finland	Central Baltic Sea	Gulf of Finland	Northeast Gulf of Riga	Gulf of Riga	Central Baltic Sea
Sampling Duration	1979 - present				1993 - present	1979 - present	1993 - present	1960 - present
Sampling Frequency	August				up to 10 times per year	monthly to weekly in non-ice months	at least 3 times per year	seasonally (May, August, October)
Sampling Gear (diameter)	WP-2 Net (6 cm)				Judy Net (6 cm)		WP-2 Net (7 cm)	Judy Net (6 cm)
Sampling Mesh (µm)	100 µm				before 2005 90 µm, since 2005 100 µm		100 µm	160 µm
Sampling Depth (m)	Surface-thermocline, thermocline-halocline, halocline-bottom (if no clines then 0 to bottom)				0 to bottom		0 to 6	0 to 100
Contact Person	Maiju Lehtiniemi				Arno Põllumäe		Anda Ikauniece	Gunta Rubene
Contact's Email Address	Maiju.Lehtiniemi@ymparisto.fi				arno@sea.ee		anda.ikauniece@lhei.lv	Gunta.Rubene@bior.gov.lv
Associated Persons	Siru Tasala					Maria Põllupüü, Mart Simm		Solvita Strāķe
Associated Institutions	Finnish Meteorological Institute FMI				Estonian Marine Institute, University of Tartu		Latvian Institute of Aquatic Ecology (LHEI)	Institute of Food Safety, Animal Health and Environment (BIOR)

Ocean Region	Baltic Sea						
Country	Poland			Germany	Sweden		
Sampling / Monitoring Programme	HELCOM Monitoring			Leibniz Institute for Baltic Sea Research, Warnemünde (IOW)	SMHI / HELCOM Monitoring		
Report Section	Section 6.6			Section 6.7	Section 6.8		
Sampling Site Name	Gdańsk Basin	Southern Gotland Basin	Bornholm Basin	Arkona Basin	Anholt East	Släggö	Å17
WGZE Site Number	3	8	9	40	41	42	43
Sampling Location	Gdańsk Basin	Southern Gotland Basin	Bornholm Basin	Southern Baltic Sea	Kattegat	Skagerrak	Skagerrak
Sampling Duration	1979-present			1979 - present	1998 - present	2007- present	
Sampling Frequency	3-6 times per year			3 times per year	fortnightly	monthly	
Sampling Gear (diameter)	WP-2 Net (3 m)			WP-2 Net (3 m)	WP-2 Net (5 m)		
Sampling Mesh (µm)	100µm			100 µm	90 µm		
Sampling Depth (m)	0 to bottom			0 to 25	0 to 25		
Contact Person	Piotr Margonski			Lutz Postel	Lars Johan Hansson		
Contact's Email Address	pmargon@mir.gdynia.pl			lutz.postel@io-warnemuende.de	lars.hansson@smhi.se		
Associated Persons					Marie Johansen		
Associated Institutions	Institute of Meteorology and Water Management (IMGW)			Federal Maritime and Hydrographic Agency of Germany (BSH)	Swedish Meteorological and Hydrological Institute (SMHI)		

Ocean Region	North Sea and English Channel				
Country	Norway	Germany	United Kingdom		
Sampling / Monitoring Programme	IMR / Norwegian Coastal Long-term Monitoring Programme of Environmental Quality	Alfred-Wegener-Institut Helmholtz Zentrum für Polar- und Meeresforschung (AWI) and Deutsches Zentrum für Marine Biodiversitätsforschung (DZMB)	MSS Inshore Ecosystem Monitoring Program		Plymouth Marine Laboratory (PML)
Report Section	Section 7.1	Section 7.2	Section 7.3	Section 7.4	Section 7.5
Sampling Site Name	Arendal Station 2	Helgoland Roads	Stonehaven	Loch Ewe	Plymouth L4
WGZE Site Number	44	45	46	47	48
Sampling Location	Northern Skagerrak	Southeast North Sea	Northwest North Sea	Northwest Scotland	English Channel
Sampling Duration	1994 - present	1975 - present	1997 - present	2002 - present	1981 - present
Sampling Frequency	twice per month	Every Monday, Wednesday, and Friday	Weekly (2 weeks per year)		Weekly (40 weeks per year)
Sampling Gear (diameter)	WP-2 Net (5 cm)	Apstein and Calcofi	Bongo Net (40 cm)		WP-2 Net
Sampling Mesh (µm)	100 µm	100 µm, 60 µm	200 µm		200 µm
Sampling Depth (m)	0 to 6	0 to bottom	0 to 6	0 to 3	0 to 6
Contact Person	Tone Falkenhaug	Maarten Boersma	Kathryn Cook		Angus Atkinson
Contact's Email Address	Tone.Falkenhaug@imr.no	Maarten.Boersma@awi.de	Kathryn.cook@scotland.gsi.gov.uk		aat@pml.ac.uk
Associated Persons	Lena Omli	Jasmin Renz	John Fraser, Susan Robinson		Elaine Fileman, Claire Widdicombe, Rachel Harmer, Andrea McEvoy, Roger Harris, Tim Smyth
Associated Institutions	Institute of Marine Research (IMR)	Bundesamts für Seeschifffahrt und Hydrographie (BSH)	Marine Scotland Science (MSS)		Plymouth Marine Laboratory, PML

Ocean Region	Bay of Biscay and western Iberian Shelf						
Country	Spain					Portugal	
Sampling / Monitoring Programme	Zooplankton Ecology Group / University of the Basque Country (ZEG/UBC)	Instituto Español de Oceanografía (IEO) - Spain ; s e Ries temporales De oceanografía en el norte de España (RADIALES)				Instituto Português do Mar e da Atmosfera (IPMA)	Center of Marine Sciences (CCMAR U ALG)
Report Section	Section 1	Section 2	Section 3	Section 4	Section 5	Section 6	Section 7
Sampling Site Name	Bilbao and Urdaibai Estuaries	Santander Transect	Gijón/Xixón	A Coruña	Vigo	Cascais	Guadiana Lower Estuary
WGZE Site Number	49	6	5	3	3	3	5
Sampling Location	Inner Bay of Biscay	Southern Bay of Biscay	Southwestern Bay of Biscay	Northwest Iberian Shelf	Northwest Iberian Shelf	Southwestern Iberian Shelf	southern Iberian Peninsula
Sampling Duration	1997-present	1991 - present	2001 - present	1990 - present	1994 - present	2005 - present	1997-present
Sampling Frequency	Monthly	Monthly	Monthly	Monthly	Monthly	Monthly	Monthly, or every 2-3 months
Sampling Gear (diameter)	Ring Net (25 m)	Juday Net (6 cm)	WP-2 Net (8 m)	Juday Net (6 cm)	Bongo Net (40 cm)	WP-2 Net (6 cm)	WP-2 Net (40 cm)
Sampling Mesh (µm)	200 µm	200 µm	200 µm	197196:200 µm; 1996-present 200 µm	200 µm	200 µm	200 µm
Sampling Depth (m)	Mid depth, horizontal tow	0 to 6	0 to 100	0 to 6	0 to 95	0 to 6	0.5m , horizontal tow
Contact Person	Fernando Villate	Carmen Rodriguez	Angel Lopez Urrutia	Maite Alvarez Ossorio	Ana Miranda	Antonina dos Santos	Maria Alexandra Chicharo
Contact's Email Address	fernando.villate@ehu.es	carmen@st.ieo.es	alop@gi.ieo.es	maite.alvarez@co.ieo.es	ana.miranda@vi.ieo.es	antonina@ipma.pt	mchichar@ualg.pt
Associated Persons	Ibon Uriarte, Arantza Iriarte	Juan Bueno, Ángel López Urrutia	Juan Bueno & Ángel López Urrutia	Antonio Bode	Gerardo Casa, Antonio Bode	A. Miguel P. Santos	Joana Cruz Radhouan Ben-Hamadou , Pedro Morais , Ana Faria , David Pilo , Renata Goncalves , Teja Muha , Susana Ferreira , Joao Pedro Encarnacao, Vanessa Neves , Luis Chicharo
Associated Institutions	University of the Basque Country	Instituto Español de Oceanografía				Instituto Português do Mar e da Atmosfera (IPMA)	Center of Marine Sciences (CCMAR U ALG)

Ocean Region	Mediterranean Sea						
Country	Spain		France	Italy		Croatia	Greece
Sampling / Monitoring Programme	Instituto Español de Oceanografía (IEO) - Spain		Laboratoire d'Océanographie de Villefranche (LOV)- France	SZN-Italy	UNITS-Italy / OGS-Italy	IZOR-Croatia	HCMR-Greece
Report Section	Section 9.1	Section 9.2	Section 9.3	Section 9.4	Section 9.5	Section 9.6	Section 9.7
Sampling Site Name	Málaga Bay	Baleares Station	Villefranche Point B	Gulf of Naples LTER-MC	Gulf of Trieste LTER	Stončica	Saronikos S11
WGZE Site Number	5	3	8	9	60	61	62
Sampling Location	Alboran Sea	Balearic Sea	Cote d'Azur	Gulf of Naples	Northern Adriatic Sea	Central Adriatic Sea	Aegean Sea
Sampling Duration	1992-2000, 2010-present	1994 - present	1966 - present	198 - present	1970 - present	199 - 1991; 1995 - present (unprocessed)	198 - present
Sampling Frequency	quarterly	monthly (up until 2006); after 2007 every 3 months	daily pooled by week	biweekly (198-1990), weekly (1995 - present)	monthly	monthly (with gaps)	seasonally (198-1998); monthly after 1999
Sampling Gear (diameter)	Double bongo net (40 cm)	Bongo net (20 cm)	Regent, Juday-Bogorov & WP2 nets	Nansen Net (113 m)	WP-2 Net	Hensen Net (73 cm)	WP-2 Net
Sampling Mesh (µm)	200 µm	100/250 µm	60, 80 & 200 µm	200 µm	200 µm	80 µm	200 µm
Sampling Depth (m)	0 to bottom	0 - 100	0 - 75	0 - 8	0 - 15	0 to 100	0 to 75
Contact Person	Lidia Yebra	Mª Luísa Fernández de Puellas	Lars Stemmann	Maria Grazia Manacchi	Serena Fonda-UmaniValentina Tirelli	Olja Vidjak	Ionna Siokou; Soultana Zervoudaki
Contact's Email Address	lidia.yebra@ma.ieo.es	mlufernandez@ba.ieo.es	stemmann@obs-vlfr.fr	grazia@szn.it	s.fonda@units.it; vtirelli@ogs.trieste.it	vidjak@izor.hr	isiokou@hcmr.gr; tanya@hcmr.gr
Associated Persons	Jesús M. Mercado, Dolores Cortés, Sébastien Putzeys	Mª Luísa Fernández-Puelles, Magdalena Gálvez	Gabriel Gorsky	Iole Di Capua	Alessandra de Olazábal	Natalia Bojanić	Soultana Zervoudaki, Epaminondas Christou
Associated Institutions	Instituto Español de Oceanografía (IEO)	Instituto Español de Oceanografía (IEO)	Observatoire Océanologique de Villefranche-sur-Mer (OOV)	Stazione Zoologica Anton Dohrn di Napoli (SZN)	UNITS-Italy (University of Trieste); 1970-2005; OGS-Italy (Istituto Nazionale di Oceanografia e di Geofisica Sperimentale; 2006-present)	Institut Za Oceanografiju i Ribarstvo (IZOR)	Hellenic Centre for Marine Research (HCMR)

Ocean Region	North Atlantic Basin
Country	United Kingdom
Sampling / Monitoring Programme	Continuous Plankton Recorder
Report Section	Section 10
Sampling Site Name	CPR Surveys
WGZE Site Number	* CPR Standard Areas
Sampling Location	Trans-Atlantic Basin
Sampling Duration	1946 - present
Sampling Frequency	Monthly (with gaps)
Sampling Gear (diameter)	CPR (1.24 cm)
Sampling Mesh (µm)	270 µm
Sampling Depth (m)	sub-surface (7-10 m)
Contact Person	Priscilla Licandro
Contact's Email Address	prli@sahfos.ac.uk
Associated Persons	Claudia Castellani, Martin Edwards, Rowena Stern
Associated Institutions	Sir Alister Hardy Foundation for Ocean Science (SAHFOS)



ICES

International Council for
the Exploration of the Sea

CIEM

Conseil International pour
l'Exploration de la Mer